Nephrotoxicity biomarkers in vivo and in vitro: Identification and validation of biomarkers for the detection of substance-induced acute and sub-acute renal damage

Vom Fachbereich Biologie der Technischen Universität Darmstadt

zur Erlangung des akademischen Grades

eines Doctor rerum naturalium

genehmigte Dissertation von
Diplom-Biologe Tobias Christian Fuchs
aus Darmstadt

Referent:	Prof. Dr. Paul G. Layer
Koreferent:	Prof. Dr. Heribert Warzecha
Externer Referent:	Philip G. Hewitt, PhD

Tag der Einreichung: 08.01.2013
Tag der mündlichen Prüfung: 07.03.2013
Darmstadt 2013
D17

Ich wohne in meinem eignen Haus
Hab Niemandem nie nichts nachgemacht
Und – lachte noch jeden Meister aus
Der nicht sich selber ausgelacht.

-Friedrich Nietzsche-

Unsere Wissenschaft ist in jedem Augenblick nur die Hypothese dessen,
was bis zu diesem Augenblick kein Experiment falsifiziert.
Die endgültige wissenschaftliche Summe wird nie mehr sein als das geltende
Vorurteil in dem Moment, in dem die Menschheit verlischt.
(translated from the Spanish)

-Nicolás Gómez Dáliva-

I went to the woods because I wished to live deliberately, to front only the essential facts of life, and see if I could not learn what it had to teach, and not, when I came to die, discover that I had not lived. I did not wish to live what was not life, living is so dear; nor did I wish to practice resignation, unless it was quite necessary. I wanted to live deep and suck out all the marrow of life, to live so sturdily and Spartan-like as to put to rout all that was not life, to cut a broad swath and shave close, to drive life into a corner, and reduce it to its lowest terms, and, if it proved to be mean, why then to get the whole and genuine meanness of it, and publish its meanness to the world; or if it were sublime, to know it by experience, and be able to give a true account of it in my next excursion.

-Henry David Thoreau-

TABLE OF CONTENT

DANKSAGUNG

Wie im Allgemeinen üblich darf in einer Dissertation eine Danksagung nicht fehlen. In dieser wird den Personen gedankt, welche einen nicht unerheblichen Anteil an der vorgelegten Arbeit haben. Dies bedeutet jedoch nicht, dass man sie auch zwingend in der Referenzierung findet. Vielmehr handelt es sich um die eigentlich wichtige und grundlegende Unterstützung, die eine Arbeit wie die Doktorarbeit erst ermöglicht und die bis auf diese wenigen Zeilen nicht weiter wahrgenommen wird. Dieser besagte Beitrag, welchen ich hier an dieser Stelle für meine Arbeit niederlegen möchte, ist an sich nicht ausreichend in Worte zu fassen um es hier adäquat darstellen zu können, und doch unternehme ich den Versuch wie viele vor mir, den Menschen zu danken, ohne es im Detail hier näher ausführen zu können, in der Hoffnung jede Person weiß für sich, wie wichtig eben ihr individueller Beitrag für mich und diese Arbeit war.

Somit möchte ich den wissenschaftlichen und akademischen Betreuern und Gutachtern für ihre Unterstützung und Förderung danken, die ihren inhaltlichen Beitrag und Anteil hat, welcher mit in die tägliche Arbeit eingeflossen ist. Somit vielen Dank an meinen Doktorvater Prof. Paul G. Layer für die Bereitschaft, meine externe Doktorarbeit von Seiten der TU-Darmstadt aus zu betreuen und für die positiven Feedbacks. Dank auch an Prof. Heribert Warzecha, welcher sich bereit erklärt hat, als Zweitgutachter zu fungieren. Mein Dank an Dr. Stefan O. Müller für die kritische Begutachtung meiner Arbeitsfortschritte während des Lab-meetings sowie für die Anerkennung meiner Leistungen bei der Nominierung und Betreuung im Student Excellence Program der Firma Merck KGaA.
Einen ganz besonderen Dank möchte ich an meinen fachlichen Betreuer Philip Hewitt, PhD richten, welcher immer eine offene Tür und ein offenes Ohr hatte, sei es fachlich oder privat. Vielen Dank Phil für die Zusammenarbeit, Diskussionen, Anregungen, das entgegengebrachte Vertrauen und die vielen DVDs, die ich mir von dir ausleihe durfte, sowie die fantastischen *movie nights*. Ich habe die Zeit als einer deiner *Students* wirklich sehr genossen und nehme sehr viel aus der Zeit bei dir mit.

Ebenfalls danken möchte ich Dr. Barbara Emde, durch die ich sehr viel im Bezug auf *Study Reports and -designs*, GLP-konforme Rohdatentabellen und dergleichen gelernt habe. Danke für deine tatkräftige Unterstützung sowohl bei der täglichen Arbeit als auch bei den kleinen Alltagssorgen.
Danke auch an Dr. Stefanie Czasch und Dr. Anja Knippel für die Zusammenarbeit bei der histopathologischen und immunhistochemischen Auswertung der Studien und die offene(n) Tür(en) bei „pathologischen Fragen“.
Abschliessend möchte ich allen Mitarbeitern bei Merck danken, welche Anteil haben an dieser Arbeit. Danke an das Team der *Rodent Toxikology*, *Clinical Pathology* und *Histopathology*. Auch wenn ich hier nicht jedem von euch einzeln danken kann, möchte ich doch, dass ihr wisst, wie viel Spaß mir die Zusammenarbeit mit euch allen gemacht hat und wieviel ich von euch und euren Erfahrungen lernen konnte. Danke an Jörg Hiller für die tatkräftige Fürsorge bei allen Arten von IT-Problemen. Und Danke für die Späße, Schwätzchen und Capsules zwischendurch, die selbst Schwierigkeiten mit dem PC freundlicher haben erscheinen lassen.

Meinen Dank möchte ich ebenfalls an Prof. Robert Russel (Universität Heidelberg) und Dr. Gordana Apic (CEO Cambridge Cell Networks) für die angenehme und fruchtbare Zusammenarbeit in „unserem“ BMBF geförderten Projekt richten. Ich habe sehr viel aus unserer Zusammenarbeit mitgenommen und besonders unsere Meetings in sehr guter Erinnerung.

Bei den Personen, denen man danken möchte, nein danken muss, handelt es sich aber nicht nur um Kollegen, Betreuer, oder gar Vorgesetzte. Es handelt sich auch um Mitstreiter, welche einen begleitet und geholfen haben und die, dadurch dass sie das gleiche Schicksal teilen, einen ganz eigenen Anteil und Beitrag leisten. Danke Christina Schmitt für die vielen anregenden und hilfreichen Diskussionen. Hier sind mir besonders das gedankliche Durchspielen von Studiendesigns und die daraus resultierende Analyse im Gedächtnis geblieben. Danke, Kathleen Boehme, für dein fantastisch pragmatisches Verständnis in Sachen Statistik sowie deine

Toleranz und Resistenz meinen Scherzen gegenüber. Danke an Birthe Lauer, die mir gezeigt hat, dass Hartnäckigkeit sich auszahlen kann.

Danke an Germaine L. Truisi, die mir so manches Lächeln aufs Gesicht zaubern konnte mit ihren fantasievollen, sprachlichen Auswüchsen und Eigenkreationen. Danke Germaine, für dein Engagement in der Organisation von ausserbetrieblichen Gruppenaktivitäten sowie die einfach schöne und angenehme Zusammenarbeit.
Danke auch an Yasmin Dietz, mit der ich mich trotz farblicher Unterschiede sehr gut verstanden habe. Wir sind das lebende Beispiel, dass Zusammenhalt und Kommunikation auch solche Hürden überwinden kann und einfach Spaß macht.
Ebenfalls möchte ich natürlich meinen „studentischen Schützlingen“ danken für die gute Arbeit, die ihr geleistet habt, welche mich als inoffiziellen Betreuer in einem umso besseren Licht hat erscheinen lassen. Danke an Katharina Frick, Esther Johann und Andreas Gado. Ich hoffe, ihr konntet ebenso viel von mir lernen wie ich von euch. Und natürlich auch mein Dank an die ehemaligen Doktoranden, welche mich als Schützling betreut, gefördert und angeleitet haben. Danke Jens Hrach und Julia Pieh für eure Unterstützung zu den Anfangszeiten als Doktorand.

Nun kommt der schwerste und doch zugleich der erfreulichste Teil der Danksagung. Wie dankt man der Famile, die immer, ausnahmslos und bedingungslos für einen da ist, wenn es darauf ankommt?
Meine Familie ist klein und wie üblich bei kleinen Gruppen, rückt man näher zusammen, weiß mehr zu schätzen, was man hat, sorgt und kümmert sich mehr um den anderen. In diesem Sinne möchte ich meiner Mama danken, dass sie immer und ohne Ausnahme da war und mich unterstützt, gefördert und angetrieben hat. Diese Arbeit ist nicht etwa zwischen 2009 und 2012 entstanden, sondern hat ihren Anfang in den 90ern bei den alltäglichen Kämpfen in der Grundschule, als es an die Erledigung der Hausaufgaben ging. Danke hierfür und danke dafür, dass du mir immer alles ermöglicht hast, auch wenn damit das ein oder andere eigene Opfer verbunden war.
Ebenso gilt mein Dank meiner Tante Sandra, welche immer ein offenes Ohr hatte und bei Bedarf für ein bisschen Zerstreuung gesorgt hat. Danke für die vielen schönen Gespräche über Lokalpolitik und Wirtschaft, die neuesten Reise- und Modetrends oder die angesagtesten Darmstädter Cafes und Restaurants bei einem Kaffee und Wein auf dem Luisenplatz oder bei dir nach einer „Glühbirnentausch-Aktion“.

Dass das Leben wie eine Schachtel Pralinen ist, hat sich ja in der Zwischenzeit herum gesprochen. Auch mit Danksagungen verhält es sich so. Bei mir ist es jedoch so, dass es eine Praline gibt, die immer erst ganz zum Ende genussvoll celebriert wird. Diese Praline in meiner Danksagung ist meine Frau.
Ich danke dir Nadine für deine Liebe, Unterstützung, die aufmunternden Worte, den Rückhalt und den Verzicht auf viele Wochenenden und Urlaube. Die Zeit der Doktorarbeit war nicht immer leicht und rückblickend glaube ich fast, dass es für dich noch schwerer war als für mich. Immerhin hatte ich ja neben den typischen Unsicherheiten, die eine Doktorarbeit so mit sich bringt, der vielen Stunden Arbeit und der generellen mageren Anerkennung sowie dem fehlenden Verständnis dafür, was man eigentlich den Tag über so tut, immer das Glück zu wissen, das ich etwas für mich tue. Du hingegen hattest all das in gleichem Masse und oben drauf noch mich. Trotzdem hattest du immer ein strahlendes Lachen auf dem Gesicht. Dieses Lachen, was mehr als ansteckend ist, hat mir sehr oft über das ein oder andere Schuldgefühl hinweggeholfen und mich positiv nach vorne schauen lassen. Aber nicht nur durch deine fantastisch liebenswerte Art, sondern auch durch dein Fachwissen hast du mir so manchens Excel-Dilemma erspart. Auch wenn ich Fragen hatte und einen unabhängigen und unbelasteten Blick auf ein Problem gebraucht habe, hast du mir häufig geholfen und potentielle Lösungen aufgezeigt. Um es einfach mit drei Worten zu sagen: „Danke für alles!“

ABBREVIATIONS[1]

AA	Aristolochic acid
ADME	Absorption, Distribution, Metabolism, and Excretion
AhR	Arylhydrocarbonreceptor
AKI	Acute kidney injury
AmpB	AmphotericinB
APAP	Acetyl-para-Aminophenol (Paracetamol)
ATP	Adenosintriphosphat
BMBF	German Federal Ministery of Education and Research (*Bundesministerium für Bildung und Forschung)*
β2m	Beta-2-microglobulin
BUN	Blood-urea nitrogen
CAS-Nummer	Chemical Abstract Services-number
CHN	Chinese herb nephropathy
CKD	Chronic kidney disease
CNS	Central nervouse system
Crea	Creatinine
C_t	Threshold Cycle
CYP	Cytochrom-P450-Monooxygenase
d	Day
DAB	3,3-Diaminobenzidine
DOX	Doxorubicin
DMSO	Dimethyl sulfoxide
DNA	Desoxyribonucleic acid
ELISA	Enzym-linked Immunosorbent Assay
EMA	European Medicines Agency
etc.	et cetera
EU	European Union
FAO	Fatty acid Oxidation
FDA	Food and Drug Administration
FDR	False Discovery Rate
FET	Fluoreszenz-Energytransfer
FXR	Farnesoid-X-Rezeptor

[1] Genesymbols and their related gene names, mentioned in the text and tables, are listed in the appendix and not in the list abbreviations. Genesymbols are written in respect to the "Guidelines for Nomenclature of Genes, Genetic Markers, Allelles, and Mutations in Mouse and Rat"(www.informatics.jax.org/mgihome/nomen/gene.shtml), beginning with an uppercase letter, followed by all lowercase letters/numbers (e.g. Timp1).

GLP	Good Laboratory Practice
GST	Glutathion-S-Transferase
HD	high dose
HPRT	Hypoxanthin-Guaninphosphoribosyltransferase
IHC	Immunohistochemistry
IMI	Innovative Medicines Initiative
ITF	Innovation Task Force
Kim-1	Kidney injury molecule-1
LD	low dose
LDA	lineare discrimination analyse
LOWESS	Locally Weighted Polynomial Regression
d-MAN	d-Mannitol
MD	mid dose
MET	Metformin
MoA	Mode of Action
mRNA	Messanger RNA
MSR	Merck Serono Research
NADPH	Nicotinamidadenindinucleotidphosphat
NEAA	Non essential amino acid
NGAL	Neutrophil gelatinas-associated lipocalin/ Lipocalin-2
NOAEC	No Observed Adverse Effect Concentration
NOAEL	No Observed Adverse Effect Level
NOEL	No Observed Effect Level
NRC	National Research Council
NRK-52E	Normal Rat Kidney cell line; clone 52E
NSAID	Non-steroidal anti-inflammatory drug
Nt	Nucleotide
OAT	Organic anionentransporter
OCT	Organic cationentransporter
OECD	Organisation for Economic Cooperation and Development
PBS	Phosphate Buffered Saline
PCA	Principal Component Analysis
PCR	Polymerase chain reaction
PMDA	Pharmaceutical and Medical Devices Agency
PPAR	Peroxisome proliferator-activated receptor
PSTC	Predictiv Safety Testing Consortium
PUR	Puromycin
QMS	Quality Management System

RNA	Ribonucleic acid
ROS	Reactive Oxygen Species
Rpm	Rounds per minute
PTC	Proximal tubular cells
TD	Toxicodynamic
Timp-1	Tissue inhibitor of matrixmetalloproteases-1
TK	Toxicokinetic
TLC	Thin layer chromatography
TMB	3,3´,5,5´-Tetramethylbenzidin
UGT	UDP-Glucuronosyltransferase
USA	Unite States of America
VAN	Vancomycin
VEGF	Vascular endothelial growth factor
v/v	Volume to Volume
w/o	without

SUMMARY

The major aims of this work included the evaluation of urinary protein markers, transcriptional analysis of the underlying mechanism of Vancomycin-induced nephrotoxicity based on gene expression analysis, the evaluation and generation of reliable transcriptional biomarkers. In addition, the utility of an in vitro test system to produce in vivo like responses to nephrotoxin treatment was tested. Therefore, several questions, important for the further enhancement of preclinical safety assessment as well as the understanding of the underlying mechanism of drug-induced nephrotoxicity, were addressed.

For urinary biomarker analysis three well known nephrotoxins (Vancomycin, Cisplatin and Puromycin) were used. The urinary proteins Kim-1, Clusterin and Osteopontin were clearly identified as the most predictive biomarkers for tubular degeneration, while β2-microglobulin and Cystatin C can be used to discriminate glomerular induced proteinuria. In addition, exploratory urinary biomarkers like Timp-1, NGAL, Calbindin and VEGF showed great potential to deliver further information about the underlying mechanism of toxicity, the area of damage or potential gender differences. However, there are several limitations associated with these new markers and therefore, further investigations and improvements are still needed. The urine dipstick assay for Kim-1, as a quick and easy to use method, was compared to the multiplex Luminex assay. The data showed a clear limitation in sensitivity when there are only slight alterations in urinary Kim-1 levels. In cases where there are strong changes, the results showed a good correlation and can therefore be recommended as general screening tool.

More traditional detection systems, in this case immunohistochemical analysis, can help the identification of early renal changes in a reliable way. This could be especially shown for Kim-1 and Clusterin, while the interpretation of renal expression of Osteopontin was hindered because of strong basal expression and therefore background staining.

The transcriptomic analysis was performed primarily to obtain further insights into the underlying mechanism of Vancomycin-induced nephrotoxicity. Several potential key pathways and processes, which can be considered to be a good starting point for further investigations, were identified. For example, the inflammatory processes, characterized by an activation of the complement system, leukocyte extravasations and several processes involving the transcription factor NF-κB, seems to play an important role in the nephritis induced by Vancomycin. In addition, a Fas-induced and caspase-dependent apoptosis was identified, which overlaps to the already mentioned inflammatory processes. The regenerative properties of the kidney, also reflected by the urinary protein biomarkers as well as almost all histo- and clinical-pathological observations, can be due to the important position of integrin-signaling and Rho-GTPase-induced actin remodeling. These processes lead to cellular shape restoration and cell migration.

The hypothesis that transcriptional changes reflect renal (and other organs) pathological changes is well accepted. Therefore, a commercial test system provided by Compugen Ltd. (based on the measurement by SYBR® green detection of several specific genes, in combination with a related software tool) was tested for its predictive power. Three independent rat studies were chosen for this approach, namely Gentamycin, 3-pyrrolidineacetic acid, 5-[[[4_-[imino[(methoxycarbonyl) amino]methyl] [1,1_-biphenyl]-4-yl]oxy]methyl]-2-oxo-, methyl ester,(3S-trans) (FP007SE/ BI-3), and aristolochia acid. The results indicated a good reflection of Gentamycin induced nephrotxicity, while FP007SE and aristolochic acid delivered unclear results. Several animals within the FP007SE and aristolochic acid studies were identified as positive for renal insult, but without any histopathological correlation. Because of the time- and/or dose-dependent increase in incidence, it was hypothesized that a real prediction, i.e. identification of substance induced alteration with no manifested morphological changes, could be possible.

Three published transcriptional biomarker lists (containing, 4 genes, 19 genes, and 45 genes) were evaluated for their potential to predict the outcome of our Vancomycin study. In addition, the methodological independence of such publicly available biomarker lists could be assessed. From these three gene lists a new “best predictor” biomarker list was created, by also taking the observations from the mechanistic gene expression analysis into account. This final list contains 40 individual transcripts which were grouped into 10 functional categories and reflect the biological reality in more detail. These can now be used in further exploratory or pre-clinical routine studies for the prediction of rodent specific nephrotoxicity.

Finally, a proof-of-principal investigation was conducted with the aim to study whether or not a renal cell line (NRK-52E) can reflect transcriptional changes in a comparable way to those observed in rat in vivo after treatment with nephrotoxins. 192 Significantly altered genes were identified over all positive substances (AmphotericinB, Doxorubicin, Puromycin, and Paracetamol); where 44 genes (~23%) have been frequently reported in the literature to be associated with renal cell damage. Nine of these genes, including Cd44, Cyr61 and Cdkn1a, were of special interest since they were some of the most prominently deregulated in vivo genes and a possible mechanistic relation was identified within this study.

ZUSAMMENFASSUNG

Das primäre Ziel dieser Arbeit umfasste die Evaluierung von urinären protein- und gewebebasierten transkriptionellen Biomarkern, die Analyse von Genexpressionsveränderungen zur näheren Charakterisierung des toxikologischen Mechanismus von Vancomycin und *einen proof-of-principal* Ansatz mit dem Ziel des Nachweises der Vergleichbarkeit von Genexpressionsveränderungen nach Behandlung mit Nephrotoxinen in der renalen Zelllinie NRK-52E und Nierengewebe der Ratte. In diesem Sinne konnten noch offene Fragen bezüglich der oben genannten Bereiche, welche sowohl für die weitere Verbesserung und Entwicklung von toxikologischen Sicherheitsbeurteilungen als auch für das Verständnis der zugrunde liegenden toxischen Mechanismen, beantwortet bzw. neue Lösungsansätze aufgezeigt werden. Für die Untersuchung der urinären Proteinbiomarker wurden drei gut beschriebene Nephrotoxine - nämlich Vancomycin, Cisplatin und Puromycin - verwendet. Die Proteine Kim-1, Clusterin und Osteopontin konnten über alle drei Studien als die prädiktivsten Biomarker für tubuläre Degenerationen identifiziert werden. Für glomeruläre Schäden war der Nachweis mit β2-microglobulin und Cystatin C am bedeutendsten. Weitere explorative urinäre Proteinbiomarker wie z.B. Timp-1, NGAL, Calbindin oder VEGF zeigten ebenfalls das Potential, weitere Informationen über den zugrunde liegenden Mechanismus, den Bereich der Schädigung innerhalb des Nephrons oder aber geschlechtsspezifische Reaktionen zu detektieren. Dies muss jedoch in weiteren Studien näher untersucht werden. Für die Messung der einzelnen Proteine wurde ein multiplexing immunoassay verwendet, welcher die parallele Detektion von mehreren Proteinen in einer Probe erlaubt, sowie ein Urinteststreifen für Kim-1, welcher als schnelle und einfache Methode evaluiert wurde. Das Ergebnis war eine limitierte Sensitivität, welche sich in kein bis geringen Änderungen des Urin-Kim-1 Levels bei leichten tubulären Veränderungen wiederspiegelte. Im Falle von starken tubulären Einflüssen waren die ermittelten Daten jedoch gut vergleichbar, womit durchaus eine Empfehlung zur Verwendung des Teststreifens als Standardanalyse gegeben werden kann.

Zusätzlich zum Nachweis der Proteine im Urin wurden die drei prädikativsten Marker auch mittels immunohistochemischer Analysen evaluiert, mit dem Ergebnis, dass sowohl renal expremiertes Kim-1- und Clusterin-Protein zum frühen und spezifischen Nachweis von tubulären Schäden verwendet werden kann. Die Interpretation von renal expremiertem Osteopontin-Protein war durch die stärkere Hintergrundfärbung erschwert, aber dennoch möglich.

Die transcriptomics-Analysen, welche u.a. zum Ziel hatten, den mechanistischen Hintergrund von Vancomycin-induzierten Nierenschäden, über den auf molekularer Ebene noch relativ wenig bekannt ist, zu untersuchen, lieferte mehrere potentiell wichtige Signalwege und Prozesse, welche in künftigen wissenschaftlichen Untersuchungen näher betrachtet werden sollten. So wurde der Einfluss von inflammatorischen Prozessen näher beschrieben. Charakteristische Mechanismen, welche als Schlüsselfunktion der Vancomycin-induzierten Nephritis identifiziert wurden, waren die Aktivierung des Komplementsystems und Leukozyten-Extravasation unter Beteiligung des Transkriptionsfaktors NF-κB. Darüber hinaus konnte die Fas-vermittelte und Caspase-abhängige Apoptose näher charakterisiert werden, welche einige Parallelen zu den bereits erwähnten inflammatorischen Prozessen vermuten lässt. Die auffallende Regeneration des geschädigten renalen Gewebes nach behandlungsfreien Perioden konnte auf den Einfluss von Integrin-vermittelten Signalwegen zurückgeführt werden, welche unter Beteiligung von Rho-GTPasen in der Actin-Neubildung und -Umgestaltung involviert sind. Diese Prozesse führten zur Wiederherstellung der charakteristischen zellulären Form sowie der Wiederbesiedlung durch migrierende Zellen. Da die den Ergebnissen zugrunde liegenden Daten größtenteils auf Genexpressionsveränderungen beruhen, lässt sich dementsprechend keine finale Aussage über den Mechanismus machen. Es wurden jedoch mehrere wissenschaftlich gestütze Hypothesen aufgestellt, welche für weitere Untersuchungen als Anhaltspunkt in Betracht gezogen werden sollten.

Im Gegensatz dazu ist die Verwendung von transkriptionellen Alterationen als Biomarker zur Reflextion von renalen pathologischen Veränderungen ohne weiteres möglich. Aus diesem Grund wurde zum einen ein Testsystem der Firma Compugen Ltd., basierend auf einer SYBR® green Messung von 6 Transkripten in Kombination mit einem Softwarepacket auf ihre Prädiktivität getestet. Drei unabhängige Rattenstudien unter Verwendung von Gentamycin, 3-pyrrolidineacetic acid, 5-[[[4_-[imino[(methoxycarbonyl) amino]methyl] [1,1_-biphenyl]-4-yl]oxy]methyl]-2-oxo-, methyl ester,(3S-trans) (FP007SE/ BI-3) und Aristolochiasäure wurden hierfür herangezogen. Es zeigte sich innerhalb der Gentamycin-Studie eine gute Übereinstimmung der histopothologischen Befunde mit den Ergebnissen des Testsystems, während innerhalb der FP007SE- und Aristolochiasäure-Studie ambivalente Resultate auftraten. Diese waren derart, dass einzelne Tiere als positiv affektiert eingestuft worden, ohne dass eine entsprechende Korrelation auf histopathologischer Ebene nachweisbar war. Da jedoch die Inzidenz mit der Zeit und/oder Dosis anstieg, konnte geschlussfolgert werden, dass es sich hierbei um eine Prädiktion von substanzinduzierten Veränderungen auf molekularer Ebene handelt, welche noch keine Ausprägung auf morphologischer Ebene hat.

Zusätzlich zu diesem Ansatz wurden auf Basis der Genexpressionsdaten der Vancomycin-Studie, drei Transkriptbiomarkerlisten auf ihre Prädiktivität und methodische Souveränität hin untersucht. Auf Grundlage der Untersuchung und des Vergleiches dieser Listen, welche aus 4-, 19-, und 45 Genen bestand, sowie der Einbeziehung der Erkenntnisse aus den mechanistischen Analysen, konnte eine finale Biomarkerliste abgeleitet werden. Diese aus 40 Transkripten bestehende Liste wurde in 10 funktionale Kategorien unterteilt, um eine mechanistisch-toxikologische Ableitung zu ermöglichen. Diese so establierte Liste kann im Folgenden für weitere exploratorische oder aber präklinische Standardstudien verwendet und weiter optimiert werden.

Eine proof-of-principal Analyse basierend auf einem in vitro Testsystem wurde durchgeführt mit dem Ziel, den Nachweis zu erbringen, ob die renale Zellinie NRK-52E vergleichbare Genexpressionsveränderungen nach Behandlung mit Nephrotoxinen aufweist, wie bei Verwendung von renalem Gewebe behandelter Ratten beobachtet wurde. Es konnten 192 signifikant veränderte Transkripte identifiziert werden, wobei 44 (~23%) dieser bereits häufig in der Literatur im Zusammenhang mit renalen zellularen Schäden in vivo erwähnt wurden. Für neun dieser Gene konnte eine besondere Evidenz aufgezeigt werden, da diese eine mechanistische Relation sowohl zueinander als auch der zugrunde liegenden Pathologie zuließen.

1 Introduction

1.1 Toxicogenomics and Biomarker Discovery

1.1.1 Toxicology

"All things are poison, and nothing is without poison; only the dose permits something not to be poisonous" (german: *Alle Dinge sind Gift und nichts ist ohne Gift; allein die Dosis macht, dass ein Ding kein Gift ist.)* [Marquardt et al., 2004]. No other sentence is as closely related to toxicology as this *dictum* from Philippus Theophrastus Aureolus Bombast von Hohenheim (also known as Paracelsus). It still reflects the general principals of modern toxicology. Toxicology can be described as the study of mechanisms, treatments, symptoms and detection of adverse events of chemical and biological compounds on living organisms and the environment. These harmful effects on health depend on the route and time of exposure as well as the concentration to which the organism is exposed [Marquardt et al., 2004]. Over the last few decades toxicology has evolved in to an independent, complex and varied scientific discipline. The main task of modern toxicology is to assess and describe the risk of the exposure to humans and the environment and to approximate the potential magnitude of an insult as well as to discover the underlying mechanism. Protection, precautions and treatment of adverse events are also part of the toxicologist's range of tasks. Applications in toxicology include testing of potential drug candidates in the pre-clinical development, implementation of measures for industrial safety, identification and treatment of adverse events in clinical toxicology, and clarification of the harmful impact of environmental chemicals in the field of ecotoxicology [Hodgson, 2010]. For the detection and classification of any kind of insult, toxicology is divided in several subfields, focused on a multitude of potential endpoints. These range from the general detection of compounds and there metabolites in body fluids and tissue, changes of the general health condition, clinical-chemical parameters, pathological/ morphological tissue alterations up to lethality [Forth, 2001]. To achieve this, there are many layers of possible testing methods available to the toxicologist: in silico (computational based simulations), in vitro (based on cell- and tissue cultures) and in vivo (based on animal testing) methods. Currently the regulatory standard for the approval of novel drugs is the use of animal models, on which most of the methods in toxicology are based [Hayes, 2007]. In vivo studies are designed to translate the intended medical conditions to a mechanism of the drug and to approximate the potential risk for humans. When a substance is administered to an animal, many chemical and physiological changes can occur. Therefore, it can interact at many places throughout the whole body, and effects upon one process in one organ can cause unexpected consequences in another. By studying adverse effects of chemicals or drugs by using animals is critical because such complexity cannot be duplicated in in vitro systems. However, the question of the cellular interaction on a molecular level remains mostly unanswered, predominantly because most traditional methods rely on analyzing only the resulting pathology. Despite intensive efforts, unexpected side effects after the application and exposure of humans to chemicals and drugs cannot be guaranteed. Figure 1-1 gives an overview of a toxicokinetic (TK) and toxicodynamic (TD) workflow and the field in which modern molecular toxicology can deliver additional information.

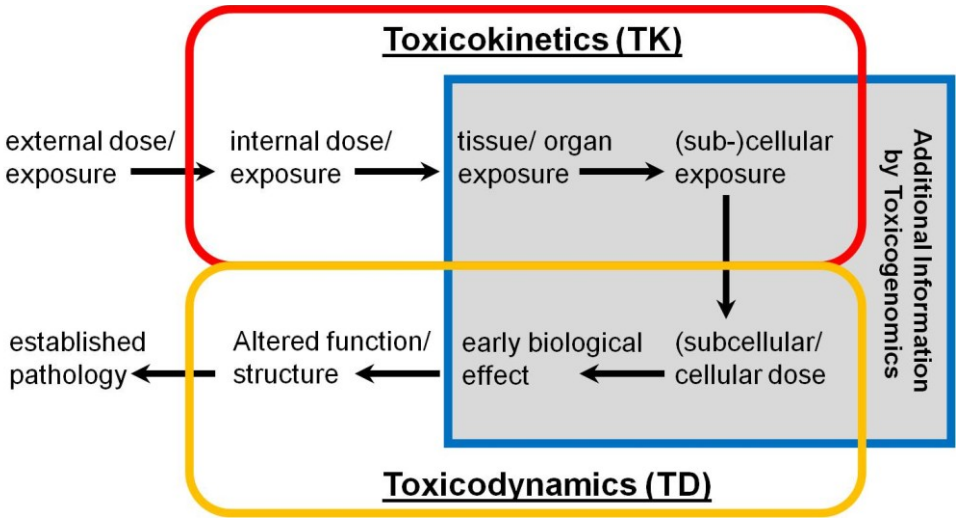

Figure 1-1 Overview of additional usefulness of molecular toxicology. The term toxicokinetic includes the uptake, transport, metabolism, transformation, sequestration and excretion of a compound, while toxicodynamic gives information about the binding, interacting and toxic effects of a compound to the organism. Especially on the (sub-)cellular and early effect level, novel technologies can deliver further information about the properties of a studied compound.

In addition, the question arises about the ethical use of animal testing. In this context the 3R-prinicals were first suggested by William Russel and Rex Burch in 1959 [Russel et al., 1959]. The maxim of this principal is that dependent on the current state of the art in technology; animal tests should be refined to obtain as much information as possible and concurrently to minimize suffering of the test animals. In addition animal tests or even the number of used animals should be reduced and if possible replaced by alternative methods (in silico or in vitro). Therefore, it is a major challenge in toxicology to establish and use state of the art methods and technologies to increase the quality and density of information produced, with simultaneous consideration of the regulatory requirements and the validity of the data. The development of novel alternative methods for animal testing and the establishment of new methods to increase the productivity of animal tests as well as to deliver further information besides traditional approaches comprise molecular and cellular biology. These new methods and an increased understanding of molecular mechanisms will result in fewer wrongly classified compounds in early phases of drug/chemical development. Figure 1-2 gives an overview of a simplified decision tree in a toxicological approach. If clear signs of toxicity appear in two different species, normally the developmental process will stop. If no signs of toxicity are observed, the compound enters the clinical phases. In "real-life" this is usually in between these two scenarios. Based on the all available data the drug developmental process will continue or stop. This can lead, as a consequence, to the loss of a potentially safe drug, which does not enter clinical trials. Or, on the other hand to the development of a toxic drug, which will fail in later phases of clinical development, something that is extremely expensive. In addition, toxicology is confronted with a problem of increasing costs in clinical and pre-clincal studies, prolonged developmental times as well as failure of drug candidate in late phases of drug development [Allen et al., 2008]. The United States Food and Drug Administration (US-FDA) reacted to this trend in 2004 with a White paper [FDA, 2004] in which this problem was summarized and the suggestion of integrating novel technologies into the drug developmental process was formulated. In 2007 the establishment of novel technologies was powered by the report "Toxicity Testing in the 21st Century: A Vision and a Strategy" from the National Research Council (NRC). Also the European Medical Agency (EMA) joined in this venture by founding the Innovation Task Force (ITF), who offers their expertise in the application and handling of new technologies within the EMA and to serve as a consultant and center of information concerning regulatory requirements [EMA, 2009].

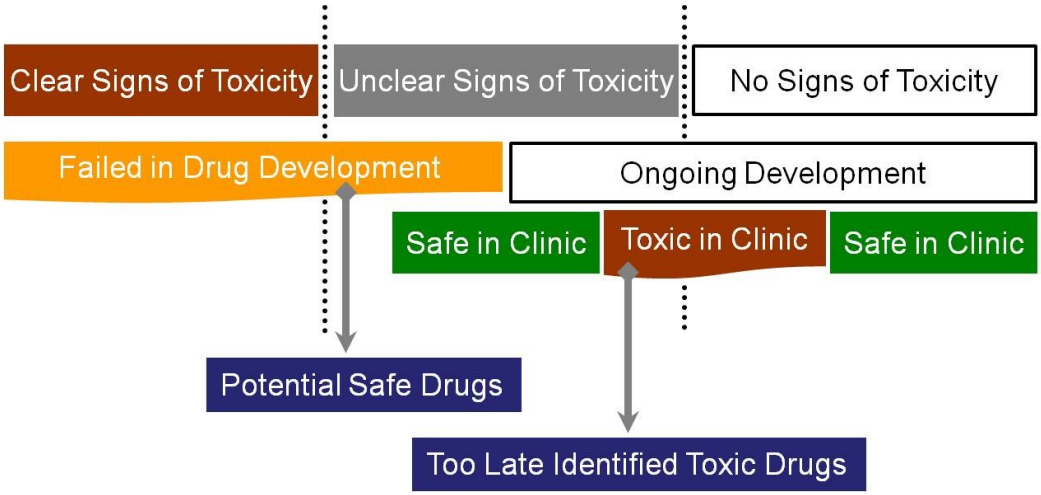

Figure 1-2 Decision tree in toxicology. Depending on the toxicological results, a drug-developmental process can be stopped or be continued. If clear signs of toxicity appear in two different species, normally a compound will fail. If no signs of toxicity are observed, the compound enters clinical development [modified by Fuchs et al., 2011a].

A new research approach of "integrative biology", also called "systems biology", aims to understand the entire biological nature of a cell, tissue, organ or even an organism [Pujol et al., 2010]. In contrast to the reductionist approach of classical biology, which focuses on selected partial aspects; it should be made possible to understand the entire system in a better way and to make more reliable predictions of potential toxicoloigal outcomes. Omics technologies represent a subset of the methods used in systems biology. With these methods it is possible to analyze global changes in cellular systems or tissues on a transcriptional (Genomics), protein (Proteomics) or endogenous metabolite (Metabolomics) level. By parallel detection of changes in the expression level of thousands of genes (Transcriptomics) several kinds of interactions and early changes caused by compounds, pathogens or the environment can be identified.

1.1.2 Toxicogenomics

The term "toxicogenomics" is an amalgamation of the word "toxicology", which describe the science of compound induced adverse/ toxic effects on living systems or the environment, and the word "genomics" which is a hyponym for the genetic discipline focused on studying the whole genome of an organism [Waters et al., 2004]. It is a relatively young branch of toxicology which is defined as the investigation between the structure and activity of the genome and adverse biological effects with exogenous stressors [Aardema et al., 2002].

Toxicogenomics deals with the discovery and understanding of the influence of toxins on the regulation of genes and their involvement in a potential adverse outcome. The focus is formally, but not limited to, the study of messenger RNA (mRNA) which can be changed depending on the treatment with toxins (Figure 1-3). The aim of toxicogenomics analysis is to identify the mode of action (MoA) by which a compound or class of compounds cause a toxic or adverse effect [Edwards et al., 2008]. However, the detection of genomic alterations, e.g. changes of transcriptomics, makes it possible to study global changes and to derive a holistic pathway which can describe potential mechanisms which subsequently lead to morphological/ physiological changes. In this case transcriptional alterations can be based or be correlated to the MoA, the phenotype and/or the toxicological mechanism.

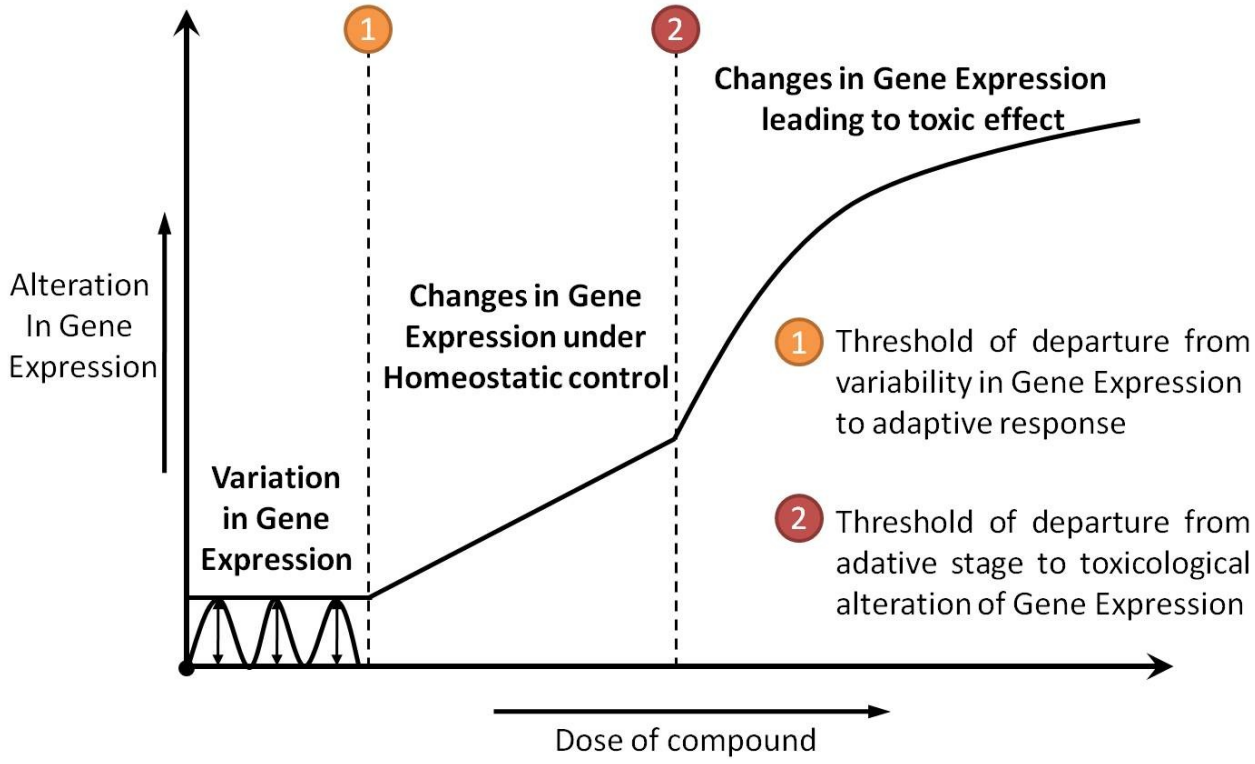

Figure 1-3 Alteration in gene expression depending on the dose of a compound. Depending on the exposure of a living system to a xenobiotic, adaptive systems try to stabilize the homeostatic status. After exceeding of a threshold, gene expression changes can be related to toxic effects [adapted by Fuchs et al., 2013].

Figure 1-4 gives an overview of different groups of transcript classification and there meaning for analysis. In this case it should be mentioned that it is important to distinguish between the pharmacological/ toxicological effect of a drug and their action. The effect is the measurable or observable consequence of the MoA or secondary mechanisms. The action itself is the biochemical/ physiological mechanism of the drug, which underlies the response in an organism to the drug.

The effect is the measurable or observable consequence of the MoA or secondary mechanisms. The action itself is the biochemical/ physiological mechanism of the drug, which underlies the response in an organism to the drug.

In addition to the identification of characteristic molecular pathways specific transcripts, involved in one of the classes mentioned above, can be used as mechanistic or predictive bioindicators or biomarkers for organ- or disease-specific toxicological alterations. [A more detailed discussion on biomarkers will be given in 1.1.3.1 Definition of Biomarkers]. In 2005 a published Guideline be the FDA [FDA, 2005] suggested that data from these kind of technologies could be submitted on a voluntary basis and shall promote the pharmaceutical industry to use them in routine drug development. In the last few years many new projects were initiated to evaluate the suitability of Omics technologies, including toxicogenomics, in the field of pharmaceutical and chemical safety assessments.

Some of these initiatives include; the “EU Innovative Medicines Initiative” (IMI,) founded in Europe (2008), the “National Toxicology Program” in the USA (2004) and the “Conditioning and usage of hepatic in vitro systems for the identification of liver carcinogens using toxicogenomics methods” by the German Federal Ministry of Education and Research (BMBF) in Germany (2007). This development of public funded projects, as well as individual academic and industrial research investigations is still in progress. Several cooperations are still running or planned for the future. Table 1-1 gives an overview of some important, planned, passed or progressing projects and their aims.

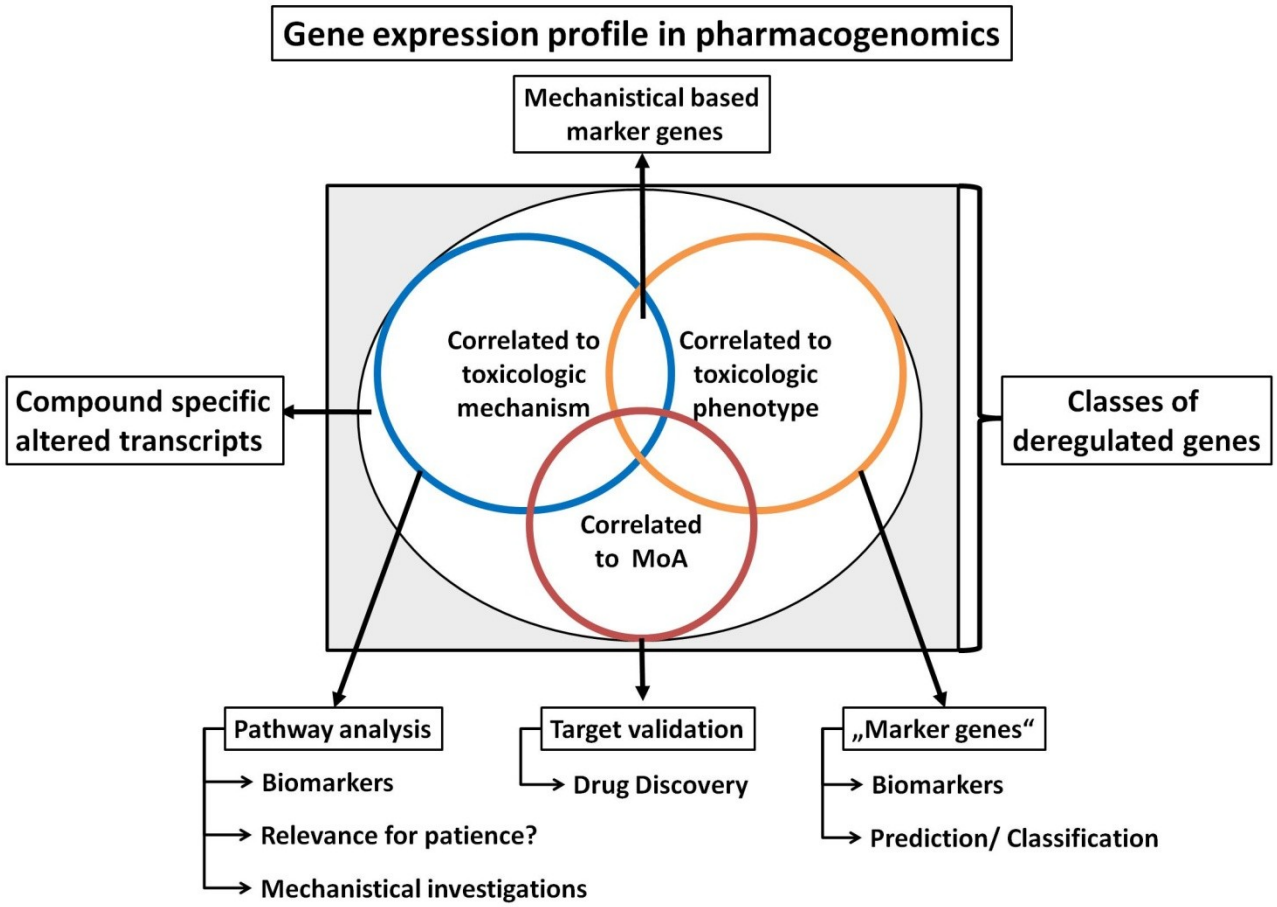

Figure 1-4 Classification of gene expression profiles. Transcript alteration after compound exposure can be related to several changes. On one hand transcripts can correlate to the toxic mechanism. These kinds of transcripts can be used to analyse the pathway induced by a potential drug candidate or serve as mechanistic biomarkers. On the other hand alterations can also be correlated to the Mode of Action (MoA) [adapted by Fuchs et al., 2013].

Another field of application of these Omics technologies is the comparison of test models. In this case differences in the sensitivity of species, strains, genders, age groups or even in vitro and in vivo models can be discovered and can be incorporated into risk assessment processes.

Table 1-1 Overview of national and international initiatives which focus on biomarker discovery using omics-technologies.

Consortium or international initiative	Describtion	References
7th Framework Programme (EU)	In the 7th Framework Programme all research-related EU initiatives are bundled. The initiative already runs is Predict-IV, focused on the establishment of new *in vitro* toxicity screening model including toxicogenomic, toxicoproteomic and metabolomic observation.	www.predict-iv.toxi.uni-wuerzburg.de
Critical Path Initiative (US-FDA)	In March 2004 the Critical Path Initiative was founded. In addition to the release of a white paper by the US-FDA was the reaction to a decline in the number of medical product submitted for approval. The effort to stimulate the development of the scientific processes through which a medical product can be transferred from the discovery phase to the "proof of concept" into the market release.	www.fda.gov/oc/initiatives/criticalpath/
Critical Path Institute/ Predictiv Safety Testing Consortium (USA)	The Critical Path Institute (C-Path) has the goal to identify and therefore reduce toxic effect by drug interactions and to improve therapeutic outcomes. Several working groups focused on nephrotoxicity, hepatotoxicity, and genotoxicity were established, working on the identification of novel biomarkers for the early detection of these toxicities.	www.C-Path.org/pstc.cfm
Toxicogenomics Project (Japan)	In 2002 the Toxicogenomics Project was founded with the aim to create a toxicology database for Nephro- and Hepatotoxicity that enables forward and reverse toxicology. The cooperative research project joined private and national companies.	www.tgp.nibio.go.jp
International Life Science Institute/ Health and Environmental Sciences Institute (international)	As a non-profit institution of the International Life Science Institute (ILSI) the Health and Environmental Sciences Institute (HESI) was initiated as an international forum for e.g. safety assessment and toxicology to enhance the understanding of the underlying scientific issues. Several working groups are working on different kinds of toxicity. The most developed results were published by the "Nephrotoxicity Working Group" who started the first systematic approach to understand the mechanism of nephrotoxicity and to identify diagnostic biomarkers using genomics technologies.	www.ilsi.org www.hesiglobal.org
Innomed Consortium (EU)	The InnoMed PredTox project was a joint collaboration between the European Commission and Industry to enhance drug safety. 3 technology providers, 3 academic institutions and 10 pharmaceutical companies analysed hundreds of samples by using toxicogenomics, metabonomics and -proteomics technologies to discover biomarkers for nephro- and hepatotoxicity and to pre-validate biomarkers identified. Also the toxic mechanism of the failed drug-candidates provided by the pharmaceutical partners was studied.	www.innoMed-PredTox.com
Netherlands Toxicogenomics Centre (Netherland/ international)	The Netherlands Toxicogenomics Center (NCT) is a collaboration of international academic and industrial partners. The First projects of the NTC were started in 2004 with the aim to increase the basic understanding of toxicological mechanisms by using toxicogenomics technologies. In this case the main focus was to develop new alternative methods that reflect the risks of chemical compounds in a similar or even better way than traditional animal testing approaches.	http://www.toxicogenomics.nl/

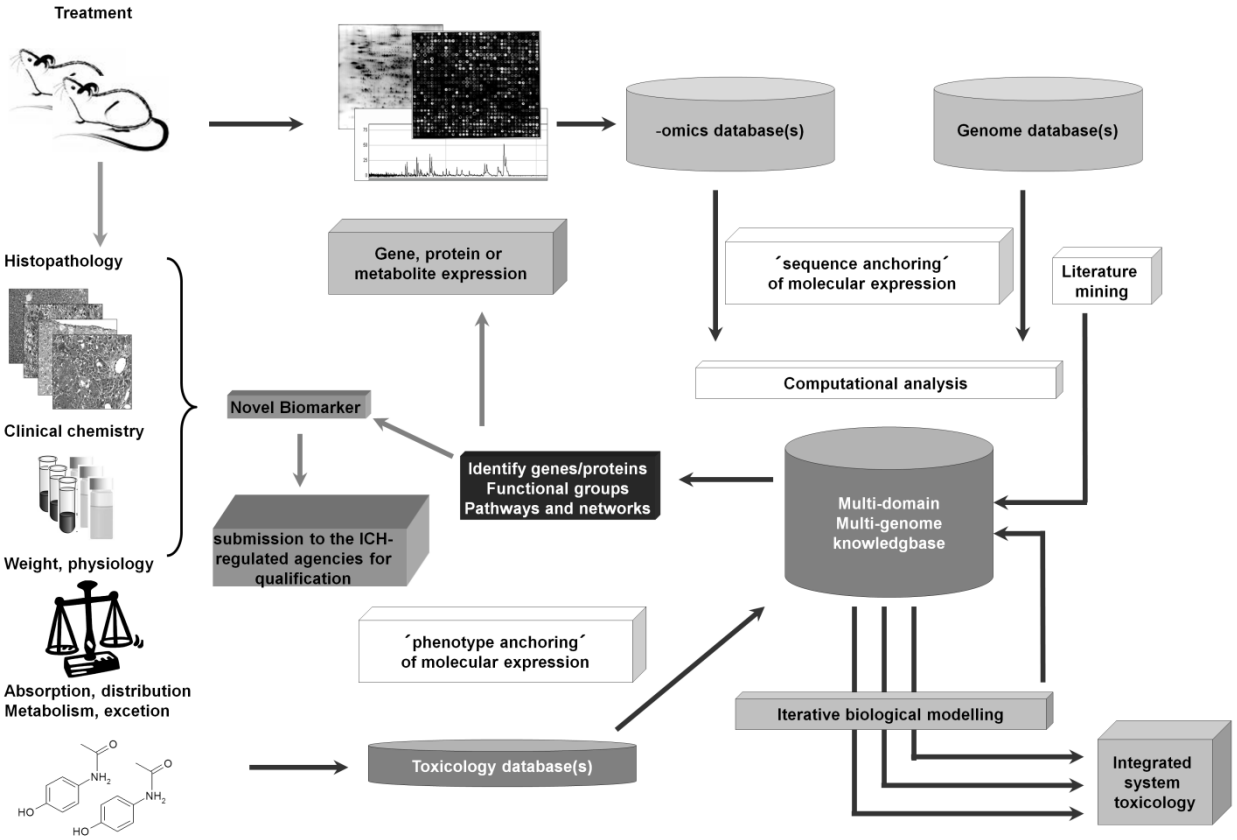

Figure 1-5 Integration of toxicogenomics in toxicological routine studies. Shown is an integrated approach for the inclusion of novel Omics data in the toxicological safety assessment and the identification and implementation of novel biomarkers into the standard battery or for the submission to the FDA/EMA qualification process. Figure adapted by Fabre et al., 2009.

All of this takes into account the already mentioned 3R-prinicpal, by which the earlier identification of characteristic gene expression profiles can lead to the replacement of a long-term toxicity study by short-term or single dose studies or by a reduction in the number of animals needed per study. The usefulness of an integrated approach of toxicogenomics into the drug development process and the risk assessment of drug candidates in pre-clinical trials is illustrated in Figure 1-5. The use of toxicogenomics in combination with in vitro screening systems can also be a powerful tool which can enable the prioritization of a high number of potential drug candidates. Here, the most promising candidates can be studied first in vitro which can reduce the number of animal studies performed. Subsequently, the optimum range of dosing can be approximated so that high dosing and unnecessary suffering of the test animals can be avoided. Not only in drug development but also in the risk assessment of chemicals, cosmetics and nutritional supplements these novel technologies have been established [Cunningham et al., 2003; Oberemm et al., 2005]. By passing the new EU chemical regulation REACH (Registration, Evaluation, Authorization and Restriction of Chemicals) on June 1st of 2007, toxicogenomics and in vitro systems gained in importance [European Commision, 2007]. Independent of the use of toxicogenomics in pharmaceutical drug development or chemical risk assessment, it has to be mentioned that the experimental design of a toxicogenomics study has to be planned very carefully, because experience clearly shows that relatively minor changes can have a strong impact on the transcriptome [Fuchs et al., 2013]. The number of microarrays used, time points of treatment, replicates as well as statistical analysis has to be accurately defined at the beginning of the experiment.

1.1.3 Biomarkers in Toxicology

1.1.3.1 Definition of Biomarkers

Biomarkers in general can be defined as measurable, biological indicators of the actual condition of a living system. Therefore, they can deliver information about a normal biological, pathological or pharmacological process. The use of biomarkers is not limited to safety assessment (safety biomarkers) but can also be used for efficiency evaluation in drug targeting and lead discovery/ optimization [Wang, 2008]. Consequently biomarkers can be traditional parameters like blood-pressure, weight loss or pyrexia. But also single molecules which show a increase or decrease in abundance in a tissue or body fluid can serve as biomarkers for a disease, for example. An increase in blood glucose level in diabetes mellitus or the appearances of phenylketons in urine in case of phenylketonuria are examples of such biomarker molecules. Novel molecular biomarkers are defined as parameters that can be discovered by using technologies such as toxicogenomics and proteomics.

Biomarkers can be identified on the in vivo and in vitro level. Independent of the model or technology used, different questions can be addressed by gene expression profiling concerning biomarker discovery (see Figure 1-4). In case of toxicogenomics, pathway analysis, target validation or the identification of potential, surrogate biomarkers can be studied. Figure 1-4 gives an overview of the single fields of transcriptional analysis and there overlap. Mechanistically based biomarkers, for example, can be defined as altered transcripts related to the underlying mechanism and the toxicologic/ pathologic phenotype.

Biomarker techniques are not limited to transcriptomics but they can also include proteomics, metabolomics or functional assays. Biomarkers range from simple biofluid biochemical endpoints to more complex assessments. In the following description biomarkers will be used synonymously for protein or transcriptional biomarkers, if not mentioned otherwise.

There are some fundamental characteristics a good safety biomarker must have, independent of the molecular class, the used technology or the matrix used for detection[2]:

- Indicative after active observable damage or real predictive (biomarkers should be appear prior to histopathalogical changes)
- Highly sensitive in correlation with the area and severity of damage
- Specific for a organ, tissue or special kind of injury/ mechanism
- Independent of age, gender and other external factors (e.g. diets, exercise)
- Ideally it should be accessible in body-fluids like urine or blood (if this is not possible also peripheral tissue is acceptable for potential translational usability)
- It should be bridge across species and be translational for humans
- The mechanism of biomarker induction/ release should be known

In the past a combined strategy for biomarker discovery has proven successful. The increased role of biomarkers in pharmaceutical drug development is reflected by the number of FDA approvals using biomarkers to enhance the scientific outcome of these studies. The use of biomarkers in drug development is formally based on the aim to

[2] The following list is adapted by Robinson et al., 2008.

accelerate the development of potential drug candidates and simultaneously to enhance our knowledge of the safety profile. This can lead in consequence to a cost reduction because of a fewer drug failures in late phases of the clinical drug development. Therefore, it is of major interest for pharmaceutical companies to identify novel sensitive and specific safety biomarkers and develop cost efficient detection methods which can be easily implemented in both routine preclinical and clinical studies [Marrer et al., 2009].

There are a multitude of biomarkers used in the drug developmental process. In the field of personalized medicine, for example, disease specific biomarkers are used for a pre-selection of patients by assessing whether it is likely they will respond or not to a specific drug [Hodgson et al., 2009]. Diagnostic biomarkers can be used to identify a given pathological stage, while prognostic biomarkers enable the monitoring of a progression of a disease or healing process [Arthur et al., 2008]. Biomarkers have been used to assess the absorption, distribution, metabolism and excretion (ADME) of compounds by measuring transporters or xenobiotic metabolizing enzymes [Grossman, 2009]. By studying these processes, drug-drug interactions or the half-life in plasma of certain substances can be extrapolated to individual patients groups.

In toxicology it is the aim to identify biomarkers specific for certain mechanisms and/ or organ specific toxicities that can be implemented in early preclinical phases. Furthermore, predictive biomarkers could be used to predict compound-induced injury based on molecular events, even before morphological change appear. Biomarkers based on gene expression analysis are promising candidates because the appearance of mRNA are not directly linked to physiological processes but they are usually responded as a functional upstream processor and therefore appear very early. As mentioned above a good marker has to be specific and sensitive for a defined damage and/ or tissue. Consequently a biomarker should be sensitive enough to detected even small alterations. Furthermore, an ideal biomarker should also reflect different stages of an insult to enable one to monitor a time- and/ or dose-dependent progression [Huzarewich et al., 2010].

For preclinical safety evaluations it is also of importance that the biomarkers are easy to detect and to be able to screen hundreds of samples in an easy, fast and cost efficient way [Hewitt et al., 2004]. Of special interest for the translatability to clinical trials, but also for preclinical studies taking account of the 3R principals (Toxicogenomics and Biomarker Discovery), is the accessibility of biomarkers in a non-invasive way. The challenge of using body fluids is to make sure that the origin of the biomarker is based on a target specific mechanism or the target is the origin of the biomarker itself. Interference of a biomarker with other organs or mechanisms can lead to reduced sensitivity or specificity which can lead to false positive or false negative results, respectively.

1.1.3.2 Traditional biomarkers for the detection of renal damage

In toxicological studies it is routine to examine organs and tissues histopathologically after a defined and strictly regulated period of time. In this case it is possible to observe the area or the extent of damage visually. This is the reason why histopathology is the “gold standard” in the detection of substance induced organ damage [CDER, 2006]. The major limitation in histopathalogical assessments is the large number of animals needed to observe a time-course for example. In this case an individual animal per time point would be needed. Therefore, clinical-chemical (clinical-pathological) parameters were used for many years to allow interim observations without further need of additional animals. For example, most of the parameters for the detection and monitoring of renal function are serum parameters, first serum creatinine (SerCrea) and blood urea nitrogen (BUN) [Fuchs et al., 2011b]. The importance of these markers is reflected in their routine use in clinical trials for monitor chronic kidney disease (CKD). Both compounds are

metabolites which normally are eliminated by the kidney, where they are freely filtered by the glomerulus and then enter the urine. If the function of the kidney is affected, the glomerular filtration rate (GFR) decreases and the amount of creatinine and BUN in the blood increase [Stevens et al., 2006]. The major disadvantage of these markers is that they are linked to renal function. Because the kidneys have high capacities to compensate mass loss, a decline of functionality is only detectable after the loss of 2/3 of healthy renal tissue [Pfaller et al., 1998; Amin et al., 2004]. This means that these markers cannot be detected in acute renal injury (AKI) were the function of the kidneys is normally not or only slightly affected.

Additionally, these kidney clinical-chemical parameters have proved to be sensitive for detecting other physiological or pathological conditions and are therefore considered to be unspecific. BUN as well as serum creatinine are described to increase after congestive heart failure or shock [Schrier, 2008]. Also normal physiological or anatomical differences can affect these markers. Creatinine level, a break-down product of muscle tissue, strongly depends on age, gender; weight and muscle mass [Fuchs et al., 2011a+b]. Another disadvantage of these markers is that they give no further information about the area of damage within the kidney. A localization of the initial part within the nephron where damage takes place is therefore not possible.

Urine analysis is also a common method to determine several other parameters to achieve further information about the health status of the kidney. Visual (urine volume, cloudiness, coloration), olfactory (odor) and chemical analysis, such as the detection of osmolarity, pH value, electrolytes, glucose level or total amount of urinary protein can be performed [Fuchs et al., 2011b]. All of these parameters can deliver further information about any renal damage but are not or only have limited suitability for the early detection of acute renal alterations.

Other renal specific enzymes have also been measured as markers for renal function. One example of such an enzyme is γ-glutamyltransferase (GGT), located in the brush border of proximal tubular cells. An increase of this enzyme in urine is a warning of a direct break-down of the tubular epithelia [Greco et al., 1985; Liangos et al., 2007].

1.1.3.3 Novel protein and transcriptional biomarkers

With an increasing awareness for the need and the key benefits of organ specific safety biomarkers, multiple national and international projects were founded by different academic/ industrial institutions, as well as a health authorities, to evaluate the capability of omics-technologies to enhance our toxicological knowledge and to identify novel, sensitive and specific biomarkers.

One of the first projects was the *HESI Application of Genomics to Mechanism-Based Risk Assessment Technical Committee*" founded in 1999 by merger of the *International Life Sciences Institute / Health and Environmental Sciences Institute*" (ILSI/HESI) and several partners from industry as well as public and academic research facilities. The project group of the ILSI/HESI-Nephrotoxicity Working Group had set itself the task of identifying renal specific biomarkers, on a transcriptional and protein level, by microarray analysis. Therefore, gene expression data were generated from three rat toxicity studies with three well described model compounds and in addition compared with traditional toxicological end points, including histopathology and clinical-chemical parameters [Amin, et al., 2004; Kramer et al., 2004; Thompson et al., 2004]. Male Sprague Dawley rats were treated with 2, 20, 80 or 240 mg/kg Gentamycin (7 days), 0.3, 1 or 5 mg/kg Cisplatin (single dose) and 5 or 20 mg/kg puromycin (21 days). Several, important deregulated genes could be identified including Havcr1, Clu, Spp1 and Lcn2. Subsequently, a significant increase in the urinary level of Clusterin, α-GST, μ-GST und RPA-1 could be detected, some of which had better diagnostic performance over the traditional markers SerCrea and BUN. As a consequence, the Nephrotoxicity Working Group submitted a claim in

May 2008 to the US-FDA and EMA for the use of these four urinary proteins as potential biomarkers for the early detection of nephrotoxicity.

The European contribution to the identification of novel safety biomarkers was initiated in 2005 by the forerunner of the Innovative Medicine Initiative (IMI) in the form of the Innomed/PredTox (Predictive Toxicology) project, which aimed to improve the safety profile of novel drug candidates [Innomed-PredTox Project 2005-2009]. This cooperation, consisting of 12 pharmaceutical companies, three universities and two small technology suppliers, investigated 16 compounds with known nephrotoxic and hepatotoxic safety profiles. Of particular interest was the fact that only two out of the 16 compounds were well described "model compounds" (gentamycin and troglitazone) while the other 14 compounds were rejected drugs from the pharmaceutical partners which failed during drug development because of nephrotoxic, hepatotoxic effects or both. Also in this initiative the overall aim was to identify and evaluate the usefulness of specific biomarkers by using a combination of traditional and omics techologies to enhance the prediction in preclinical rat toxicity studies. The test compounds were administered to male Wistar rats in two doses for up to 1, 3 and 14 days [Suter et al., 2011].

The largest toxigocenomics project that has been funded is the Toxicogenomics Project in Japan (TGPJ). This 5 year collaboration project started in 2002 with the National Institute of Health Sciences and 17 pharmaceutical companies, with the aim to elucidate the interrelationship between gene expression changes and toxicants and to build up a publicly available database. Here, 150 chemicals were used for studying gene expression changes in rats (kidney and liver) and rat/ human primary hepatocytes [Toxicogenomics Project in Japan, 2002-2007]. A database was created by providing almost all gene expression data as well as histopathological and clinical-pathological data (TG-GATES DB). This kind of information allows the researcher to study the mechanism of a compounds toxicity, to identify biomarkers, or build up computer-based prediction models from all information of thousand of samples and therefore millions of transcript datapoints [Kondo et al., 2009].

Another project, finally leading to the first qualification process of novel safety biomarkers, is based on the approach of the Predictive Safety Testing Consortium (PSTC) funded in 2006 by the Critical Path Institute (C-Path) [PSTC-webpage]. The project members, consisting of world leading pharmaceutical companies and public institutions under the roof of the regulatory agency US-FDA, aimed to validate novel biomarkers and methods to enhance the usefulness in routine preclinical safety approaches. Five areas of interest were defined; carcinogenicity, hepato-, nephro-, myo- and vasculotoxicity.

The nephrotoxicity working group investigated 8 nephrotoxic compounds (gentamycin, cisplatin, puromycin, Vancomycin, doxorubicin, furosemid, lithiumcarbonat and tracolimus) as well as 2 hepatotoxic compounds (methyapyrilen and α - Naphthyisocyanat) which served as negative controls. Male Sprague-Dawley and Wistar rats were treated with 4 different doses up to 14 days. As a result of toxicological observations and omics studies 23 potential urinary protein biomarkers and many transcriptional biomarkers were validated. In the following qualification process 7 out of the 23 urinary biomarkers were qualified by the FDA, EMA and PMDA for the use in acute rat toxicity studies up to 14 days [Fuchs et al., 2011b].

Table 1-2 gives an overview of the urinary protein biomarkers analyzed in this study with their qualification status and their ability to detected renal damage of specific nephron segments.

An increasing number of in vitro based projects have been funded over the last few years. The main problem with in vitro models, especially models based on cell lines, is that they deliver only limited significance for the underlying mechanism of the in vivo situation. This becomes particularly obvious by the fact that biomarkers identified in vivo are not necessarily translational into the in vitro situation [Dere et al., 2006]. Subsequently, there are no consistent biomarkers described so far which deliver reliable data over in vivo and in vitro models or even between different in

vitro models. Even primary cells, directly isolated from the tissue of interest, show significant differences by comparing gene expression profiles with those from the whole organ treated with the same toxin [Boess et al., 2003].
Therefore, on one hand it is possible to identify and evaluate specific endpoint biomarkers, based on fundamental cellular functionalities for a defined in vitro model, in which particular attention may be given to the specific mechanism. In this case the studied endpoint must be very detailed in its content. On the other hand, the stringent comparison of already mentioned omics- data on a global basis and subsequently a detailed characterization of the used in vitro model can enhance the usability of a given in vitro system for a more holistic and global, mechanistically analysis [Tuschl et al., 2009].
Beside the already mentioned TGPJ project, several other projects have focused on different in vitro models, like the European ACuteTox-Project. It started a trial to optimize and revalidate in vitro testing strategies to predict human acute toxicity [Clemedson, 2008]. This integral EU project started in 2005 under the 6th Framework program of which also the Innomed/ PredTox project belongs. During the course of this project no omics-technologies were used, but different cytotoxicity assays, like the detection of intracellular ATP, neutral red uptake, cytokine release or substance induced alterations of the transepithelial electrical resistance in combination with different cell lines. PredictIV, another EU funded project, was initiated within the 7th Framework program. PredictIV is more focused on biomarker discovery and is analyzing a direct comparison of the in vivo and in vitro systems [PredictIV-webpage]. The methodology includes genomics and proteomics but also kinetic observations based on different cell systems. The aim is to identify the most suitable in vitro test system for human hepato- nephro- and neurotoxicity, with an integrated in vitro exposure measurement. Additionally, the systems shall be tested for their ability to mimic long-term repeated dose studies.

In the following section, the ten urinary protein biomarkers evaluated in this project shall be shortly presented. For more detailed information, refer to the literature given in (Table 1-2).

Table 1-2 Overview of the measured biomarkers, the presumed prediction of the damage-location and their status of acceptance by the US-FDA and EMA. Exploratory biomarkers are not accepted but with promising results in pre-clinical observation. (PT= proximal tubule, DT= distal tubule, CD= collecting duct)

Measured markers and the acceptance state by US-FDA/ EMA		
Protein	**Regulatory status**	**References**
PT damage		
Cystatin C	Accepted	Colle, et al., 1990; Conti, et al., 2006; Schaefer et al., 1994; Uchida et al., 2002; Vaidya et al., 2008b, Fuchs et al., 2011a, Fuchs et al., 2012, Dieterle et al., 2010
Kim-1	Accepted	Ichimura et al., 2008; Liangos et al., 2007; Prozialeck et al., 2007; Rached, et al., 2008; Sieber, et al., 2009; Vaidya, et al., 2008; van Timmeren et al., 2007; Wang, et al., 2008; Zhou et al., 2008, Fuchs et al., 2011a, Fuchs et al., 2012, Dieterle et al., 2010
β_2-microglobulin	Accepted	Chen et al., 2008; Gatanaga et al., 2006; Hofstra et al., 2008; Morel et al., 2005; Rached, et al., 2008; Zhu et al., 2009, Fuchs et al., 2011a, Fuchs et al., 2012, Dieterle et al., 2010
α–GST	Exploratory	Prozialeck et al., 2009; Usuda et al., 1998; Lebeau et al., 2005; Thukral et al., 2005; Branten et al., 2000; Bruning et al., 2001; Kilty et al. 1998, Fuchs et al., 2011a, Fuchs et al., 2012,
Timp-1	Exploratory	Chromek et al., 2003; Chromek et al., 2004; Horstrup et al., 2002; Huang et al., 2001; Kharasch et al., 2006; Rached, et al., 2008; Sieber, et al., 2009; Wang, et al., 2008; Wasilewska et al., 2008, Fuchs et al., 2011a, Fuchs et al., 2012
DT damage		
Calbindin	Exploratory	Takashi et al., 1998; Hoffmann et al., 2010 Fuchs et al., 2011a, Fuchs et al., 2012
general damage		
Clusterin	Accepted	Dvergsten et al., 1994; Hidaka et al., 2002; Ishii et al., 2007; Rached, et al., 2008; Shannan et al., 2006; Sieber, et al., 2009; Wang et al., 2008, Hoffmann et al., 2010; Fuchs et al., 2011a; Fuchs et al., 2012
Osteopontin	Exploratory	Alchi et al., 2005; Lim et al., 2004; Rached, et al., 2008; Wang, et al., 2008; Hoffmann et al., 2010; Fuchs et al., 2011a; Fuchs et al., 2012
NGAL	Exploratory	Flo et al., 2004; Bennett et al., 2008; Mishra et al., 2004; Mishra et al., 2003; Rached, et al., 2008; Sieber, et al., 2009; Vaidya, et al., 2008; Wang, et al., 2008; Wheeler et al., 2008; Hoffmann et al., 2010; Fuchs et al., 2011a; Fuchs et al., 2012
VEGF	Exploratory	Avihingsanon et al., 2006; Kim et al., 2005; Ogutmen et al., 2006; Peng et al., 2007; Shihab et al., 2001; Vaidya, et al., 2008; Wakelin et al., 2004; Hoffmann et al., 2010; Fuchs et al., 2011a; Fuchs et al., 2012

Cystatin C

The 13 kDa Cystatin C protein is a major inhibitor of extracellular cystein proteases, expressed in nucleated cells [Manabe et al., 2011]. Because of its small size and its relatively constant blood level, which is in contrast to creatinine and independent of muscle mass, gender and age, it is freely filtered from the glomerulus and almost completely reabsorbed [Uchida et al., 2002, Fliser et al., 2001, Bokenkamp et al., 1998]. Before Cystatin C was identified as a potential urinary protein biomarker for nephrotoxicity, it was used as a serum parameter for the estimation of the glomerular filtration rate.

The fact that Cystatin C also can be used as urinary protein biomarker is based on its almost complete lysosomal degradation. Therefore, the urinary Cystatin C level will increase when the proximal tubular cells, containing the highest amount of lysosomes, are degraded and therefore no absorption can take place. There is some evidence that urinary Cystatin C only shows alteration after proximal tubular damage [Conti et al., 2006], however, it has also been shown that Cystatin C increases in glomerular induced proteinuria [Dieterle et al., 2010]. A definitive mechanism for this observation has not been formulated so far.

Kidney Injury Molecule-1

The protein encoded from the Havcr1 gene, known as kidney injury molecule-1 (Kim-1) or T-cell immunoglobulin mucin (Tim-1) is probably the most promising of the new urinary protein biomarker. It is a 100 kDa, transmembrane glycoprotein of the immunoglobulin superfamily, and is involved in several intra- and intercellular processes. Kim-1 was first described in relation to an immune response, especially Th1 and Th2 mediated immunity [Mcintire et al., 2003, Mariat et al., 2005, Curtiss et al., 2007], or as a receptor for the hepatitis A virus [Kaplan et al., 1996].

During acute kidney injury, Kim-1 has been postulated to be involved in cell regeneration, due to its structural similarity to cell adhesion molecules like integrins, selectins and cadherins [Fagotto et al., 1996, Sastry et al., 1993]. The expression of Kim-1 is limited to proliferating and dedifferentiated epithelial cells of the S3 segment of the proximal tubulus [Ichimura et al., 1998]. This gives further support to the hypothesis that Kim-1 is related to regenerative processes after a renal insult. In addition, Kim-1 has a very low expression in healthy kidneys, therefore an early upregulation (both transcript as well as protein) and its detectability in urine, are additional advantages. In contrast to other urinary proteins, Kim-1 is not secreted into the tubular convolute. After damage to proximal tubule cells of the S3 segment, the ectodomain is cleaved by matrix metalloproteases (MMP) and the soluble form of Kim-1 is shed into the urine [Bailly et al., 2002]. However, the whole mechanism of the induction and repair functions of Kim-1 in relation to other survival and apoptotic factors is not yet fully understood. In addition to the already mentioned regenerative processes, Kim-1 may also play a role in the prevention of kidney injury [Fuchs et al., 2011] via clearance of apoptotic cells. Kim-1 has phosphatidylserine receptor properties and can recognize the epitopes on the surface of apoptotic cells by conversion of epithelial cells to a phagocytic phenotype [Ichimura et al., 2008].

β2-microglobulin

β2-microglobulin (β2m) is a plasma protein, expressed on the surface of nucleated cells and functions as a soluble subunit of the major histocompatibility complex class I (MHC-I) and has therefore an antigen-presenting role. β2m has not been described to be upregulated in renal cells after an insult, nor on mRNA neither on protein level. Therefore, its physiological role is not related to its property as a biomarker of kidney injury. The specificity of β2m for renal damage seems to be based on the fact that it is released into the blood in response to cellular turnover. Because β2m is only an 11.8-kDa monomeric protein it is freely filtered by the glomerulus. By entering the tubular convolute β2m is absorbed by proximal tubular cells and catabolized by lysosomal degradation [Miyata et al., 1998]. Like Cystatin C, β2m has

been described to appear in the urine after the proximal tubular protein reabsorption complex is disturbed by tubular cell break-down induced by nephrotoxin exposure [Chapelsky et al., 1992]. Therefore, β2m has been classified as a specific urinary protein biomarker for proximal tubular damage [Rached et al., 2008, Hofstra et al., 2008, Gatanaga et al., 2006]. However, because of the non-renal origin of β2m there is some evidence that this filtered protein may lack sensitivity for the detection of proximal tubular damage [Hoffmann et al., 2010, Fuchs et al., 2012] and could also be used as a biomarker for glomerulus induced proteinuria [Dieterle et al., 2010].

Alpha Glutathione *S*-transferases

Several classes of Glutathione *S*-transferases (GSTs) have been described. They are involved in detoxification processes, by conjugation of GSH to xenobiotics. Consequently, the highest expression of these important cytosolic Phase II xenobiotic metabolism enzymes is seen in the liver, kidneys, gut, lungs and heart. However, general GSTs, such as α-GST, are expressed in almost all tissues. Very high amounts of α-GST are expressed in liver hepatocytes and in renal proximal tubular cells, leading and having been used as a sensitive marker for liver tissue damage following acute liver injury and acute kidney injury [Beckett et al., 1985, Redl et al., 1995]. It has been reported that α-GST enters the urine after drug-induced proximal tubular cell break-down and can be therefore used as biomarker for proximal tubular damage [Bruning et al., 2001, Lebeau et al., 2005, Branten et al., 2000, Usuda et al., 1998].

The fact that α-GST shows an overlap in expression between kidney and liver cells and exclusive kidney damage without any impact on the liver is very rare, a rise in blood α-GST during hepatic insult cannot be excluded. Consequently, it must be assumed that also an increase in urinary α-GST may also be to hepatotoxicity. For this reason the submission from the ILSI/HESI consortium to qualify α-GST as an acute kidney injury biomarker was rejected [EMA, 2010].

Tissue Inhibitor of Matrix Metalloproteases-1

The tissue inhibitor of matrix metalloproteases-1 (Timp-1) is a specific inhibitor of MMPs, which are related to the extracellular matrix equilibrium [Brew et al., 2000]. Timp-1 shows the highest affinity of the Timp family and therefore the strongest binding to MMP-9. The interruption of the equilibrium of these two molecules can lead to different pathological outcomes. Consequently, the deregulation of MMPs can cause an accumulation of Timps and lead to the progression of renal injury, and is often observed during tubulointerstitial fibrosis [Horstrup et al., 2002].

Timp-1 itself is a 28.5 kDa glycoprotein expressed in several different cell types, including fibroblasts, osteoblasts and epithelial cells and consequently appears in many tissues and body fluids [Lambert et al., 2004]. Therefore, an elevation of Timp-1 in urine could also be observed as a consequence of acute and chronic organ toxicities [Liu et al., 2006]. In addition to the inhibition of MMPs, Timp-1 also has been described to stimulate cell proliferation, as well as preventing apoptosis [Schnaper et al., 1995]. As for all ubiquitous proteins with a size below the filtration barrier of the glomerulus, the origin of Timp-1 in urine still needs to be confirmed, because tissue remodeling processes and damage in other tissues can also elevate the amount of Timp-1 in the blood and subsequently in urine [Barton et al., 2003].

Calbindin

Calbindin or Calbindin28k (~28kDa) belongs to the vitamin D-dependent calcium-binding protein family. This family is characterized and further sub-divided based on the number of Ca^{2+}-binding EF-hand domains. Physiologically, they are involved in the transport of calcium ions [Kojetin et al., 2006]. Members of this family have been observed in the kidney and intestine. In rat, the localization of Calbindin was found at epithelial cells of the distal tubules, where they are responsible for the transport of Ca^{2+} ions out of the primary urine back into the tubular cells. Based on the

localization, and (pre-) clinical observations, Calbindin can be assumed to be a promising urinary biomarkers specific for distal tubular injury [Hasegawa et al., 1993, Takashi et al., 1998, Hoffmann et al., 2010]. Even though there has been promising data reported, there are still questions, which have to be addressed. Calbindin has been described to decrease in relation to drug-induced renal insult, on both the gene expression as well as protein expression level [Matheis et al., 2011, Wang et al., 2008, Hoffmann et al., Fuchs et al., 2012]. Owing to its involvement in calcium homeostasis and that extracellular calcium is an important factor of cellular stress; further mechanistic studies should be performed to investigate this interaction.

Clusterin

Clusterin, also named glycoprotein 80, apolipoprotein J or serum protein 40, is a glycoprotein expressed in many different tissues and secreted in body fluids. Therefore, Clusterin, which formally appears as an abdimer, is involved in many different physiological processes, including lipid transport, cell aggregation and the complement system [Rosenberg et al., 1995, Shannen et al., 2006]. The highest expression of Clusterin has been observed in differentiating and proliferating cells [French et al., 1993]. Clusterin also has anti-apoptotic, as well as pro-apoptotic properties, depending on the intracellular form [French et al., 1994, Hara et al., 2001, Trougakos et al., 2005]. Based on these characteristics, Clusterin has been identified in several studies focused on kidney diseases, like glomerulonephritis, renal tumors but also in drug-induced tubular damage, as a good biomarker, both on the transcript as well as protein level [Correa-Rotter et al., 1998, Eti et al., 1993, Hidaka et al., 2002, Witzgal et al., 1994, Yang et al., 2007]. The fact that Clusterin is upregulated on the protein level and is secreted directly into the urine after renal insult, is one of the major benefits of this protein.

Osteopontin

The gene product of the Spp1 gene, Osteopontin, also known as secreted phosphoprotein 1, uropontin or early T-lymphocyte activation-1, is a multifunctional glycoprotein. It was discovered in 1986 from osteoblasts [Oldberg et al., 1986]. Osteopontin is involved in the mineralization process of bones, where the highest expression can be observed. However, it is also expressed in several other epithelial cells such as liver, lung, urinary bladder, skin, pancreas and kidney [Brown et al., 1992] The molecular mass of Osteopontin is on average 44 kDa, but varies depending on its glycosylation and phosporylation state. In case of kidney damage the physiological function of Osteopontin seems to be related to regeneration of cells after an insult and the accumulation of macrophages and monocytes, responsible for the clearance of apoptotic cells [Xie et al., 2001]. Osteopontin has also been reported to have anti-apoptotic properties and has been reported to be involved in several tumors. The mechanism leading to a protective effect against apoptosis involves the activation of NF-κB, by interacting with αvβ2 integrin of endothelial cells [Mazzali et al., 2002]. Additionally, Osteopontin is also involved in the prevention of kidney stones, by inhibition of the formation of oxalate crystals [Wesson et al., 2003].

The specific upregulation of Osteopontin in renal tissue was shown in preclinical rat disease models, including nephrocarcinoma, interstitial nephritis, glomerulonephritis, [Xie et al., 2001, Persy et al., 1999] as well as in drug-induced kidney injury [Iguchi et al., 2004, Thukral et al., 2005, Wang et al., 2008]. Subsequently, the increase in Osteopontin protein has also been observed in urine [Khan et al., 2002, Shui et al., 2007]. Owing to the localization of the Osteopontin protein, which has been described to be the highest in the descending limb of the loop of henle within rat kidneys, it is used as a marker for damage to the loop of Henle. However, the release of Osteopontin seems also take place after proximal and distal tubule damage, and can be therefore classified as a general tubular marker [Hoffmann et al., 2010].

Lipocalin-2/ NGAL

Lipocalin-2 or Neutrophil gelantinace associated lipocalin-2 (NGAL) is a member of the lipocalin family. Members of this family are characterized by their small, β-barrel structure containing eight β-strands [Flower et al., 1993]. This calyx enables the Lipocalin members, which are formally localized extracellularly, to bind small hydrophobic molecule and translocate them into cells [Kjeldsen et al., 1993, Goetz er al., 2002]. In case of NGAL, it is responsible for the transport of siderphores, which are produced by prokaryotes during an infection, leading to a reduction of iron uptake of the bacteria and as a consequence to an inhibition in their growth [Goetz er al., 2002, Flo et al., 2004]. Therefore, NGAL is strongly involved in the immune response after an infection, which is also reflected by expression of this protein by neutrophils and epithelial cells as an early response to cellular stress. Within the kidney the expression of NGAL, both mRNA and protein, is very low when no pathological alterations are taking place, while in cases of tubular damage it is strongly elevated [Mishra et al., 2004]. An increase in NGAL could be observed in many renal diseases [Wagener et al., 2008, Mishra et al., 2003, Ding et al., 2007, Bennett et al., 2008]. There is evidence that NGAL has a protective effect on renal cells. It has been shown that the NGAL protein, administered exogenously, has a protective effect against ischemic kidney injury in mice [Mori et al., 2005]. The response of NGAL to renal injury is very early and therefore highly sensitive. However, the fact that NGAL is expressed in several tissues during acute stress and released into the blood, together with the small size of this protein, means that it freely enters the tubular convolute and consequently the urine, leads to the assumption that there is a lack in specificity.

Vascular Endothelial Growth Factor

Vascular endothelial growth factor (VEGF or VEGF-A) is a member of multipotent cytokines [Ferrara et al., 2001]. By alternative splicing the VEGF gene can be transcribed into six different isoforms [Neufeld et al., 1999]. The physiological function of VEGF is wide, including the increase vascular permeability, support of vascular survival, the stimulation of endothelial cell differentiation and cell proliferation, mediation of endothelium-dependent vasodilatation and prevention of apoptosis [Ferrara et al., 2001, Neufeld et al., 1999]. In addition, VEGF is also involved in matrix remodeling, expression of adhesion molecules and chemotaxis of monocytes [Schrijvers et al., 2004]. Therefore, VEGF has been described to have renal protective properties [Matsumoto et al., 2003]. Consequently, VEGF has been described in a multitude of renal diseases to show an increase (transcriptionally and on protein level), for example in diabetic nephropathy [Braun et al., 2001], high protein-induced nephropathy [Schrijvers et al., 2002], nephron reduction [Flyvbjerg et al., 2002] and glomerulonephritis [Matsumoto et al., 1997a+b+c, Matsrumoto et al., 1999, Matsumoto et al., 2001]. VEGF has been described to be produced by adjacent podocytes. It is required to maintain normal fenestrated endothelial function of the glomerulus and is particularly important for normal functioning of the glomerular basement membrane [Sugimoto et al., 2003]. However, less information is available for the performance of VEGF in preclinical rat toxicity studies to serve as a urinary biomarker. Data available so far do not show a clear conclusion for the performance of VEGF [Hoffmann et al., 2010, Fuchs et al., 2012].

1.2 The Kidney

1.2.1 General Function of the Kidney

The kidney is the major organ of excretion of xenobiotics (drugs, chemicals, environmental toxins) as well as their metabolites. The general functionalities of the kidney are based on blood filtration, secretion and reabsorption of molecules by the glomerulus and the tubular system. The whole mechanism of filtration of water and soluble reabsorption is a complex interaction of the highly specialized tubular cells and salt gradients over the different segments of the kidney. At this point a detailed description is not warrented. Single aspects are described in the special sections 1.2.2 Morphology and Cell types of the Kidney.

The kidney has a high metabolic activity and transporter capacity which enables the metabolic inactivation of compounds as well as increases their water solubility, enabling an enhanced elimination *via* the urine. Therefore, the kidney is essential for the regulation of the water-, electrolyte and acid-base homeostasis within the body. Furthermore, the kidney is responsible for the synthesis of the hormone erythropoietin and in this case is directly involved in the formation of erythrocytes [Sands et al., 2005]. Another central position of the kidney is based on the synthesis of the endopeptidase renin, which is the major stimuli of the renin-angiotensin-aldosterone system, which is the most important regulator of the blood pressure and in cases of the need of water storage.

1.2.2 Morphology and Cell types of the Kidney

1.2.2.1 Macroscopic Structure

The kidney is a paired, bean-shaped organ, which is located in the abdominal cavity. Each kidney has a concave and convex surface. The renal hilum, located at the concave surface is the point at which the ureter and the renal vein leave the organ, while the renal artery enters it. The whole kidney is surrounded by the renal capsule, a fibrous tissue. Morphologically the kidney can be divided into the lighter, superficial area of the renal cortex and the darker, deep medulla. Both structures together build up the renal lobes. These structures build the renal pyramids which contain the surrounding cortex a portion of the medulla (Figure 1-6). At the end of these pyramids the renal papilla enters the minor calyces which again enter the major calyx to release the urine into the renal pelvis [Schmidt et al., 2004].

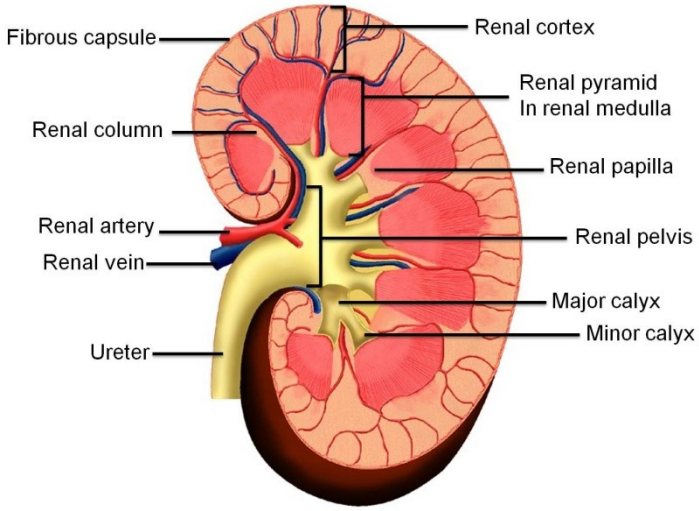

Figure 1-6 The Kidney. Shown is a multilobular left kidney with a coronal section. The anatomic structure, including the renal cortex and medullar forming the renal pyramids, the calyxces, the renal pelvis, artery and vein as well as the ureter are displayed [modified by Standford School of Medicine, 2012].

1.2.2.2 The Nephron

The nephron is the functional subunit of the Kidney (Figure 1-7). The total number of nephrons in humans is about 1 million, while rat only have approximately 30,000. Depending on their location within the kidney it can be discriminated between common cortical (formally located in the cortex) and juxtamedular (formally located in the medulla) nephrons [Schmidt et al., 2004]. The nephron is the area where the primary urine is built up as well as where essential blood components like glucose, amino acids and salts are reabsorbed. Both types of nephrons can be sub-divided in four major sections which differ in their functions, locations and out of this in their cell types.

The blood filtration occurs in the glomerulus. During this process the primary urine enters the tubular system. It can be roughly separated in to the proximal tubulus, the loop of henle and the distal tubulus. The final urine enters the collecting ducts which lead to the renal calyces. In the following sections the single parts of the nephron shall be described in more detail depending on their significant as major targets of compound induced renal damage.

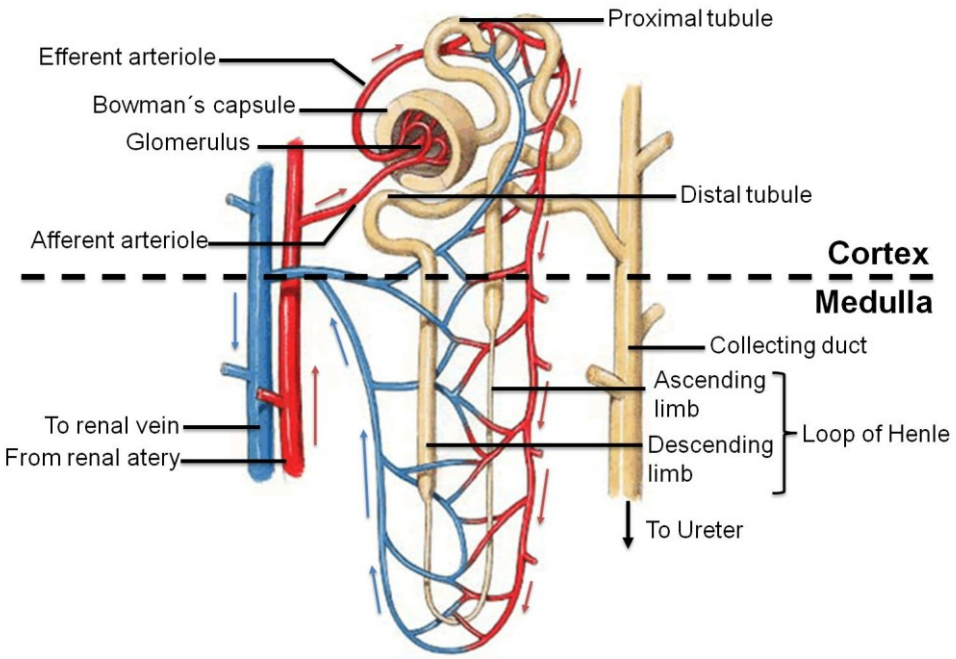

Figure 1-7 The nephron. Given is a nephron with its specific subunits, the glomerulus within the Bowman´s capsule, the proximal tubule, the Loop of Henle (roughly subdivided in the ascending and descending linb), the distal tubule and the collecting duct. Also shown is the renal system of tiny blood vessels traveling alongside the nephron, the Preitubular capillaries [modified by Ken Pitts, 2011]

1.2.2.3 The Glomerulus

The glomerulus, or the renal corpuscle, consists of two structures, the Bowman´s capsule and the actual glomerulus. In the proper sense the glomerulus describes a capillaries bed between the arterioles Vas affernece and Vas efference. The glomerulus is enclosed in the Bowman´s capsule, a cup-like sac, which is one of the filtration barriers responsible for the filtration of the blood. Figure 1-8 gives a schematic overview of the anatomic structure as well as the buildup of the barrier forming compartments within the Bowmans capsule.

The Bowman´s capsule has an outer parietal and an inner visceral layer. Both composed of squamous epithelium, while the visceral layer is lined by podocytes which contact the capillary bed, forming filtration slits by their foot processes [Schmidt, 2004]. Therefore, three filtration barriers can be discriminated: The fenestrated capillaries (barrier for cellular components), the glomeruli basal membrane (pore size: 240 – 340 nm) and the visceral layer (filtration slits: ~25 nm). All layers together provide barrier properties of the glomerulus for molecules >70 kDa [Greaves, 2011]. Therefore, in healthy kidneys, molecules exceeding this size cannot enter the primary urine. Beside this molecular size exclusion, the electrical charge also plays a pivotal role. Uncharged or positively charged molecules are filtered more easily. The reason for this is the negatively charged surface of the endothelial cells. Albumins for example have a molecular mass 66 (on average) and are therefore under the barrier properties of the glomerulus. Because of the strong negative charge the impermeability of the glomerular barriers for albumin is still at 99.97% [Klinke, 2004]. The primary urine formed by the glomerulus enters the proximal tubular system (1.2.2.4 The Tubular System), in which essential compounds and water are reabsorbed.

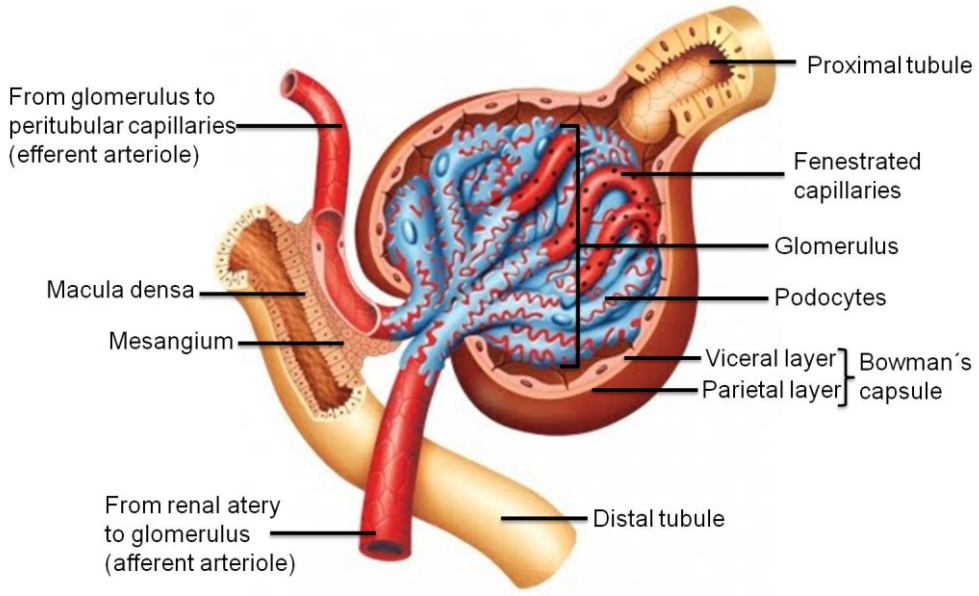

Figure 1-8 The Glomerulus. A schematic drawing shows the afferent and efferent arteriole entering and leaving the glomerulus. The glomerulus is covered by podocytes within the Bowman´s capsule. In addition the Macula densa and the Mesangial cells between the distal tubule and the glomerulus is given. [modified by Haussecker, 2012].

1.2.2.4 The Tubular System

Directly behind the glomerulus the primary urine enters the proximal tubulus. This tubular part can be subdivided into two sections, the pars convoluta and the pars recta. The pars convoluta are confined entirely to the renal cortex while the pars recta descend into the outer medulla. [Boron et al., 2008]. Regarding functional properties and ultrastructure the proximal tubules can also be divided into three segments (S1, S2 and S3) where the segments S1 and S2 belong to the pars convoluta and S3 segment belongs to the pars recta. Although the cellular complexity increases from the S1 to the S3 segments, the cellular structure is similar over the individual segments. The proximal tubular cells (PTCs) are characterized by a luminal surface covered with densely packed microvilli. This brush border increases the luminal surface, depending on there resorptional functionality and a putative flow sensing within the lumen [Wang, 2006]. In addition the PTCs are highly packed with mitochondria which are needed to supply energy to various ATP-dependent transport processes but also protein synthesis. One of the key ATP-dependent transport processes is the sodium transport out of the PTCs via the Na/ K-ATPase. This energy consuming transport builds-up a concentration gradient which therefore leads to water reabsorbtion by passive diffusion, following the sodium along its concentration gradient. In addition, various secretion processes are taking place. Most of the ammonium eliminated in the urine is formed in the proximal tubule by cleaving of glutamine to α-ketoglutarate [Rennke et al., 2009]. But also a multitude of drug is transported by the proximal tubules into the lumen to allow the elimination via the urine.

The next tubular region is the so called loop of Henle. The main function of the loop of Henle is to create a concentration gradient in the medulla by achieving a high sodium concentration near the collecting ducts in order to reabsorb water passively by moving down its concentration gradient [Eaton et al., 2004].

Therefore, this part can be roughly divided into two portions; the descending limb, which is the first part after the proximal tubulus and the ascending limb of the loop of Henle. Subdivisions into five parts depending on there morphological structure and the location within the kidney are prominent:

1. Thick descending limb
2. Thin descending limb
3. Thin ascending limb
4. Thick ascending limb
5. Cortical thick ascending limb

Both the thick and thin descending limbs are highly permeable to water while the permeability for urea and ions is quite low. In the renal medulla a sharp bend is the border from the descending and the ascending limbs. The thin ascending limb is characterized by its impermeability to water but not to ions. Similarly, the thick ascending limb is responsible for the reabsorption of Na^+, K^+ and Cl^{2+} by the passive transport via NKCC2 (Na-K-2Cl symporter) [Lytle et al., 1995]. The final area of the loop of Henle, the cortical thick ascending limb, drains the urine into the distal tubular convolute.
The distal tubular cells (DTCs) are responsible for the regulation of several electrolytes like Na^+, K^+ and Ca^{2+} and also the pH by absorbing and secreting bicarbonate and protons. In contrast to the PTCs the DTCs do not have an apical brush border and are under strong hormone control. Therefore, aldosterone increases sodium reabsorption. Sodium and potassium levels are also controlled by secreting K^+ and absorbing Na^+.
Followed by the distal tubule, the urine enters the collecting duct. In this compartment, which is formally not part of the nephron, the fine adjustment of concentration via water absorption is performed. All the processes in the collecting duct are controlled by the hormones aldosterone and antidiuretic hormone (ADH).

1.3 Nephrotoxicity

The kidney is one of the most affected target organs of xenobiotic-induced organ toxicity [Emeigh-Hart et al., 2005]. A very large number of therapeutic compounds (aminogykosides, NSAIDs, ACE inhibitors) as well as chemicals (heavy metals like cadmium and cobalt) lead to excessive tissue damage in renal tissue. The high rate of substance-induced renal damage can be explained by the central role of the kidney in xenobiotic elimination processes. Therefore, a high number of drugs are eliminated *via* the kidney excreted through the urine. Additionally, the high blood flow rate of the kidney, which is about 1.2 liters per minute (1700 liter per day), that corresponds to a value of 25% of the cardiac output, leads to an extraordinary exposure to xenobiotic compounds [Klinke et al., 2004].

The kidney has, beside liver and gut, one of the highest activities of phase I and phase II xenobiotic metabolizing enzymes [Lohr, 1998]. Consequently, several harmless compounds can be activated and toxified within the kidney itself [Emeigh-Hart et al., 2005]. Also extrarenal, hepatic activated substances can enter the kidney.

Based on the physiological functionality of the kidney to reabsorbed essential blood components, the cells of the proximal and distal tubulus are very rich in active and passive transporters. This leads to the fact that several xenobiotic compounds are taken up by the tubular cells, which can lead to the accumulation of these compounds (aminoglykosids, platinum complexes) – potentially increasing toxicity [Anzai et al., 2007].

The glomerulus filters approximatly 120 mL primary urine per minute. This leads to a total daily amount of ~170 L primary urine entering the tubular system, which is concentrated down to ~1.5 L daily urinary output. This means as a consequence the concentration of xenobiotics can also increase up to 100 fold compared the serum level. Combined with the metabolic activity and the transport capacity even very small administered doses can exceed tolerable concentrations within renal tissue. All this leads to an increasing number of acute kidney injury (AKI) and chronic kidney diseases (CDK). AKI describes the reversible insufficiency of the glomerular and tubular excretion function. Consequently, anuria tubular symptoms can appear [Marquardt et al., 2004]. Overall, 1-7% of patients with a long-term hospitalization develop AKI [Hou et al., 1983; Edwards et al., 1994; Nash et al., 2002; Liangos et al., 2006] while the number in patients in an intensive care unit increases up to 25% [Chertow et al., 1998; de Mendonca et al., 2000]. 50-70% of adults and 30% of pediatric patients with AKI die of the disease annually [Minejima et al., 2011]. One of the reasons for AKI is the nephrotoxic potential of a multitude of drugs. The number which can lead to drug-induced AKI varies in literature. Between 8 and 60% of the reported cases can lead back to Nephrotoxins [Hou et al., 1983, Nash et al., 2002; Uchino et al., 2005]. This underpins the importance of identifying and evaluating novel methods for the early prediction of renal damage, not only in toxicology but in clinical trials.

Pathological changes associated with AKI or general nephrotoxicity can be caused by several factors and include a multitude of different mechanisms. The manifested pathology can vary depending on the underlying effect on renal cells and the area within the nephron. This may be due to the heterogenic construction of the nephron, which includes several different cell types which are separated and have defined localizations within the kidney. It can be discriminated between pre-, intra-, and post-renal causes, while compound induced renal damage accounts for the group of intra-renal causes. A general overview is given in Figure 1-9. A common pre-renal cause of acute kidney injury is azotemia, which can be induced by diuretics or other antihypertensive drugs [Wilcox, 1999]. Intrarenal toxicity can manifest after cardiovascular damage, direct tubular injury, interstitial damage and glomerular injury.

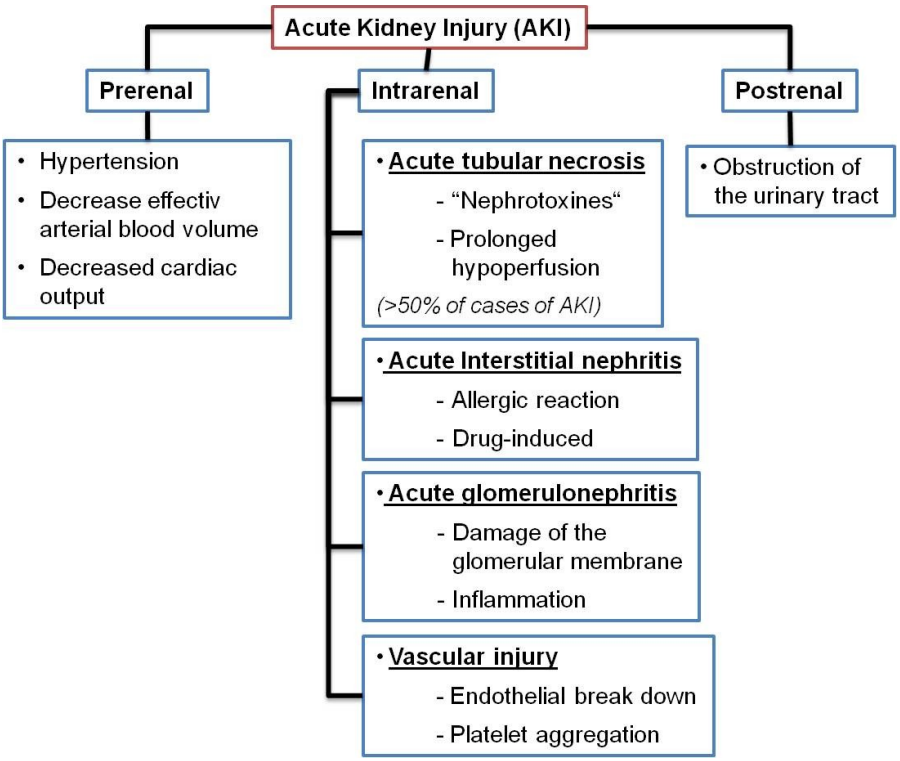

Figure 1-9 Overview of the three major causes of acute kidney injury (AKI). Pre-, intra- and, postrenal causes can be discriminated. The most important alteration in case of drug-induced kidney injury is the intrarenal acute tubular necrosis. [modified by Dermirjian et al., 2012]

While vascular injury, associated with primary endotheilial damage, leading to platelet aggregation/ consumption and consequently to renal vascular injury [Choudhury et al., 2006], tubular injury is characterized by direct injury of tubular cells. This damage itself can be caused by toxic, inflammatory, ischemic or obstructive mechanisms.

A common cause of drug-induced renal interstitial inflammation is an increasing number of lymphocytes, monocytes, eosinophils and plasma cells within the renal interstitium [Choudhury et al., 2006]. This can be induced by compounds leading to immune reactions, which then localizes within the interstitium. Another cause is the binding of renal tubular cell antigens by drugs. Also in some glomerular alterations, inflammatory processes have been described to play a pivotal role [Kleinknecht, 1995]. Drugs that alter the glomeruli and subsequently lead to an elevated permeability often cause proteinuria. Glomerular damage can be caused by different mechanisms. Therefore, glomerulonephritis, which describes the inflammation of the membranous tissue and glomeruloslerosis, which is the scarring of small renal blood vessels, can be discriminated. These pathologies are all acute events. However, chronic nephrotoxicity must not be forgotten, and describes the situation of prolonged exposure of the kidney to a compound. The underlying mechanisms of the compounds used within this project will be described in more detail under 1.3.1 Nephrotoxins.

1.3.1 Nephrotoxins

Four general mechanisms leading to renal damage are known, based on the role of the kidney within an organism and the functional properties (see Figure 1-10), whereby it should be noted that in most cases a combination of these will appear in an in vivo situation. First, a compound can enter the cell by diffusion or by active uptake and can interact there, without metabolism, with intracellular macromolecules. Another possibility is the intracellular formation of reactive oxygen species (ROS), which causes oxidative stress and cellular damage. On the other hand a compound can

be metabolized intrarenally to form toxic metabolites which can interact with cellular compartments or lead to lipid oxidation. The last possibility of a direct mechanism leading to drug-induced kidney injury is via extrarenal toxification (usually hepatic) of drugs which subsequently enters the kidney [Greaves, 2011]. Because of the central role of the kidney within the body several other secondary mechanisms can be lead to AKI or CKD based on the extrarenal organ damage, such as hepatorenal syndrome [Arroyo et al., 1996].

In the following section the used compounds within this scientific approach shall be introduced and the underlying mechanism, as far as known, shall be described in more detail.

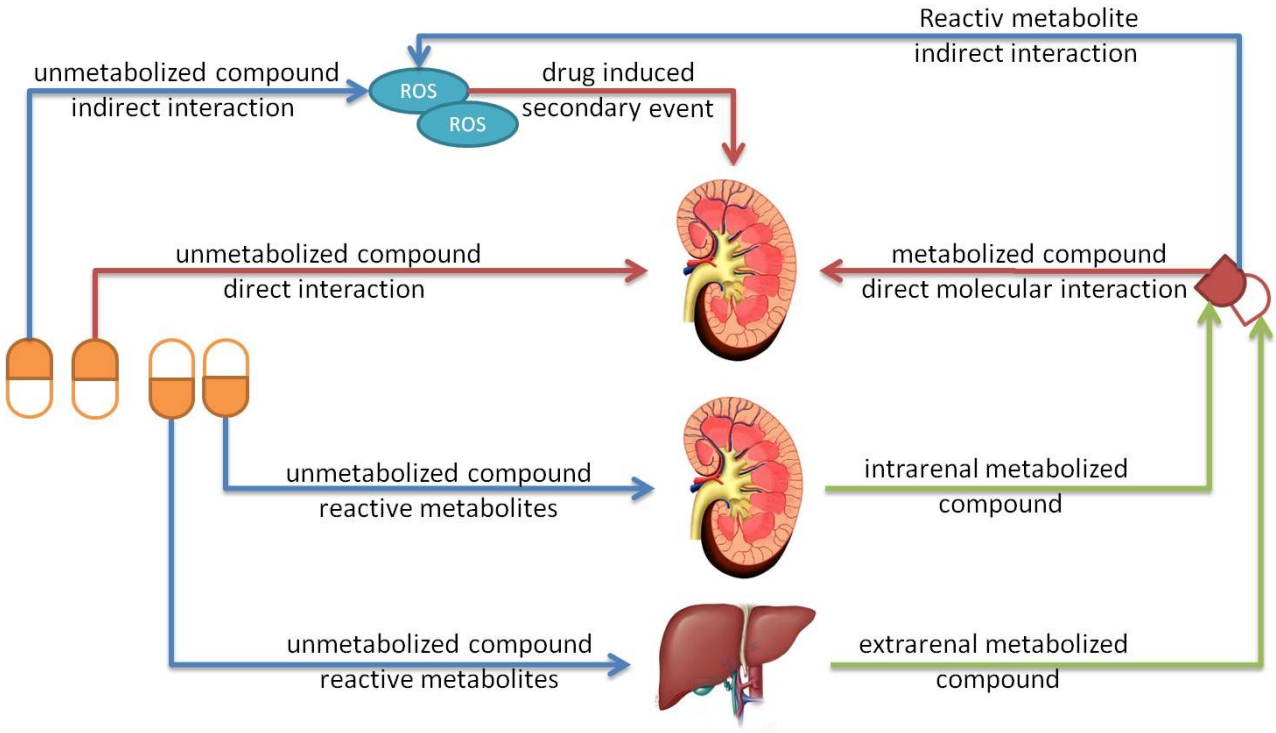

Figure 1-10 General mechanisms of drug-induced renal damage. Based on the structure, the physicochemical properties, the toxicokinetic and toxicodynamics a drug can directly interact with cellular compartments or induce secondary cellular responses, like ROS. Other drugs maybe intra- or extrarenally activated and therefore lead to renal injury. The blue arrows indicate steps without direct, harmful impact on the kidney. The red arrows show direct detrimental effect of either the drug or its metabolites. The green arrows indicate metabolic activation of the original drug.

Compounds used in vivo

- Vancomycin

  Vancomycin is a large, rigid glycopeptides that inhibit bacterial cell wall peptidoglycan synthesis. The mechanism is based on its three-dimensional structure, containing a cleft into which the L-lysine-D-alanyl-D-alanine amino acid sequence fits, which is highly specific for bacterial cell walls [Reynolds et al, 1989].

  Vancomycin is a known nephrotoxin, if special importance in nosocomial infection patient populations. [Toyoguchi et al., 1997]. Because Vancomycin is a drug of last resort for gram-positive bacterial infections [Cui et al., 2006] nephrotoxic side effects have been frequently reported in humans. The nephrotoxicity varies from in 0–17% in case of Vancomycin monotherapy and 7-35% in cases of co-administration with other antibiotics (e.g., aminoglycoside) [Rybak et al., 2009]. However, the full mechanism of toxicity is still not completely understood. The basic mechanism of Vancomycin nephrotoxicity depends on an energy-dependent uptake from the blood over the basolateral membrane of tubular cells [Dieterich et al., 2009]. It is suggested that Vancomycin alters the energy dependent renal reabsorption function of the proximal tubule cells, by

detrimentally affecting mitochondrial function [King et al, 2004]. Oxidative stress might be involved in the pathogenesis of Vancomycin induced renal damage as mitochondria represent a major site of ROS production. In addition, the induction of several antioxidants, serving as potential protective factors, has been reported [Celik et al., 2005]. Vancomycin is reported to show pathological changes in tubulus of kidney in animals treated intraperitoneal (i.p.) with 200 mg/kg/day. Cellular oedema, cell necrosis and tubular atrophy were the most evident changes [Naghibi et al., 2007]. Therefore, 300 mg/kg/day Vancomycin (i.p.) was used in this study to induce server toxic effects. As a low dose, were no-to-minimal alterations were expected, 50 mg/kg/day Vancomycin was used.

- Cisplatin

Platinum compounds are widely used drugs for the treatment of several kinds of cancers [Kelland, 2007]. The most common members of the group of platinum compounds are Cisplatin, oxaliplatin and Carboplatin. The cytotoxic potential of this class of compounds is based on their ability to induce DNA cross-links [Poklar et al., 1996; Rudd et al., 1995]. Cisplatin, for example, reacts preferably with the N_7-atom of adenine and guanine because of the high electophilicity of the water-Cisplatin complex. In this way intra- and inter-strand links are formed, eventually leading to an inhibition of DNA synthesis [Huang et al., 1995; Takahara et al., 1996]. Additionally, Cisplatin induces point mutations and the generation of superoxide radicals, as well as inhibiting DNA repair mechanisms and telomerase activity [Barabas et al 2008]. Apoptosis has also been reported, and it is worth noting that several signaling and apoptosis pathways are induced by Cisplatin. Therefore, p53, p21 or caspase dependent and independent pathways, as well as Bax, FasL and other death agonistic molecules, can be involved in Cisplatin induced apoptosis. The exposure of tubular cells to Cisplatin activates several signalling pathways that lead to tubular cell injury and death but also induces injury in renal vasculature. This results in decreased blood flow and ischemic injury of the kidneys, contributing to a decline in glomerular filtration rate (GFR). These events, taken together, culminate in the loss of renal function during Cisplatin nephrotoxicity and can be considered to be a multifactorial process, finally triggering acute renal failure [Pabla et al., 2008].

The dose limiting effect in the administration of Cisplatin is the nephrotoxic potential, specifically the severe injury of the S3 segment of the proximal tubulus [Cristofori et al., 2007]. The basolateral drug transport via the organic cation transporter-2 (OCT2) seems to play a key role in the accumulation of Cisplatin in proximal tubular epithelial cells. After entering the PTCs Cisplatin is activated by an aquation reaction, i.e. substitution of the two chloride groups with hydroxyl ligands, which only enables binding to two sites in DNA.

In clinical trials, Cisplatin nephrotoxicity is often seen after 10 days of administration and is manifested as higher serum creatinine, reduced serum magnesium and potassium levels as well as a lower glomerular filtration rate. The long-term effects of Cisplatin on renal function are not completely understood, but it is expected that Cisplatin treatment may lead to sub-clinical, permanent reduction in GFR [Koch Nogueira et al., 1998].

Because of the high specificity of Cisplatin to cause damage to the proximal tubular cells, mainly of the S3 segment, this compound has been used to study the specific, but slight effects, on this area. Therefore, the high dose used was chosen as 0.6 mg/kg based on the dose-rang finding study [Fuchs et al., 2012] where 0.5 mg/kg caused no tubular necrosis or degeneration, while 1 mg/kg lead to moderate to massive alterations after 28 days of treatment. The low dose was 0.3 mg/kg and was chosen to observe if even no to minimal histopathological alterations can be detected at early time points by the evaluated urinary biomarkers.

- Puromycin

  Puromycin is an aminonucleoside antibiotic, which inhibits protein synthesis in vivo as well as in cell-free systems [Darken, 1964]. As an aminoacyl-tRNA analogue, it leads to the premature release of unfinished polypeptide chains as polypeptidyl-puromycin derivatives. In addition, Puromycin serves as an acceptor of the peptidyl chain from peptidyl-tRNA in the P site, in a reaction in which peptidyl chains are attached to the free ammonium group of Puromycin catalyzed by peptidyl transferase [Azzam et al, 1973].

  To date the nephrotoxic mechanism of Puromycin is not yet understood. However, it is known that it induces a nephritic syndrome in humans [Kihara et al., 1995]. The MAP kinase pathway, which induces apoptotic processes, is also known to be involved in the development of renal damage after Puromycin treatment [Servais et al., 2008]. Puromycin is described to induce PPARγ in podocytes, which is the primary event in early development of glomerulosclerosis, as this increase is counter regulated and might promote podocyte healing and repair [Kiss-Toth et al, 2008]. Based on literature data from repeated dose studies using Puromycin [Nosaka et al., 1997; Amin et al. 2004] and a previous performed in-house dose range finding study a high dose of 30 mg/kg and a low dose of 10 mg/kg were used.

- Gentamycin

  The broad spectrum antibiotic, Gentamycin, is produced by fungi suchas *Mikromonospora purpurea* and *Mikromonospora echinospora.* This aminoglycoside antibiotic, consisting of a mixture of three slightly different compounds, is hydrophilic because of several OH-groups, which leads to a strongly reduced uptake into body cells, with the exception of proximal tubular cells [Aktories *et al.*, 2011]. Therefore, Gentamycin only works for the treatment of extracellular pathogenic germs. The importance of this antibiotic is its wide spectrum of effect, reaching from gram-negative rods to gram-positive cocci. Because of the missing reabsorption after oral application, the efficiency is limited to local function. However, by intra muscular injection the reabsorption of Gentamycin is about 90% [Mutschler *et al.*, 2008]. Because of its relatively low plasma binding, Gentamycin is usually glomerular filtrated and eliminated in the urine without changes [Aktories*, et al.*, 2011]. Even for Gentamycin, one of the most studied nephrotoxic drugs on the market, the underlying toxic mechanism is still not yet completely understood. It is known that glomerular atrophy, tubular fibrosis/ necrosis as well as epithelial oedema of proximal tubules and inflammation are associated with Gentamycin induced-renal damage [Ozbek et al., 2009; Balakumar et al., 2010]. On a molecular basis, a multitude of processes seems to be involved in the outcome of renal damage. For example, lysosomal phospholipidosis and apoptosis, which have been suggested to play key roles [Ali, 1995; El Mouedden et al., 2000]. In addition, inflammatory driven renal damage, initiated by Gentamycin–induced tubular cell necrosis, leads to a progression in renal pathogenesis [Geleilete et al., 2002]. Also oxidative stress induced by ROS seems to play a pivotal role in the renal cortex, eventually leading to renal deterioration [Walker et al., 1999]. Finally, it has been reported that Gentamycin-induced nephrotoxicity seems to be associated with the over expression of NFκB- and p38/ MAPK pathways [Ozbek et al., 2009]

- Aristolochic acid

  Aristolochic acid (AA) is a mixture of structurally related nitrophenanthrene carboxylic acid derivatives, primarily AA I and AA II, which occur as secondary metabolites in plants of the genus *aristolochia*. It is described to be a rodent carcinogen and a highly nephrotoxic compound [Mengs et al., 1982, Mengs et al., 1993]. In humans, exposure to AA has been linked to the pathogenesis of Chinese herb nephropathy (CHN), a

rapidly progressive interstitial nephropathy associated with the intake of Chinese herbs mistakenly containing *Aristolochia fangchi* [Depierreux et al., 1994, Vanherweghem et al., 1993]. Based on the striking similarities to CHN, including an association with increased risk for the development of urothelial malignancies, AA has also been suspected to be a causative agent for Balkan endemic nephropathy, a chronic tubulointerstitial kidney disease which occurs in geographically limited areas of the Balkan region, presumably through contamination of flower with seeds of *Aristolochia clematitis* growing on the fields [Grollman et al., 2007]. AA mediated nephrotoxicity in rodents is characterized by progressive loss of the proximal tubule brush border and necrosis of the renal tubule epithelium within the outer stripe of the outer medulla and the medullary rays [Lebeau et al., 2005]. The mechanism of AA nephrotoxicity and carcinogenicity is not fully understood but is thought to involve metabolic activation to a cyclic N-acylnitrenium ion which forms covalent DNA adducts [Debelle et al., 2004, Yang et al., 2007].

- FP007SE (BI-3)
  BI-3 3-pyrrolidineacetic acid, 5-[[[4'-[imino[(methoxycarbonyl) amino]methyl] [1,1'-biphenyl]-4-yl]oxy]methyl]-2-oxo-, methyl ester,(3S-trans) is a compound used in the previously described Innomed/Predtox project. This compound was selected for the project based on previous knowledge of its toxicity to the liver and kidney. Doses were suggested on the basis of a previous 4 week toxicity study at Boehringer Ingelheim Pharma GmbH & Co.KG. During this study clear liver and kidney toxicities were shown at 1000 mg/kg/day. 100 mg/kg/day were selected as a low dose, based on that 30 mg/kg/day was derived as NOAEL and 180 mg/kg/day showed first signs of toxicity. 1000 mg/kg/day were chosen as the high dose. Important information about the nephrotoxic potential of BI-3 was published in 2011 [Hoffmann et al., 2011; Matheis et al. 2011].

Compounds used in vitro

- Acetyl-*para*-Aminophenol
  Acetaminophen (Paracetamol) is a popular analgesic and antipyretic drug widely used in the treatment of pains, headaches and fever [Prescott, 2000]. In contrast to other common analgesics like ibuprofen or aspirin, acetaminophen has no effect on platelet function or anti-inflammatory properties and is therefore not a member of non-steroidal anti-inflammatory drugs or NSAIDs [Marquad et al., 2004]. In standard doses Acetaminophen is a very safe drug. However, because of its wide availability, overdoses, accidental or suicidal, are very common [Hobson, 1997]. Acetaminophen is thought to act primarily in the central nervous system (CNS), increasing the pain threshold by inhibiting both isoforms of cyclooxygenase, COX-1 and COX-2, enzymes involved in prostaglandin synthesis [Graham et al., 2005]. Acetaminophen does not inhibit COX in peripheral tissues and therefore has no peripheral anti-inflammatory affects. In contrast to aspirin, acetaminophen indirectly blocks COX in a way that this blockade is ineffective in the presence of peroxides [Boutaud et al., 2002]. This might explain why acetaminophen is effective in the central nervous system and in endothelial cells but not in platelets and immune cells which have high levels of peroxides. Studies also report that acetaminophen selectively blocks a variant of the COX enzyme that is different from the known variants COX-1 and COX-2. This enzyme is now referred to as COX-3 [Chandrasekharan et al., 2002].
  Acetaminophen toxicity is mostly reported in context of excessive liver, but also kidney, damage after overdosing [Tarloff et al., 1996]. Acetaminophen itself is not toxic. However, approximately 90 to 95% of a dose is metabolized in the liver via the cytochrome P450 enzyme pathways, followed by conjugation with

glucuronic acid, sulfuric acid or cysteine. An intermediate metabolite (NAPQI) is hepatotoxic and most likely nephrotoxic and can accumulate after the primary metabolic pathways have been saturated.

- Doxorubicin

  Doxorubicin is a widely used, quinine-containing anthracycline antibiotic, used in cancer treatment. The mechanism of action is based on the intercalation of Doxorubicin into DNA double stands and by the inhibition of macromolecular biosynthesis [Fornari et al., 1994]. Therefore, DNA replication is inhibited by Doxorubicin by stabilization of the topoisomerase II complex, built after it has broken the DNA chain for replication. The structure of Doxorubicin can be divided into two major groups, a planar aromatic chromophore which intercalates between two base pairs and the daunosamine (six membered sugar) which fits into the minor groove of the double helix and interacts with further base pairs [Frederick et al., 1990]. Its use in chemotherapy is limited by several side effects, including cardiac-, testicular-, pulmonary- and nephrotoxicity [Singal et al., 1987; Fadillioglu et al., 2003]. The area of kidney injury includes tubular atrophy and glomerular capillary permeability [Wapstra et al., 1999].

  So far it is believed that the major processes within renal tissue related to Doxorubicin toxicity is the formation of free radicals, protein oxidation, iron-dependent oxidative damage of cellular macromolecules and lipid/membrane peroxidation mediated by an imbalance in oxidant-antioxidant homeostasis [Liu et al., 2007]. On potential source of free radicals described to play a role, is nitric oxide syntheses (NOS) via a stimulation of NO production [Radi et al., 1991]. In addition, mitochondrial toxicity as well as transmembrane arginine transport on a subcellular level is described for doxorubicin [Cendan et al., 1995].

- Amphotericin B

  The polyene antifungal drug, AmphotericinB is a widely used fungicide for internal and external treatment. It is ~95% bound on plasma proteins like albumin, which leads to an almost complete distribution within the whole organism [Marquardt et al., 2004; Brajtburg et al., 1996]. Its fungistatic activity is based on its high affinity against ergosterol, a steroid integrated exclusively within the membrane of fungi. AmphotericinB induces the formation of a membrane pore, leading to the loss of the membrane integrity by perforation. Subsequently, mono- and bivalent ions, notably sodium and calcium ions, start to leak out due to increased permeability. Because the specificity of AmphotericinB to bind exclusively to ergosterol is low, mammalian cell membranes, containing cholesterol, are also attacked leading to reduced membrane integrity. Because of the continuous loss of ions, which play a crucial role in the functionality of the kidney, apoptosis of renal tubular cells is induced as a consequence. However, the affinity to ergosterol compared to cholesterol is significant higher [Brajtburg et al., 1996; Sawaya et al., 1995]. Why the major side effect of AmphotericinB is nephrotoxic is not yet completely understood. One hypothesis for the selective side effects in vivo is the relative low pH of renal cells, which is around 5.5 – 6. This causes a reduced uptake of calcium ions. Walev and colleagues could show that cells treated with AmpothericinB recovered when an extracellular pH of 7-7.4 was used, while the cellular damage showed a further procession at a pH of 6.6 [Walev et al., 1996].

- Puromycin

  See the description of Puromycin under 1.3.1 Nephrotoxins.

- d-Mannitol

  Mannitol, as well as its isomer sorbitol, is alcoholic sugars, often used as sweeteners for people with diabetes or as general food supplements [Roempp et al., 1992]. In addition, Mannitol is used in several medical

applications, like cardiopulmonary bypasses [Carcoana et al., 2003], Alzheimer´s disease, chemotherapy [Ikeda et al., 2002], and cystic fibrosis [Jaques et al., 2008]. One of the most important applications is its use in patients with oliguric renal failure [Atherton et al., 1968]. Because of the free filtration and the inability of the PTCs and DTCs to reabsorb Mannitol from the tubular lumen after i.v. administration, the sodium and water reabsorption *via* its osmotic effect is decreased. Subsequently, a decrease in extracellular fluid volume takes place because of an increase in sodium and water excretion. Therefore, no direct nephritic potential of Mannitol has been described so far.

- Metformin

  Metformin is an antihyperglycemic agent, which improves glucose tolerance in patients with type 2 diabetes, lowering both basal and postprandial plasma glucose [Mutschl et al., 2001]. Metformin is not chemically or pharmacologically related to any other classes of oral antihyperglycemic agents. Unlike sulfonylureas, Metformin does not produce hypoglycaemia in either patients with type 2 diabetes or normal subjects and does not cause hyperinsulinemia [Bodmer et al., 2008]. With Metformin therapy, insulin secretion remains unchanged while fasting insulin levels and daylong plasma insulin response may actually decrease. Metformin improves insulin sensitivity by increasing insulin receptor binding as well as peripheral cellular insulin uptake and decreasing intestinal glucose absorption and hepatic gluconeogenesis [Bailey, 1993]. Anaerobic glycolysis is stimulated and insulin action at the receptor or post receptor level is increased. No direct nephritic potential of Mannitol has been described so far.

1.4 In vivo - and in vitro - Methods in Toxicology

The most widely used test models in toxicological studies are mice (*mus musculus*) and rats (*Rattus norvegicus* forma domestica). Several rat strains, with different pheno- and genotypes, as well as transgenic animals are bred in order to meet the different study requirements. Other animal models like canine, monkey and mini-pigs are common in toxicological safety assessment. In general, modern toxicology is still based on animal testing to get reliable and regulatory accepted data. Because it is not yet possible to simulate the whole complexity of the in vivo situation in an in vitro model there is a need on one hand to develop better in vitro test systems and, on the other hand, to develop novel methods and technologies to increase the output of animal studies. These novel approaches have to go hand-in-hand with traditional toxicological observations to evaluate the usefulness and the added value of novel parameters and/ or technologies (see 1.1.2). There are a multitude of endpoints, based on several biological classes of molecule and test systems which can deliver further toxicologically relevant information. The complexity of the model systems can span from whole organisms down to subcellular compartments, the complexity of the used technologies can range from whole genome sequencing to single gene detection. Figure 1-11 gives an overview of a pre-selection of methods and models with increasing / decreasing complexity and reliability. With the increasing complexity of the methods the amount of data, and therefore the bioinformatics and scientific challenge of analyzing and interpreting, increases. Global microarrays for example deliver huge amounts of data points per sample, which makes it necessary to filter out the information of interest. Single gene or protein analysis on the other hand deliver less information, but are much easier to handle and be implemented into early decision making.

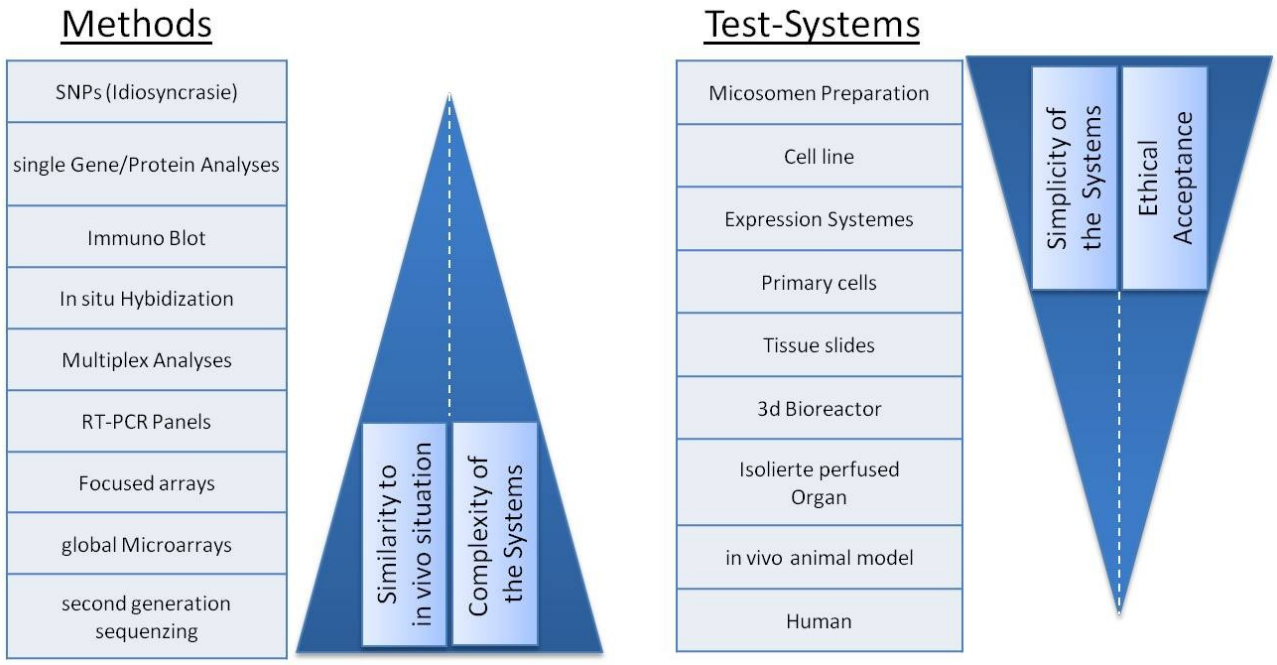

Figure 1-11 In drug development, the used test-systems und methods. Methods as well as test-systems are ordered based on there complexity in handling as well as their reflection of the in vivo system (in more detail to reflect the human situation) [modified from Brandon et al., 2003].

Consequently there are several test systems available which can deliver relevant and high quality information on test compounds and therefore aid in the decision to go on or stop the development of a potential drug candidate.

The benefit of in vitro models includes their ethical acceptance, their cost efficiency and their higher throughput which enables the testing of many of compounds in parallel. On the other hand the question answered by the models has to be

very specific and the available information generated can be very limited. This is the reason why in vitro models in routine are formally used for a pre-selection of potential drug candidates based on e.g. general cytotoxicity, genotoxicity, specific organelle toxicity or interference of the drug with metabolic enzymes or transporters. As in vitro systems the perfused kidney, renal tissue slices, isolated nephrons, primary cells and cell lines with renal characteristics haven been established [Pfaller et al., 1998]. For routine toxicological assessments, cell lines and primary cells are the most efficient models used, based on a combination of easy handling and complexity.

Several different cell lines are available to study renal related alterations in vitro. Therefore, available cell lines, like LLC-PK1 (swine), NRK-52E (rat), MDCK (canine), OK (opossum), HK-2 (human), RPTEC/ hTERT1 (human), have been frequently used to assess cytotoxicity, transepithelial electrical resistance, tight junction proteins and inulin uptake [Duff et al., 2002, Rached et al., 2008, Jennings et al., 2009, Wieser et al., 2008, Wiesinger et al., 2012]. The analysis of the whole genome transcriptomics, using renal cell lines, to evaluate there usability has not yet been fully addressed.

For the examination of nephrotoxic effects on mRNA in in vitro systems, the permanent cell line NRK-52E cells were used. This cell line was described the first time in 1966 and was generated from the cell line NRK-49F. In contrast the NRK-52E cells show epithelial morphology and are characterized by an almost complete set of diploid chromosomes (only 4% tetraploid). In the past the influence of a polyploidy set of chromosomes on the gene regulation could be clearly shown, making these cells more preferable for gene expression analysis [Gottlieb, 2003; Chen, 2006]. Additionally, several studies have focused on the mechanism of nephrotoxicity and nephrocarcinogenicity using NRK-52E cells [Leussink et al., 2003; Rached et al., 2008; Ahn et al., 2010]. In this case publications are available describing ROS-induced cell apoptosis by nephropathy inducing reagents [Xiong, 2006]. Furthermore, based on NRK-52E cells, the influence of cadmium on the cell cycle, especially on the G2/ M-Phase blocking, could be shown and the impact of the increased activity of p53 causing in a increased expression of cell cycle kinases, such as p27 and p21 and a reduction of Cdk1 and Cdk2, has been reported [Xie et al., 2006].

1.5 Aim of the work

In the last few decades several studies were published that delivered further insights in to the detection of drug-induced nephrotoxicity. Taken together, the outcome of these studies was that several urinary proteins can be used for the detection of acute nephrotoxicity in rodent toxicity studies up to 14 days of treatment. These proteins must be discriminated between qualified (accepted by the FDA/ EMA) and exploratory (recommended for further evaluations) biomarkers.
The aim of the in vivo studies was to validate the already qualified urinary protein biomarkers and to prove that the described exploratory markers can also deliver additional information or to increase the sensitivity and/or specificity of the panel already qualified. Additionally, several questions regarding these markers shall be answered:

1. How the markers behaved in both genders?
2. Can the markers be used for sub-acute toxicity studies, i.e., after 28 days of treatment?
3. Which of the qualified/ exploratory markers deliver reliable results?
4. How are the diagnostic properties related to histopathological findings?
5. How can a recovery period influence the excretion of these urinary biomarkers?

In addition, several alterations on the transcriptional level have been observed and a multitude of potential gene expression biomarkers have been proposed in the last few years. Subsequently, novel transcriptional biomarkers were identified, characterized and shown to deliver further mechanistic information and to enlarge the availability of biomarkers for renal safety assessment with the potential to serve as translational biomarkers for human and other species. Therefore, already published mRNAs biomarkers shall be tested for their predictivity of nephrotoxicity and to see if there is an improvement over the already published biomarkers. In addition, we aimed to evaluate what the best combination of altered genes is for predicting different pathological phenotypes. Mechanistic analysis of Vancomycin-induced nephrotoxicity shall be performed to obtain on one hand further insights on the underlying toxic processes of this compound and on the other hand the potential to show generic alterations which themselves could be used for the detection of drug-induced kidney injury.

The aim of the in vitro studies was to test whether the results of the in vivo study can be mimicked and search for in vitro specific kidney markers. Since a lot of information about altered transcripts in rat after treatment with nephrotoxins is available, the question arose whether or not these findings can be translated and used on in vitro level. Therefore, the applicability of NRK-52E cells, a rat cell line, to work in combination with transcriptional biomarkers shall be addressed by whole genome transcriptomics as a proof-of-principal analysis.

2. Materials and Methods

2.1 Materials

2.1.1 Chemicals and Reagents

Table 2-1 Cell culture reagents

Name	Provider	Registered office
CASY®Ton	Schärfe System GmbH	Reutlingen Germany
DMEM, w/o glucose and sodium pyruvat, w/i L-glutamin, pyridoxine HCl and phenolred	Gibco/ Invitrogen	Karlsruhe, Germany
DMEM, w/i 4.5g/L glucose, L-glutamin and phenolred, w/o sodium pyruvat	Gibco/ Invitrogen	Karlsruhe, Germany
DMEM F12 (1:1), w/i L-glutamin, 15 mM Hepes, glucose and phenolred	Gibco/ Invitrogen	Karlsruhe, Germany
Epidermal growth factor, final 10 ng/mL (EGF)	Sigma Aldrich	Steinheim, Germany
Fetal calf serum (FCS)	Hyclone/ Perbio	Logan, USA
Ham´s F12, w/i L-glutamin	Gibco/ Invitrogen	Karlsruhe, Germany
Hydrocortisone, final 36 ng/ml	Sigma Aldrich	Steinheim, Germany
Insulin, Transferrin, Selenium final 5 µg, 5 µg, 5ng (ITS)	Sigma Aldrich	Steinheim, Germany
PBS Dulbeccos w/i Ca, Mg	Gibco/ Invitrogen	Karlsruhe, Germany
PBS Dulbeccos w/o Ca, Mg	Gibco/ Invitrogen	Karlsruhe, Germany
Penicillin (10 kU/ ml)-Streptomycin (10 mg/ ml) solution	Sigma Aldrich	Steinheim, Germany
Trypsin/ EDTA-solution (0.5%)	Sigma Aldrich	Steinheim, Germany
Trypsin/ EDTA-solution (0.25%)	Sigma Aldrich	Steinheim, Germany

Table 2-2 Kits and reagents for biochemical assays

Name	Provider	Registered office
Agencourt® RNAClean™ XP	Agencourt/ Beckman Coulter	Beverly, USA
CellTiter-Glo® Luminescent Cell Viability Assay	Promega	Madison, USA
Coomassie Brilliant Blue G250	Merck KGaA	Darmstadt, Germany
Ethanol Lichrosolv®	Merck KGaA	Darmstadt, Germany
MessageAmp™ II aRNA Amplification Kit	Ambion/ Applied Biosystems	Austin, USA
Rat RENA-Strip Kit	BioAssay Works®	Ijamsville, USA
RNeasy Mini Kit	Qiagen	Hilden, Germany

Name	Provider	Registered office
RNase-free DNase Set	Qiagen	Hilden, Germany
RNA 6000 Nano Kit	Agilent Technologies	Waldbronn, Germany
RNA 6000 Pico Kit	Agilent Technologies	Waldbronn, Germany
Schreddercolumn, QIAshredder	Qiagen	Hilden, Germany
WideScreen® Rat Kidney toxicity assay Panel 1	Merck Millipore (Novagen®)	Billerica, USA
WideScreen® Rat Kidney toxicity assay Panel 2	Merck Millipore (Novagen®)	Billerica, USA

Table 2-3 Reagents for molecular biological studies

Name	Provider	Registered office
Cy3-Streptavidin	Amersham Biosciences/ GE Healthcare	Buckinghamshire, England
DEPC water	Ambion/ Applied Biosystems	Austin, USA
E1BC buffer	Illumina Inc.	San Diego, USA
Ethanol Lichrosolv®	Merck KGaA	Darmstadt, Germany
High Temperature Wash buffer	Illumina Inc.	San Diego, USA
HybE1 buffer	Illumina Inc.	San Diego, USA
β-Mercaptoethanol	Sigma Aldrich	Steinheim, Germany
Nuklease free water	Ambion	Austin, USA
Propanol	Merck KGaA	Darmstadt, Germany

Table 2-4 Substances and solutions for *in vitro* toxicity studies

Name	Provider	Registered office
DMSO	Sigma Aldrich	Steinheim, Germany
AmphotericinB	Sigma Aldrich	Steinheim, Germany
Paracetamol	Sigma Aldrich	Steinheim, Germany
Doxorubicin	Fluka/ Sigma Aldrich	Steinheim, Germany
Puromycin	Sigma Aldrich	Steinheim, Germany
Metformin (1,1-Dimethylbiguanid)	Sigma Aldrich	Steinheim, Germany
d-Mannitol	Sigma Aldrich	Steinheim, Germany

2.1.2 Cell lines

The used rat cell line NRK-52E (ATCC Bestellnummer: CRL-1571™) was purchased from ATCC (Manassas, USA).

2.1.3 Consumables

Table 2-5 Consumables

Name	Provider	Registered office
Combitips plus, 2, 2,5, 5, 10 mL Eppendorf	Eppendorf	Hamburg, Germany
PCR reaction tubes 0,2 ml	Eppendorf	Hamburg, Germany
Pipettes, serological, 1, 2, 5, 10, 25, 50 ml	Nunc (Thermo Fisher Scientific)	Langenselbold, Germany
Pipette tips, non-sterile, 100-300 µl	Brand	Wertheim, Germany
Pipettenspitzen, RNase-free, sterile, 10REACH, 20P, 100E, 200, 300, 1000E	MolecularBioProducts	San Diego, USA
Reaction tubes, Safe-Lock Tubes, RNase-free, 1,5 mL und 2 ml	Eppendorf	Hamburg, Germany
Reaction tubes, Falcon tubes, Plastik, 15 ml	Greiner bio-one	Frickenhausen, Germany
Reaction tubes, Falcon tubes, Plastik, 50 mL (steril)	BD Biosciences	Franklin Lakes, USA
Roundbottem plate 96-Well	Bilatec AG	Viernheim, Germany
Thermosprint® PCR-plate, 96-Well	Bilatec AG	Viernheim, Germany
6-Well plate, Multiwell™ 6-Well, sterile	Becton Dickinson Labware	Franklin Lakes, USA
96-Well plate, steril, black with transparent bottem	Becton Dickinson Labware	Franklin Lakes, USA
96-Well plate, transparent, sterile	Becton Dickinson Labware	Franklin Lakes, USA
96-Well plate, sterile, white with transparent bottom	Becton Dickinson Labware	Franklin Lakes, USA
96-Well plate, white, for luminometric assays	Nunc (Thermo Fisher Scientific)	Langenselbold, Germany
Cellculture flask, Cellstar, T25	Greiner bio-one	Frickenhausen, Germany
Cellculture flask, Cellstar, T75	Greiner bio-one	Frickenhausen, Germany
Cellculture flask, Cellstar, T175	Greiner bio-one	Frickenhausen, Germany
Cell scraper, sterile	Corning Inc.	New York, USA

2.2 Instruments

Table 2-6 Instruments

Name	Provider	Registered office
ADIVIA 1650, Autoanalyzer	Siemens Medical Solutions Diagnostics GmbH	Bad Nauheim, Germany
ADVIA 120	Siemens Medical Solutions Diagnostics GmbH	Bad Nauheim, Germany
Agilent Bioanalyzer 2100	Agilent Technologies	Waldbronn, Germany
Agilent Bioanalyzer Priming Station	Agilent Technologies	Waldbronn, Germany
BeadChip® Hyb Cartridge (Hybridisierungskammer)	Illumina Inc.	San Diego, USA
Incubator Hera cell	Heraeus GmbH	Hanau, Germany
CASY TTC Zellzählsystem	Schärfe System GmbH	Reutlingen, Germany
Chemiluminometer Lumistar Galaxy	BMG Lab Technologies	Offenburg, Germany
Clinitek 100	Siemens Medical Solutions Diagnostics GmbH	Bad Nauheim, Germany
Stainless steel balls	Qiagen	Hilden, Germany
Hybridisationoven	Illumina Inc.	San Diego, USA
Little Dipper® Illumina® BeadChips Prozessor	SciGene Corp.	Sunnyvale, USA
Illumina BeadArray Reader	Illumina Inc.	San Diego, USA
Illumina Sentrix® HumanRef-12 V1 BeadChip Arrays	Illumina Inc.	San Diego, USA
Luminex® 200 Total System	Luminex Corp.	Austin, USA
Hybex™ Microarray Incubation System	SciGene	Sunnyvale, USA
Microplatespektrophotometer MWG Discovery HT-R	AVISO	Jena, Germany
Laminar-flow steril bench Herasafe	Heraeus GmbH	Hanau, Germany
Automated Glass Coverslipper Leica CV5030	Leica Microsystems	Wetzlar, Germany
Microscope Axiovert 25	Zeiss	Jena, Germany
Microscope Leica	Leica	Wetzlar, Germany
Microscope Olympus, BX40G	Olympus Optical CO, Ltd	Hamburg, Germany
Microcentrifuge 5415R	Eppendorf	Hamburg, Germany
Mirax Scanner	Carl Zeiss	Jena, Germany
Multifuge® 3S-R	Heraeus (Thermo Fisher Scientific)	Langenselbold, Germany
Multichanelpipette 10-300µl	Eppendorf	Hamburg, Germany
NanoDrop ND-1000	NanoDrop Technologies	Wilmington, USA
NanoDrop ND-2000	NanoDrop Technologies	Wilmington, USA
Pipettes 2-1000µl	Eppendorf	Hamburg, Germany
Pipettes 2-1000µl	Gilson	Middleton, USA
Pipetting controler, Pipetus®-akku	Hirschmann Laborgeräte	Eberstadt, Germany
pH-Meter 766 Calimatic	Knick GmbH & Co. KG	Berlin, Germany

Name	Provider	Registered office
QIAcube	Qiagen	Hilden, Germany
Refractometer	Küss	Hamburg, Germany
Reinstwasseraufbereitungsgerät Pure Lab Plus	ELGA	Celle, Germany
Shaker Titramax® 101	Heidolph Instruments	Schwabach, Germany
Shaker Phero-shaker	BIOTEC-FISCHER GmbH	Reiskirchen, Germany
Spectralphotometer Polarion	Tecan Germany GmbH	Crailsheim, Germany
Steril benchank Hera®safe	Thermo Fisher Scientific (Heraeus)	Waltham, USA
Theonyx Liquid Performer	AVISO	Jena, Germany
Thermomixer comfort	Eppendorf	Hamburg, Germany
Thermocycler, Mastercycler gradient	Eppendorf	Hamburg, Germany
Thermocycler, Primus 96 advanced	PEQLab GmbH	Erlangen, Germany
Tissue Lyzer	Qiagen	Hilden, Germany
Vacuubrand suction pumpe BVC 01	Vacuubrand GmbH & CoKG	Wertheim, Germany
Vacuum conzentrator (Concentrator 5301)	Eppendorf	Hamburg, Germany
Ventana Discovery Immunostainer	Roche diagnostics	Mannheim, Germany
Ventana Discovery E-bar lable printer	Roche diagnostics	Mannheim, Germany
Vortexer for Agilent-Chips	IKA® Werke GmbH	Staufen, Germany
Vortexer Vortex Genie 2	Scientific Industries	Bohemia, USA
Lab balance Navigator	Ohaus	Giessen, Germany
Lab balance Sartorius BP211D	Sartorius	Göttingen, Germany
Waterbath Julabo SW22	Julabo GmbH	Seelbach, Germany

2.3 Software

Table 2-7 Software for data analysis

Name	Provider	Registered office
BeadScan	Illumina Inc.	San Diego, USA
GenomeStudio 1.1.1	Illumina Inc.	San Diego, USA
ChemDraw® Ultra 8.0	Cambridge Soft Corporation	Cambridge, USA
2100 Expert software	Agilent Technologies	Waldbronn, Germany
Expressionist® Analyst Pro Version 5.3.2	Genedata AG	Basel, Schweiz
GraphPad Prism v. 5.02	GraphPad Software	San Diego, USA
GeneGo's MetaCore™ v. 5.3	GeneGo	St. Joseph, USA
Ingenuity´s IPA™ v. 8.6	Ingenuity Systems, Inc.	Redwood City, USA
Microsoft Office 2007 Standardpackage	Microsoft Corps.	Redmond, USA
Microsoft Office 2003 Standardpackage	Microsoft Corps.	Remond, USA
Mirax Viewer Version 1.12.22.0	Zeiss	Jena, Germany
OriginLab v. 7.0	OriginLab	Northampton, USA
Abode Photoshop Elements 8.0	Adobe Systems Inc.	San Jose, USA
Abode Acrobat 9 Standard	Adobe Systems Inc.	San Jose, USA
ToxWiz v. 2.5	Cambridge Cell Networks	Cambridge, UK

2.4 Rat toxicity studies

In the following section the in vivo rat toxicity studies which were investigated will be described in more detail.

2.4.1 28-day rat toxicity studies

The 28-day rat studies were performed in the AAALAC certified Toxicology facility at Merck Serono, Darmstadt, Germany. All studies were applied and performed according Article 8 paragraph 1 of the German Animal Protection Welfare Act (DA4/Genehmigung 204). The treatment of the animals, sample collection and preparation, as well as measurements of all standard parameters, were done under „Good Laboratory Practice“ guidelines. All non standard parameters, like gene expression analysis and the detection of urinary biomarkers, as well as immunohistochemistry were performed according to the Merck internal Quality Management System (MSR-QMS). All animal related activities were carried out by specialized staff, registered at the Darmstadt Regional Council (DA 4/P V 54-19c20/15).

Dose range finding study

Before the final studies were conducted, a dose range finding study was carried out under the same conditions as planned for the main studies. The aim of the dose range finding studies was to detect the optimal doses for gene expression analysis as well as for the detection of urinary protein biomarkers. Therefore, 6 rats (3♂ + 3♀) per group were treated with 4 doses of the 3 model nephrotoxic compounds (based on literature data), with the same treatment pattern as described in the following section ”*Study Design”*. Urine, blood and organ collection were performed after 28 days of treatment. Histopathological observations were carried out routinely for kidney, urethra, bladder and all organs with macroscopic alterations. Significant results of the dose range finding study are reported by Fuchs et al., 2012.

Based on the findings of clinical-chemical parameters, together with the results of the urinary protein biomarker analysis, doses for the main studies were selected (Table 2-9).

All results reported in this document are exclusively based on the main studies which will be described in more detail below.

Main 28 day rat toxicity study

All studies were performed according to Good Laboratory Practice (GLP) and in compliance with the German Law on the Protection of Animals (German Welfare Act, Article 8a). Wistar rats, 10 weeks old, purchased from Charles River Laboratories (Sulzbach, Germany) were randomly divided into groups of 10 animals (5♂ + 5♀). Rats were individually housed in type III isolated ventilated Makrolon® cages with a 12 h light/ dark cycle. Standard laboratory chow (Provimi Kliba 3433.0, Aalen, Germany) and tap water were provided *ad libitum*.

Study Design

Based on the data from the dose range finding study the doses for the main studies were chosen. Rats were treated with either Vamcomycin (Ratiopharm, Ulm, Germany) at dose levels of 50 mg/kg bw or 300 mg/kg bw; or cis-

diamindichloridplatinum(II) (Cisplatin) (medac GmbH, Hamburg, Germany) at 0.3 mg/kg bw or 0.6 mg/kg bw; or Puromycin (Invivogen, Tolouse, France) at 10 mg/kg bw or 30 mg/kg bw. To reduce the total number of animals only 2 dose groups (low dose (LD) and high dose (HD)) were used. Table 2-9 gives an overview of the used doses and abbreviations used.

In the Vancomycin study the high dose were chosen to show massive changes in renal tissue the low dose was expected to show none to minimal changes in histopathology and traditional parameters. The dosing within the Cisplatin study was chosen to induce only mild alterations in high dose animals and no changes in traditional toxicological methods in the low dose group. Within the Puromycin study moderate to massive changes were expected after high dose treatment, while the low dose should show only minimal effects.

Four time points and the intervals of treatment were chosen, as well as a general overview of the study design, including the observed parameters for the single studies as shown in Figure 2-1. 10 Rats (5♂ + 5♀) per dose group and time point were treated with Vancomycin or Cisplatin i.p. daily for 7 days and then only once per week. Puromycin animals were treated i.p. daily for 14 days and then twice per week.

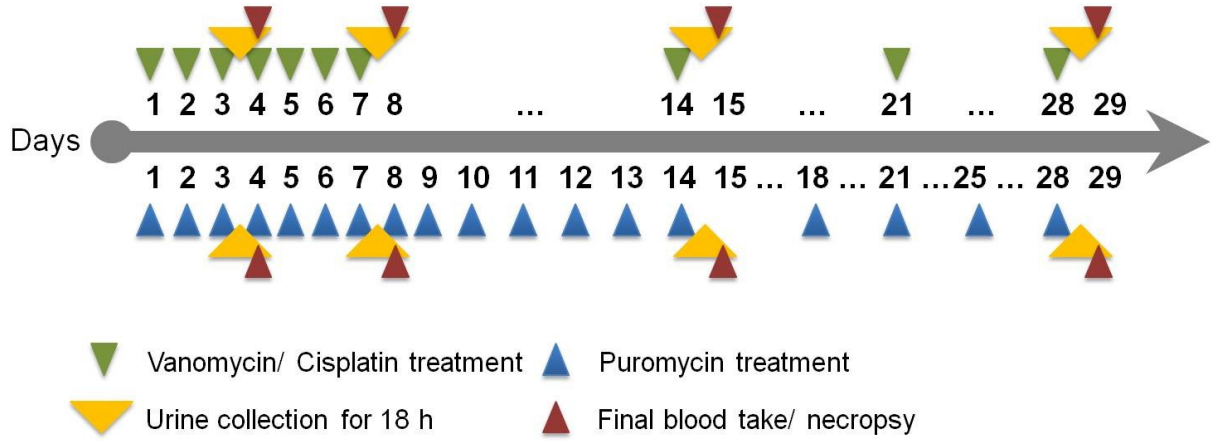

Figure 2-1 Schema of treatment and sample collection of all three main studies. Animals were treated daily for one week and then once per week up to 28 days (Vancomycin, Cisplatin) or daily for 14 days and the twice per week (Puromycin). Sample collection was performed on days 4, 8, 15 and 29.

These treatment patterns allowed us to analyze acute changes caused by daily dosing and at the same time to study recovery periods which can still lead to significant injury after 28 days.

In all studies urine was collected under cooled conditions on days 3/4, 7/8, 14/15 and 28/29 for analysis of standard clinical-chemical parameters and novel urinary protein biomarkers. Therefore, animals were housed in individual metabolism cages for 18h (fasted with free access to water) and urine was collected under cooled conditions. For standard clinical chemical analysis the urine was used immediately. For the detection of urinary protein biomarkers urine was stored at -80°C until required. Subsequent to the urine collection a final blood take, by punctuation of the sublingual vein under light isofluorane anesthesia, was made. Animals were sacrificed by CO_2 asphyxiation and organs were collected for histopathological examination. All organs were fixed in formalin. Tissues for histopathological observations (kidney, ureter, bladder, and all organs with abnormal observations in gross pathology) were embedded in paraffin. Beside organ collection for standard histopathology, renal tissue was collected for gene expression analysis. For this the upper half of the left kidney was dissected and snap-frozen in liquid nitrogen and then stored at -80°C.

An overview of the performed analysis for each individual study is given in Table 2-8.

Table 2-8 Overview of analysis performed for each individual study. In addition to the displayed analysis, histopathological, clinical chemical and hematological analyses were performed for each study.

Vancomycin
● Luminex® xMAP® (urinary protein biomarker)
● RENA-strip™ Dipstick Assay (urinary Kim-1)
● Immunohistochemistry (Kim-1, Clusterin, Osteopontin)
● Illumina Whole genome analysis

Cisplatin
● Luminex® xMAP® (urinary protein biomarker)
● RENA-strip™ Dipstick Assay (urinary Kim-1)

Puromycin
● Luminex® xMAP® (urinary protein biomarker)
● RENA-strip™ Dipstick Assay (urinary Kim-1)
● Immunohistochemistry (Kim-1, Clusterin, Osteopontin)

Substance application

The used compounds in these studies are well described nephrototoxins, so called model compounds (see 1.3.1 Nephrotoxins used in this study). Because stability information was available for these commercially available substances the Central Dispensory (ZDP) of the Non-Clinical Safety Department, Merck Serono, Darmstadt prepared the solutions daily under room temperature and minimal light exposure. The used dilutions of Vancomycin were prepared with water for injection (wfi), for Cisplatin and Puromycin 0.9% saline was used.

Animals of the control groups were treated with either 0.9% saline or wfi in the highest volume of the substance treated animals.

Table 2-9. Used dose levels for the intraperitoneal treatment of the rats in all three studies. The dose levels were evaluated by the results of a dose range finding study.

Nephrotoxine	low dose	high dose	Route of application	Vehicel
Cisplatin	0.3 mg/kg bw	0.6 mg/kg bw	i.p.*	0.9% saline
Puromycin	10 mg/kg bw	20/30 mg/kg bw[#]	i.p.*	0.9% saline
Vancomycin	50 mg/kg bw	300 mg/kg bw	i.p.*	wfi**

* i.p.: intraperitoneal; ** wfi: water for injection; [#] treatment with 30mg/kg daily on days 1-14, then twice per week with 20 mg/kg.

Sample collection and necropsy

As the major focus for these studies, the kidneys were collected first to avoid RNA degradation caused by autolysis. Therefore, the peri-renal capsule was removed and the upper half of the left kidney was snap-froozen in liquid nitrogen. Terminal body weights, as well as kidney and liver weights, were recorded. Only kidney, ureter, bladder, liver and organs showing macroscopic alterations were investigated histopathologically. Special attention was paid to not exceed the fixation time of the kidney over 48 hours, because of the need to use these tissues for future immunohistochemical analysis.

2.4.2 Additional rat in vivo studies investigated

Innomed/ PredTox

Within the 6th Framework program the Innomed/PredTox project undertook several studies to identify and evaluate novel biomarkers and technologies to enhance the diagnosis of nephrotoxicity. Within this project the failed drug candidate 3-pyrrolidineacetic acid, 5-[[[4_-[imino[(methoxycarbonyl) amino]methyl] [1,1_-biphenyl]-4-yl]oxy]methyl]-2-oxo-, methyl ester,(3S-trans) (FP007SE/ BI-3) was used to study nephrotoxicity. Several omics-data [Matheis et al. 2011], as well as traditional clinical and histopathological observations are already published. Renal tissue of this project was used to investigate 6 transcripts provided by Compugen Ltd. for their ability to predict developing acute kidney injury.

University of Wuerzburg

At the University of Wuerzburg, several studies were performed which focused on renal damage. Two of these studies were used to evaluate the transcriptional biomarkers from Compugen Ltd. to test their diagnostic performance.

Gentamycin

The first study used Gentamycin as one of the most common model compounds for the induction of renal tubular damage. Data from clinical pathology and histopathology, as well as urinary protein biomarker excretion, are already publically available [Hoffmann et al., 2011]. Rats were treated daily with Gentamycin (i.p.) for up to 7 days. Urine was collected on days 1, 3, and 7 with a final necropsy on day 8. Kidneys were histopathologically analysed and a part was snap-frozen in liquid nitrogen for gene expression analysis.

Aristolochic acid

Study Design.

In this study the doses were chosen based on publically available data which show, that ≥5 mg/kg aristolochic acid cause massive tubular degeneration and necrosis after 28 day treatment. The used study had a run-time of 12 days using the same concentrations like reported by Mengs and Stotzem, 1993 [Mengs et al., 1993]. This approach was chosen to get no to minimal renal changes in histopathological observations. With novel methods like, the measurement of urinary protein biomarkers and transcriptional analysis it was tested if it is possible to predict nephrotoxicity before histopathological alterations manifest on morphological level.

In this study Male Wistar rats, 6–8 weeks old, weighing approximately 200 g were purchased from Harlan-Winkelmann (Borchen, Germany) and were randomly divided into three groups of five animals. Animals were kept in macrolon® cages (five animals per cage) on a 12 h light/dark cycle and allowed free access to standard laboratory chow (SSniff, Soest, Germany) and tap water. Rats were treated with AA (27 % AAII and 65 % AAI; Sigma, Taufkirchen, Germany) at dose levels of 0.1, 1 and 10 mg/kg bw per day. AA was administered by gavage, five days per week over two weeks. Control animals received an equal volume of tap water. The animals were housed in individual metabolic cages during the study. Urine was collected at 24 h and on days 5 and 12. Blood samples were taken from the retro-orbital plexus under light isoflourane anaesthesia on days 1 and 5 for clinical chemistry. The animals were sacrificed by CO_2 asphyxiation and blood was collected by cardiac puncture 24 h after administration of the final dose.

Blood samples and aliquots of urine were immediately used for routine clinical chemistry analyses. The remaining urine and plasma was stored at -20°C until further analysis. Organs (liver, kidney and bladder) were removed and weighed. The left kidney was partitioned transversely in a ratio of approximately 2:1; the larger part was stored in formalin. The remainder and the right kidney were snap frozen in liquid nitrogen and stored at −80 °C. The liver and bladder were stored in formalin.

Urine and plasma analyses were carried out at the Laboratory for Clinical Chemistry, University of Wuerzburg, on a Vitros 700XR (Ortho-Clinical Diagnostics, Neckarsgemuend, Germany) using standard protocols for the determination of these parameters according to the manufacturer's instructions. The following parameters were determined in urine: glucose, GGT (γ-glutamyl transferase), total protein, creatinine and osmolality. For blood samples the following parameters were determined in plasma: creatinine, urea, total bilirubin, aspartate aminotransferase, alanine amino transferase, GGT, alkaline phosphatase and total protein.

2.5 Histopathology

Preparation of paraffin tissue section for Hematoxilin/ Eosin (HE) staining

The preparation of the tissue sections was performed by experienced personnel to guarantee the high quality of the sections. The procedures were performed according standard operation protocols (SOPs). The organs were embedded in paraffin and sections for standard Hematoxilin/ Eosin (HE) staining were prepared. The intersection plane of the organs is shown in Table 2-10. The thickness of the slices was approximalty 2µm.

Table 2-10 An overview of organs and the intersection plane routinely assessed within the Vancomycin, Cisplatin and Puromycin nephrotoxicity studies.

Organ and tissue	Intersection plane
Kidney	transversal in the hilus region, longitudinal
Bladder	Longitudinal
Ureter	Transversal
Liver	transversal, (1x Lobus sinister lateralis, 1x Lobus dexter medialis)
Organs with macroscopic alterations	representative areale

Hematoxilin/ Eosin (HE) staining

The HE staining was performed in an automated way using the Leica AutoStainer XL in combination with coverslipautomat CV5030. Before staining the slides were deparaffinized by using xylol. The slides were then rehydrated with decreasing alcohol concentrations and water. After the staining with hemalaun, the slides again had to be dehydrated with xylol with additional alcohol incubations in between to cover the slides with entellan, a xylol containing mounting medium. A detailed overview is given in Table 2-11.

Table 2-11 Individual steps which were performed for Hematoxilin/ Eosin staining of tissue slides. The whole procedure was performed in an automated manner.

Step	Reagents/ Dye	Time
1	Xylol	2 min.
2	Xylol	2 min.
3	Iso-Propanol	3 min.
4	Ethanol 96%	3 min.
5	Ethanol 80%	3 min.
6	Ethanol 70%	3 min.
7	VE-H_2O	3 min.
8	Hämalaun	4 min.
Wash	tap-H_2O	2 min.
Wash	tap-H_2O	2 min.

Step	Reagents/ Dye	Time
Wash	tap-H_2O	2 min.
12	Eosin	1 min.
13	Ethanol 96%	10 sec.
14	Ethanol 96%	10 sec.
15	Iso-Propanol	1 min.
16	Iso-Propanol	1 min.
17	Iso-Propanol/Xylol	2 min.
18	Xylol	2 min.

The analysis of the HE stained tissue slides were performed by Dr. Stefanie Czasch, pathologist at Global Non-Clinical Safety at Merck Serono, Darmstadt.

In addition the kidney samples were reviewed by Dr. Jürgen Hellmann, Dr. Anja Knippel and Dr. Gundi Müller, pathologists at Global Non-Clinical Safety at Merck Serono, Darmstadt.

2.6 Immunohistochemistry

Because the tissue was fixed in formalin and embedded in paraffin, the slides had to be prepared in a multi-step procedure, which can vary depending on the protein biomarker studied. In a first step the epitopes must be made available for antibody binding, including deparaffinization and demasking. Additional steps can be required to block or quench endogenous enzymes or biotin prior to antibody staining in order to prevent unspecific binding. In this study an indirect method, including streptavidin and biotin labeling, was used for the detection of renal Kim-1, Clusterin and Osteopontin. Figure 2-2 gives an overview of the general principal of the method.

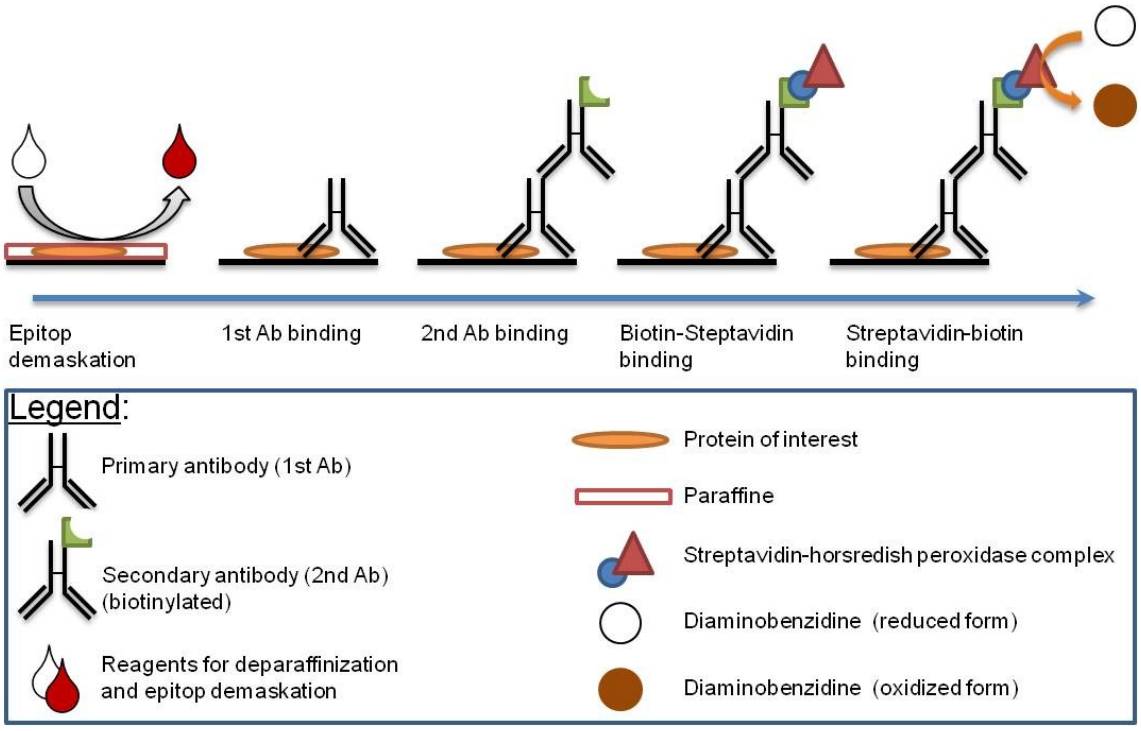

Figure 2-2 Schematic workflow of an immunohistochemical protein staining. In a first step, the protein was demasked and deparaffinized. The slide was incubated with the first antibody (1st Ab) addressed against the protein of interest, and the biotinylated second antibody (2nd Ab), against the 1st Ab. The staining reaction was catalyzed by a streptavidin linked horseradish peroxidase, by oxidization of Diaminobenzidine.

After preparing the renal tissue sections, the slides were incubated with an unlabeled primary antibody specific for the target protein. In a second step a secondary antibody against the primary antibody was used. This secondary antibody has to be raised against the animal species in which the primary antibody was raised. Additionally, it must be biotinylated for the subsequent labeling and staining reaction. A detailed list of used antibodies and the performed steps is given in Table 2-12 and Table 2-13.

The tissue then was incubated with a streptavidin/ horseradish peroxidase-complex which has a high affinity to biotin and specifically binds to the biotinylated secondary antibody. Horseradish peroxidase (HRP) is the catalyzing enzyme used to start the staining reaction initiated by the addition of the substrate diaminobenzidine (DAB). The transparent dye, DAB, reacts with H_2O_2 catalyzed by the HRP leading to a turnover of the transparent form into an insoluble brown complex which precipitates in the area of high protein abundance. Finally, a counter staining was performed using hematoxilin and bluing reagents, each in order to show unspecific binding of the antibody's backbone. As quality controls the immunohistochemical staining procedure was accompanied by an isotype as well as non 1st Ab controls in order to show unspecific binding of the antibody's backbone.

Table 2-12 Overview of the used primary and secondary antibodies for immunohistochemical analysis of Kim-1, Clusterin and Osteopontin. In addition the used isotype antibodies are shown, used in the same final concentration as the primary antibodies.

Antibodies	Cell Conditioning	Dilution	Incubation Time	Host	Provider
primary antibodies					
Kim-1	/	1:100	1h	Goat	R&D Systems
Clusterin	CC1	1:100	1h	Goat	Santa Cruz Biotechnology
Osteopontin	CC1	1:100	1h	Rabbit	Rockland Inc.
secondary antibodies					
Anti-goat		1:200	1h	Donkey	Santa Cruz Biotechnology
Anti-rabbit		1:200	1h	Goat	Rockland Inc.
isotype antibodies					
normal goat IgG			1h	Goat	R&D Systems
normal rabbit IgG			1h	Rabbit	Santa Cruz Biotechnology

All immunohistochemical stainings were performed using the automated Ventana Discovery immunostainer in combination with the DAB-Map® detection Kit. The immunohistostainer follows individual staining protocols identified by a barcode on each slide. All steps of immunohistochemistry were performed automatically, except for the application of primary and secondary antibodies. An overview of the single steps performed is given in Table 2-13.

Table 2-13 The individual steps which were performed for immunohistochemical staining of Kim-1, Clusterin and Osteopontin on renal tissue slides. The whole procedure was performed in an automated manner.

Step	Reagents/ Dye	Time
1	Deparaffinization	8 min.
2	cell conditioning	20 min.
3	Application of inhibitor D	4 min.
4	Titration of 1st Ab	60 min.
5	Titration of 2nd Ab	20 min.
6	Application of Blocker D	2 min.
7	Application of SA-HRP D	16 min.
8	Application of DAB and H_2O_2	8 min.
9	Application of Copper D	4 min.
10	counterstaining (Hematoxilin)	6 min.
11	Application of bluing reagents	6 min.

2.7 Cell Biological Methods

2.7.1 Culture of the permanent cell line NRK-52E

The NRK-52E cells were cultured at 37°C and 5 % CO_2 in DMEM high glucose medium (4.5 mg/mL glucose). As supplements 10% FCS, 1% NEAA and 1% Pen/Strep were added. The cells were maintained in cell culture flasks until 80-100 % confluence. Subsequently, the cells were passaged or used for individual experiments. For passaging the cell layer was washed with 10 mL PBS without Mg/Ca and then incubated with Trypsin-EDTA solution (0.5% trypsin) for 10 seconds. The Trypsin-EDTA was removed and the cells were incubated at 37°C and 5% CO until the cells detached from the cell culture flask. The cell suspension was taken up in pre-warmed cell culture medium and the cell number was determined by using the Casy® Cellcounter by diluting the cell suspension 1:500 in CasyTon™. The appropriate number of cells was diluted in medium and plated in multi-well plates for the experiments. For routine cultivation the cell suspension was split at ratios between 1:20 up to 1:100, depending on the cell density and the experimental needs. Detailed information about the used cell numbers and volumes are given in Table 2-14.

Table 2-14 Overview of cell number, volume of medium and trypsin used for maintenance and treatment of different applications of NRK-52E cells.

Culture vessel	Area of growth	Cell number [cell/ mL]	Volume	Volume of Trypsin	Application
T175 Flask	175 cm²	-	20 mL	2 mL	Routine culture
T75 Flask	75 cm^2	-	10 mL	1 mL	Routine culture
96-Well	0,32 cm²	$4x10^5$	0.1 mL	-	Cell viability assays
6-Well	9,5 cm²	$2x10^6$	1.5 mL	-	Gene expressions analysis

2.7.2 Cell treatment

To evaluate and characterize the response of the NRK-52E cells to different drugs, cytotoxicity / cell viability assays were performed. The cells were cultured in 96-well plates and treated with a minimum of 5 concentrations of each compound. Intracellular ATP content, as well as the neutral red uptake (NRU), was evaluated. The cells were cultured in cell culture flasks as described under “Culture of the permanent cell line NRK-52E“. Before each experiment, cells were seeded in the appropriate cell culture plate at the density needed and cultured for a minimum of 24 h at 37°C and 5 % CO_2.

The compounds used for the experiments with NRK-52E cells were dissolved in DMSO or PBS and used at a final dilution of 1:200 in cell culture medium. This results in a final DMSO concentration of 0.5 % (v/v). The treatment of the cells was conducted every 24 h. All experiments were performed independently three times by use of different cell passages, and the cells were not used for longer than 18 passages from time of thawing.

The results of the cytotoxicity tests were then used for choosing the final concentrations for gene expression analysis. This was conducted by logistic fitting of the dose response curves derived from the data from 72 h treatment. The TC_{20} value is the concentration at which the viability of the cells was reduced by 20%. This concentration was defined as the high dose, while the low dose was chosen as the "non observed adverse effect concentration (NOAEC)" based on the dose response curve. For the gene expression experiments the compounds were diluted 1000-fold in cell culture medium to avoid any influence by DMSO. The final resulting DMSO concentration was therefore 0.1 % (v/v).

2.7.3 Cytotoxicity assays

Detection of ATP depletion

The determination of intracellular ATP concentration, as a measure of a cells reduced metabolic activity, was used. Therefore, the *CellTiter-Glo®* assay by Promega was used [CellTiter-Glo®-Bulletin, 2011]. The principal of the detection of intracellular ATP content reside in the universal functions of ATP as one of the most important energy stores. ATP is produced, inter alia, within the cells in the mitochondria and cannot leave the healthy cell because of the intact membrane integrity. Additionally, ATP is only synthesized by healthy and living cells. If cell damage takes place, for example caused by a toxic insult, the membrane integrity gets lost and the already produced ATP is released. Subsequently, no further ATP production is performed leading to a total or a reduction in intracellular ATP content.

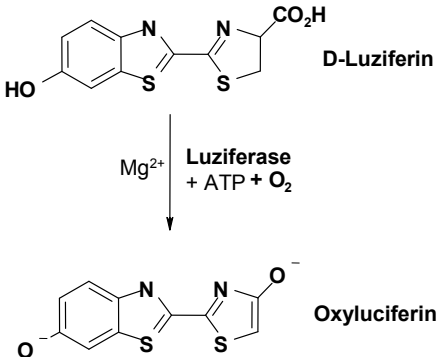

Figure 2-3 Reaction used to determine the intracellular ATP content by using the CellTiter-Glo® assay. The reaction of D-Luciferin catalyzed by air-oxygen, Mg^{2+}, Luciferase and the intracellular ATP. The whole reaction results in a luminescence light signal which can be measured.

In addition, an impact of the test compound directly on the mitochondria can lead to a reduction in ATP synthesis by influencing the oxidative chain reaction at the mitochondria membrane, which also leads to a reduced intracellular ATP level.

The detection process is based on the conversion of D-Luciferin to Oxyluciferien. This reaction is catalyzed by Luciferase and involves air-oxygen, magnesium cations and ATP (Figure 2-3). The source of ATP, in this case, is the intracellular ATP, which is therefore the limiting factor for the reaction. By cell lyses, the ATP content is released under controlled conditions. This can be used directly to correlate the emitted bioluminescence light signal to the impact of drug treatment on ATP and as a signal of cell death [Crouch, 1993].

For the procedure, cells were seeded in a white 96-well plate. The lyophilized CellTiter-Glo® substrate was reconstituted in 10 mL CellTiter-Glo® buffer and then mixed 1:2 with cell culture medium. Here, the basal medium, without supplements, was used. The supernatant was aspirated and 100 µl of the CellTiter-Glo® reagent/ cell culture mix was added into each well. The cells were incubated for approximately 10 min under light rotation (300 rpm) at RT until the cells were completely lyzed. Immediately, the plate was measured using a luminometer [CellTiter-Glo®-Bulletin, 2011]. Each data point was evaluated in triplicate, including blank (well without cells) and the vehicle control (cells treated with DMSO/ PBS).

The resulting data were analyzed by calculation of the arithmetic mean over all triplicates and the subtraction of the blank value. Afterwards, the mean values of the treatments were related to the corresponding vehicle control to generate

relative values which were used as the cell viability. For determination of the TC_{20} and NOAEC level the mean of the three biological replicates was used.

Neutral red uptake

The neutral red uptake assay (NRU) provides a quantitative estimation of viable cells within a cell culture. The NRU method itself was originally developed by Borenfreund and Puerner (1985) [Borenfreund et al., 1985]. It is based on the property of living cells to take up the weakly cationic dye by penetration through cell membranes of viable cells by non-ionic diffusion and accumulation. The supravital neutral red dye then binds to the anionic surface of the lysosomal matrix by electrostatic hydrophobic bonds [Winckler et al., 1974; Nemes et al., 1979]. If cellular membrane integrity is lost, the dye also can enter the cell debris.

The neutral red stock (4 mg/mL) was diluted 1:80 with cell culture medium to achieve a final concentration of 50 µg/mL. The diluted dye was centrifuged for 10 min at 100 x g to remove crystallized precipitates. Cells were seeded in black 96-well plates and treated as described in “Culture of the permanent cell line NRK-52E“ and "Cell treatment“. After the appropriate time of treatment, the supernatant was replaced with 200 µl of neutral red/ medium mixture. The cell culture was incubated for 3 h at 37°C and 5 % CO_2. Subsequently, the supernatant was aspirated and the cells were carefully washed with pre-warmed PBS. After the soluble (extra cellular) neutral red dye was removed, the viable cells were lyzed and the intracellular neutral red dye was solubilized. 300 µl Of 1 % acetic acid in 50 % Ethanol were pipette in each well and placed on a shaker (300 rpm) at RT for 10 min, or until the neutral red dye formed a homogeneous solution. The absorbance of neutral red was read at a wavelength of 540 nm using a photospectrometer. As described for ATP-depletion, each data point was evaluated in triplicate, including blank (well without cells) and the vehicle control (cells treated with DMSO/ PBS).

It has been shown that quantified neutral red is linearly related with cell number [Borenfreund et al., 1985], therefore the determined absorbance was directly used to calculate the relative viability based on the corresponding vehicle control. The resulting data were analyzed by calculation of the arithmetic mean over all triplicates and the subtraction of the blank value. Afterwards, the mean value of the treatments was related to the corresponding vehicle control to generate relative values, as a measure of cell viability.

2.8 Biochemical Tests

2.8.1 Urinary Protein biomarkers

2.8.1.1 Luminex® xMAP® Technology

The Luminex® xMAP® technology is a novel method for the multiplexed detection of analytes, e.g. proteins, in a single sample. It is based on two well established methods, a classical sandwich-ELISA and flow-cytometry. The assay itself is performed in a 96-well microtiter plate which allows a higher throughput of samples and easy handling. The samples, including the proteins of interest, in this case Kim-1, Timp-1, VEGF, α-GST, CystatinC, Clusterin, Osteopontin, Lipocalin-2/ NGAL, β2-microglobulin and Calbindin, were mixed with different types of special beads. Each bead type has an individual color ID which is characterized by their specific mixture of a red and an infrared dye (Figure 2-4A). On the surface of each individual bead type, antibodies are coated against one of the protein to be detected (Figure 2-4B). In the case of the used WideScreen® assays polyclonal antibodies against the specific urinary proteins are spotted on the beads. Immediately after a first incubation step, in which the analytes were captured by their antibodies on the different beads, a secondary, polyclonal antibody against the 1st Ab was added.

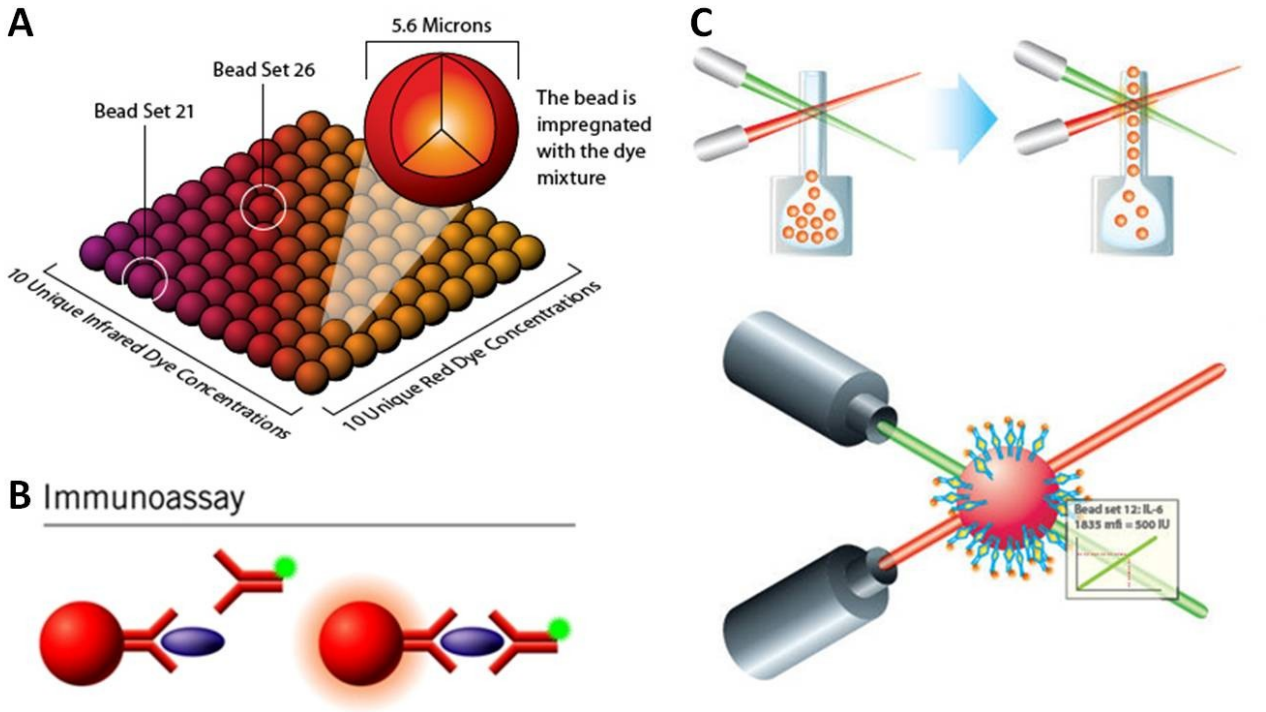

Figure 2-4 (A) the building up of up to hundred beads filled with different concentrations of two different dyes (red and infrared). (B) On each individual bead type, characterized by their specific mixture of dyes, an antibody against the analytes of interest is coated which then can be detected by a soluble secondary antibody conjugated to a fluorophore. (C) The principal of detection is based on the amount of sample, including the analytes of interest and leading the fluid through two lasers (red and green). The red laser identifies the bead type and therefore the identity of the analytes, the green laser quantifies the secondary antibody coupled light signal [modified by Virocore, 2012 and teomed, 2012]

The secondary antibody is biotinylated, ensuring a signal amplification of the Streptavidin-Pyroerytrin-complex (SA-PE) needed for the fluorescence detection. The multiplexed quantification is performed by two laser-systems. A green laser detects the Pyroerytrin (PE)-conjugate. The fluorescence intensity is proportional to bound protein. This can be used to quantify the total amount of protein via a standard curve. A second laser detects the red fluorescence signal to identify the bead type and therefore the quantified analytes (Figure 2-4C). From this multiple proteins can be detected in parallel in one sample in a more sensitive and sample saving way.

For a detailed description of the whole procedure see [Hoffmann et al., 2011]. For specific information on used urine dilution factors, urine and buffer volumes refer to Table 2-15.

The settings for the measurement are as follows:

Volume per measurement: 50µL

Bead count per measurement: 100

Timeout: 60 seconds

DDGate: 7500 - 15500

Table 2-15 The used dilution factors, and volumes for the WideScreen® Rat Kidney toxicity panel 1 and panel 2.

	WideScreen® Rat Kidney Toxicity Assay			
	Panel 1		**Panel 2**	
	Dilution	**Volume** [Urine : Buffer]	**Dilution**	**Volume** [Urine : Buffer]
Standard	1:2	40µL : 40µL	1:50	2 µL : 98 µL
Slight increase	1:10	8µL : 72µL	1:1000	1µL (1:10): 99µL
Strong increase	1:100	1µL : 99µL	>1:10000	case-by case

2.8.1.2 Kim-1 detection via the RENA®-strip Dipstick Assay

The RENA-strip dipstick assay, purchased from BioAssay Works, is based on thin layer chromatography. This so called lateral flow assay enables the detection of urinary Kim-1 by the lateral flow of diluted urine samples in combination with colloidal gold-conjugated antibodies specific for rat Kim-1. The urine sample comes in contact with two test bands driven by capillary force. The first is the test band with the specific antibodies against Kim-1. The second band is a control band, containing IgG specific conjugated antibodies, to ensure the right function of the test system. By passing a field containing soluble conjugated antibodies a complex of the immobilized anti-Kim-1 antibodies, Kim-1 itself and the soluble detection antibodies is formed leading to the appearance of a red band urinary Kim-1 is present. The test principal is shown in Figure 2-5.

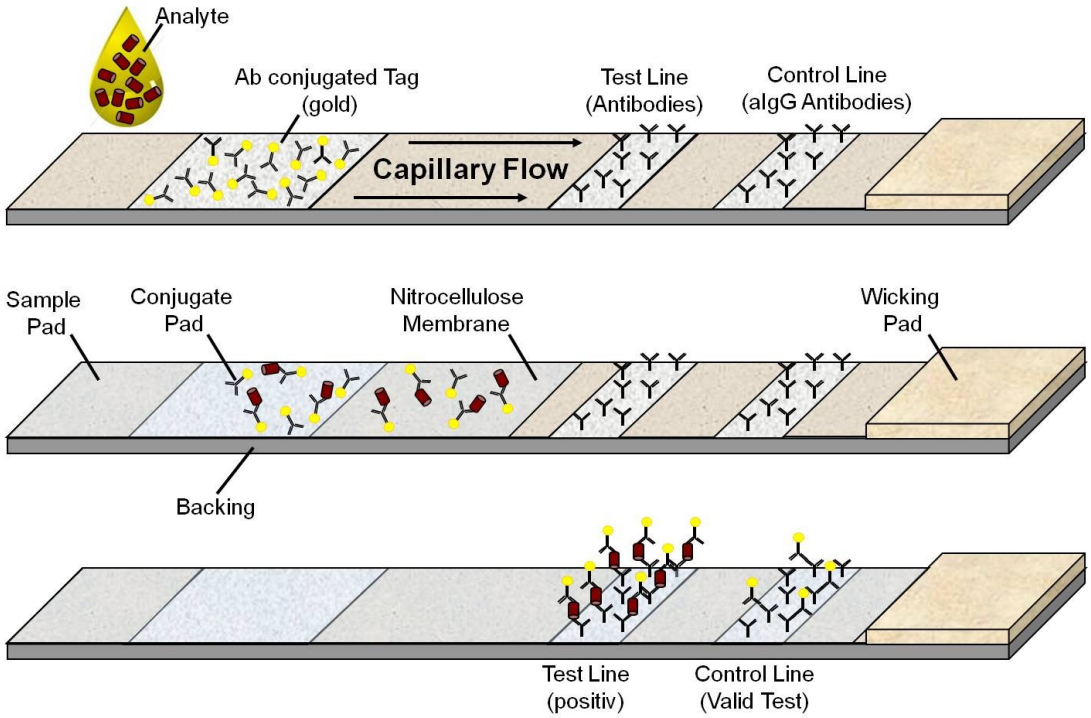

Figure 2-5 The principal of the lateral-flow technology, where the RENA-strip® dipstick assay is based on. The urine containing the analyte is moved by the capillary flow over an area containing gold-conjugated antibodies against rat Kim-1. In the following the test line with immobilized antibodies against Kim-1 is passed. Finally, the control with anti IgG antibodies is used as quality control. [modified by Cytodiagnostic, 2012]

The band can be analyzed semiquantitatively or quantitatively using a lateral-flow reader. The urine samples were diluted 1:2 in borat test tubes before they were exposed to the test-strips. The test-strips were incubated for 15 min at RT before measurement with the lateral flow reader purchased from BioAssay Works. The Sandwich Assay protocol was used, by which the intensity of the test band with the control band was evaluated. The resulting value was multiplied with the lot-specific multiplication factor to get the Kim-1 concentration in nanogram per milliliter.

2.8.2 Hematological parameters

Within the department of clinical pathology of Merck Serono, Non-Clinical Development a hemogram was prepared for each individual animal, using standard operation protocols. The measurements were conducted by qualified employees of Merck Serono, following “good laboratory practice” (GLP).

2.8.3 Clinical-chemsitry Parameters

Within the department of clinical pathology of Merck Serono, Non-Clinical Development standard clinical-chemical parameters in serum and urine were measured for each individual animal, using standard operation protocols. The measurements were conducted by qualified employees of Merck Serono, following “good laboratory practice” (GLP).

2.9 Molecular biological Methods

In the following section, the procedure of gene expression analysis, including RNA purification (see 2.9.1 RNA Isolation from renal tissue and cell lines), sample processing (see *cRNA-Synthesis*), and the hybridization (see 2.9.3.2 Sample hybridization) will be described in more detail. Figure 2-6 gives an overview of the general workflow necessary for the evaluation of global gene expression profiling using the Illumina bead arrays.

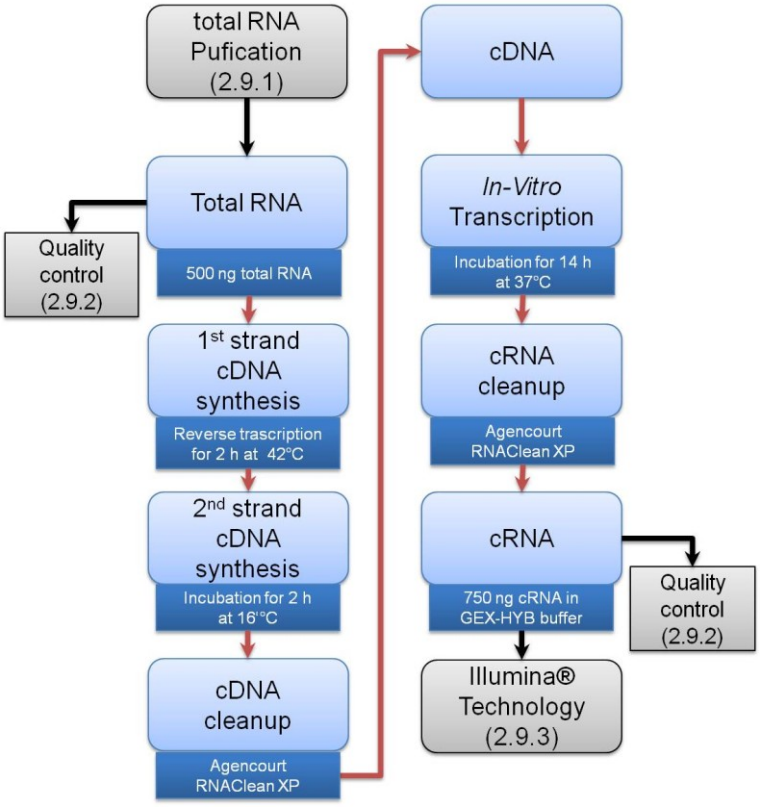

Figure 2-6 General workflow of the whole procedure of gene expression profiling by using the Illumina Sentrix bead array. In a first step, the total RNA was isolated from the biological sample e.g. tissue or cells. Then the quantity and quality of the isolated total RNA was conducted. If the RNA quality showed a RIN of >7 the concentration of total RNA was set to 500 ng in 11µl nuclease free water. Subsequently, the first and second strand cDNA synthesis was performed in two separated cycles over 2 hours, the first at 42°C and the second at 16°C. The synthesized cDNA was cleaned up by Agencourt beads and directly used for the in vitro transcription (IVT) at 37°C for 14 hours. After the cRNA was synthesized an additional clean up using Agencourt beads was performed in a similar way. The purified cRNA was quantified and the quality was evaluated before 750 ng cRNA were hybridized on the Illumina RatRef12 v.1 Chips for 20 hours at 58°C. The Chips were then washed in an automated manner on the Little Dipper platform.

2.9.1 RNA Isolation from renal tissue and cell lines

The isolation procedure was performed on the QiaCube® system in an automated manner. The protocols used were identical to the procedure described in the manual [RNeasy Plus Mini, 2010]. The isolation is based on silica columns plus the elimination of genomic DNA by the gDNA eliminator column, both included in the *RNeasy Plus Mini* Kit. In the following the procedure for renal tissue and cell lines will be described in more detail.

Renal Tissue

The upper part of the left kidney was used for RNA analysis (Sample collection and necropsy). For RNA isolation it must be avoided to thaw the frozen kidney tissue because of a loss of RNA quality due to RNA degradation. Therefore, the tubes were transferred in liquid nitrogen. Pieces of kidney tissue of ~30 mg were transferred into a 2 mL reaction tube and 350 µL RLT buffer (containing 1‰ (v/v) β-Mercaptoethanol) were added. A 5 mm diameter RNase-free, stainless steel ball was put into the reaction tube, placed into the TissueLyser® and processed at 30Hz for 2 min to lyse and homogenize the tissue sample. The lysate was used as starting material for the RNA isolation.

Permanent Cell lines

The cell culture medium was removed and the cell layer was washed two times with 1mL pre-warmed PBS (with Mg^{2+}/Ca^{2+}) per well. Immediately after the final washing step 350 µL RLT buffer (containing 1‰ (v/v) β-Mercaptoethanol) were added and the cells collected using a "rubber policeman". Subsequently, the cell lysate was transferred to a shredder column and centrifuged for 3 min at full speed to homogenize the lysate. The lysate was then used as starting material for the RNA isolation.

General procedure of the RNeasy mini Plus Kit

The whole lysate was transferred onto a gDNA eliminator column to remove genomic DNA. The flow-through was collected and 350 µL 70% ethanol added. The whole sample was transferred onto a spin column and centrifuged at 10,000 rpm for 30 sec. The captured total RNA was washed once by adding 350 µl RW1 buffer and twice with 500µL RPE buffer, with centrifugation steps in between. After the second washing step using RPE buffer, the spin column was centrifuged at full speed for two minutes to dry the silica membrane. The RNA was eluted by adding 40µL RNase-free water and analyzed via NanoDrop™ (*Determination of RNA concentration via NanoDrop™* ***System***) and Bioanalyzer (*Determination of quality via the Agilent Bioanalyzer*). For storage the RNA samples were kept at -80°C.

2.9.2 RNA-Analysis

Determination of RNA concentration via NanoDrop™ System

For the quantification of total RNA or cRNA the NanoDrop™ spectrophotometer was used. For this cuvette-free measurement 1 µL sample was pipetted on the sample tablet, which includes a fiber optic. By closing the machine the fiber optic makes contact with the liquid surface by which it is opened between the upper and lower part of the sample drop. A xenon flashlight penetrates the sample and is detected by a silicium CCD chip. The result is a UV-Vis spectrum in the wavelength from 200-750 nm. For the calculation of the concentration the absorption at 260 nm was used. An OD = 1 corresponds to a RNA amount of 33 µg/mL. The ratio of absorption at A260 nm/ A280 nm was used as quality control. This parameter reveals information about impurities with proteins or aromatic hydrocarbons, like phenol which has its maximum absorption at 280 nm. In clean RNA samples the ration should be about 1.8 and 2.0 [Thermo Scientific, 2008].

Determination of quality via the Agilent Bioanalyzer

After the quantification of the total RNA and cRNA samples (Determination of RNA concentration via NanoDrop™ ***System***) the quality of the RNA was determined. It was important to determine the suitability of the samples for further cRNA synthesis (see Determination of quality via the Agilent Bioanalyzer) or the hybridization step (see Illumina® Technology). Therefore, the Lab-on-a-Chip-Technology from Agilent Technologies was used. The Agilent Bioanalyzer uses a special chip system based on electrophoretic measurements. The measuring principle is based on a microfluidic technique, which leads to the measurement of RNAs and RNA fragments, by the management of small amounts of liquid in a miniaturized channel system (Figure 2-7).

For example, the building of the Aglient RNA 6000 Nano chip, used for both species of RNA mentioned above, includes a system of small, closed channels and wells, which are etched into a plastic microchip. Under pressure or elctrocinetic forces the samples transverse the channels in a controlled way. In separation channels, the single compounds of the sample were separated for detection. The detection of individual RNA fragments is performed by a fluorescence dye which is added together with the gel matrix into each individual well [Agilent, 2010].

By using the 2100 Expert software the detected fluorescence signals are transformed in to electropherograms or gel-like pictures for simplification of the analysis. Subsequently, the transformed data was used to calculate a concentration value as well as a quality parameter, the so called RNA Integrity Number (RIN). The concentration was calculated by the area under the electropherogram in comparison to a standard ladder, included on each chip (Figure 2-8). The observed concentration data were used to pre-validate the concentrations measured using the NanoDrop system. Finally, the concentrations determined via the NanoDrop system were used only for concentration level adjustment for cRNA synthesis and hybridization of cRNA on the Illumina chips, because the data are more reliable than the concentrations determined by the Agilent Bioanalyser. The detection of RNA and cRNA samples, as already mentioned above, was performed using the Agilent RNA 6000 Nano chip and the corresponding Agilent RNA 6000 Nano kit. The qualitative range of the system is about 25 - 500 ng/µL RNA. The Agilent RNA 6000 Nano chip allows the parallel analysis of 12 samples. The used reagents were equilibrating at room temperature before use, according the user manual.

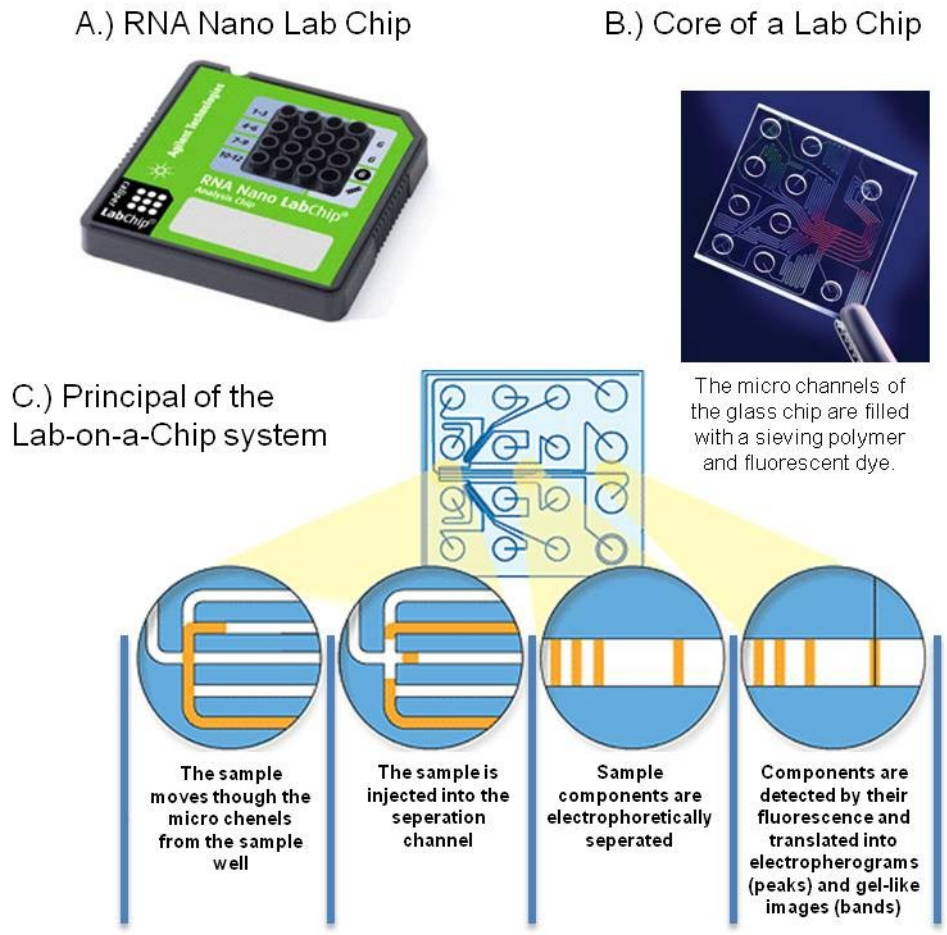

Figure 2-7 Agilent Lab-on-a-chip based technology of the RNA Nano LabChip (A) and its build up with the channel system (B). The measuring principal (C) is based on an electrophoretic separation of the sample components and the detection by a fluorescence dye [Abb. Modified by Agilent, 2010, ESD, 2009, IMB Microarray Facility, 2010].

As a first step, 500 µL Agilent RNA 6000 Nano gel matrix was pipette into a centrifuge filter column and centrifuged for 10 min at 1,500 g. 65 µL gel was mixed with 1 µl Agilent RNA 6000 Nano fluorescence dye by vortexing.

The gel-dye mix was centrifuged at RT and 13,000 g. The Agilent RNA 6000 Nano chip was put into the priming station and 9µL of gel-dye mix were pipette into the cavity marked by "G". The Priming Station was closed for 30 sec. to distribute the gel-dye mix in the channels of the chip.

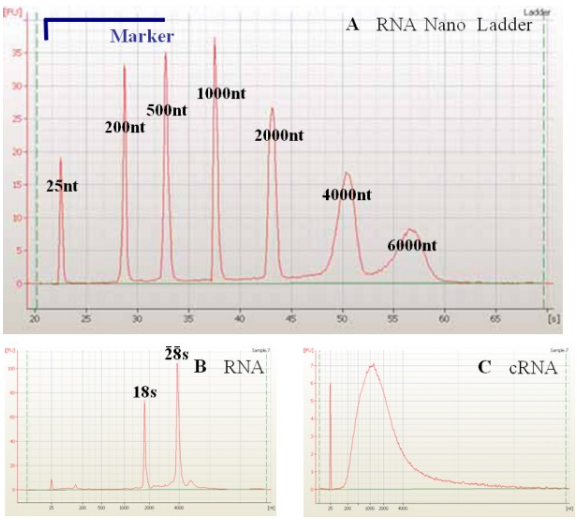

Figure 2-8 Electropherograms of total RNA (B) and cRNA (C) as well as the corresponding RNA-Ladder (A) determined by using the RNA 6000 Nano chip on the Agilent Bioanalyzer. [modified by Agilent, 2006]

Additionally, 9 µL were pipette into the upper gel wells. In all sample wells, including the well for the ladder, 5 µL RNA 6000 Nano Marker were placed. 1 µL sample or ladder was put into each well and the whole chip was vortexed for 60 sec. at 2,400 rpm [Agilent, 2006].

The chip was introduced into the Bioanalyser machine and the measurement was started.

For total RNA an electropherogram should have two prominent peaks, the ribosomal RNA (rRNA) subunits of the 18s and 28s, at 1800nt or 3800nt. (Figure 2-8).

In this measurement two quality parameters are included. First, the 2100 Expert software automatically calculated the ratio of 28s to 18s rRNA. A high quality RNA sample has a ratio of > 2.0 while with increasing degradation of the RNA the ratio decreases. Because the 28s/18s ratio depends on a variability of the included RNA concentration, it is hard to define a threshold for RNA quality. Therefore, a second quality parameter can be used. The so called RNA Integrity Number (RIN), also delivers information on the degradation of the RNA sample. The RIN value is based on the electrophoretic staining of the RNA sample. The value is between 1 and 10, while 1 means highly degradated RNA and 10 RNA with optimal quality (Figure 2-9). This method includes the determination of the presence or absence of degradation products, based on the Agilent RNA Integrity Database (RINdb). The basis of the RINdb are the analysis of 1300 RNA samples from different tissues of rat, mouse and human with different qualities, which were assigned a RIN value. By using bioinformatic, neuronal network analysis of the underlying electropherograms, this adaptive and fault-tolerant learning system, allows us to calculate specific properties, such as signal areas, -intensities or –ratios of the electropherograms. Figure 2-9 shows the electropherograms of samples with RINs from 10 to 1 [Mueller et al., 2010, Schroeder et al., 2006]. Therefore, the RIN value is a highly reproducible parameter for the determination of the RNA quality because it includes the whole electropherogram for the calculation [Mueller et al., 2010, Schroeder et al., 2006]. Furthermore, the RIN enables the definition of thresholds based on individual experiences for specific downstream applications, like real-time PCR or microarray analysis.

For the microarray experiments presented here, only samples with RINs of >7 were used. This value is based on the experience that no significant alterations based on the RNA degradation are expected in the following measurements. Because the RIN cannot be calculated for biotinylated cRNA because the samples are already fragmented, the quality check limited to study of the electropherograms manually. Typically, electropherograms of well processed cRNA show a wide spectrum, reaching from 250 – 5500 nt with its peak at 1000 – 1500nt (Figure 2-8).

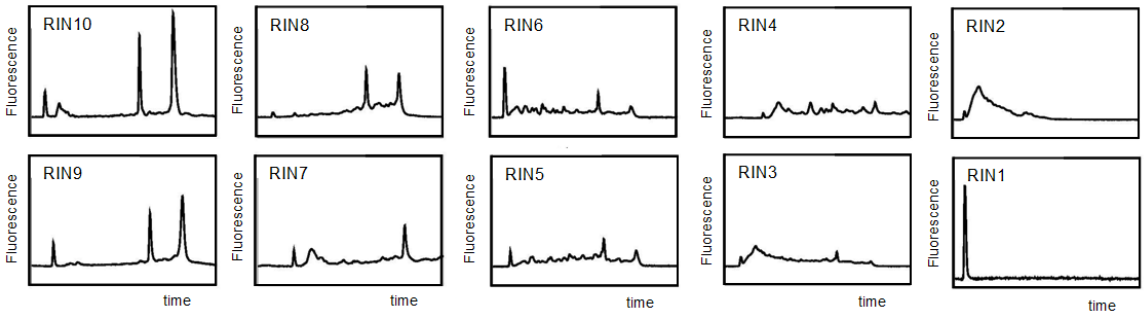

Figure 2-9 Electropherogramms of total RNA samples with decreases in RNA integrity displayed by the RNA integrity number (RIN). RIN 10 gives a typical electropherogram of complete, intact RNA and a RIN of 1 shows completely degraded RNA with only on peak at the beginning of the plot indicating the shift to shorter RNA fragments. [modified by Schroeder et al., 2006].

2.9.3 Illumina® Technology

In 2005 Illumina marketed a novel technology for the analysis of global gene expression changes [Illumina, 2010]. The Sentrix® BeadChip is based on 50 base pairs oligonucleotide sequences, which are labeled with a 29 base address sequence. By standard oligonucleotide synthesis, gene specific sequences, based on the NCBI (*National Center for Biotechnology Information Reference Sequence)* reference sequence database, are produced [Barnes et al., 2005]. A special multi-step algorithm was used to integrate parameters like the absence of repetitive genomic sequences, inequality to other gene sequences, melting temperature and self-complementarily [Illumina, 2006]. After synthesis, these oligonucleotide sequences were covalently coated on 3 µm silica beads. On average each bead contains more than 10^8 copies of a specific oligonucleotide of an individual transcript and is present approximately 30 times in each sample field of the array [Kuhn et al., 2004]. This repetition of sequences and beads serves as internal technical replicates and therefore help to make the system stable and deliver reliable and reproducible data. Another characteristic of the Sentrix® Bead Array system is the random distribution of the beads in wells, which are etched on to sample fields (Figure 2-10) [Steemers et al., 2005]. To address this, the 29 base address sequence is used in a decoding procedure to identify the final positions of the beads/ transcripts. For this purpose Illumina developed a decoding algorithm, which is based on sequential hybridization and re-hyridisation of the address sequence [Gunderson et al., 2004]. A great advantage of the Illumina Bead Chips is the fact that 12 samples can be processed on parallel on the same Chip. This allows a higher throughput and a reduction in time and costs.

The RNA was isolated from the renal tissue or cell lines as described under “RNA Isolation from renal tissue and cell lines”. After isolation the RNA was quantified and the quality was determined (see *Determination of RNA concentration via NanoDrop System*). RNA samples with a sufficient quantity and high quality were used for cRNA synthesis (see *Determination of quality via the Agilent Bioanalyzer*). The cRNA also was quantified and qualified and afterwards hybridized on the BeadChips (see Illumina® Technology). After washing and staining the BeadChips were scanned with the BeadScan by a confocal laser-scanning technology.

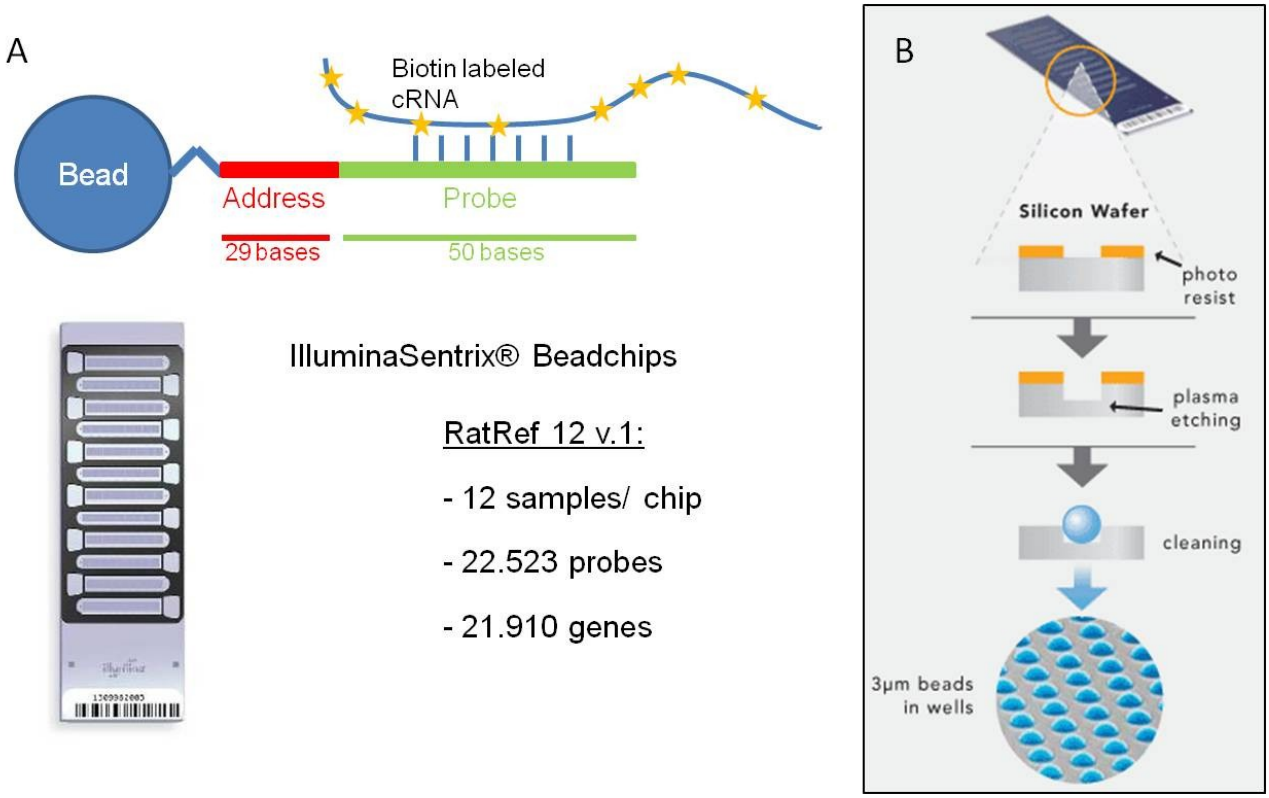

Figure 2-10 Shown is the (A) Construction of the bead with its coated addresses and probe sequences, as well as (B) the developmental process of a *Illumina Sentrix® BeadChip*. [Figure modifid by Illumina, 2010, Illumina, 2006]. The RatRef-12 v.1 chip allows the parallel hybridization of 12 samples per chip and the determination of approximately 22,000 genes per sample. By a plasma etching process, ~3 µm cavities were prepared on a silica dish to immobilize the beads on each chip.

cRNA-Synthesis

For the cRNA synthesis a modified protocol was used, including the Illumina TotalPrep RNA Amplification Kit from Ambion Inc., in combination with the Agenourt RNAClean XP from Beckman Coulter Inc.

500 ng Total RNA per sample was used in 11 µL nuclease free water in a 0.2 mL 96 well plate. In a first step, single stranded cDNA was synthesized from the mRNA containing total RNA sample by using the oligo-dT primer and a reverse transcriptase. Table 2-16 shows the preparation of the master mixes used in the procedure. 9µl 1st strand synthesis master mix were added to each sample well and incubated at 42°C for two hours.

Subsequently, for the 2nd strand synthesis, the single stranded cDNA converted to double-stranded cDNA. The second strand master mix was prepared directly prior to use and 20 µL were dispensed into each sample well. For the 2nd strand synthesis the samples were incubated for additional two hours at 16°C. For cDNA purification a modified procedure was used. The cDNA reaction mixture was completely transferred into a round bottom plate and 180 µL of Agencourt RNACleanXP bead solution was added to each individual sample. The mixture was incubated at RT for 5 min before the plate was placed on a magnetic separator for a minimum of 10 min. The liquid was discard avoiding contact to the cDNA-containing beads. The beads then were washed 3 times with 200 µL 70% ethanol before elution of cDNA by adding 20 µL nuclease free water. The purified double stranded cDNA was again transferred in a 0.2 mL 96-well plate for the IVT reaction. During the IVT reaction, biotinylated UTP-nucleotides were incorporated by an amplification reaction creating multiple copies of cRNA. 7.5 µL IVT Master Mix were dispensed into each sample well and the reaction was incubated for 14 h at 37°C. Following the IVT reaction, samples were cleaned as described for the cDNA, by using 80% ethanol except 70% ethanol. Afterwards the cRNA was quantified and checked for quality.

Table 2-16 The single components used for 1st and 2nd stand master mix of the reverse transcription of the total RNA samples, as well as the in vitro transcription (IVT) master mix. The volumes are given for a single reaction of either 20 µL (1st strand RT), 100 µL (2nd strand RT) or 25 µL (IVT).

1st Strand Reverse Transcription Master Mix for 1 sample (20 µL reaction volume)	
Amount	**Component**
1 µL	T7 Oligo(dT) Primer
2 µL	10X First Strand Buffer
4 µL	dNTP Mix
1 µL	RNase Inhibitor
1 µL	Array Script (reverse transcriptase)

2nd Strand Master Mix for 1 sample (100 µL reaction volume)	
Amount	**Component**
63 µL	Nucelase-free Water
10µL	10X Second Strand Buffer
4µL	dNTP Mix
2µL	DNA Polymerase
1µL	RNase H

IVT Master Mix for 1 sample (25 µL reaction volume)	
Amount	**Component**
2.5 µL	T7 10 Reaction Buffer
2.5 µL	T7 Enzyme Mix
2.5 µL	Biotin-NTP Mix

Sample hybridization

For hybridization, 750 ng cRNA in 5 µL nuclease-free water was used. The *GEX-HYB* and *GEX-HCB buffers* were equilibrated at 58°C for 10 min to completely dissolve the salts present. Subsequently, the buffers were cooled down to room temperature. 10 µL *GEX-HYB buffer* were pipette into each cRNA sample and denatured for 5 min at 65°C. The reservoirs of the hybridization chambers were filled with 200 µM *HEX-HCB buffer* to ensure a humid atmosphere during the hybridization process. The cRNA sample was vortexed and 15 µL sample was applied to each array of the *BeadChip*. The chips were placed into the hybridization chamber and incubated for 20 h at 58°C under slight shaking (speed 5) in the hybridization oven.

The buffers needed for the washing and staining steps are shown in Table 2-17. The chips were directly transferred from the hybridization chamber into a bath of 250 mL *E1BC buffer*. The foil was removed under the fluid surface and put into a new dish with *E1BC buffer*. The chips were placed into the Little Dipper® and the program was started. In a first step, the Chips were dipped for 10 min in 55°C warm high-Temperature wash buffer. This was followed by a 5 min washing step in 250 mL fresh *E1BC buffer* and thereafter in 250 mL 100% ethanol for 10 min. After an additional washing step in E1BC for 2 min each chip was dipped into 4 mL of *Block E1 buffer* for 10 min at 22°C.

Table 2-17 Buffers and reagents for the hybridization procedure of the Illumina bead arrays.

Buffer	Formulation
E1BC	- 800 mL DEPC water - 2.4 mL *E1BC*-Stock
High Temperature-Wash buffer	- 630 mL DEPC water - 70 mL *High Temperature*-Wash buffer Stock
Block E1-buffer containing Strepatividin-Cy3	- 500 mL *Block E1*-Buffer - 500 µl Streptavidin-Cy3-Stock (1 mg/ ml)

Finally, the chips were stained in Block E1 buffer containing Streptavidin-Cy3 for 10 min under light dipping movements. After the staining step the chips were finally washed in 250 mL *E1BC buffer* for 5 min and centrifuged at 275 g at room temperature for drying. The chips were directly transferred into the Illumina Bead Array Reader and scanned at 532 nm and a resolution of 0.8 µm.

2.9.4 Quantitative RT-PCR

0.2 U/mL SuperScript™ II Reverse Transcriptase (Invitrogen, Karlsruhe, Germany), 0.3 µg/µl random hexamer primers (Roche, Mannheim, Germany), 10 mM deoxy-NTPs (Roche, Mannheim, Germany) and 40 U/µL RNAsin (Promega GmbH, Mannheim, Germany) were used to transcribe 4 µg of total RNA to cDNA in 30 µL for 60 minutes at 42°C. Transcription of selected genes (Compugen nephrotoxicity signature) was quantified in triplicates using custom-made oligonucleotides (Sigma Aldrich, Steinheim, Germany) on the ABI Prism 7000 Sequence Detection System (Applied Biosystems, Darmstadt/Germany).

Table 2-18 Oligonucleatides for the transcriptional biomakers included in the Compugen Ltd. Panel. Ccng1 and Isg20 were present as two different splice variants. Actv, Actg, Hprt1 and Ywhaz were used as housekeeping genes.

gene symbol	Forward primer → 5´- 3´	Reverse primer → 5´- 3´
Biomarker transcripts		
Ccng1 (splice variant 1)	CAGAATTGCTGCCTCAATCTAGTCC	GGTTTTGCAGATGTACTCGGTTCC
Ccng1 (splice variant 2)	GAGATCCAAGCACTGAAGTATGTAGAGT	TCAGGAGTACAGTGGATACATTTCTCTT
Ei24	AATCTAGGCTGCCTCCTGGAG	AGGTCAATTATACAAGGCATGACTTTAG
Isg20 (splice variant 1)	GGGCCACAATGGAGCTCTAC	ACAGGTCTCATTCATGGAAAACTATG
Isg20 (splice variant 2)	ACAGCCTGATGCAGACAGC	TCTGGTTCATTATCAAGGGAAGTTG
Tnfrsf12a	GATCTGGGTAGGTGGTTGTTGG	CGCACACCCTTATAAAAGTCCC
Housekeepertranscripts		
Actb	GGGAAATCGTGCGTGACATT	GCGGCAGTGGCCATCTC
Actg2	TACCCTATTGAGCACGGCAT	CGCAGCTCGTTGTAGAAGGT
Hprt1	GCGAAAGTGGAAAAGCCAAGT	GCCACATCAACAGGACTCTTGTAG
Ywhaz	CAAGCATACCAAGAAGCATTTGA	GGGCCAGACCCAGTCTGA

Forty cycles were run with the following parameters: 50ºC for 2 min, 95ºC for 10 min, and then 40 cycles of 95ºC for 15sec, followed by 60ºC for 1 min, except for Ccng1 splice variant 2 for which the annealing temp was 62ºC for

transcription using SYBR® green chemistry (Applied Biosystems, Darmstadt, Germany). cDNAs were stored at -80°C and diluted 1:20 in TE-buffer (10mM Tris pH=8, 1mM EDTA) and PCR reactions were performed with 5 µL of diluted cDNA in 20 µL reactions. On every plate an 8 point standard curve, prepared by reverse transcription of universal rat RNA (Stratagene, Heidelberg, Germany), was included.

2.10 Statistics and mathematical evaluation

2.10.1 General statistical average and error values

Student´s T-Test

The student´s T-Test, developed in 1908 by Wiliam Sealy Gosset, within the Guiness brewery for quality control of the brewing process, is a mathematical hypothesis testing method. This statistical test follows a Student´s distribution (probability distribution) if the null hypothesis is supported. The null hypothesis says that the mean of both samples (e.g. control and treated group) are equal. For the calculation of the probability, the mean and variance of both samples are used. In addition, the probability distribution depends on the degrees of freedom, which is calculated by the number *n* of independent observations minus the number of parameters taken in account into the analysis [Draghici, 2003]. The number of degrees of freedom for the evaluation of the p-value is given by two unpaired samples *n+m-2*. Based on the t-ratio and by using the degrees of freedom the probability (p-value) can be evaluated out of the probability distribution by using tables or statistics software. The t-ratio is the difference between sample means divided by the standard error of the difference, calculated by combining the SEMs of the two groups. Therefore, the p-value is used to show whether the difference between the mean of two groups is likely to be due to chance. Small p-values indicate that the probability that the means of both distributions are equal (null hypothesis) is quite low [Rudolf et al., 2008]. In practice a threshold for the significance level is defined, normally 0.05 or 0.01. That means that a p-value of 0.05 indicates a 5% error probability to reject the null hypothesis incorrectly.

ANOVA

In contrast to the student´s t-test, the analysis of variance (ANOVA) allows the comparison of multiple groups or conditions in parallel [Draghici, 2003]. The simplest form of an ANOVA is to compare two groups which correspond to the t-test. It can be discriminated between unifactorial (one-way ANOVA) and multifactorial (n-way ANOVA) analysis of variance, which are different in the number of factors included into the analysis. A simple ANOVA is based on the comparison of the variability between different testing groups and the variability within the testing groups. The requirements for an ANOVA are the same as for a t-test, including variance homogeneity and normal distribution of the data. The underlying probability distribution is the F-distribution. The mathematical principle of a unifactorial ANOVA is the partitioning of the square sum of the total variance (S_{total}), which means the square sum of all differences of the individual observations from the global mean [Draghici, 2003].

$$S_{total} = S_{fault} + S_{cont}$$

Equation 1 The fundamental technique of an analysis of variance is a partitioning of the **sum of squares** (S) into components related to the individual observations

In this case S_{fault} is the square sum of variance within the testing group (replicates) [Draghici, 2003], which in principal is excepted to be relatively small, because the differences between the replicates of a testing group takes place by experimental/ technical error and the biological variation. The S_{cont} stands for the variance of the groups around the global average (variation between the groups) and characterizes the variance of the defined condition, like time,

treatment and gender. By using the degrees of freedom, the mean square error for S_{fault} and S_{cont} can be calculated [Draghici, 2003]:

$$(A)MS_F = \frac{SS_{fault}}{N-k} \quad (B)MS_{cont} = \frac{SS_{cont}}{k-1}$$

Equation 2 Calculation of the mean square error of the variance within (A) the groups and (B) between the groups to evaluate the F-value by using a analysis of variance (ANOVA). k = number of conditions, N = total number of measurements within the dataset, Sfault Square sum of the intra-group variance, Scont Square sum of the inter-group variance

Based on the F-value and the degrees of freedom *k*-1 and N-*k* the p-value can be evaluated [Draghici, 2003]. In principal this procedure is identical for multifactorial analysis of variance, with the difference that multiple factors/ conditions (e.g. treatment, gender and time) can be taken into account within one analysis.

$$F = \frac{MS_{cont}}{MS_F}$$

Equation 3 Equation for the calculation of the F-value by a unifactorial analysis of variance. MS_{cont} = mean square error of the inter-group variance, MS_F = the mean square error of the intra-group variance

In this work the one-way ANOVA was used to compare the results of the urinary protein measurement, the clinical pathological and hematological results of the groups treated with nephrotoxic model compounds with the groups treated with the vehicle (control groups). The calculations were conducted using the GraphPad Prism Software (version 5) by GraphPad Software Inc. (San Diego, USA).

2.10.2 Calculation of renal functional property values

The calculation of renal parameters that reflect the renal functional properties are based on the comparison of concentrations of different components in urine and in blood. Out of the ratio from these two observations the clearance and therefore the glomerular filtration rate can be estimated. There are a multitude of equations for the calculation of the glomerular filtration rate, all of which have advantages and disadvantages. To calculate the creatinine clearance, which is widely used in (pre-) clinical trials, the urinary output was multiplied by urinary creatinine concentration, divided by the concentration of creatinine in serum (Equation 4).

$$creatinine\ clearance = \frac{1000 \times V_{urine} \times c_{uCrea}}{c_{sCrea}}$$

Equation 4 To calculate the renal clearance of creatinine the urinary volume (V_{urine}) was multiplied by 1000, for unit correction, and the urinary concentration of creatinine (c_{uCrea}) and then divided by the concentration of creatinine in serum. The units used within the calculation were V_{urine} [mL/ 18h], c_{uCrea} [mmol/L], c_{sCrea} [µmol/L].

2.10.3 Receiver Operating Characteristic curve

The Receiver Operating Characteristic curve (ROC curve) is a statistical method to determine the sensitivity (True Positive Rate) and 1-specificity (False Positive Rate) of a diagnostic test in relation to a specific outcome. In our case, the ROC curves were used to evaluate the performance of novel urinary protein biomarker to detect histopathological alterations. The sensitivity reflects the fraction of animals with pathological kidney damage that the urinary biomarker correctly identifies as positive. On the other hand the specificity is the fraction of animals without pathological alteration that the biomarker correctly identifies as negative. Therefore, it is a binary classification system, as its discrimination threshold is variable. By interpretation of the data it has to be kept in mind that in this work the histopathological evaluation serves as the "gold-standard" and the calculated values only reflect how urinary biomarker excretion cover histopathological findings. As quantitative values, the area under the ROC curve (AUROC) was evaluated as the overall ability of the biomarker to discriminate between those animals with pathological renal damage and those without. A perfect result, i.e., no false negative or false positive measurements, has an AUROC of 1.0. For the worst case, the analysis of a distinct biomarker will give a result that of a probability of 50% to predict the pathology by the biomarker. In this case the calculated AUROC will have a value of 0.5. All calculated values will lie between these borders. We decided to highlight values with an AUROC > 0.9 as good biomarkers with a satisfying diagnostic performance. However, also biomarkers below 0.9 can be of value.

By using GraphPad Prism we calculated the sensitivity and specificity using each individual value of the dataset as the potential cutoff value. Therefore, many pairs of sensitivity and specificity were calculated. If a higher threshold is chosen the specificity of the test will increase, but sensitivity will be lost. By using a lower threshold, the sensitivity of the test will be enhanced but it will lose specificity.

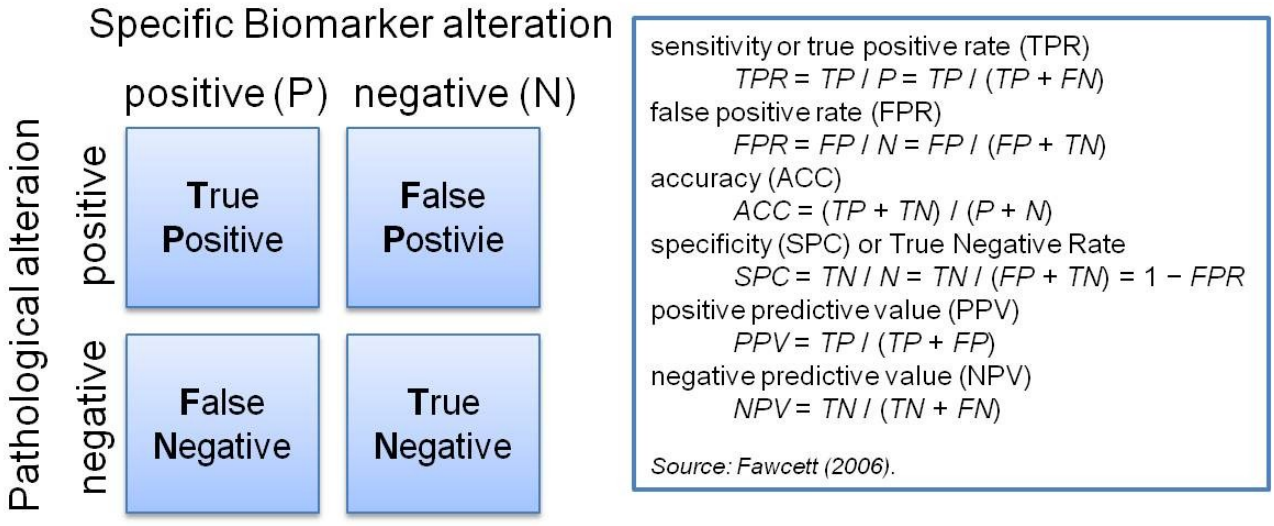

Figure 2-11 A schematic overview of the principle of classification rates for the urinary protein biomarker measurement compared to pathological alterations observed by histopathology. If an animal shows pathological alteration and also the biomarkers deliver a positive result it's a true positive (TP) outcome. If the biomarker delivers a negative result it is false negative (FN). If animals shows no pathological alterations and also the biomarkers do not show any changes the result is true negative (TN). In the other case, if the biomarker indicates an alteration it is a false positive (FP). Out of these possibilities the sensitivity, accuracy and specificity can be deduced.

2.10.4 Challenge of statistical analysis of omics-data

The challenge in analysing whole genome gene expression data lays in the enormous amount of single data points produced by these genomic technologies. Therefore, specialized computational analyses are needed to identify the relevant information in a reliable way and to make it possible to bring the data into a biological context. The field of bioinformatics, which is a branch of computational biology, addresses the analysis and management of biological data. The analysis of thousands of transcripts within a microarray experiment can be performed using different general approaches, depending on the aim of analysis. Four general categories are available for analysing genomics data[3]:

1. Class discovery
2. Class comparison
3. Class prediction
4. Mechanistic analysis

The class discovery is a general and unbiased look at the data, and enables the discovery of group classes. The principle of this analysis approach is the grouping of similar effects of the gene expression pattern, to discover differences and similarities of e.g. pathology groups. This method can be used to get a first overview of the dataset or to check whether an analysis influences the clustering of the data in relation to each other. The advantage of this method is that class discovery is an unsupervised method, which leads to classification on their similarity in expression pattern, independent of the group. The mathematical approach used within this study was the principal component analysis. Because of the complex mathematical algorithms underlying these statistical approaches, only the principal of the analysis will be explained. However, it has to be mentioned that the individual clusters created by these methods do not necessarily have any toxicological or biological meaning. To determine whether a clustering is relevant, further analyses are required.
The class comparison gives further information by comparison of for example untreated with treated animals/ cells to identify treatment related differences. In general, almost all parameters of a study can by analysed by this method to evaluate their impact of the observed gene expression alteration. The most important factor is that a reliable control group is available. Each departure from the normal biological/ physiological phenotype/ genotype can be assumed to be related to the compound treatment and therefore predicted as patho-toxicologically relevant. Also biological and technical variability has to be taken into account, for which a wide variety of statistical tools can be used. The statistical tests used within this study include the t-test (two group comparison) and the analysis of variance (multiple group comparison) already described above. However, in case of whole genome gene expression analysis one problem occurs when using these statistical tests. Normally, a significance level is assumed to be $p \leq 0.05$. Because of the high number of genes (~22,000genes) detected within in one experiment (multiple testing), applying a 95% confidence limit on gene selection ($p \leq 0.05$) will lead, by chance, to 500 genes detected as significantly altered. To avoid this problem a more stringent gene selection is warranted, by using p-value threshold of $p \leq 0.01$ together with a fold-change (FC)-ranking, which describes a ratio of treated vs. control groups. This approach was expected to deliver reliable results by an enhanced reproducibility and a balanced sensitivity and specificity [Shi et al., 2008]. In addition, the q-value by Benjamini and Hochberg [Benjamini et al., 2001] was used to minimize misclassification by only taking the p-value into account. The q-value is a measure of the false discovery rate, and is therefore a control statistic used to correct in a list of rejected hypothesis the expected proportion of incorrect rejected null hypothesis.

[3] Fuchs et al., 2012

The class prediction analysis deals with the supervised, computation prediction of a toxicological outcome based on the gene expression pattern. The assumption of this kind of testing is that similar pathologies lead to comparable effects on the gene expression level. There are two different approaches which can be used to build up such a classification model:

1. Gene ranking
2. Use of rational defined gene lists

By ranking genes, a computational algorithm finds the ideal set of genes that can discriminate between different phenotypes or pathologies. In this case the ideal gene set is defined by a minimized misclassification rate, i.e. a minimum false positive and a minimum false negative classification (Figure 2-11). A multitude of mathematical models can be used, including the analysis of variance (ANOVA) [Bushel et al., 2002], the support vector machine weight (SVM) [Mundra et al., 2008] and the recursive feature elimination (RFE) [Furlanello et al., 2003]. In the second approach an already defined gene list (e.g. by mechanistic link or an already classified and published gene list) can be used to build a classification model. In this work three gene lists were used, taken from the literature, to evaluate their usability to predict nephrotoxicity, independent of the used method. Many algorithms can be used to build up the rules for the classification model, such as discriminant analysis [Nguyen et al., 2002, Orr et al., 2002, Antoniadis et al., 2003, Le et al., 2003], classification and regression trees [Boulesteix et al., 2003], support vector machines [Ramaswamy et al., 2001, Brown et al., 2000], and k-nearest neighbours [Theilhaber et al., 2002]. In general, all these algorithms are developing a rule based on the gene expression data. For an unknown compound, this rule can be then used to predict the class of the compound without any further information.

Quality control of microarray data

On each Illumina bead array six different quality controls are present which can be used within the GenomeStudio software from Illumina. These controls include the control of the laboratory processes of cRNA syntheses, hybridization and background up to the generation of the fluorescence signal.

Firstly, the expression of housekeeping genes can be checked. 14 Different species specific housekeepers are present with two oligonucleotide probes on each array. To check the quality of the hybridization process three controls, a Cy3, a high and a low stringent hybridization control were used. The Cy3 control is composed of six different oligonucleotide probes on each chip and the corresponding Cy3 oligonucleaotides, which are included in the *HybE1* buffer. This enables the control of the hybridization process, independent of the RNA quality and the preparation process. In contrast, the low stringent control contains only four different probes and each of them are characterized by 2 mis-matched pairs, leading as a consequence to only a very minimal signal in case of an optimal hybridization. The high stringent control does not have any mis-matched pairs and are characterized by a high GC-content, leading to a very strong signal.

Another control is composed of biotinylated oligonucleotides, and is also included within the *HybE1* buffer. This control enables the quality check of the secondary staining reaction of the Cy3-dye. For determination of unspecific background hybridization reactions also 20 different randomized oligonucleotides are included, which do not match to any sequence within the genome of the used species. In addition, unspecific binding reactions of the dye, as well as cross reactivity, were detected by this control.

Based on these controls with the GenomeStudie software, the detection limit was defined and transcripts near the background were excluded from the analysis [Illumina, 2004]. No further analysis was conducted within this software tool. The signal intensity values were exported from each individual probe and uploaded within the Genedata Analyst

software for further analysis. Therefore, in a first step the data were visualized by log-log-plots and box-plot analysis to evaluate the general distribution of the data and to identify potential outliers.

Normalization of microarray data

To enable comparability of gene expression data generated under different conditions, such as technology, time points or experiments, the data has to be normalized [Draghici, 2003]. Such differences between arrays also can appear by using different protocols, amounts or quality of mRNA, Scanner setups, cRNA synthesis or hybridization assays. A multitude of special algorithms are available to transform gene expression data to eliminate or reduced systemic errors, which can lead to discrepancies in signal intensities [Knudsen, 2004]. In general, there are linear and non-linear methods. Linear methods are mean or median normalization methods, and adjust the intensity signals by the average signal. Here, housekeeper genes can be used as reference points to transform all values relative to these genes. In general, these methods are preferable if the data shows a parallel shift in log-log-plots to the midline (bisector). For datasets showing a non-linear curve shape in the log-log-plot, like a banana-shaped curve, the non-linear methods are preferable.

In this study the Genedata Analyst software was used to normalize the gene expression data. Within the rat in vivo study only slight differences between the individual experiments were detected, with a linear curve shape. Therefore, the linear *Central Tendency normalization* method was used, with the median as a setting factor. The median is the value of a dataset, separating the higher half of the processed values from the lower half. In contrast to the arithmetic mean, the median is a more robust method in respect of outliers. For each experiment/ array, all probes are shifted by a constant sum, such that the median of the normalized data values in each experiment equals the target value, in case of this study 100. The generated/ calculated new values show stable differences between each other compared to the differences of the original/ non-normalized data. In case of the in vitro data a point wise division was used to normalize the datasets. This was possible because it can be assumed that the corresponding vehicle, derived from the same passage, is the same biological replicate, so that the ratio of the treated cells and the vehicle control subtract the effects/ processes present in the untreated cells.

Global Data analysis

Principal component analysis (PCA)

The principal component analysis (PCA) is a vectorial approach, which can be used in toxicogenomics for class discovery. It is a visualization tool which aims to reduce the number of multidimensional dataset to fewer dimensions (2D/ 3D) with a minimization of loss of information [Draghici, 2003]. It is a mathematical procedure that uses an orthogonal transformation to convert a set of observations of possibly correlated variables into a set of values of linearly uncorrelated variables – the so called principal components. In a microarray dataset each experiment and each individual gene represents a single dimension. For example, in the Vancomycin study reported here, containing 72 different experiments with ~20,000 genes, the regular results without PCA would be a data cloud of 72 experiments in a 20,000 dimensional space. Within the PCA, the dimensions become regarded as important dimensions, which strongly vary between the experiments/ data. Dimensions with only a low variation within the datasets are often neglected. The statistical properties are first order, so the variance of the data is used within the PCA to build the whole dataset in to a novel coordinate system with fewer dimensions. The direction of the new axes of the coordinate system, are Eigen

values of a square matrix, in this case a correlation matrix of the data. By using the genes of different experiments within the PCA, each experiment will be displayed in a graph as a single point. Therefore, the PCA can identify a tendency of a dataset, as well as outliers [Draghici, 2003]. It has to be mentioned that not all axes carry an equally weight within the PCA. The mathematical transformation is defined in such a way that the 1st principal component accounts the most variability of the original data as possible and has therefore the largest possible variance. The same is true for the 2nd component under the constraint that it be orthogonal (uncorrelated), to the preceding components.

Transcription Factor Analysis in IPA

Transcriptional analysis was conducted by using the Ingenuity Transcription Factor Analysis in IPA®. The analysis is based on two independent values, a z-score, which can be used as a numerical value of the regulatory influence of the individual transcription factors (TF) and an overlap score (Fisher´s Exact Test p-value) indicating whether there is a statistically significant overlap of the underlying dataset and the genes regulated by this TF. The regulation z-score describes transcriptional regulators that are able to describe observed alterations on gene expression and infer their activation state. This predictive process is based on relationships (edges) in the molecular interaction network within the datasets and is associated with the literature derived information within the IPA-database of the expected deregulation, which can be named as “activating” or “inhibiting”. For the z-score, the calculated value must be interpreted to be predictive for the activation state of the activated TF when the parameters given in Table 2-19 are matched.

Table 2-19 Given is the principal of relation of the evaluated z-score and the underlying basic approach for interpretation. Ehe expected (in literature descibed associated relationships) regulation directions of the transcription regulators can be either “activating” or “inhibiting”. Dependent on the evaluated observed gene regulation over all downstream genes (up; down), the sign of the calculated z-score reflects the overall predicted activation state of the transcription factor (<0: inhibited; >0 activated). In practice, the z-score is considered to be significant if it is ≥ 2 or ≤ -2.

Regulation direction associated with relationship	calculated z-score based on the observed gene deregulation	Mean observed gene regulation over all downstream transcripts	Predicted activation state of transcription regulator
activating	≥ 2	up	activated
activating	≤ -2	down	inhibited
inhibiting	≤ -2	up	inhibited
inhibiting	≥ 2	down	activated

Analysis of qRT-PCR data by Compugen’s classifier

Average C_t values were calculated from triplicate measurements for each sample. The standard curve was used to transform the average C_t to RNA expression levels. The geometric mean of the four housekeeping genes expression levels was calculated for each sample, and this value was used as a normalization factor that accounts for the relative total RNA amount per sample. The RNA expression was further normalized for each marker, so that the geometric mean of the control samples expression levels is a predetermined value (the geometric mean of the control samples used to train the classifier, see below). A Random-Forest classifier was used to determine the toxicity status for each sample. Both the 4-marker and the 6-marker classifiers use an additional gender parameter, and give numerical results between 0 and 1. Any sample with a value above 0.4 was considered toxic. A toxicity score was calculated for each group of

samples (control, low, medium and high dose), as the percentage of toxic samples in the group. All calculations were done using MS-Excel, the classifiers were created and run using R software, embedded in Excel.

3 Results and Discussion

3.1 Identification of nephrotoxic effects in vivo

In the following sections results from different methods will be presented and described which evaluate the advantages and disadvantages of some qualified and exploratory biomarkers in different test settings (see 3.1.1 Results and Discussion for the evaluation of urinary protein biomarkers). General histo- and clinical-pathological methods as well as hematological, immunohistochemical and gene expression data were analyzed to characterize the underlying pathology and to evaluate the performance of these urinary protein biomarkers for their ability to detect substance induced nephrotoxicity and renal recovery in a gender independent way. After describing the relevant findings for each individual study the results from all methodologies are discussed.
In a second step gene expression analysis of the Vancomycin study was conducted to obtain a mechanistic understanding as well as transcription based biomarker identification (see 3.1.3 Gene expression analyses of renal tissue).

3.1.1 Results and Discussion for the evaluation of urinary protein biomarkers

3.1.1.1 Results (Vancomycin)

Histopathological observation (Vancomycin)

Gross pathological kidney-related findings were restricted to high dose animals (300 mg/kg) at all time points. The main macroscopic observations were a bilateral pale discoloration, enlargement of the whole organ and a granular surface. A holistic overview of the results is summarized in Table 3-1.
On day 4 in all animals of the high dose treated group (300 mg/kg), treatment-related effects in the kidneys were observed. The animals showed a mild to moderate tubular degeneration, which was mainly located in the proximal tubules. The tubules were characterized by dilation, showing a flattened basophilic tubular lining epithelium with single cell necroses and intraluminal sloughing cells. Moreover, all animals treated with 300 mg/kg Vancomycin revealed minimal to moderate eosinophilic casts.
On day 8 the treatment related tubular degeneration showed an increasing severity (up to massive) in male and female rats. However, in general almost all findings were more pronounced in male than in female rats. Also moderate to massive tubular dilation was found in male rats, but in female rats this effect was only mild. Still present were minimal to moderate cellular and eosinophilic casts. In addition, mixed cellular inflammatory infiltrates were diagnosed in all high dose treated animals, both in the interstitium and intraluminal in damaged tubules.
The first tubular degeneration observation in a low dose treated animal (50 mg/kg) was found on day 15 without any further findings. All high dose treated animals (300 mg/kg) showed minimal to massive tubular degeneration in both genders, more pronounced in males, at day 15 but with a lower severity compared to day 8.
A clear reduction in cellular and eosinophilic casts was also observed, although some animals still showed minimal to mild effects. Minimal to mild tubular dilation was only observed in individual animals. In all high dose treated male rats, but not in females, minimal to moderate mixed cellular interstitial inflammatory infiltrates in the interstitium and intraluminal were observed in damaged tubules.

Table 3-1 Incidence summary of Vancomycin treatment-related kidney histophatology findings. The number of animals in each group of five is shown in parentheses. / ≙ lesion not observed, + ≙ minimal, ++ ≙ mild, +++ ≙ moderate, ++++ ≙ massive, and +++++ ≙ high severity of lesion

		Vancomycin [mg/kg]					
Observation		**Male**			**female**		
in Kidney	**time**	**0**	**50**	**300**	**0**	**50**	**300**
Tubular Degeneration	**day 4**	/	/	++ (3/5) +++ (2/5)	/	/	++ (4/5) +++ (1/5)
	day 8	/	/	+++ (2/5) ++++ (3/5)	/	/	++ (3/5) +++ (2/5)
	day 15	/	/	++ (3/5) +++ (1/5) ++++ (1/5)	/	+ (1/5)	+ (1/5) ++ (4/5)
	day 29	/	+ (4/5)	+++ (1/5) ++++ (2/5) +++++ (2/5)	/	+ (3/5)	++ (2/5) +++ (1/5) ++++ (2/5)
Tubular Dilatation	**day 4**	/	/	+ (1/5) ++ (2/5)	/	/	/
	day 8	++ (1/5)	/	+++ (2/5) ++++ (3/5)	/	/	++ (2/5)
	day 15	/	/	+ (1/5) ++ (2/5)	/	/	+ (1/5)
	day 29	/	/	+++ (1/5) ++++ (4/5)	/	/	++ (3/5) +++ (1/5) ++++ (1/5)
Eosinophilic Casts	**day 4**	/	/	++ (5/5)	/	/	+ (3/5) ++ (1/5) +++ (1/5)
	day 8	/	/	++ (5/5)	/	/	+ (5/5)
	day 15	/	/	+ (2/5) ++ (1/5)	/	/	+ (1/5) ++ (1/5)
	day 29	/	/	++ (5/5)	/	/	++ (5/5)
Cellular Casts	**day 4**	/	/	/	/	/	/
	day 8	/	/	++ (1/5) +++ (4/5)	/	/	+ (5/5)
	day 15	/	/	++ (2/5) +++(1/5)	/	/	+ (1/5)
	day 29	/	/	+ (1/5)	/	/	+ (1/5)
Basophilic Tubules	**day 4**	/	/	/	/	/	/
	day 8	/	+ (3/5)	/	/	+ (1/5)	/
	day 15	/	+ (5/5)	/	/	/	/
	day 29	+ (2/5)	/	/	/	++ (1/5)	/
Infiltrates	**day 4**	+ (1/5)	/	/	/	/	/
	day 8	/	/	++ (1/5) +++ (4/5)	/	/	+ (1/5) ++ (4/5)
	day 15	/	/	+ (2/5) ++ (1/5) +++ (2/5)	/	/	/
	day 29	/	/	++ (3/5) +++ (2/5)	/	/	+ (2/5) ++ (1/5)

On day 29, in seven (4♂ + 3♀) low dose treated animals (50 mg/kg) minimal tubular degeneration without further findings were observed. In all ten high dose treated animals (300 mg/kg) mild to severe tubular degeneration, concomitant to mild to massive tubular dilation was observed. Consequently, mild eosinophilic casts were detectable in all high dose treated animals (300 mg/kg). Mixed cellular inflammatory infiltrates were again diagnosed in nearly all high dose animals with a higher degree of severity in males. Treatment related findings in other organs were limited to deposits of fibrin on the liver capsule in both gender accompanied by mixed cellular infiltrates. In addition, individual focal small hepatocellular necroses and mixed cellular infiltrates in the serosa of the urinary bladder were observed. All these findings were considered to be a sequela of the i.p. application of the test item.
In summary, histopathologically Vancomycin related changes in the kidneys e.g. tubular degeneration, dilation, cellular and eosinophilic casts, were restricted to the high dose animals of all time points with an increase from day 4 to day 8. After 15 days of treatment, in addition to the findings in the high dose group, one low dose female rat revealed minimal tubular degeneration. After 29 days, nearly all low dose rats showed minimal tubular degeneration in addition the strong findings in the high dose group.

Clinical, clinical-pathological and hematological observation (Vancomycin)

Only significant observation or relevant parameters in case of the underlying evaluation are shown. Over all the parameters, determined effects were more pronounced in male rats compared to females. As shown in Table 3-2 the body weight was decrease in high dose treated male and female rats (300 mg/kg) over all time points. In contrast, kidney weights showed an increase in all animals treated with 300 mg/kg Vancomycin, from day 3 on. The low dose treated rats (50 mg/kg) showed no relevant alterations in body or kidney weight. Statistical significance could not be determined for any time or dose group for these two parameters.
Significant effects were observed for creatinine and blood urea nitrogen (BUN) levels. Significant increases were observed in high dose (300 mg/kg) treated male rats from day 7 on. Female rats showed, on day 7 and day 29, the strongest increase in serum creatinine and BUN, while also the other time points showed slight elevated serum levels. In addition, several low dose (50 mg/kg) treated animals showed slight and partly significant decreases in these two parameters.
Renal functionality was calculated using three different parameters, which are routinely used to evaluate the health status of the kidney. First the urinary excretion of sodium and calcium were analysed (Figure 3-1). Changes in urinary sodium excretion were only observed in male and female rats treated with high doses (300 mg/kg) of Vancomycin. A decrease in urinary excretion of sodium appeared after 4 and 28 days of treatment, while on day 8 and day 15 no changes occurred. For urinary excretion of calcium significant alterations in low dose (50 mg/kg) treated animals were limited to female rats after 28 days of treatment. In high dose (300 mg/kg) treated female rats a slight, but significant decrease on day 4 and a non significant increase at day 14, while male rats showed no alterations on day 4 but a strong and significant increase on day 15 followed by a decrease on treatment day 28. The creatinine clearance (Crea Clear) was used as an estimation of the glomerular filtration rate (GFR). Therefore, all significant and relevant observations were limited to high dose (300 mg/kg) treated animals with two exceptions.

Table 3-2 Summary of the body and kidney weight determined for male and female rats treated with 50 mg/kg and 300 mg/kg Vancomycin for up to 28 days. The data of the control group are displayed in each table. Significant changes were indicated with * $p < 0.05$, ** $p < 0.01$, *** $p < 0.001$ (ANOVA + Dunnett)

		Vancomycin [mg/kg]					
		Male			Female		
	Time	0	50	300	0	50	300
body weight [g]	day 3	251.5 ± 4.65	262 ± 8.51	238 ± 5.79	171.75 ± 3.4	167.8 ± 10.26	166.6 ± 6.07
	day 7	282.8 ± 9.07	278.6 ± 10.06	251.2 ± 10.47	182.2 ± 4.44	180.8 ± 6.18	170.2 ± 3.9
	day 14	304.4 ± 18.61	313.4 ± 11.80	270.6 ± 15.65	186.6 ± 6.27	182.8 ± 5.45	178.8 ± 4.82
	day 28	338.2 ± 22.97	337.2 ± 10.08	310.6 ± 8.88	194.6 ± 5.94	191 ± 5.83	190.2 ± 3.96
kidney weight [g]	day 3	2.04 ± 0.15	2.078 ± 0.18	2.73 ± 0.21	1.35 ± 0.06	1.23 ± 0.06	1.77 ± 0.35
	day 7	2.22 ± 0.11	2.06 ± 0.11	4.79 ± 1.00	1.37 ± 0.06	1.38 ± 0.10	1.84 ± 0.26
	day 14	2.27 ± 0.04	2.43 ± 0.21	2.59 ± 0.34	1.37 ± 0.05	1.44 ± 0.13	1.57 ± 0.26
	day 28	2.48 ± 0.34	2.62 ± 0.13	4.69 ± 1.35	1.45 ± 0.05	1.52 ± 0.04	2.7 ± 0.52

A strong increase in variability was observed on treatment day 7 in male rats and a slight, but significant, increase in Crea Clear on day 28 in females. However, almost all high dose groups showed a significant decrease in these two parameters except female rats on day 7 and 14 in Crea Clear.

Several dose and time dependent changes were observed in urinary parameters (Table 3-4). In addition, a dose and time dependent decrease in urinary volume was observed, which was most prominent in high dose (300 mg/kg) treated animals on day 29, for both genders. In control animals a time dependent effect was determined also, leading to a lowered urinary excretion on day 14. This is probably due to the changing of the treatment schedule, leading to a lowered fluid volume. On day 29, the animals had adapted to the weekly treatment pattern.

Several other relevant urinary components showed strong effects (Table 3-4). Urinary glucose showed significant increased levels earliest on day 3 in male rats of the high dose group (300 mg/kg). In female rats no relevant effects were observed up to day 14, while on day 29 the urinary glucose level in male and female rats treated with 300 mg/kg Vancomycin, increased up to the 10-fold of the corresponding control animals.

The measurement of urinary protein showed statistically significant changes only on day 28 in high dose animals (300 mg/kg). However, also at the earlier time points relevant dose dependent elevations were observed. The most prominent finding was in one high dose female rat on day 3, which showed a urinary protein excretion of 3.3 g/L (data not shown). This leaded to a high mean and standard deviation for the whole group (Table 3-4).

Table 3-3 Summary of clinical pathology serum parameter determined for male and female rats treated with saline, 50 mg/kg and 300 mg/kg Vancomycin for up to 28 days. The data of the control group are displayed in each table. Significant changes were indicated with * $p < 0.05$, ** $p < 0.01$, *** $p < 0.001$ (ANOVA + Dunnett)

		Vancomycin [mg/kg]					
		Male			female		
	time	0	50	300	0	50	300
Creatinine [mg/dL]	day 3	0.12 ± 0.03	0.14 ± 0.02	0.43 ± 0.26	0.19 ± 0.03	0.19 ± 0.02	0.41 ± 0.20
	day 7	0.11 ± 0.02	0.10 ± 0.03	1.13 ± 0.57 *	0.30 ± 0.06	0.27 ± 0.05	0.41 ± 0.07 *
	day 14	0.24 ± 0.01	0.23 ± 0.01	0.38 ± 0.10 *	0.28 ± 0.01	0.25 ± 0.03 *	0.45 ± 0.28
	day 28	0.23 ± 0.02	0.24 ± 0.04	1.45 ± 0.56 **	0.30 ± 0.07	0.22 ± 0.06	1.20 ± 0.65 *
BUN [mg/dL]	day 3	37.71 ± 4.48	27.14 ± 3.33	84.07 ± 55.43	34.95 ± 5.72	35.31 ± 6.29	72.54 ± 40.21
	day 7	30.63 ± 2.36	27.14 ± 0.99 *	151.33 ± 41.19 **	33.51 ± 7.14	34.11 ± 6.29	56.33 ± 14.86 *
	day 14	27.98 ± 3.39	28.11 ± 0.89	46.72 ± 7.29 **	34.83 ± 3.32	31.83 ± 1.95	66.18 ± 49.12
	day 28	25.22 ± 3.21	29.07 ± 5.58	159.50 ± 46.45 **	34.95 ± 3.10	32.19 ± 6.74	162.38 ± 58.99 **
Glucose [mg/dL]	day 3	80.00 ± 11.15	86.49 ± 6.62	94.42 ± 9.24	84.69 ± 14.24	87.93 ± 13.02	83.6 ± 8.22
	day 7	81.44 ± 11.14	91.17 ± 11.99	104.15 ± 18.08 *	85.77 ± 7.92	80.72 ± 11.21	96.94 ± 9.13
	day 14	98.74 ± 11.14	113.51 ± 11.75	109.19 ± 23.72	89.37 ± 9.75	94.78 ± 17.77	94.06 ± 4.30
	day 28	110.63 ± 13.52	109.91 ± 20.74	107.03 ± 15.84	92.61 ± 14.67	93.33 ± 9.13	108.11 ± 21.43

Table 3-5 gives an overview of the significant hematological findings. Almost all relevant findings were limited to animals treated with 300 mg/kg Vancomycin. The major effect was on white blood cells (WBC), probably due to their crucial role of inflammatory processes during kidney injury. A slight increase in numbers of red blood cells and platelets were limited to day 3 and day 7 in male rats of the high dose groups (300 mg/kg). Female rats showed slight and partially significant decreases in these two parameters. The most prominent findings were observed in white blood cells in both genders on days 7, 14 and 28. This effect in WBCs was limited to an increase in neutrophils, lymphocytes and monocytes. However, also basophils, and large unstained cells showed slight dose dependent alterations, which were limited to individual animals.

Table 3-4 Summary of clinical pathology urinary parameter determined for male and female rats treated with saline, 50 mg/kg and 300 mg/kg Vancomycin for up to 28 days. The data of the control group are displayed in each table. Significant changes were indicated with * $p < 0.05$, ** $p < 0.01$, *** $p < 0.001$ (ANOVA + Dunnett)

		Vancomycin [mg/kg]						
		Male				female		
	time	0	50	300		0	50	300	
Volumen [mL]	day 3	27.48 ± 4.98	22.98 ± 7.42	13.28 ± 4.07	**	8.76 ± 3.10	11.12 ± 2.82	6.28 ± 3.44	
	day 7	27.76 ± 5.05	19.16 ± 6.42	* 13.78 ± 3.52	**	12.26 ± 5.87	10.22 ± 5.10	12.02 ± 2.69	
	day 14	19.32 ± 4.04	18.88 ± 2.12	18.2 ± 4.97		8.30 ± 3.40	7.74 ± 3.34	8.42 ± 3.96	
	day 28	21.04 ± 6.03	22.28 ± 1.21	8.58 ± 6.3	**	14.44 ± 5.02	12.92 ± 5.10	4.85 ± 1.96	**
Glucose [mg/dL]	day 3	3.28 ± 1.33	4.5 ± 1.45	6.81 ± 2.34	*	8.72 ± 3.24	7.64 ± 4.66	9.80 ± 6.96	
	day 7	3.64 ± 3.64	4.72 ± 0.82	7.68 ± 3.51	*	7.06 ± 3.64	7.75 ± 5.44	10.74 ± 8.36	
	day 14	5.12 ± 1.12	5.98 ± 0.78	5.19 ± 1.78		7.35 ± 2.74	11.68 ± 5.04	12.29 ± 12.03	
	day 28	5.87 ± 1.33	11.78 ± 5.51	63.17 ± 17.16	***	4.22 ± 0.97	9.33 ± 4.47	44.32 ± 19.52	***
total protein [mg/dL]	day 3	19.58 ± 7.15	21.3 ± 7.09	26.78 ± 6.16		12.04 ± 5.70	8.88 ± 3.93	83.96 ± 139.75	
	day 7	22.52 ± 22.52	37.92 ± 21.04	36.2 ± 11.22		12.88 ± 7.30	13.10 ± 10.61	12.82 ± 4.78	
	day 14	39.22 ± 7.45	40.36 ± 10.21	30.76 ± 17.33		13.94 ± 4.24	16.66 ± 8.58	13.78 ± 3.83	
	day 28	39.98 ± 12.30	40.3 ± 13.72	74.58 ± 23.28	*	8.76 ± 2.12	13.12 ± 5.04	38.23 ± 9.42	***
Creatinine [mg/dL]	day 3	27.03 ± 6.46	38.83 ± 18.85	52.21 ± 14.43	*	52.32 ± 19.27	40.85 ± 12.81	85.00 ± 64.72	
	day 7	26.39 ± 6.44	38.54 ± 6.23	47.16 ± 7.68		52.15 ± 29.86	64.91 ± 45.83	42.57 ± 10.75	
	day 14	48.95 ± 9.67	48.76 ± 4.56	53.97 ± 15.00		56.85 ± 13.43	71.17 ± 42.67	60.54 ± 22.50	
	day 28	47.9 ± 11.98	41.59 ± 3.14	87.6 ± 51.82	*	37.14 ± 8.14	47.61 ± 21.66	74.46 ± 19.09	**

Table 3-5 Summary of hematological parameter determined for male and female rats treated with saline, 50 mg/kg and 300 mg/kg Vancomycin for up to 28 days. The data of the control group are displayed in each table. Significant changes were indicated with * $p < 0.05$, ** $p < 0.01$, *** $p < 0.001$ (ANOVA + Dunnett)

		Vancomycin [mg/kg]					
		Male			female		
	time	0	50	300	0	50	300
RBC [counts/pL]	day 3	8.10 ± 0.19	8.15 ± 0.29	8.64 ± 0.23 **	8.06 ± 0.43	7.91 ± 0.40	8.38 ± 0.21
	day 7	8.18 ± 0.18	8.39 ± 0.25	8.81 ± 0.24 **	8.14 ± 0.19	8.10 ± 0.30	7.94 ± 0.59
	day 14	8.66 ± 0.52	8.40 ± 0.42	7.88 ± 0.39 *	7.89 ± 0.57	8.13 ± 0.47	7.63 ± 0.27
	day 28	8.32 ± 0.42	8.67 ± 0.39	8.04 ± 0.32	8.13 ± 0.25	7.98 ± 0.43	7.62 ± 0.09 *
PLT [counts/nL]	day 3	913 ± 104	1010 ± 98.62	921 ± 127	895 ± 74	876 ± 135	1060 ± 78 *
	day 7	896 ± 62	904 ± 62	1063 ± 129 *	946 ± 126	996 ± 63	1314 ± 99 ***
	day 14	815 ± 118	879 ± 133	1039 ± 132 *	877 ± 127	944 ± 166	978 ± 118
	day 28	899 ± 110	888 ± 119	857 ± 81	929 ± 83	847 ± 68	1071 ± 134
WBC [counts/nL]	day 3	6.40 ± 0.77	8.60 ± 1.76 *	7.32 ± 1.16	3.90 ± 1.19	3.56 ± 0.67	4.98 ± 1.05
	day 7	7.62 ± 0.93	7.90 ± 2.69	16.76 ± 2.52 ***	4.00 ± 1.11	4.94 ± 1.47	6.44 ± 1.25 *
	day 14	6.16 ± 1.11	5.70 ± 0.59	9.48 ± 2.31 **	3.96 ± 1.71	5.66 ± 0.88	6.60 ± 1.80 *
	day 28	5.56 ± 1.12	6.30 ± 1.11	9.34 ± 2.14 **	3.76 ± 0.51	3.50 ± 0.99	7.12 ± 0.46 ***
NEU [counts/nL]	day 3	0.96 ± 0.14	1.53 ± 0.70	1.33 ± 0.19	0.48 ± 0.13	0.62 ± 0.14	0.79 ± 0.14 **
	day 7	1.38 ± 0.24	1.34 ± 0.35	7.78 ± 1.65 ***	0.51 ± 0.14	0.99 ± 0.72	1.30 ± 0.67
	day 14	1.29 ± 0.72	0.95 ± 0.30	2.80 ± 0.72 **	0.73 ± 0.38	0.92 ± 0.46	1.50 ± 0.66
	day 28	0.96 ± 0.35	1.26 ± 0.43	3.15 ± 1.15 ***	0.70 ± 0.17	0.54 ± 0.18	2.75 ± 0.57 **
Lymph[counts/nL]	day 3	5.13 ± 0.79	6.60 ± 1.63	5.53 ± 1.14	3.23 ± 1.09	2.75 ± 0.68	3.85 ± 0.98
	day 7	5.88 ± 0.83	6.06 ± 2.22	7.73 ± 1.28	3.28 ± 1.12	3.70 ± 0.87	4.84 ± 0.96 *
	day 14	4.56 ± 0.89	4.49 ± 0.46	6.20 ± 2.22	3.06 ± 1.29	4.43 ± 1.04	4.78 ± 1.36
	day 28	4.33 ± 0.79	4.68 ± 0.72	5.68 ± 1.20	2.85 ± 0.54	2.78 ± 0.83	3.94 ± 0.80

		Vancomycin [mg/kg]					
		Male			female		
	time	0	50	300	0	50	300
EOS [counts/nL]	day 3	0.12 ± 0.04	0.16 ± 0.06	0.15 ± 0.03	0.07 ± 0.02	0.06 ± 0.01	0.12 ± 0.06
	day 7	0.11 ± 0.04	0.15 ± 0.07	0 25 ± 0.12 *	0.06 ± 0.01	0.08 ± 0.04	0.07 ± 0.02
	day 14	0.10 ± 0.04	0.09 ± 0.02	± 0.08	0.06 ± 0.02	0.08 ± 0.02	0.10 ± 0.08
	day 28	0.11 ± 0.05	0.11 ± 0.04	0.14 ± 0.02	0.09 ± 0.02	0.05 ± 0.02	0.13 ± 0.06
BASO [counts/nL]	day 3	0.04 ± 0.01	0.08 ± 0.04	0.09 ± 0.02 *	0.02 ± 0.02	0.03 ± 0.01	0.05 ± 0.02 *
	day 7	0.04 ± 0.03	0.06 ± 0.05	0.14 ± 0.07 *	0.02 ± 0.01	0.03 ± 0.01	0.05 ± 0.02 *
	day 14	0.05 ± 0.02	0.03 ± 0.01	0.04 ± 0.01	0.02 ± 0.01	0.04 ± 0.04	0.04 ± 0.02
	day 28	0.04 ± 0.02	0.05 ± 0.01	0.05 ± 0.03	0.03 ± 0.01	0.03 ± 0.01	0.03 ± 0.01
MONO[counts/nL]	day 3	0.13 ± 0.04	0.19 ± 0.03 **	0.18 ± 0.02 *	0.07 ± 0.03	0.07 ± 0.02	0.13 ± 0.04 *
	day 7	0.16 ± 0.07	0.24 ± 0.06	0.73 ± 0.19 ***	0.08 ± 0.04	0.10 ± 0.05	0.14 ± 0.08
	day 14	0.14 ± 0.03	0.12 ± 0.03	0.25 ± 0.08 *	0.09 ± 0.03	0.14 ± 0.02	0.14 ± 0.07
	day 28	0.10 ± 0.02	0.16 ± 0.04	0.25 ± 0.10 **	0.07 ± 0.01	0.07 ± 0.04	0.20 ± 0.03 ***
LUC [counts/nL]	day 3	0.02 ± 0.01	0.03 ± 0.01	0.04 ± 0.02	0.01 ± 0.01	0.01 ± 0.00	0.01 ± 0.01
	day 7	0.02 ± 0.01	0.04 ± 0.02	0.10 ± 0.08 *	0.02 ± 0.01	0.03 ± 0.02	0.03 ± 0.02
	day 14	0.02 ± 0.01	0.02 ± 0.01	0.06 ± 0.04	0.02 ± 0.02	0.03 ± 0.01	0.04 ± 0.02
	day 28	0.02 ± 0.01	0.02 ± 0.01	0.05 ± 0.02 *	0.03 ± 0.01	0.03 ± 0.02	0.06 ± 0.03

Abbreviation: RBC = red blood cells, PLT = platelets, WBC = white blood cells, NEU = neutrophils, Lymph = Lymphocytes, EOS = eosiniphils, BASO = basophils, MONO = monocytes, LUC = large unstained cells.

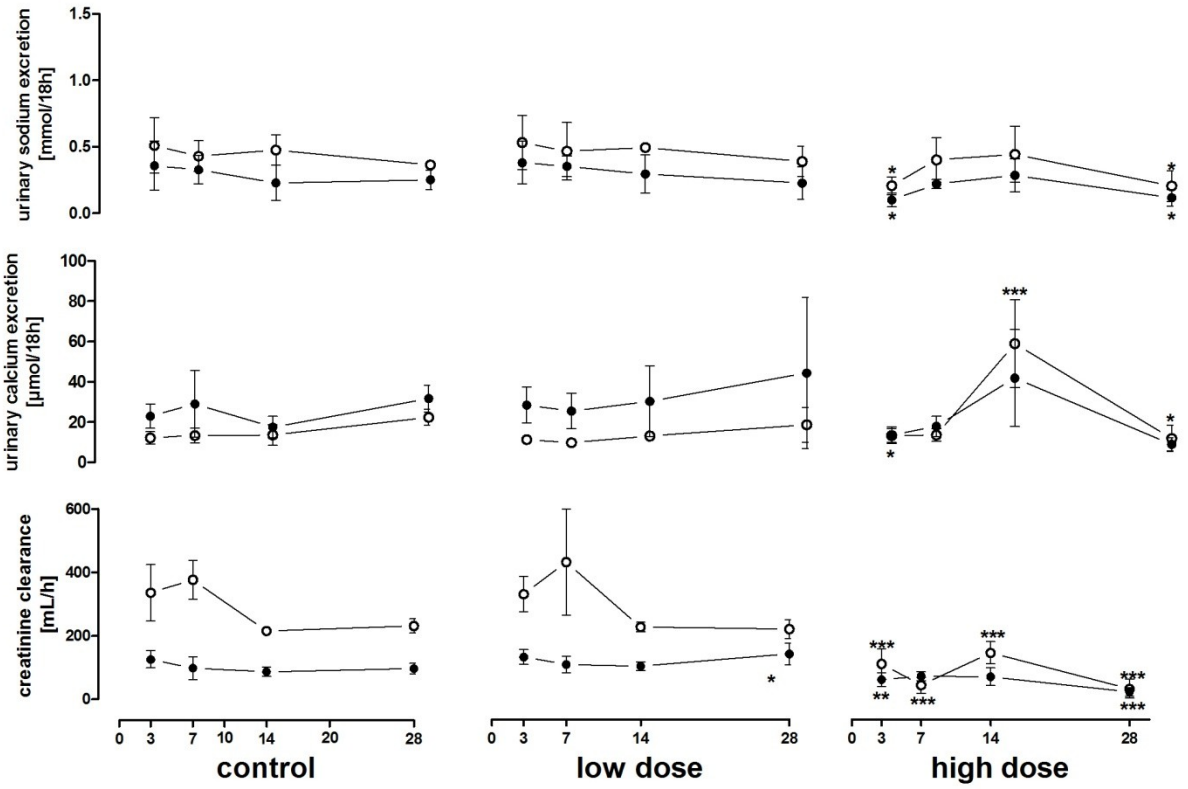

Figure 3-1 Urinary sodium and calcium excretion, as well as the creatinine clearance for male (○) and female (●) rats treated with either saline (control), 50 mg/kg Vancomycin (low dose), or 300 mg/kg Vancomycin (high dose). Data are presented for both genders individually by mean ± SD. Significant changes are indicated with * $p < 0.05$, ** $p < 0.01$, *** $p < 0.001$ (ANOVA + Dunnett).

Detection of novel qualified and exploratory urinary proteins (Vancomycin)

In Vancomycin treated rats a clear dose and treatment schedule dependency in urinary protein biomarker excretion was observed. In addition, differences in the excretion of specific biomarkers between genders were observed.

In male rats a strong increase in urinary Kim-1, Osteopontin, Calbindin and Clusterin was observed (Figure 3-2a, -g, -h, -i) in the high dose group (300 mg/kg). Kim-1 showed a further increase from day 4 to day 8 with a massive decrease in Kim-1 excretion on day 15 compared to the earlier time points. On day 29 urinary Kim-1 levels rose again. In the low dose group (50 mg/kg) only two of the four animals with histopathological findings showed an increase in urinary Kim-1 level (Figure 3-2a). The urinary excretion level of Ostoepontin in male rats treated with 300 mg/kg Vancomycin showed a strong and significant increase over all four time points (Figure 3-2g). The highest magnitude of urinary Osteopontin was measured on day 4 with a constant decrease over up to day 29. The four low dose animals (50 mg/kg) on day 29 showed a slightly enhanced elevation of urinary Ostoepontin. Calbindin also showed significantly increased level at all time points in the high dose group (300 mg/kg) while in contrast to Osteopontin the strongest increase was observed on day 29 (Figure 3-2h). Also on day 4 a strong increase was observed followed by a slight increase on day 8 and 15. In the low dose group (50 mg/kg) only 3 animals on day 29 showed a marked increase. Significant excretion levels of urinary Clusterin were only determined on day 4 and day 29 (Figure 3-2i). The magnitude of urinary Clusterin was also strongly elevated on day 8 but with a very high variation between individual animals.

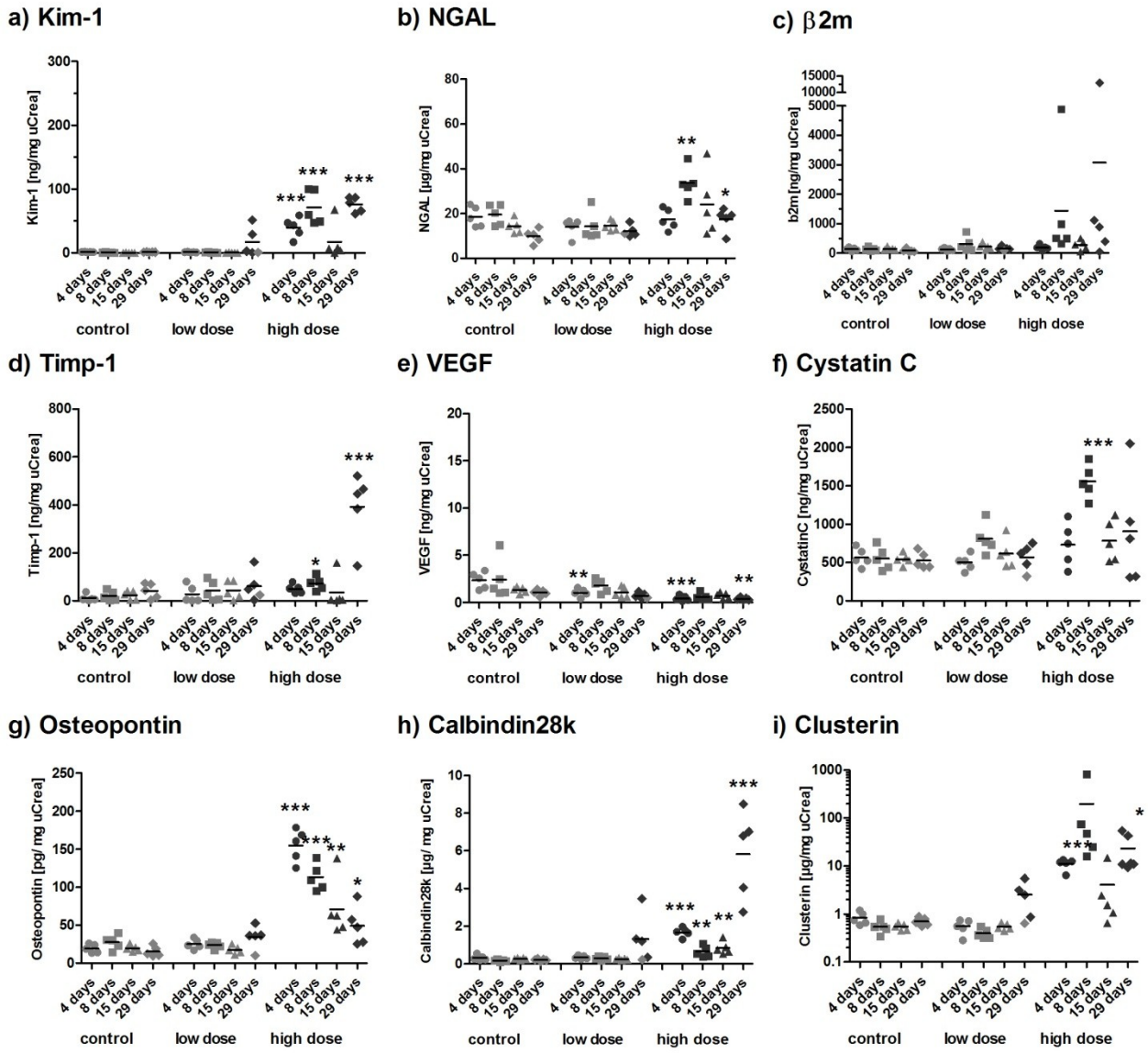

Figure 3-2 Excretion of (a) Kim-1, (b) NGAL, (c) b2m, (d) Timp-1, (e) VEGF, (f) CystatinC, (g) Osteopontin, (h), Calbindin28k, (i) Clusterin in urine of male rats treated with Vancomycin (low dose: 50 mg/kg; high dose: 300 mg/kg)for 3 days (dots), 7 days (squares), 14 days (triangle), and 28 days (rhombus). Data are presented as individual animals and as the mean (bar; n=5). The light grey signs indicate no tubular degeneration; the darker grey indicates tubular degeneration (based on histopathology). * $p < 0.05$, ** $p < 0.01$, *** $p < 0.001$ (ANOVA-Dunnett).

On day 29 of the low dose group (50 mg/kg) three animals showed a strong increase while one animal with histopathological findings showed no alteration.The biomarkers NGAL, β2m, Timp-1 and CystatinC also showed strong and significant alterations in there urinary level, but not to the same extent as the other biomarkers. NGAL, for example showed no increase on day 4 and a strong and significant increase on day 8 in animals treated with 300 mg/kg Vancomycin (Figure 3-2b). On day 29 also a significant increase was observed, but this was matched by a decrease in urinary NGAL level in the control animals on day 15 and day 29. In the low dose group (50 mg/kg) no alterations were observed. In contrast β2m was increased at all time points of high dose treated animals (300 mg/kg) but without any statistical significance (Figure 3-2c). This is probably due to one animal on day 8 and one animal on day 29 showing a marked increase far above the other animals (up to 60 fold of the urinary level in the control animals), resulting in an extraordinary higher mean. On day 8, one animal showed a slight increase in the low dose group (50 mg/kg) even though no histopathological findings were recorded for this rat. The low dose animals on day 29 with tubular degeneration showed no alterations.

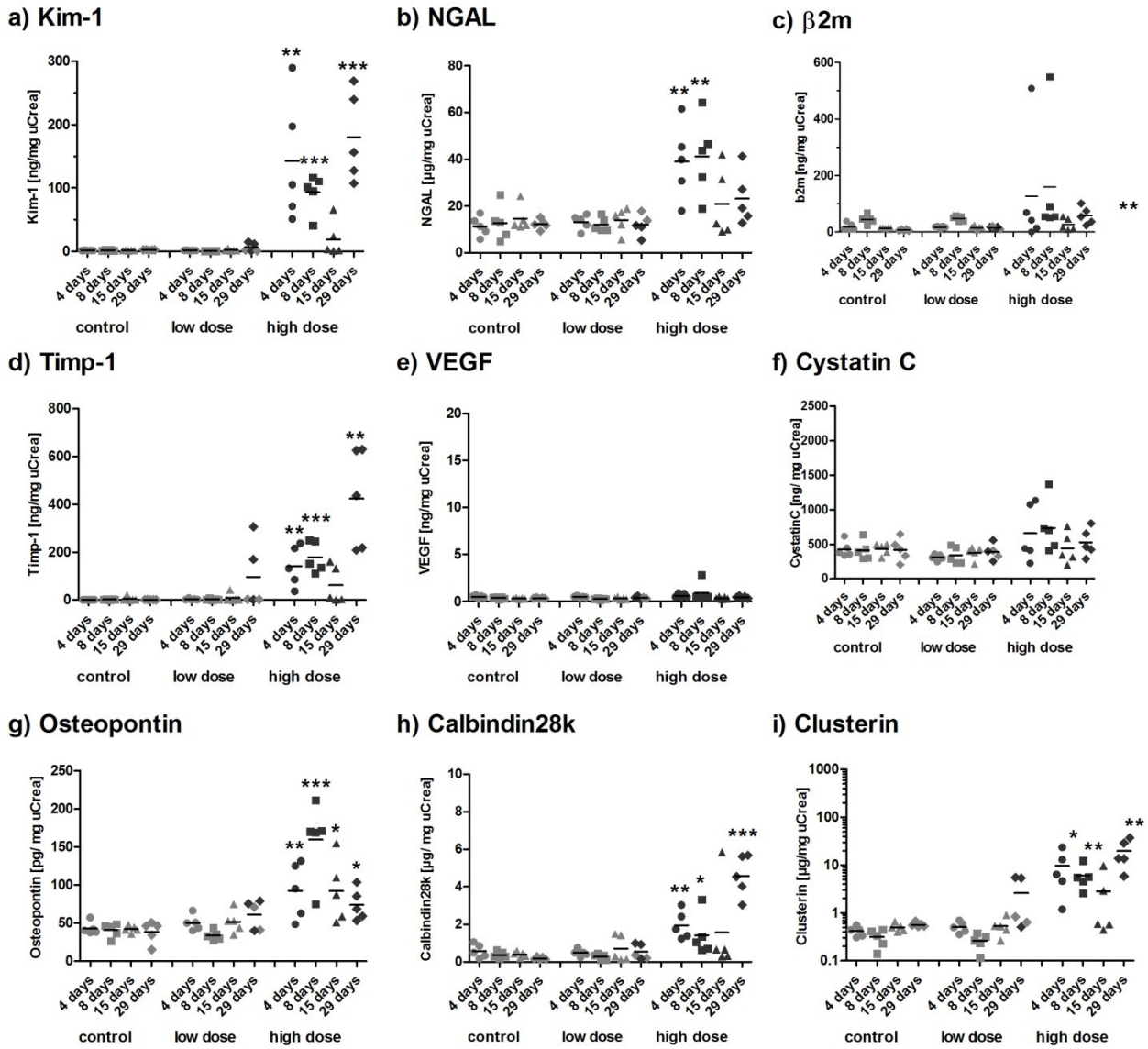

Figure 3-3 Excretion of (a) Kim-1, (b) NGAL, (c) b2m, (d) Timp-1, (e) VEGF, (f) CystatinC, (g) Osteopontin, (h), Calbindin28k, (i) Clusterin in urine of female rats treated with Vancomycin (low dose: 50 mg/kg; high dose: 300 mg/kg) for 3 days (dots), 7 days (squares), 14 days (triangle), and 28 days (rhombus). Data are presented as individual animals and as the mean (bar; n=5). The light grey signs indicate no tubular degeneration found within this animal, the darker grey indicates tubular degeneration observed (based on histopathology). * $p < 0.05$, ** $p < 0.01$, *** $p < 0.001$ (ANOVA-Dunnett).

For Timp-1 a time-dependent increase in urinary excretion in the control groups (up to 3 fold on day 29 compared to day 4) was detected (Figure 3-2d). In addition, a treatment dependent increase on days 4, 8 and 29 of the high dose (300 mg/kg) treated animals was observed. While day 4 delivered no statistical significance, day 8 and 29 showed significant enhancement of urinary Timp-1. The increase was strongest on day 29. Only one animal on day 15 showed an increased level of Timp-1. Low dose animals (50 mg/kg), at all time points, showed a slight increase with an enhanced variability within the group compared to the control group. The highest and only significant excretion of urinary CystatinC was observed in animals treated with 300 mg/kg for 7 days (Figure 3-2f).

However, all groups of high dose treated animals showed higher average CystatinC excretion then the control group. In addition the variance within the groups of altered CystatinC level increased. Independent on any observed histopathology animals of the low dose group (50 mg/kg) showed an increase on day 8, while the affected animals on day 29 showed no alteration.

In contrast to all other markers mentioned above, the urinary biomarker VEGF showed a dose-dependent decrease over all time points (Figure 3-2e). In addition a time-dependent decrease down to a half of the excretion was detected in the control animals. α-GST was not analysed because most of the animals of the control group lay below the detection range of the WideScreen™ assay.

In female rats treated with Vancomycin, Kim-1, NGAL, Timp-1, Osteopontin, Calbindin and Clusterin showed dose dependent changes in urinary excretion, with statistical significance (Figure 3-3a, -b, -d, -g, -h, -i).

In rats treated with 300 mg/kg Vancomycin urinary Kim-1 was elevated in all animals on days 4, 8, and 29, while day 4 showed a higher magnitude than day 8 together with a higher intragroup variance (Figure 3-3a); the group mean was the highest on day 29. On day 15, only two animals showed an increase in Kim-1 excretion, even though all five animals showed renal tubular damage. In low dose treated animals (50 mg/kg) slight changes were limited to two of the three animals described to have tubular degeneration. NGAL was statistically significant elevated on days 4 and 8 in the high dose group (300 mg/kg), while day 15 and 29 levels were only slightly increased (Figure 3-3b). No alterations in low dose (50 mg/kg) treated animals were observed. Comparable to Kim-1, Timp-1 showed an increase in high dose treated animals (300 mg/kg) on days 4, 8 and 29, while the magnitude of increase was the highest at the latest time point (Figure 3-3d). In addition, the same two animals of the low dose group (50 mg/kg) exclusively showed an increase in urinary Timp-1. As described for male rats, Osteopontin was statistically significantly increased at all time points of the high dose treated animals (300 mg/kg). The highest urinary excretion was observed on day 8 while the magnitude of increase on days 4 and 15 was comparable. The excretion on day 29 was still elevated but slightly below the value of days 4 and 15. In low dose treated animals (50 mg/kg) the mean of animals treated for 28 days was also slightly increased, while only two of the treated animals (same animals already mentioned from Kim-1 and Timp-1) showed an increase. However, one animal not found to indicate morphological changes within the kidney showed a comparable increase of urinary Osteopontin. Calbindin showed a strong increase on day 4 in rats treated with 300 mg/kg Vancomycin, while the urinary level decreased on day 8 compared to day 4 (Figure 3-3h). The highest magnitude in Calbindin excretion was at the latest time point. In low dose treated aminals (50 mg/kg) only two animals on day 15, without any histopathological correlation, and the same two animals (female rat 97 and 99) as already mentioned, showed a slight alteration. The urinary Clusterin level were statistically significantly elevated in the high dose groups on days 4, 8, and 29 (Figure 3-3i). Only two animals on day 15 showed an increase compared to the control animals. In low dose treated animals (50 mg/kg) again the same two animals showed an increase in urinary Clusterin, while the others, independent if histopathological observations, showed no alteration.

Further significant alterations in urinary biomarker excretion in female rats were limited to high dose treated animals (300 mg/kg) on day 29, which showed an elevated level of β2m. In addition, one animal on day 4 and day 8 showed a very strong increase in β2m. Urinary levels of VEGF and CystatinC showed no significant alterations, however in the high dose groups on days 4 and 8 CystatinC levels were increased in some animals.

To evaluate the diagnostic performance of these urinary biomarkers to reflect histopathological changes, Receiver Operation Characteristic (ROC) analyses were performed (Table 3-6).

Table 3-6 Area-under-the-receiver-operator-characteristic curve (AUROC) for detection of Vancomycin induced nephrotoxicity. The area under the curve is used as a measure for the overall ability of a biomarker to discriminate animals without histopathological findings in kidney from those with signs of tubular damage (degeneration/ necrosis). Markers with a good diagnostic performance (AUROC > 0.90) are highlighted in bold. In addition the 95% confidence interval and the p-value are displayed. * = measurement by Luminex® xMAP®, ** = measurement by RENA®-Sticks, # = classical clinical-pathology parameter determined by standard procedures.

Kidney Biomarker	Male			Female		
	AUROC	95% CI	p-value	AUROC	95% CI	p-value
KIM-1*	**0.95**	**0.89 - 1.02**	**<0.0001**	**0.90**	**0.80 - 1.01**	**<0.0001**
Timp-1*	0.74	0.60 - 0.87	0.0022	**0.94**	**0.87 - 1.01**	**<0.0001**
VEGF*	0.89	0.81 - 0.97	0.0001	0.67	0.52 - 0.81	0.0292
$ß_2$-Microglobulin*	0.76	0.63 - 0.90	0.0007	0.70	0.56 - 0.85	0.0084
Clusterin*	**0.98**	**0.95 - 1.01**	**<0.0001**	**0.94**	**0.88 - 1.00**	**<0.0001**
Cystatin C*	0.73	0.59 - 0.88	0.0027	0.68	0.53 - 0.83	0.0196
Lipocalin-2/ NGAL*	0.69	0.54 - 0.83	0.0145	0.76	0.62 - 0.91	0.0006
Osteopontin*	**0.98**	**0.95 - 1.00**	**<0.0001**	**0.94**	**0.87 - 1.00**	**<0.0001**
Calbindin *	**0.98**	**0.96 - 1.00**	**<0.0001**	0.88	0.78 - 0.97	0.0001
KIM-1**	0.86	0.76 - 0.96	<0.0001	0.81	0.69 - 0.94	<0.0001
BUN#	**0.91**	**0.81 - 1.01**	**<0.0001**	**0.91**	**0.82 - 0.99**	**<0.0001**
Serum Creatinine#	**0.96**	**0.91 - 1.01**	**<0.0001**	0.87	0.78 - 0.96	<0.0001

In addition detection by using the Luminex® xMAP® technology an alternative detection method for Kim-1, based on a Dipstick assay, was analysed. Based on the AUROC, Kim-1 (m: 0.95; f: 0.90), Clusterin (m: 0.98; f: 0.94), Osteopontin (m: 0.98; f: 0.94) and BUN (m: 0.91; f: 0.91) performed the best, while BUN showed the lowest AUROC of the four markers mentioned. Relevant gender differences were observed for Timp-1 (m: 0.74; f: 0.94), Calbindin (m: 0.98; f: 0.88), VEGF (m: 0.89; f: 0.67) and serum creatinine (m: 0.96; f: 0.87). β2m (m: 0.76; f: 0.70), CystatinC (m: 0.73; f: 0.68) and NGAL (m: 0.69; f: 0.76) perfomed poorly. The AUROCs of Kim-1 (m: 0.86; f: 0.81) determined by using the Dipstick assay were good but below the values of the Luminex® xMAP® measurement.

In general it has to be mentioned that rats on day 15, independent of the sex showed the smallest changes in almost all urinary biomarkers. This is in good correlation to the histopathological findings.

Evaluation of expression of Kim-1, Clusterin and Ostoepontin protein in renal tissue (Vancomycin) - immunohistochemical analysis

Kim-1 and Clusterin showed no staining in untreated animals, while Osteopontin showed a slight but constant basal expression within corical and medullar tissue of the kidney (Annex 1).

Representive pictures for Kim-1, Clusterin and Osteopontin stained kidney sections fom male and female rats treated with 300 mg/kg Vancomycin are shown in Figures 3-4, 3-5-, 3-6, 3-7, 3-8, 3-9). The low dose treated animals (50 mg/kg) showed no relevant changes compared to the control animals, except for animals treated for 28 day, which showed slightly increased staining compared to the time matched control animals. For each individual finding an overview is given spanning from the cortex to the medullary papilla and a detailed picture of the cortical zone and the medullary zone. To show the most specific observations in some pictures the inner or the outer zone of medulla is shown.

Kim-1

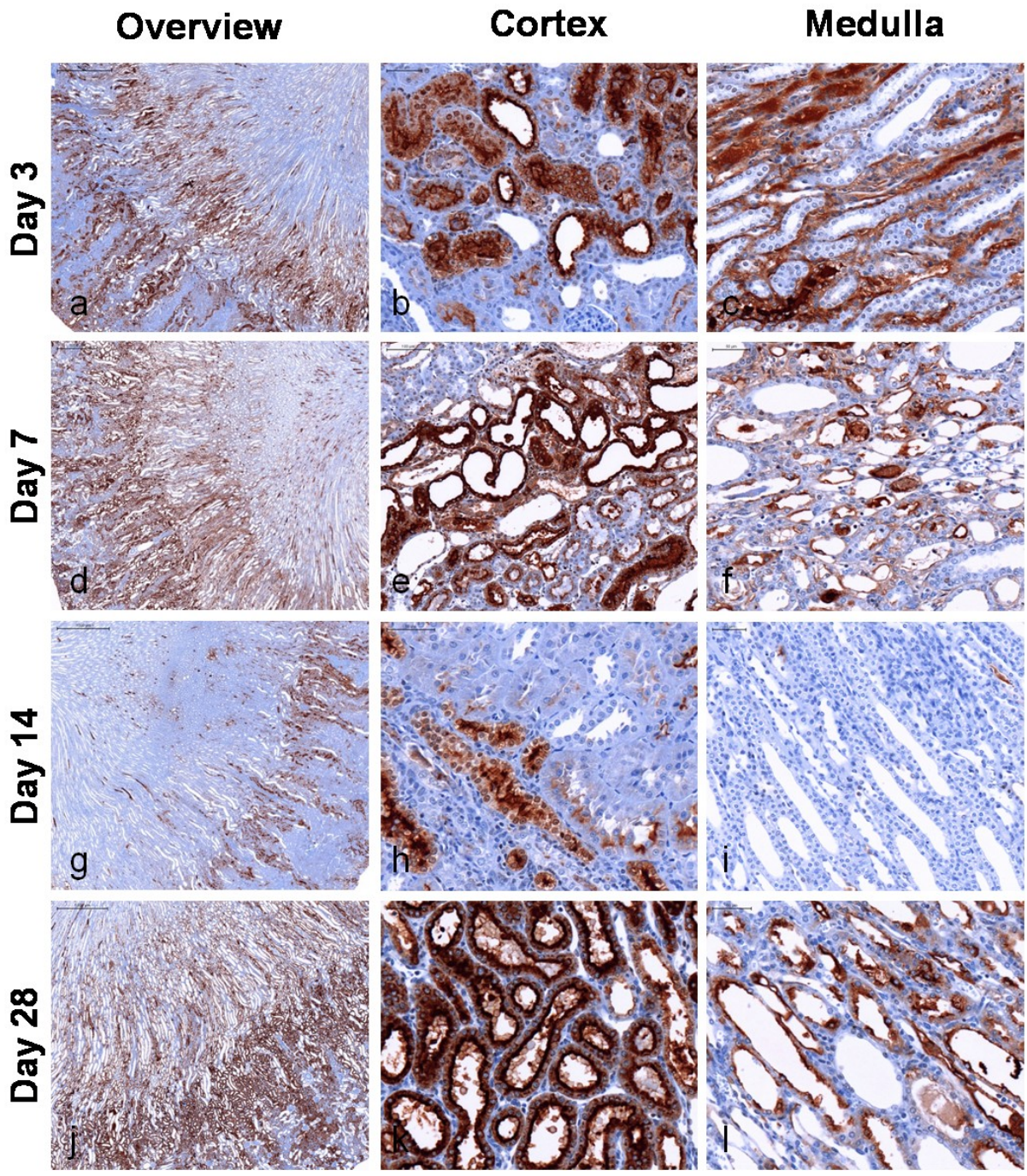

Figure 3-4 Location of Kim-1 protein in renal tissue of male rats treated with 300 mg/kg Vancomycin is shown for each time point of necropsy. An overview picture for each time point (a, d, g, j) shows the whole area from the cortical zone to the medullary papilla. In addition two detailed pictures, either of the cortex (b, e, h, k) or the medulla(c, f, i, l) is given. The magnification of the overview was ~10 times and of the detailed pictures ~70 times.

In male rats the area of Kim-1 expression was in the cortical zone, reaching into the outer zone of the medulla (Figure 3-4). In general Kim-1 showed a very dark staining and therefore a strong increase in Kim-1 protein. The highest expression was found at the apical membrane of proximal tubular cells.

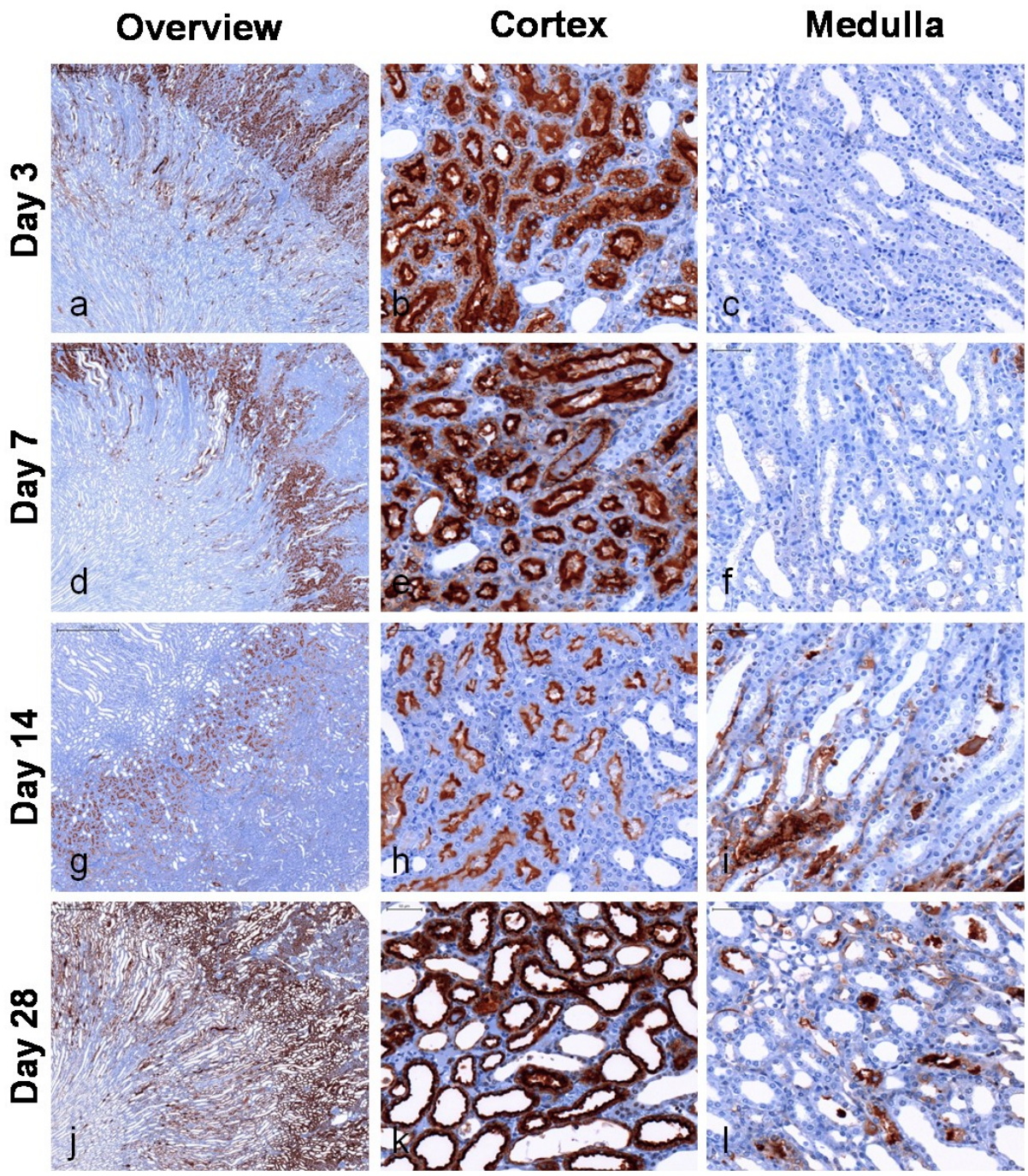

Figure 3-5 Location of Kim-1 protein in renal tissue of female rats treated with 300 mg/kg Vancomycin is shown for each time point of necropsy. An overview picture for each time point (a, d, g, j) shows the whole area from the cortical zone to the medullary papilla. In addition two detailed pictures, either of the cortex (b, e, h, k) or the medulla(c, f, i, l) is given. The magnification of the overview was ~10 times and of the detailed pictures ~70 times.

Most of the medullar staining is located intraluminal and therefore is not a direct protein expression located in this area, but a translocation from the proximal tubules by flow in.

The earliest increase in Kim-1 protein expression was on day 3 with a further increase of protein amount on day 7 (Figure 3-4a-f). Even though there was strong tubular degeneration and dilatation on day 7, the expression of Kim-1 was still located on the apical membrane of the proximal tubules. Also the expression in the outer zone of the medulla showed a high magnitude of expression. However, the staining within cells decreased from day 3 to day 7 and was

replaced by prominent intraluminal amounts of Kim-1 (Figure 3-4 c, f). On day 14 a strong reduction of Kim-1 protein compared to the earlier time points was observed (Figure 3-4 g-i). Only individual areas within the cortex were observed still expressing Kim-1. No to minimal amount of intraluminal Kim-1 protein was detected in the medulla. The amount of Kim-1 protein found on day 28 of high dose (300 mg/kg) Vancomycin treatment, showed an additional increase compared to all other time points (Figure 3-4 j-l). In this group also intracellular Kim-1 was observed in the medullary zone.

In female rats treated with 300 mg/kg Vancomycin for up to 28 days, the renal expression of Kim-1 protein gave comparable results as reported for male rats. The most prominent difference between both sexes was the location of Kim-1 expression.

In female rats Kim-1 was found in the cortical area, without prominent findings in the medulla. Therefore, on day 3 high amount of Kim-1 protein was found in the proximal tubules, while only slight amount of intraluminal Kim-1 protein was observed in the medulla (Figure 3-5. a-c). On day 7 a slight reduction of Kim-1 protein was found compared to day 3, but still with a high and specific expression in the cortex. As reported for male rats, on day 14 only a minimal stain of renal Kim-1 protein could be observed.

In addition, minimal staining of Kim-1 in the medulla was found. However, this staining was limited to cellular casts and proteinaceous droplets. In good relation to male rats, the strongest expression of Kim-1 protein and over the largest area over the tissue was observed on day 28 (Figure 3-5 j-l). In this group also minimal amounts of intracellular Kim-1 protein were found in the medullary zone.

Clusterin

The intrarenal expression of Clusterin showed no gender specific differences in the location of expression, but a treatment and severity-dependent alteration (Figure 3-6 a-l; Figure 3-7 a-l). In contrast to Kim-1, especially for female rats, the area of Clusterin was not primarily limited to the cortical area. On the contrary, the majority of Clusterin protein was found on the cortico-medullary boundary.

On day 3 of high dose (300 mg/kg) Vancomycin treatment in male rats, Clusterin expression was found, with specific tubular staining in the cortical and medullary zone (Figure 3-6 b-c). Significant areas of the cortex remained unstained, also showing no damaged tissue, while the outer medullary zone showed the strongest staining (Figure 3-6 a). On day 7 the expression of renal Clusterin protein in males showed a strong increase in the medulla, but also in the cortical zone (Figure 3-6 d). The medullar staining included intracellular as well as intraluminal parts (Figure 3-6 f). Only minimal amounts of Clusterin protein was detected on day 14, in both cortical and medullary zone (Figure 3-6 g). Clusterin protein staining often correlates with inflammation (Figure 3-6 h). Clusterin in the medulla was formally limited to intercellular or intraluminal fluidal accomulations (Figure 3-6 i). On day 28 male rats showed an increase in Clusterin protein expression compared to day 3 and day 14. However, the area and intensity of Clusterin protein staining was below that observed on day 7 (Figure 3-6 j-l). In female rats (Figure 3-7) the expression pattern of renal Clusterin was comparable to males (Figure 3-6), although the expression area in the cortical zone was slightly higher in female rats (Figure 3-7). On day 3 a high Clusterin expression was observed, both cortical and medullary (Figure 3-7 a-c). The cortical expression of Clusterin in male and female rats was observed in both proximal and distal tubular cells.

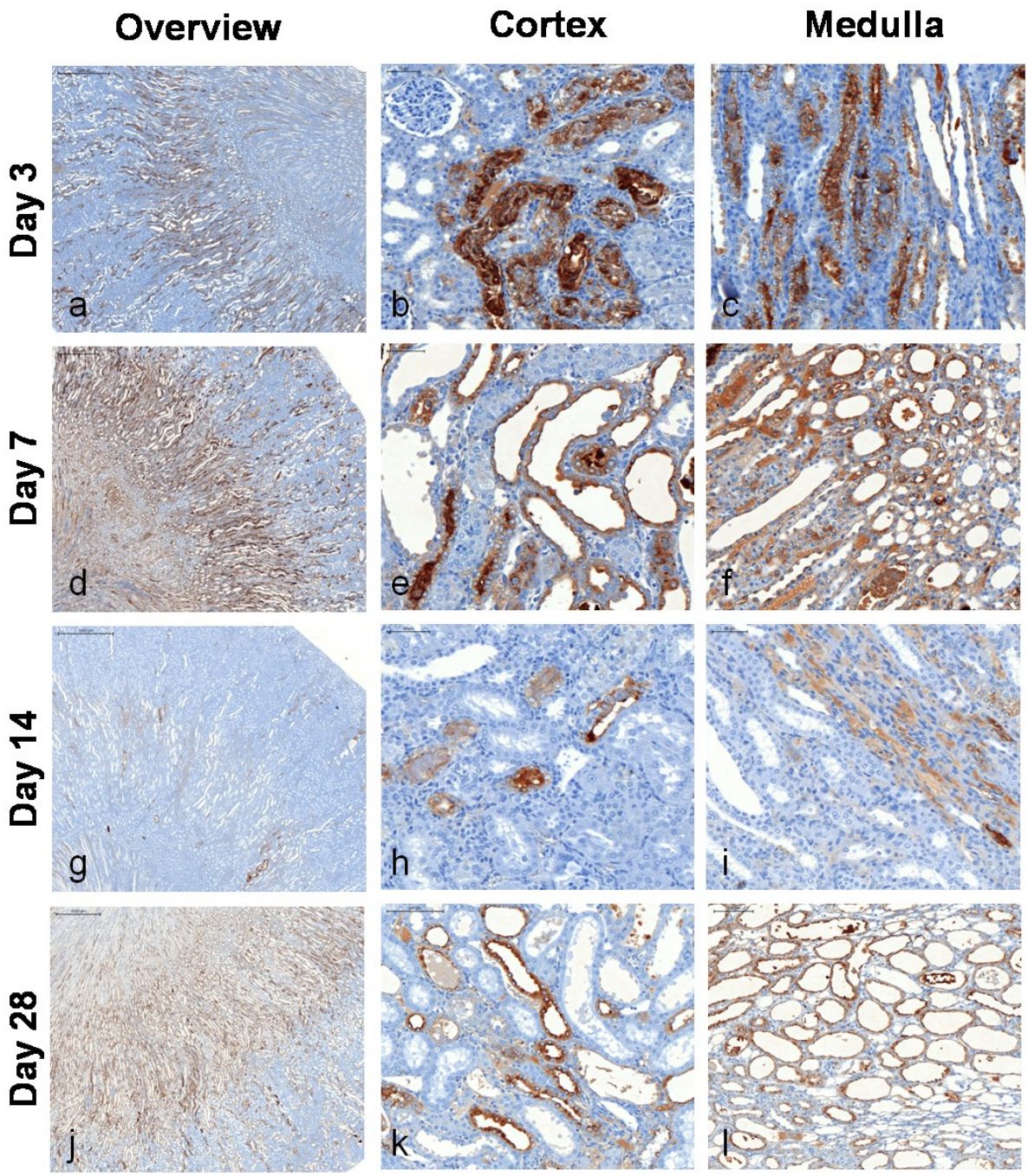

Figure 3-6 Location of Clusterin protein in renal tissue of male rats treated with 300 mg/kg Vancomycin is shown for each time point of necropsy. An overview picture for each time point (a, d, g, j) shows the whole area from the cortical zone to the medullary papilla. In addition two detailed pictures, either of the cortex (b, e, h, k) or the medulla(c, f, i, l) is given. The magnification of the overview was ~10 times and of the detailed pictures ~70 times.

The staining of Clusterin in the outer medullar and inner medullary zone was often, but not exclusively, limited to intracellular staining. Very low amounts of intraluminal Clusterin was observed (Figure 3-7 c). On day7 the Clusterin amount showed a reduction in female rats treated with 300 mg/kg Vancomycin, mainly in the medullary area. An additional reduction in renal clusterin protein expression compared to day 3 was observed on day 14, while the difference between day 7 and day 14 was only marginal (Figure 3-7 g-h).

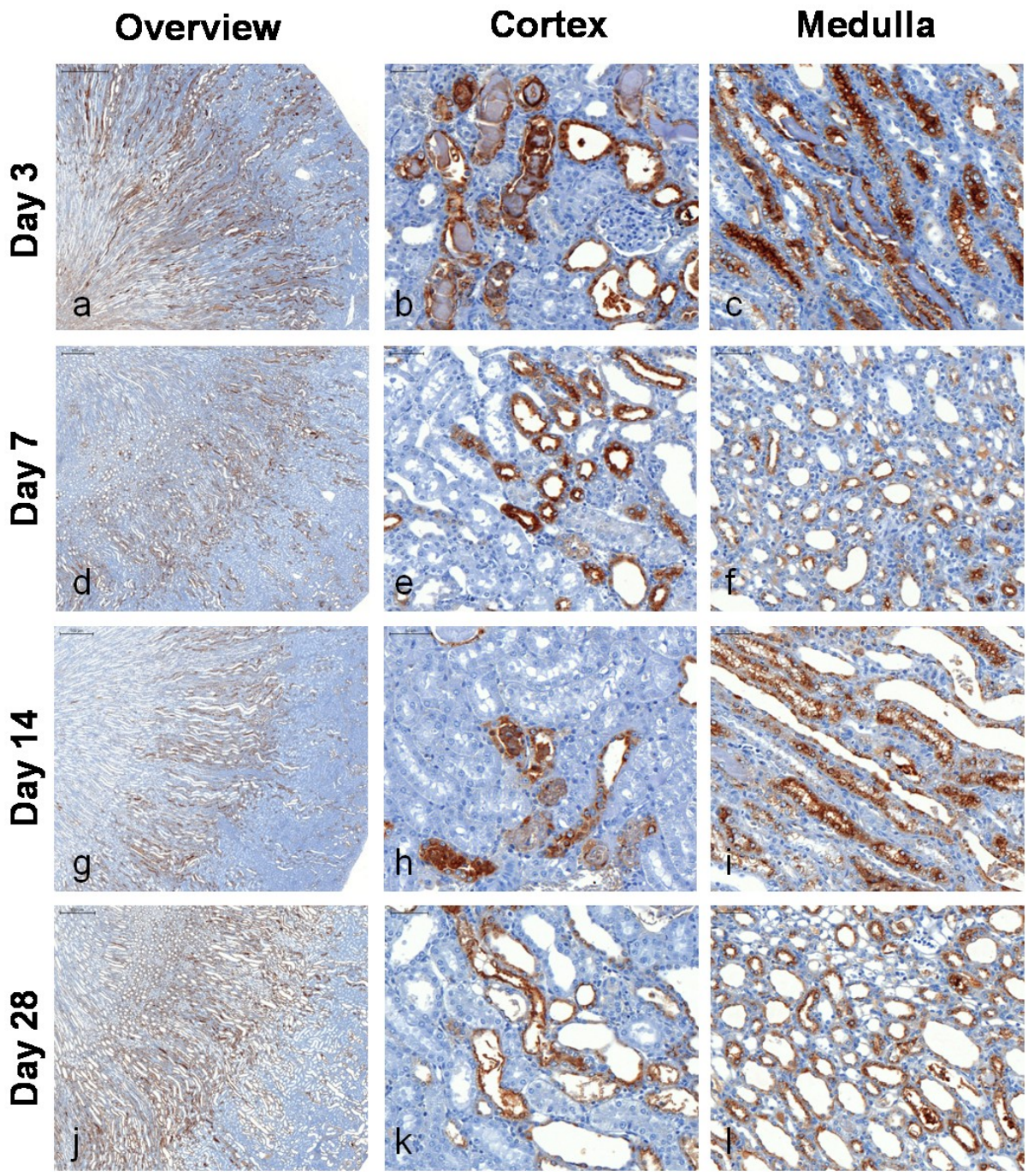

Figure 3-7 Location of Clusterin protein in renal tissue of female rats treated with 300 mg/kg Vancomycin is shown for each time point of necropsy. An overview picture for each time point (a, d, g, j) shows the whole area from the cortical zone to the medullary papilla. In addition two detailed pictures, either of the cortex (b, e, h, k) or the medulla(c, f, i, l) is given. The magnification of the overview was ~10 times and of the detailed pictures ~70 times.

The expression in the medullary zone remained constant, while the corical Clusterin expression was further reduced compared to day 3 and 7 (Figure 3-7 h). The increase on day 28, already described for male rats (Figure 3-6 j-l), was also observed in female (Figure 3-7 j-l) rats, although not as strong.

Osteopontin

In contrast to Kim-1 and Clusterin, Osteopontin was found in higher amounts in renal tissue of animals treated with water for injection or 0.9% saline. A constant low level expression of Osteopontin protein within proximal tubular cells of the cortex and a strong extracellular accumulation over the medullary zone down to the medullary pelvis was observed in both genders (see 5.1 Annex 2). In addition, the bladder also showed strong staining of the extracellular matrix over the whole organ (Annex 2).

However, in male rats treated with 300 mg/kg Vancomycin for three days, a slight but noticeable increase was observed (Figure 3-8 a-c). The main locations of expression were the cortical tubules and the tubular cells of the outer medullary zone (Figure 3-8 b-c). In addition, a staining of the extracellular matrix within the medullar was seen, leading to stronger stains within this area (Figure 3-8 a, c). On day 7, a further increase in male rats of renal Osteopontin was seen (Figure 3-8 d). This increase was caused by staining of proteinaceous droplets within the proximal tubules and of the extracellular matrix within the medulla (Figure 3-8 e-f). The intracellular amount of Osteopontin within renal cells of male rats was unchanged at this time. Over the whole kidney a strong reduction in Osteopontin expression in male rats treated with 300 mg/kg Vancomycin for 14 days was observed (Figure 3-8 g). However, the stained protein was still above the basal expression. Also on day 14 the stain was characterized by proteinaceous droplets and extracellular matrix staining (Figure 3-8 h, i). But also intracellular Ostoepontin was detected in the cortical tubular cells (Figure 3-8 h). On day 28 of Vancomycin treatment with 300 mg/kg, the intensity of Osteopontin staining observed in male rats were between day 3 (Figure 3-8 a) and day 7 (Figure 3-8 d) with a stronger relocation into the medullary area (Figure 3-8 j). Therefore, the remaining Osteopontin at the cortex was limited to luminal accumulations with only individual intracellular staining (Figure 3-8 k). In contrast, the medulla showed very strong extracellular staining over the whole tissue (Figure 3-8 j, l).

In female rats treated with 300 mg/kg Vancomycin, the expression of Osteopontin on day 3 was more pronounced than in male rats of the same time point (Figure 3-9 a-c). This was seen in corical, proximal tubules and in medullary distal tubular cells (Figure 3-9 b, c). Also in female rats a strong staining of the extracellular matrix was observed. Compared to day 3 a reduction of renal Osteopontin over the whole tissue was detected (Figure 3-9 d), while the expression in the proximal tubular cells remained constant. In the medullary zone, especially in the inner area, the amount of strongly stained extracellular matrix components increased strongly (Figure 3-9 f). In contrast to male rats treated with 300 mg/kg Vancomycin for 14 days (Figure 3-8 g-h), the amount of Osteopontin protein in females did not decrease compared to the earlier observations (Figure 3-9 g-h). The staining of Osteopontin, especially in the medullary zone, showed no alteration compared to day 7 (Figure 3-9 f, i). However, the expression within the cortex was slightly reduced but still present in the proximal tubular cells as well as the luminal (Figure 3-9 h). The expression of Osteopontin after 28 days of high dose (300 mg/kg) treatment showed the lowest staining in female rats (Figure 3-9 j-l). The intracellular expression within cortico-tubular cells was reduced to a level near to that in control animals (Figure 3-9 k). However, a very prominent amount of intraluminal Ostoepontin, within proteinaceouce droplets as well as at the extracellular matrix, was observed.

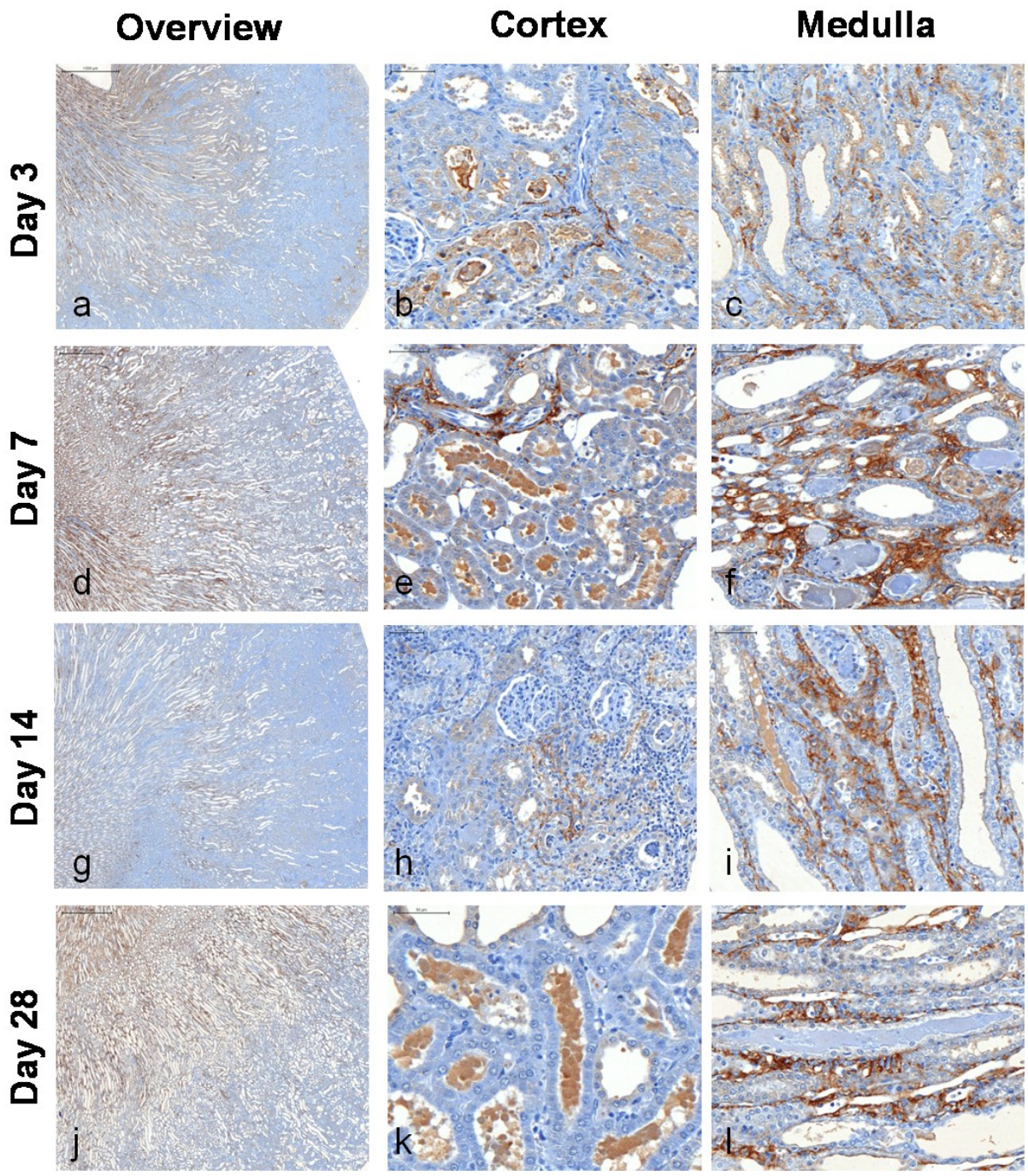

Figure 3-8 Location of Osteopontin protein in renal tissue of male rats treated with 300 mg/kg Vancomycin is shown for each time point of necropsy. An overview picture for each time point (a, d, g, j) shows the whole area from the cortical zone to the medullary papilla. In addition two detailed pictures, either of the cortex (b, e, h, k) or the medulla(c, f, i, l) is given. The magnification of the overview was ~10 times and of the detailed pictures ~70 times.

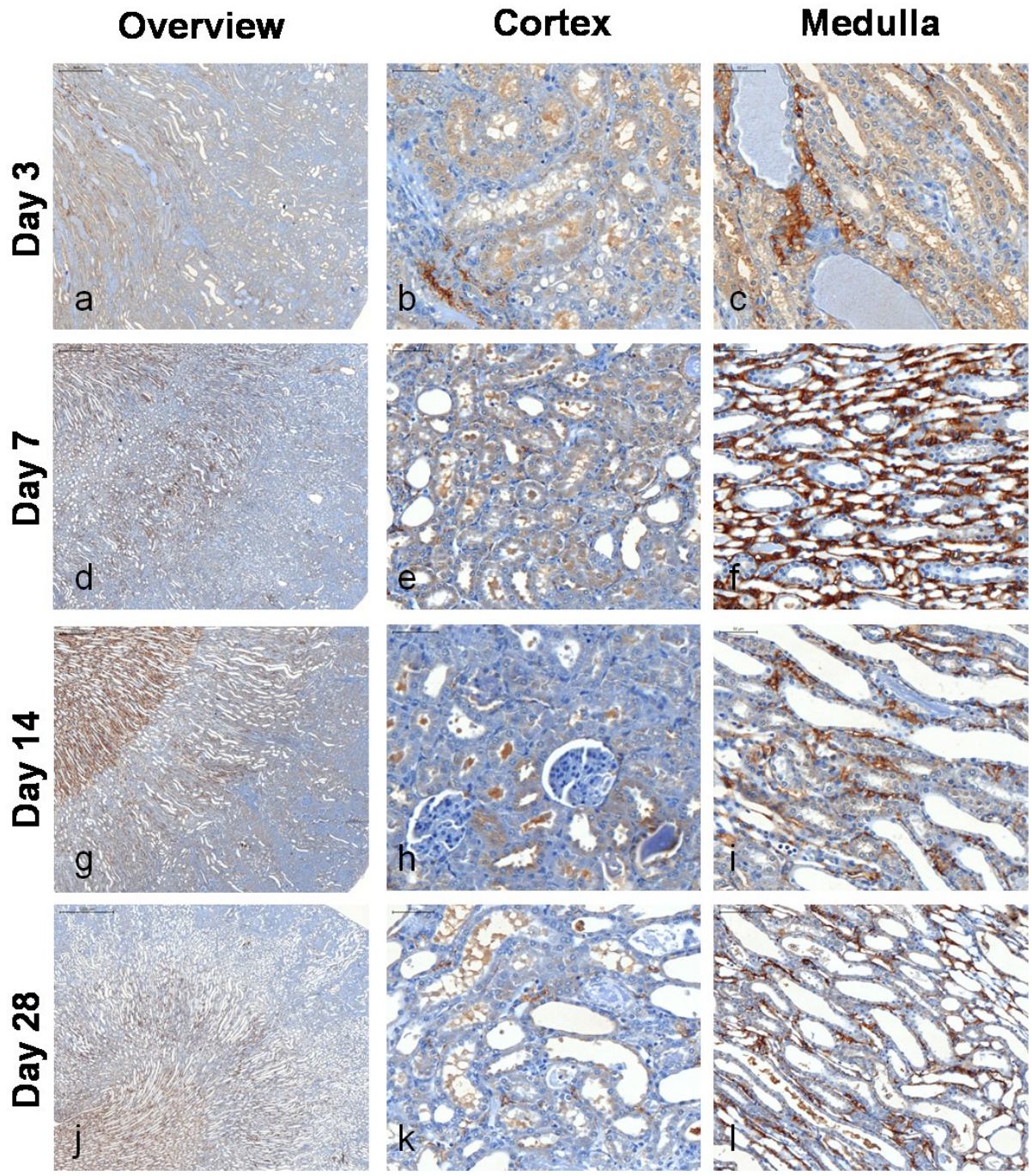

Figure 3-9 Location of Osteopontin protein in renal tissue of female rats treated with 300 mg/kg Vancomycin is shown for each time point of necropsy. An overview picture for each time point (a, d, g, j) shows the whole area from the cortical zone to the medullary papilla. In addition two detailed pictures, either of the cortex (b, e, h, k) or the medulla(c, f, i, l) is given. The magnification of the overview was ~10 times and of the detailed pictures ~70 times.

Expression of the corresponding mRNA of novel urinary protein biomarkers (Vancomycin)

To evaluate if the increase in urinary proteins or renal protein expression was also reflected by gene expression changes, the corresponding data was extracted from the whole genome dataset (3.1.3 Gene expression analyses of renal tissue)

and fold-changes against the average control animals were calculated. The results are given in Figure 3-10 (male) and Figure 3-11 (female).

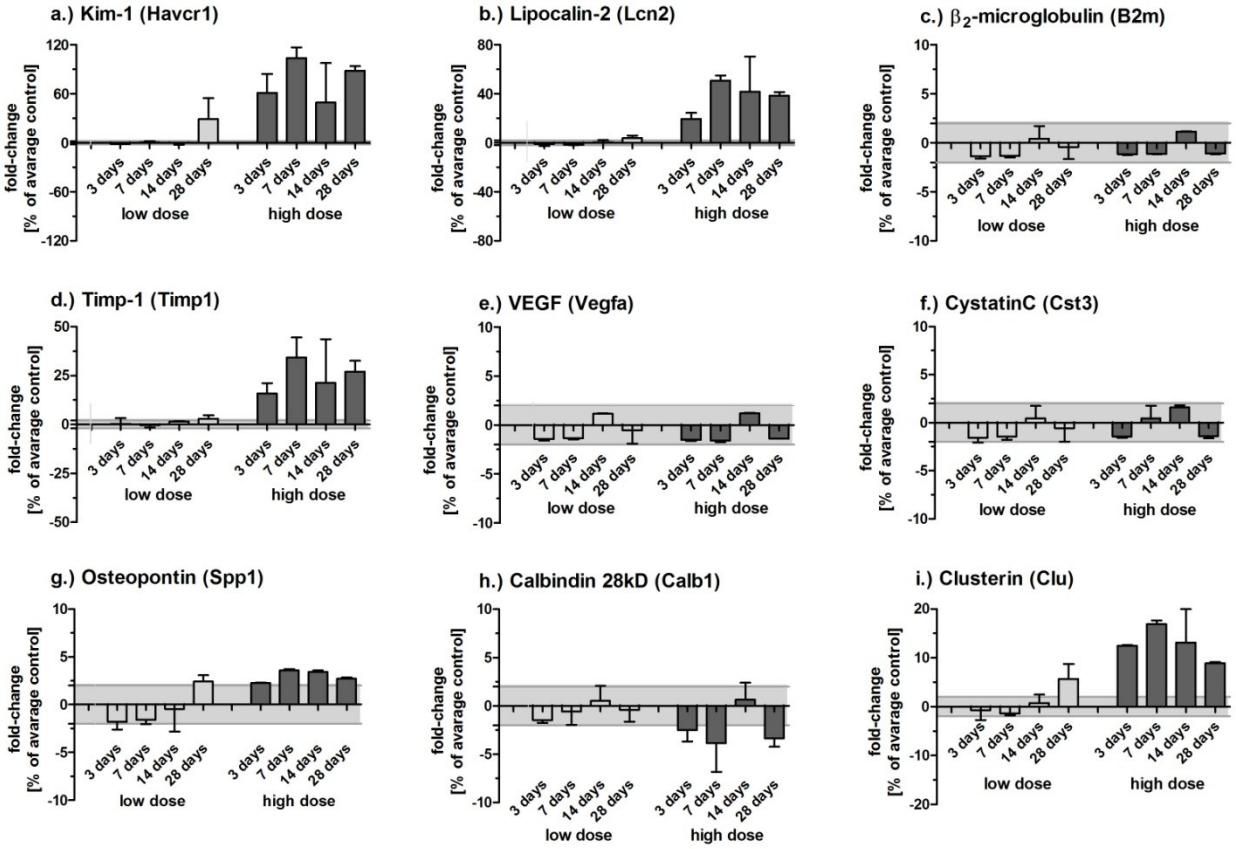

Figure 3-10 Gene expression changes of (a) Kim-1, (b) Lipocalin-2, (c) β2m, (d) Timp-1, (e) VEGF, (f) CystatinC, (g) Osteopontin, (h), Calbindin , (i) Clusterin determined in renal tissue of male rats treated with Vancomycin (low dose: 50 mg/kg (light grey); high dose: 300 mg/kg (dark grey)) for 3 days, 7 days, 14 days, and 28 days. In parenthesis the gene symbols are shown. Data are presented as means of the fold-changes over the average of the time matched control animals (bar ± SD; n=3). The range for -2 to +2 is indicated as light grey bands to indicate the strength of alteration.

In both genders almost all gene expression changes appeared in the high dose group (300 mg/kg) of Vancomycin treated animals. Exceptions were the animals of the low dose group (50 mg/kg) treated for 28 days with Vancomycin. This was found in both sexes, but was more pronounced in male rats. The highest fold-change in male rats was observed for Kim-1 (Figure 3-10 a), reaching up to ~107-fold on day 7. On days 3, 14 and 28 a fold-change of ≥ 50 was measured. However, on day 14 the variation within the group of three animals was the highest reaching from 7 to 102 fold induction. Other transcripts showing strong induction were Lipocalin-2 (up to 50-fold), Timp-1 (up to 35-fold) and Clusterin (up to 17-fold) (Figure 3-10 b, d, g). All of these transcripts showed the highest intragroup variance after 14 days of treatment; even this was not nescessarily the lowest value observed. Therefore Lipocalin-2 showed a comparable fold-change on day 14 and 28 (40-fold) (Figure 3-10 b) and Clusterin showed a 5-fold lowered value on day 28 compared to day 14 (Figure 3-10 i). Only a slight increase in the expression level for male rats was observed for Osteopontin reaching to a maximum of 3.5-fold with the lowest values on day 3 (2.2) and day 28 (2.7) (Figure 3-10 g). In constrast to the transcripts mentioned above, no increased variation within the 14 day high dose (300 mg/kg) treatment group could be observed. Calbindin showed no dose- or time-dependent increase but a decrease in gene expression (Figure 3-10 h). Therefore a repression of -2.5 on day 3, -3.8 on day 7, and -3.4 on day 28 was detected. No

changes were observed for day 14. No alterations on mRNA level were found for β2m, VEGF, and CystatinC, nor in the low (50 mg/kg) neither in high dose (300 mg/kg) treated animals (Figure 3-10 c, e, f).

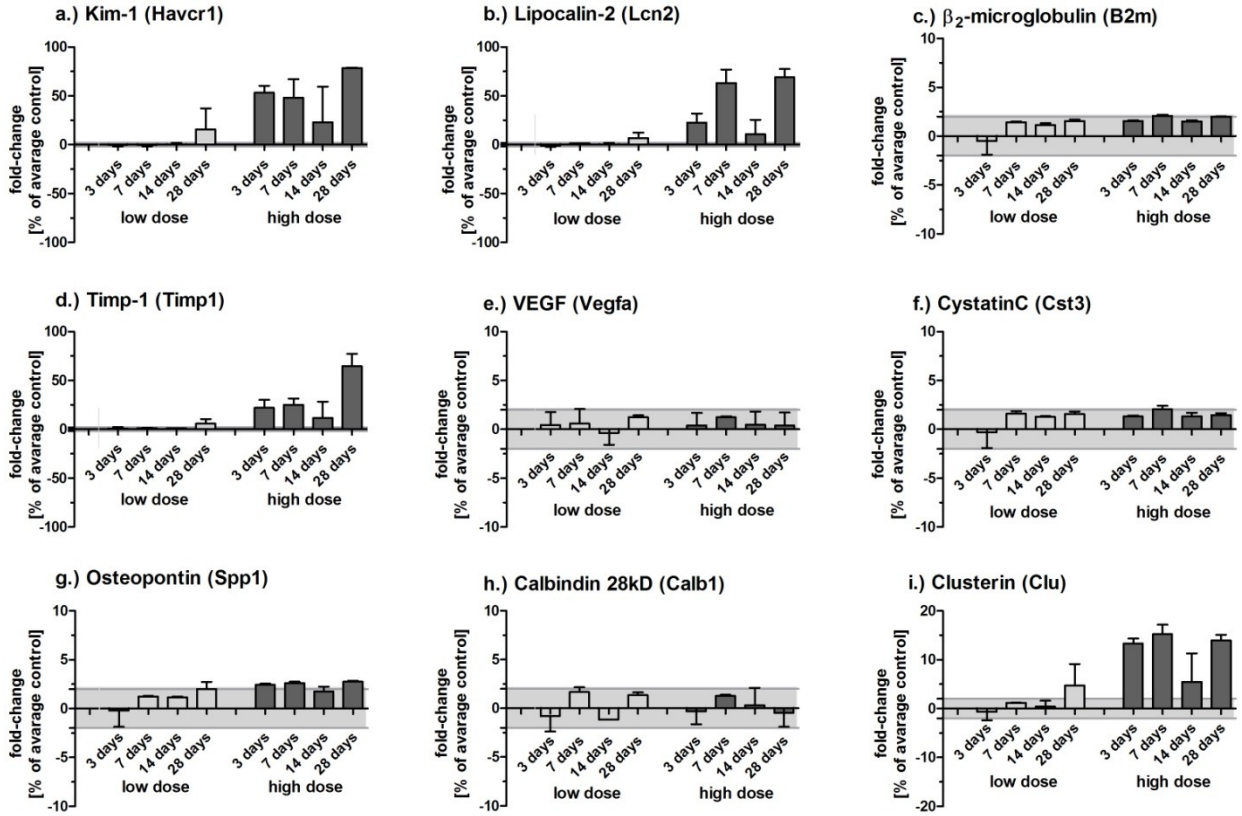

Figure 3-11 Gene expression changes of (a) Kim-1, (b) Lipocalin-2, (c) β2m, (d) Timp-1, (e) VEGF, (f) CystatinC, (g) Osteopontin, (h), Calbindin , (i) Clusterin determined in renal tissue of female rats treated with Vancomycin (low dose: 50 mg/kg (light grey); high dose: 300 mg/kg (dark grey)) for 3 days, 7 days, 14 days, and 28 days. In parenthesis the gene symbols are shown. Data are presented as means of the fold-changes over the average of the time matched control animals as the mean (bar ± SD; n=3). The range for -2 to +2 is indicated as light grey bands to indicate the strength of alteration.

In female animals the highest fold-indiction was also observed from Kim-1 (~78-fold), but at the latest time point (Figure 3-11 a). In addition, no prominent increase from day 3 (~53-fold) to day 7 (~48-fold) was observed. However, as observed for male rats, the Kim-1 gene expression on day 14 showed a strong variation, from 1.4- to 65- fold. Also comparable to male rats, Lipocalin-2 (up to ~70-fold), Timp-1 (up to ~65-fold) and Clusterin (up to ~15-fold) showed the most prominent alterations at the transcript-level (Figure 3-11 b, d, i). Lipocalin-2 showed only a small induction on day 14 (~11-fold) compared to days 7 (~63-fold) and 28 (~70-fold). However, no increased variance for the 14 day high dose (300 mg/kg) treatment group was detected (Figure 3-11 b). Timp-1 remained relativly constant from day 3 (~22-fold) to day 7 (~25-fold), with a smaller increase on day 14 (~11-fold) (Figure 3-11 d). Timp-1 showed the highest expression in female rats treated with 300 mg/kg Vancomycin on day 28 of treatment (~65 fold). In addition, the gene expression of Clusterin showed a different expression pattern over time compared to male rats. On days 3 (~13-fold), day 7 (~15-fold) and 28 (~14-fold) a relatively constant fold-change increase was observed, while on day 14 the fold-induction was only 5.5-fold (Figure 3-11 i). The gene expression of Osteopontin showed only slight alterations, of approximately 2.5-fold on days 3, 7 and 28 with no change seen on day 14 to (Figure 3-11 g).

Females showed no alterations on mRNA level for β2m, VEGF or CystatinC in the low (50 mg/kg) and high dose (300 mg/kg) treated animals (Figure 3-11 c, e, f). In addition, Calbindin 28kD remained unchanged over time and dose (Figure 3-11 h).

3.1.1.2 Discussion and Conclusion (Vancomycin)

Within this study Vancomycin at doses of 50 mg/kg (low dose) and 300 mg/kg (high dose) caused severe renal damage specifically to the tubular system. This was reflected by the strength of response of several of the urinary protein biomarkers. In addition, the traditional parameters, serum creatinine and blood urea nitrogen, showed a strong response, probably due to the severity of nephrotoxicity induced. The fact that beside these two parameters also urinary glucose showed a dose and treatment dependent increase (Table 3-4), without stong alterations on serum level (Table 3-3) clearly indicates the detrimental functional effect on proximal tubular cells. Under physiological conditions, renal proximal tubular cells reabsorb tubular glucose by the Na^+/glucose co-transporter SGLT1 in the S3 segment or the SGLT2 in the S1/2 segment [Wright et al., 2007]. Other effected urinary parameters, like urinary output, which showed a time and dose dependent decrease, mainly in male rats, and the strong increase in urinary total protein excretion, corroborate these findings. However, compared to the increase in urinary protein biomarkers, the change in total urinary protein was only observed on day 28 of high dose (300 mg/kg) treated animals [Fuchs et al., 2011]. In contrast to urine volume, urinary creatinine excretion also showed some significant changes. Therefore, it was decided to normalize urinary protein biomarkers with urinary creatinine. This should take in to account any variations in urinary volume and composition. Several publications have focused on novel urinary protein biomarkers and used this kind of normalization, which results in a better comparability to publicly available data.
Several indications of inflammatory processes, within the hemogram (Table 3-5) as well as cellular infiltration within renal tissue (Table 3-1) were observed. A major impact was observed on white blood cells, while red blood cells showed only slight changes. Inflammatory processes are described to play a key role in several kinds of renal injury and diseases, although the mechanism(s) are not yet completely understood on a molecular level. A mechanistic evaluation of inflammatory processes in Vancomycin induced nephrotoxicity is presented in section 3.1.3 Gene expression analyses of renal tissue.
The strong effects caused by Vancomycin correlates well with the dose range finding study. Data of this study are already reported [Fuchs et al., 2012].

The best performing urinary biomarkers were Kim-1, Clusterin and Osteopontin, as reflected by the AUROC values (Table 3-6). Kim-1, one of the most promising urinary biomarkers to bridge between different species and renal diseases, showed a good correlation to the histopathological findings in both genders (AUROC values ♂ 0.95; ♀ 0.90). However, the magnitude of urinary Kim-1 increase in female rats was much higher (Figure 3-2a; Figure 3-3a), which was not reflected histopathologically (Table 3-1). In contrast, male rats showed a higher treatment dependent induction of Havcr1 transcripts, which is the related gene to the Kim-1 protein, compared to female rats (Figure 3-10; Figure 3-11). An important observation in urinary Kim-1 excretion as well as for several other urinary biomarkers (see below) was the absence (or only a weak) increase after 14 days. The 7 days that was treatment free up to day 14 reflected a recovery of the damaged renal tissue. This was also obvious when referring the histopathological observations (Table 3-1). The fact that no further increase in urinary Kim-1 could be detected showed that this biomarker has the potential to function as a monitoring parameter for renal health status, but also a limitation of sensitivity. Because of this

discrepancy between the observed minimal to mild tubular effects at this time point, and the lack of increase in urinary Kim-1, the detection of only slight renal injury seems not to be possible by using this urinary biomarker. However, because only the ectodomain of Kim-1, which is a transmembran receptor, is released into urine, the question arrises if the total amount of Kim-1 protein within the kidney is reduced or only the shedding of the ectodomain is inhibited. By immunohistochemical analysis of renal Kim-1 protein, it could be shown that the total expression of Kim-1 protein depends on the underlying renal damage. Therefore, the absence of urinary Kim-1 elevation on treatment day 14 is a direct result of the lowered expression of Kim-1 protein within the kidney. Overall the detection of renal Kim-1 protein seems to be more sensitive than the detection of urinary protein. Therefore, the screening of Kim-1 by using tissue arrays is a valide method for the assessment of renal diseases and drug induced insults. In both male and female rats, generally the major origin of Kim-1 expression is located in the renal cortex but with a wider spread in males compared to female rats. The stronger limitation in female rats can be due to the fact that the severity in females was lower than that of male rats. In addition, even on day 3 male rats treated with 300 mg/kg Vancomycin showed a similar impact on renal tissue to females, and showing the same widespread expression of Kim-1. Therefore, the location of Kim-1 synthesis seems to be slightly different between sexes and can be assumed to be a major reason for the different magnitude in urinary Kim-1 excretion. The difference in the amount of renal Kim-1 can also be assumed to be involved in the progression of insult. Kim-1 is described to be involved in the regulation of Th1 and Th2 cell-mediated immunity [Mcintire et al., 2003; Mariat et al., 2005; Curtiss et al., 2007], which itself can lead to an increased insult on renal tubular cells. It has been described that Kim-1 is involved in the progress of Cisplatin induced nephrotoxicity [Nozaki et al., 2011]. Finally, the deterioration in the state of renal health observed on day 28 of treatment, independent of two additional recovery periods is also well reflected by the urinary Kim-1 excretion as well as in renal Kim-1 expression either on protein or on mRNA level. This points to the fact that Kim-1 can be used independently of the duration of the treatment or the interval of drug application because it´s exclusive link to the condition of the kidney.

High similarities to Kim-1 excretion were observed for Clusterin, which is also one of the FDA, EMA and PMDA accepted urinary biomarkers [Fuchs et al., 2011]. Compared to Kim-1 the ROC analysis delivered better values for Clusterin (♂ 0.98; ♀ 0.94), which could be due to the higher urinary excretion of Clusterin on treatment day 14 compared to the control animals (Figure 3-2i Figure 3-3i) and the higher total magnitude of urinary Clusterin. Therefore, the only minimal to mild histopathological observation (Table 3-1) are better reflected by urinary Clusterin, leading to a higher sensitivity of this biomarker. This is especially true for male rats, but also with some limitation for females. In contrast to renal Kim-1 expression, Clusterin showed an expression within renal tissue over almost all different tubules. Therefore, the specificity of Clusterin is weaker than Kim-1 because the location of the kidney injury cannot be finally linked to any specific tubular segment. Renal Clusterin protein expression reflected the urinary excretion of the protein very well. The protein expression of Clusterin was strongly reduced on day 14 and was linked to the lowered urinary excretion of this protein. The total amount of urinary Clusterin was much higher (up to 1000-fold) compared to Kim-1, reflecting the tubular specific damage caused by Vancomycin treatment. Therefore, combining the measurement of Kim-1 and Clusterin can be used to distinguish between proximal tubular alterations and general tubular damage.

The urinary excretion of Clusterin, after 28 days of treatment, including three recovery periods, delivered values between that of day 3 and day 7 for male rats and the highest values in females (Figure 3-2i; Figure 3-3i). This was not reflected by protein expression in renal tissue or on the gene expression level, were male rats showed the lowest expression of Clu over all high dose (300 mg/kg) animals (Figure 3-10i). In renal tissue the strongest staining was observed for male rats on day 7 and for females on day 3. This may be an indication of a different mechanism of involvement of Clusterin in the progression of renal injury, even only truth for a small time shift. Because Clusterin is

described to be involved in a multitude of cellular processes, including, immune response via the complementary system [Correa-Rotter et al., 1992], apoptosis [French et al., 1994; Hara et al., 2001], growth, proliferation and differentiation [French et al., 1993; Witzgall et al., 1994], it can not be described which is the major factor for the reduced amount of renal protein. The fact that the urinary amount stayed relatively unaltered can be explained by the massive break-down of cells at this time point and as a consequence the release of the still present protein into the primary urine.

Osteopontin, which performed the best within this study, is in contrast to Kim-1 and Clusterin not qualified by the FDA, EMA and PMDA. The calculated AUROC (♂ 0.98; ♀ 0.94) values were identical to that of Clusterin and therefore above the evalulated values of Kim-1. However, the excretion pattern of urinary Osteopontin showed a clear difference over time in relation to the other two markers. The first two time points showed a perfect correlation to the histopathological findings, with the highest increase on day 3 in male rats with a slightly lowered increase on day 7 (Figure 3-2 g) and the time dependent increase from day 3 to day 7 in females (Figure 3-3 g). Urinary Osteopontin excretion showed only a slight increase on treatment day 14 and an additional decrease in day 28. This increase at this late time point delievered statistically significantly elevated level of Osteopontin, the strength of which was not reflected by the magnitude of this urinary protein. The reason for this became clear by evaluating the amount and distribution of Osteopontin in renal tissue. While at the first two time points the majority of renal Osteopontin was observed to be intracellular in tubular cells, with an increased amount of extracellular Osteopontin on day 7, at the later time points the staining of Osteopontin was almost completely limited to the extracellular matrix. Because Osteopontin is described to bind to collagen [Chen at al., 1992] this urinary protein biomarker has a clear limitation for usability in chronic rodent studies where interstitial fibrosis takes place. Although the protein expression within the kidney remained constant over the treatment time, the release into urine was reduced. Additionally, the immobilized Osteopontin bound to collagen can bridge different phases of regeneration, as observed on day 14 in male rats (Figure 3-2 g). Ostepontin can be released with collagen in cases of regeneration and the related degradation of collagen fibers (Figure 3-8 d-f, g-i). This will lead to an underestimation of the regeneration of renal tissue but also will increase the sensitivity compared to other biomarkers, e.g. Kim-1, which showed no significant increase on day 14. The fact that only small fold-inductions of Spp1, the Osteopontin related gene, were observed (Figure 3-10g, Figure 3-11g), together with the higher basal expression of renal protein, indicates that the amount of expressed Osteopontin in renal tubular cells is constantly higher compared to Kim-1 and Osteopontin. Therefore, it can be hypothesised that Osteopontin can be used for a very early prediction of drug-induced tubular damage. Further studies will be needed with earlier time point e.g. the first hours after drug application, to evaluate the potential of Osteopontin and to define the framework for a potential qualification of this valuable biomarker. The potential involvement of Osteopontin in the progression of kidney injury should be taken into account. The fact that Osteopontin is described to be involved in neutrophil migration by chemotoxis of a cleavage product (Kim et al., 2008) can increase inflammatory processes by Osteopontin accumulation within renal tissue. Additionally, it has been reported that the activation of NF-κB, by binding to αvβ3 integrin of endothelial cells, leads to a protective effect of Osteopontin against apoptosis [Mazzali et al., 2002].

Another well performing (non-qualified) urinary biomarker was Calbindin (♂ 0.98; ♀ 0.88). In contrast to Kim-1, which is proximal tubular specific and Clusterin/ Osteopontin which are specific for general tubular damage, Calbindin is described to be specific for distal tubular and collecting duct injury. In comparison to the three biomarkers mentioned above, the different in diagnostic performance between male and female rats was more pronounced for this biomarker. Distal tubular damage, which is rarely reported for Vancomycin treatment, therefore the slight but significant increase in urinary Calbindin at the earlier time points and the massive increase on treatment day 28 point to the fact that distal tubular damage takes place as a secondary effect caused by the predominant proteinuria on day 28. However, the fact

that the calculated AUROC values and in general the increase in urinary Calbindin (Figure 3-2 h, Figure 3-3 h) showed a good correlation to tubular degeneration, without any discrimination of the different types of tubules, show the high sensitivity of this urinary biomarker. An obvious influence of urinary calcium concentrations on the excretion of Calbindin could be excluded; even though Calbindin is a family member of vitamin D-dependent calcium-binding proteins [Fuchs et al., 2011]. Because in other studies it has been reported that Calbindin showed a dose-dependent decrease [Hoffman et al., 2010] it can be hypothised that beside kidney calcification, as reported for Ciclosporin A [Aicher et al., 1997] also other mechanisms related to renal damage are involved in the excretion of Calbindin. Therefore, the regulation of Calbindin expression seems to be exclusively regulated by alternative pathways, such as by induction though the parathyroid hormone, which is a key molecule in calcium homestasis [Hemmingsen et al., 2009]. This assumption is supported by the observation that serum phosphate, an inducer of the parathyroid hormone [Nakajima et al., 2009], was increased in dose-dependent manner on day 28 (data not shown).

The induction of Calbindin protein seems not to be regulated on gene expression level, because of the absence of any increase in mRNA. Male rats of the high dose (300 mg/kg) group showed a decrease in Calb1 mRNA without any effect on urinary protein level. Taken together Calbindin performed very well in this study and the fact that it is one of the few described urinary biomarkers which are specific for distal tubular damage, makes this urinary biomarker an important addition to the panel of urinary biomarkers.

A gender dependent response was observed for Timp-1, also a non qualified biomarker, with a clearly better performance in female rats (♂ 0.74; ♀ 0.94). While the increase in male rats was only very slight, except on treatment day 28, and the basal excretion of Timp-1 protein was higher compared to female rats, the correlation of increased amount of urinary Timp-1 to histopathological findings was poor. This discrepancy between both genders could not be confirmed by transcriptional analysis. In this case the measurement of Timp1 mRNA delivered the best correlation to the histopathological findings - when both genders were taken into account. Another difference was the increase in urinary Timp-1 protein in male rats with aging, while the amount of Timp-1 in females stayed constant. It has been reported that differences in Timp-1 and MMP-9, the strongest inhibited matrix metalloprotease of Timp-1 protein, in male and female rats are present in rat aortic smooth muscle cells [Woodrum et al., 2005]. However, because it can be assumed that the functional role of Timp-1/ MMP-9 on the regulation of extracellular matrix degradation, is similar in almost all tissues expressing Timp-1, this protein can delivered additional information in relation to the development of tubulointerstitial fibrosis, by accumulation of Timp-1 and the resulting imbalance between this protein and MMPs [Schnaper et al., 1995]. This is in line with the observation of the highest increase of urinary Timp-1 protein in male rats on day 28, with the increasing amounts of fibrotic fibers within high dose (300 mg/kg) treated animals over time and to the strongly lowered increase of Osteopontin mentioned above. In contrast to Osteopontin, Timp-1 is therefore a potential candidate to monitor chronic kidney diseases, which already has been reported with increasing amount of urinary Timp-1 [Liu et al., 2006]. Besides its extracellular inhibitory activity, Timp-1 has in addition anti-apoptotic and pro-proliferatory properties [Schnaper et al., 1995].

In contrast to the biomarkers mentioned so far, which are more or less exclusively expressed within renal tissue, Cystatin C, a qualified biomarker, is not described to be elevated in renal damage. Cystatin C is considered to be a proximal tubular biomarker, based on the physiological process of reabsoption of freely circulating Cystatin C by proximal tubular cells. If this functional capacity is limited by cellular break-down an increase in urinary Cystatin C can be detected. Therefore, the general mechanism of increase in urine is comparable to elevated urinary glucose excretion if serum glucose remains constant. The extra renal origin of the Cystatin C is also reflected by analyzing transcriptional changes. However, the performance of Cystatin C within this Vancomycin study was quite poor (♂ 0.73; ♀ 0.68). Only in male rats treated for 7 day with 300 mg/kg Vancomycin was a significant elevation in urinary Cystatin C observed.

The poor performance of this extra renal urinary biomarker was highlighted by the creatinine showed a strong decline in all high dose (300 mg/kg) treated animals. Thus less Cystatin C can enter the tubular lumen leading to no or only weak alterations in urinary excretion. This assumption was confirmed by comparison of the increase in urinary Cystatin C in male low dose (50 mg/kg) treated animals for 7 days and the related creatinine clearance/ GFR which also showed an increase in filtration properties. Therefore, the specificity of Cystatin C as a functional biomarker for proximal tubular damage is questionable. However, Cystatin C is widely used as alternative method to creatinine clearance because of the dependency of this parameter on age, gender and muscle mass [Fuchs et al 2011]. The parallel detection of Cystatin C in serum and urine to calculate the Cystatin C clearance would give the benefit of being able to evaluate the renal function on the filtration level. In addition, only minimal gender differences in the basal excretion of Cystatin C were observed. This fact is important because of the physiological proteinuria described for rats, leading to a higher excretion of urinary total protein in male rats (Table 3-4). The amount of Cystatin C seems not to be strongly affected by this physiological process. Independently, it has been reported that urinary Cystatin C has been used in clinical studies for the detection of structural and functional renal tubular impairment in adults and children without any observed influence of the glomerular filtration rate [Herget-Rosenthal et al., 2007]. Therefore, further investigations are needed to avoid the underestimation of the potential of this qualified biomarker.

β2m is a qualified functional urinary biomarker which is released into the blood during cellular turnover. Therefore, the results derived for β2m in this study were similar to Cystatin C. The diagnostic performance was poor in both male and female rats (♂ 0.76; ♀ 0.70), even if individual animals showed a large increase (Figure 3-2c Figure 3-3c). In contrast to Cystatin C the observed gender difference in the basal urinary excretion was more prominent, reaching ~6-fold higher level in male rats, but this was also masked by the fluctuation within the GFR in male rats.

By taking the observations of Cystatin C and β2m together it is more likely that these two urinary biomarkers can potentially be used as predictors of glomerular damage. Because of the increase in protein load by break-down of the filter barrier a saturation of the transport properties of tubular cells will lead to an increase in urinary protein. This is in good correlation to previously reported findings, by comparing the diagnostic performance of these biomarkers with only glomerulare observations [Dieterle et al., 2010]. Finally, an intrarenal influence of Cystatin C and β2m can be excluded because of no time or dose dependent alterations on gene expression level.

Lipocalin-2, also known as NGAL, also showed poor diagnostic performance within this study (♂ 0.69; ♀ 0.76). Although this urinary protein biomarker is not yet qualified by the regulatory authorities for preclinical or clinical use; it is one of the most promising urinary parameters studied in clinical trial settings [Mishra et al., 2003, Ding et al., 2007, Wagener et al., 2008]. The disadvantage of NGAL is its involvement in the acute phase response [Hoffmann et al., 2010]. Because of its systemic expression and the free glomerulation filtering, systemic inflammatory processes can lead to an increase in urinary excretion of NGAL. Therefore, the complete health status of the test subject has to be monitored to exclude sepsis and other inflammatory processes. In case of this study the observed increase in urinary NGAL delivered good results for treatment day 7 for male rats and on treatment day 3 and 7 for females. Because of the limited magnitude of increase in relation to the basal excretion of NGAL, the discrimination between affected and non affected animals was not always possible. In addition, the fact that no massive increase in urinary NGAL was observed, even though there were prominent systemic and renal inflammatory processes observed (Table 3-1, Table **3-5**) together with severe histopathological findings, lead to the suggestion that different extra- and intrarenal factors influenced the expression and excretion of NGAL. The impact of specific drug induced mechanisms was previously reported for Gentamicin, Ochratoxin A and BI-3 [Hoffman et al., 2010], and NGAL was only a good predictor for gentamicin induced nephrotoxicity.

In contrast to the findings of urinary NGAL protein, the fold-induction of Lcn2, the corresponding transcript, delivered a much better prediction of the health status of the kidney, in both male and female rats. Because Lcn2 has been reported in several independent toxicogenomics approaches [Dieterich et al, 2009, Kondo et al., 2009, Wang et al., 2008], it can be suggested that changes at the mRNA level in response to cell damage are not necessarily paralleled by increased protein levels and active secretion/leakage into the tubular convolute. Additionally, there is major evidence suggesting that Lcn2 is located in the distal tubule of the nephron, while the protein is also located in the proximal tubule, so the protein is probably reabsorbed [Paragas et al., 2011]. Therefore, the specificity of NGAL mRNA is also questionable.

Finally, the non qualified vascular endothelial growth factor (VEGF) showed differences between the genders (♂ 0.89; ♀ 0.67). While female rats showed no alteration in urinary VEGF, it can be suggested that in general the source of VEGF seems to be intra-renal, and was confirmed by the absence of any alterations on gene expression level in male and female rats. However, its performance for identifying acute or chronic kidney disease seems to be limited. It was already reported that VEGF lead to a slowdown in progression of renal injury by reducing renal fibrosis [Kang et al., 2001], and preserves renal microvessel structure [Leonard et al., 2008]. In contrast to female rats, males showed a slight dose-dependent decrease in urinary VEGF that may explain the better diagnostic potential in males. However, because the decrease in urinary VEGF has been described in the context of idiopathic membranous glomerulonephritis (MGN) [Honkanen et al., 2000] and the AUROCs were calculated by using tubular degeneration as the comparator, this high AUROC seems to be calculated by chance in respect of the comparator. However, because MGN is caused by immune complex formation in the glomerulus, formed by antibodies binding to antigens in the basement membrane, leading to activation of the C5b –C9 complements a membrane attack complex (MAC) is formed on the glomerular epithelial cells [Beck et al., 2010]. In HE staining light microscopically observations, the glomeruli seem to be unaffected by Vanomycin.

So far, many contradictory findings were reported for urinary VEGF to detecte AKI. However, because of the central role in reno-protection and the potential to serve as an intrinsic biomarker for glomerular damage, further investigations are needed to identify potential endpoints which can be predicted by VEGF in a sensitive and specific way.

3.1.1.3 Results (Cisplatin)

Histopathological observation (Cisplatin)

In gross pathology bilateral pale discoloration of the kidneys was found earliest on day 8 in individual low (0.3 mg/kg) and high (0.6 mg/kg) dose treated male rats. In addition, rats treated with 0.6 mg/kg Cisplatin showed an enlargement of the kidneys. From day 15 on also individual female rats showed pale discoloration as well as kidney enlargement and a granular surface of the kidney, especially in the high dose group (0.6 mg/kg). The same observations were observed on day 29. An overview of the results is summarized in Table 3-7.

Microscopically, no Cisplatin-related alterations were detected in animals treated with 0.3 mg/kg, at any time point. Therefore, all further data and descriptions refer to animals treated with 0.6 mg/kg Cisplatin.

The earliest findings (on day 4) were minimal multifocal single cell necroses or tubular cells in two of the five male rats. On day 8 minimal to moderate tubular degeneration and up to mild tubular necroses were more prominent, still limited to male rats. In contrast, on day 15 one female and all male rats showed minimal to moderate multifocal tubular degeneration. In addition, the female rats and one male rat showed concomitant multifocal tubular dilation, while tubular necroses were present in the female and three male rats. On day 15 also minimal and a mild infiltration with mononuclear inflammatory cells were present in one male and one female, respectively. The last time point (day 29) showed comparable findings to those on day 15. Also, all five male animals showed minimal to moderate multifocal tubular degeneration, while females revealed no specific findings. In addition to the tubular insult, minimal to mild eosinophilic casts were present in single animals of the high dose treated animals (0.6 mg/kg) on days 8, 15 and 29.

Treatment-related findings in other organs were observed, as early as day 8. Gastro-intestinal alterations, like focal erosion of the gastric mucosa with focal edema, hemorrhage and mixed cell infiltration were detected. Subsequently, in individual animals the forestomach mucosa showed mild epithelial hyperplasia and the ceacum showed focal mild submucosal hemorrhages. The same findings were seen on day 15 but not on day 29. In addition, animals treated for 14 days also mild to moderate lymphoid depletion in the thymus were present in three male and one female rat.

Beside tubular degeneration, also regeneration attempts of the tubular lining epithelium were observed. These epithelial cells were characterized by large pale cells showing anisocytosis and anisokaryosis. The tubular damage was located in the S3 segment of the proximal tubules (pars recta). The severity of the findings in high dose treated animals (0.6 mg/kg) increased up to day 15. Kidney findings on day 29, related to Cisplatin treatment, were comparable to those on day 15.

Clinical, clinical-pathological and hematological observation (Cisplatin)

Only significant observation or relevant parameters in case of the underlying evaluation are shown. The tables for all three studies (Table 3-8, Table 3-9, Table 3-10) show the same parameters to allow comparison between the different compounds, even though some parameters show no relevant effects in one or two compounds.

Table 3-7 Incidence summary of Cisplatin treatment-related kidney histophatology findings. The number of animals in each group of five is shown in parentheses. / ≙ lesion not observed, + ≙ minimal, ++ ≙ mild, +++ ≙ moderate, ++++ ≙ massive, and +++++ ≙ high severity of lesion

		Cisplatin [mg/kg]					
		male			female		
	time	0	0.3	0.6	0	0.3	0.6
Tubular Degeneration	**day 4**	/	/	/	/	/	/
	day 8	/	/	+ (3/5) ++ (1/5) +++ (1/5)	/	/	/
	day 15	/	/	+ (2/5) ++(2/5) +++ (1/5)	/	/	+++ (1/5)
	day 29	/	/	+ (4/5) +++ (1/5)	/	/	/
Tubular Dilatation	**day 4**	/	/	/	/	/	/
	day 8	/	/	+ (1/5)	/	/	/
	day 15	/	/	++ (1/5)	/	/	++ (1/5)
	day 29	/	/	+++ (1/5)	/	/	/
Tubular Necrosis	**day 4**	/	/	+ (2/5)	/	/	/
	day 8	/	/	+ (4/5) ++ (1/5)	/	/	/
	day 15	/	/	+ (1/5) ++ (1/5)	/	/	+ (1/5)
	day 29	/	/	+ (1/5)	/	/	/
Cellular Casts	**day 4**	/	/	/	/	/	/
	day 8	/	/	+(2/5)	/	/	/
	day 15	/	/	+(1/5)	/	/	/
	day 29	/	/	/	/	/	/
Basophilic Tubules	**day 4**	/	/	+ (1/5)	/	/	/
	day 8	/	+ (1/5)		/	/	/
	day 15	+ (1/5)	+ (2/5)	+ (1/5)	/	+ (1/5)	+ (1/5) ++(1/5)
	day 29	/	+ (1/5)	+++ (1/5)	/	+ (1/5)	+ (2/5)
Infiltrates	**day 4**	/	+ (1/5)	/	/	/	/
	day 8	/	/	+ (1/5)	/	/	/
	day 15	/	/	+ (1/5)	/	/	+ (1/5) ++(1/5)
	day 29	/	/	/	/	/	/

Table 3-8 Summary of body and kidney weight determined for male and female rats treated with 0.3 mg/kg and 0.6 mg/kg Cisplatin up to 28 days. The data of the control group are displayed in each table. Significant changes were indicated with * $p < 0.05$, ** $p < 0.01$, *** $p < 0.001$ (ANOVA + Dunnett)

		Cisplatin [mg/kg]					
		Male			female		
	time	0	0.3	0.6	0	0.3	0.6
body weight [g]	day 3	261 ± 11	261 ± 12	256 ± 8	170 ± 6	170 ± 9	170 ± 6
	day 7	297 ± 4	276 ± 9 *	262 ± 17 ***	192 ± 11	175 ± 11 *	166 ± 6 **
	day 14	314 ± 11	300 ± 12	262 ± 22 ***	192 ± 5	195 ± 7	180 ± 20
	day 28	349 ± 14	329 ± 20	313 ± 30 ***	207 ± 6	204 ± 5	202 ± 15
kidney weight [g]	day 3	2.02 ± 0.09	2.02 ± 0.22	1.95 ± 0.04	1.38 ± 0.11	1.30 ± 0.13	1.29 ± 0.04
	day 7	2.24 ± 0.07	2.08 ± 0.17	2.04 ± 0.36	1.48 ± 0.07	1.37 ± 0.16	1.32 ± 0.11
	day 14	2.34 ± 0.21	2.18 ± 0.25	2.05 ± 0.19	1.51 ± 0.13	1.48 ± 0.10	1.51 ± 0.19
	day 28	2.34 ± 0.11	2.28 ± 0.16	2.16 ± 0.24	1.49 ± 0.07	1.46 ± 0.14	1.51 ± 0.23

As observed by the limited histopathological findings in female rats treated with 0.3 and 0.6 mg/kg Cisplatin, almost all dominant, statistical significant or biological relevant alterations in the clinical pathological parameters were limited to male rats. In addition, in female rats a considerable fluctuation over time was observed with often increased parameters on day 3 and day 14 and decreases on day 7 and day 28 (Table 3-8, Table 3-9, Table 3-10). In contrast, the hematological analysis showed in females strong and significant effects but below the observed effects in males (Table 3-11). A strong reduction in body weight on days 7, 14 and 28 in male rats treated with 0.6 mg/kg Cisplatin was observed. Also low dose treated male rats (0.3 mg/kg) showed reduced (non significant) body weight. In female rats a significant body weight reduction was only determined on day 7 in both dosing groups. Day 14 and 28 also showed slightly decrease weights. In contrast, the kidney weights showed no relevant alterations in both genders. In serum parameters, especially in creatinine and BUN, most findings were in the low dose (0.3 mg/kg) treated male rats (Table 3-9). Therefore, a reduction in serum creatinine was observed on day 3 and day 7 in both dosing groups. No relevant alteration at the later time points appeared.

BUN also was reduced in male rats on day 3, but was followed by an increase on day 7. The slightly elevated level in BUN stayed relatively constant up to day 28. In female rats the most prominent effects on BUN were limited to days 7 and 14 of both low (0.3 mg/kg) and high dose (0.6 mg/kg) treated animals. However, statistical significance could only be calculated for high dose animals (0.6 mg/kg) on day 29. In male rats serum glucose levels were also elevated in both dosing groups, with the highest values observed on day 7. Female rats showed the fluctuation mentioned above within the serum glucose level (Table 3-9).

Table 3-9 Summary of clinical pathology serum parameter determined for male and female rats treated with saline, 0.3 mg/kg and 0.6 mg/kg Cisplatin for up to 28 days. The data of the control group are displayed in each table. Significant changes were indicated with * $p < 0.05$, ** $p < 0.01$, *** $p < 0.001$ (ANOVA + Dunnett)

		Cisplatin [mg/kg]					
		Male			female		
	time	0	0.3	0.6	0	0.3	0.6
Creatinine [mg/dL]	day 3	0.25 ± 0.02	0.14 ± 0.02 ***	0.18 ± 0.02 ***	0.29 ± 0.04	0.21 ± 0.04	0.21 ± 0.03
	day 7	0.23 ± 0.02	0.14 ± 0.04 ***	0.21 ± 0.03	0.28 ± 0.03	0.16 ± 0.03	0.20 ± 0.05
	day 14	0.24 ± 0.03	0.26 ± 0.02	0.27 ± 0.07	0.27 ± 0.05	0.29 ± 0.03	0.37 ± 0.20
	day 28	0.25 ± 0.02	0.24 ± 0.02	0.26 ± 0.04	0.28 ± 0.02	0.28 ± 0.03	0.25 ± 0.03
BUN [mg/dL]	day 3	33.15 ± 3.46	29.79 ± 2.50	29.07 ± 3.17	35.19 ± 5.00	34.95 ± 5.39	36.75 ± 3.90
	day 7	30.27 ± 1.88	32.91 ± 2.45 **	41.56 ± 6.72	30.75 ± 2.26	35.19 ± 1.97	36.27 ± 5.74
	day 14	31.59 ± 2.19	30.15 ± 2.63	34.35 ± 7.15	30.39 ± 3.28	35.31 ± 1.61	50.2 ± 44.83
	day 28	27.62 ± 1.80	28.11 ± 4.52 *	34.83 ± 3.34	32.07 ± 2.46	38.31 ± 3.10	33.03 ± 1.90 **
Glucose [mg/dL]	day 3	85.41 ± 13.58	90.09 ± 6.98	92.97 ± 11.86	71.35 ± 10.48	81.08 ± 8.83	80.36 ± 2.05
	day 7	88.65 ± 10.30	106.67 ± 8.20 *	116.40 ± 10.16 **	90.81 ± 6.57	89.73 ± 9.74	84.33 ± 7.36
	day 14	104.15 ± 13.33	108.11 ± 10.74	115.68 ± 18.35	102.7 ± 14.64	95.50 ± 4.93	108.47 ± 18.35
	day 28	119.28 ± 4.66	108.47 ± 19.84	112.79 ± 15.43	107.39 ± 12.72	77.48 ± 6.62 **	95.50 ± 10.89

Urinary excretion was not significantly effected in either gender (Table 3-10). However, a slightly reduced urinary volume was determined in high dose (0.6 mg/kg) treated male rats, while female rats only showed a relevant decrease in urinary volume on day 7. All high dose (0.6 mg/kg) treated male rats, independent of the time, showed a slight increasing tendency in urinary glucose. The most pronounced outcome was detected for male rats treated with 0.6 mg/kg Cisplatin for 7 days. Female rats showed no relevant alteration in urinary glucose. Also urinary total protein delivered no time- or dose-dependent alterations. Only a slight, but not statistical significant, increase in low (0.3 mg/kg) and high (0.6 mg/kg) dose treated animals on day 7 and 28 in male rats was observed. In addition, a very strong and statistical significant reduction in urinary total protein in female rats treated for 29 day with either 0.3 mg/kg or 0.6 mg/kg Cisplatin was observed. The level of urinary creatinine showed no statistical significant alterations but slight fluctuations between individual animals and dose groups (Table 3-10). These fluctuations correlated with the variation in urinary volume.

Table 3-10 Summary of clinical pathology urinary parameter determined for male and female rats treated with saline, 0.3 mg/kg and 0.6 mg/kg Vancomycin for up to 28 days. The data of the control group are displayed in each table. Significant changes were indicated with * $p < 0.05$, ** $p < 0.01$, *** $p < 0.001$ (ANOVA + Dunnett)

		Cisplatin [mg/kg]					
		Male			female		
	time	0	0.3	0.6	0	0.3	0.6
Volumen [mL]	day 3	15.30 ± 8.51	16.72 ± 9.49	12.92 ± 4.30	8.32 ± 4.33	8.24 ± 3.70	8.38 ± 3.97
	day 7	15.68 ± 15.68	17.36 ± 7.07	11.32 ± 10.22	16.68 ± 7.23	13.60 ± 5.82	9.60 ± 2.55
	day 14	26.24 ± 11.44	21.96 ± 9.14	14.84 ± 1.60	13.56 ± 5.49	10.66 ± 6.26	12.18 ± 7.01
	day 28	21.28 ± 8.21	14.64 ± 4.53	17.04 ± 8.47	9.96 ± 4.37	15.12 ± 6.38	12.75 ± 3.00
Glucose [mg/dL]	day 3	7.82 ± 5.24	6.81 ± 3.47	8.40 ± 1.65	9.01 ± 7.24	8.97 ± 3.39	8.29 ± 4.03
	day 7	6.23 ± 6.23	6.16 ± 1.66	20.25 ± 14.87 *	7.10 ± 3.41	5.30 ± 2.30	7.03 ± 1.24
	day 14	5.08 ± 1.90	5.66 ± 2.29	5.73 ± 0.78	7.89 ± 4.30	9.23 ± 4.32	7.78 ± 4.56
	day 28	6.56 ± 2.21	9.55 ± 2.22	8.04 ± 3.06	7.78 ± 3.03	4.97 ± 1.66	6.44 ± 0.97
total protein [mg/dL]	day 3	60.80 ± 36.17	43.52 ± 25.22	48.10 ± 14.40	15.78 ± 9.79	12.06 ± 4.10	12.22 ± 6.70
	day 7	38.26 ± 38.26	42.86 ± 12.6	51.04 ± 24.45	10.40 ± 5.11	7.88 ± 2.71	10.78 ± 3.03
	day 14	39.14 ± 26.51	32.4 ± 11.93	26.98 ± 17.68	11.18 ± 5.12	12.92 ± 5.71	10.38 ± 5.38
	day 28	37.76 ± 10.13	44.04 ± 7.43	43.78 ± 20.05	13.02 ± 5.61	4.60 ± 3.01 **	6.18 ± 1.18 *
Creatinine [mg/dL]	day 3	68.25 ± 37.13	53.94 ± 29.00	59.71 ± 19.50	67.72 ± 44.31	56.12 ± 18.07	58.21 ± 25.47
	day 7	49.30 ± 49.30	46.51 ± 14.09	98.25 ± 71.50	41.64 ± 19.27	35.49 ± 13.63	46.21 ± 11.21
	day 14	38.10 ± 15.06	43.50 ± 15.49	47.57 ± 1.64	47.34 ± 21.86	55.71 ± 22.78	46.44 ± 20.69
	day 28	52.06 ± 22.98	74.81 ± 22.47	63.29 ± 25.41	60.90 ± 26.94	40.07 ± 11.49	46.70 ± 5.67

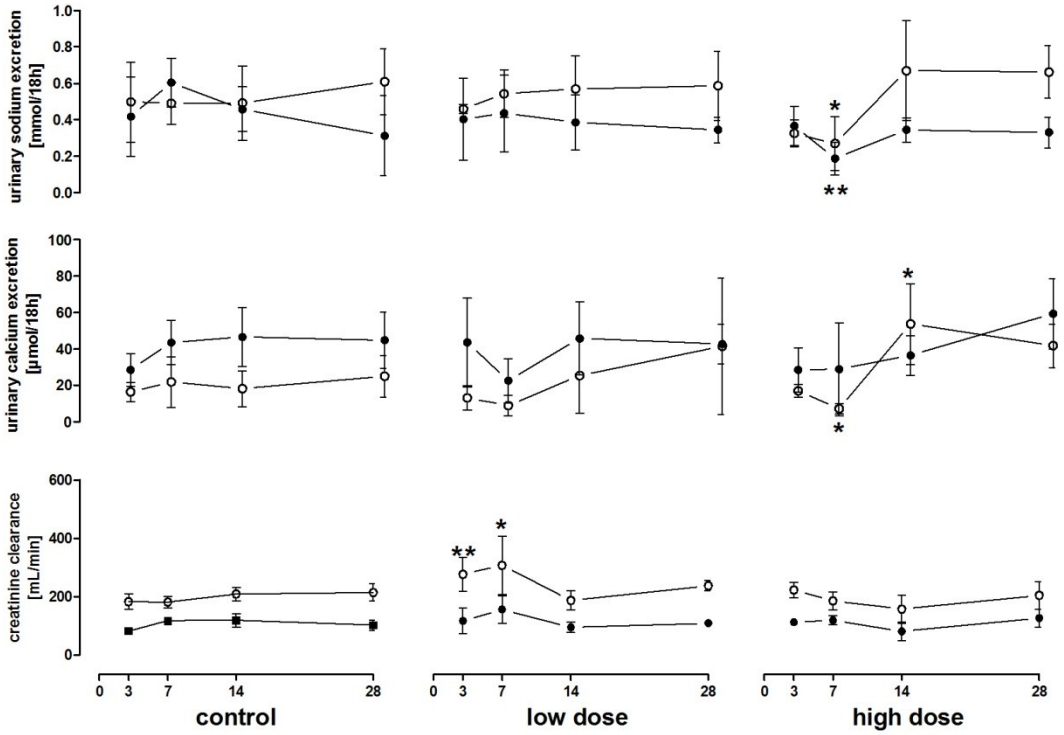

Figure 3-12 Urinary sodium and calcium excretion, as well as the creatinine clearance for male (○) and female (●) rats treated with either saline (control), 0.3 mg/kg Cisplatin (low dose), or 0.6 mg/kg Cisplatin (high dose). Data are presented for both genders individually by mean ± SD. Significant changes were indicated with * $p < 0.05$, ** $p < 0.01$, *** $p < 0.001$ (ANOVA + Dunnett).

The renal functional properties were only mildly affected by Cisplatin treatment with either 0.3 mg/kg or 0.6 mg/kg (Figure 3-12). A strong, significant reduction in urinary sodium excretion was observed after 7 days of high dose (0.6 mg/kg) treatment in both genders, followed by a slight (non significant) increase on treatment day 14 in male rats. In contrast, urinary calcium excretion in male rats showed a decrease on day 3 with an additional significant increase on day 14. Significant changes in creatinine clearance where limited to male rats treated with 0.3 mg/kg Cisplatin. A significant increase in creatinine clearance was observed after 3 and 7 days of treatment with a return to the normal by day 14. The glomerular filtration rate showed no changes in low dose (0.3 mg/kg) treated animals but a slight decrease on day 7 and day 14 of high dose (0.6 mg/kg) treated male rats. Only the decrease on day 14 delivered statistical significance.

The most prominent findings within the Cisplatin study were hematological alterations. In contrast to the observation within the Vancomycin study, Cisplatin caused a decrease in absolute cell counts. RBCs were only affected in male high dose (0.6 mg/kg) treated animals on day 29, while female rats showed no relevant changes. The total counts of platelets showed a strong and dose-dependent decrease in both genders on day 14, while on day 29 male rats showed a tendency of an increase, and female rats still showed a decrease. The strongest effects were observed for WBC, in a time- and dose-dependent manner. A strong decrease in WBCs was earliest detected on days 3 and day 7 in low (0.3 mg/kg) and high (0.6 mg/kg) dose treated animals of both genders. At later time points a decrease in cell counts was still present but less strong. The most effected white blood cell sub-population in Cisplatin treated animals were the neutrpophils, eosinophils and basophils. But also lymphocytes showed a reduction in total cell count. No changes were observed for monocytes.

Table 3-11 Summary of hematological parameter determined for male and female rats treated with saline, 0.3 mg/kg and 0.6 mg/kg Cisplatin for up to 28 days. The data of the control group are displayed in each table. Significant changes were indicated with * < 0.05, ** < 0.01, *** < 0.001 (ANOVA + Dunnett)

		Cisplatin [mg/kg]					
		male			female		
	time	0	0.3	0.6	0	0.3	0.6
RBC [counts/pL]	day 3	8.22 ± 0.23	8.24 ± 0.40	8.11 ± 0.31	8.17 ± 0.41	7.78 ± 0.17	7.96 ± 0.29
	day 7	8.28 ± 0.38	8.35 ± 0.42	8.57 ± 0.51	7.85 ± 0.25	8.02 ± 0.28	8.32 ± 0.51
	day 14	8.26 ± 0.40	8.22 ± 0.24	8.34 ± 0.40	7.98 ± 0.19	8.01 ± 0.20	7.81 ± 0.28
	day 28	8.56 ± 0.13	8.41 ± 0.26	8.19 ± 0.17 *	7.96 ± 0.15	8.03 ± 0.29	7.67 ± 0.51
PLT [counts/nL]	day 3	890 ± 64	905 ± 71	930 ± 72	977 ± 123	850 ± 45	949 ± 71
	day 7	899 ± 98	1020 ± 128	979 ± 63	947 ± 144	983 ± 97	1043 ± 141
	day 14	939 ± 23	837 ± 78 *	691 ± 60 ***	936 ± 119	855 ± 91	714 ± 78 **
	day 28	800 ± 79	824 ± 19	966 ± 126	921 ± 85	877 ± 29	846 ± 31
WBC [counts/nL]	day 3	8.00 ± 1.09	5.64 ± 1.40 *	5.36 ± 1.50 *	5.90 ± 1.74	4.72 ± 0.79 *	3.84 ± 1.32 **
	day 7	8.20 ± 1.20	6.50 ± 1.17 *	4.28 ± 0.76 ***	6.16 ± 1.83	3.84 ± 0.79	3.32 ± 0.75 **
	day 14	7.38 ± 1.47	6.72 ± 1.26	5.06 ± 1.51 *	7.20 ± 0.92	5.70 ± 1.20	4.20 ± 1.37
	day 28	7.66 ± 1.81	7.82 ± 0.26	5.66 ± 0.70 *	4.84 ± 0.69	3.86 ± 0.71	4.20 ± 0.55
NEU [counts/nL]	day 3	2.12 ± 0.88	0.77 ± 0.32 **	0.79 ± 0.18 **	0.87 ± 0.36	0.84 ± 0.56	0.43 ± 0.12
	day 7	1.37 ± 0.37	0.74 ± 0.21 **	0.63 ± 0.21 **	1.78 ± 1.30	0.51 ± 0.24 *	0.37 ± 0.17 *
	day 14	1.26 ± 0.12	1.14 ± 0.38	1.05 ± 0.78	1.75 ± 0.35	1.03 ± 0.32 **	0.74 ± 0.31 ***
	day 28	1.89 ± 0.96	1.42 ± 0.26	1.20 ± 0.49	1.01 ± 0.21	0.70 ± 0.21	0.69 ± 0.17 *
Lymph [counts/nL]	day 3	5.41 ± 0.39	4.61 ± 1.05	4.31 ± 1.39	4.76 ± 1.43	3.66 ± 0.56	3.23 ± 1.15
	day 7	6.38 ± 0.93	5.53 ± 0.93	3.43 ± 0.50 ***	4.10 ± 0.79	3.14 ± 0.64	2.80 ± 0.65 *
	day 14	5.80 ± 1.28	5.26 ± 0.82	3.78 ± 0.74 *	5.08 ± 0.70	4.41 ± 1.06	3.24 ± 0.99 *
	day 28	5.41 ± 0.85	6.02 ± 0.37	4.14 ± 0.51 *	3.60 ± 0.62	2.99 ± 0.76	3.34 ± 0.39

		Cisplatin [mg/kg]					
		male			female		
	time	0	0.3	0.6	0	0.3	0.6
EOS [counts/nL]	day 3	0.24 ± 0.09	0.11 ± 0.04 **	0.10 ± 0.04 **	0.10 ± 0.04	0.09 ± 0.01	0.06 ± 0.01 *
	day 7	0.20 ± 0.03	0.10 ± 0.02 **	0.09 ± 0.06 **	0.12 ± 0.05	0.05 ± 0.02 *	0.04 ± 0.02 **
	day 14	0.14 ± 0.03	0.07 ± 0.03 **	± 0.04 **	0.17 ± 0.16	0.07 ± 0.02	0.05 ± 0.03
	day 28	0.13 ± 0.02	0.13 ± 0.04	0.10 ± 0.03	0.10 ± 0.04	0.07 ± 0.02	0.06 ± 0.01
BASO [counts/nL]	day 3	0.07 ± 0.02	0.03 ± 0.01 **	0.02 ± 0.02 **	0.06 ± 0.03	0.03 ± 0.01	0.02 ± 0.01 **
	day 7	0.07 ± 0.02	0.04 ± 0.02 **	0.02 ± 0.01 ***	0.05 ± 0.03	0.02 ± 0.01	0.02 ± 0.01 **
	day 14	0.07 ± 0.03	0.04 ± 0.02	0.03 ± 0.01 *	0.04 ± 0.02	0.03 ± 0.02	0.02 ± 0.01
	day 28	0.07 ± 0.03	0.05 ± 0.01	0.03 ± 0.02	0.04 ± 0.02	0.03 ± 0.00	0.02 ± 0.01
MONO [counts/nL]	day 3	0.12 ± 0.04	0.08 ± 0.04	0.12 ± 0.03	0.09 ± 0.03	0.10 ± 0.03	0.09 ± 0.05
	day 7	0.15 ± 0.04	0.10 ± 0.03	0.10 ± 0.03	0.10 ± 0.07	0.07 ± 0.02	0.06 ± 0.03
	day 14	0.10 ± 0.05	0.15 ± 0.08	0.13 ± 0.05	0.12 ± 0.04	0.14 ± 0.06	0.12 ± 0.11
	day 28	0.15 ± 0.08	0.16 ± 0.04	0.13 ± 0.06	0.07 ± 0.02	0.05 ± 0.02	0.07 ± 0.03
LUC [counts/nL]	day 3	0.03 ± 0.01	0.01 ± 0.01 *	0.01 ± 0.01 **	0.02 ± 0.02	0.01 ± 0.01	0.01 ± 0.01
	day 7	0.03 ± 0.01	0.02 ± 0.00	0.01 ± 0.01 ***	0.01 ± 0.01	0.01 ± 0.00	0.01 ± 0.00
	day 14	0.02 ± 0.01	0.02 ± 0.01 **	0.01 ± 0.01	0.02 ± 0.01	0.01 ± 0.01	0.01 ± 0.01
	day 28	0.02 ± 0.01	0.03 ± 0.00	0.02 ± 0.01	0.02 ± 0.01	0.01 ± 0.01	0.01 ± 0.01

Abbreviation: RBC = red blood cells, PLT = platelets, WBC = white blood cells, NEU = neutrophils, Lymph = Lymphocytes, EOS = eosiniphilics, BASO = basophilics, MONO = monocytes, LUC = large unstained cells.

Detection of novel qualified and exploratory urinary proteins (Cisplatin)

In animals treated with either 0.3 mg/kg or 0.6 mg/kg Cisplatin for up to 28 days the urinary excretion of the evaluated biomarker only changed in some limited cases. In male rats urinary Kim-1 showed the most prominent and statistically significant alterations, which was time and dose dependent (Figure 3-13a). The low dose (0.3 mg/kg) treated male rats showed no alteration, while the high dose treated animals (0.6 mg/kg) showed a significant increase, earliest on day 4. However, on this day of urine collection, histopathological observed tubular degeneration/ necrosis were only found in two of the five animals. Kim-1 was increased in the urine of all animals on day 4; with higher levels observed on day 8, where all five animals showed tubular alterations was higher. Animals treated for 15 and 29 days showed a time-dependent decrease compared to day 8, but was still significantly elevated.

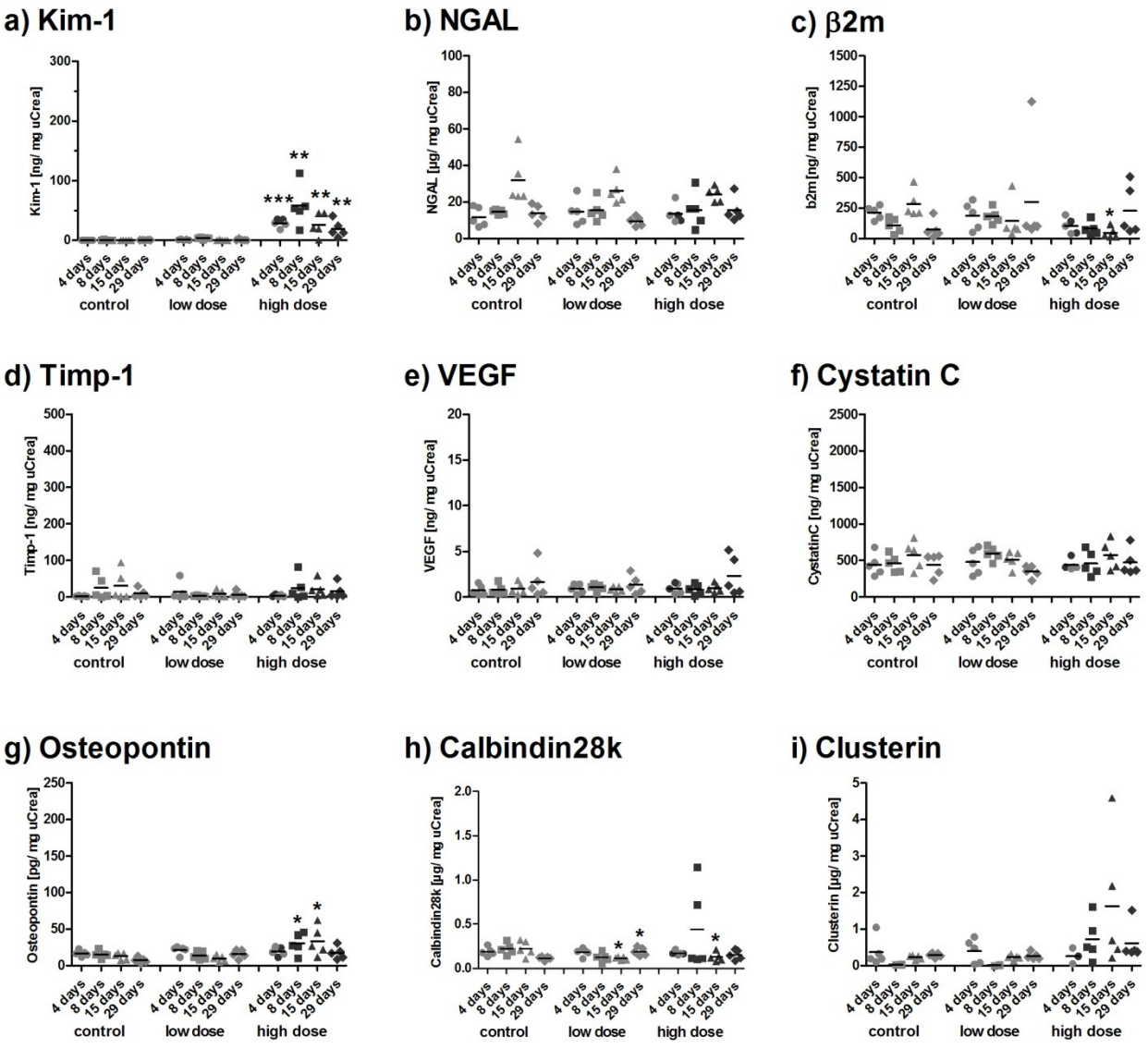

Figure 3-13 Excretion of (a) Kim-1, (b) NGAL, (c) b2m, (d) Timp-1, (e) VEGF, (f) CystatinC, (g) Osteopontin, (h), Calbindin28k, (i) Clusterin in urine of male rats treated with Cisplatin (low dose: 0.3 mg/kg; high dose: 0.6 mg/kg) for 3 days (dots), 7 days (squares), 14 days (triangle), and 28 days (rhombus). Data are presented as individual animals and as the mean (bar; n=5). The light grey signs indicate no tubular degeneration found within this animal, the darker grey indicates tubular degeneration observed. * $p < 0.05$, ** $p < 0.01$, *** $p < 0.001$ (ANOVA-Dunnett).

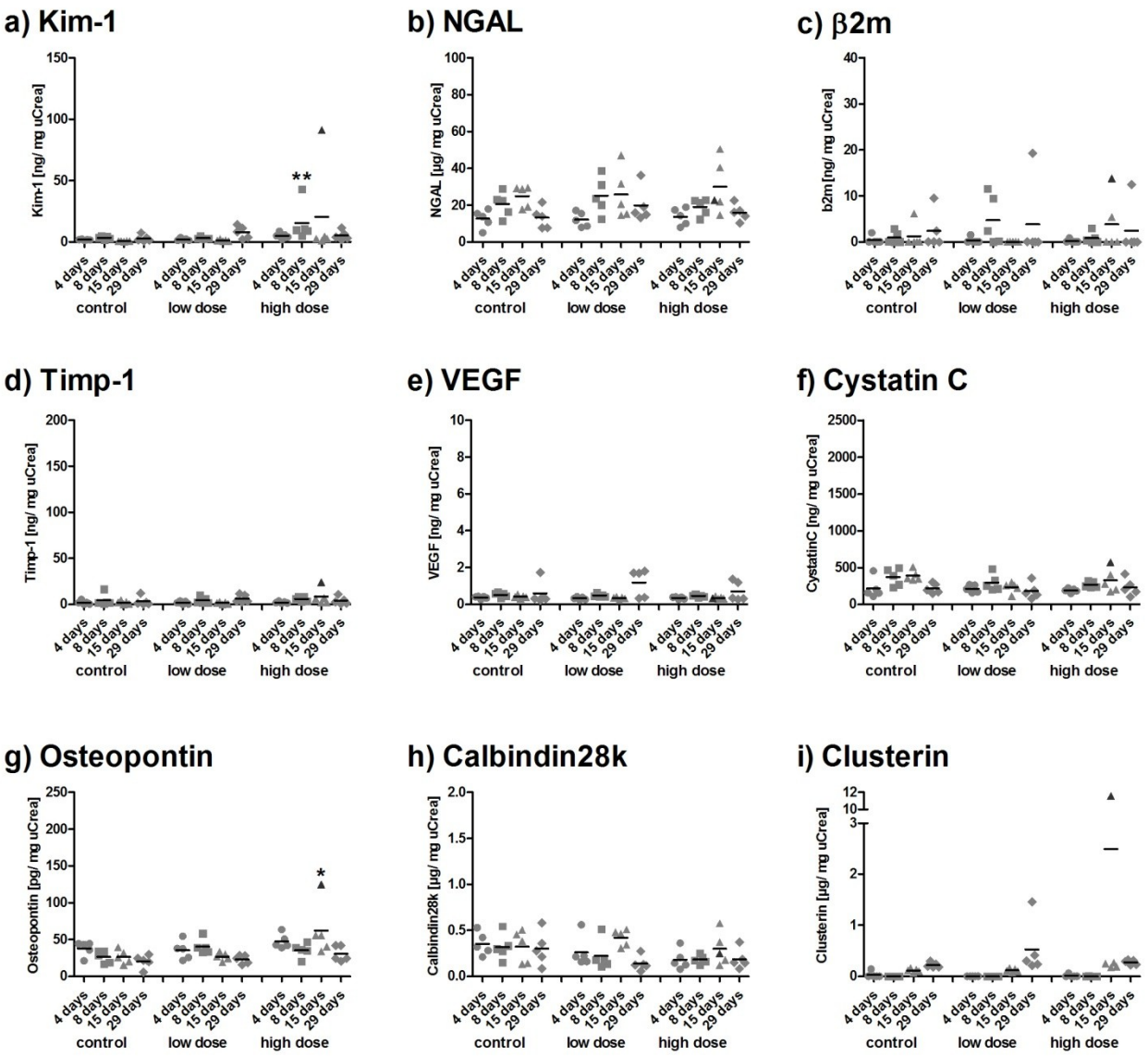

Figure 3-14 Excretion of (a) Kim-1, (b) NGAL, (c) b2m, (d) Timp-1, (e) VEGF, (f) CystatinC, (g) Osteopontin, (h), Calbindin28k, (i) Clusterin in urine of female rats treated with Cisplatin (low dose: 0.3 mg/kg; high dose: 0.6 mg/kg) for 3 days (dots), 7 days (squares), 14 days (triangle), and 28 days (rhombus). Data are presented as individual animals and as the mean (bar; n=5). The light grey signs indicate no tubular degeneration found within this animal, the darker grey indicates tubular degeneration observed. *p < 0.05, **p < 0.01, *** < 0.001 (ANOVA-Dunnett).

Other urinary biomarkers showing statistical or biological significant changes were β2m, Osteopontin, Calbindin and Clusterin (Figure 3-13c, -g, -h, -i). In case of urinary β2m excretion no time or treatment-related elevation in urinary level were observed. However, because of the strong variation in opposite directions, the significant result obtained for the high dose treated animals on day 15 should be rejected because of the lack of biological relevance. The low dose treated male rats (0.3 mg/kg) showed no alterations over time, while animals of the high dose treated group (0.6 mg/kg) showed an increase of urinary Osteopontin on day 8 and day 15 in individual animals, while no alterations were observed on days 4 or 29, independent of the observed histopathological outcome (Figure 3-13g). Animals of the control group showed a decrease in urinary Calbindin level on day 29 leading as a consequence to a calculated p-value of <0.05 in low dose treated animals (0.3 mg/kg (Figure 3-13h). In contrast, animals on day 15 of the same treatment group showed a significant decrease compared to the corresponding control group. Also on day 15 in high dose treated groups (0.6 mg/kg) a statistically significant decrease was observed. However, two animals on day 8 showed a very

strong increase, while the other animals, which showed the same severity of renal damage, had no elevated Calbindin. In contrast, Clusterin showed no statistically significant changes over the single time points of the high dose treated animals (0.6 mg/kg), although a relevant time-dependent increase from day 4 to day 15 was observed. On day 29 urinary Clusterin levels were still enhanced on average, but below the level of day 15. The other biomarkers, NGAL, Timp-1, VEGF and CystatinC (Figure 3-13 b, -d, -e, -f) showed no biological or statistical significant or biological relevant changes.

In female rats the only limited changes in urinary biomarkers was observed. Statistically significant findings were measured for Kim-1 in high dose treated animals (0.6 mg/kg) on day 8 (Figure 3-14a), and Osteopontin of the same treatment group on day 15. The only female rat showing tubular degeneration and necrosis was clearly identified by Kim-1, Osteopontin and Clusterin (Figure 3-14a, -g, -i). The urinary excretion of Kim-1 for example was approximatly 50-fold higher than the corresponding control and ~35 fold of the other animals of the same group.

Table 3-12 Area-under-the-receiver-operator-characteristic curve (AUROC) for detection of Cislpatin induced nephrotoxicity. The area under the curve is used as a measure for the overall ability of a biomarker to discriminate animals without histopathological findings in kidney from those with signs of tubular damage (degeneration/ necrosis). Markers with a good diagnostic performance (AUROC > 0.90) are highlighted in bold. In addition the 95% confidence interval and the p-value are displayed. The AUROC for female rats were not calculated because of only one animal with biological important histopathological findings. * =measurement by Luminex® xMAP®, ** = measurement by RENA®-Sticks, #= classical clinical-pathology parameter determined by standard procedures.

Kidney Biomarker	Male			Female		
	AUROC	95% CI	p-value	AUROC	95% CI	p-value
Kim-1*	**0.95**	**0.89 - 1.00**	**<0.0001**	/	/	/
Timp-1*	0.68	0.53 - 0.82	0.0337	/	/	/
VEGF*	0.57	0.41 - 0.73	0.3891	/	/	/
$ß_2$-Microglobulin*	0.69	0.53 - 0.85	0.0203	/	/	/
Clusterin*	0.81	0.68 - 0.95	0.0003	/	/	/
Cystatin C*	0.53	0.37 - 0.70	0.6757	/	/	/
Lipocalin-2/ NGAL*	0.56	0.40 - 0.72	0.4755	/	/	/
Osteopontin*	0.75	0.60 - 0.90	0.0028	/	/	/
Calbindin *	0.58	0.41 - 0.75	0.3291	/	/	/
Kim-1**	0.82	0.69 - 0.96	0.0001	/	/	/
BUN#	0.74	0.57 - 0.91	0.0036	/	/	/
Serum Creatinine#	0.55	0.38 - 0.72	0.5659	/	/	/

Osteopontin showed for the same individual female rat an elevation in urine of nearby 6-fold of the control and still 3-fold to the other animals of the same treatment group. However, NGAL, β2m, Timp-1, VEGF, CystatinC and Calbindin showed no or only weak changes for this female rat (Figure 3-14 b, -c, -d, -e, -f, -h). To evaluate the performance of these urinary protein biomarker ROC curves were calculated. However, because only one female rat showed histopathological changes, it was not possible to calculate ROC curves. The results of this analysis are given in Table 3-12. In male rats, Kim-1 performed well when using both technologies tested (the Luminex® xMAP® technology (m: 0.95) as well as the Dipstick assay (m: 0.82)). Clusterin (m: 0.81) was below the defined threshold of 0.90 while Osteopontin showed an AUROC of 0.75 and was therefore the third-best parameter determined within the Cisplatin study. The other novel urinary protein biomarkers showed AUC values below 0.70 (Timp-1: 0.68; VEGF: 0.57; ß2m: 0.69; CystatinC: 0.53; NGAL: 0.56; Calbindin: 0.58). The traditional clinical-pathological parameters showed inconsistent results. BUN showed an AUC of 0.74 while serum creatinine had the lowest value, with no diagnostic

potential (m: 0.55). Kim-1 and Clusterin were the only markers indicating significant or biologically relevant alterations in the kidney, while Osteopontin gave a relevant hint only on day 8 and day 15.

3.1.1.4 Discussion and Conclusion (Cisplatin)

The doses of Cisplatin were chosen to induce only mild histopathological changes in high dose and no to minimal changes in low dose animals. The main aim was to see whether the urinary protein biomarkers can be used for detection of such small changes or predict early developing changes. As shown in the section 3.1.1.3 the expected mild changes were induced, especially in male rats. The lack of observations in females, except for one rat, indicates a higher resistance of females to cisplatin-induced nephrotoxicity after long-term treatment.

The only mild renal alterations are reflected among other things by the lack of changes in kidney weight (Table 3-8). That did not mean that no strong systemic alterations were caused by Cisplatin treatment. Therefore, the strong decrease in body weight of male rats treated with 0.6 mg/kg Cisplatin clearly indicates degree of toxicity caused (Table 3-8). Also female rats treated with the same dose showed an effect after 7 days of daily treatment. However, the recovery periods lead to only a slight but still present lowered body weight compared to the control group at later time points. The most obvious systemic changes were neutropenia, a reduction of white blood cells including neutrophils, lymphocytes, eosinophils, basophils and large unstained cells, in both genders (Table 3-11). This effect can be attributed to the pharmacological function of Cisplatin, which acts as an inhibitor of proliferation and the hematotoxicity of Cisplatin has been previously reported [Khynriam et al., 2001]. In contrast, the platelet count was slightly increased in both genders on days 3 and 7 with a strong and statistical significant decrease on day 14. The thromocytosis, observed at the earlier times, can be explained by very early anemia. The involvement of nephritis in this phenotypical outcome is unlikely because of the lack of dominant infiltrates (Table 3-7) and the general signs of systemic inflammatory seen histopathologically.

The histopathological findings within renal tissue were well reflected by several biomarkers. The best biomarker in this case was Kim-1 (Figure 3-13 a), as identified by ROC analysis for male rats (Table 3-12). This urinary protein, which is described to be specific for proximal tubular damage, more precisely of the S3 segment [Zhang et al., 2009] delivered a AUC of the ROC of 0.95 (0.89-1.00). This underlines the importance of this biomarker, as well as showing a clear indication for the mechanism of cisplatin induced nephrotoxicity [Kroning et al., 2000], which is also described to specifically hit the part of the S3 segment by enhanced accumulation within this area [Arany et al., 2003]. Beside the S3 segment also slight effects on the S1 segment of the proximal and the distal tubulus have been described [Arany et al., 2003; Kroning et al., 2000]. Therefore, the low concentration used within this study seems to hit exclusively the S3 segment, which was clearly seen by the increase in urinary Kim-1. Beside Kim-1 only Clusterin showed a relatively good performance of 0.81 (0.68-0.95). Osteopontin, which was one of the best urinary biomarker within the Vancomycin study, had the third highest AUC of 0.75 (0.60-0.90) of the evaluated urinary protein biomarker. Based on the slight effects on the kidney seen within this study, it was not unexpected that some biomarkers for general tubular damage, like Timp-1, NGAL and VEGF, performed poorly. The same is the case for Calbindin, which is specific for distal tubular and collecting duct injury, which also showed a poor performance. Taken together, these results clearly show the great benefit of using a panal of urinary biomarker, specific for different areas within the nephron. We can conclude that for Cisplatin nephrotoxicity, the area of damage was limited to the S3 segment of the proximal tubular convolute.

In case of female rats treated with either 0.3 mg/kg or 0.6 mg/kg, even though no ROC curves could be calculated because of the lack of positive histopathological findings, the performance of some of the biomarkers were quite good (Figure 3-17). Kim-1, Osteopontin and Clusterin showed a clear increase in the individual female rat (Figure 3-17 a, g, i) identified to be positive for moderate tubular degeneration, mild dilatation, minimal necrosis as well as mild basophilic tubules and infiltrates (Table 3-7). The urinary excretion of β2m and CystatinC, both described to be specific for proximal tubular damage, showed no relevant alterations in urinary excretion level. This is reflected by the AUC for male rats (0.69 (0.53-0.85) for β2m and 0.53 (0.37-0.70) for Cystatin C) and by the fact that in female rats the affected animal did not show a relevant increase of these proteins compared to the others (Figure 3-14 c, f). This gives further indication of the questionable specificity of these two urinary biomarkers to be proximal tubular specific.

Kim-1, Osteopontin and Clusterin all performed better than the traditional serum parameters, creatinine and BUN, with AUC values in male rats of 0.55 (0.38-0.72) and 0.74 (0.57-0.91), respectively. The better value for BUN reflects the slight dose-dependent increase observed in low dose (0.3 mg/kg) treated animals. In contrast, the reduction in serum creatinine, especially in the first week of daily administration, can be due to the reduction in body weight and therefore the reduced muscle mass. This was confirmed because male rats, characterized by an increased creatinine clearance (Figure 3-12) and a strong reduced body weight (Table 3-8), showed a much stronger reduction (Table 3-9). The poor performance of the traditional parameters clearly shows the benefits of the novel biomarkers. The sensitivity of functional parameters like the creatinine clearance can be categorized as low for the predictivity of very early and slight insults to renal tissue. The effect of a decrease in urinary sodium and calcium excretion (Figure 3-12) can be interpreted as the physiologic response to a decrease in renal perfusion to control hypovolemia, which is reflected by the decline in urinary output (Table 3-10). In contrast to the situation within the Vancomycin study, where the increase in urinary glucose level was determined to be caused by proximal tubular break-down, in Cisplatin treated animals the increase (Table 3-10) seems to be caused by an increase in blood sugar level (Table 3-9), which was observed specifically on day 7. Therefore, the only prominent treatment related alteration in renal function can defined by a slight increase in creatinine clearance in low dose (0.3 mg/kg) treated animals on days 3 and 7 and the alterations within the electrolytes in high dose (0.6 mg/kg) treated animals.

In summary, the novel urinary protein biomarkers, evaluated within this study to allow the detection of only mild renal injury, can be used, but with several limitations. Kim-1, which has a special significance within this study because of its toxicity target, Clusterin and Osteopontin can be defined as the most promising urinary biomarker. The benefit of the combined determination of these three urinary protein biomarkers is the overlapping specificity of the nephron area, enabling the identification of the major location of damage. Because of the major changes in Kim-1, the location could be further sublocalized as proximal tubular specific. Additionally, further evidence was given by the data presented, that the usefulness of β2m and Cystatin C to function as biomarkers for proximal tubular damage is strongly limited.

3.1.1.5 Results (Puromycin)

Histopathological observation (Puromycin)

Gross pathological kidney-related findings were restricted to high dose animals (30/20 mg/kg) after 14 and 28 days of treatment. The main macroscopic observations on days 15 and 29 were a bilateral pale discoloration, enlargement of the whole organ and a granular surface. In addition, minimal accumulation of fluid in the abdomen and the thorax of high dose (30/20 mg/kg) treated animals was observed as early as day 8. An overview of the results is summarized in Table 3-13.

On day 4 no animal of any group showed effects in the kidneys. On day 8 a minimal vacuolation of the glomerular tufts was observed in one male rat and two females of the high dose (30/20 mg/kg) treatment group. Animals treated for 14 days with high dose (30/20 mg/kg) Puromycin showed mild to moderate multifocal glomerular vacuolations, as well as mild to massive tubular degeneration. In addition, mild to moderate tubular dilatation was observed in both sexes. The severity was slighty more pronounced in male rats then in females of the same dose group. After 29 days of treatment with 30/20 mg/kg (high dose) Puromycin, only one individual male rat survived with mild vacuolation of glomerular tufts, moderate tubular degeneration but without dilatation. Female rats of the same dose group showed minimal to mild vacuolation of glomerular tufts, minimal tubular degeneration. Minimal tubular dilation was also observed in one female rat. Severity of the lesions was slightly more pronounced in the males.

Beside the described findings also mild to moderate eosinophilic casts were observed in all male and female rats treated with 30/20 mg/kg Puromycin for 14 and 28 days. Basophilic tubules were described without a strong treatment dependency.

Clinical, clinical-pathological and hematological observation (Puromycin)

Only significant observation or relevant parameters in case of the underlying evaluation are shown. The tables for all three studies show the same parameters to allow comparison between the different compounds even though some parameters show no relevant effects in one or two compounds.

In almost all clinical-pathological parameter, female rats showed a stronger or even earlier alteration compared to the corresponding male animals (Table 3-14- Table 3-17). A slight reduction in terminal body weight was observed on day 3 in both genders.

A statistically significant reduction in body weight in female rats was observed after only 7 days of high dose (30/20 mg/kg) treatment, and remained constant up to day 29. Male rats treated with the same doses showed a significant decrease in body weight only on days 14 and 28 (Table 3-14). The kidney weight was less affected then the body weight in both genders. On day 8 a significant decrease in both genders was observed, while the later time points showed a specific increase in kidney weight. Statistical significance in male rats was limited to day 7 after treatment with 30/20 mg/kg Puromycin.

Table 3-13 Incidence summary of Puromycin treatment-related kidney histophatology findings. The number of animals in each group of five is shown in parentheses. / ≙ lesion not observed, + ≙ minimal, ++ ≙ mild, +++ ≙ moderate, ++++ ≙ massive, and +++++ ≙ high severity of lesion

		Puromycin [mg/kg]					
		male			Female		
	time	0	10	30/20	0	10	30/20
Tubular Degeneration	**day 4**	/	/	/	/	/	/
	day 8	/	/	/	/	/	+ (1/5)
	day 15	/	/	+++ (4/5) ++++ (1/5)	/	/	++ (5/5)
	day 29	/	/	+++ (1/1)	/	+ (1/5)	+ (5/5)
Tubular Dilatation	**day 4**	/	/	/	/	/	/
	day 8	/	/	/	/	/	/
	day 15	/	/	++ (3/5) +++ (1/5)	/	/	++ (5/5)
	day 29	/	/	/	/	/	+ (1/5)
Eosinophilic Casts	**day 4**	/	/	/	/	/	/
	day 8	/	/	+++ (1/5)	/	/	+ (2/5)
	day 15	/	/	+++ (5/5)	/	/	+++ (5/5)
	day 29	/	/	+++ (1/1)	/	+ (2/5)	++ (3/5) +++ (2/5)
Basophilic Tubules	**day 4**	/	+ (2/5)	+ (2/5)	/	/	+ (1/5)
	day 8	/	/	+ (2/5)	+ (1/5)	/	/
	day 15	+ (2/5)	/	+++ (1/5)	/	/	/
	day 29	/	+ (3/5)	/	/	+ (1/5)	/
Glomerular Damage	**day 4**	/	/	/	/	/	/
	day 8	/	/	+ (1/5)	/	/	+ (1/5)
	day 15	/	/	++ (1/5) ++ (2/5)	/	/	++ (5/5)
	day 29	/	/	++ (1/1)			+ (4/5) ++ (1/5)

Females showed significant alterations on days 8, 15 and 29. In serum, both traditional parameters showed time dependent changes in both sexes, but more pronounced in female rats (Table 3-15).

Serum creatinine significantly decreased on days 3 and 7 in low (10 mg/kg) and high dose (30/20 mg/kg) treated female rats, while in male rats the same alteration was earliest observed on day 7. In contrast, both genders showed a strong increase in serum creatinine on day 15 in high dose groups (30/20 mg/kg) while the low dose (10 mg/kg) treated animals showed no alteration. On day 29 a slight, non significant increase was observed in both sexes and dose groups. BUN significantly increased only on days 14 and 28 in male and female rats after high dose (30/20 mg/kg) Puromycin treatment.

Table 3-14 Summary of body and kidney weight determined for male and female rats treated with 10 mg/kg and 30/20 mg/kg Puromycin for up to 28 days. The data of the control group are displayed in each table. Significant changes were indicated with * $p < 0.05$, ** $p < 0.01$, *** $p < 0.001$ (ANOVA + Dunnett). Because only one male rat on day 28 survived, no statistics could be performed. Strong changes were indicated with (*) based on comparison groups found to be significant altered

		Puromycin [mg/kg]						
		Male			Female			
	time	0	10	30/20	0	10	30/20	
body weight [g]	day 3	255 ± 6	248 ± 6	249 ± 6	170 ± 4	166 ± 6	165 ± 6	
	day 7	275 ± 14	271 ± 8	261 ± 12	178 ± 5	173 ± 7	165 ± 2	**
	day 14	281 ± 13	281 ± 11	255 ± 5 **	182 ± 10	172 ± 9	167 ± 7	*
	day 28	307 ± 14	321 ± 10	227 (*)	180 ± 6	184 ± 10	155 ± 9	***
kidney weight [g]	day 3	2.16 ± 0.07	2.11 ± 0.05	2.06 ± 0.18	1.39 ± 0.06	1.37 ± 0.06	1.43 ± 0.10	
	day 7	2.20 ± 0.13	2.06 ± 0.07	1.90 ± 0.30 *	1.49 ± 0.13	1.36 ± 0.08	1.33 ± 0.10	*
	day 14	2.15 ± 0.14	1.93 ± 0.17	2.15 ± 0.13	1.41 ± 0.11	1.33 ± 0.09	1.59 ± 0.13	*
	day 28	2.16 ± 0.12	2.33 ± 0.18	2.22	1.36 ± 0.06	1.45 ± 0.15	1.67 ± 0.23	*

In contrast to male rats females showed a slight but statistically non significant increase in low dose (10 mg/kg) treated animals on day 3 followed by a decrease after high dose treatment (30/20 mg/kg). Serum glucose levels showed only mild changes over time and dose, with the exception of male rats treated with 30/20 mg/kg Puromycin for 14 days and one individual rat on day 29 (Table 3-15), which showed a strong decrease in serum glucose level. The major alterations in urinanalysis were focused on days 15 and 29 (Table 3-16). However, some effects were also observed at day 4, for example a halfing in urine volume of male rats treated with 30/20 mg/kg Puromycin. In general the decrease in urinary output was more pronounced in male rats than in females but with the strongest impact on days 15 and 29 in both sexes where it was reduced to nearly 25% in males and 50% in females. Comparable to the serum glucose level also urinary glucose (Table 3-16) showed only slight changes. Therefore, a slight but non statistically significant increase was observable in male rats of the high dose (30/20 mg/kg) treatment group on day 4. In contrast, female rats showed a significant decreased urinary glucose level, both in low (10 mg/kg) and high (30/20 mg/kg) treated animals While urinary glucose levels remained relatively constant on day 8 a strong impact in female rats was observed on day 15 in high dose (30/20 mg/kg) animals, where a 3-fold increase was observed. Only individual male rats on day 28 showed a marked increase in urinary glucose level. The most prominent finding in urinary parameters was the increase in urinary total protein. While in male rats no changes after 4 or 8 days was observed, female rats showed a non-significant increase on day 8. Subsequently, an extremely strong increase was found in both genders after high dose (30/20 mg/kg) Puromycin treatment on day 15 (~30-fold increase in male (~16.0 g/L) and ~330-fold increase in female rats (~26.6 g/L)) compared to the corresponding control animals.

Table 3-15 Summary of clinical pathology serum parameter determined for male and female rats treated with saline, 10 mg/kg and 30/20 mg/kg Puromycin for up to 28 days. The data of the control group are displayed in each table. Significant changes were indicated with * $p < 0.05$, ** $p < 0.01$, *** $p < 0.001$ (ANOVA + Dunnett). Because only one male rat on day 28 survived, no statistics could be performed. Strong changes were indicated with (*) based on comparison groups found to be significant altered.

		Puromycin [mg/kg]					
		Male			female		
	time	0	10	30/20	0	10	30/20
Creatinine [mg/dL]	day 3	0.19 ± 0.01	0.19 ± 0.01	0.19 ± 0.01	0.25 ± 0.02	0.19 ± 0.02 **	0.14 ± 0.02 ***
	day 7	0.21 ± 0.02	0.16 ± 0.02 *	0.17 ± 0.04 *	0.24 ± 0.03	0.19 ± 0.04	0.17 ± 0.04 *
	day 14	0.23 ± 0.02	0.20 ± 0.03	1.26 ± 0.82 **	0.23 ± 0.03	0.23 ± 0.03	0.56 ± 0.18 ***
	day 28	0.21 ± 0.01	0.23 ± 0.03	0.32	0.26 ± 0.04	0.27 ± 0.04	0.31 ± 0.07
BUN [mg/dL]	day 3	27.74 ± 1.67	29.43 ± 2.21	29.79 ± 2.50	30.63 ± 2.44	34.95 ± 3.92	28.71 ± 1.07
	day 7	28.11 ± 2.38	27.98 ± 2.27	34.71 ± 8.03	30.99 ± 1.62	31.71 ± 3.07	34.35 ± 4.04
	day 14	28.59 ± 2.06	31.83 ± 3.63	345.91 ± 211.81 **	34.35 ± 1.87	37.23 ± 5.70	194.21 ± 46.72 ***
	day 28	27.74 ± 2.95	30.03 ± 1.85	56.45 (*)	31.47 ± 2.02	33.03 ± 2.72	43.48 ± 6.03 ***
Glucose [mg/dL]	day 3	79.28 ± 9.87	83.60 ± 12.65	84.69 ± 10.89	81.08 ± 14.53	76.04 ± 8.10	78.92 ± 4.49
	day 7	83.60 ± 13.76	83.24 ± 12.05	90.45 ± 6.55	86.49 ± 5.25	65.95 ± 6.45 *	71.35 ± 5.78
	day 14	103.06 ± 19.42	83.96 ± 8.70	74.78 ± 17.99 *	79.28 ± 6.98	78.56 ± 5.78	88.29 ± 15.66
	day 28	113.15 ± 14.49	96.22 ± 10.24	86.49 (*)	84.69 ± 7.85	80.72 ± 7.79	77.84 ± 6.16

The low dose (10 mg/kg) treated animals remained unaltered. While the high amount of urinary protein was constant in female rats, the male rats at this time point showed a further increase in urinary protein (~54.6 g/L) on day 28 of treatment (up to ~148-fold) (Table 3-16). In contrast, the level of urinary creatinine showed only mild changes over time and dose. A slight decrease in low dose (10 mg/kg) treated animals of both sexes and a significant increase in high dose (30/20 mg/kg) treated male rats was seen on day 4. In addition, a slight increase in both genders appeared after 14 days of high dose (30/20 mg/kg) treatment and in low dose (10 mg/kg) treated female rats. The most prominent increase was observed for the surviving male rat treated for 28 days with 30/20 mg/kg Puromycin. The renal functional properties showed the most relevant disturbances after 14 days of high dose (30/20 mg/kg) Puromycin treatment (Figure 3-15). A strong decrease in urinary sodium excretion was detected on both genders after low (10 mg/kg) and high dose (30/20 mg/kg) treatment. In female rats the decrease remained low up to day 29 in the high dose (30/20 mg/kg) group. Urinary excretion of calcium showed a strong increase on days 4 and 8 in animals treated with 30/20 mg/kg Puromycin, followed by a strong decrease on day 15.

Table 3-16 Summary of clinical pathology urinary parameter determined for male and female rats treated with saline, 10 mg/kg and 30/20 mg/kg Puromycin for up to 28 days. The data of the control group are displayed in each table. Significant changes were indicated with * < 0.05, ** < 0.01, *** < 0.001 (ANOVA + Dunnett). Because only one male rat on day 28 survived, no statistics could be performed. Strong changes were indicated with (*) based on comparison groups found to be significant altered.

		Puromycin [mg/kg]								
		Male				female				
	time	0	10		30/20		0	10		30/20	
Volumen [mL]	day 3	20.04 ± 6.90	22.72 ± 6.45		10.74 ± 2.20	*	9.26 ± 4.63	12.92 ± 3.66		8.78 ± 3.72	
	day 7	16.88 ± 7.16	17.76 ± 4.04		15.18 ± 5.68		8.2 ± 3.05	11.7 ± 5.05		8.46 ± 4.94	
	day 14	24.84 ± 10.44	18.76 ± 3.79		6.88 ± 2.94	**	12.8 ± 1.99	7.42 ± 4.25		6.8 ± 2.96	***
	day 28	23.60 ± 6.81	15.88 ± 5.54		5.50	(*)	11.22 ± 6.41	10.6 ± 5.3	*	6.94 ± 1.84	*
Glucose [mg/dL]	day 3	5.41 ± 3.12	4.32 ± 0.99		7.21 ± 2.21		10.09 ± 4.70	4.68 ± 0.99	*	6.85 ± 2.96	
	day 7	6.49 ± 2.05	5.05 ± 0.81		6.13 ± 3.02		7.57 ± 3.22	4.50 ± 1.04		6.13 ± 1.61	
	day 14	5.77 ± 4.11	4.32 ± 0.99		6.13 ± 2.73		5.05 ± 0.81	7.93 ± 3.51		14.77 ± 4.66	**
	day 28	4.32 ± 0.99	6.85 ± 2.96		10.81	(*)	6.49 ± 2.73	5.77 ± 2.96		7.21 ± 1.27	
total protein [mg/dL]	day 3	43.22 ± 21.00	32.70 ± 24.19		42.40 ± 11.48		14.78 ± 8.26	6.78 ± 2.11		11.42 ± 5.01	
	day 7	44.40 ± 13.57	42.08 ± 13.74		53.36 ± 21.73		12.92 ± 4.40	10.50 ± 2.20		29.90 ± 28.57	
	day 14	48.04 ± 28.02	40.36 ± 13.93		1603.06 ± 586.51	***	8.64 ± 1.38	19.16 ± 9.59		2656.06 ± 788.6	***
	day 28	37.12 ± 16.76	143.58 ± 56.91	**	5458.60	(*)	11.90 ± 5.99	101.54 ± 127.86		2801.82 ± 436.65	***
Creatinine [mg/dL]	day 3	40.52 ± 15.78	29.72 ± 10.35		63.05 ± 11.63	*	55.71 ± 23.23	34.98 ± 9.83		52.32 ± 19.45	
	day 7	48.05 ± 14.22	44.02 ± 9.62		57.45 ± 25.97		52.64 ± 12.27	35.99 ± 9.76		57.77 ± 12.11	
	day 14	42.51 ± 21.09	41.76 ± 9.48		60.16 ± 17.31		42.17 ± 6.38	72.95 ± 40.33		68.43 ± 25.24	
	day 28	36.61 ± 6.93	62.24 ± 24.41		108.41	(*)	53.74 ± 23.25	57.34 ± 42.48		59.1 ± 17.42	

In low dose (10 mg/kg) treated animals only a minimal increase in urinary calcium excretion was observed after 8 days. Creatinine clearance showed an increase on day 4 in males and in females on day 8 in high dose (30/20 mg/kg) animals, while a strong decrease was observed on day 15, and stayed low up to day 29.

In contrast to the hematological findings reported in animals treated with Vancomycin (Table 3-5) or Cisplatin (Table 3-11), Puromycin treated rats showed very strong effects were observed in red blood cells and platelets and only minor changes were seen for white blood cells (Table 3-17). Statistically significant findings in the count of RBCs were limited to high dose (30/20 mg/kg) treated female rats, which showed a slight increase on day 4 and a strong decrease on day 29.

Table 3-17 Summary of hematological parameter determined for male and female rats treated with saline, 0.3 mg/kg and 0.6 mg/kg Cisplatin for up to 28 days. The data of the control group are displayed in each table. Significant changes were indicated with * < 0.05, ** < 0.01, *** < 0.001 (ANOVA + Dunnett).

	Puromycin [mg/kg]						
	Male			female			
Time	0	10	30/20	0	10	30/20	
RBC [counts/pL]	8.43 ±0.35	8.00 ±0.35	8.44 ±0.63	8.19 ±0.16	8.27 ±0.26	8.58 ±0.05	**
	9.25 ±0.39	8.78 ±0.27	8.82 ±0.45	8.51 ±0.25	8.66 ±0.41	8.44 ±0.46	
	8.49 ±0.37	9.04 ±0.19	9.31 ±1.54	8.09 ±0.18	8.55 ±0.33	8.42 ±0.47	
	8.86 ±0.35	9.05 ±0.35	6.48	8.54 ±0.33	8.78 ±0.27	6.44 ±0.27	***
PLT [counts/nL]	909 ±100	964 ±60	960 ±112	936 ±96	957 ±123	1046 ±80	
	803 ±135	901 ±74	968 ±51 *	934 ±64	910 ±51	1239 ±154	***
	882 ±95	1054 ±87	1617 ±146 ***	1001 ±125	989 ±102	1534 ±137	***
	904 ±107	979 ±88	1804	786 ±62	896 ±172	1423 ±307	***
WBC [counts/nL]	6.17 ±1.31	4.8 ±1.54	4.77 ±1.29	5.05 ±2.35	5.74 ±0.54	5.54 ±1.18	
	7.29 ±2.33	9.23 ±1.59	7.30 ±0.87	5.60 ±1.35	5.43 ±1.49	5.73 ±2.28	
	6.97 ±0.98	7.76 ±1.19	13.29 ±12.61	4.77 ±0.83	5.03 ±0.90	4.76 ±2.73	
	7.04 ±2.04	6.56 ±1.07	5.73	5.27 ±2.26	5.60 ±1.68	6.08 ±1.50	
NEU [counts/nL]	1.16 ±0.28	0.69 ±0.23 *	0.74 ±0.24 *	1.07 ±0.79	0.74 ±0.27	0.68 ±0.06	
	1.86 ±0.72	1.52 ±0.26	1.43 ±0.30	1.32 ±0.67	1.15 ±0.55	1.19 ±0.29	
	1.33 ±0.37	1.41 ±0.29	4.93 ±6.48	1.01 ±0.51	0.91 ±0.09	1.54 ±1.13	
	1.54 ±0.68	1.29 ±0.28	1.09	1.11 ±0.34	1.10 ±0.27	1.30 ±0.61	
Lymph [counts/nL]	4.69 ±1.05	3.87 ±1.24	3.84 ±1.39	3.68 ±1.85	4.72 ±0.60	4.52 ±1.10	
	4.98 ±2.07	7.26 ±1.56	5.57 ±0.75	3.92 ±1.12	4.01 ±1.58	4.28 ±2.17	
	5.30 ±0.66	5.90 ±0.95	7.63 ±5.81	3.51 ±0.74	3.83 ±0.87	2.97 ±1.50	
	5.12 ±1.24	4.96 ±0.79	4.27	3.90 ±1.99	4.14 ±1.38	4.51 ±1.12	

	Puromycin [mg/kg]						
	Male			female			
Time	0	10	30/20	0	10	30/20	
EOS [counts/nL]	0.10 ±0.02	0.08 ±0.04	0.08 ±0.04	0.11 ±0.05	0.07 ±0.01	0.09 ±0.05	
	0.16 ±0.08	0.14 ±0.05	0.09 ±0.02	0.09 ±0.04	0.10 ±0.02	0.05 ±0.01	
	0.11 ±0.04	0.16 ±0.08	0.07	0.11 ±0.04	0.11 ±0.04	0.03 ±0.03	*
	0.12 ±0.04	0.12 ±0.02	0.09	0.1 ±0.06	0.15 ±0.07	0.07 ±0.02	
BASO [counts/nL]	0.06 ±0.02	0.06 ±0.04	0.05 ±0.02	0.05 ±0.03	0.07 ±0.02	0.07 ±0.04	
	0.08 ±0.04	0.08 ±0.02	0.07 ±0.02	0.07 ±0.02	0.05 ±0.02	0.05 ±0.02	
	0.07 ±0.04	0.09 ±0.03	0.08 ±0.09	0.05 ±0.02	0.06 ±0.02	0.03 ±0.03	
	0.05 ±0.01	0.05 ±0.01	0.03	0.05 ±0.04	0.06 ±0.04	0.03 ±0.01	
MONO [counts/nL]	0.14 ±0.04	0.09 ±0.05	0.07 ±0.02	*	0.13 ±0.05	0.12 ±0.05	0.15 ±0.03
	0.19 ±0.05	0.19 ±0.04	0.12 ±0.04		0.16 ±0.08	0.12 ±0.05	0.13 ±0.05
	0.14 ±0.05	0.16 ±0.02	0.49 ±0.55		0.08 ±0.02	0.1.0 ±0.03	0.17 ±0.16
	0.17 ±0.10	0.12 ±0.03	0.22		0.11 ±0.05	0.13 ±0.06	0.15 ±0.06
LUC [counts/nL]	0.03 ±0.03	0.01 ±0.01	0.01 ±0.01		0.01 ±0.01	0.02 ±0.01	0.03 ±0.00 *
	0.02 ±0.01	0.04 ±0.02	0.03 ±0.01		0.03 ±0.02	0.02 ±0.01	0.03 ±0.03
	0.02 ±0.00	0.04 ±0.02	0.08 ±0.08		0.01 ±0.00	0.01 ±0.01	0.02 ±0.02
	0.02 ±0.00	0.01 ±0.01	0.04		0.01 ±0.01	0.01 ±0.01	0.02 ±0.01

Abbreviation: RBC = red blood cells, PLT = platelets, WBC = white blood cells, NEU = neutrophils, Lymph = Lymphocytes, EOS = eosiniphilics, BASO = basophilics, MONO = monocytes, LUC = large unstained cells.

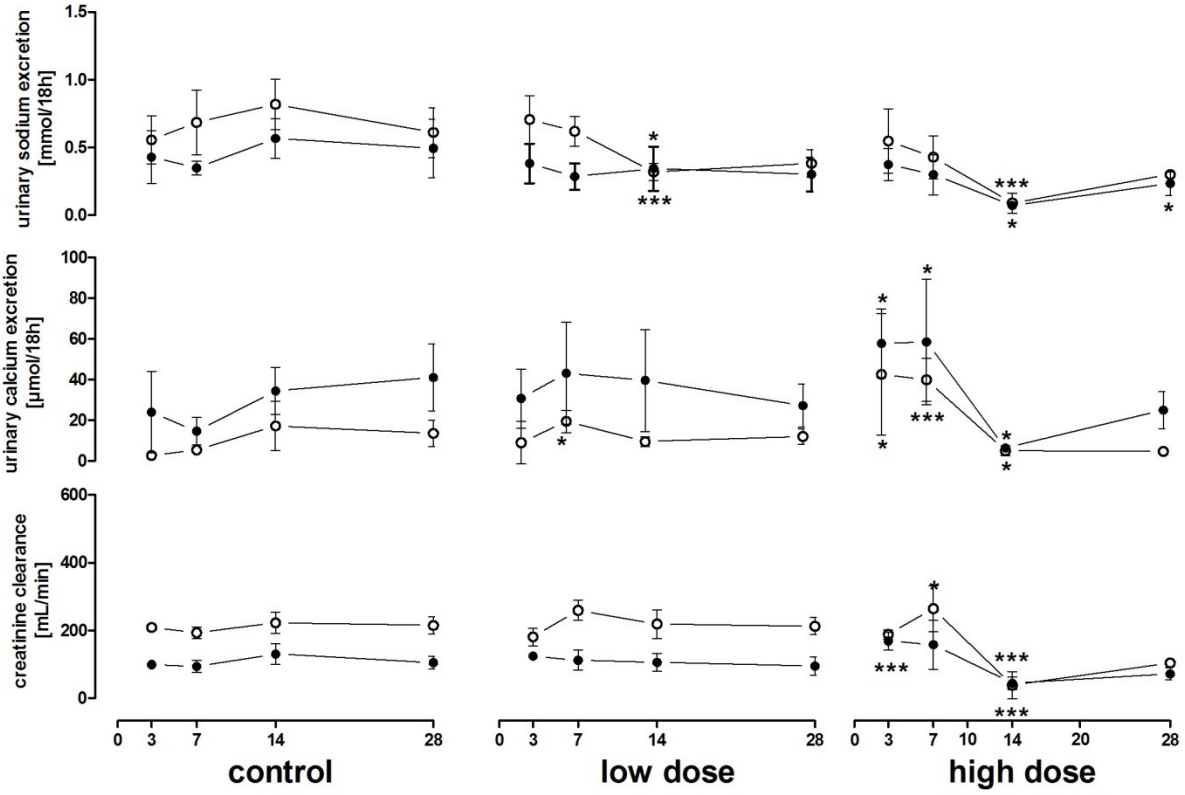

Figure 3-15 Urinary sodium and calcium excretion, as well as the creatinine clearance calculated for male (○) and female (●) rats treated with either wfi (control), 10 mg/kg Puromycin (low dose), or 30/20 mg/kg Puromycin (high dose). Data are presented for both genders individually by mean ± SD. Significant changes were indicated with * $p < 0.05$, ** $p < 0.01$, *** $p < 0.001$ (ANOVA + Dunnett).

The most prominent alteration was the strong, time- and dose-dependent increase in total platelet count. This effect was most pronounced after 15 days of high dose (30/20 mg/kg) treatment and remained relatively constant up to day 29. Statistically significant or biologically relevant findings in the white blood cell populations were limited to individual observations of changed neutrophils, eosinophils, monocytes and large unstained cells. The data is summarised in Table 3-17.

Detection of novel qualified and exploratory urinary proteins (Puromycin)

In animals treated with 30/20 mg/kg (high dose) Puromycin for up to 28 days the urinary excretion of the evaluated biomarker increased after days 14 and day 28 after high dose treatment (30/20 mg/kg) (Figure 3-16, Figure 3-17). In contrast to the treatment schedule of Vancomycin and Cisplatin, Puromycin was administered daily for up to 14 days followed by dosing twice per week. In addition, no statistical analysis could be conducted for high dose (30/20 mg/kg) treated male rats on day 29 because only one animal survived. The strongest increase in both genders was observed for urinary Cystatin C (Figure 3-16f, Figure 3-17f), and Clusterin (Figure 3-16i, Figure 3-17i) after treatment for 14 and 28 days with 30/20 mg/kg Puromycin. These were also the only time points were renal tubular degeneration, dilatation and glomerular vacuolization were observed.

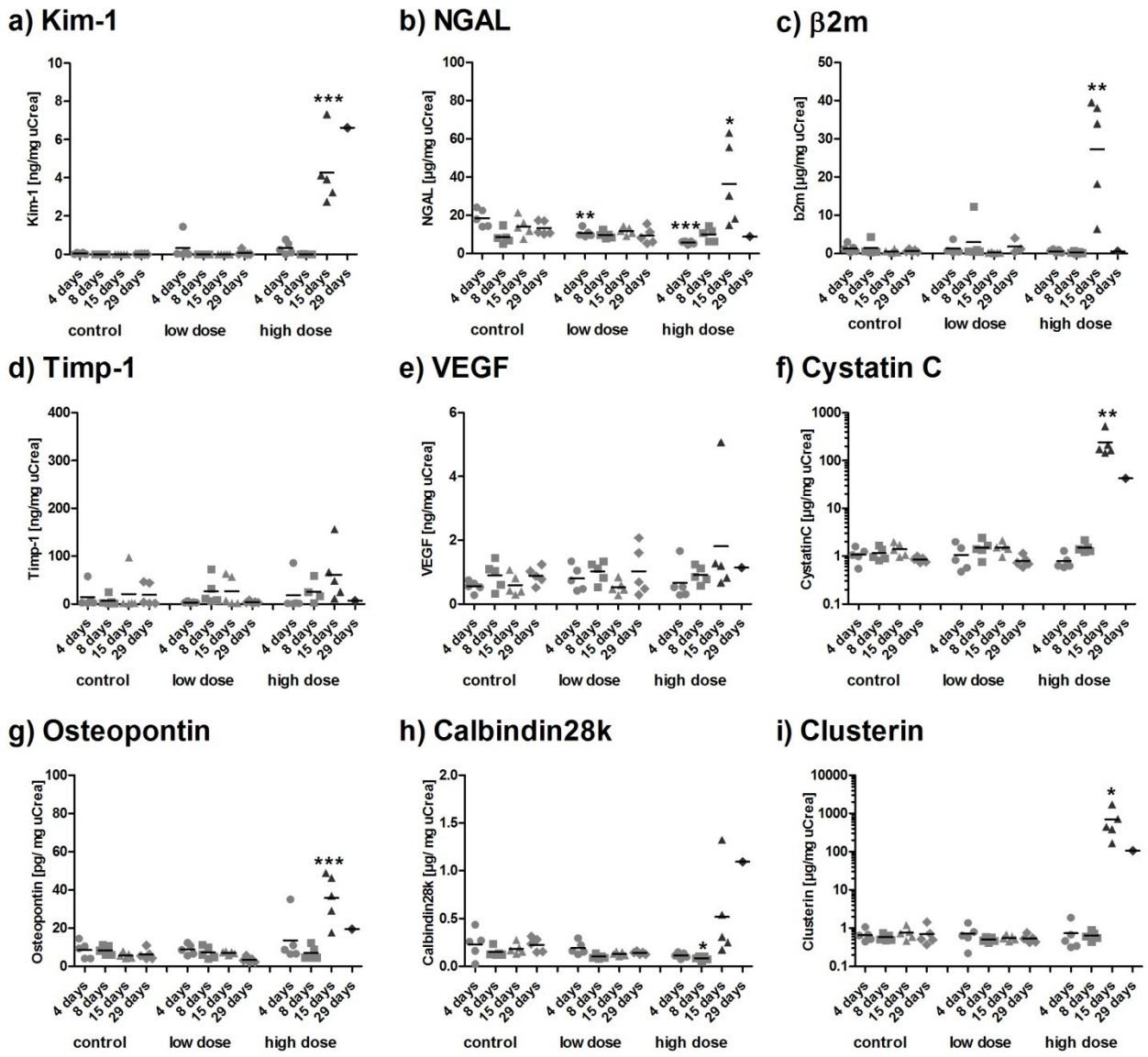

Figure 3-16 Excretion of (a) Kim-1, (b) NGAL, (c) b2m, (d) Timp-1, (e) VEGF, (f) CystatinC, (g) Osteopontin, (h), Calbindin28k, (i) Clusterin in urine of male rats treated with Puromycin (low dose: 10 mg/kg; high dose: 30/20 mg/kg) for 3 days (dots), 7 days (squares), 14 days (triangle), and 28 days (rhombus). Data are presented as individual animals and as the mean (bar; n=5). The light grey signs indicate no tubular degeneration found within this animal, the darker grey indicates tubular degeneration observed. * $p < 0.05$, ** $p < 0.01$, *** $p < 0.001$ (ANOVA-Dunnett).

One exception was was one female animal on day 8 treated with 30/20 mg/kg, which showed mild tubular degeneration and necrosis. However, this animal did not show any increase in any of the evaluated biomarkers.

β2m also showed a strong increase in the pathologically affected high dose (30/20 mg/kg) animals, but with a stronger variation between individual animals (Figure 3-16c, Figure 3-17c). However, the individual male rat on treatment day 28 showed no alteration. Male rats in general showed a large variation over all dosing groups (Figure 3-16c), while female rats were characterized by a higher excretion of urinary β2m.

In comparison to Vancomycin and Cisplatin treatment the increase in Kim-1 (Figure 3-16a, Figure 3-17a) after Puromycin treatment, was much lower. However, because of the very low background of Kim-1 protein and the minimal variablility, this slight increase still lead to significant increases in both male and female rats.

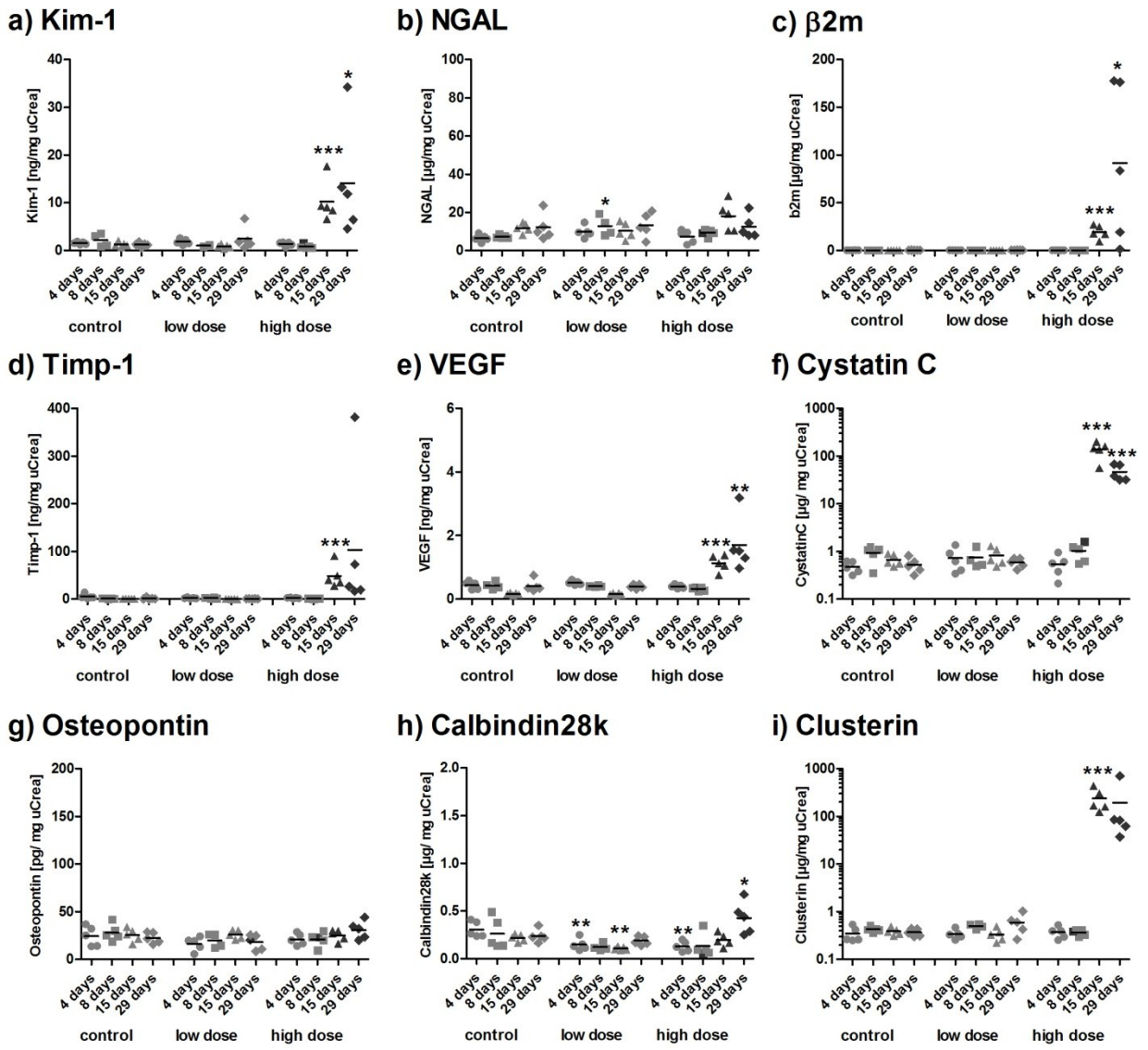

Figure 3-17 Excretion of (a) Kim-1, (b) NGAL, (c) b2m, (d) Timp-1, (e) VEGF, (f) CystatinC, (g) Osteopontin, (h), Calbindin28k, (i) Clusterin in urine of female rats treated with Puromycin (low dose: 10 mg/kg; high dose: 30/20 mg/kg) for 3 days (dots), 7 days (squares), 14 days (triangle), and 28 days (rhombus). Data are presented as individual animals and as the mean (bar; n=5). The light grey signs indicate no tubular degeneration found within this animal, the darker grey indicates tubular degeneration observed. * $p < 0.05$, ** $p < 0.01$, *** $p < 0.001$ (ANOVA-Dunnett).

Gender specific increases in individual urinay biomarkers were detectable. For example, Osteopontin only showed a statistically significant increase in male rats on days 15 and 29 of high dose (30/20 mg/kg) Puromycin treatment, while Timp-1 only increased significantly in female rats.

NGAL also showed a significant increase in male rats treated with 30/20 mg/kg Puromycin for 14 days, while the remaining animal on day 29 showed no alteration in urinary NGAL excretion (Figure 3-16b). In contrast, NGAL showed no significant increase within the groups where histopathological alterations were described. However, a statistically significant increase was seen on treatment day 7 of female animals administered with 10 mg/kg Puromycin. Low dose (10 mg/kg) treated animals on day 4 and day 15 as well as high dose (30/20 mg/kg) treated animals on day 4 showed a significant decrease in Calbindin. However, animals which showed tubular degeneration and/or glomerular vacuolization did not show any decrease of Calbindin. In contrast, animals from the Puromycin high dose (30/20 mg/kg) treatment group on day 28 showed a statistically significant increase.

In male rats no prominent or statistically significant alterations in VEGF were observed. However, one animal showed an increase in urinary VEGF level of 10-fold (Figure 3-16f). This animal was the only one that showed a massive glomerular vacuolization and moderate eosinophilic casts. In contrast, female rats showed a statistically significant elevation of VEGF after 14 and 28 days of treatment, in a time dependent manner (Figure 3-17f).

Table 3-18 Area-under-the-receiver-operator-characteristic curve (AUROC) for detection of Puromycin induced nephrotoxicity. The area under the curve is used as a measure for the overall ability of a biomarker to discriminate animals without histopathological findings in kidney from those with signs of tubular damage (degeneration/ necrosis). Markers with a good diagnostic performance (AUROC > 0.90) are highlighted in bold. In addition the 95% confidence interval and the p-value are displayed. The AUROC for female rats were not calculated because of only one animal with biological important histopathological findings. * =measurement by Luminex® xMAP®, ** = measurement by RENA®-Sticks, #= classical clinical-pathology parameter determined by standard procedures.

Kidney Biomarker	Male			Female		
	AUROC	95% CI	p-value	AUROC	95% CI	p-value
Kim-1*	**1.00**	**1.00 – 1.00**	**<0.0001**	**0.93**	**0.79 – 1.00**	**<0.0001**
Timp-1*	0.82	0.69 – 0.95	0.0119	**0.90**	**0.78 – 1.00**	**<0.0001**
VEGF*	0.77	0.60 – 0.93	0.0341	0.88	0.72 – 1.00	<0.0001
$ß_2$-Microglobulin*	**0.93**	**0.82 – 1.00**	**0.0006**	**1.00**	**1.00 – 1.00**	**<0.0001**
Clusterin*	**1.00**	**1.00 – 1.00**	**<0.0001**	**0.93**	**0.80 – 1.00**	**<0.0001**
Cystatin C*	**1.00**	**1.00 – 1.00**	**<0.0001**	**1.00**	**1.00 – 1.00**	**<0.0001**
Lipocalin-2/ NGAL*	0.88	0.70 – 1.00	0.0028	0.61	0.41 – 0.81	0.2355
Osteopontin*	**0.99**	**0.97 – 1.00**	**<0.0001**	0.68	0.52 – 0.84	0.0623
Calbindin *	**0.93**	**0.85 – 1.00**	**0.0006**	0.76	0.62 – 0.91	0.0053
Kim-1**	0.65	0.48 – 0.82	0.2231	0.85	0.75 – 0.95	0.0003
BUN#	**1.00**	**1.00 – 1.00**	**0.0003**	**0.96**	**0.91 – 1.00**	**<0.0001**
Serum Creatinine#	**1.00**	**1.00 – 1.00**	**0.0003**	**0.90**	**0.80 – 1.00**	**<0.0001**

Female rats showed no alteration in urinary Osteopontin at any time point or dose group (Figure 3-16g), while male rats showed a clear dose- and pathology-dependent increase, specifically on day 14 (Figure 3-17g).

The results of the ROC analysis are given in Table 3-18.

Based on the area-under-the-ROC-curves (AUROC), Kim-1 (m: 1.00; f: 0.93), Cystatin C (m: 1.00; f: 1.00), β2m (m: 0.93; f: 1.00) and Clusterin (m: 1.00; f: 0.93) performed the best. However, the traditional parameters BUN (m: 1.00; f: 0.96) and serum creatinine (m: 1.00; f: 0.90) also performed well within this study. Based on the results of the ROC-analyses a strong gender specific diagnostic performance of the urinary biomarker was observed, with a better performance in male rats observed (Table 3-18). Osteopontin (m: 0.99; f: 0.68) and Calbindin (m: 0.93; f: 0.76) showed a much better performance in male rats then in females. Even the calculated AUROC values for NGAL (m: 0.88; f: 0.61) were below the set threshold of 0.9, but the diagnostic performance was much better in male then in female rats treated with Puromycin. In constrast, Timp-1 (m: 0.82; f: 0.90) showed a slightly higher AUROC in females. Also better performance in female rats was seen for VEGF (m: 0.77; f: 0.88) which was below the threshold, but still indicated a good performance.

A poor performance was observed for Kim-1 (m: 0.65; f: 0.85) when determined by using the Dipstick assay, which was far below the values of the Kim-1 Luminex® xMAP® measurement.

Evaluation of expression of Kim-1, Clusterin and Osteopontin protein in renal tissue (Puromycin)

The Puromycin study showed in addition to tubular damage also glomerular effects. The markers evaluated performed very well by urinary analysis, as reflected by ROC analysis (Table 3-18).

The protein expression in control animals showed no time-dependent alteration. Kim-1 and Clusterin showed no staining in untreated animals, while Osteopontin delivered a slight but constant basal expression within corical and medullar tissue. An overview of control animals is shown in the 5.1 Annex 1.

Representive pictures for Kim-1, Clusterin and Osteopontin stained kidney for male and female rats treated with 30/20 mg/kg Puromycin are shown in the figures below. The low dose treated animals (10 mg/kg) showed no relevant changes compared to the control animals. For each individual finding an overview is given spanning from the cortex to the medullary papilla and a detailed picture of the cortical zone and the medullary zone. To show the most specific observations in some pictures the inner or the outer zone of medulla is also shown.

For Puromycin treated rats it was expected that tubular damage would only appear as a secondary process caused by excessive glomerular damage.

Kim-1

Male rats treated with 30/20 mg/kg Puromcin for 3 (Figure 3-18 a-c) and 7 (Figure 3-18 d-f) days showed no staining within the cortical or medullary zone. Therefore, no difference compared to the control animals was seen. After 15 days a strong increase in tubular Kim-1 proteins appeared, limited to individual proximal tubules (Figure 3-18 g). The staining was exclusively found intracellular and not in any proteinaceouse casts (Figure 3-18 h) within the cortex. In contrast, the staining of Kim-1 within the medullary zone was limited to intraluminal accumulation, down to the pelvis (Figure 3-18 i). On day 28 male rats still showed a high expression of renal Kim-1 protein; although below the intensity observed on day 14 (Figure 3-18 j, k). The intraluminal Kim-1 in the medulla was still present, but also reduced compared to the earlier time point (Figure 3-18 l).

In contrast to male rats, females treated with 30/20 mg/kg Puromycin for up to 28 days, showed a slight but significant increase in renal Kim-1 proteins within proximal tubular cells as early as three days of treatment (Figure 3-19 b). However, the staining was limited to individual cells belonging to one or neighboring tubules (Figure 3-19 a). No staining in the medullar was detected. After 7 days of treatment the expression of renal Kim-1 protein was reduced compared to day 3, but still above the expression seen in control animals (Figure 3-19 d, e). No Kim-1 was found in the medullary zone (Figure 3-19 f). On day 15 a strong increase in Kim-1 protein was observed in the cortex. In contrast to male rats at the same time point, the staining of Kim-1 within the renal cortex was wide spread (Figure 3-19 g, h). In addition, slight staining of Kim-1 was also observed within intraluminal proteinaceouse droplets (Figure 3-19 h). Medullary staining was still limited to intraluminal accumulation (Figure 3-19 i). Comparable to male rats, the area and the intensity of Kim-1 expression after 28 days of 30/20 mg/kg Puromycin treatment was also reduced in females (Figure 3-19 j). However, distinct areas of Kim-1 expression were detected in proximal tubular regions (Figure 3-19 k).

Also after 28 days massive proteinaousos casts were found, which showed no to only minimal staining of Kim-1 proteins. Only in the medullary zone, individual droplets were found (Figure 3-19 l) including Kim-1 stain.

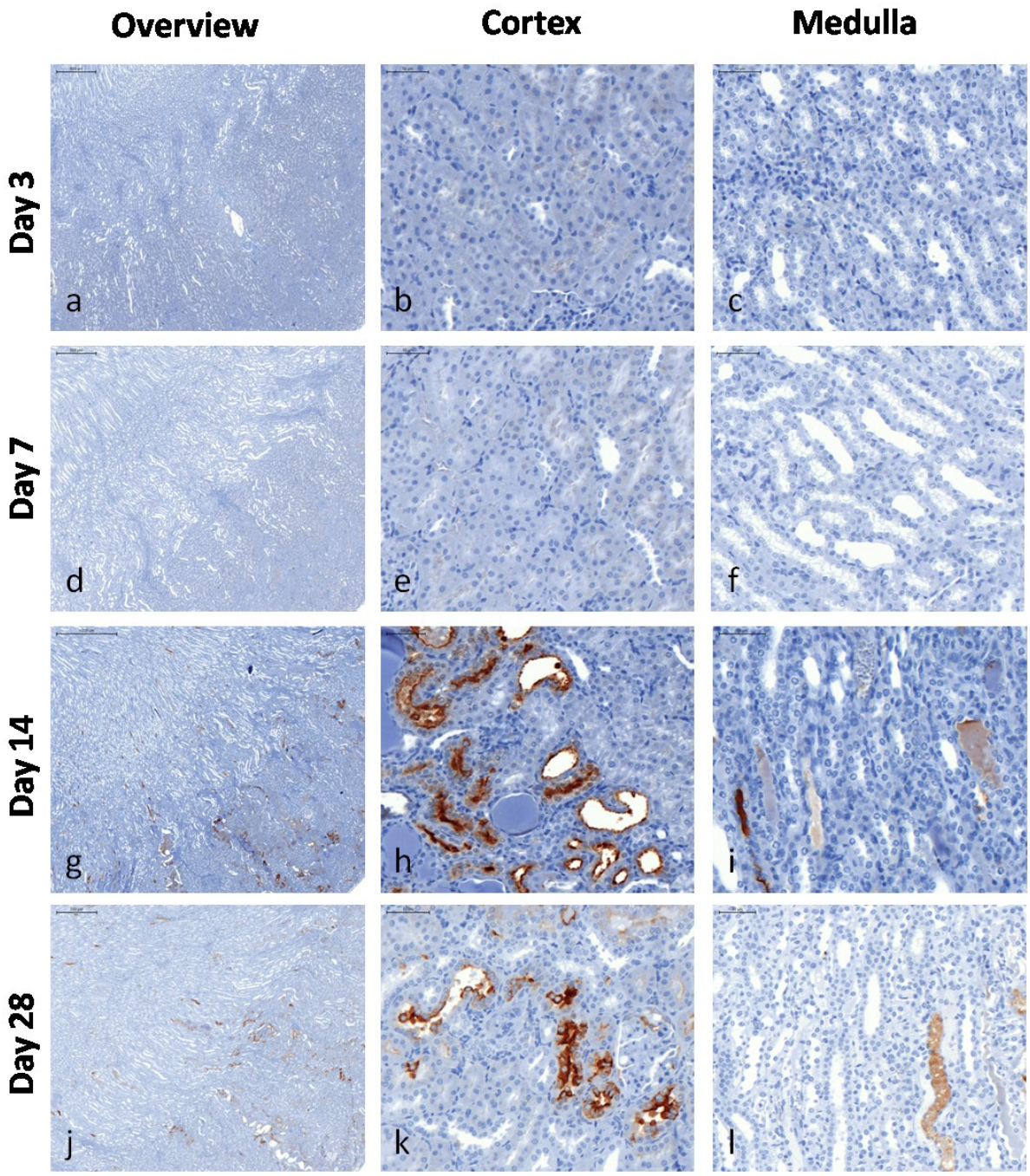

Figure 3-18 The location of Kim-1 protein in renal tissue of male rats treated with 30/20 mg/kg Puromycin is shown for each time point of necropsy. An overview picture for each time point (a, d, g, j) shows the whole area from the cortical zone to the medullary papilla. In addition, two detailed pictures, either of the cortex (b, e, h, k) or the medulla (c, f, i, l) are given. The magnification of the overview was ~10 times and of the detailed pictures ~70 times.

Clusterin

The expression of clusterin in male rats after 30/20 mg/kg Puromycin treatment showed no alterations up to seven days, neither in the cortex neither nor in the medulla (Figure 3-20 a-f). After 14 days of treatment individual tubules showed slight, but not prominent, expression of renal Clusterin (Figure 3-20 g, h). The staining in the cortical zone was limited to cells and was not found in any proteinaceouce casts within the tubular lumen (Figure 3-20 h).

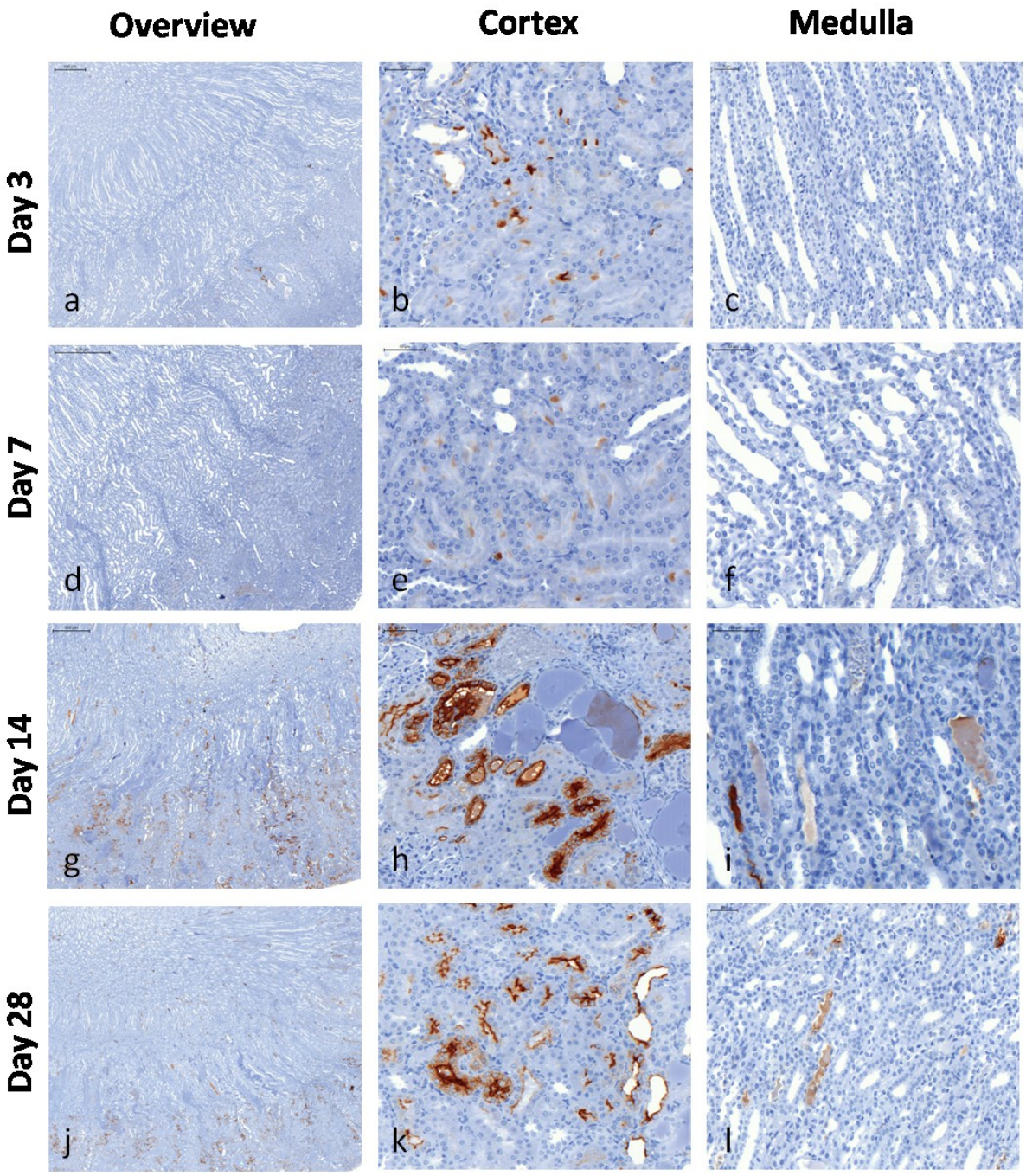

Figure 3-19 The location of Kim-1 protein in renal tissue of female rats treated with 30/20 mg/kg Puromycin is shown for each time point of necropsy. An overview picture for each time point (a, d, g, j) shows the whole area from the cortical zone to the medullary papilla. In addition, two detailed pictures, either of the cortex (b, e, h, k) or the medulla (c, f, i, l) is given. The magnification of the overview was ~10 times and of the detailed pictures ~70 times.

In contrast, the medullary luminal staining, especially in the inner medullary zone, was more pronounced (Figure 3-20 g, i). On day 29, the staining was comparable to day 15 in intensity and area, with the exception that the tubular lumen in the medullary zone showed more diffuse, but weaker stained fluids (Figure 3-20 j-l). In female rats treated with 30/20 mg/kg Puromycin also no increase in renal Clusterin expression on days 4 and 8 were observed, neither in the cortex nor in the medulla (Figure 3-21 a-f). On day 14 an increase in Clusterin was detected in individual tubules, without any staining of proteinaceous casts (Figure 3-21 g, h).

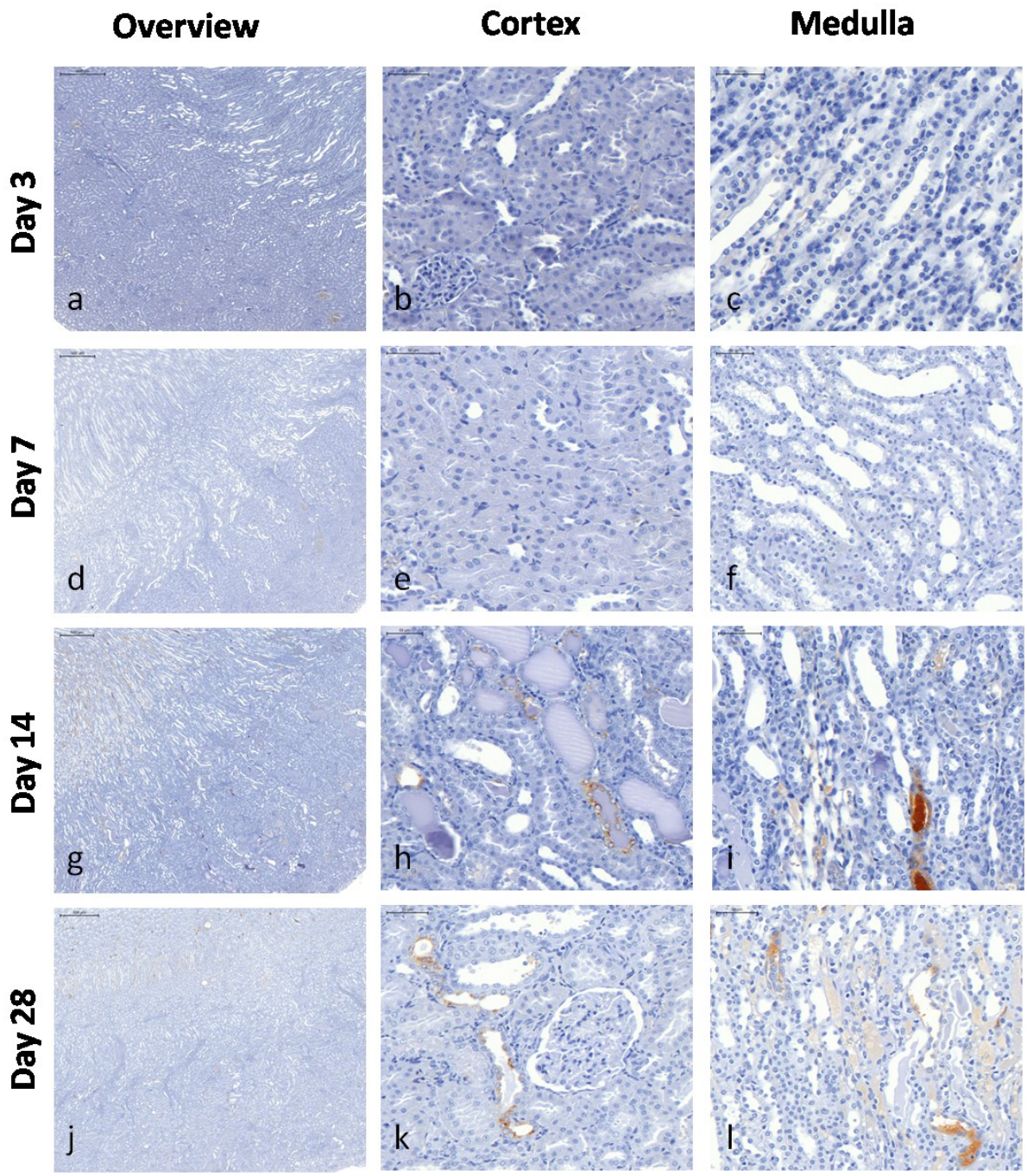

Figure 3-20 The location of Clusterin protein in renal tissue of male rats treated with 30/20 mg/kg Puromycin is shown for each time point of necropsy. An overview picture for each time point (a, d, g, j) shows the whole area from the cortical zone to the medullary papilla. In addition, two detailed pictures, either of the cortex (b, e, h, k) or the medulla (c, f, i, l) is given. The magnification of the overview was ~10 times and of the detailed pictures ~70 times.

As already described for male rats, also, the staining within the medullary zone of females was limited to intraluminal fluids (Figure 3-21 i). After 28 days of treatment, the intensity of Clusterin expression increased slightly compared to day 14 and the staining was still located in the same areas.

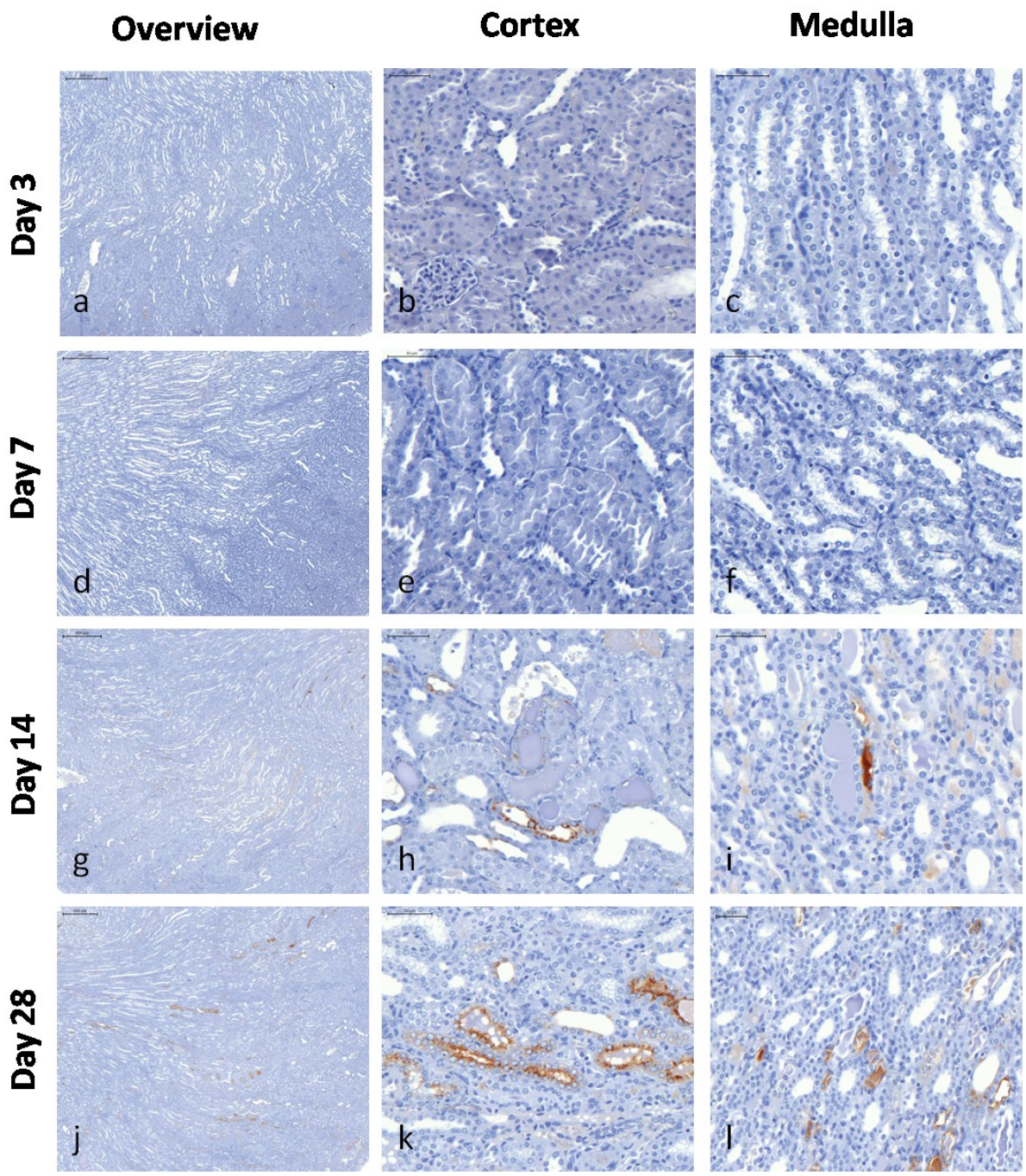

Figure 3-21 The location of Clusterin protein in renal tissue of female rats treated with 30/20 mg/kg Puromycin is shown for each time point of necropsy. An overview picture for each time point (a, d, g, j) shows the whole area from the cortical zone to the medullary papilla. In addition, two detailed pictures, either of the cortex (b, e, h, k) or the medulla (c, f, i, l) is given. The magnification of the overview was ~10 times and of the detailed pictures ~70 times.

Osteopontin

The basal expression of Osteopontin in male and female rats was much more pronounced then for Kim-1 and Clusterin. However, in male rats treated with 30/20 mg/kg Puromycin for three days a slight but significant increase in renal, cortical Osteopontin was observed (Figure 3-22 a, b). Also in the medullary zone, significant amount of Osteopontin protein was found, both intra- and extracellular (Figure 3-22 c).

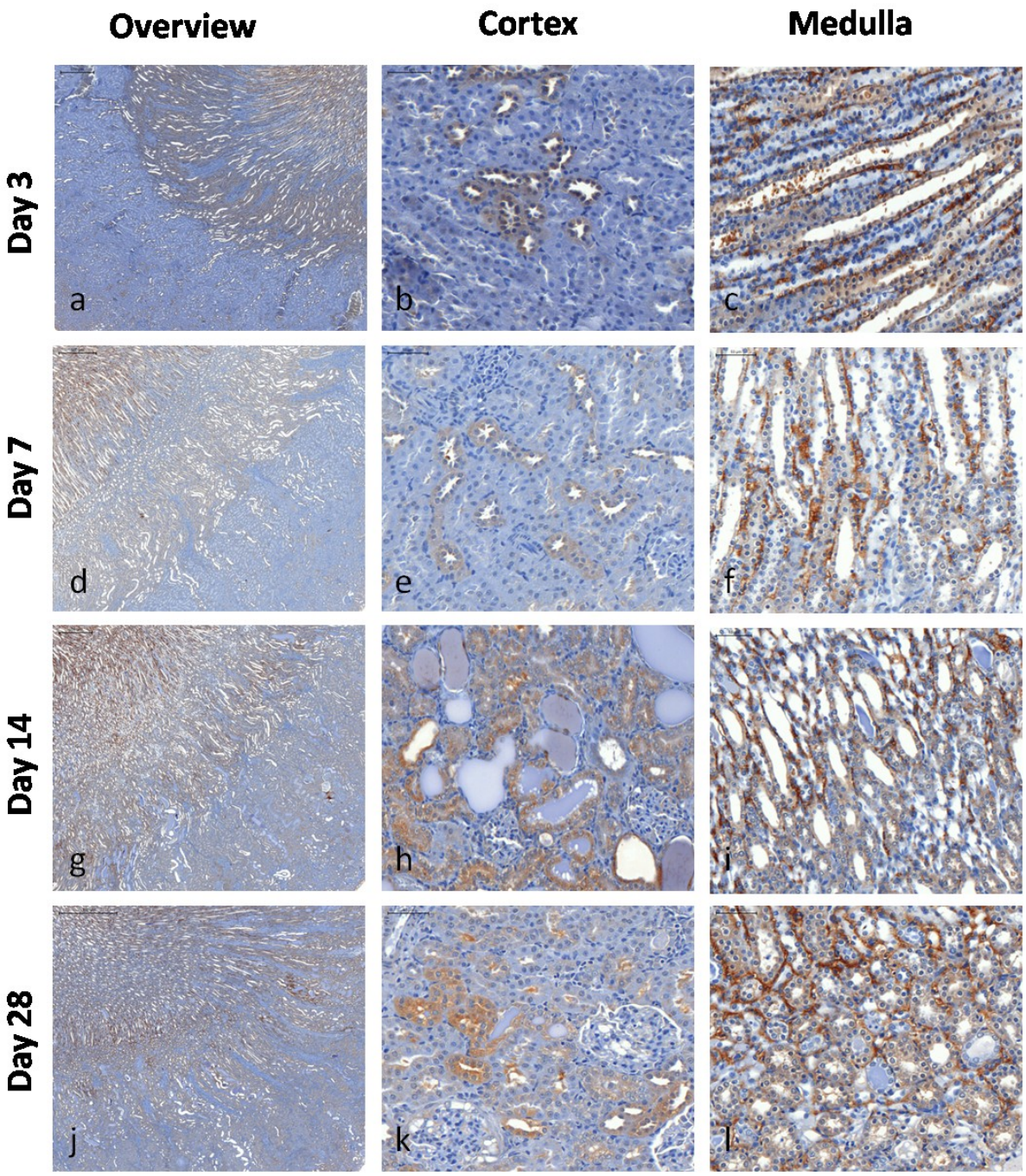

Figure 3-22 The location of Osteopontin protein in renal tissue of male rats treated with 300 mg/kg Vancomycin is shown for each time point of necropsy. An overview picture for each time point (a, d, g, j) shows the whole area from the cortical zone to the medullary papilla. In addition, two detailed pictures, either of the cortex (b, e, h, k) or the medulla (c, f, i, l) is given. The magnification of the overview was ~10 times and of the detailed pictures ~70 times.

These expression patterns remained constant from day 4 to day 8 (Figure 3-22 d-f). On day 14 the intensity and the area covered by Osteopontin staining increased strongly compared to days 4 and 8 (Figure 3-22 g- j). Not only minimal staining of tubular casts in the cortical or medullarly zone was found (Figure 3-22 h), but strong staining of the extracellular matrix was found (Figure 3-22 j). Compared to day 15 the expression of renal Osteopontin was slightly reduced on day 29, although the location of staining remained unaltered (Figure 3-22 j-l).

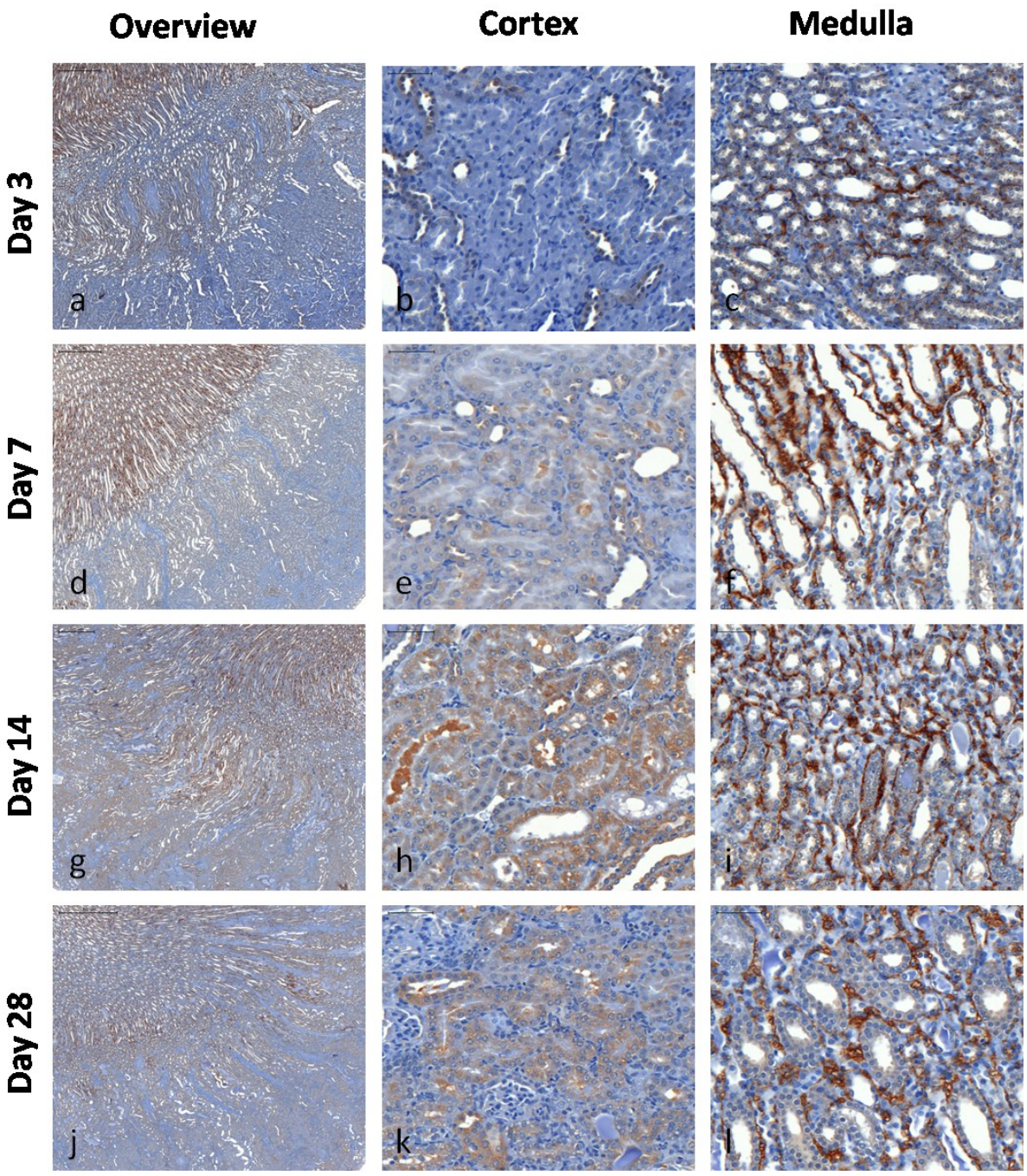

Figure 3-23 The location of Osteopontin protein in renal tissue of male rats treated with 30/20 mg/kg Puromycin is shown for each time point of necropsy. An overview picture for each time point (a, d, g, j) shows the whole area from the cortical zone to the medullary papilla. In addition, two detailed pictures, either of the cortex (b, e, h, k) or the medulla (c, f, i, l) is given. The magnification of the overview was ~10 times and of the detailed pictures ~70 times.

In female rats, the expression of renal Osteopontin showed no relevant alteration after three days of high dose (30/20 mg/kg) Puromycin treatment in the cortex (Figure 3-23 a, b). However, the staining of the inner medullary zone appeared to be slightly stronger, especially in the extracellular matrix (Figure 3-23 a, c). After seven days of treatment, the intensity of staining further increased, both in the cortex and the medulla (Figure 3-23 d-f). As already described for male rats, on day 15 the intensity and area of Osteopontin expression reached the highest degree. Therefore, cortical Osteopontin protein was found both intracellular and intratubular (Figure 3-23 h). The intensity of medular staining

remained unaltered compared to day 7 (Figure 3-23 i). On day 28, a decrease compared to day 14 over all renal compartments was observed; showing an expression still above day 3 levels (Figure 3-23 j-l).

3.1.1.6 Discussion and Conclusion (Puromycin)

The doses of 10 mg/kg (low dose) and 30/20 mg/kg (high dose) were chosen to induce mild to moderate glomerular damage in high dose and no to minimal glomerular alterations in low dose animals. Almost all of the biomarkers within this study are described to be specific for tubular damage; however there is some evidence that several of urinary markers can also be used to detect glomerular alteration.

As shown in section "Histopathological observation (Puromycin)", the expected moderate changes on the glomerulus were only weakly observed, while tubular alterations appeared more prominently then expected. However, the results were generally in line with the observations from the dose range finding study [Fuchs et al., 2012]. Because of the presense of both glomerular vacuolization and tubular damage, the interpretation of the underlying changes in urinary protein profiles is much more complex then for the studies of Vancomycin (see 3.1.1.1 Results (Vancomycin)) or Cisplatin (see 3.1.1.3 Results (Cisplatin)). It was assumed that any differences observed between the Vancomycin derived results (specific tubular damage only) and the results from the Puromycin treated animals, are caused by a glomerular change.

The fact that the body weigth showed a time- and dose-dependent decrease reflects the strong impact of the Puromycin treatment on the animals, even before renal alterations were observed by histopathology. The alteration in kidney weight, which showed a decrease on day 8 and an increase on days 15 and 29 in high dose (30/20 mg/kg) treated animals, gives evidence that Puromycin can have an effect on the kidney, even before histopathological alterations are observed, as was the case on treatment day 7. The increase in kidney weight can be due to a hydronephrosis and therefore lead to an increased volume of primary urine within the tubular system. Hydronephrosis describes the situation where the urine collecting system of the kidney is dilated [Merck Manuals Home Health Handbook, 2007]. These findings are in good correlation with the decrease in urinary output (Figure 3-15) and with the absence of marked alterations in white blood cells (Table 3-17), because of the non-inflammatory characteristics of this nephrosis. Because the ureter and bladder were always within normal limits (data not shown), the cause of the hydronephrosis must be assumed to be related to the kidney. Therefore, the moderate to massive break-down in tubular cells and the prominent appearance of tubular degeneration (Table 3-13) can point to the fact that apoptotic cells lead to the obstruction of the collecting system of the kidney [Yang et al., 2001]. However, the presense of a hydronephrosis can also explain the strong alterations in sodium and calcium excretion, which appeared also in low dose (10 mg/kg) treated animals, as well as the impairment of the renal function as displayed by the creatinine clearance. The imbalance in electrolytes, as well as the decrease in glomerular filtration rate, can have a strong impact on the evaluated urinary protein biomarkers and therefore their predictivity.

In general, the male rats were more sensitive to Puromycin treatment than females. This was reflected over almost all evaluated parameters. The two urinary protein biomarkers most excpected to be affected are Cystatin C and β2m, both described to be not of renal origin [Fuchs et al., 2011]. Both biomarkers are assumed to show an increase specifically after tubular damage, by a reduced reabsorption after renal tubular break-down. There is already some evidence that they are more specific in case of glomerular damage induced proteinuria [Dieterle et al., 2010]. Within this study, this was the case for Cystatin C, which showed and very marked and highly specific increase in all rats described to have histophatological alterations. Because the source of Cystatin C is not renal but systemic, the detection of this individual protein, even highly specific, could not be shown to bring a higher sensitivity compared to the general determination of total urinary protein. Subsequently, as it is the case for urinary albumin, which can be used to discriminate between glomerular and tubular associated proteinuria, the detection of an individual non-renal, urinary protein, can give further information about the area of damage or can in some cases be more sensitive than the detection of total protein in urine.

In addition, the diagnostic performance determined by ROC analyses clearly reflects the good correlation of the increase in urinary Cystatin C with the histopathological observations (Table 3-18). Because of the appearance of both glomerular and tubular damage, no clear assignment for the origin of the urinary Cystatin C is possible. However, by comparying the underlying pathologies and the diagnostic performance of Cystatin C over all three studies, the hypothized specificity of Cystatin C for glomerular damages is supported. Subsequently, it was also reported that Cystatin C is expressed within the proximal tubular cells [Togashi et al., 2011]. Even though the amount of renal Cystatin C protein was not altered after Cisplatin treatment, it can be hypothized that the break-down of proximal tubular cells leads to a release of intracellular Cystatin C, which then entered the urine.

β2m is described to follow the same mechanism as Cystatin C, and showed a marked and statistically significant increase. The reason for the stronger variation between individual animals is currently not clear. The fact, that β2m is affected by other physiological conditions reflects the physiological proteinuria described for male rats [Appenroth et al., 1986]. Therefore, the basal excretion of β2m in male rats was always higher and characterized by a stronger variability between the animals, also when no histopathological alterations were observed. Subseqeuntly, it can be hypothized that the strong and statistically significant decrease in creatinine clearance, which is considered to be a suitable parameter for the glomerular filtration rate, has a stronger influence on β2m then on Cystatin C. This assumption is underlined by the fact that in contrast to Cystatin C no prominent renal expression of β2m itself has been described so far. However, the strong increase, as well as the good AUROC values, indicates that β2m is a good marker to detect the underlying renal pathology caused by puromycin. The fact that β2m is one of the FDA/ EMA/ PMDA qualified biomarkers for acute rat toxicity gives further evidence for the use of this marker in routine toxicological studies.

The remaining urinary protein biomarker, which performed well in both genders were Kim-1 and Clusterin. Based on a direct comparison of these two qualified protein biomarkers, it becomes obvious that tubular damages took place, with a strong impact to the proximal tubular cells. This is suported by the increase in urinary Kim-1, which is specific for the S3 segment of the proximal tubulus. In contrast, urinary Clusterin, which showed a very strong elevation of >100-fold over the control animals, indicates general tubular insult. The increase in urinary Kim-1 was further supported by the expression of renal Kim-1 protein, which showed strong and specific staining of individual proximal tubulus. In this case it is notable that female rats showed a higher concentration of urinary Kim-1, even though the observed renal damage was weaker than seen in the males. Additionally, female rats showed individual cells expressing Kim-1 protein as early as day 3 (Figure 3-19), even though no histopathological observations were observed. Because of the high specificity of the immunohistochemical analysis and the relatively small area of expression, these very slight effects might be overlooked during histopathology assessments. However, the urinary Kim-1 levels also showed a very slight increase in animals on day 4. Based on the absence of comparable alterations within the control animals, these slight events seem to be treatment related. This leads to the conclusion that the immunohistochemical analysis of Kim-1 protein within renal tissue is highly sensitive and therefore also a potential method for screening by tissue array analysis.

The level of renal expression of Clusterin protein was below that observed for Kim-1. This is remarkable, because of the very high amounts of urinary Clusterin excretion seen. This can be explained by the property of Clusterin, that after the specific upregulation in renal tissue after an insult, it is directly secreted into the urine [Solichova et al., 2007]. Consequently, the intracellular levels of Clusterin protein can be lower. Additionally, Clusterin is expressed in a multitude of tissues and secreted into many different bodyfluids [Jones, 2002]. The origin of the urinary Clusterin is not nescessarily from the kidney. Especially in this study, were a strong impairment of the renal clearance was observed, together with some effects on other organs (data not shown), this assumption can not be rejected. That there is an

increase in renal Clusterin expression, together with the high diagnostic performance, also within the Vancomycin and Cisplatin studies, makes this qualified urinary biomarker specific and sensitive for the prediction of general tubular damage.

A strong gender difference was observed for urinary Osteopontin excretion, performing much better in male rats treated with Puromycin than in females. Male rats showed a pathology-dependent increase on days 15 and 29, while female rats showed no changes at all. By comparing the alterations in urinary Osteopontin level with the renal protein expression, it becomes clear that also female rats showed an increase in renal Osteopontin expression. Subsequently, the question arises why the urinary amount of Osteopontin remained constant. While in male rats the staining of collagen-bound Osteopontin, which was specifically observed in the medullary zone, showed only a slight increase, the staining intensity within females was much stronger. This could be observed the earliest on day 8, where also a slight increase in intracellular expression of Osteopontin within cortical tubular cells was seen. The fact that female rats builded up a higher amount of extracellular matrix proteins like collagen, can explain the absence of an increase of urinary Osteopontin, because it was trapped within the medullary zone and the bladder. The gender specific up-regulation of profibrotic factors can be due to renin, which has been described to mediate profibrotic effects by specific receptor binding [Ruester et al., 2006]. Because it is known that the Renin-Angiotensin system showed different responses of androgens and oestrogens on normal and diseased kidney, it has been hypothized that oestrogen playes a key role in an superior renal function and higher resistiance to renal injury of females. In addition, female rats have been shown to have a much stronger proteinuria (Table 3-16), one of the major causes for interstitial fibrosis [Ruester et al., 2006]. Finally, urinary Osteopontin delivered only good results in male rats and therefore underestimated the renal injury in females.

The urinary protein biomarker Calbindin also showed a higher sensitivity and specificity in male rats. However, female rats showed more significant alterations, specifically decreases, than males. In general the positively diagnosed animals of high dose treatment on days 14 and 28, gives evidence that Calbindin showed a pathology-dependent increase in both genders. However, application dependent effects, leading to a reduction in urinary Calbindin masked this effect in female rats. One possible reason for the decrease in urinary Calbindin is based on hydronephrosis. Calbindin is strongly associated with the intraluminal and intracellular calcium homeostasis, based on its role as a calcium binding protein. The hydronephrosis-induced imbalance in calcium can be seen to be inversely related. Therefore, the increase in calcium excretion (Figure 3-15) is linked to the decrease in urinary Calbindin (Figure 3-16h, Figure 3-17h). However, the lack of a strong increase in animals with tubular and/or glomerular damage can also be based on the sensitivity and specificity of Calbindin to detect distal tubular damage. Because it was expected that the primary effect of Puromycin was glomerular damage and tubular alterations only appeared as a secondary effect caused by proteinuria, the distal tubulus may be only weakly affected in female rats, as supported by the histopathological observations (Table 3-13). In contrast Timp-1 performed better in female rats the in males. While female rats showed a strong increase in urinary Timp-1 in all animals affected by either tubular damage or glomerular vacuolation, males only showed a tendency in high dose treated animals on day 15. Two differences between the genders may play a role in the underlying results. Firstly, there was a difference in the control animals observed over time. Male rats showed a constant increase in urinary Timp-1 from day 3 to day 28, while the urinary Timp-1 level in female remained constant. Therefore, differences in the normal growing of the kidney of the juvenile rats seem to have slightly different mechanisms between the sexes. Timp-1, a specific inhibitor of matrix metalloproteases (MMPs), is involved in the degradation of the extracellular matrix [Brew et al., 2000]. In healthy tissue Timp-1 and the MMP binding partners ensure equilibrium of formation and degradation of extracellular matrix [Fuchs et al., 2011]. Because a stronger formation of fibrotic tissue was observed in female rats (Figure 3-23), the equilibrium of this steady state seems to have been interrupted and

therefore lead to this specific pathological outcome. Consequently, the involvment of Timp-1 in this process of extracellular matrix formation can due to the absence of urinary Timp-1 in male rats. However, it is not clear if the absence or presence of Timp-1 is caused by the difference in the development of fibrotic tissue or the reason for it. By analyzing the diagnostic performance of urinary VEGF to detect Puromycin induced renal damage; there were also gender specific differences. Both male and female rats showed elevated AUC in ROC analysis, but still below the defined threshold of a well performing biomarker. However, female rats showed a slightly better AUROC (0.88 and a 95%CI of 0.72-1.00). Also the two high dose female groups on treatment days 14 and 28 showed statistically significant results with only low variations, even though the increase was only low, giving further evidence that this urinary biomarker can deliver reliable information. Because VEGF has been described to be specific for tubular damage in chronic cyclosporine nephrotoxicity [Shihab et al., 2001], or tracolimus induced nephrotoxicity [Ogutmen et al., 2006], it can be concluded that the increase in urinary VEGF was caused by the tubular degeneration. Subsequently, this would not explain why no stronger increase in male rats was observed and why no increase in urinary VEGF was detected within the Vancomycin and/or the Cisplatin study. Because of the involvement of VEGF in a multitude of cellular and renal processes, including the promotion of cell proliferation, differentiation and survival of endothelial cells, the mediation of endothelium-dependent vasodilatation, the induction of microvascular hyperpermeability and the participation in interstitial matrix re-modeling [Schrijvers et al., 2004]. Its role in cell proliferation and differentiation as a reason for its increased release is unlikely because of the absence of basophilic tubules in female rats and in this case a lower regeneration as observed in males. Consequently, beside the tubular specificity, there is also some evidence that VEGF may be predictive for glomerular alteration. It has also been reported to play a key role in diabetic nephropathy [Kim et al., 2005] and glomerulonephritis [Matsumoto et al., 1997b, Ostendorf et al., 1999]. The underlying data can be interpreted as a response to the glomerular damage, because only in our Puromycin studies were these effects, together with the increase in urinary VEGF, observed. The gender difference observed gave further evidence to the role of VEGF in extracellular matrix remodeling. Because VEGF has been described to reduce renal fibrosis and stabilizes renal function, the increase could be a reaction of the increase in connective tissue in female rats. As an increase of VEGF was only observed in Puromycin treated rats, and showed a fundamentally different pathology than the other model compounds, further investigations have to be performed to idenfity the major reason for the observed increase in urinary VEGF.

Because of the lack of specific treatment dependent increase and the resulting low diagnostic performance, NGAL delivered no reliable information in the Puromycin induced renal damage. The reason for this observation is probably due to the low impact of Puromycin on the distal tubular. There is some evidence suggesting that the transcript of the Lcn2 gene, encoding for the NGAL protein, is usually expressed in the distal tubule of the nephron, while the protein itself is also located in the proximal tubule, so the protein is probably reabsorbed after leaving the distal tubular cells [Paragas et al., 2011]. By an absence of strong impact on the distal tubular cells it could be therefore assumed that no or only slight induction of NGAL takes place. The involvement of NGAL in inflammatory processes, NGAL is expressed by neutrophilic and epithelial cells as a first response to cellular stress and, therefore, is considered to be an acute-phase protein, can point to a higher specificity in Nephritic then in Nephrotic pathological outcomes.

3.1.1.7 Results of two different technologies for urinary Kim-1 measurement

The data of Kim-1 detection by using the Luminex® xMAP® technology are already reported above (Figure 3-2- Figure 3-17). Additionally the diagnostic performance of urinary Kim-1 determined by the RENA-Stipe® has been shown in Table 3-6 to Table 3-18. In Cisplatin treated animals, which showed weaker pathological alterations within the kidney (Table 3-7), an increase in urinary Kim-1 earliest on day 14 in high dose (0.6 mg/kg) treated male rats was observed (Figure 3-24 c). In this group also three animals without tubular degeneration showed an increase. The highest increase in male rats treated with 0.6 mg/kg Cisplatin was observed after 7 days, while no relevant increase after 15 days was seen. On day 29 urinary Kim-1 determination using the RENA-Strip® showed a slight enhancement in urinary level. In female rats treated with either 0.3 mg/kg or 0.6 mg/kg Cisplatin for up to 28 days, only one animal on day 15 showed renal tubular degeneration as well as dilatation and necrosis (Table 3-7). This individual animal showed a clear elevation in urinary Kim-1 within the RENA-strip™ assay (Figure 3-24 d).

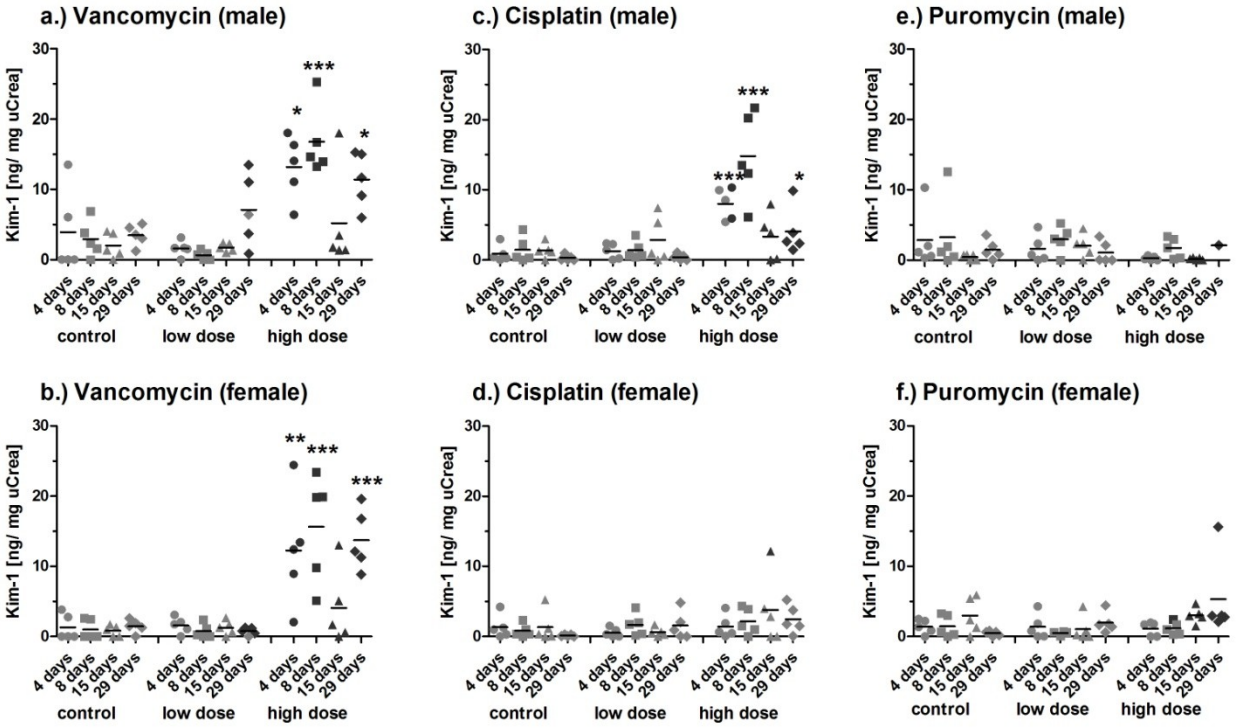

Figure 3-24 Excretion of Kim-1 in urine of male and female rats treated with Vancomycin (low dose: 50 mg/kg; high dose 300 mg/kg; Cisplatin (low dose: 0.3 mg/kg; high dose: 0.6 mg/kg) or Puromycin (low dose: 10 mg/kg; high dose: 30/20 mg/kg) for 3 days (dots), 7 days (squares), 14 days (triangle), and 28 days (rhombus). Kim-1 was determined by a rapid urinary dipstick assay (RENA-strip™). Data are presented as individual animals and as the mean (bar; n=5). The light grey signs indicate no tubular degeneration found within this animal, the darker grey indicates tubular degeneration observed. * $p < 0.05$, ** $p < 0.01$, *** $p < 0.001$ (ANOVA-Dunnett).

In contrast to Kim-1 measurement by using the WideScreen™ Rat Kidney Toxicity Assay, the determination by using the RENA-strip™ delivered no statistically significant alteration in urinary Kim-1 level after Puromycin treatment (Figure 3-24 e, f). The only animal showing an increase in urinary Kim-1 was 1 female rat of the high dose (30 mg/kg) group treated for 28 days. However, this animal did not show stronger histopathological changes then the others, showing only mild tubular degeneration and minimal glomerular vacuolization. By a direct mathematical comparison using linear regression (Figure 3-25 a, c, e) and Bland-Altman analysis (Figure 3-25 b, d, f), some differences between the RENA-Strip® dispstick and the Luminex® xMAP® based Widescreen™ assay become clear.

The Pearson correlation of the Luminex® xMAP® and the RENA-Strip™ technology was 0.772 within the Vancomycin study while the coefficient of determination (r^2_{fit}) was 0.596 (Figure 3-25 a). In contrast, a good linearity was observed by processing the data by a Bland-Altman analysis (Figure 3-25 b). The data points showed a clear tendency to an increased positive difference (Luminex® xMAP® minus RENA-Strip™) with a total increase on average. However, this results in a bias in urinary Kim-1 detection by these two technologies of 23 ng/mg urinary creatinine and a 95% limit of agreement of + 120/-75 ng/ mg urinary creatinine.

The results of the analysis of the Cisplatin data delivered comparable results. The Pearson correlation was 0.836 (r^2_{fit} = 0.699) (Figure 3-25 c). Even the linear regression showed better results within this study, also the linearity within the Bland-Altman plot was more pronounced (Figure 3-25 d). However, the bias as well as the 95% limit of agreement was high within this study and resulted in values of 52.8 (bias) and +263/-157 (± 1.96SD) ng/ mg urinary creatinine of Kim-1.

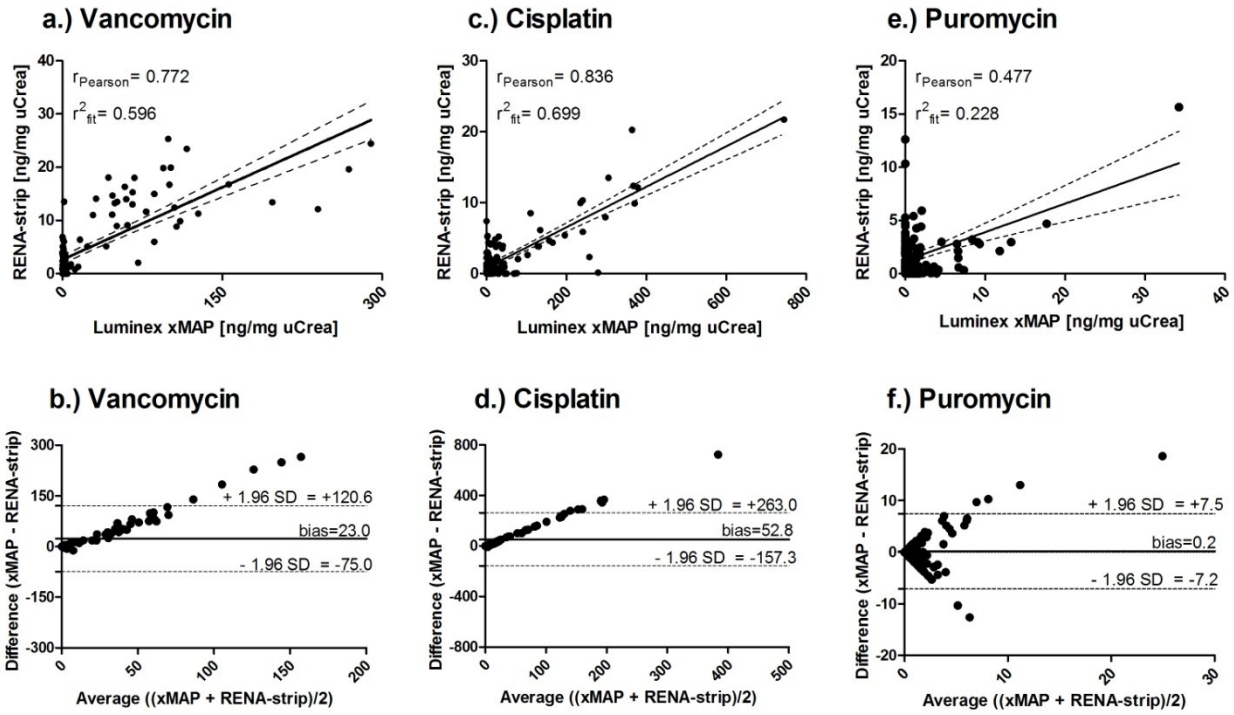

Figure 3-25 Bland-Altman analysis and Linear regression of Kim-1 determined by using the WideScreen™ Rat Kidney Toxicity Assays (Luminex® xMAP®) and the RENA-strip™ dipstick assay (RENA-strip™). Both analyses are shown using absolute, normalized (normalization was conducted against urinary creatinine) value of all animals from the Vancomycin (a-b), Cisplatin (c-d) or Puromycin (e-f) treatment. The Bland-Altman-Plot gives the average values on the x-axis and the differences of the two methods on the y-axis. The solid line indicates the mean difference or bias, broken lines indicate the 95% confidence limit of the bias. Linear regression is displayed by individual animals and a solid line represents the regression line. The broken line represents the 95% confidence interval. Additionally, the Pearson correlation (r_{Person}) and the coefficient of determination (r^2_{fit}) is given.

Within the datasets of puromycin, where only a limited increase in female rats in urinary Kim-1 level was determind by both the Luminex® xMAP® and the RENA-strip™ based approach, the results of the linear regression as well as the Bland-Altman analysis are different from the analysis of the Vancomycin and the Cisplatin study. This results in a lower coefficient of correlation and linear regression ($r_{Pearson}$ = 0.477; r^2_{fit} = 0.228). In contrast, the Bland-Altman plot delivered no linear tendency, but a high variation around 0. Subsequently the biases as well as the 95% limit of

agreement were much lower the described for the other evaluations (0.2 (bias) +7.5/ -7.2(± 1.96SD)) ng/ mg urinary creatinine of Kim-1.

3.1.1.8 Conclusion of comparison of two different technologies for Kim-1 detection

In summary, both Kim-1 assays evaluated delivered comparable results. However, there are several discrepancies between the Luminex® based multiplexing assay and the rapid RENA-strip® dipstick assay. The most important difference is the lower sensitivity of the Dipstick assay for urinary Kim-1. This leaded to lower AUROC values, suggesting that the histopathological observations are less well reflected.

Within the Vancomycin and Cisplatin studies, the urinary excretion of Kim-1 caused by treatment was observed in both the WideScreen™ and RENA-strip™ assays. In addition, both assays were sensitive enough to record the renal recovery, which occured after the first week without daily Vancomycin treatment. It is important to note that the observed tubular alterations within this study were very marked, allowing the poorly sensitive RENA-strip® dipstick assay to monitor changes in Kim-1. However, the excellent linearity within the Bland-Altman plot showed that the differences between the two detection methods were smaller. Therefore, the increase in urinary Kim-1 detected by the Luminex® based WideScreen™ assay was much greater compared to the RENA-strip™ assay.

The lack of Kim-1 determined by the RENA-strip™ assay witin the Puromycin study confirms the poor sensitivity of this assay. Kim-1 expression within the renal tissue was shown clearly and the observed pathological alterations were actually greater than the severity observed in the Cisplatin study.

Dependent on the study requirements both assays can be used with some limitations to detect renal damage. However, based on the data presented here, the Luminex® based WideScreen™ assay is the preferred assay for multiple reasons. Firstly, the sensitivity of the assay is above the observed sensitivity of the RENA-strip™ dipstick assay. In addition, the benefit of measuring multiple proteins in one sample at the same time (multiplexing) also enhances the applicability of this assay. Finally, the histopathological alterations were better predicted by the WideScreen™ assay. Taken together, the WideScreen™ assay is recommendable as a tool to monitor renal health status, during the course of an in vivo study without the need for additional animals.

In contrast, the dipstick assay delivers a fast and reliable result if marked effects in the proximal tubulus are present. Therefore, it is feasible that in very early phases of safety evaluation the RENA-strip dipstick assay could be included in to the standard panel of tests to get immediate results witout any time delay. However, in contrast to the WideScreen™ assays, this dipstick assay cannot be recommended as a stand alone method for decision making, but in combination with other methods to get additional hints about the status and the progression of renal damage.

3.1.2 Final Conclusion of the evaluation of urinary protein biomarkers

The data presented from all three 28 day rat toxicity studies clearly showed that Kim-1 and Clusterin performed the best from the set of qualified urinary protein biomarkers. In addition, Osteopontin, an exploratory biomarker, also delivered highly predictive results. However, this biomarker has the disadvantage of only performing well when no fibrosis appears during the progress of renal insult. An increase of renal Osteopontin protein expression can be used to indicate an increase in protein content, although this methodology is not ideal for screening, due to the strong background levels. In contrast, the renal protein expression of Kim-1 and Clusterin has the potential to be used by tissue array applications.
It was shown that several of the urinary protein biomarkers clearly reflect the actual health status of the kidney, including regenerative processes. Therefore, it can be concluded that these biomarker can be used to monitor the progression of renal damage in a non-invasive way. In addition, further information can be delivered about the area of damage within the nephron. For both the Vancomycin and Puromycin studies the traditional serum parameters, creatinine and BUN, also performed well. Therefore, the information about the area of damage is a major advantage of these novel urinary biomarkers. For example, within the Cisplatin study, only Kim-1 identified renal proximal tubular break-down in a highly specific and sensitive way.
Other biomarkers showed a tendency for gender specific differences. Timp-1, for example, was more predictive in females for all three model nephrotoxins. This could be due to physiological differences between the genders in kidney growth, reflected by the time dependent increase in urinary Timp-1 in male control animals. Calbindin showed a better predictivity in males. In the Cisplatin and Puromycin studies Calbindin showed treatment dependent decreases in animals with no renal damage. Therefore, further research is needed to evaluate the underlying mechanisms of this protein in renal pathologies. Because of its unique position as a specific distal tubular damage marker, this urinary protein biomarker can deliver important information about the location and progression of nephrotoxicity.
The two qualified urinary protein biomarker, Cystatin C and β2m, which are described to be of non renal origin, performed very poorly in the studies discussed here. Therefore, the assumption that the disturbance of reabsorption of these proteins by tubular degeneration leads to an increase in urinary protein must be questioned. This mechanism may be relevant in some kinds of drug-induced nephrotoxicity, but based on the data we have generated it seems to be more likely due to alternative mechanisms, such as the release of intracellular Cystatin C by tubular cells undergoing degradation. β2m also seems to increase in the case of prominent proteinuria by glomerular vacuolization and can be therefore used as glomerular specific urinary biomarker.
NGAL showed a poor performance in all studies. The only relevant increase in urinary NGAL was observed after 3 and 7 days of Vancomycin treatment (after massive tubular degeneration). Therefore, it could be suggested that NGAL can be used only for the very early changes, (i.e. the first days). In addition, the strong involvement of NGAL in inflammatory processes and the risks of false positive results lead to the assumption that this urinary protein has more disadvantages then benefits and should therefore not been used in 28 day rat toxicity studies.
The exploratory biomarker VEGF showed some evidence of importance in glomerulopathies. However, further experience by testing this urinary protein biomarker in real life situations will be necessary to evaluate whether a specific pathology or mechanism can be linked to urinary VEGF release.
Beside the performance of the urinary proteins as non-invasive biomarkers, the transcripts of the ten used proteins were evaluated. It was found that the transcripts of some of the biomarkers performed better on the transcriptional level than the urinary proteins. Beside Kim-1 and Clusterin showing very good results on the mRNA level, also Timp-1 reflected the histopathological changes very well in both male and female rats. Osteopontin showed a treatment-dependent increase in transcripts, but was weaker than the observed increase in Osteopontin protein. Nevertheless, the increase

over the control group was predictable for the underlying pathological alterations and it can be assumed that, in contrast to the Osteopontin protein, these changes are independent of expression of profibrotic factors. The down regulation of Calbindin mRNA in animals with tubular damage is only partly reflected by the urinary protein content. However, it is in good agreement to other observations reported for transcriptional biomarkers in nephrotoxicity, including the Innomed/PredTox project [Matheis et al., 2011].

In conclusion, the implementation of Kim-1, Clusterin and Ostoepontin into routine testing for nephrotoxicity is strongly recommended. In addition, Cystatin C and total urinary protein seem also to be excellent markers to detect potential impairments of the glomerulus. For the question of the best technology to employ, the decision strongly depends on the needs. If strong renal effects are expected or the results are needed within very short time, the RENA-strip™ assay can be recommended, being aware of the poor sensitivity of this assay. For a higher sensitivity and the benefit of the multiplexed detection of several proteins, the best solution would be a standard multiplexing assay, like the WideScreen™ Rat Kidney Toxicity Assay (now Milliplex xMAP assay). In addition, the evaluation of transcriptional biomarkers should also be addressed in pre-clinical safety assessment, based on the good performance of some of the transcripts presented here.

3.1.3 Gene expression analyses of renal tissue

The aim of the gene expression analysis, using renal tissue from rats treated with different doses of Vancomycin for different time points, was to evaluate i) the potential molecular mechanisms in male and female rats which may play a key role of the upcoming and established Vancomycin-induced kidney injury and ii) to evaluate potential transcriptional surrogate biomarkers for their usability and the mechanistic connectivity to the underlying mechanism.

3.1.3.1 Global Analysis

As already described a clear dose-dependency as well as a specific treatment dependent pattern in renal response on Vancomycin treatment was observed. In a first step, the whole genome transcriptomics data derived from the Genome Studio were normalized by median adjustment, after the whole dataset was analysed by box-plot and Log-Log plot using the Genedata Analyst Software tool. Based on the profile display and the background controls included on each array of a RatRef bead chip, all values with a signal intensity of <70 were excluded from the analyses for background correction.

All remaining transcripts were analyzed by a principal component analyses (PCA) for potential class discovery. The PCAs were compared for a.) gender differences, b.) treatment effects and c.) severity of tubular degeneration (Figure 3-26). A clear gender difference was observed, especially along component 3, with an increase in similarity along component 1 (Figure 3-26 a). In addition, a clear separation of the high dose (300 mg/kg) treated animals was observed, with the exception of four animals, all from treatment day 14 (Figure 3-26 b). Finally, the severity of tubular degeneration was overlaid to the PCA resulting in a clear serverity-dependent separation of animals without histopathological findings (Figure 3-26 c). Only animals with moderate findings or higher (≥ +++) were completely separated from the animals without findings. Individual animals with only minimal or mild (+ or ++) changes clusterd together near the unaffected animals. Taking all these observations together, the major factor that affects gene expression is based on the histopathology and not on the gender or the application of treatment to the test animals. Subsequently, by comparison of the gender differences (Figure 3-26 a) and the histopathology (Figure 3-26 c) the response of male and female rats after Vancomycin treatment shows a similar progression. It is not expected that within one species / strain that any gender difference on gene expression level would be seen. Therefore, to discover whether or not the response in male and female rats within individual pathway or transcripts is identical all following analysis were performed for male and female rats separately.

The fact that the low dose (50 mg/kg) treated animals clustered together with the animals of the control group is a reflection of only minor individual findings of histopahtological alterations within this group (Table 3-1). The duration of treatment seems to be not directly important for the outcome of the PCA, only that the health status of the kidney altered with time. Based on the observation already described, a time-dependency from days 3 and 7, as well as a recovery effect, were expected for treatment day 14.

To enable the analysis of the outcome of each individual time, all high dose (300 mg/kg) treatment groups were tested by a t-test against the corresponding control group by setting the threshold at $p \leq 0.01$ and $q \leq 0.01$.

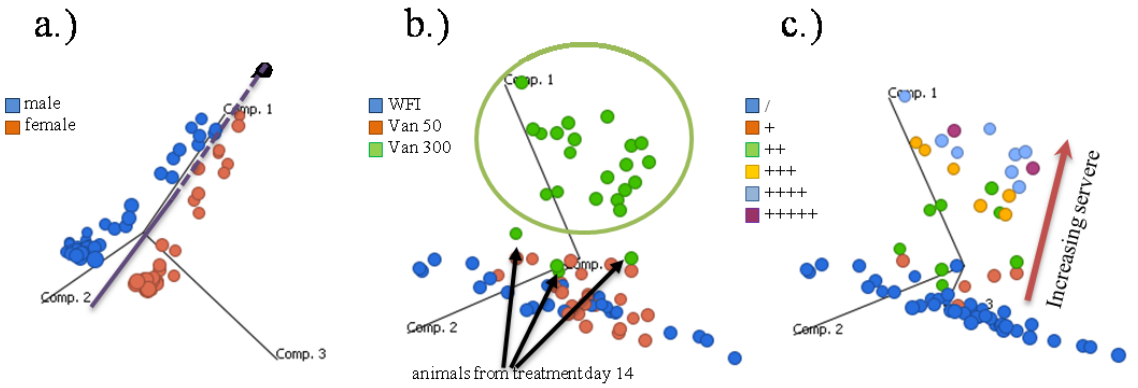

Figure 3-26 Principal component analysis (PCA) of the global gene expression dataset from renal tissue from male and female rats treated with water for injection (WFI), 50 mg/kg or 300 mg/kg Vancomycin. Each individual dot represents one individual experiment including all remaining transcripts. The position within the coordinate system give rationales about similarities or differences, whereas component 1 has the highest impact, followed by component 2 and component 3. a.) an overview on gender differences (blue = male, red = female). The solid violet line indicates the strong separation between male and females while the dotted line indicates only a slight separation. b.) Shown is the position of the treatment groups within the PCA (blue = control (WFI), red = low dose (50 mg/kg Vancomycin), green = high dose (300 mg/kg Vancomycin). The green circle indicates the clear separation of the high dose group from the control and low dose group. c.) reflection of the histopathological observed tubular degeneration within the PCA (blue = no findings, red = minimal, green = mild, yellow = moderate, light blue = massiv, violet = servere). The arrow indicates the direction of increasing server.

Female rats treated with 300 mg/kg Vancomycin showed more significantly altered genes compared to male rats. The difference was the smallest on day 7 were 4386 genes were altered in males while females showed 7995 alterations (~180 % increase). The strongest effect with ~440% (♂ 584, ♀ 2575) more altered genes was observed on day 14. On treatment days 3 and day 28 female rats showed ~190% (♂ 2583, ♀ 4918) and ~200% (♂ 2546, ♀ 5071) altered transcripts (Figure 3-27), respectively.

To check whether all these significantly altered genes deliver a reliable and reproducible result with a biological relevance, each group was divided by the corresponding control group to generate fold-changes (FC). The cutoff was set at FC ≥ 1.5 and FC ≤ -1.5 to see only slightly altered transcripts, which can have a mechanistic relevance. Only approximately 37-74% of the significantly altered genes showed an FC above the threshold, depending on the time and gender. Subsequently, in all eight groups the percentage of the male rats was above the value calculated for the females (Figure 3-27).

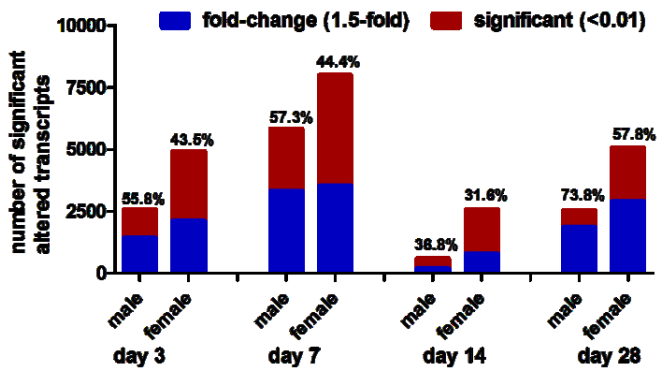

Figure 3-27 Significantly altered transcripts with a $p \leq 0.01$ and $q \leq 0.01$ for each individual time point for male and female rats. Out of these groups the fold-changes against the corresponding control groups were calculated with a threshold of $FC \geq 1.5$. The given percentages reflect the proportion of the fold-induced genes from the whole group of significant altered genes.

However, the higher number of altered genes in female rats, together with the already described differences in histopatholigcal severity (Table 3-1) and urinary protein biomarker excretion (Figure 3-2, Figure 3-3, Table 3-6), gives further evidence for alternative mechanisms occuring in females.

3.1.3.2 Mechanistic Analysis

The underlying list of altered transcript for each individual time point and sex, were uploaded into the Ingenutiy pathway software tool and the most prominently altered canonical pathways were analysed. The transcripts and fold-changes from the individual pathways are given in the Annex 2, Table 5-1 to Table 5-17. In addition, transcription factors in toxicological mechanisms were analysed within the IPA software tool. The analysed pathways were included into one of the following categories: Inflammation, apoptosis/ cell cycle, or recovery/ rearangement. The results of the comparison of the progression over the studied time points in both sexes are given in Table 3-19. It was not excpected that all transcripts would be included in these pathways, because several regulatory steps in the signaling pathways are not happening on the gene expression level. By comparing the different conditions, several differences were discovered in case of gender differences of Vancomycin induced nephrotoxicity. Firstly, the complement system seems to play a pivotal role in this drug-induced renal damage [White et al., 2012]. The individual components of the complement system remained constantly altered from day 3 to day 28. In male rats this was more pronounced then in females, which showed a stronger variation reaching from 31% on day 14 to 40% on days 7 and 28. Therefore, the recovery period, which already was described, was also reflected in female rats, while male rats showed no changes in the upregulation of the complement components. This can be assumed to be one reason for the lower severity observed in female rats, because the role of the complement system, which is a casade of enzyme activations that bridges between the innate and the acquired immune response, leads to the clearance of immune complexes and apoptotic cells, and the activation of inflammation. Three activation pathways were described for the complementary system, while all of them converge into a final pathway, including several activation steps (shown in Figure 3-28). At the end of the cascade, the component C7, C8 and C9 form the membrane attack complex (C5b6789; MAC) which integrates into the cell membrane and initiates cell lysis. The complement system has already been described to have an important role in ischemic AKI [Arumugam et al., 2004] as well as in drug-induced AKI [Quigg, 2003]. It also has been described in the special case of Vancomycin-induced nephrotoxicity in mice [Dieterich et al., 2009]. A comparison of the gene expression changes of the data generated from our study and the publicly available dataset shows that the initial pathways where limited to the classical and the alternative pathway, while the Lectin pathway (not shown), which is independent of a Antigen-Antibody complex and is initiated by mannose binding lectin, seems not to be involved in either species. The major difference between rats and mice seems to be in the formation of the MAC, because no alterations on gene expression for the components C7 and C9 where observed in mice, while C8 was down-regulated. However, because of the higly complex nature of this mechanism no deeper mechanistic analysis was possible based only on the gene expression data. Neverthless, the data generated within this study gave clear evidence that the complement system is strongly involved in the progression of Vancomycin-induced renal damage.

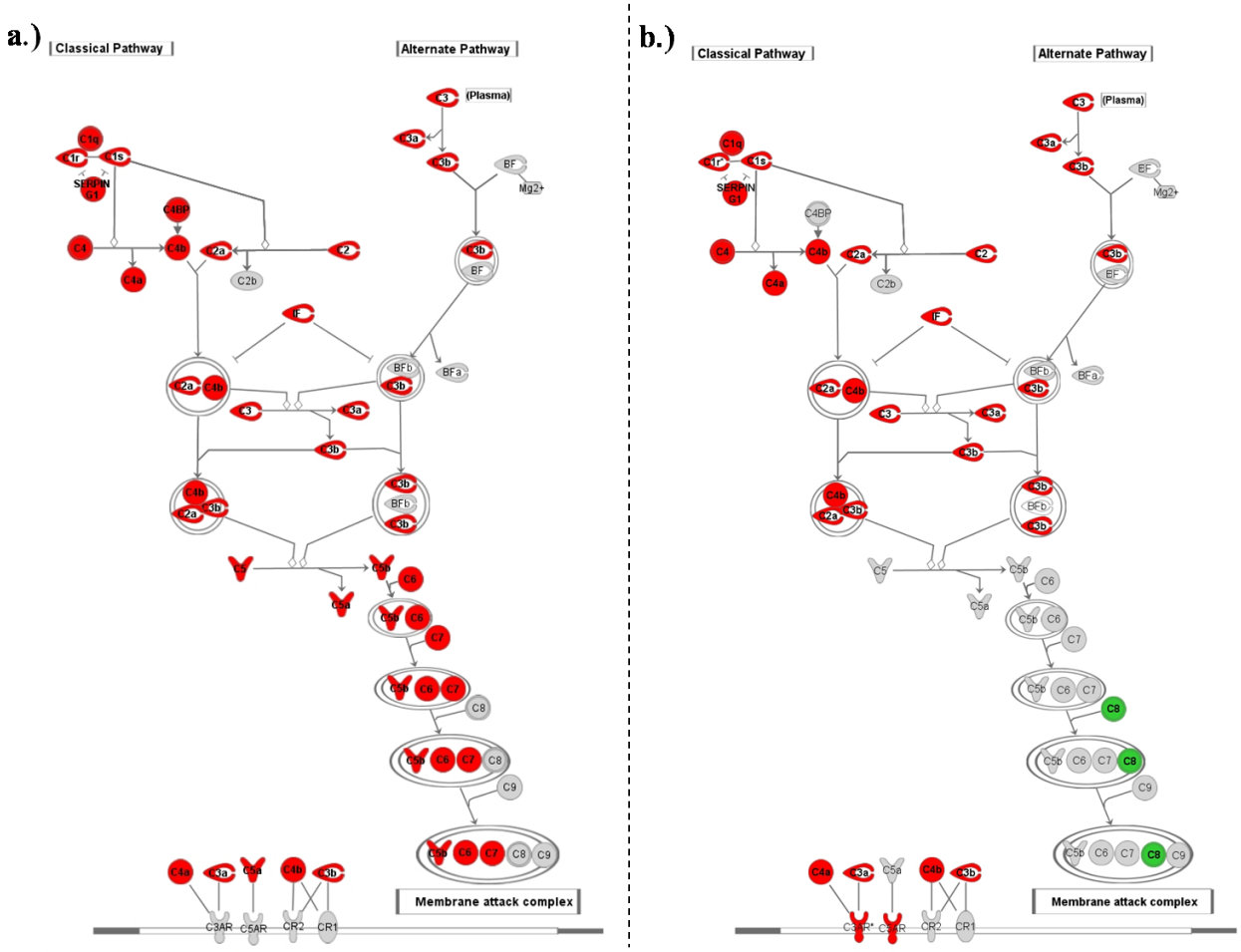

Figure 3-28 Shown are the classical and the alternative pathway of the complement system for a.) the underlying gene expression dataset generated out of the Vancomycin study and b.) a public available dataset of mice treated with 400 mg/kg Vancomycin (i.p.) (Dieterich et al., 2009). Red indicates that the transcripts showed a fold-change of ≥ 1.5 ($p \leq 0.01$, $q \leq 0.01$) and green indicates that the transcripts showed a fold-change of ≤ -1.5 ($p \leq 0.01$, $q \leq 0.01$). Grey displays that the transcripts are not present in the dataset presented here. Within the rat toxicity study (a) almost all components of the complement systems are significant up-regulated both in the classical as well as the alternative pathway. In the study used mice, also many transcripts were up-regulated; even though several key transcripts are not increasingly expressed within renal tissue.

It cannot be assumed that the complement system is one of the initial factors leading to tubular damage, but an important factor leading to an amplification of the initial insult. It already had been demonstrated that the filtration of complement components into the renal tubular system, as is the case during proteinuric renal damage, leads to tubular inflammation and injury [Lenderink et al., 2007]. The fact that the observed injury in female rats was below that observed in male rats in correlation to the presents of the complementary system, makes these pathways potential targets for AKI prevention. Therefore, inhibition of individual complement components could be shown to protect proximal tubules in a rat model of proteinuric kidney disease against renal dysfunction [He et al., 2005].

For the detection of drug-induced renal damage, the components of the complement system also seem to be usefull, as early transcriptional biomarkers. Consequently, the components C2, C3 and C4 are the most recommendable due to there central and initial function. This is supported by observations of C3 upregulation in Cyclosporin-induced proximal tubular cell break-down [Kim et al., 2007]. In addition, these transcripts have a strong benefit of bridging between species because of the high conservation of the complement system, as could be shown by comparing rat and mouse gene expression pattern. In addition the already described biomarker Clusterin interactes directly with the complement system in case of renal injury [Correa-Rotter et al., 1992]. Clusterin has an inhibitory effect on the complement system and the MAC activity, and therefore can be assumed to have a renoprotective function. However, it is not clear if the

regulation of the complement system and clusterin are directly linked, or if apoptotic and remodeling processes, where clusterin is also involved, are regulating both independently.

The involvement of inflammatory processes, which is a normal reaction to cell damage, is also underlined by the extravasation of leukocytes (Table 3-19). This process describes the migration of leukocytes from blood to tissue during inflammation, and occurs in several steps. In general, three major processes are involved; the capture and tethering of endothelial cells and leukocytes, the chemokine mediated rolling and firm adhesion of the leukocytes to the underlying endothelial cells, and the transmigration of leukocytes through spaces between the cells. Important chemokines include IL-1, TNF-α and Cxcl8, among others [Janeway et al., 2005, Aplin et al., 1998]. During this processes several adhesion molecules, like P/E-Selectin, β2-integrin, JAMs or ICAM-1, are invovled. Because of the important role of adhesive molecules and the ECM, it is not suprising that Timp-1 is involved in this process, by inhibition of MMP-9, secreted by leukocytes to degrade the basement membrane to avoid uncontrolled ECM degradation [Agrawal et al., 2006, Clark et al., 2011]. During tissue damage this process is also used by monocytes during there development into macrophages and an earlier increase in female rats is known, and could be one explanation for the weaker Vancomycin-induced nephrotoxicity in female rats.

Because both the complement system and the leukocyte extravasation are part of the acute-phase response, the IL-6 signaling, which is an important regulator of lymphocyte stimulation and acute-phase response, was also investigated. This signaling cascade can be driven by either IL-6-type cytokines, targeting signal transducers and activators of transcription (Stat) family and tyrosine kinases of the Janus Kinase (JAK) family [Haan et al., 2006, Murray et al., 2007], or by activation of the extracellular signal-regulated kinases (ERK1/2) of the mitogen activated protein kinase (MAPK) pathway [Singh et al., 2006]. Both of these pathways have already been discussed to play a pivotal role in different mechanisms of drug-induced nephrotoxicity. Cisplatin-induced nephrotoxicity, for example, has already been described to be regulated by a MAPK-dependent p38 induction [Francescato et al., 2009], while also a JAK/STAT mediated inhibition of Cisplatin-induced apoptosis has been reported [Salahudeen et al., 2008]. Neverthless, independent of the underlying mechanism, the results of the IL-6 signaling gave further evidence of the importance of acute phase pathways and inflammatory processes in early phases of Vancomycin-induced nephrotoxicity. In addition, it was found that in this study Stats seems to play a pivotal role in the response of renal cells to Vancomycin-induced tubular damage (Table 3-20). Beside inflammation, also cell death and cell cycle control are very important factors. Because apoptosis is a very common event in compound-induced toxicity, this signaling pathway was evaluated in more detail (Table 3-19). Apoptosis is a highly coordinated and energy-consuming process, which involves the activation of special cysteine proteases (Caspases), and can be discriminated between two major pathways, the intrinsic and the extrinsic pathways. It is not possible to discriminate between these two pathways only by analyzing gene expression data. Especially the intrinsic pathway, which is triggered by a change in mitochondrial transmembrane potential, leads to a release of two main groups of pro-apoptotic proteins from the intermembrane space into the cytosol. These important regulators, cytochrome c (CytC), Smac/Diablo and the serine protease high temperature requirement protein A2 (Htra2/Omi), will not be necessarily deregulated in the gene level. However, based on the data presented here, there is some evidence that the extrinsic singaling pathway was strongly involved in the observed apoptotic processes (Figure 3-29).

Table 3-19 The number of invovled transcripts in several pathways as percentage of the total number transcripts. In addition, the p-value is given in parentheses. The percentages were color coded as follow: white = < 10%; grey = 10%-20%; green = 20%-30%; yellow = 30%-40%; orange = 40%-50%; red = > 50%. The pathways were grouped in to three categories: Inflammation, Apoptosis/ cell cycle and Recovery/ Rearangement. Only genes altered in animals treated with 300 mg/kg Vancomycin (high dose) were analyzed.

Pathways								
	male				**female**			
Inflammation	**3d**	**7d**	**14d**	**28d**	**3d**	**7d**	**14d**	**28d**
complement system	**40%** (1.78E-08)	**40%** (2.56E-05)	**40%** (4.18E-06)	**43%** (8.50E-08)	**37%** (1.71E-05)	**40%** (2.90E-5)	**31%** (3.10E-06)	**40%** (2.29E-05)
Leukocyte extravasation	**12%** (4.34E-03)	**25%** (5.01E-08)	**26%** (7.98E-11)	**18%** (2.87E-05)	**25%** (7.71E-11)	**28%** (3.23E-10)	**17%** (1.72E-08)	**27%** (1.46E-09)
IL-6 Signaling	**16%** (1.18E-03)	**28%** (1.79E-05)	**26%** (9.77E-06)	**23%** (2.04E-5)	**27%** (1.52E-06)	**31%** (6.98E-07)	**18%** (2.41E-05)	**29%** (4.85E-06)
Apoptosis/ cell cycle								
Apoptosis Signaling	**13%** (2.95E-2)	**28%** (2.00E-05)	**28%** (1.06E-06)	**19%** (2.26E-03)	**29%** (1.38E-07)	**32%** (7.29E-07)	**24%** (5.84E-09)	**32%** (1.28E-07)
Death Receptor signaling	**12%** (5.85E-02)	**21%** (2.63E-03)	**28%** (4.04E-05)	**15%** (5.22E-02)	**28%** (2.52E-05)	**29%** (1.06E-04)	**20%** (5.69E-05)	**31%** (2.20E-05)
Cell Cycle control of chromosomal replication	**36%** (4.56E-07)	**45%** (3.93E-07)	**42%** (5.55E-07)	**52%** (3.28E-11)	**45%** (3.51E-08)	**45%** (4.50E-07)	**26%** (1.10E-04)	**55%** (1.90E-10)
Recovery/ Rearangement								
Integrin Signaling	**8%** (2.39E-01)	**22%** (8.76E-06)	**25%** (8.93E-10)	**15%** (3.35E-03)	**24%** (8.06E-10)	**26%** (1.28E-08)	**19%** (7.88E-11)	**27%** (2.16E-09)
Signaling by Rho Family GTPases	**8%** (1.13E-01)	**22%** (8.47E-07)	**20%** (8.78E-08)	**15%** (2.55E-04)	**22%** (1.26E-09)	**21%** (2.73E-06)	**13%** (2.89E-06)	**22%** (1.05E-07)
HMGB1 signaling	**17%** (2.25E-04)	**33%** (1.06E-08)	**29%** (7.38E-08)	**27%** (5.03E-08)	**30%** (8.00E-09)	**32%** (5.45E-08)	**25%** (1.80E-10)	**32%** (3.33E-08)

The Fas-receptor, also known as the death-receptor, which is the initial point of the transmembrane receptor-mediated extrincic signaling, was upregulated in male and female rats over all time points. This receptor triggers, after binding of a ligand, Caspase 8/10, which were also upregulated, and can then initiate the execution pathway, resulting in caspase 3 mediated characteristic cytomorphological features, such as chromatin condensation, DNA fragmentation, membrane blebbing and cell shrinkage [Elmore, 2007]. Alternativly, Caspase 8/10 can also activate Bid or Bax, both pro-apoptotic factors in a p53 dependent manner, which as a consequence ends in the intrinsic pathway of apoptosis. Because the activation of p53 is based on a phosphorylation, the increase in p53 mRNA observed specifically in male rats, is not necessarily correlated with an elevation in activity.

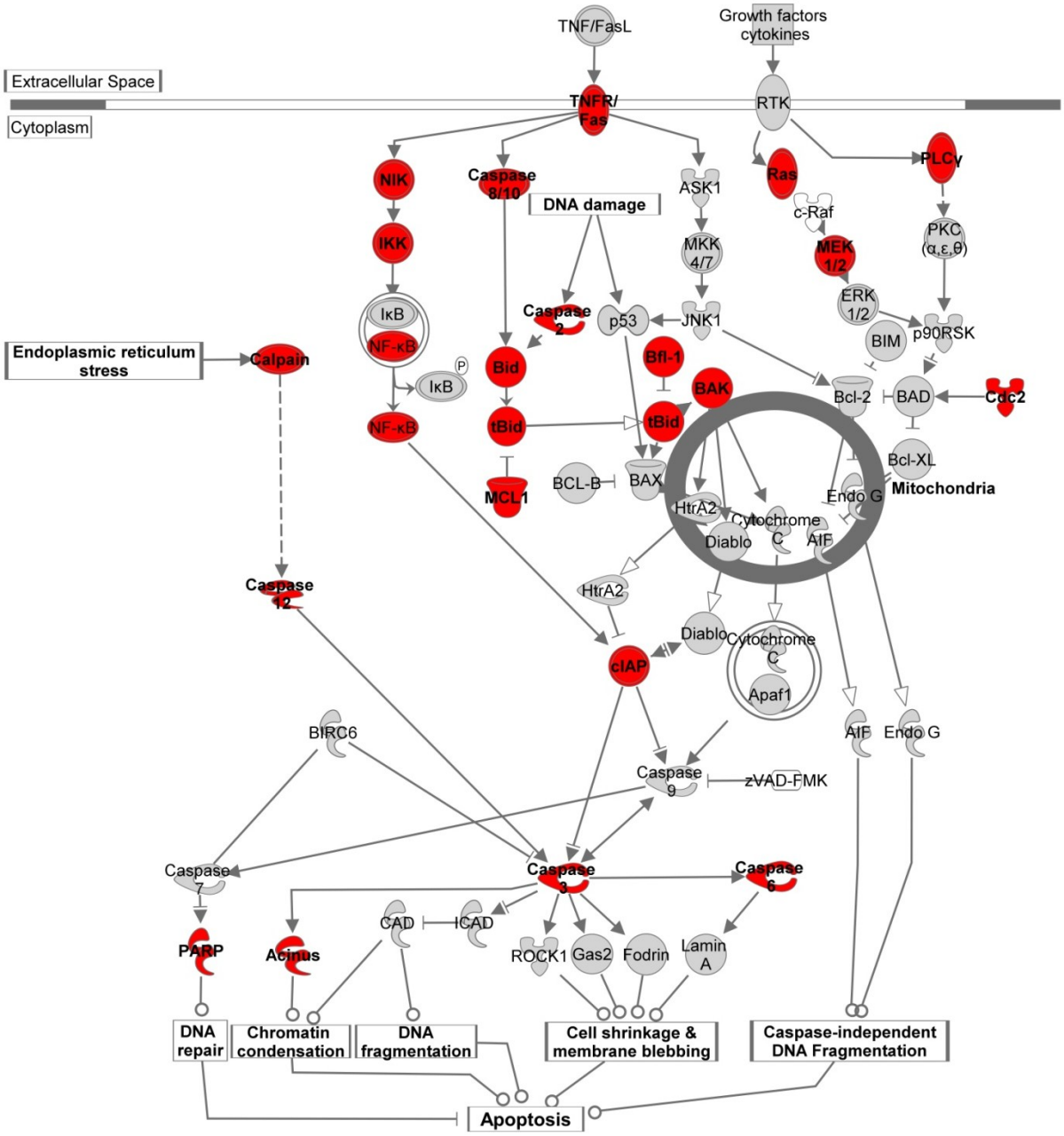

Figure 3-29 Apoptosis signalling; intrinsic and the extrinsic pathways. Red indicates that the transcripts showed a fold-change of ≥ 1.5 ($p \leq 0.01$, $q \leq 0.01$). Grey displayes that the transcripts are not present in the our dataset. Within this toxicity study almost all Caspases were significantly up-regulated. In addition, several components related to the extrinsic pathway and a separate ER stress mediated pathway was activated.

The analysis of downstream genes regulated by p53 gave some evidence that this transcription factor is not prominently involved in the response of renal cells to Vancomycin-induced cell death (Table 3-20). However, by comparing the ratios of involved molecules for male and female rats over all time points (Table 3-19), it become obvious that apoptotic processes occured earlier in female rats, particularly on day 3 (m: 13%; f: 29%). While male rats showed a similar invovlment, earliest on day 7 (m: 28%; f: 32%). To underline the assumption that the extrinsic pathway may be predominant, also the ratio of the Death Receptor signaling is shown in Table 3-19, reflecting comparable patterns in the number of altered transcripts. Beside the activation of Caspase 8/10, the Fas receptor has also been described to increase the activation of the NIK protein, which itself can initiate a singaling cascade by phosphorylation, involving NF-κB [Malinin et al., 1997, Sakurai et al., 2003]. Since NF-κB is a very common transcription factor, strongly related to processes of immuigenicity, it is also an important mediater of apoptosis by increasing the activity of cIap, which

itself is able to activate several Caspases (Caspases 3 and 9) [Shen et al., 2007]. The role of NF-κB could only be shown for male rats on treatment days 3 and 28 (Table 3-20). For all other groups, it was not possible to calculate any scores. Taken this together with the observation of early inflammatory processes in females, which can be assumed to be involved in cell death and in the clearance of apoptotic cells, this can be one reason for the general lower progress in female rats compared to male. In addition to the already mentioned Caspases, Caspase 12 showed also an upregulation in all high dose (300 mg/kg) treated animals (Figure 3-29). Caspase 12 activation is related to endoplastic reticulum (ER) stress caused by hypoxia, glucose starvation and perturbation of calcium homeostasis [Yoneda et al., 2001]. Since it has been described that Vancomycin is involved in complex formation of the ERp57 protein, which is mainly localized in the ER, with calreticulin there is some evidence of a potential involvement of ER stress in Vancomycin-induced renal insult [Frasconi et al., 2001]. This is supported by the findings that the ERp57/Calreticulin complex is associated with cell death and differentiation [Panaretakis et al., 2008]. Even though apoptosis is a relatively general mechanism it is a highly predictive indicator of cellular stress and should be always evaluated in case of the detection of organ specific toxicity. Therefore, it was not unexpected that the public dataset from Dieterich and colleagues [Dieterich et al., 2009], showed similar results to ours. To summarise, Vancomycin-induced apoptosis in rodent kidney seems to be a Fas-receptor mediated and Caspase dependent mechanism.

The cell cycle control of chromosomal replication, which showed the highest number of genes being deregulated, indicates a high proliferative activity (Table 3-19). In addition, a strong gender difference was observed. While male rats showed the lowest ratio, reflecting in this case cyclin-dependent kinases (Cdk), cell division cycle (Cdc) members and other molecules involved in the formation of the origin recognition complex (ORC), after 3days of treatment (m: 36%; f: 45%), female rats showed the lowest ratio on day 14 (m: 42%; f: 26%). Comparable data were observed on days 7 (m: 45%; f: 45%) and 28 (m: 52%; f: 55%). Based on these results it can be assumed that the induction of proliferation in male rats took longer to manifest after an insult. In addition, the replication of renal cells lead to a strong recovery on day 14 in both genders, but because of the stronger pathological outcome in male rats, the transcripts involved in cell cycle chromosomal replication, remained at an elevated level. Consequently, the highest ratios were observed in the latest time point where also the most prominent effects were observed histopathologically (Table 3-1). It has been reported that Vancomycin is directly involved in cellular proliferation of proximal tubule cells. Here, Vancomycin lead to an increased incorporation in BrdU, followed by the accumulation of cells in the G_2/M phase of the cell cycle [King et al., 2004]. In our dataset, key components of the G_2/M phase of the cell cycle were significantly deregulated, namely Cdk1, CyclinA and –B, as well as Cdc25a.

Beside the inflammatory and apoptotic processes, remodeling and recovery processes play an additional and fundamental role in the outcome and progression of Vancomycin-induced nephrotoxic mechanisms. Three major processes are involved in the regeneration of tubular cells after toxic insult; migration/anchoring, proliferation and repair of physiological functions [Nony et al., 2003]. Proliferation was observed by the changes in cell cycle control of chromosomal replication. By evaluating several pathways it becomes obvious that in case of migration/ anchoring, integrin mediated signaling plays the most important role in the renal reorganization after Vancomycin-induced tubular damage. Integrins are heterodimeric adhesion receptor glycoproteins on the cell surface, which mediate cell migration and adhesion by interaction with the cytoskeleton, the ECM and other cells [Hynes, 1992]. Integrins can bind several ECM molecules, such as cellular receptors, fibronectin, laminins or collagens and subsequnelty lead to the (re-) attachement of the cells to the basement membrane after they have detached because of an insult to the basement membrane. Additionally, integrins are responsible for the signal transduction from the extracellular space into the cell. The most prominent fold-change alterations in our dataset from both genders were observed for α1-integrin, α4-integrin

and β1-integrin, while male rats additionally showed an up-regulation of α5-integrin, β4-integrin, β6-integrin, and β7-integrin. Based on the fact that integrins are composed of one α and one β subunit and each combination has its specific binding and signaling properties, this is potentially an important factor explaining the sex differences. The interaction, which is realized by the cytoplasmic tails of the integrins with intracellular signaling/ regulatory molecules, can induce several different pathways and therefore different cellular effects. Signaling molecules described to be involved in integrin signaling are mitogen-activated protein (MAP) kinase as well as focal adhesion kinase (FAK) and integrin-linked kinase (ILK) signaling cascades [Juliano, 1994, Delcommenne et al., 1998]. In the data presented here, both in male and in female rats, many transcripts showed an up-regulation in almost all of these signaling pathways. Male rats showed almost no upregulation of molecules involved in integrin signaling on day 3 and an elevation on days 7 and 14, while female rats showed comparable number of involved transcripts on days 3, 7 and 28 (Table 3-19). This is remarkable, because in both genders eosinophilic casts were observed at the earliest on day 3 and therefore the detachment of necrotic cells already appeared at this early time point. On day 28, where the strongest pathological effects were observed in both genders, it was expected that mechanisms of repair and reorganization also showed the highest presence and activity. This was only the case in female rats, while males showed a reduction compared to days 7 and 14. Beside the integrin-driven activation of ERK/MAPK or JNK/SAPK mediated transcription, the growth factor receptor PI3K or Wnt-signaling, are also strongly related to the cytoskeleton dynamics of filaments which is a nessecary process that allows cellular migration. The polarization of tubular cells, which is one of the first reactions of cells to toxin induced cell stress, is also susceptible to actin remodeling. Sublethal cell damage and cell loss is hypothized to initiate a migratory response in the denuded area of the nephron followed by an increasing proliferative activity to replace lost cells [Nony et al., 2003]. To underline the importance of integrin signalling, the signalling by Rho Family GTPases and the Actin Nucleation by ARP-WASP complex is also involved in cellular reorganization processes, especially the actin nucleation. The signaling by Rho Family GTPases, which regulates a multitude of cell biological processes, including transcriptional regulation via AP-1, morphogenesis, reorganization of the actin cytoskeleton, neutrophil activation, phagocytosis, mitogenesis, and apoptosis [Boureux et al., 2007, Ellenbroek et al., 2007, Hall et al., 1998], and the High Mobility Group-B1 (HMGB1) signalling, which is a special mechanism of cellular stress and injury. Because this pathway is related to gene expression regulation of fibrolysis and cell adhesion, but also in the cellular immune response, it can be seen as a link between inflammatory reactions and the repair processes.

The Rho family is a subfamily of GTPases. Three members of this family have been studied more extensively, namly Cdc42, Rac1 and Rho. While Cdc42, described to be associated with the formation of filopodia, gene expression was unaffected by Vancomycin treatment, Rac1 and Rho were strongly elevated. Rac1, which is related to actin polymerization to form lamellipodia, has also been reported to induce cell proliferation in an NFκB-mediated process. In contrast, Rho is a regulator of focal adhesion and actin filament bundling into stress fibers. The formation of stress fibers has already been described for other compounds causing nephrotoxic insult on tubular cells, including Cisplatin [Imamdi et al., 2004], (1,2-dichlorovinyl)-L-cysteine [de Graauw et al., 2007] and chromium compounds [Dartsch et al., 1998], and therefore underlining the importance of these Rho-mediated cellular responses. Several proteins have been identified as targets of Rho.

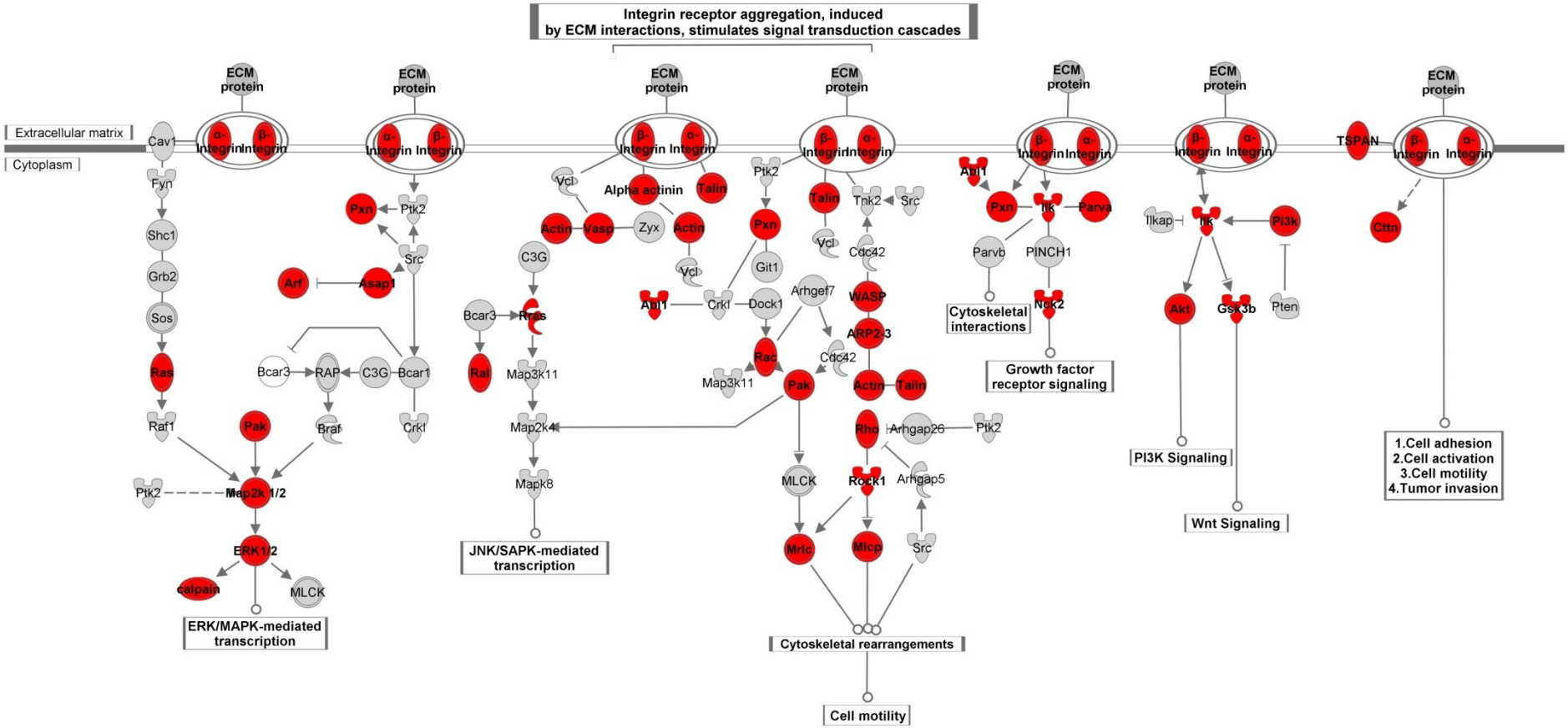

Figure 3-30 Overview of intergrin-mediated signaling pathways. Within this general overview only interactions of integrin with proteins of the extracellular matrix (ECM) are displayed. The signaling cascade leading to cytoskeletal rearrangement and cell motility, including Rac1, Rho and Rock as key players, is most pronounced. However, all shown integrin-mediated cascades are characterized by the upregulation of several molecules and can therefore be assumed to activate the individual downstream processes. Red indicates that the transcripts showed a fold-change of ≥ 1.5 ($p \leq 0.01$, $q \leq 0.01$). Grey displays that the transcripts are not present in the dataset. The ECM proteins are displayed in grey, even though it is sure that they are present.

Because of its central position in downstream regulation, Rock is important. Rock activates Mlc, leading to actomyosin contractility, or LIMK, which results in inhibition of Cofilin and causes actin polymerization. Rock has also been reported to phosphorylate intermediate filaments, like desmin or vimentin [Sin et al., 1998, Inada et al., 1999]. The latter has been frequently reported to be associated with drug-induced renal damage. It is noteworth that the key player within the interaction network also showed an increase on the gene expression level. Since all the downstream processes and signalings lead to recovery, repair and reorganization, the lowered pathological findings in female rats compared to male rats can be due to a higher turnover of dieing cells and new migrating cells. In addition, the repair of damaged cells can be assumed to be more effective when there is a stronger activation of integrin signaling molecules (Table 3-19).

The HMGB-1 signaling pathway is not directly linked to integrin-signaling, but involved in assembly of nucleoprotein complexes, maintenance of nucleosome structure and regulation of gene transcription. The genes described for this mechanism are related to cell adhesion and fibrolysis. In general, the HMGB-1 signaling pathway can be classified as being related to inflammation. There are two potential origins for HMGB-1, a DNA binding protein that also can be associated with cell surface receptors [Ellerman et al., 2007]. One potential source of HMGB-1 is by secretion from macrophages and monocytes after stimulation with toxins. During infiltration of the renal tissue, it is likely that the underlying inflammatory processes lead to the release of HMGB-1. This relation to the inflammatory processes becomes obvious when comparing the ratio pattern of the HMGB-1 signaling and the inflammatory processes, except the complement system. The second mechanism of HMGB-1 release is by necrotic cells. This could be an explanation why the HMGB-1 signaling is still relatively active on day 28 in male rats. Even though a high severity on renal tubular cell damage was observed (Table 3-1) the apoptotic signaling was reduced at this time point. Therefore, it could be assumed that the underlying insult is probably caused by necrosis. Subsequently, the release of HMGB1 has to come mainly from this source, especially as the leukocyte extravasation, was reduced on day 28 of Vancomycin treatment. Once released HMGB-1 protein can activate inflammatory cells through binding of IL-1, TNF-α, IFN-γ, LPS or HMGB1 itself to their own receptors (IL-1R, TNFR1, TLR4, IFN-γR and RAGE, respectively) and conseqeuntly activate the MAPK-signaling or the NF-κB pathway. In addition, HGBM-1 can activate cell surface receptors on various cell types, including epithelial cells, through JNK, Akt, ERK1/2, PI3K and p38 mediated signaling. HGMB-1 has also been described to interacte with Rho, Rac1 and Cdc42. These proteins, as already described above, are related to cellular reorganization, rearrangement and mortility. It can be hypothized that the activation of these key players results in the infiltration of further macrophages. Cells activated by HMGB-1 result in the upregulation of adhesion molecules like VCAM1, ICAM1 and RAGE. It has also been described that HMGB-1 interacts with the membrane receptors and the extracellular matrix of lamellopodia, and is involed in the release of MMPs by REAG-mediated MAPK activation. Taking all this in account, the role of HMGB-1 in drug-induced kidney damage seems to have been underestimated. There is only limited information about the involvement of HMGB-1 in drug-induced kidney injury. In case of renal ischemia reperfusion injury, the important role of HMGB-1 as a pro-inflammatory cytokine was shown [Wu et al., 2010], and also the expression of HMGB-1 in proximal tubular cells has been described [Lu et al., 2011]. Research on the potential underlying mechanisms of drug-induced nephrotoxicity, specifically tubular nephritis, and the involvement of HMGB-1 protein needs to be addressed in the future.

Finally, a transcription factor analysis was conducted to identify key transcription factors responsible for alterations in gene expression. The most common, toxicologically relevant transcription factors were analysed first; namely Ahr, Myc, NF-κB, and p53. Even though the physiological ligand of the cytosolic aryl hydrocarbon receptor (Ahr) has not yet been discovery, its functional role in physiology and toxicology has extensively been studied [Okey et al., 2007]. It is known that Ahr plays a pivotal role in development of T-cells [Li et al., 2001] and hepatocytes [Walisser et al., 2005],

hematopoiesis and lymphoid systems [Gasiewicz et al. 2010]. In addition, it is strongly involved in the induction of the xenobiotic metabolizing enzymes, mainly Cyp1A1 and Cyp1B1 [Harrigan et al., 2004]. However, in the dataset presented here, where Ahr was significantly down regulated in male rats on treatment days 7 28 (Table 3-20), Ahr has been related to the upregulation of several collagen proteins, TGF-β, Actn1, Fn1, A2m and Spp1. Since renal fibrosis is mediated mostly by the fibrogenic cytokine TGF-β [Branton et al., 1999], and the other factors mentioned above are also strongly involved in the development of fibrogenic tissue, there is some evidence that Ahr is involved in the build up of renal fibrosis. This is supported by reports that Ahr-deficient mice are characterized by extensive fibrosis in the heart and kidneys [Sauzeau et al., 2010]. Even though the mechanistic role of Ahr in the development of renal fibrosis is not yet understood; the results indicate an involvement of the Ahr-receptor within the progression of fibrogenic tissue building. Ahr is known to interact with the Ahr-interacting protein (AIP) in an Hsp90-mediated process, which enhances the Ahr function [Bell et al., 2000]. Since Hsp90 (Hsp90aa1) is down-regulated by Ahr when active [Moennikes et al., 2004], and that Hsp90 is increased during drug-induced nephrotoxcity, the inhibition of Ahr can be seen as one potential source of this Hsp90 increase.

In contrast to Ahr, the transcription factor Myc, involved in a multitude of processes, showed no functional activation at any time point. However, this transcription factor showed a strong upregulation on the mRNA level in all dose groups, reaching from +3.0 to +7.1 fold in male rats and +2.5 to +9.3 fold in females. Taken together with the very high number of related downstream genes (m: 134 to 220; f: 144 to 218), this gives further evidence of the important role of Myc in Vancomycin-induced kidney damage. In addition, a treatment-dependent upregulation of Myc was been observed in NRK-52E cells after treatment with several nephrotoxins (see 3.2 Identification of potential surrogate transcriptional biomarkers in vitro).

The transcription factor NF-κB, which already has been mentioned as being involved in inflammatory processes and apoptosis induction (Table 3-19), was assumed to play a key role because of the advanced nephritis. However, the calculation of the z-scores was only possible for male rats treated for 3 and 28 days with 300 mg/kg Vancomycin. Nevertheless, these groups of animals showed the higest z-score of all evaluated transcription factors. NFκB is related to several already described biomarkers, namely, Clu, Lcn2, and Spp1, as well as several exploratory transcriptional biomarkers, like Cd44, Cyr61, Fn1, Hmox1, or A2m, (3.1.4 Testing of two panels of potential transcriptional biomarkers), there is some evidence that NF-κB plays a pivotal role in the development of renal tubular responsiveness to drug induced alterations. This is supported, again only for male rats, by the activation status of RelA (p65), a binding partner of NF-κB, which also increases NF-κB activity [Bettelli et al., 2005, Gewurz et al., 2012].

Finally, the major apoptosis inducing transcription factor p53 was assessed. No significant involvement in the gene expression regulation could be evaluated, in male or female rats. Therefore, it must be assumed that the apoptotic processes taking part into the kidneys during Vancomycin treatment follows a p53-independent pathway. It has been shown for Cisplatin nephrotoxcity, that Src, a proto-oncogen, interacts with phosphorylated PKCδ, which itself regulates MAPK-mediated apoptosis without activation of p53 [Pabla et al., 2011].

Beside these traditional toxicological related transcription factors, the dataset was screened for specific and significant altered factors (Table 3-20). The findings were more pronounced in male rats compared to females.

Table 3-20 The predicted activation or inhibition of common toxicological and study specific transcription factors (TF) to evaluate there involvement in gene regulation during Vancomycin induced nephrotoxicity. The values represent z-scores calculated by the IPA software tool and the p-value of the individual dataset (in parentheses). The z-score gives the tendency of regulation, while the p-value gives a measure whether there is a statistically significant overlap between the dataset and the genes regulated by the TF. Z-score ≥ 2 and ≤ -2 were assumed to be predictive. Values between 2 and -2 are displayed in grey. Green indicates inhibition, red indicates activation.

	Male				Female			
TFs (common)	**3d**	**7d**	**14d**	**28d**	**3d**	**7d**	**14d**	**28d**
Ahr	-1.76 (4.03E-15)	**-2.07 (4.28E-17)**	-1.07 (3.22E-11)	**-2.36 (6.66E-16)**	-1.84 (1.60E-10)	-1.81 (5.25E-11)	1.93 (3.09E-07)	-1.40 (1.45E-10)
Myc	-0.92 (1.01E-30)	-1.42 (1.50E-46)	-0.84 (1-08E-40)	-0.60 (2.89E-42)	-0.82 (6.30E-43)	-0.51 (9.71E-42)	0.45 (2.54E-43)	0.43 (4.45E-46)
NF-κb	**5.04 (5.37E-14)**	/ (7.91E-21)	/ (3.36E-15)	**4.02 (1.60E-20)**	/ (1.01E-16)	/ (1.85E-14)	/ (8.76E-13)	/ (1.59E-15)
p53	-1.78 (3.59E-36)	-0.45 (7.22E-51)	0.41 (2.94E-50)	-0.60 (1.43E-45)	0.04 (5.73E-51)	0.18 (2.60E-48)	-0.30 (6.87E-41)	0.252 (1.30E-49)
TFs (specific)								
PPARα	**-4.01 (1.50E-30)**	**-4.88 (1.19E-27)**	**-3.19 (2.04E-10)**	**-4.89 (1.53E-37)**	**-3.70 (1.23E-14)**	**-2.13 (4.55E-14)**	**-2.39 (9.15E-11)**	**-3.94 (1.89E-16)**
PPARγ	**-2.77 (2.77E-11)**	**-3.75 (7.25E-12)**	**-2.05 (4.91E-05)**	**-3.45 (2.30E-13)**	**-2.60 (1.77E-05)**	/ (2.24E-04)	-1.11 (4.80E-05)	**-2.43 (3.29E-08)**
PPARδ	**-2.80 (2.91E-09)**	**-3.50 (7.72E-08)**	/ (2.01E-05)	**-3.09 (4.60E-10)**	**-2.29 (6.57E-05)**	-1.82 (2.32E-05)	/ (1.79E-04)	**-3.93 (6.42E-58)**
RelA	**3.33 (5.53E-11)**	**3.13 (1.88E-17)**	/ (3.18E-13)	**3.07 (2.85E-14)**	/ (1.88E-13)	/ (6.78E-10)	/ (3.02E-09)	/ (4.42E-12)
Smad3	**3.25 (1.04E-08)**	**2.71 (5.10E-09)**	**2.05 (2.20E-06)**	**3.13 (1.60E-12)**	**2.42 (2.50E-06)**	**2.14 (1.02E-04)**	**2.01 (2.91E-07)**	**2.31 (1.19E-05)**
Stat1	**3.28 (2.01E-09)**	**2.55 (5-83E-17)**	/ (3.74E-12)	**3.43 (9.87E-12)**	/ (2.44E-13)	/ (1.75E-11)	/ (2.75E-12)	/ (2.59E-11)
Stat3	**2.99 (2.36E-14)**	**3.11 (1.53E-23)**	/ (8.10E-16)	**3.35 (1.54E-21)**	**2.07 (3.90E-15)**	**2.44 (4.53E-15)**	/ (2.60E-12)	**2.10 (4.03E-15)**

PPARα, PPARδ and PPARγ belong to the family of peroxisome proliferator-activated receptors (PPAR). All these transcription factors showed an inhibition in male and female rats on treatment days 3 and 28, while male rats in addition showed significant alterations on day 7. The most pronounced inhibition was observed for PPARα predominantly on day 14, which reflects the general pattern caused by the recovery of the renal tissue. All of these PPARs are ubiquitary expressed, while PPARα is expressed in high amounts within kidney, liver, gut and heart [Tyagi et al., 2011].

The role of PPARs in renal disease is not yet fully understood. Beside their major role in energy homeostasis, more specific in β-oxidation, they have been described to be also involved in tissue repair and inflammation [Escher et al., 2000, Berger et al., 2002]. PPARα, PPARδ, and PPARγ have been described to have protectiv effects against ischemia/ reperfusion and nephrotoxin induced cortical necrosis as well as inflammatory processes [Baud et al., 2002, Berger et al., 2002]. However, PPARα seems to be the most potent protector in case of renal damage. Within the kidney PPARα is primarily expressed in proximal tubular cells. Therefore, is has also been described that PPARα ligands prevents Cisplatin nephrotoxicity, by inhibition of renal fatty acid oxidation (FAO) and pyruvate dehydrogenase complex (PDC) activity [Li et al., 2004]. It has been hypothized that the anti-inflammatory properties of PPARs, by suppressing anoikis and inflammatory infiltration in proximal tubular epithelia, are also responsible for the protective effect [Letavernier et al., 2005]. However, PPARα has been described to inhibit NF-κB [Baud et al., 2007], while PPARδ protein increases the activity of the NF-κB complex [Di-Poi et al., 2002]. Because NF-κB also has curative properties by clearance of apoptotic and necrotic cells by macrophages, this can also be assumed to be a mechanism of PPAR protection. A potential explanation for the observed differences between the sexes could be the less strong inhibition in females, subsequently leading to a higher protection of tubular cells.

The most dominant activated transcription factor was Smad3. Smad3 is a member of the Smad family of proteins, and is related to inflammation, fibrosis, apoptosis and accelerated wound healing [Ashcroft et al., 1999, Inazaki et al., 2004]. This transcription factor is induced by TGF-β and is involved in cell signalling. Since TGF-β itself is known to cause renal tubular damage in a Smad3 -independent mechanism, it is hard to discriminate whether or not the interaction of these two molecules is important in Vancomycin-induced nephrotoxicity [Dai et al., 2003]. For the interaction it has been report that the sensitivity to TGF-β-induced apoptosis is regulated by crosstalk between the Akt/PKB serine/threonine kinase and Smad3 [Conery et al., 2004]. However, the fact, that smad3 seems to be significantly activated supports the important role of this transcription factor. The combination of an upregulation of TGF-β (as observed in our study), lead to an activation of several molecules related to the extracellular matrix, like collagens, Timp1, Vim, Fbln1 and Spp1. Additionally, TGF-β itself can be induced by TGF-β activated Smad3, lead to an upregulation of Tgfb1 and Tgfb2 gene expression. In case of drug-induced nephrotoxicity, the interaction of TGF-β and Smad3 has been studied by the progression of chronic cyclosporine nephrotoxicity [Islam et al., 2001, Tao et al., 2011]. It could be shown that sodium depletion, as it was the case for treatment day 3 and day 28 (Figure 3-1), enhances fibrosis and TGF-β expression [Shihab et al., 1997]. The involvement in inflammatory processes became obvious when taking into account that Smad3 and RelA can bind each other [Wang et al., 2011]. RelA, which already has been described as an interaction partner of NF-κB, is strongly related to inflammatory processes [Sanz et al., 2010]. It can be assumed, that the regulatory molecules TGF-β, Smad3, NF-κB and RelA act in a feedback control system because TGF-β/ Smad signaling has been described to be suppressed by NF-κB/RelA [Bitzer et al., 2000].

Finally, the last specific and significant activated transcription factor belongs to the Signal Transducer and Activator (Stat)-family. In mammals seven Stats have been described [Ihle, 2001]. They are involed in several regulatory pathways and signaling cascades. They are most frequently related to Janus kinases (JAK) resulting in the expression of several growth factors and cytokines subsequently leading to cell differentiation, migration and proliferation as well as apoptotic processes [Aaronson et al., 2002]. In our data, Stat1 and Stat3 showed a significant activation in male rats on treatment days 3, 7 and 28 (Table 3-20). In female rats only Stat3 was significantly activated on days 3, 7 and 28. It is remarkable that Stat1 and Stat3 showed such high z-scores because these two Stats have been described to be strongly related to IL-6 activation [Takeda et al., 1998, Dawn et al., 2004], which itself is involved in a pathway already described above (Table 3-19). Beside the induction of inflammatory responses, Stat3 is also related to induced

proliferation of renal cells after an insult [Arakawa et al., 2008] and can be therefore assumed to be involved in the recovery of renal tissue, as observed within this study (Table 3-1).

Both Stats have been described to have an important role in nephrotoxicity, especially Cisplatin-induced renal damage [Tadagavadi et al., 2010]. The invovlemant of the MAPK-signaling, significant altered after Vancomycin-treatment, indicates a central position of this pathway. In general, almost all of the transcription factors directly influence each other and delievered a more complex interaction network (Table 3-21). This gives further evidence that the similarity in downstream genes and biological mechanisms is of essential importance in Vancomycin-induced nephrotoxicity.

Table 3-21 Relationships between the most relevant transcription factors identified in renal tissue after Vancomycin treatment. The relationships were summarized as follow: a: activation, b: regulation of binding, e: expression, i: inhibition, l: localization, m: modification, p: phosphorylation, pd: protein-DNA interaction, pp: protein-protein interaction, pr: proteolysis, tl: transclocation, tc: transcription. For the identification of the interactions the Ingenuity pathway analysis software IPA® as used.

	NF-κb	**PPARα**	**PPARγ**	**PPARδ**	**RelA**	**Smad3**	**Stat1**	**Stat3**
NF-κb	a, b, tl	a, e, i, pp, tc	a, e, i,pp, tc	a	a, e, l, m, pp, b, tc, tl	a	a, p, pp, b,	pp, b,
PPARα	a, e, i, pp, tc	a, e, i, l, pd, pp, tc, tl	a, e, pp, tc	a, tc	pp, b	-	-	-
PPARγ	a, e, i,pp, tc	a, e, pp, tc	a, e, i, p, pd, pp, pr, b, tc, tl	a, e, tc,	a, e, pp, b,	p, pp, b,	a, e, pd	pp
PPARδ	a	a, tc	a, e, tc,	a, e, pp, tl	pp	e, tc	e	-
RelA	a, e, l, m, pp, b, tc, tl	pp, b	a, e, pp, b,	pp	a, e, m, p, pp, pr, b, tc, tl	p, pp	pp	l, pp, tl
Smad3	a	-	p, pp, b,	e, tc	p, pp	a, i, m, p, pp, pr, b, tc	a, e, pp	pp
Stat1	a, p, pp, b,	-	a, e, pd	e	pp	a, e, pp	a, m, p, pp, pr, b, tc, tl	a, e, p, p, b
Stat3	pp, b,	-	pp	-	l, pp, tl	pp	a, e, p, p, b	a, e, i, m, p, pd, pp, pr, b, tc, tl

The highest number of relationships was observed for each individual transcription factor by interaction with themselves, which indicated the strong feedback control mechanism of gene expression. However, also several relationshipts could be observed for NF-κB-PPARα/ PPARγ, NF-κB-RelA, NF-κB-Stat1 and RelA-PPARγ. The Stats showed the major interaction between themselves, while PPARα showed interactions with NF-κB, RelA and the other PPARs. All this gives further evidence for the central role of NF-κB as a mediator of multiple processes, including inflammation, proliferation, apoptosis and cell growth and recovery.

Since Vancomycin-induced nephrotoxicity can inhibited by targeting superoxide dismutase [Nishino et al., 2002, Nishino et al., 2003], it is assumed that oxidative stress may play a role in cellular damage caused by Vancomycin. A key transcription factor in case of oxidative stress is Nrf2, but showed no increase in gene expression or any significant elevation by transcription analysis. However, several molecules regulated by this transcription factor or otherwise

related to oxidative stress, reactive oxygen species (ROS) or in the response to oxidative stress and the maintenance of normal cellular redox states were significantly altered. The upregulated genes were the superoxide dismutase 3 (Sod3), heme oxygenase-1 (Hmox1), thioredoxin-disulfide reductase, xanthine dehydrogenase (Xdh), gluthathione peroxidase 2 (Gpx2), peroxidase 2 (Prdx2), and NAD(P)H dehydrogenase quinone 1 (Nqo1). In addition, NF-κB1 and NF-κB2, RelA, Stat3, Jun, and Fos, involved in many processes like inflammation, proliferation, and apoptosis, showed an upregulation that was dependent on the severity of damage. Also an upregulation of the chaperone and stress response proteins Hsp90, chaperonin containing Tcp1 (Cct7), FK506 binding protein 5 (Fkbp5) and peptidylprolyl isomerase B (Ppib) was observed. Downregulation was observed for catalase (Cat), gluthathione peroxidase 1 (Gpx1), glutamate-cysteine ligase (Gclc), aflatoxin aldehyde reductase (Afar), cytochrome P450 2E1 (Cyp2E1), gluthathion S-transferase alpha 5 (Gsta5). In summary, the gene expression changes suggested that an oxidative stress response has been induced by Vancomycin treatment, presumably to help reduce the harmful impact of ROS on renal cells.

3.1.4 Conclusion about Gene expression analyses

Several potential key players in the progression of Vancomycin induced nephrotoxicity have been identified and discussed. However, the underlying results are based on gene expression data only. Subsequently, the results only show one part of a broader picture and should be seen as a starting point of further studies.

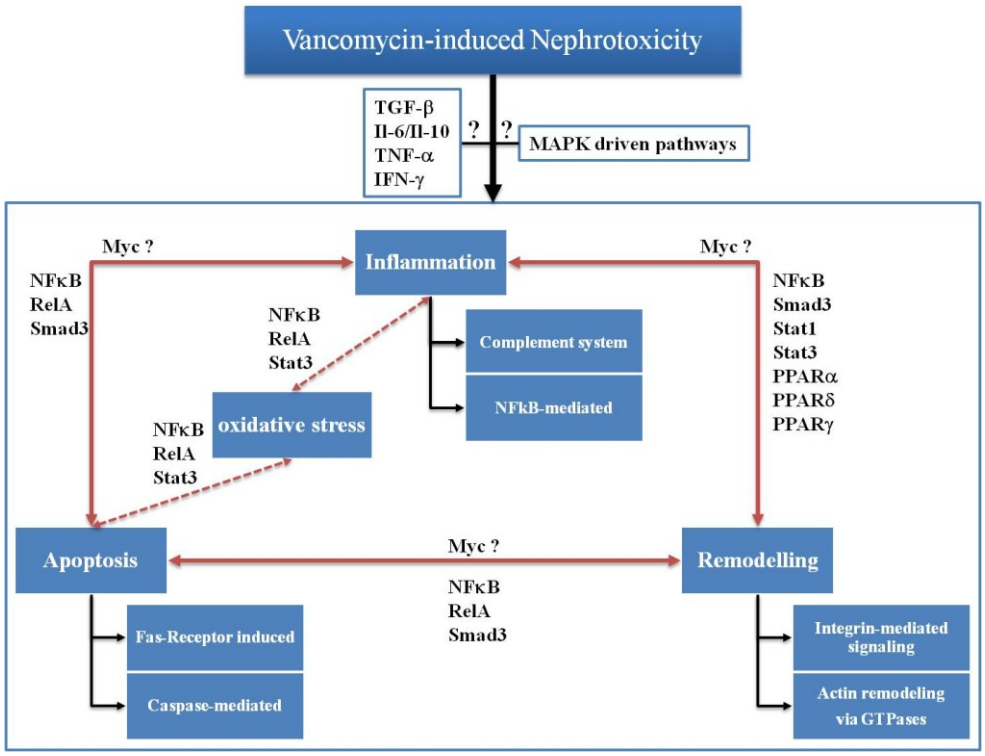

Figure 3-31 Pathway from the underlying gene expression data generated from renal tissue after Vancomycin treatment. The three major processes (inflammation, apoptosis, remodeling) are shown with the two major biological mechanisms involved. In addition, the individual processes were linked based on identified transcription factors, including oxidative stress.

It could be shown that the three major processes – inflammation, apoptosis and remodeling/ regeneration (Figure 3-31) - are the most prominent alterations observed, which were confirmed by the in-life parameters as well as histopathological evaluations (see 3.1.1.1 Results (Vancomycin)). Subsequently, further molecular biological/ toxicological alterations could be identified. For example, the complement system seems to play a pivotal role in Vancomycin induced renal tubular damage. Since similar gene expression alterations were reported for several compound-induced renal alterations, this process seems not to be Vanyomycin specific [Kim et al., 2007, Pan et al., 2009]. This highly conserved acute response showed also a more or less constant activation in male and female rats. In addition, the detection of complement components could therefore be assumed to have a degree of diagnostic potential, especially as the complement pathway is highly regulated and conserved across species. Another factor which appears frequently over all the evaluated biological responses is the involvement of the transcription factor NF-κB, which also induces complement component 3, and -4b. Since NF-κB is a key molecule in inflammatory processes, which was present in a treatment dependent manner, but it may also influence apoptosis and regeneration. By taking into account that NF-κB regulates a multitude of genes not directly related to inflammatory processes and that several of these were also degregulated within this study, it is very likely that it may also be involved in these biological events. Furthermore,

the way in which this transcription factor counterbalance the beneficial anti-apoptotic properties and the detrimental pro-inflammatory activity, gives strong evidence for an involvement of NF-κB within this interplay of life and death signals. Another important question, related to cell death and survival, is how the apoptotic program is regulated. In this case, our data suggest that the induction of apoptosis is primarily induced by the Fas-receptor (FasR). Since the Fas-receptor is activated by Fas-ligands (FasL) which belongs to the tumor necrosis factor (TNF) family, needs further investigation. Further evidence is given by the fact that TNF-α has been described to activate a p53-dependent apoptosis mediated by NF-κB. Therefore, it can be hypothized that an alternative FasR/ TNF-α dependent pathway of apoptosis exists without the activation of p53 by NF-κB. However, the apoptotic process itself seems to be caspase-dependent because of the upregulation of initiation as well as effector caspases. Consequently, any alteration in mitochondrial function, characterized by increased oxygen and ATP production described for Vancomycin, is not leading to the release of the apoptosis inducing factor (AIF) and the initiation of a caspase-independent apoptosis. Caspase 12 has been reported to be related to endoplasmic reticulum stress, although it is more likely that the up-regulation of Caspase 12 is due to the inflammation. In contrast to the possible ER-stress, there is much more evidence for an involvement of oxidative stress in Vancomycin induced nephrotoxicity, triggered by NF-κB, RelA and Stat3. Kidney remodelling, which includes cell proliferation, migration and differentiation, is the most comprehensive process during renal tubular cell injury. Apoptosis and cellular clearance by inflammatory cells like macrophages are fundamental processes in healing of the kidney. Therefore we concentrated on processes directly involved in the repopulation of denuded tubular areas, the cell-cell signaling mediated migratory processes and the recovery of the cellular shape and properties including the building up of a functional extracellular matrix. Here, integrin-mediated pathways seem to play the most important role and are involved in many different downstream signalling events. One pathway which was most pronounced was the GTPase-dependent actin nucleation. This process is of importance for differentiation, migration and cellular shape recovery, and was driven by de GTPases Rho, Cdc42 and Rac1. Many of these cellular processes are not exclusively important in renal tubular cell recovery, but also in the motility of monocytes and magrophages infiltration. The same is true for the potential involvement/ influence of HMGB1, which on one hand can be induced by secretion from macrophages or by release from necrotic tubular cells. In summary, the gene expression data gave further insights in potential processes and signaling pathways of Vancomycin induced nephrotoxicity. The data gave strong evidence of an involvement of Stat3, Smad3, and Myc in Vancomycin-induced nephrotxicity. Because the data presented are exclusively based on the measure of mRNAs and not on proteins, this approach has to be seen as a hypothesis building one. The results were meant to give a statistically significant starting point for further investigation. Therefore, the Fas-receptor mediated apoptosis, the influence of NF-κB on inflammation, apoptosis and recovery has to be addressed. In addition, the background on PPAR inhibition as a potential origin of renal cell protection needs further work. Independent of the analyzed processes, the MAPK pathway has to be considered, because of the strong evidence for its involvement in Vancomycin-induced nephrotoxicity. Because the data point to some similarities in Vancomycin and Gentamycin-induced renal damage, the involvement of the MAPK-signaling can be partially extrapolated. Thus it can be hypothized that the p38-MAPK pathway may be involved in renal insult induced by Vancomycin. In addition, the increase of NF-κB protein, which seems to be responsible in Gentamycin induced inflammatory processes of interstitial nephritis, could also be transfered to Vancomycin nephrotoxicity. Since this pathway can be initialized by TNF-α and TGF-β and is mediated by p38/ MAPKα, this pathway is likely to be involved. However, because the majority of regulatory steps takes place in form of phosphorylation events on protein level, analysis on gene expression level only deliveres limited information and needs additional studies.

3.1.5 Evaluation of putativ transcriptional biomarkers in vivo

In the following section transcriptional biomarkers for the identification/ prediction of compound induced nephrotoxicity, taken from renal tissue, were evaluated. A commercialized set of genes in combination with a Random Forest classifier were evaluated for their applicability to detected renal damager. This system, consisting of the protocol for the SYBR®-green based qRT-PCR as well as the analyzing software, was provided by Compugen Ltd. In this approach three independent studies were used (see 2.4.2Additional rat in vivo studies investigated). In a second step these transcriptional biomarkers, as well as other sets of genes derived from public available datasets (TG-GATEs) as well as from literature were tested for their ability to predict renal insult within a whole genome dataset.

Compugen Ltd. Classification model:

For testing the Compugen Ltd. based classification system for nephrotoxicity, three independent rat studies (Gentamycin, FP007SE/ BI-3, aristolochic acid) were used. Animals within the Gentamycin study showed no histopathological alterations within the control group after 7 days of treatment. All five low dose (60 mg/kg) treated animals showed mild to high severity of proximal tubular necrosis while all high dose (120 mg/kg) treated animals showed a high severity of lesions after the treatment period [Hoffmann et al., 2010]. These results could be reflected by using the Compugen classification model. However, only 3 out of the five animals from the original study could be used for testing, All three tested control animals showed classification values between 0.1 and 0.2 and therefore were far below the classifier threshold of 0.4, subsequently leading to a toxicity value of 0% (0 of 3 animals) (Figure 3-32a). In low (60 mg/kg) as well as in high (120 mg/kg) dose treated animals all three rats delivered values above the threshold (0.6-0.8) leading as a consequence to a classification of 100 % (3 of 3 animals). However, no differences were observed between animals only showing mild insults compared to animals with a high severity of lesions (data not shown). Both classifiers, the 4 gene and the 6 gene (including two splice variants of Ccng1 and Isg20; see Table 2-18), delivered the same classification.

In contrast to the Gentamycin study were only one time point of tissue collection was performed (Figure 3-32a), three different time points were evaluated within the FP007SE study. The histopathological observations within the FP007SE study showed 2 animals of the control group with minimal necrosis within the proximal tubulus after 3 days of treatment. In the low dose group (100 mg/kg) one animal showed minimal necrosis after treatment day 1 and two animals after treatment day 3. However, at the latest time point no animals were observed showing renal alteration. In high dose (1000 mg/kg) treated animals no changes were observed after 1 day of treatment and only one animal showed minimal proximal tubular necrosis after 3 days.

However, after 14 days of treatment 2 rats showed moderate and one animal showed severe tubular damage. Within the classification model by Compugen Ltd., in contrast to the Gentamycin study, on day 2 and day 4 a toxicity value of 20% was calculated. This indicates that in both groups one animal was classified as positive for renal insult (Figure 3-32b). While in the control group studied after 4 days (classifier value: ~0.49) the positive classified animal had mild necrosis, the animal on day 2 (classifier value: 0.52-0.56) was not described to show any pathological alterations. However, a good time and dose dependent increase in toxicity values, and therefore in the number of positive classified animals per group, was measured.

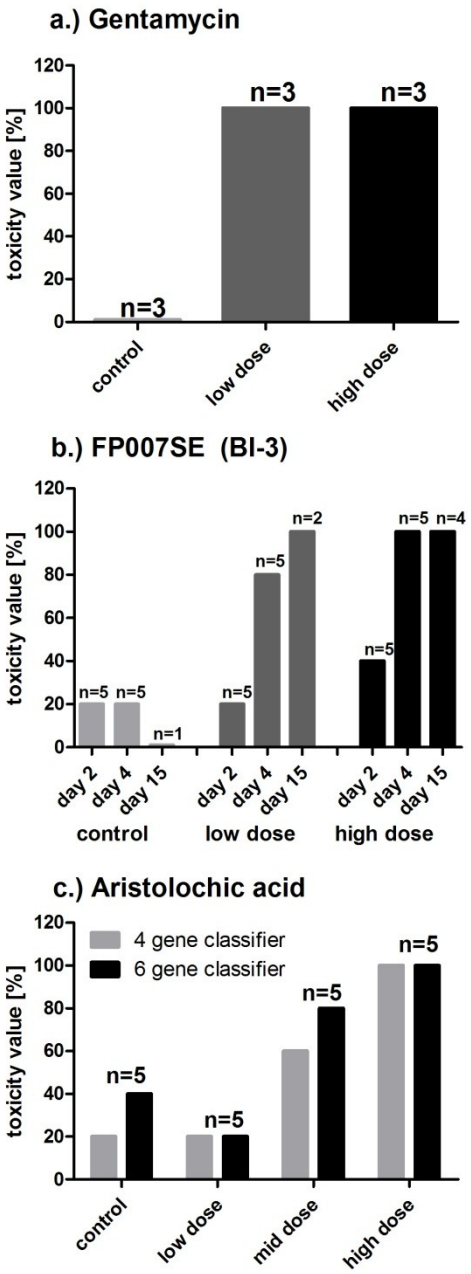

Figure 3-32 The toxicity values derived by the classification model from Compugen Ltd. based on the quantification of 4 genes. The classifier calculated individual classification value of each individual animal. If the value lay above the threshold defined by Compugen Ltd. (0.4) the animal was assumed to be possitiv (toxic affected). Out of this the toxicity value for the treatment group was calculated be the number of positiv classified animals against all animals. Renal tissue of three independent studies were used: a.) Gentamycin, b.) FP007SE (BI-3), c.) aristolochic acid. Because the samples were provided by the University of Wuerzburg, for any reason not for all treatment groups all samples were available. Therefore the total number of used samples (n) is displayed in each individual graph.

A disadvantage of this result was the lack of coverage of the evaluated toxicity values by histopathological observation. One animal of the low dose (100 mg/kg) treatment group on day 2 was correctly classified (toxicity value 20%), however two animals positively classified on day 15 with classification values in the 6 / 4 gene classifier of 0.37 / 0.4 and 0.57 / 0.58, showed no histopathological findings. On day 4, low dose (100 mg/kg) treated animals also showed classification values above the threshold and must be therefore assumed to be positive. Similarly, in high dose (1000 mg/kg) animals, where two animals treated for two days and four animals treated for four days were positively classifiered without necrotic findings within the kidneys. Therefore, these results are categorised as false positives. However, there is some evidence that the measured classification and toxicity value could be a real prediction of the developing nephrotoxicity. This hypothesis is supported by the fact those animals without proximal tubular necrosis, even though they are above the threshold, showed smaller classification values. Therefore, the alterations caused by treatment with FP007SE were specifically established on molecular/ transcriptional level and had not yet lead to renal necrosis.

Witin the study using aristolochic acid (AA), described to be a rodent carcinogen and a highly nephrotoxic compound, no histopathological alterations were observed at any time point. However, the classification model showed a clear dose-dependent increase in the prediction of incidence of renal damage. In contrast to the other two studies, the 6 gene and the 4 gene classification model showed slight differences for the control and the mid dose (1 mg/kg) groups. In the 6 gene classifier two animals of the control group were predicted to be positive (40% toxicity value) while only one animal in the 4 gene classifier lay above the threshold (20% toxicity value) (Figure 3-32c). Subsequently, only one of these two animals showed a high classification score while the second was a borderline. In the low dose (0.1 mg/kg) treated group only one animal was above the threshold (20% toxicity value), independent of the used classifier. In the mid dose (1 mg/kg), either 4 animals in the 6 gene (80% toxicity value) or 3 animals in the 4 gene (60% toxicity value) classifier were above the threshold. Independent of the classifier, the high dose (10 mg/kg) treated animals were predicted as positive in 100% of the cases (5 of 5 animals).

These results deliver further evidence that this transcriptional panel provided by Compugen Ltd. could have the potential to really predict renal damager, even before histopathological alterations take place. By assuming this hypothesis, the prediction of a developing AA induced kidney injury can be seen as successful. The fact that the mid- and high dose samples were increasingly classified as nephrotoxic deliver additional information about the solidity of this early prediction. To take into account that the measured values of the gentamycin study, where clear histopathological findings were observed, and the FP007SE were some findings could be covered by histopathological observed necrosis, these findings give further hints to the great benefit of transcriptional biomarkers, especially in the early stages of developing kidney damage. Nevertheless, it must also be mentioned that the detected transcripts are involved in a multitude of signaling pathways and pathological processes. Especially in carcinogenicity, this is of special interest as Ccng1, a member if the cyclin family, is involved in the eukaryotic cell cycle and in addition is inducible by p53 [Endo et al., 1996; Okamoto et al., 1996]. It also was described to be directly involved in renal tumorigenesis [Stemmer et al., 2007]. Tnfrsf12a, a member of the tumor necrosis factor receptors, was also described to be involved in tumor formation, not only in kidney, but in several organs, such as liver [Mei et al., 2006], esophageal [Wang et al., 2006] and skin [Ahlborn et al., 2008]. While Isg20, an exonuclease with specificity to ssRNA, seems to be not directly involved in carcinogenic pathway but in inflammatory processes, the inactivation of Ei24 has been described to be associated with the formation of invasive cervical carcinoma [Mazumder et al., 2011] because of its role as an apoptosis-inducing factor [Chen et al., 2002].

In summary, changes in gene expression could be observed much earlier than the increase of marker proteins in urine. Together, the data generated by the qRT-PCR based classification model suggests that the 4 gene classifier delivered comparable results to the 6 gene classification model. Further investigations are needed using additional nephrotoxins as well as non nephrotoxic compounds to validate the utility of these transcriptional biomarkers. To check whether these transcripts also can be used independently of the underlying method the transcripts were analysed based on the Vancomycin study (see below).

Independency of transcripts used in the Compugen Ltd. Classification model

To evaluate if the transcripts used within the Compugen Ltd. Classifier can also be used directly as potential biomarkers, the intensity values were extracted from the whole genome dataset generated from the samples of the Vancomycin study. The intensity values of the control groups were averaged (n=3) (arithmetric mean) and relative ratio values of each treated animal were calculated against the average of the corresponding time matched control group. The ratios were then averaged (geometric mean) and the data were displayed as $\log_2$ normalized values in Figure 3-33. To evaluate the relationship of gene expression pattern, the deregulations were ploted against the histopathological observations of tubular degeneration. The increase in Ccng1 mRNA was only slightly related to histopathology in female rats, while male rats showed no alteration (Figure 3-33a). In addition, the magnitude of Ccng1 induction was low, reaching only an level of $\log_2(1)$, a quasi doubling, in animals with moderate to massive tubular degeneration. However, Ccng1, has been described in several studies to be upregulated in renal tissue after gentamycin, Batcitracin and Cisplatin induced nephrotoxicity [Ozaki et al., 2009, Wang et al., 2008]. When Vancomycin was administered daily at 160 mg/kg i.v. for up to 5 days, no alteration of Ccng1 was observed [Wang et al., 2008]. In contrast Isg20 has not been reported in case of drug induced nephrotoxicity.

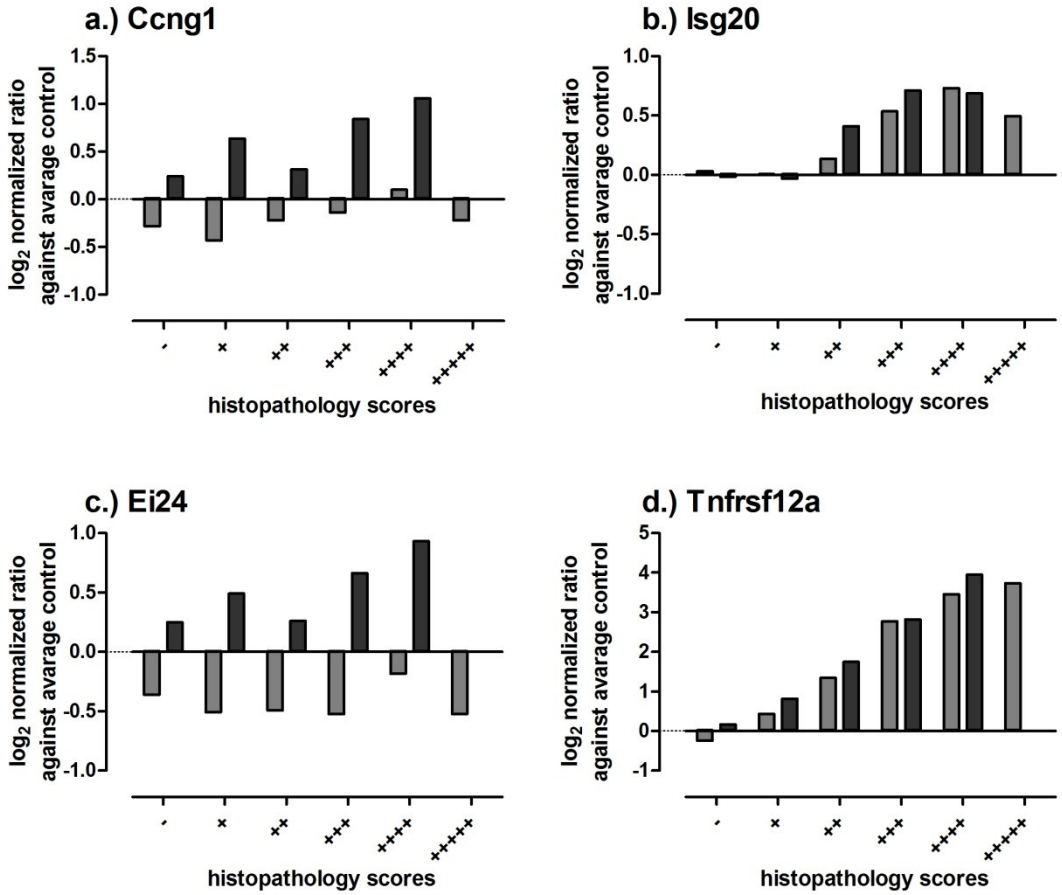

Figure 3-33 Deregulations of a.) Ccng1, b.) Isg20, c.) Ei24, and d.) Tnfrsf12a over the histopathological findings (tubular degeneration) from the Vancomycin study. The data are presented as the log_2 normalized ratios of the averages (geometric mean) over each individual group against the average of the corresponding time match control group as bars (lighter grey = male rats; dark grey = female rats). - ≙ lesion not observed, + ≙ minimal, ++ ≙ mild, +++ ≙ moderate, ++++ ≙ massive, and +++++ ≙ high severity of lesion.

Because of its involvement in inflammatory processes, which also play a pivotal role in renal damage and by the fact that it is expressed by vascular endothelial cells [Imaizumi et al., 2008], like VEGF, it can be assumed that this transcript can have the potential to deliver further information in special cases of renal alteration. Within our Vancomycin study, Isg20 showed a clear tendency in both male and female rats from mild to high severe of damage, however it has a limited potential as a biomarker because of the low magnitude of increase, which was always below $log_2(1)$ (Figure 3-33b). A similar situation occurred for Ei24, which also has not been reported to be responsive to drug induced renal damage. However, there are several reports of the involvement of Ei24 in case of p53-dependent apoptosis [Burns et al., 2001; Mork et al., 2007]. Ei24 showed a similar regulation pattern to Ccng1, also with the specific gender differences and the low magnitude of increase (Figure 3-33c). In contrast to Isg20 and Ei24, Tnfrsf12a has been described in several approaches with the aim to identify potential biomarkers for nephrotoxicity. For example, Tnfrsf12a has been described to be upregulated in e.g. compound A induced nephrotoxicity [Kharasch et al., 2006] as well as in ischemic acute renal failure [Yuen et al., 2006]. Within our panel of genes, Tnfrsf12a showed the best correlation to histopathological observations (Figure 3-33d).

Based on our results, it can be concluded that Tnfrsf12a can be used as an exploratory transcriptional biomarker for drug-induced renal damge. However, further work on Ccng1, Isg20 and Ei24 is needed before a final decision can be made.

3.1.4 Testing of two panels of potential transcriptional biomarkers

Beside the transcripts used within the Compugen Ltd. based assay, there are many other potential transcriptional biomarkers published. In almost all cases these genes were discovered through large cooperation's [Fuchs et al., 2011]. However, in most of the cases these lists of potential transcriptional biomarker were generated and proven by the consortia / cooperation partners themselves, but there are fewer reports of the validation of these biomarkers in an independent way. Within the following sections two of these biomarker lists were used to evaluate the applicability of these biomarkers to identify renal damage in our Vancomycin study. The two biomarker lists which will be used in the following are based on the Toxicogenomic Project in Japan (TG-GATEs) reported by Minowa and colleques [Minowa et al., 2012] and a literature based biomarker panel [Wang et al., 2008].

Evaluation of a multigene biomarker panel identified by the Toxicogenomic Project in Japan

The scientific approach within the Toxicogenomics Project in Japan was based on the measurement of whole genome transcriptional changes in kidney from rats treated with 41 nephrotoxic and non-nephrotoxic compounds. Two different approaches were used, either a single treatment with an observation time of 24h or daily dosing (intravenously or orally) for 28 days. Male Sprague-Dawley rats were treated with three different doses (low, middle, and high) of each compound. In the single treatment regime renal tissue was collected at 3, 6, 9 and 24h; in the repeated dosing regime on days 4, 8, 15 and 29. Gene expression profiles were generated from kidney total RNA using Affymetrix DNA microarrays. For more detailed information refere to Minowa et al., [2012]. The identification of the relevant genes was based on a computational classification model. The model resulted in a list of 19 probes (Table 3-22) with a reported sensitivity of 93% and a selectivity of 90%.

Table 3-22 Originally identified transcripts of the TG-GATEs classification model with their rank of classification. In addition the Affymetrix Probe ID is given.

Rank	Probe ID	Gene symbol	Gene title
1	1387965_at	Havcr1	Hepatitis A virus cellular receptor 1
2	1368420_at	Cp	Ceruloplasmin
3	1368627_at	Rgn	Regucalcin (senescence marker protein-30)
4	1368497_at	Abcc2	ATP-binding cassette, sub-family C, member 2
5	1370445_at	Pla1a	Phospholipase A1 member A
6	1371785_at	Tnfrsf12a	Tumor necrosis factor receptor superfamily, member 12a
7	1383605_at	LOC360919/ LOC684913	Similar to alpha-fetoprotein
8	1379889_at	Lamc2	Laminin, gamma 2
9	1377092_at	EST	EST
10	1379340_at	Lamc2	Laminin, gamma 2
11	1390579_at	RGD1305222	Similar to RIKEN cDNA 1810029B16
12	1387382_at	Hnmt	Histamine N-methyltransferase
13	1370422_at	Ripk3	Receptor-interacting serine-threonine kinase 3
14	1367856_at	G6pd	Glucose-6-phosphate dehydrogenase
15	1370333_a_at	Igf1	Insulin-like growth factor 1
16	1367712_at	Timp1	TIMP metallopeptidase inhibitor 1
17	1367977_at	Snca	Synuclein, alpha
18	1374070_at	Gpx2	Glutathione peroxidase 2
19	1383675_at	EST	EST

The individual transcripts were exctracted out of the Illumina RatRefv.1.0 whole genome dataset generated from our Vancomycin study. However, Ceruloplasmin (rank 2), Insulin-like growth factor 1 (rank 15) and EST (rank 19) were not present on the Illumina microarray. In addition, γ-Laminin, which was present in the gene list twice with different probes, was only included once (ILMN_1368403). The expressed sequence tag (1377092_at) was found to be synonymous with the suppressor of cytokine signaling 3 (Socs-3).

The intensity values of the control groups were averaged (n=3) (arithmetric mean) and relative ratio values of each treated animal were calculated against the average of the corresponding time matched control group. The ratios were then averaged (geometric mean) and the data were displayed as $\log_2$ normalized values in Figure 3-33. To evaluate the relation of gene expression pattern the deregulations were plotted against the histopathological observations of tubular degeneration (Figure 3-34a-o).

Several of the evaluated transcripts showed renal damage related changes. The earliest and strongest up regulation was observed for Havcr1, Tnfrsf12a, Lamc2, Timp1 and Gpx (Figure 3-34a, e, f, j, l). Because of the close functional relationship between Havcr1, Timp1 and Lamc2, in the interaction with extracellular matrix components and other cofactors and their involvement in cellular repair, attachment, migration and organization [Huo et al., 2010, Hellman et al., 2006, Mizushima et al., 1998, Miner et al., 1999], it can be assumed that these processes start immediately after an insult, even though only minimal histopathological degenerations can be observed. Therefore, these transcriptional biomarkers can be used to detect moderate/mild changes in renal cells. Because no strong differences between male and female rats were observed, which can be due to the general mechanism of cellular repair, they also can be used independently of the sex. Tnfrsf12a is a receptor for Tnfsf12/Tweak and a weak inducer of apoptosis [Tran et al., 2005]. However, Tnfrsf12a was also reported to be involved in angiogenesis and endothelial proliferation [Wiley et al., 2001]. Furthermore, it is involved in the modulation of cellular adhesion to matrix proteins [Meighan-Mantha et al., 2000]. In summary, this transcript seems to play an impotant role in nephrotoxicity. This is underlined by the fact that Compugen Ltd. identified this biomarker independently (3.1.4 Testing of two panels of potential transcriptional biomarkers).

Gpx (glutathione peroxidase) is one of two isoenzymes responsible for the majority of the glutathione-dependent hydrogen peroxide reducing activity [Prabhakar et al., 2005, Ng et al., 2007]. Gpx is involved in the oxidative stress response, specifically induced by reactive oxygen species (ROS) [Miyamoto et al., 2003], a further indication for the mechanism of Vancomycin induced nephroptoxicity. However, beside this strongly up regulated transcript, there are also insult-dependent down regulated genes within this biomarker list. These include Rgn, Hnmt and Snca (Figure 3-34b, g, k). While Hnmt, a histamine N-methyltransferase inactivating histamine and functions as an anti-inflammatory factor, showed only minimal differences between male and female rats, Rgn and Snca showed a marked decrease in gene expression only in male rats. These differences can point to a potential gender difference in the mechanism of Vancomycin induced nephrotoxicity. Rgn, a calcium-binding protein, has an important role in calcium homeostasis and therefore in modulating Ca^{2+} signaling and Ca^{2+}-dependent enzyme activities and processes [Lai et al., 2011]. Since it is known that elevated intracellular calcium levels can induce apoptosis [Mattson et al., 2003] it can be hypothized that a decrease in renal Rgn can lead to less calcium-binding and therefore to an accumulation of Ca^{2+}, finally leading to apoptosis. In addition, it has been reported that Rgn knockout mice were highly susceptible to receptor-mediated apoptosis [Ishigami et al., 2002] and therefore underline the anti-apoptotic role of Rgn. The decrease of Snca also lead to a reduction of an anti-apoptotic factor. Snca has been described to reduce caspase-3 activity [Li et al., 2005] to inhibit the proteasome formation [Tanaka et al., 2001], a decrease will probably lead to an increase in apoptotic events. In summary, the decrease in gene expression could only be observed at later stages when mild to moderate changes already were established.

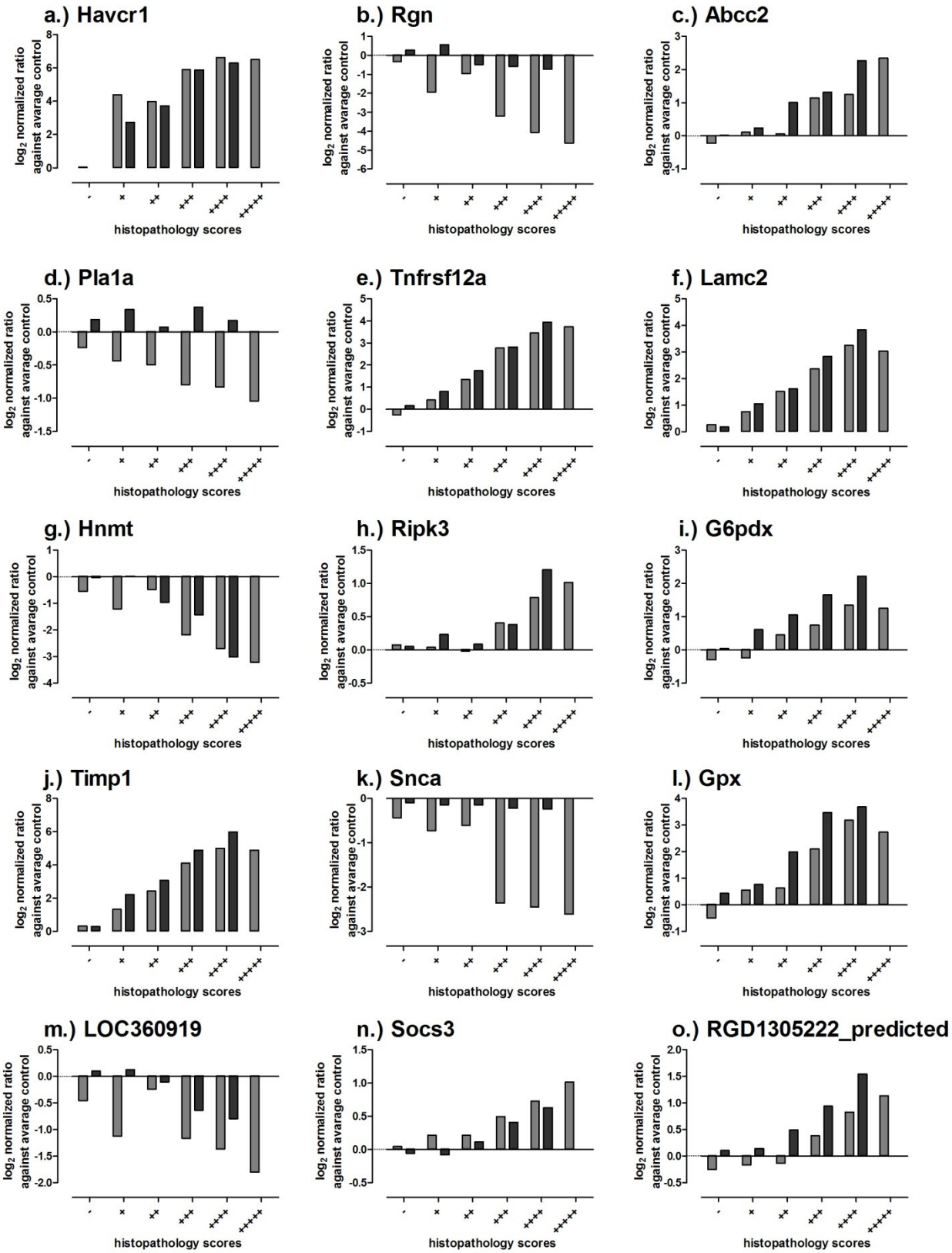

Figure 3-34 Gene deregulation of a.) Havcr1, b.) Rgn, c.) Abcc2, d.) Pla1a, e.) Tnfrsf12a, f.) Lamc2, g.) Hnmt, h.) Ripk3, i.) G6pdx, j.) Timp1, k.) Snca, l.) Gpx, m.) LOC360919, n.) Socs3, o.) RGD1305222_predicted over the histopathological findings (tubular degeneration) from the Vancomycin study. The data are presented as the $\log_2$ normalized ratios of the averages (geometric mean) over each individual group against the average of the corresponding time match control group as bars (lighter grey = male rats; dark grey = female rats). - ≙ lesion not observed, + ≙ minimal, ++ ≙ mild, +++ ≙ moderate, ++++ ≙ massive, and +++++ ≙ high severity of lesion.

Beside the transcriptional biomarkers mentioned above, also Abcc2 (Figure 3-34c) and G6pdx (Figure 3-34i), showed a gender-independent increased gene expression in relation to the observed severity, although they were not as sensitive. The increase reached $\log_2(1)$ earliest when mild to moderate tubular degeneration were observed histopathologically. Similar to Ccng1, Isg20 and Ei24 are included in the Compugen Ltd. assay (Figure 3-33a-c), also Pla1a, Ripk3, LOC360919, Socs3 and RGD1305222_predicted (Figure 3-34d, h, m, n, o) showed a clear tendency in altered gene expression in relation to histopathological observation, but with a relative low magnitude of deregulation. This finding can be due to the specific mechanism of Vancomycin-induced nephrotoxicity or based on the fact that the discovery of these transcripts was based on a computational classification model, which does not necessarily identify genes with strong alterations.

Evaluation of a literature based biomarker panel

A list of 48 transcripts, generated by Wang and collogues by doing literature search, delivered a transcript biomarker candidate list and tested against 4 nephrotoxicants (Bacetracin, Gentamycin, Cisplatin, Vancomycin) and 3 hepatotoxicants (4,4-Diaminodiphenylmathane, Ketoconazole, 1-Naphthyl isothiocyanate), delivered promising results [Wang et al., 2008]. However, only male Sprague-Dawley rats were treated orally, intravenously or subcuntaneously daily with one of the model compounds for up to five days with kidney tissue collection on days 1, 3 and 5. Therefore, no data are available about the performance of the transcript panel in more long term treatment or in female rats. As mentioned for the gene set identified by Minowa and colleagues (Table 3-22) not all transcripts were present on the Illumina RatRef.v1.0 whole genome array. Ceruloplasmin (Cp), glutamate-ammonia ligase (Glul) and solute carrier family 21, member 1 (Slc21a1) were not included.

The benefit of using a larger panel of transcripts, like in this approach, is the possibility to group specific transcripts by their reported or expected function. Consequently, the pattern of transcripts within such groups can deliver further information about the underlying toxicological processes. The results of the altered genes were grouped and presented in Table 3-24 and Table 3-23.

The most obvious observation in both male and female rats is the early and strong increase in genes of the group “regeneration/ repair/ remodeling”. In this group five transcripts showed an increase in renal gene expression even after only minimal histopathological observations were recorded. These five genes are Clu, Havcr1, Lcn2, Timp2 and Spp1 All of which can be also determined on the urinary protein level. In addition female rats showed an increase in gene expression for Fn1 and Ctss within this group. However, the majority of changes in these transcriptional biomarkers were earliest established when mild to moderate tubular degeneration were observed. This is the case over all functional groups used within this analysis. The increase of pro-apoptotic factors in the functional group “apoptosis/ necrosis/ oxidative stress”, including Jun or the decrease of anit-apoptotic factors like Rgn, started to change when moderate tubular degeneration was observed. This is true for male rats (Table 3-24), where many more down regulated transcripts were measured, while female rats (Table 3-25) only showed down regulation of Odc and Ghr, both involved in cell growth and proliferation [Chi et al., 2006, Jeay et al., 2001]. The group “acute phase/ inflammatory” gave additional information about the underying renal injury and the processes affeceted. In this case A2m and Cd44 delivered the earliest and most pronounced results in both male and female rats. A2m, a protease inhibitor and cytokine transporter, is described to be increased, on a protein level, in nephritic syndrome. In case of longstanding chronic renal failure A2m can lead to amyloid [Picken, 2009]. This can be due to the function of A2m as an inhibitor of MMP, comparable to Timp1 [Webster et al., 2006].

Table 3-24 Transcriptional biomarker list reported by Wang and colleques [Wang et al., 2008] for the male rats of the Vancomycin study. The data are presented as the log_2 normalized ratios of the averages (geometric mean) over each individual group against the average of the corresponding time match control group. Log_2 values are color coded as follow: ≤ -2 dark green, -2 to-1 light green, -1 to 1 yellow, 1 to 2 orange, ≥ 2 red. The values are displayed over the histopathological findings (tubular degeneration). - ≙ lesion not observed, + ≙ minimal, ++ ≙ mild, +++ ≙ moderate, ++++ ≙ massive, and +++++ ≙ high severity of lesion

Gene Category	Histopathological scores [tubular degeneration]					
	-	+	++	+++	++++	+++++
Apoptosis/necrosis/oxidative Stress						
Anxa5	-0.29	-0.39	1.29	1.53	2.70	2.28
Hmox1	-0.02	0.13	0.64	1.74	1.88	2.20
Jun	-0.08	-0.21	1.06	1.40	1.57	1.13
Hmox2	-0.57	-0.48	-0.16	-0.69	-0.50	-0.57
Gadd45a	-0.42	-0.38	-0.34	-1.16	-0.85	-0.75
Odc	-1.03	-1.43	-0.31	-1.65	-0.83	-1.20
Calb1	-0.20	-0.09	0.29	-1.11	-1.26	-1.67
Ghr	-0.30	-0.36	-1.30	-2.10	-1.91	-1.71
Cat	-0.45	-0.66	-0.21	-1.43	-1.88	-2.13
Rgn	-0.33	-1.15	-0.84	-2.31	-4.28	-4.61
Acute phase/ inflammatory						
A2m	-0.04	0.36	2.11	2.55	3.65	3.53
Cd44	-0.04	0.10	1.26	2.51	2.93	2.63
Vcam1	-0.23	-0.49	0.70	0.47	1.63	0.79
Cd24	-0.16	-0.07	0.55	0.49	1.16	0.63
Ccnd1	-0.37	-0.38	-0.18	-0.07	0.42	0.55
Ccng1	-0.25	-0.53	-0.13	-0.30	-0.11	-0.21
IgKc	0.04	-0.09	-0.12	-0.03	0.07	0.02
Regeneration/repair/remodeling						
Clu	-0.26	2.81	3.17	3.64	4.05	3.16
Havcr1	-0.18	4.52	4.39	6.20	6.64	6.50
Lcn2	-0.59	2.31	3.51	4.58	5.66	5.33
Timp1	0.06	1.81	2.68	4.10	5.17	4.90
Fn1	-0.43	-0.64	1.75	2.24	3.07	2.38
Spp1	-0.62	1.41	1.45	1.21	1.76	1.42
Ctss	-0.45	-0.38	1.12	1.14	1.93	0.65
Igfbp1	-0.69	0.66	0.56	1.00	1.66	0.87
Vim	-0.11	-0.21	0.43	0.70	1.72	0.95
Mt1a	-0.28	-0.08	-0.25	-0.32	-0.11	-0.15
Tmsb10	0.03	0.28	0.17	0.29	0.35	0.51
Cst3	-0.09	-0.43	0.06	-0.39	0.20	-0.37
Hormon/metabolism/transport						
Mgp	0.10	0.19	1.17	1.79	2.76	2.01
Cyr61	-0.04	-0.17	0.13	1.35	2.51	2.62
Bmp1	0.07	-0.09	0.09	0.04	0.57	0.14
Slc22a1	-0.37	-0.01	-0.41	-0.28	-0.54	-0.24
Ugt1a1	-0.29	-0.53	-0.28	-0.41	-0.60	-0.14
Vegfa	-0.36	-0.27	-0.16	-0.52	-0.54	-0.48
Aldh1a1	-0.40	-0.31	-0.54	-0.64	-1.04	-0.94
Gstm2	-0.20	-0.88	0.02	-1.06	0.28	-0.55
Bmp4	-0.31	-0.54	-0.21	-1.04	-0.69	-1.04
Cyp2d22	-0.34	-0.56	-0.17	-0.95	-1.09	-1.37
G6pc	-0.14	-0.16	-0.32	-0.78	-1.56	-2.07
Slc22a6	-0.48	-0.04	-0.90	-1.57	-2.07	-1.50
Oat	-0.10	-0.53	-0.05	-1.72	-1.73	-2.02
Nphs2	-0.38	-0.14	-1.21	-1.64	-1.95	-1.59
Ngfg	-0.65	-0.34	-1.24	-3.32	-3.38	-3.49
Egf	0.02	-0.18	-0.92	-2.43	-3.70	-4.71

Table 3-25 Transcriptional biomarker list reported by Wang and colleques [Wang et al., 2008] for the female rats of the Vancomycin study. The data are presented as the log_2 normalized ratios of the averages (geometric mean) over each individual group against the average of the corresponding time match control group. Log_2 values are color coded as follow: ≤ -2 dark green, -2 to-1 light green, -1 to 1 yellow, 1 to 2 orange, ≥ 2 red. The values are displayed over the histopathological findings (tubular degeneration). - ≙ lesion not observed, + ≙ minimal, ++ ≙ mild, +++ ≙ moderate, and ++++ ≙ massive lesion

Gene Category	Histopathological scores [tubular degeneration]				
	-	+	++	+++	++++
Apoptosis/necrosis/oxidative Stress					
Anxa5	0.16	0.44	1.45	2.26	2.84
Hmox1	0.02	0.16	1.05	1.53	1.80
Jun	0.13	0.58	1.03	1.69	1.67
Hmox2	-0.11	0.17	0.34	0.48	0.56
Gadd45a	0.04	0.37	0.07	0.19	0.26
Odc	-0.25	0.12	-2.01	-2.77	-1.31
Calb1	-0.12	0.33	0.26	0.43	-0.12
Ghr	0.03	0.02	-1.00	-1.04	-0.97
Cat	0.01	0.13	-0.21	0.05	-0.55
Rgn	0.29	0.27	-0.55	-0.63	-0.60
Acute phase/ inflammatory					
A2m	0.00	0.11	1.27	3.92	3.03
Cd44	0.03	0.38	1.53	2.64	2.31
Vcam1	0.11	0.71	1.15	1.90	1.65
Cd24	0.25	0.84	0.93	1.56	1.65
Ccnd1	0.15	0.71	0.39	0.68	2.04
Ccng1	0.28	0.67	0.33	0.82	1.01
IgKc	-0.06	-0.16	-0.20	-0.38	-0.24
Regeneration/repair/remodeling					
Clu	0.20	1.77	3.60	4.00	3.81
Havcr1	-0.11	3.01	4.74	5.93	6.29
Lcn2	0.08	2.67	3.94	6.15	6.18
Timp1	0.31	1.92	4.12	4.92	6.12
Fn1	0.55	1.26	1.75	3.26	3.01
Spp1	0.24	1.22	1.16	1.38	1.49
Ctss	0.33	1.32	1.08	2.31	2.14
Igfbp1	0.21	0.73	1.02	1.70	1.19
Vim	0.53	0.80	0.51	1.86	1.89
Mt1a	0.14	0.27	0.32	1.01	0.33
Tmsb10	-0.15	-0.18	-0.01	-0.03	-0.09
Cst3	0.38	0.62	0.40	1.13	0.47
Hormon/metabolism/transport					
Mgp	0.37	1.55	1.45	2.84	2.69
Cyr61	0.59	0.95	1.27	2.10	2.63
Bmp1	0.23	0.28	0.35	0.96	0.62
Slc22a1	0.16	0.31	0.39	0.58	0.99
Ugt1a1	0.08	0.50	0.53	1.03	1.32
Vegfa	0.08	0.30	0.22	0.28	0.14
Aldh1a1	0.12	0.54	0.17	0.32	0.06
Gstm2	0.33	0.24	0.33	0.36	0.16
Bmp4	0.04	0.35	0.22	0.29	0.09
Cyp2d22	-0.10	-0.04	-0.06	-0.14	-0.28
G6pc	-0.03	0.07	-0.23	-0.32	-1.45
Slc22a6	0.13	0.53	-0.46	-0.57	-0.50
Oat	0.20	0.26	-0.21	-0.12	-1.22
Nphs2	0.40	0.85	-0.60	-0.81	-0.34
Ngfg	0.10	0.15	-1.08	-1.37	-1.92
Egf	0.23	-0.01	-0.59	-1.63	-3.72

In addition, A2m seems to be strongly related to the induction and function of the complementary system. The A2m protein includes multiple domains with homology to the complement component C3 in human [Doan et al., 2007] and can act as a negative regulator of the lecitin pathway of the complementary system [Ambrus et al., 2003].

Cd44 is a cell-surface glycoprotein, also described to be involved in cell-cell interations, cell adhesion and migration [Goodison et al., 1999]. Furthermore, it seems to play a pivotal role in lymphocyte signaling [Taher et al., 1996, Ilangumaran et al., 1998]. Cd44 has a close relationship to Osteopontin, which can act as a ligand of the Cd44 receptor. Osteopontin modulates the Cd44-dependent chemotaxis or peritoneal macrophages [Zhu et al., 2004] and functions by binding to Cd44 and initiating a survival signal via a phospahtidylinositol 3-kinase/Akt pathway [Lin et al., 2001]. However, changes were only detectable when mild tubular degenerations were present. In contrast to the gene category group “apoptosis/ necrosis/ oxidative stress”, where male rats showed more deregulations, within the group “acute phase/ inflammatory” female rats showed more de-regulations, more specifically up-regulation of transcripts. Subsequently, Vcam1, Cd24, Ccnd1 and Ccng1 showed an up-regulation but only when massive tubular degenerations occurred (Table 3-26). This is remarkable because female rats showed a generally lower renal injury. Even in male rats identified with servere degenerations, these transcripts showed no alteration. Based on the general biological function as cell adhesion molecules (Vcam1, Cd24) and regulators of cyclin-dependent kinases, it was expected that no marked differences between the sexes will be present. However, this can be seen as a hint on differences in the mechanistic response of male and female rats, as a consequence leading to differences in the nephrotoxic outcome. Further mechanistic investigations on this hypothesis are required.

Within the last group “Hormone/ metabolism/ transport”, comparable differences between male and female rats were observed as described for the group “Apoptosis/ necrosis/ oxidative Stress”. This includes the similar increase in gene expression of two transcripts, in this case Mgp and Cyr61 and a relatively strong and widespread decrease in mRNA level within male renal tissue. Mgp is an extracellular matrix protein involved in the inhibition of tissue calcification [Schurgers et al., 2008], for example in arteries [Luo et al., 1997]. Calcification is a common cause of tubular interstitial nephritis as well as acute tubular necrosis [Loh et al., 2009], which is important to detect at very early stages. In contrast, the secretory protein encoded by Cyr61 plays an important role in a multitude of processes, such as cell proliferation, differentiation, apoptosis and ECM formation [Lee tal., 2007, Si et al., 2006, Todorovic et al., 2005, Lau, 2011]. It is a member of the Igfbp-family and is described to interact with Vegfa and Vegfc, MMP1, MMP3, as well as with Integrin-α1 and -α3. Even though it has been described in several scientific publications with the aim to identify nephrotoxicity [Mishra et al., 2003, Ichimura et al., 2004], the major role of this molecule in the developing and establishing renal injury has not yet been discovered.

3.1.5 Final resumee on gene expression biomarkers

Several of the reported transcripts can be used as predictive/ descriptive transcriptional biomarkers, delivering reliable results. Furthermore, the very early detection, when only minimal histopathological observations are present, indicate the high sensitivity of these transcriptional biomarkers. The benefit of the unbiased measurement of a panel of transcripts together with the advantage of grouping the transcripts into functional units can deliver additional information about the health status of the kidney. However, the major disadvantage of this approach is the risk of a misinterpretation by relying on predefined groups. In addition, transcripts like A2m, Cd44, Clu and Cyr61 can be grouped in multiple functional units. The fact that for almost all transcripts several functions were described in the literature makes this a major challenge of defining a transcriptional biomarker panel. Therefore, for any toxicological routine study, a combined approach of measuring urinary proteins, which has to be preferred because of the non-invasive character of this determination, at several interim time points and a final determination of the gene expression changes of the corresponding mRNA species can significantly enhance the drug development process. In addition these data will be available earlier than the sometimes very time consuming histopathological reporting. This approach has the best chance to be applied in early acute studies, where routinely no histopathology is available or in more long-term studies, by evaluation of additional time points. In both cases alteration on urinary protein or renal transcriptional changes can be used as a flag of the initiation of renal damage before sever histopathological changes have occured.

As an outlook, based on the data presented here and further literature search the following list of transcriptional biomarkers can be extracted and recommended for further evaluation. This list of 40 transcripts were grouped into 10 functional categories (Apoptosis, Cell Cycle, Proliferation, Cytosceleton, Transporter and metabolism, Metal Ion Binding, Oxidativ Stress, Tissue Remodeling, Extracellular Matrix, Inflammation) whereby individual transcripts can be present in more than one of these groups. Beside the already described and evaluated transcripts within the biomarker panels several additional transcripts were included based on the results of the gene expression data of our study and literature data of promising biomarkers. For example, the complement components C3 and C4 were included based on their abundance and potential importance for inflammation induced renal cell damage [Brown et al., 2007]. In addition, Nqo1, a cytoplasmic 2-electron reductase, often described to be upregulated in the case of drug-induced renal oxidative stress [Aleksunes et al., 2010], was included. Finally, Hsp90aa1 was described to play a pivotal role in proliferatory processes after toxic insults. Subsequently, it is also an important interaction partner with several transcription factors; themselves involved in cellular responses after a renal insult (see 3.1.3.2 Mechanistic Analysis).

This gene list can be considered as a starting point to evaluate the usefulness of transcriptional biomarkers in pre-clinical routine studies. It is important to remember that the studies performed to identify theses transcripts for the detection of renal damage are based on well known and highly potent nephrotoxiciants. Therefore, novel drugs/chemical candidates, with an often weaker toxicological profile and less specific nephrotoxic potential can lead to altered sensitivity and specificity. As a consequence, this list of potential transcriptional biomarkers has to be validated further with many more test compounds.

Table 3-27 Final transcriptional biomarker list for routine use in pre-clinical rat toxicity studies. The 40 individual transcripts were grouped into functional categories, while the transcripts can be present in more then one category.

Gene Symbol	Unigene	Description
Apoptosis		
Anxa5	Rn.3318	Annexin A5
Calb1	Rn.3908	Calbindin 1
Casp3	Rn10562	Caspase 3
Casp12	Rn.81078	Caspase 12
Cd24	Rn.6007	CD24 molecule
Cd44	Rn.1120	Cd44 molecule
Cdkn1a	Rn.10089	Cyclin-dependent kinase inhibitor 1A
Clu	Rn.1780	Clusterin
Gadd45a	Rn.10250	Growth arrest and DNA-damage-inducible, alpha
Ghr	Rn.2178	Growth hormone receptor
Hmox1	Rn.3160	Heme oxygenase (decycling) 1
Jun	Rn.93714	Jun oncogene
Nqo1	Rn.11234	NAD(P)H dehydrogenase, quinone 1
Rgn	Rn.10006	Regucalcin (senescence marker protein-30)
Tnfrsf12a	Rn.105040	Tumor necrosis factor receptor superfamily, member 12a
Cyr61	Rn.22129	Cysteine-rich, angiogenic inducer, 61
Cell Cycle		
Ccng1	Rn.5834	Cyclin G1
Cdkn1a	Rn.10089	Cyclin-dependent kinase inhibitor 1A
Egf	Rn.6075	Epidermal growth factor
Gadd45a	Rn.10250	Growth arrest and DNA-damage-inducible, alpha
Proliferation		
Cd24	Rn.6007	CD24 molecule
Cdkn1a	Rn.10089	Cyclin-dependent kinase inhibitor 1A
Clu	Rn.1780	Clusterin
Egf	Rn.6075	Epidermal growth factor
Hmox1	Rn.3160	Heme oxygenase (decycling) 1
Hsp90aa1	Rn.119867	Heat shock protein 90, alpha (cytosolic), class A member 1
Odc	Rn.874	Ornithine decarboxylase 1
Timp1	Rn.25754	TIMP metallopeptidase inhibitor 1
Cytosceleton		
Lamc2	Rn.9278	Laminin, gamma 2
Tmsb10	Rn.5983	Thymosin, beta 10
Vim	Rn.2710	Vimentin
Transport and metabolism		
Abcc2	Rn.10265	ATP-binding cassette, subfamily C (CFTR/MRP), member 2
Gpx	Rn.3503	Glutathione peroxidase 2
G6pd	Rn.11040	Glucose-6-phosphate dehydrogenase
Nqo1	Rn.11234	NAD(P)H dehydrogenase, quinone 1
Metal Ion Binding		
Cp	Rn.32777	Ceruloplasmin
Ctss	Rn.11347	Cathepsin S
Hmox1	Rn.3160	Heme oxygenase (decycling) 1
Lcn2	Rn.11303	Lipocalin 2
Rgn	Rn.10006	Regucalcin (senescence marker protein-30)

Gene Symbol	Unigene	Description
Oxidativ Stress		
Clu	Rn.1780	Clusterin
Hmox1	Rn.3160	Heme oxygenase (decycling) 1
Nqo1	Rn.11234	NAD(P)H dehydrogenase, quinone 1
G6pd	Rn.11040	Glucose-6-phosphate dehydrogenase
Tissue Remodeling		
Fn1	Rn.1604	Fibronectin 1
Lamc2	Rn.9278	Laminin, gamma 2
Havcr1	Rn.11154	Hepatitis A virus cellular receptor 1
Spp1	Rn.8871	Secreted phosphoprotein 1
Timp1	Rn.25754	TIMP metallopeptidase inhibitor 1
Vim	Rn.2710	Vimentin
Ngfg	Rn.11331	Nerve growth factor, gamma subunit
Nphs2	Rn.86433	Nephrosis 2, idiopathic, steroid-resistant
Tmsb10	Rn.5983	Thymosin, beta 10
Cyr61	Rn.22129	Cysteine-rich, angiogenic inducer, 61
Extracellular Matrix		
Cd44	Rn.1120	Cd44 molecule
Cyr61	Rn.22129	Cysteine-rich, angiogenic inducer, 61
Havcr1	Rn.11154	Hepatitis A virus cellular receptor 1
Lamc2	Rn.9278	Laminin, gamma 2
Mgp	Rn.2379	Matrix Gla protein
Timp1	Rn.25754	TIMP metallopeptidase inhibitor 1
Ngfg	Rn.11331	Nerve growth factor, gamma subunit
Inflammation		
A2m	Rn.198688	Alpha-2-macroglobulin
C2	Rn.98333	Complement component 2
C3	Rn.11378	Complement component 3
C4a	Rn.155573	Complement component 4A
Casp3	Rn10562	Caspase 3
Casp12	Rn.81078	Caspase 12
Ccng1	Rn.5834	Cyclin G1
Cd44	Rn.1120	Cd44 molecule
Clu	Rn.1780	Clusterin
Ctss	Rn.11347	Cathepsin S
Lcn2	Rn.11303	Lipocalin 2
Hnmt	Rn.13145	Histamine N-methyltransferase

3.2 Identification of potential surrogate transcriptional biomarkers in vitro

The aim of this evaluation was to check wether or not it is possible to identify transcriptional biomarkers in a renal cell line with the potential to bridge to the in vivo situation. Therefore, four nephrotoxic and two non-nephrotoxic compounds were administered to NRK-52E cells for up to 72h as a proof-of-principal.

3.2.1 In Vitro Cytotoxicity Assay

Before gene expression analysis could be performed the right concentration of the test compounds had to be evaluated. This was necessary to avoid a concentration too low to induce any significant gene expression changes a too high a concentration so that no enough cells survive the treatment time. Therefore, a dose range finding experiment were performed by measure the intracellular ATP concentration, used as an indirect measurement of cell viability. In addition, the neutral red uptake assay (NRU) was conducted to check if differences in the cellular responsiveness appear by using different cell viability/ toxicity assays.

Dose range finding in vitro

The intracellular ATP content can provide information about the viability of the cells as well as give any evidence of a potential effect on the mitochondria. To discovery whether or not a compound affects the mitochondria, an additional cytotoxicity or cell viability assay must be performed in parallel. For each individual compound, a series of a minimum 5 concentrations in 4 technical replicates were used. Each experiment was repeated a minimum of 3 times by using different passages of NRK-52E cells. These passages were used as biological replicates to ensure validity of the results. The TC_{20} values were calculated for the ATP Test after 72h of treatment, while the cells were treated every 24h (three treatment periods). Here the TC_{20} value is the concentration of the test compound required to reduce the ATP content by 20% compared to the corresponding vehicle control and calculated by plotting the relative cell viability values on a logarithmic scale and perform a sigmoidal fit (Table 3-28). Subsequently, the TC_{20} values were used as a high dose (HD) concentration. An example of such an approach is given in Figure 3-35.

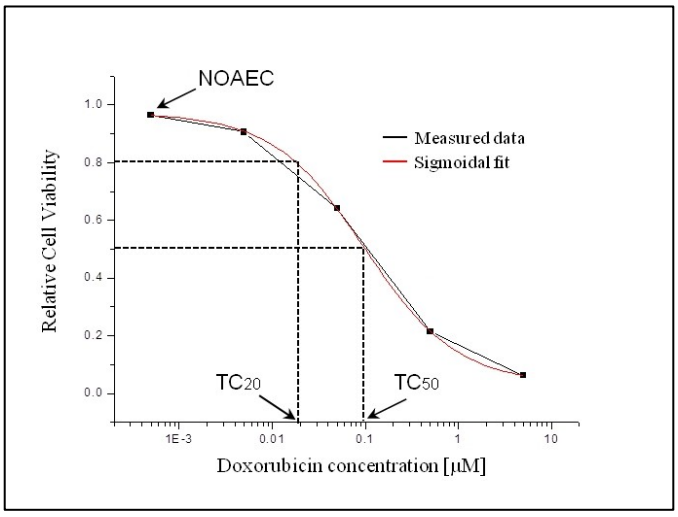

Figure 3-35 Example of the evaluation of the NOAEC, TC_{20}, and TC_{50} based on the relative cell viability determined by intracellular ATP content. Dose response curve of Doxorubicin ploted on a logarithmic scale. In this example five concentrations were used to and the NOAEC was directly evaluated from the curve by chosing a concentration without any alteration. The sigmoidal curve was calculated and generated by using the Origin® software. The TC_{50} value is the half maximal toxic concentration where 50% of the cells are dead. In contrast, the TC_{20} is defined by the concentration where 80% of the cells are alive and 20% are dead.

The low dose concentration was chosen to cause no adverse effect (no-observed-adverse-effect-concentration (NOAEC)). In contrast, the concentrations for Paracetamol were extrapolated directly from the measured data without calculation of the TC values. As negative compounds, Metformin and d-Mannitol were used. As expected no cytotoxicity was observed for these compounds. Therefore, Merck internal standard concentrations for cytotoxcity assay were used. The calculated values for the used model compounds (Puromycin, Paracetamol, Doxorubicin, Amphotericin B, Metformin and d-Mannitol) are given in Table 3-28. In addition to the evaluated concentrations used for the gene expression experiment, also the TC_{50} value is shown. Doxorubicin (TC_{50}: 0.1µM) and Puromycin (TC_{50}: 0.5µM) are the most potent compounds used within this experiment. While Paracetamol (TC_{50}: 5000µM) showed only marked effects in the millimolar concentration range. This was expected because Paracetamol itself is not nephrotoxic but some of its metabolites, specifically para-Aminophenol. Amphotericin B has also shown a high potency to induce proximal tubular damage in vitro (TC_{50}: 1.5µM). In addition, for all nephrotoxic model compounds the difference between the observed NOAEC and the TC_{20} was higher (~5-10 fold) than between the TC_{20} and the TC_{50} (~2-5 fold). In this case the steepest curve was observed for Puromycin, indicating a very tight range of toxicity and underlines the high cytotoxic potential of this drug.

Table 3-28 Overview of the calculated concentrations from the dose range finding study. The low dose (LD) was determined by evaluation of the non-observed-adverse-effect-concentration (NOAEC). As high dose the calculated TC_{20} was used. In addition the TC_{50} is displayed

Compounds	Abbreviation	NOAEC [µM] low dose (LD)	TC_{20} [µM] high dose (HD)	TC_{50} [µM]
Puromycin	Pur	0.025	0.35	0.5
Paracetamol	APAP	500*	2000*	5000*
Doxorubicin	Dox	0.001	0.02	0.1
Amphotericin B	AB	0.5	5	1.5
Metformin	Met	20**	100**	/
d-Mannitol	Man	20**	100**	/

* Concentrations for Paracetamol could not be calculated because of only slight cytotoxicity. The used concentrations were based on direct observations of the measured viability.

** Concentrations for Metformin and d-Mannitol could not be calculated because of the lack of cytotoxic effects. The used concentrations were based on Merck internal standard concentrations.

. / = not calculatable.

By comparison of the intracellular ATP content and the neutral red uptake it was obvious that the variance between the individual biological replicates was much higher by using the NRU assay than within the ATP assay (Figure 3-36).
Paracetamol only showed slight cytotoxicity in both assays (Figure 3-36a). At concentration > 2 mM a stronger decrease could be observed, and increased up to ~20% cell viability at 1 M. Because this concentration is far too high to be specific for nephrotoxic effects, it was decided only to use concentrations ≤ 2 mM (Table 3-28). Paracetamol is mainly metabolized/ activated in the liver and can produce toxic metabolites. The most important metabolite is N-acetyl-p-benzo-quinone imine (NAPQI), which is primarily responsible for the toxic (hepatotoxic) effect of paracetamol. Beside the liver, the kidney also metabolizes Paracetamol. The general mechanism of toxification by a Phase 1 reaction including Cytochrom P450-dependent monooxygeneses is comparable in both organs [Lee et al., 1996; Manyike et al., 2000]. In the kidney, Paracetamol is metabolized within the proximal tubular cells or the inner renal medullar by the Cytochrom P450-system or the prostaglandin-H peroxide synthetase to NAPQI, leading to tubular/ papillar necrosis. Another toxic metabolite formed in the kidney is p-Aminophenol, described to cause necrosis of the pars recta and the glomerulus [Carpenter et al., 1981].

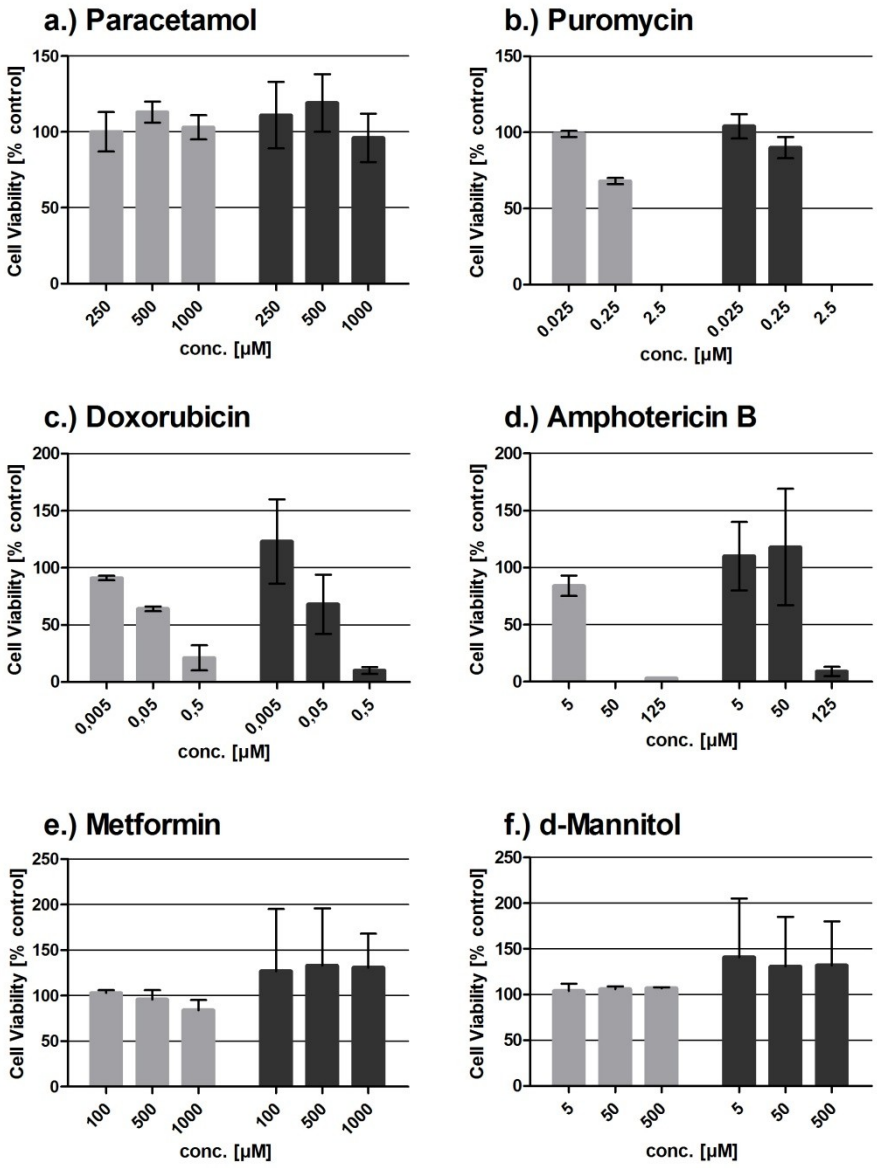

Figure 3-36 Cell viability after treatment with three concentrations of a.) Paracetamol, b.) Puromycin, c.) Doxorubicin, d.) Amphotericin B, e.) Metformin, and f.) d-Mannitol determined with either the determination of the intracellular ATP content (light grey) or the neutral red uptake (dark grey).

Based on the cytotoxicity assays by direct comparison of Paracetamol and its metabolite p-Aminophenol (data not shown) it was assumed that the NRK-52E cells are not able to metabolize Paracetamol in a sufficient manner. This was verified by gene expression analysis of several hepatic and renal metabolizing enzymes from Phase 1 and Phase 2 (data not shown). NRK-52E cells are not strongly inducible after treatment with cytochrome P450 inducers like 3-Methylcholandren, β-Naphtoflavon or Dexamethasone. Paracetamol was included into the set of nephrotoxic compound with the aim to check whether or not the slight toxicity can be used to detected highly sensitive transcriptional biomarkers.

In contrast, Puromycin showed very strong cytotoxicity in both the ATP and NRU assays (Figure 3-36b). However, some differences between the used assays were observed. The calculated viability after treatment with 0.25 µM Puromycin resulted in a cell viability of ~60% when using the ATP-assay, while still ~90% of the cells were alive as

measured in the NRU assay. The effect of Puromycin on the mitochondria is well described; more dominant for cells of the glomerulus than the proximal tubular cells [Hagiwara et al., 2006].

Doxorubicin, which is described to cause mitochondrial toxicity [Goormaghtigh et al., 1990] showed no to only slight differences between the two used cytotoxicity assays (Figure 3-36c). However, because the value within the NRU assay at concentrations of 5 nM was about ~125% viability while the ATP assay delivered a value of near 100% viability, it cannot be finally clarified if there is a slight impact on the mitochondria.

In contrast, a very strong difference between these two assays was observed for Amphotericin B (AB) (Figure 3-36d). A treatment with 50 µM AB lead to a relative cell viability of near 0% when using the ATP assay, while the same concentration did not lead to any alteration within the NRU assay. Here the very high sensitivity of the detection of the intracellular ATP assay becomes clear. The potential effect of AB can be explained by several mechanisms. Thus the changes of intracellular Ca^{2+} content, caused by the pore-building potential of AB, may play a role in the ongoing mitochnondrial damage [Murchison et al., 2000].

The negative controls, Metformin and d-Mannitol, showed no relevant alterations in either assay. Therefore, the highest concentration chosen was 100µM.

3.2.2 Gene expression analysis of NRK-52E cells

The aim of this apporach was to evaluate the capability to use NRK-52E cells for the detection of transcriptional biomarkers with the potential to bridge between the in vitro and the in vivo situation.

3.2.2.1 Identification of in vivo nephrotoxicity biomarker in vitro

Gene expression data was derived from whole genome profiles using the Illumina RatRef v.1 Beadarray. In a first step, a general overview of the gene expression pattern was investigated (i.e., box-plot and Log-Log plot). Based on the profile display and the background controls included on each array of a RatRef v.1 bead array, all values with a signal intensity of < 60 were excluded from the analyses for background correction. Statistically significant genes were selected by student's t-test with a p-value cutoff of $p < 0.01$ for each individual compound. Subsequently, only the positive compounds, which were described to be nephrotoxic, were used. The transcripts from these groups were then further filtered by selecting genes that showed a deregulation of ≤ -1.5 or ≥ 1.5 fold. The remaining four gene lists, from each compound, were used to create a Venn diagram. From this a total number of 192 genes were identified to be common across all 4 compounds (Figure 3-37). Out of these 192 altered transcripts, 128 genes were down-regulated ($FC \leq -1.5$), 64 genes were up-regulated ($FC \geq 1.5$). This shows a first obvious deviation from the in vivo data, where the majority of transcripts showed an up-regulation. In addition, the magnitude of fold-changes was low compared to the in vivo situation, although still statistically significant. The fold-change only exceeded ± 10 in some individuals (Figure 3-37).

The heatmap, which is based on a 2-dimensional hierarchical clustering, automatically sorting transcripts as well as samples with a positive correlation together, gives further evidence for the high sensitivity of transcriptional changes. Thus the 192 genes grouped all high dose treated cell samples together. In addition, the low dose of Doxorubicin, which was the most potent compound, also clustered near to the high dose treatments. However, the fold-changes were far below those observed for the high dose treated samples. In contrast, Puromycin, showed a slightly different pattern. The

high dose Puromycin treated samples clustered together with the low dose groups of Paracetamol and Amphotericin B, while the low dose Puromycin samples were categorized in the same group as d-Mannitol, a negative compound. This discrepancy can be explained in two different ways. Puromycin is described to induce glomerular damage, but also proximal tubular degeneration and necrosis, while the other compounds primarily target proximal tubular cells. Therefore, it can be hypothized that the mechanism of Puromycin toxicity is quite different from the others.

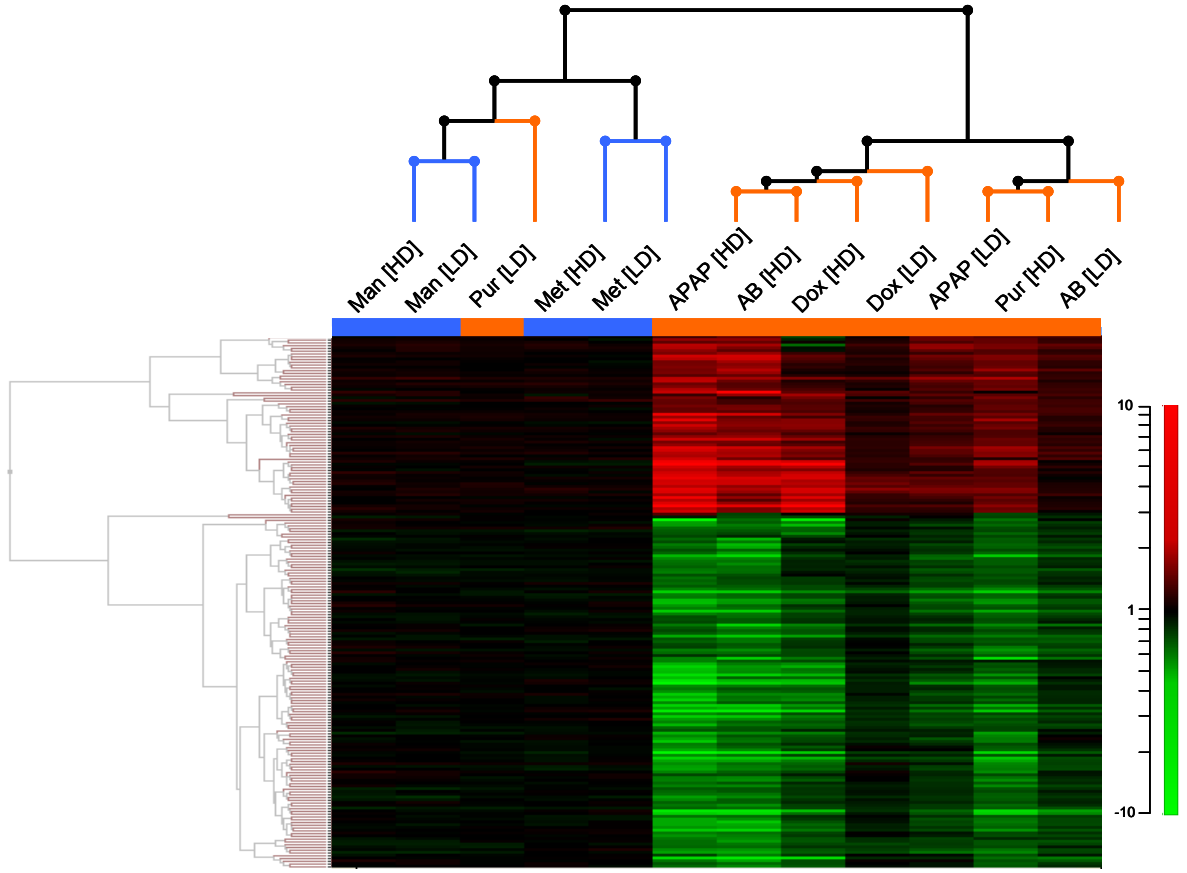

Figure 3-37 2-Dimensional hierarchical cluster of the fold-changes of 192 genes which were significantly altered after 72h treatment of NRK-52E cells with high doses of Paracetamol (APAP), Puromycin (Pur), Doxorubicin (Dox), Amphotericin B (AB). In addition, the fold-changes of the negative comopunts Metformin (Met) and d-Mannitol (Man) were included. 128 genes showed a down regulation (green) and 64 an up-regulation (red). The orange lines identify the positive, while the blue lines the negative compounds. Significance was determined by a students t-test ($p < 0.01$) and a fold-induction of ≤ -1.5 and ≥ 1.5 against the vehicle control.

It is also possible that the steepness of the dose-response curve evaluated for Puromycin is a reason for this discrepancy. However, all the three replicates of Puromycin treated samples, both high dose and low dose treatment groups (data not shown), were very similar. The data showed that also the low dose treated samples showed a deregulation of the identified transcripts, even though there was no effect on cellular ATP levels observed. This points to the fact that the genes reacted to stress very early and have therefore the potential to act as predictive in vitro biomarkers. The negative compounds Metformin and d-Mannitol, as well as the low dose dose Puromycin treated samples, showed no alteration in gene expression pattern at all.

The identified 192 transcripts were analyzed for their involvement in specific biological processes. Therefore, a network analysis was conducted by using the IPA® software tool. It was found that from the total number of 19 identified networks, the nine highest are connected over one or even more molecules present in the networks (Table 3-29). The score only is a numerical value used to rank the networks according their degree of relevance to the eligible molecules within the network. The score is based on a calculation of a right-tailed Fisher´s Exact Test und therefore is not a

measure of the biological relevance or quality of the network. The building up of networks by IPA® is based on data mining and did not take into account which type of sample or tissue were analyzed. However, IPA can be used to get an impression on which processes the genes of a dataset are involved and to develop hypotheses for the further network analyses.

Predictably, most of the identified functional networks were related to general cellular processes like Cell-To-Cell contacts, cell cycle development and metabolic pathways. Therefore, it was obvious that the system lacked the complexity of the in vivo situation. However, there is evidence for the involvement of some transcripts in relation of renal insult in vivo. For example, Col3a1 was already described to play a pivotal role in the development of interstitial fibrosis [Bielesz et al., 2010] as well as in chronic Cyclosporin induced nephropathy [Oleggini et al., 2000]. In vivo Col3a1 shows an up-regulation at the transcriptional level, while in this study it was strongly down regulated. This can be due to the fact that the matrix accumulation in the progression of renal interstitial fibrosis is triggered by several growth factors, such as TGF-β, which is induced by the renin-angiotensin system [Fukagawa et al., 1999]. Gstm5, Igfbp6 and Asns gave further evidence of some similarities between the response of renal cells in vivo and the NRK-52E cells in culture. Although Gstm5 is not reported to be altered in rat in vivo, however, the family member Gstm1 was identified in several studies [Ozaki et al., 2009, Thomson et al., 2004]. Importantly, within the Ingenuity IPA software tool these two transcripts are used synonymously. In addition, the protein product, µGST, is also used as an exploratory urinary biomarker, described to be specific for the distal tubulus [Fuchs et al., 2011, Rouse et al., 2011]. Similarily, Igfbp6, also is not reported in case of nephrotoxicity, but the family member Igfbp1 is reported relatively often. For example, it is described to be up-regulated in Cisplatin-induced nephrotoxicity [Huang et al., 2001] as well as mercuric chloride, 2-bromoethylamine hydrobromide, hexachlorobutadiene, mitomycin, amphotericin, and puromycin, where it showed a time- and dose-related change [Thukral et al., 2005]. Asns, an asparagine synthase, is responsible for the synthesis of asparagine and has been described to be constantly up regulated in isolated primary rat proximal tubular cells compared to fresh renal tissue. However, it was also described to be up regulated in male Sprague-Dawley rats after induction of acute renal failure by Ischemia/ Reperfusion and treatment of Mercuric chloride [Yuen et al., 2006]. In addition, other common genes (Table 3-29) which were not previously described as nephrotoxic biomarkers were included in the networks.

Based on these results, further investigations were performed to discover all potential in vivo biomarkers in vitro. Therefore, the generated gene list was evaluated for the overlap of the transcripts with reported, relevant findings within in vivo based nephrotoxicity biomarkers. For this the software tools GeneGo Metacore®, Ingenuitys IPA® and ToxWiz® from Cambridge Cellnetwork as well as intensive literature search was conducted.

A list of 44 genes, which are well described potential transcriptional biomarkers, was identified (Figure 3-38).

Eight out of the 44 transcripts were found to be more frequently mentioned in case of treatment related deregulations in case of drug induced renal insult [Sanz et al., 2011, Amin *et al*., 2004; Davis et al., 2006; Thompson *et al*., 2004, Huang et al., 2001, Dieterich et al., 2009, Akcay et al., 2009, Wang et al., 2008, Fuchs et al., 2011]. These transcripts (Tnfrsf12a, Cxcl1, Cd44, Odc1, Cdkn1a, Ccng1, Cyr61 and Fn1), are of special interest and therefore as displayed with bold lines in Figure 3-38. These eight transcripts, taken together, were present in five of the nine connected networks. Tnfrsf12a, Cxcl1 and Cd44 were included in the “Network 5”, and are involved in Cell-To-Cell integrations, specifically over the cell surface [Takahashi et al., 2005]. Cyr61 and Fn1 showed a relationship to “Network 1”. This network, which was the highest ranked network, contained the most found transcripts and subsequently the most cross connections.

Table 3-29 Top 9 networks found within the IPA® database. The score, based on a p-value calculation, of the likelihood that a network is significantly, and not by random change, identified, for each functional network is shown. Also the number of molecules and the transcripts themselves within the dataset included within the specific networks are shown. Common genes are shown in bold.

ID	Score	Top Functions	Focus Molecules	Molecules from the list in Network
1	**40**	Cell-To-Cell Signaling and Interaction, Tissue Development, Dermatological Diseases and Conditions	22	Aldh2, C5orf13, Calcoco1, **Col3a1**, Cyr61, Fcgrt, Fn1, Gsta4, **Gstm5**, Hla-e, Htra1, **Igfbp6**, Iitga3, Krt15, Mgst1, Rragd, S100a1, Serpinf1, Slc7a7, Tagln, Tf, Vwf
2	**39**	Amino Acid Metabolism, Small Molecule Biochemistry, Vitamin and Mineral Metabolism	22	Aars, **Asns**, Atf4, Baz1a, Ccne2, Cdc6, Cdkn1a, Cep70, Csdc2, Gars, Lrp8, Mcm10, Meis1, **Mthfd1**, Mthfd2, Ndrg2, Pik3ip1, Rbp1, RGD1564040, Rgs2, Rrm2, Slc20a1,
3	**30**	Cell Cycle, Lipid Metabolism, Small Molecule Biochemistry	18	Cryab,Cycs,Edn1,Enc1, Fam189b, Fbxo2, Gamt, Maged2, Myc, **Nme3**, Nme7, Nop56, Nppb,Odc1, **Pink1**,Ptgs1, Sfxn1, Slc12a2
4	**27**	Cell-To-Cell Signaling and Interaction, Cellular Assembly and Organization, Cellular Function and Maintenance	17	Ampd3, Arhgef19, Bhmt, Cnksr3, Ech1,**Fhl1**,Flrt3, Fmo4, Klc4, Mpzl2, **Mthfd1**, Pdk2, Pus7, Sec11c, Tm7sf2, Vkorc1, Xpa
5	**27**	Cellular Development, Cellular Growth and Proliferation, Hepatic System Development and Function	18	Ankrd1, Cd44, Cxcl2, Cxcl13, **Fhl1**, Fst, **Krt19**, Map2k6, Mmp11, Mybl1, Pcolce, S100a13, Serping1, Tnfrsf12a, Tnfsf12, Tnfsf13, Tnfsf18, **Yars**
6	**24**	Drug Metabolism, Endocrine System Development and Function, Lipid Metabolism	16	Abcc3, Aldoc, **Asns**, **Col3a1**, Fah, Fbxo6, Hist1h2ac, **Krt19**, **Nme3**, Oplah, Ptpru, Rcbtb2, Slc12a5, Slc7a5, Sox11, Stra8
7	**24**	Organismal Injury and Abnormalities, Inflammatory Disease, Respiratory Disease	15	1100001G20Rik, Adamts2, C13orf33, Cars, Col16a1, **Col3a1**, Enpp3, Grp126, Kcnmb4, Kifc2, Pomgnt11, Rnd1, Tcea3, Tmem176b, **Yars**
8	**23**	Cell Cycle, Cellular Development, Connective Tissue Disorders	15	Aen, Armcx1, Ccng1, **Col3a1**, Donson, Eelmo3, **Gstm5**, Loxl3, Rcn33, Rilpl2, Rrp9, Rtn1, Selenbp1, Skap2, Znf420
9	**19**	Cellular Movement, Cancer, Cellular Development	13	Abtb1, Aadhfe1, Boc, Cfd, Cln6, Idh1, **Igfbp6**, Lztfl1, Mettl7a, Phyh, **Pink1**, Slc17a6, Tle2

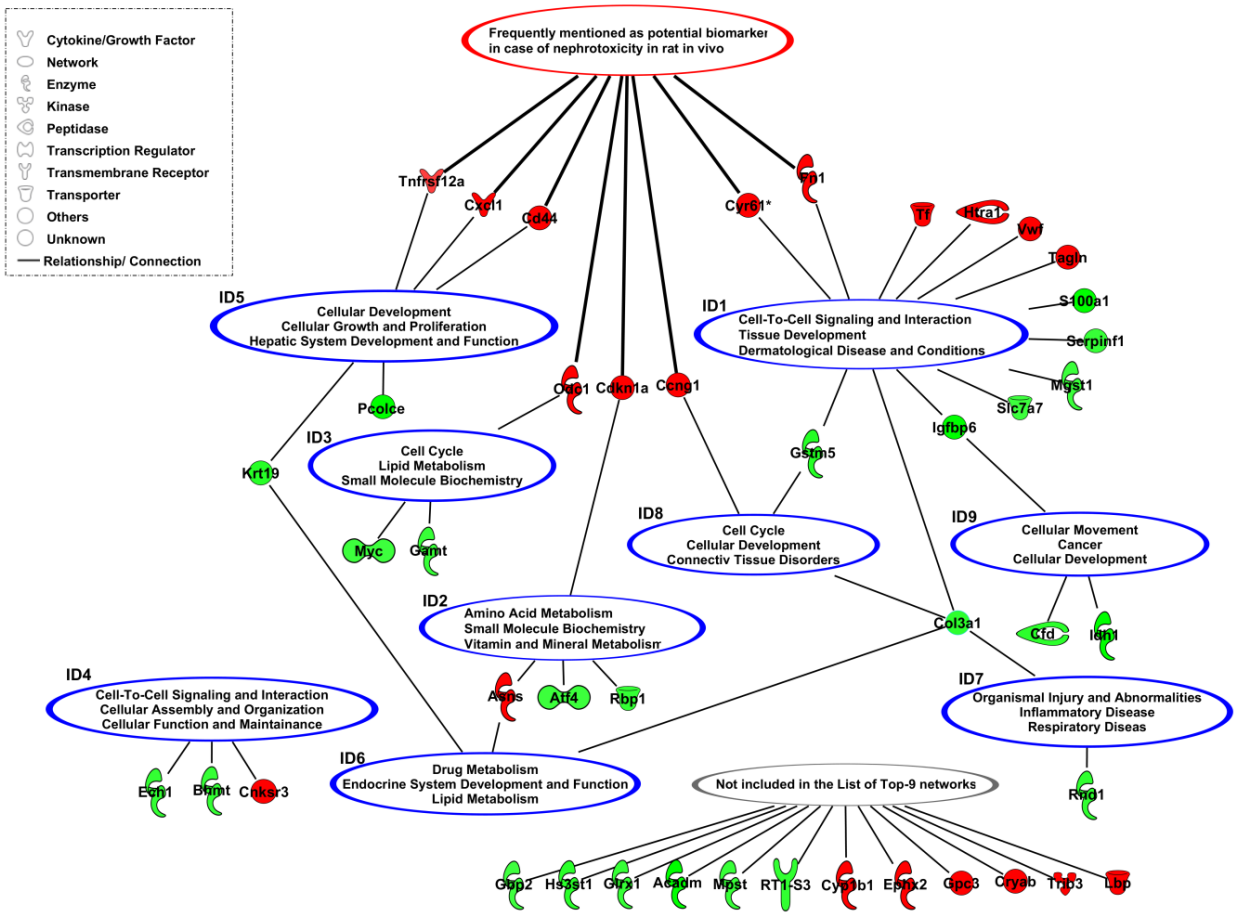

Figure 3-38 44 genes identified out of the dataset of 192 significant ($p \leq 0.01$) transcripts with a fold-change ≥ 1.5 and ≤ -1.5, to be described in case of nephrotoxicity in rat in vivo. Additionally, the 8 most frequently reported transcripts (red cycle) as well as the affiliation to the Top-9 networks (blue cycles) are displayed. Green symbols indicates the treatment dependent down regulation of the transcript, while red indicates the upregulation. The ID numbers correspond to the network numbers in Table 3-29.

Cfd, Idh1 and Igfbp6 were connected to "Network 9" while the last one is also included in "Network 1". That is also the case by observing "Network 8", were the already mentioned Ccng1, which is involved in the cell cycle, is included together with Gstm5 and Col3a1. The last two genes themselves are also part of "Network1". In general Col3a1 showed the highest number of nodes, probably due to the fundamental role of collagen in cellular growth and development. Odc1, was only included in "Network 3", and contains three described potential biomarkers, namely Odc1, Myc, and Gamt. Cdkn1a only showed a connection to "Network 2". Because the encoded protein, p21 of the Cdkn1a gene is as a cyclin-dependent kinase inhibitor involved in the regulation of the cell cycle and several other processes, it was expected that would also be a relation to "Networks 3, 5, and 8". However, the database from Ingenuity may be incomplete. The same was observed for Myc, a transcription factor described to activate various mitogenic signals, but also cell growth and apoptosis [Dominguez-Salo et al., 2007, Cotterman et al., 2008, Kanazawa et al., 2003]. The lowest numbers of transcripts were found for "Network 7", where beside Col3a1 only Rnd1, a small signaling G protein of the Rho family of GTPases [Vayssiére et al., 2000, Ridley, 2006] was present.

The fact that "Network 4" is not linked to any other network and even did not contain any of the frequently mentioned transcripts does not necessarily mean that there is no relation between this and other networks. Rather, it can be assumed that networks focused on molecules involved in Cell-To-Cell Signaling and Interaction, Cellular Assembly and Organization, Cellular Function and Maintenance are linked to networks containing Tissue Development, Cellular

development or Cellular Growth and Proliferation. Consequently also the 12 transcripts which are not part of the top-9 networks, are partly involved in proliferation of cells, like Ephx2 [Zhang et al., 2010], Gpc3 [Cano-Gauci et al., 1999], Cryab [Kumarapeli et al., 2008], Gbp2 [Gorbacheva et al., 2002], and Glrx1 [Lofgren et al., 2008] and should not be excluded from further investigation.

In summary, the significantly altered transcripts which were already described in vivo are involved in general cellular processes, like proliferation, growth and Cell-Cell integrations. Based on this observation, there is less evidence to expect that transcripts involved in e.g. oxidative stress, inflammation, or apoptosis can be used for the general prediction of nephrotoxic potential by using NRK-52E cells. It seems more likely that protein or transcripts related to general processes of cellular maintenance and recovery are a good source of biomarkers in both in vivo as well as in vitro. The set of genes generated from of the overlap over all alterations caused by the four model compounds, which are described to have different mechanisms causing renal damage, only reflect an “high level” response of the cells. Therefore, these transcripts, together with specific marker genes for the toxicological processes mentioned above, can further enhance the information about the specific underlying process resulting from treatment of NRK-52E cells with specific compounds.

The fact that cell lines like NRK-52E cells are characterized by a constant proliferation rate, it must be assumed that this can cause major differences between rats in vivo and NRK-52E cells. Therefore, the lack of any statistical significant alteration in Lcn2, Clu, or Timp1 can be due to the fact that they a constantly over expressed in NRK-52E cells and no further induction is possible. The lack of alteration on the gene expression level of these in vivo biomarkers is supported by the observations from Rached, where no to minimal alterations in Lcn2, Clu and Timp1 were observed after treatment of NRK-52E cells with either Ochratoxin A, Cisplatin, Cadmium chloride or Potassium bromated [Rached, 2009]. The fact that also no increase in Havcr1 mRNA was observed can be explained by its association with dedifferentiation and proliferative processes. It has been described that HK-2, a human immortalized renal cell line, expresses large amounts of Kim-1 protein [Bailly et al., 2002]. Thus the reason for the missing expression changes of Havcr1 in NRK-52E cells also can be due to a constant overexpression. Another possibility is the differentiation processes, while reaching confluence, lead to a break in Kim-1 gene expression.

However, based on the strong similarities found between the individual networks, the direct interactions of the 44 transcripts already described for in vivo nephrotoxicity was evaluated and is shown in Figure 3-39. 9 Genes were found in the literature to interact directly or be related to the same processes. Because of the limitation of an in vitro system, which lack complex cell-cell interactions, including different cell types and the influence of other tissues or organs, the interactions observed are involving cellular processes like proliferation, necrosis, apoptosis, direct cell-cell interactions and cell-ECM interactions. In addition, the magnitudes of fold change are given in Figure 3-40a-i. As shown in Figure 3-39, Cd44 (Figure 3-40a) has a key position within the interaction network hypothized here. It is well known that Cd44 is a cell adhesion receptor and involved in several biological processes, including support and induction of hematopoietic differentiation, cell migration, adhesion and effects on many adhesion mechanisms and interaction with cell activation signals [Lesley et al., 1993]. Two of the most prominent and relevant ligands of this receptor are hyaluronan and osteopontin, both components of extracellular fluids and matrices [Aruffo et al., 1990, Weber et al., 1996]. Osteopontin, a promising exploratory urinary protein biomarker in vivo however has poor alterations on the transcriptional level. This gives further evidence that also in this process; Osteopontin may play an important role, even though no significant induction on mRNA level was observed. Osteopontin induction within NRK-52E cells on the protein level was shown by treating the cells with cobalt chloride to mimic hypoxia [Chen et al., 2009].

Hyaluronan is a glycoaminoglycan of the extracellular matrix and is described to promote endothelial cell morphogenesis in an Odc1 (Figure 3-40b) expression dependent process by binding to Cd44 [Takahashi et al., 2005]

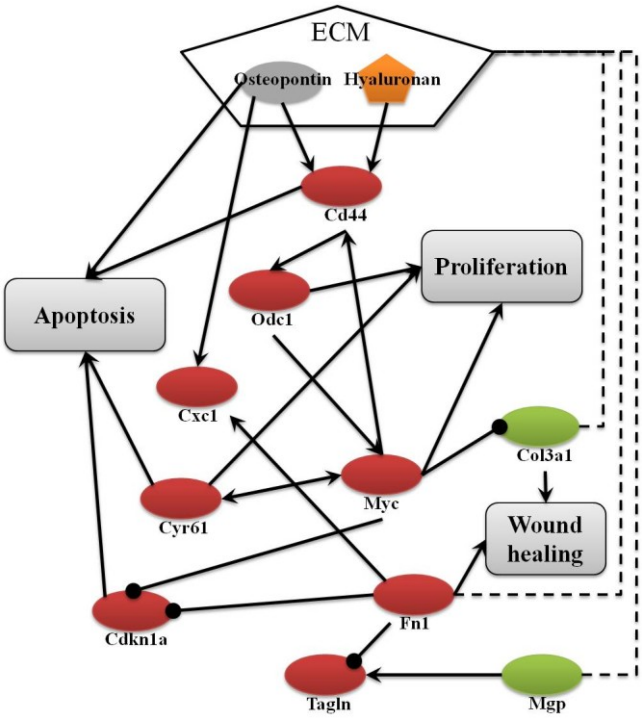

Figure 3-39 Hypothized interaction network of transcripts included in the list of 44 already described transcriptional biomarker in vivo. All 9 included genes were described in literature to interact with each other and were involved in either apoptosis, proliferation or wound healing. Red indicates up-regulation and green indicates down-regulation, as can be referenced in Figure 3-40. Arrows give activating or inducing interations while rounded lines indicate inhibitory interation or suppression. The dashed lines display the interaction or affiliation of protein to the extracellular matrix (ECM).

This is notable because Odc1 has been reported in several studies focused on nephrotoxicity as well as in hypoxia signalling [Thukral et al., 2005, Tacchini et al., 2004]. In addition, it was also reported to be up-regulated in NRK-52E cells after treatment with several nephrotoxic compounds. Hyaluronan deposition is also described to occur in areas of interstitial damage and co-localizes with de novo tubular Cd44 expression, as it is the case within the NRK-52E cells (Figure 3-40a) [Nishikawa et al., 1993, Sibalic et al., 1997]. Interleukin-8 (IL-8) induces cell arrest by a reduction of cell movement on hyaluronan, was accompanied by increased actin polymerization and a more pronounced association of Cd44 with the cytoskeleton [Azizl et al., 2000]. These findings are in good agreement to the findings observed here, where the transcripts are associated with cellular movement and development, as well as cellular assembly (Figure 3-38). Another important interaction partner of Cd44 is Fn1 (Figure 3-40d), encoding for fibronectin which is also related to the extracellular matrix in multiple processes; However, Fn1 is most frequently reported in case of interaction of endothelial cell with lymphocytes. In this case the lymphocyte Cd44 binds to the heparin-binding domain of fibronectin [Jalkanen et al., 1992]. Obviously, this cannot be the interaction taking place in this in vitro system, because of the absence of other cell types. Therefore, an alternative interaction between these proximal tubular-like cells has to be assumed which is leukocyte independent. This is in good agreement to the in vivo situation where it was shown that Cd44 is not only expressed in leukocytes entering the kidney during inflammation, but also is highly expressed by injured renal tubular epithelial cells [Florquin et al., 2002]. Fibronectin plays a crucial role in wound healing by cell adhesion, growth, migration and differentiation in vivo [Pankov et al., 2002], also in NRK-52E cells this mechanism seems to have a central role in cellular recovery. Fn1 has been described to decrease the gene expression of Transgelin (Tagln) [Hu et al., 2000]. In NRK-52E cells Tagln was observed to be up-regulated (Figure 3-40g), which is contradictory as Mgp, which has been described to induces Tagln expression [Steitz et al., 2001], was down-regulated. Therefore an alternative regulation of Tagln must be assumed. Fibronectin also induces the gene and protein expression of Myc, Mgp and in turn Cd44 (Figure 3-40c, i, a), while it decreased the expressions of Cdkn1a [Han et al., 2006, Pulai et al., 2005]. Myc itself has been described to suppress the expression of Cdkn1a and thus is capable of driving cell proliferation [de Alboran et al., 2001].

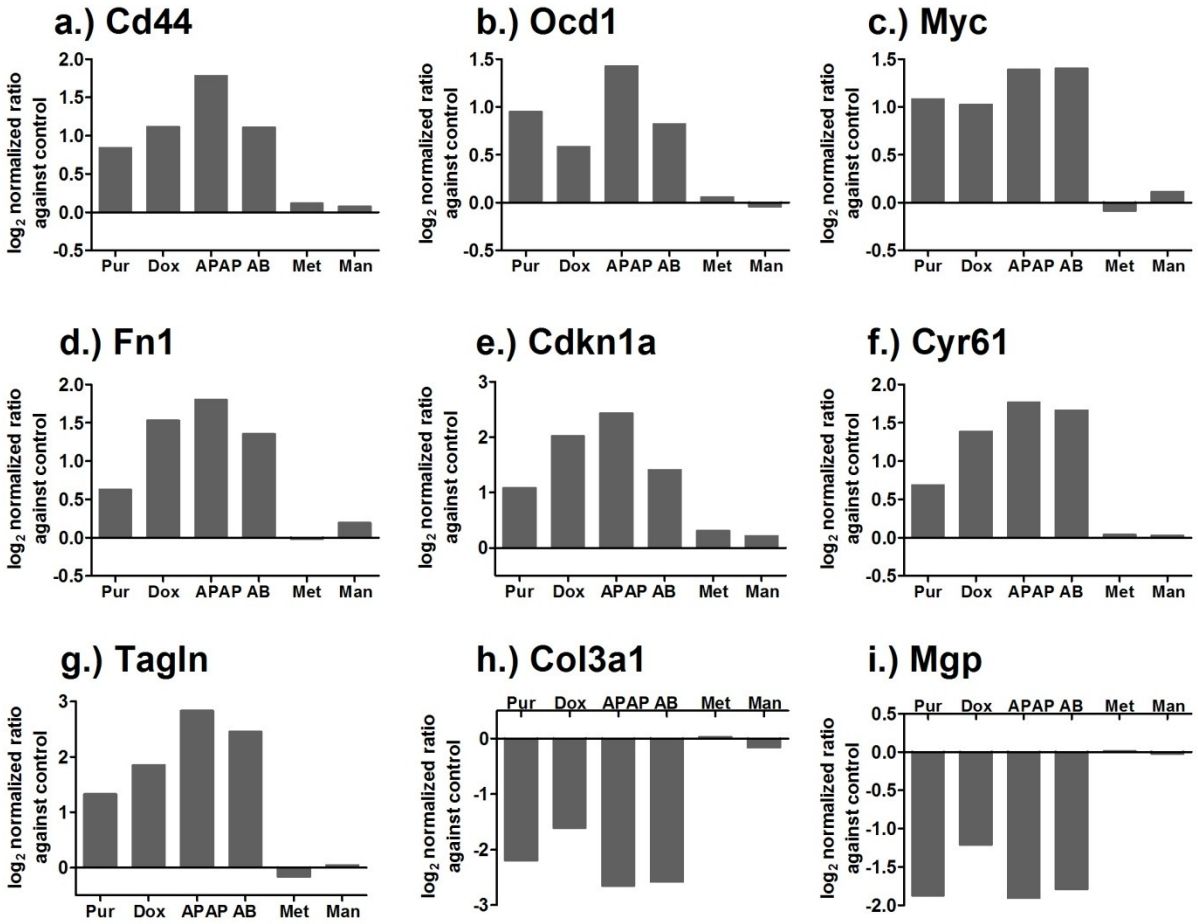

Figure 3-40 Deregulation of a.) Cd44, b.) Ocd1, c.) Myc, d.) Fn1, e.) Cdkn1a, f.) Cyr61, g.)Tagln, h.) Col3a1, i.) Mgp. The data are presented as the log_2 normalized average (geometric mean) ratios of each individual passage against the corresponding vehicle control as bars. Pur = Puromycin, Dox = Doxorubicin, APAP = Paracetamol, AB = AmphotericinB, Met = Metformin, Man = Mannitol.

Because of the multitude of factors and processes induced by Myc, it is not possible to figure out which of them may have the major impact in the progression of cellular renal break-down based on our data. However, increased expression of Myc has also been described to drive the apoptotic program by deprivation of survival factors [Askew et al., 1991, Evan et al., 1992]. Furthermore, Myc seems to play a pivotal role in cell death caused by tumor necrosis factors, chemotherapeutics and environmental stress [Basu et al., 1995, Janicke et al., 1994, Zhan et al., 1997].

In this study, and based on the identified transcripts, it is notable that the Myc target, Odc1 (Figure 3-40b), was increased [Bello-Fernandez et al., 1993]. Consequently, an increase in Odc1 would lead to increased levels of the superoxide by an elevation of the polyamine metabolism, followed by oxidative stress as a central mechanism in Myc induced apoptosis [Packham et al., 1994, Park et al., 2002]. Additionally, binding interactions between Myc and Cyr61 has been reported. Cyr61 (Figure 3-40f) or Cysteine-rich protein 61, is a member of a family of growth factor-inducible immediate-early genes. It regulates cell proliferation, adhesion, migration and differentiation in a multitude of cell types [Tong et al., 2001] and was already reported in a multitude of studies in rat. It has been assumed that Myc is involved in multiple processes by direct association with other proteins forming protein complexes to enhance the functionality of each individual complex member [Koch et al., 2007].

In case of Myc, which is a strong proto-oncogen found in several tumor cells [Finver et al., 1988, Hoffmann et al., 2002, Koscianska et al., 2007], is still inducible within NRK-52E cells, even though the cells have a high proliferative activity. By the same token, it is interesting to note that Cdkn1a was up-regulated after treatment of NRK-52E cells with 4 model nephrotoxic compounds, even though Myc and Fn1, described as inhibitors of Cdkn1a expression, are also up-regulated. It is possible that the observed alterations only take place on the transcriptional level. Because Cdkn1a is regulated by many different signaling pathways it is more likely that alternative inducing factors may play a role in the regulation of the protein expression.

For these mechanistic interactions, the strength of increase of the transcripts delivered no relevant information (Figure 3-40). In almost all cases Paracetamol lead to the strongest increases, while Puromycin often resulted in the lowest deregulation compared to the vehicle control. The strongest increase was observed for Cdkn1a, Cyr61 and Tagln, confirming the central role of these potential transcriptional biomarkers (Figure 3-40e, f, g).

3.2.3 Conclusion of transcriptional nephrotoxicity biomarkers in NRK-52E cells

The fact that several transcripts could be identified in NRK-52E cells after treatment with either Puromycin, Paracetamol, Doxorubicin or Amphotericin B, which were already described in vivo to be treatment dependently deregulated, point to the fact that these molecules play a pivotal role in the progression of renal injury and recovery. It also could be shown that several of the transcripts were mechanistically linked to cellular processes and therefore it can be hypothesized that these processes are present and of biological importance in both in vitro as well as in the kidney of treated rats. The involvement of such fundamental biological pathways including proliferation, apoptosis, and cellular recovery and reorganization can also be used to obtain further insights in to the progression of the cellular insult. Thus it can be expected that at early time points the transcripts linked to cellular stress and apoptosis will be changed and as a secondary response genes leading to proliferation and recovery will start to change.

However, these preliminary experiments only can be taken as a proof-of-principal, to check whether or not it is possible to identify in vivo linked transcriptional alterations in vitro. These results are only a starting point and need further confirmation by testing additional compounds and concentrations. Another open question is if the increase in specific genes is specific for the detection of nephrotoxic effects. This has to be evaluated by using several non-toxic as well as non-nephrotoxic compounds. It can be assumed that the major differences between these two classes of compound will be a difference in the toxic doses. The low dose treatment data generated within our study clearly showed that almost all of the 192 genes were deregulated at concentrations leading to no cytotoxicity in the ATP and NRU assays (Figure 3-37). Organ specificity is one of the major problems of in vitro toxicity assays. This is also reflected by data for Paracetamol, which is specifically described to be hepatotoxic. The concentration needed to result in cytotoxicity in vitro was very high - much higher than normally used for in vitro cytotoxicity assays. Even this high concetractions resulted in the alterations of identical genes as the other compounds in much lower concentrations, and gives further evidence of the general cellular mechanistic basis of these transcripts. NRK-52E cells have also been described to express some other molecules related to more specific toxicological processes, like Hmox1 in oxidative stress [Rached et al., 2008]. Therefore, it has to be recommended to further investigate not only the relevant transcripts, but others as displayed in Table 3-27 for in vivo studies. To enable the translation or bridging properties of transcriptional biomarkers, whether from in vitro to in vivo or from animals to human beings, it is of special interest to evaluate the same biomarkers, to get further insights on the potential to discover the safety profile of a compound.

3.3 Final Conclusion

The studies presented here deal with several questions related to the toxicological evaluation and implementation of an early, sensitive and specific detection system for drug-induced nephrotoxicity. Several rat toxicity in vivo studies were conducted to test different urinary and transcriptional biomarkers, as well as different methodological approaches. In addition, mechanistic analysis based on whole genome gene expression analysis was performed to get further insights on Vancomycin-induced nephrotxicity. Finally, a proof-of-principal investigation was carried out to evaluate the usefulness of a renal rat cell line (NRK-52E) for their applicability to detect renal cell death, employing already described in vivo gene expression biomarkers.

Ten urinary proteins were intensively studied by using urine from male and female rats treated with either Vancomycin, Cisplatin or Puromycin, in a low and a high dose, for 3, 7, 14 and 28 days. The ten urinary protein biomarkers, namely Kim-1, Clusterin, Cystatin C, β2-microglobulin, Osteopontin, Timp-1, Lipocalin-1/NGAL, VEGF, α-GST and Calbindin, were measured by a Luminex® xMAP® based multiplexed immunoassay (WideScreen™ Rat Kidney Toxicity Assay). Kim-1 was analyzed also by using a rapid urinary dipstick assay (RENA™-strips). To enable the interpretation of the resulting data in context to substance induced renal pathology, histopathological, clinical pathological and hematological analysis were conducted for each individual animal. Based on the results of a 28 day dose range finding study, different non-daily treatment schedules were used for each of the test compounds. The compounds were applied intra peritoneally for one week daily and then once per week up to 4 weeks for Vancomycin and Cisplatin. Puromycin was dosed daily for two weeks followed by twice per week. This scheduling was necessary to allow animals to survive the 4 week treatment period as well as allowing the analysis of the urinary protein pattern associated with a recovery period. . In addition, immunohistochemical analyses were performed on tissue from the Vancomycin and Puromycin studies, as well as whole genome gene expression analysis of kidneys exclusively from the Vancomycin study.

Within the Vancomycin study, which was characterized by the most pronounced tubular degeneration and also showed the strongest recovery after the change from daily to weekly treatment, the urinary protein concentrations for Kim-1, Clusterin, Osteopontin and Calbindin were strongly increased in both genders. NGAL and Cystatin C also showed a slight dose-dependent alteration in both genders, while Timp-1 showed a sex specific increase only in female rats. To see the increase of these urinary proteins in context with histopathologically observed renal tubular alterations receiver-operation-characteristic curves (ROC) were calculated and the area-under-the-ROC (AUROC) was investigated. An excellent diagnostic performance within the Vancomycin study, for both genders, was determined for Kim-1, Clusterin and Osteopontin. To evaluate the localisation of these three proteins, immunohistochemical analysis was performed. A specific and sensitive increase in renal protein was observed for Kim-1 and Clusterin, supported by the fact that Kim-1 and Clusterin are rarely expressed in healthy rats. Osteopontin also showed an elevated level in renal tissue, which further increased with increasing severity of the renal damage. This increase was seen primarily by staining of collagenous tissue, with which Osteopontin interacts. In general, the correlation of the observed tubular lesions, the evaluated renal protein levels in the tissue and the urinary excretion was very good.

When looking at the mRNA levels of the ten urinary biomarker proteins, beside an increase in Havcr1 (Kim-1 mRNA), Clu (Clusterin mRNA) and Spp1 (Osteopontin mRNA) also a strong increase in Timp1 (Timp-1 mRNA) and Lcn2 (NGAL mRNA), over the corresponding control animals, was detected. Vegfa (VEGF mRNA), B2m (β2-microglobulin) and Cst3 (Cystatin C mRNA) showed no changes on the transcriptional level. This suggests that the related transcripts from the urinary protein biomarkers can also be used / recommended, and in some cases they performed better than the urinary proteins.

Since the Vancomycin induced toxicity was massive, the Cisplatin study (mild changes on the S3 segment of the proximal tubules) was used to further evaluate the sensitivity and specificity of urinary protein biomarker excretion. The most prominent changes were observed for urinary Kim-1 excretion. In addition, Clusterin and Osteopontin also showed a relevant increase in several animals. This was also reflected by high AUROC values, underlying the diagnostic performance of these three markers. The other biomarkers remained unaltered. Since these three proteins, specific for tubular damage, also showed the best performance within the Vancomycin study, we can conclude that they are the most sensitive urinary biomarkers for tubular damage.

Less information is available about the performance of these biomarkers to predict glomerular damage; therefore Puromycin was used to induce this type of pathology. Since Puromycin caused both tubular as well as glomerular adverse effects, a final answer about the changes in urinary protein biomarker specific to glomerular alteration could not be given. However, our data give hints to the usefulness of several of the biomarkers to respond to glomerular-induced proteinuria. In animals showing pathological changes urinary Kim-1, Clusterin, β2-microglobulin and Cystatin C showed the most pronounced increase in excretion, which was also reflected by ROC analysis. Osteopontin and Calbindin showed a stronger increase in animals with histopathological findings in male rats than in female, while Timp-1 performed better in female rats. Since Kim-1 and Clusterin were shown to be highly sensitive and specific for tubular insults the elevation in β2-microglobulin and Cystatin C can be assumed to be linked to the excessive proteinuria induced by the vacuolation of the glomerular tufts, subsequently leading to an increase in excretion of these extrarenal proteins. This was partly supported in female rats by an increase in VEGF, which maybe a result of glomerular basement membrane destruction. By immunohistochemical analysis the early and specific increase in renal Kim-1 and Clusterin expression was confirmed. In addition, the gender difference in Osteopontin excretion, hypothesised to be caused by a stronger pronounced building of fibrous tissue in female rats, was also confirmed, which subsequently has to be seen as a limitation of this biomarker.

In summary, Kim-1, Clusterin and Osteopontin delivered the best diagnostic performance for drug induced tubular degeneration and necrosis. β2-microglobulin and Cystatin C can be used, in combination with the markers above, to evaluate a potential influence on the glomerulus. In addition, the immunohistochemical analysis of Kim-1 and Clusterin also can be used as an alternative and very sensitive detection method. The remaining markers (Timp-1, Calbindin, NGAL and VEGF) need further evaluation because of their inconsistent performance in reflecting the underlying renal pathologies.

The detected values for urinary Kim-1, determined by either the Luminex® xMAP® or the RENA™-strips technology, from all three test compounds, were compared by linear regression and Bland-Altman-Analysis. The results of this analysis clearly showed that the tendency in both assays was similar, although the Luminex® xMAP® based values showed a stronger magnitude of increase and therefore a higher sensitivity in detection. This was especially clear within the Cisplatin study where only mild tubular damage was observed, and the RENA™-strips were not effective. Therefore, the recommendation for preclinical routine studies would be to use the multiplex assays, which allows the detection of multiple proteins in a more sensitive manner. However, the RENA™-strips delivered reliable data in a much shorter time period and at a much cheaper cost, whereby the final decision which method to use strongly depends on the scientific and resource requirements.

Since little information is available on the cellular and molecular biological / toxicological mechanism of Vancomycin-induced nephrotoxicity, analysis of the whole gene expression profile from renal tissue was performed to build a novel hypothesis. The Illumina® RatRefv.1 beadarray was used to identify gene expression patterns in a time, dose and gender specific manner. In addition, several transcription factors were investigated, based on the initial data analysis, to improve our understanding of the involved pathways. The hematologically and histopathologically identified

inflammatory processes appear to be driven by NF-κB and RelA mediated pathways. In addition, further evidence of an involvement of the complement system was shown. For apoptotic processes, it is reasonable to assume a Fas-receptor mediated and caspase-dependent mechanism without any prominent involvement of p53. Furthermore, the recovery and rearrangement processes which take place after renal insult could be shown to include the activity of specific GTPase members - mainly Rho, Rac1 but also Cdc42, which are involved on actin nucleation of migratory processes, as well as cellular shape restoration. Within these three major general processes, the transcription factors Smad3, Stat1 and Stat3, as well as PPARα, PPARγ and PPARδ, seem to be involved. With regard to the observed higher sensitivity of male rats to Vancomycin treatment, several mechanistic differences, e.g. a later cellular recovery, gave hints to an explanation for the increased nephrotoxicity. However, a final and definitive explanation for the gender difference could not be identified, based on the gene expression data alone.

Since it could be shown within the Vancomycin study that some of the urinary protein biomarker related transcripts performed even better than the proteins, an evaluation of several gene sets were tested for their usability as transcriptional biomarkers. Three sets of transcripts were tested; one provided by Compugen Ltd., one identified from the Toxicogenomics Project in Japan (TG-GATEs) and one derived from a literature search. All showed partly overlapping mRNAs. Since the Compugen Ltd derived biomarker set only contained 6 transcripts and were never published, a test run was conducted by using three already published and described nephrotoxicity studies, namely Gentamycin, aristolochic acid and FP007SE. The performance of the Compugen Ltd. system delivered reasonable results, with some suggestion of a real predictivity. The Compugen Ltd model was used then on our Vancomycin transcriptomics data since all transcripts showed a severity-dependent alteration. The most promising gene expression change, in relation to histopathological observations, was Tnfrsf12a. The TG-GATEs prediction model consists of 19 best ranked genes, was also tested and almost all expression changes were related to an increasing severity of tubular degeneration. However, only a few genes resulted in an increase strong enough to be considered to be diagnostically useful. From these data, together with the results of the 45 genes picked from the literature, and the overall impression from the mechanistic analysis from Vancomycin, a final transcriptional biomarker list was generated containing the best performing 40 transcripts.

A proof-of-principal investigation based on an in vitro system using NRK-52E cells, and global gene expression profiling was performed. Several transcriptional alterations were observed that were also described in the in vivo approaches, both within this work as well as in literature. The mechanistic analysis showed that the transcripts Cd44, Myc, Cyr61, Cdkn1a and Fn1, involved in apoptosis, proliferation and wound healing, were identified to deliver a reliable and plausible treatment dependent response. These transcripts require further validation for their usability to serve as transcriptional biomarkers in vitro.

4 References

In alphabetical order (A → Z)

Aardema, M.J. and MacGregor, J.T. (2002) Toxicology and genetic toxicology in the new era of "toxicogenomics": impact of "-omics" technologies. Mutat Res 499, 13-25.

Aaronson, D.S. and Horvath, C.M. (2002) A road map for those who don't know JAK-STAT. Science 296, 1653-1655.

Agilent Technologies (2006). Agilent RNA Nano Kit Guide.
http://www.chem.agilent.com/Library/usermanuals/Public/G2938-90034_KitRNA6000Nano_ebook.pdf. Accessed: 25.06.2010.

Agilent Technologies (2010). Lab-on-a-Chip Products http://www.chem.agilent.com/de-DE/Products/instruments/lab-on-achip/ Pages/default.aspx. Accessed: 25.06.2010.

Agrawal, S., Anderson, P., Durbeej, M., van Rooijen, N., Ivars, F., Opdenakker, G. and Sorokin, L.M. (2006) Dystroglycan is selectively cleaved at the parenchymal basement membrane at sites of leukocyte extravasation in experimental autoimmune encephalomyelitis. J Exp Med 203, 1007-1019.

Ahlborn, G.J., Nelson, G.M., Ward, W.O., Knapp, G., Allen, J.W., Ouyang, M., Roop, B.C., Chen, Y., O'Brien, T., Kitchin, K.T. and Delker, D.A. (2008) Dose response evaluation of gene expression profiles in the skin of K6/ODC mice exposed to sodium arsenite. Toxicol Appl Pharmacol 227, 400-416.

Ahn, J., Baik, S., Ko, M., Shin, H.J., Chung H.J., and Jeong, H. (2010) Effects of Mercuric Chloride on Gene Expression in NRK-52E Cells Genomics & Informatics Vol. 8(1) 50-57

Aicher, L., Meier, G., Norcross, A.J., Jakubowski, J., Varela, M.C., Cordier, A., Steiner, S. (1997) Decrease in kidney calbindin-D 28kDa as a possible mechanism mediating cyclosporine A- and FK-506-induced calciuria and tubular mineralization. Biochem Pharmacol 53, 723-31

Akcay, A., Nguyen, Q. and Edelstein, C.L. (2009) Mediators of inflammation in acute kidney injury. Mediators Inflamm 2009, 137072.

Aktories, K., Föstermann, U., Hofmann, F. B. und K., S. (201). „Allgemeine und spezielle Pharmakologie und Toxikologie“. 10th Edition, Urban & Fischer

Alchi, B., Nishi, S., Kondo, D., Kaneko, Y., Matsuki, A., Imai, N., Ueno, M., Iguchi, S., Sakatsume, M., Narita, I., Yamamoto, T. and Gejyo, F. (2005) Osteopontin expression in acute renal allograft rejection. Kidney Int 67, 886-896.

Aleksunes, L.M., Goedken, M.J., Rockwell, C.E., Thomale, J., Manautou, J.E. and Klaassen, C.D. Transcriptional regulation of renal cytoprotective genes by Nrf2 and its potential use as a therapeutic target to mitigate cisplatin-induced nephrotoxicity. J Pharmacol Exp Ther 335, 2-12.

Ali, B.H. (1995) Gentamicin nephrotoxicity in humans and animals: some recent research. Gen Pharmacol 26, 1477-1487.

al-Kahtani, M.A., Zuleta, C., Caviedes-Vidal, E. and Garland, T., Jr. (2004) Kidney mass and relative medullary thickness of rodents in relation to habitat, body size, and phylogeny. Physiol Biochem Zool 77, 346-365.

Allen, C., Jabado, G. (2008) “Report: The Relation of Biotech and Big Pharma: Feeding the Pipeline” SANIT-Management in the Health Sector
(http://web.iese.edu/mba/health/Master/Reports/Boitech%20Pharma%20Allen%20Jabado.pdf) Accessed: 04.01.2012

Ambrus, G., Gal, P., Kojima, M., Szilagyi, K., Balczer, J., Antal, J., Graf, L., Laich, A., Moffatt, B.E., Schwaeble, W., Sim, R.B. and Zavodszky, P. (2003) Natural substrates and inhibitors of mannan-binding lectin-associated serine protease-1 and -2: a study on recombinant catalytic fragments. J Immunol 170, 1374-1382.

Amin, R.P., Vickers, A.E., Sistare, F., Thompson, K.L., Roman, R.J., Lawton, M., Kramer, J., Hamadeh, H.K., Collins, J., Grissom, S., Bennett, L., Tucker, C.J., Wild, S., Kind, C., Oreffo, V., Davis, J.W., 2nd, Curtiss, S., Naciff, J.M., Cunningham, M., Tennant, R., Stevens, J., Car, B., Bertram, T.A. and Afshari, C.A. (2004) Identification of putative gene based markers of renal toxicity. Environ Health Perspect 112, 465-479.

Amin, R.P., Vickers, A.E., Sistare, F., Thompson, K.L., Roman, R.J., Lawton, M., Kramer, J., Hamadeh, H.K., Collins, J., Grissom, S., Bennett, L., Tucker, C.J., Wild, S., Kind, C., Oreffo, V., Davis, J.W., 2nd, Curtiss, S., Naciff, J.M., Cunningham, M., Tennant, R., Stevens, J., Car, B., Bertram, T.A. and Afshari, C.A. (2004) Identification of putative gene based markers of renal toxicity. Environ Health Perspect 112, 465-479.

Antoniadis, A., Lambert-Lacroix, S. and Leblanc, F. (2003) Effective dimension reduction methods for tumor classification using gene expression data. Bioinformatics 19, 563-570.

Antoniadis, A., Lambert-Lacroix, S. and Leblanc, F. (2003) Effective dimension reduction methods for tumor classification using gene expression data. Bioinformatics 19, 563-570.

Anzai, N., Endou, H. (2007) Renal drug transporters and nephrotoxicity. AATEX 14, spezial issue, 447-452

Aplin, A.E., Howe, A., Alahari, S.K. and Juliano, R.L. (1998) Signal transduction and signal modulation by cell adhesion receptors: the role of integrins, cadherins, immunoglobulin-cell adhesion molecules, and selectins. Pharmacol Rev 50, 197-263.

Appenroth, D. and Braunlich, H. (1986) Age-dependent qualitative and quantitative changes in physiological proteinuria in rats. Z Versuchstierkd 28, 77-82.

Ferrara, N. and Gerber, H.P. (2001) The role of vascular endothelial growth factor in angiogenesis. Acta Haematol 106, 148-156.

Arakawa, T., Masaki, T., Hirai, T., Doi, S., Kuratsune, M., Arihiro, K., Kohno, N. and Yorioka, N. (2008) Activation of signal transducer and activator of transcription 3 correlates with cell proliferation and renal injury in human glomerulonephritis. Nephrol Dial Transplant 23, 3418-3426.

Arany, I. and Safirstein, R.L. (2003) Cisplatin nephrotoxicity. Semin Nephrol 23, 460-464.

Arroyo, V., Gines, P., Gerbes, A.L., Dudley, F.J., Gentilini, P., Laffi, G., Reynolds, T.B., Ring-Larsen, H. and Scholmerich, J. (1996) Definition and diagnostic criteria of refractory ascites and hepatorenal syndrome in cirrhosis. International Ascites Club. Hepatology 23, 164-176.

Arthur, J.M., Janech, M.G., Varghese, S.A., Almeida, J.S. and Powell, T.B. (2008) Diagnostic and prognostic biomarkers in acute renal failure. Contrib Nephrol 160, 53-64.

Aruffo, A., Stamenkovic, I., Melnick, M., Underhill, C.B. and Seed, B. (1990) CD44 is the principal cell surface receptor for hyaluronate. Cell 61, 1303-1313.

Arumugam, T.V., Shiels, I.A., Woodruff, T.M., Granger, D.N. and Taylor, S.M. (2004) The role of the complement system in ischemia-reperfusion injury. Shock 21, 401-409.

Ashcroft, G.S., Yang, X., Glick, A.B., Weinstein, M., Letterio, J.L., Mizel, D.E., Anzano, M., Greenwell-Wild, T., Wahl, S.M., Deng, C. and Roberts, A.B. (1999) Mice lacking Smad3 show accelerated wound healing and an impaired local inflammatory response. Nat Cell Biol 1, 260-266.

Askew, D.S., Ashmun, R.A., Simmons, B.C. and Cleveland, J.L. (1991) Constitutive c-myc expression in an IL-3-dependent myeloid cell line suppresses cell cycle arrest and accelerates apoptosis. Oncogene 6, 1915-1922.

Atherton, J.C., Hai, M.A. and Thomas, S. (1968) Effects of water diuresis and osmotic (mannitol) diuresis on urinary solute excretion by the conscious rat. J Physiol 197, 395-410.

Avihingsanon, Y., Phumesin, P., Benjachat, T., Akkasilpa, S., Kittikowit, V., Praditpornsilpa, K., Wongpiyabavorn, J., Eiam-Ong, S., Hemachudha, T., Tungsanga, K. and Hirankarn, N. (2006) Measurement of urinary chemokine and growth factor messenger RNAs: a noninvasive monitoring in lupus nephritis. Kidney Int 69, 747-753.

Aziz, K.A., Till, K.J., Zuzel, M. and Cawley, J.C. (2000) Involvement of CD44-hyaluronan interaction in malignant cell homing and fibronectin synthesis in hairy cell leukemia. Blood 96, 3161-3167.

Azzam, M.E. and Algranati, I.D. (1973) Mechanism of puromycin action: fate of ribosomes after release of nascent protein chains from polysomes. Proc Natl Acad Sci U S A 70, 3866-3869.

Bailey, C.J. (1993) Metformin--an update. Gen Pharmacol 24, 1299-1309.

Bailly, V., Zhang, Z., Meier, W., Cate, R., Sanicola, M. and Bonventre, J.V. (2002) Shedding of kidney injury molecule-1, a putative adhesion protein involved in renal regeneration. J Biol Chem 277, 39739-39748.

Balakumar, P., Rohilla, A. and Thangathirupathi, A. (2010) Gentamicin-induced nephrotoxicity: Do we have a promising therapeutic approach to blunt it? Pharmacol Res 62, 179-186.

Barabas, K., Milner, R., Lurie, D. and Adin, C. (2008) Cisplatin: a review of toxicities and therapeutic applications. Vet Comp Oncol 6, 1-18.

Barnes, M., Freudenberg, J., Thompson, S., Aronow, B. and Pavlidis, P. (2005) Experimental comparison and cross-validation of the Affymetrix and Illumina gene expression analysis platforms. Nucleic Acids Res 33, 5914-5923.

Barton, P.J., Birks, E.J., Felkin, L.E., Cullen, M.E., Koban, M.U. and Yacoub, M.H. (2003) Increased expression of extracellular matrix regulators TIMP1 and MMP1 in deteriorating heart failure. J Heart Lung Transplant 22, 738-744.

Basu, A. and Cline, J.S. (1995) Oncogenic transformation alters cisplatin-induced apoptosis in rat embryo fibroblasts. Int J Cancer 63, 597-603.

Baud, L. and Letavernier, E. (2007) PPARalpha contributes to tubular protection. J Am Soc Nephrol 18, 3017-3018.

Beck., L.B. Jr., Salant, D.J. (2010) Membranous nephropathy: recent travels and new roads ahead Kidney Int. 77(9), 765-770

Beckett, G.J., Chapman, B.J., Dyson, E.H. and Hayes, J.D. (1985) Plasma glutathione S-transferase measurements after paracetamol overdose: evidence for early hepatocellular damage. Gut 26, 26-31.

David R. Bell, D.R., Poland, A., (2000) Binding of Aryl Hydrocarbon Receptor (AhR) to AhR-interacting Protein THE ROLE OF hsp90. J Biol Chem. 275(46), 36407-36414.

Bello-Fernandez, C., Packham, G. and Cleveland, J.L. (1993) The ornithine decarboxylase gene is a transcriptional target of c-Myc. Proc Natl Acad Sci U S A 90, 7804-7808.

Benjamini, Y., Drai, D., Elmer, G., Kafkafi, N. and Golani, I. (2001) Controlling the false discovery rate in behavior genetics research. Behav Brain Res 125, 279-284.

Bennett, M., Dent, C.L., Ma, Q., Dastrala, S., Grenier, F., Workman, R., Syed, H., Ali, S., Barasch, J. and Devarajan, P. (2008) Urine NGAL predicts severity of acute kidney injury after cardiac surgery: a prospective study. Clin J Am Soc Nephrol 3, 665-673.

Berger, J. and Moller, D.E. (2002) The mechanisms of action of PPARs. Annu Rev Med 53, 409-435.

Bettelli, E., Dastrange, M. and Oukka, M. (2005) Foxp3 interacts with nuclear factor of activated T cells and NF-kappa B to repress cytokine gene expression and effector functions of T helper cells. Proc Natl Acad Sci U S A 102, 5138-5143.

Bielesz, B., Sirin, Y., Si, H., Niranjan, T., Gruenwald, A., Ahn, S., Kato, H., Pullman, J., Gessler, M., Haase, V.H. and Susztak, K. Epithelial Notch signaling regulates interstitial fibrosis development in the kidneys of mice and humans. J Clin Invest 120, 4040-4054.

Bitzer, M., von Gersdorff, G., Liang, D., Dominguez-Rosales, A., Beg, A.A., Rojkind, M. and Bottinger, E.P. (2000) A mechanism of suppression of TGF-beta/SMAD signaling by NF-kappa B/RelA. Genes Dev 14, 187-197.

Bodmer, M., Meier, C., Krahenbuhl, S., Jick, S.S. and Meier, C.R. (2008) Metformin, sulfonylureas, or other antidiabetes drugs and the risk of lactic acidosis or hypoglycemia: a nested case-control analysis. Diabetes Care 31, 2086-2091.

Boess, F., Kamber, M., Romer, S., Gasser, R., Muller, D., Albertini, S. and Suter, L. (2003) Gene expression in two hepatic cell lines, cultured primary hepatocytes, and liver slices compared to the in vivo liver gene expression in rats: possible implications for toxicogenomics use of in vitro systems. Toxicol Sci 73, 386-402.

Bokenkamp, A., Domanetzki, M., Zinck, R., Schumann, G., Byrd, D., Brodehl, J. (1998) Cystatin C – a new marker of glomerular filtration rate in children independent of age and height. Pediatrics 101(5), 875–881

Borenfreund, E. and Puerner, J.A. (1985) Toxicity determined in vitro by morphological alterations and neutral red absorption. Toxicol Lett 24, 119-124.

Boron, W.F., Baoulpaep, E.L. (2008) "Medical Physiology: A Cellular And Molecular Approaoch". 2nd Edition, Saunders/Elsevier.

Boureux, A., Vignal, E., Faure, S. and Fort, P. (2007) Evolution of the Rho family of ras-like GTPases in eukaryotes. Mol Biol Evol 24, 203-216.

Boutaud, O., Aronoff, D.M., Richardson, J.H., Marnett, L.J. and Oates, J.A. (2002) Determinants of the cellular specificity of acetaminophen as an inhibitor of prostaglandin H(2) synthases. Proc Natl Acad Sci U S A 99, 7130-7135.

Bouvier, N., Flinois, J.P., Gilleron, J., Sauvage, F.L., Legendre, C., Beaune, P., Thervet, E., Anglicheau, D. and Pallet, N. (2009) Cyclosporine triggers endoplasmic reticulum stress in endothelial cells: a role for endothelial phenotypic changes and death. Am J Physiol Renal Physiol 296, F160-169.

Brajtburg, J. and Bolard, J. (1996) Carrier effects on biological activity of amphotericin B. Clin Microbiol Rev 9, 512-531.

Brandon, E.F., Raap, C.D., Meijerman, I., Beijnen, J.H. and Schellens, J.H. (2003) An update on in vitro test methods in human hepatic drug biotransformation research: pros and cons. Toxicol Appl Pharmacol 189, 233-246.

Branten, A.J., Mulder, T.P., Peters, W.H., Assmann, K.J. and Wetzels, J.F. (2000) Urinary excretion of glutathione S transferases alpha and pi in patients with proteinuria: reflection of the site of tubular injury. Nephron 85, 120-126.

Branton, M.H. and Kopp, J.B. (1999) TGF-beta and fibrosis. Microbes Infect 1, 1349-1365.

Brew, K., Dinakarpandian, D. and Nagase, H. (2000) Tissue inhibitors of metalloproteinases: evolution, structure and function. Biochim Biophys Acta 1477, 267-283.

Brown, K.M., Sacks, S.H. and Sheerin, N.S. (2007) Mechanisms of disease: the complement system in renal injury--new ways of looking at an old foe. Nat Clin Pract Nephrol 3, 277-286.

Brown, L.F., Berse, B., Van de Water, L., Papadopoulos-Sergiou, A., Perruzzi, C.A., Manseau, E.J., Dvorak, H.F. and Senger, D.R. (1992) Expression and distribution of osteopontin in human tissues: widespread association with luminal epithelial surfaces. Mol Biol Cell 3, 1169-1180.

Brown, M.P., Grundy, W.N., Lin, D., Cristianini, N., Sugnet, C.W., Furey, T.S., Ares, M., Jr. and Haussler, D. (2000) Knowledge-based analysis of microarray gene expression data by using support vector machines. Proc Natl Acad Sci U S A 97, 262-267.

Bruning, T., Thier, R., Mann, H., Melzer, H., Brode, P., Dallner, G. and Bolt, H.M. (2001) Pathological excretion patterns of urinary proteins in miners highly exposed to dinitrotoluene. J Occup Environ Med 43, 610-615.

Burns, T.F., Bernhard, E.J. and El-Deiry, W.S. (2001) Tissue specific expression of p53 target genes suggests a key role for KILLER/DR5 in p53-dependent apoptosis in vivo. Oncogene 20, 4601-4612.

Bushel, P.R., Hamadeh, H.K., Bennett, L., Green, J., Ableson, A., Misener, S., Afshari, C.A. and Paules, R.S. (2002) Computational selection of distinct class- and subclass-specific gene expression signatures. J Biomed Inform 35, 160-170.
Bushel, P.R., Hamadeh, H.K., Bennett, L., Green, J., Ableson, A., Misener, S., Afshari, C.A. and Paules, R.S. (2002) Computational selection of distinct class- and subclass-specific gene expression signatures. J Biomed Inform 35, 160-170.

Bustelo, X.R., Sauzeau, V. and Berenjeno, I.M. (2007) GTP-binding proteins of the Rho/Rac family: regulation, effectors and functions in vivo. Bioessays 29, 356-370.

Cano-Gauci, D.F., Song, H.H., Yang, H., McKerlie, C., Choo, B., Shi, W., Pullano, R., Piscione, T.D., Grisaru, S., Soon, S., Sedlackova, L., Tanswell, A.K., Mak, T.W., Yeger, H., Lockwood, G.A., Rosenblum, N.D. and Filmus, J. (1999) Glypican-3-deficient mice exhibit developmental overgrowth and some of the abnormalities typical of Simpson-Golabi-Behmel syndrome. J Cell Biol 146, 255-264.

Carcoana, O.V., Mathew, J.P., Davis, E., Byrne, D.W., Hayslett, J.P., Hines, R.L. and Garwood, S. (2003) Mannitol and dopamine in patients undergoing cardiopulmonary bypass: a randomized clinical trial. Anesth Analg 97, 1222-1229.

Carpenter, H.M. and Mudge, G.H. (1981) Acetaminophen nephrotoxicity: studies on renal acetylation and deacetylation. J Pharmacol Exp Ther 218, 161-167.

CDER: Guidance for industry, investigators and reviewers. Exploratory IND studies. (2006). http://www.fda.gov/downloads/Drugs/GuidanceComplianceRegulatoryInformation/Guidances/ucm078933.pdf. Accessed: 15.04.2011.

Celik, I., Cihangiroglu, M., Ilhan, N., Akpolat, N. and Akbulut, H.H. (2005) Protective effects of different antioxidants and amrinone on vancomycin-induced nephrotoxicity. Basic Clin Pharmacol Toxicol 97, 325-332.

CellTiter-Glo Bulletin, (2011) http://www.promega.com/resources/protocols/technical-bulletins/0/celltiter-glo-luminescent-cell-viability-assay-protocol. Accessed: 10.06.2012

Cendan, J.C., Souba, W.W., Copeland, E.M., 3rd and Lind, D.S. (1995) Cytokines regulate endotoxin stimulation of endothelial cell arginine transport. Surgery 117, 213-219.

Chandrasekharan, N.V., Dai, H., Roos, K.L., Evanson, N.K., Tomsik, J., Elton, T.S. and Simmons, D.L. (2002) COX-3, a cyclooxygenase-1 variant inhibited by acetaminophen and other analgesic/antipyretic drugs: cloning, structure, and expression. Proc Natl Acad Sci U S A 99, 13926-13931.

Chapelsky, M.C., Nix, D.E., Cavanaugh, J.C., Wilton, J.H., Norman, A. and Schentag, J.J. (1992) Renal tubular enzyme effects of clarithromycin in comparison with gentamicin and placebo in volunteers. Drug Saf 7, 304-309.

Chen, F. and Shi, X. (2002) Intracellular signal transduction of cells in response to carcinogenic metals. Crit Rev Oncol Hematol 42, 105-121.

Chen, H.H., Chen, T.W. and Lin, H. Pravastatin attenuates carboplatin-induced nephrotoxicity in rodents via peroxisome proliferator-activated receptor alpha-regulated heme oxygenase-1. Mol Pharmacol 78, 36-45.

Chen, N., Aleksa, K., Woodland, C., Rieder, M. and Koren, G. (2008) N-Acetylcysteine prevents ifosfamide-induced nephrotoxicity in rats. Br J Pharmacol 153, 1364-1372.

Chen, T.H., Chang, C.F., Yu, S.C., Wang, J.C., Chen, C.H., Chan, P. and Lee, H.M. (2009) Dipyridamole inhibits cobalt chloride-induced osteopontin expression in NRK52E cells. Eur J Pharmacol 613, 10-18.

Chen, Y., Bal, B.,S., Gorski, J.,P. (1992) Calcium and collagen binding properties of osteopontin, bone sialoprotein, and bone acidic glycoprotein-75 from bone. J Biol Chem 267, 24871-24878

Chen, Z.J. and Ni, Z. (2006) Mechanisms of genomic rearrangements and gene expression changes in plant polyploids. Bioessays 28, 240-252.

Chertow, G.M., Levy, E.M., Hammermeister, K.E., Grover, F. and Daley, J. (1998) Independent association between acute renal failure and mortality following cardiac surgery. Am J Med 104, 343-348.

Chi, W., Song, X., Jiang, C., Liu, X., Li, W. and Wang, X. (2006) Lentiviral vector-mediated downregulation of ornithine decarboxylase inhibits tumor cell growth in vitro and in vivo. Tumour Biol 27, 243-251.

Choudhury D, and Ahmed Z. (2006) Drug-associated renal dysfunction and injury. Nat Clin Pract Nephrol 2, 80-91.

Chromek, M., Tullus, K., Hertting, O., Jaremko, G., Khalil, A., Li, Y.H. and Brauner, A. (2003) Matrix metalloproteinase-9 and tissue inhibitor of metalloproteinases-1 in acute pyelonephritis and renal scarring. Pediatr Res 53, 698-705.

Chromek, M., Tullus, K., Lundahl, J. and Brauner, A. (2004) Tissue inhibitor of metalloproteinase 1 activates normal human granulocytes, protects them from apoptosis, and blocks their transmigration during inflammation. Infect Immun 72, 82-88.

Clark, R.T., Nance, J.P., Noor, S. and Wilson, E.H. T-cell production of matrix metalloproteinases and inhibition of parasite clearance by TIMP-1 during chronic Toxoplasma infection in the brain. ASN Neuro 3, e00049.

Clemedson, C. (2008) The European ACuteTox project: a modern integrative in vitro approach to better prediction of acute toxicity. Clin Pharmacol Ther 84, 200-202.

Colle, A., Tavera, C., Laurent, P., Leung-Tack, J. and Girolami, J.P. (1990) Direct radioimmunoassay of rat cystatin C: increased urinary excretion of this cysteine proteases inhibitor during chromate nephropathy. J Immunoassay 11, 199-214.

Conery, A.R., Cao, Y., Thompson, E.A., Townsend, C.M., Jr., Ko, T.C. and Luo, K. (2004) Akt interacts directly with Smad3 to regulate the sensitivity to TGF-beta induced apoptosis. Nat Cell Biol 6, 366-372.

Conti, M., Moutereau, S., Zater, M., Lallali, K., Durrbach, A., Manivet, P., Eschwege, P. and Loric, S. (2006) Urinary cystatin C as a specific marker of tubular dysfunction. Clin Chem Lab Med 44, 288-291.

Correa-Rotter, R., Hostetter, T.H., Nath, K.A., Manivel, J.C. and Rosenberg, M.E. (1992) Interaction of complement and clusterin in renal injury. J Am Soc Nephrol 3, 1172-1179.

Correa-Rotter, R., Ibarra-Rubio, M.E., Schwochau, G., Cruz, C., Silkensen, J.R., Pedraza-Chaverri, J., Chmielewski, D. and Rosenberg, M.E. (1998) Induction of clusterin in tubules of nephrotic rats. J Am Soc Nephrol 9, 33-37.

Cotterman, R., Jin, V.X., Krig, S.R., Lemen, J.M., Wey, A., Farnham, P.J. and Knoepfler, P.S. (2008) N-Myc regulates a widespread euchromatic program in the human genome partially independent of its role as a classical transcription factor. Cancer Res 68, 9654-9662.

Cristofori, P., Zanetti, E., Fregona, D., Piaia, A. and Trevisan, A. (2007) Renal proximal tubule segment-specific nephrotoxicity: an overview on biomarkers and histopathology. Toxicol Pathol 35, 270-275.

Crouch, S.P., Kozlowski, R., Slater, K.J. and Fletcher, J. (1993) The use of ATP bioluminescence as a measure of cell proliferation and cytotoxicity. J Immunol Methods 160, 81-88.

Cui, L., Iwamoto, A., Lian, J.Q., Neoh, H.M., Maruyama, T., Horikawa, Y. and Hiramatsu, K. (2006) Novel mechanism of antibiotic resistance originating in vancomycin-intermediate Staphylococcus aureus. Antimicrob Agents Chemother 50, 428-438.

Cunningham, M.L., Bogdanffy, M.S., Zacharewski, T.R. and Hines, R.N. (2003) Workshop overview: use of genomic data in risk assessment. Toxicol Sci 73, 209-215.

Curtiss, M. and Colgan, J. (2007) The role of the T-cell costimulatory molecule Tim-1 in the immune response. Immunol Res 39, 52-61.

Cytodiagnostic Homepage (2012), http://www.cytodiagnostics.com/lateral-flow-immunoassays.php, Accessed 08.12.2012

Dai, C., Yang, J. and Liu, Y. (2003) Transforming growth factor-beta1 potentiates renal tubular epithelial cell death by a mechanism independent of Smad signaling. J Biol Chem 278, 12537-12545.

Darken, M.A. (1964) Puromycin Inhibition of Protein Synthesis. Pharmacol Rev 16, 223-243.

Dartsch, P.C., Hildenbrand, S., Kimmel, R. and Schmahl, F.W. (1998) Investigations on the nephrotoxicity and hepatotoxicity of trivalent and hexavalent chromium compounds. Int Arch Occup Environ Health 71 Suppl, S40-45.

Davis, J.W. and Kramer, J.A. (2006) Genomic-based biomarkers of drug-induced nephrotoxicity. Expert Opin Drug Metab Toxicol 2, 95-101.

Dawn, B., Xuan, Y.T., Guo, Y., Rezazadeh, A., Stein, A.B., Hunt, G., Wu, W.J., Tan, W. and Bolli, R. (2004) IL-6 plays an obligatory role in late preconditioning via JAK-STAT signaling and upregulation of iNOS and COX-2. Cardiovasc Res 64, 61-71.

de Alboran, I.M., O'Hagan, R.C., Gartner, F., Malynn, B., Davidson, L., Rickert, R., Rajewsky, K., DePinho, R.A. and Alt, F.W. (2001) Analysis of C-MYC function in normal cells via conditional gene-targeted mutation. Immunity 14, 45-55.

de Graauw, M., Le Devedec, S., Tijdens, I., Smeets, M.B., Deelder, A.M. and van de Water, B. (2007) Proteomic analysis of alternative protein tyrosine phosphorylation in 1,2-dichlorovinyl-cysteine-induced cytotoxicity in primary cultured rat renal proximal tubular cells. J Pharmacol Exp Ther 322, 89-100.

de Mendonca, A., Vincent, J.L., Suter, P.M., Moreno, R., Dearden, N.M., Antonelli, M., Takala, J., Sprung, C. and Cantraine, F. (2000) Acute renal failure in the ICU: risk factors and outcome evaluated by the SOFA score. Intensive Care Med 26, 915-921.

Debelle, F.D., Nortier, J.L., Husson, C.P., De Prez, E.G., Vienne, A.R., Rombaut, K., Salmon, I.J., Deschodt-Lanckman, M.M. and Vanherweghem, J.L. (2004) The renin-angiotensin system blockade does not prevent renal interstitial fibrosis induced by aristolochic acids. Kidney Int 66, 1815-1825.

Delcommenne, M., Tan, C., Gray, V., Rue, L., Woodgett, J. and Dedhar, S. (1998) Phosphoinositide-3-OH kinase-dependent regulation of glycogen synthase kinase 3 and protein kinase B/AKT by the integrin-linked kinase. Proc Natl Acad Sci U S A 95, 11211-11216.

Demirjian, S., Nally, J., (2012) Cleveland Clinic Homepage, Center of Continuing Education: http://www.clevelandclinicmeded.com/medicalpubs/diseasemanagement/nephrology/acute-kidney-injury/, Accessed 08.12.2012

Depierreux, M., Van Damme, B., Vanden Houte, K. and Vanherweghem, J.L. (1994) Pathologic aspects of a newly described nephropathy related to the prolonged use of Chinese herbs. Am J Kidney Dis 24, 172-180.

Dere, E., Boverhof, D.R., Burgoon, L.D. and Zacharewski, T.R. (2006) In vivo-in vitro toxicogenomic comparison of TCDD-elicited gene expression in Hepa1c1c7 mouse hepatoma cells and C57BL/6 hepatic tissue. BMC Genomics 7, 80.

Dieterich, C., Puey, A., Lin, S., Swezey, R., Furimsky, A., Fairchild, D., Mirsalis, J.C. and Ng, H.H. (2009) Gene expression analysis reveals new possible mechanisms of vancomycin-induced nephrotoxicity and identifies gene markers candidates. Toxicol Sci 107, 258-269.

Dieterle, F., Perentes, E., Cordier, A., Roth, D.R., Verdes, P., Grenet, O., Pantano, S., Moulin, P., Wahl, D., Mahl, A., End, P., Staedtler, F., Legay, F., Carl, K., Laurie, D., Chibout, S.D., Vonderscher, J. and Maurer, G. Urinary clusterin, cystatin C, beta2-microglobulin and total protein as markers to detect drug-induced kidney injury. Nat Biotechnol 28, 463-469.

Ding, H., He, Y., Li, K., Yang, J., Li, X., Lu, R. and Gao, W. (2007) Urinary neutrophil gelatinase-associated lipocalin (NGAL) is an early biomarker for renal tubulointerstitial injury in IgA nephropathy. Clin Immunol 123, 227-234.

Di-Poï, N., Tan, N.S., Michalik, L., Wahli, W., Desvergne, B., (2002) Antiapoptotic role of PPARbeta in keratinocytes via transcriptional control of the Akt1 signaling pathway. Mol Cell. 10(4), 721-733.

Doan, N. and Gettins, P.G. (2007) Human alpha2-macroglobulin is composed of multiple domains, as predicted by homology with complement component C3. Biochem J 407, 23-30.

Dominguez-Sola, D., Ying, C.Y., Grandori, C., Ruggiero, L., Chen, B., Li, M., Galloway, D.A., Gu, W., Gautier, J. and Dalla-Favera, R. (2007) Non-transcriptional control of DNA replication by c-Myc. Nature 448, 445-451.

Eaton, D.C., Pooler, J. (2004). “Vander's Renal Physiology” 6th Edition McGraw-Hill Medical.

Duff, T., Carter, S., Feldman, G., McEwan, G., Pfaller, W., Rhodes, P., Ryan, M. and Hawksworth, G. (2002) Transepithelial resistance and inulin permeability as endpoints in in vitro nephrotoxicity testing. Altern Lab Anim 30 Suppl 2, 53-59.

Dvergsten, J., Manivel, J.C., Correa-Rotter, R. and Rosenberg, M.E. (1994) Expression of clusterin in human renal diseases. Kidney Int 45, 828-835.

Edwards, N., Honemann, D., Burley, D. and Navarro, M. (1994) Refinement of the Medicare diagnosis-related groups to incorporate a measure of severity. Health Care Financ Rev 16, 45-64.

Edwards, S.W. and Preston, R.J. (2008) Systems biology and mode of action based risk assessment. Toxicol Sci 106, 312-318.

El Mouedden, M., Laurent, G., Mingeot-Leclercq, M.P., Taper, H.S., Cumps, J. and Tulkens, P.M. (2000) Apoptosis in renal proximal tubules of rats treated with low doses of aminoglycosides. Antimicrob Agents Chemother 44, 665-675.

Ellenbroek, S.I. and Collard, J.G. (2007) Rho GTPases: functions and association with cancer. Clin Exp Metastasis 24, 657-672.

Ellerman, J.E., Brown, C.K., de Vera, M., Zeh, H.J., Billiar, T., Rubartelli, A. and Lotze, M.T. (2007) Masquerader: high mobility group box-1 and cancer. Clin Cancer Res 13, 2836-2848.

Elmore, S., (2007) Apoptosis: A Review of Programmed Cell Death. *Toxicol Pathol*. 35(4), 495–516.

EMA (2009). Innovation Task Force. Stand: 23.07.2009. http://www.emea.europa.eu/htms/human/mes/itf.htm. Accessed at: 21.05.2010.

EMA, Consultation on the Qualification Opinion ILSI/HESI Submission of Novel Renal Biomarkers for Toxicity (2010)
http://www.ema.europa.eu/docs/en_GB/document_library/Regulatory_and_procedural_guideline/2010/05/WC500090466.pdf Accessed: 14.06.2012

Emeigh-Hart, S.G., Kinter, L.P. (2005) Assessing Renal Effects of Toxicants in vivo. Toxicology of the kidney, 3rd Edition, CRC Press, Boca Raton

Endo, Y., Fujita, T., Tamura, K., Tsuruga, H. and Nojima, H. (1996) Structure and chromosomal assignment of the human cyclin G gene. Genomics 38, 92-95.

Escher, P., Wahli, W., (2000) Peroxisome proliferator-activated receptors: insight into multiple cellular funktions. Mutat Res. 448,121-138.

ESD Journal Homepage- Steve Fowler (2009). Lab-on-a-Chip. http://www.esdjournal.com/articles/labchip/Lab.htm. Accessed: 25.06.2010.

Eti, S., Cheng, C.Y., Marshall, A. and Reidenberg, M.M. (1993) Urinary clusterin in chronic nephrotoxicity in the rat. Proc Soc Exp Biol Med 202, 487-490.

European Comission (2007). REACH in brief.
(http://www.ec.europa.eu/environment/chemicals/reach/pdf/2007_02_reach_in_brief.pdf.) Accessed: 21.05.2011.

Evan, G.I., Wyllie, A.H., Gilbert, C.S., Littlewood, T.D., Land, H., Brooks, M., Waters, C.M., Penn, L.Z. and Hancock, D.C. (1992) Induction of apoptosis in fibroblasts by c-myc protein. Cell 69, 119-128.

Fabre, N., Anglade, I. and Vericat, J.A. (2009) Application of toxicogenomic tools in the drug research and development process. Toxicol Lett 186, 13-17.

Fadillioglu, E., Erdogan, H., Sogut, S. and Kuku, I. (2003) Protective effects of erdosteine against doxorubicin-induced cardiomyopathy in rats. J Appl Toxicol 23, 71-74.

Fagotto, F. and Gumbiner, B.M. (1996) Cell contact-dependent signaling. Dev Biol 180, 445-454.

Fawcett, Tom (2006); *An introduction to ROC analysis*, Pattern Recognition Letters, 27, 861–874.

FDA (2004). Challenge and Opportunity on the Critical Path to New Medical Products. (http://www.fda.gov/downloads/ScienceResearch/SpecialTopics/CriticalPathInitiative/CriticalPathOpportunitiesReports/ucm113411.pdf.) Accessed at: 21.05.2010.

FDA (2005). Guidance for Industry Pharmacogenomic Data Submissions. (http://www.fda.gov/downloads/Drugs/GuidanceComplianceRegulatoryInformation/Guidances/ucm079849.pdf.) Accessed at: 21.05.2010.

Finver, S.N., Nishikura, K., Finger, L.R., Haluska, F.G., Finan, J., Nowell, P.C. and Croce, C.M. (1988) Sequence analysis of the MYC oncogene involved in the t(8;14)(q24;q11) chromosome translocation in a human leukemia T-cell line indicates that putative regulatory regions are not altered. Proc Natl Acad Sci U S A 85, 3052-3056.

Fliser, D, Ritz, E. (2001) Serum cystatin C concentration as a marker of renal dysfunction in the elderly. Am. J. Kidney Dis. 37(1), 79–83

Flo, T.H., Smith, K.D., Sato, S., Rodriguez, D.J., Holmes, M.A., Strong, R.K., Akira, S. and Aderem, A. (2004) Lipocalin 2 mediates an innate immune response to bacterial infection by sequestrating iron. Nature 432, 917-921.

Florquin, S., Nunziata, R., Claessen, N., van den Berg, F.M., Pals, S.T. and Weening, J.J. (2002) CD44 expression in IgA nephropathy. Am J Kidney Dis 39, 407-414.

Flower, D.R., North, A.C. and Attwood, T.K. (1993) Structure and sequence relationships in the lipocalins and related proteins. Protein Sci 2, 753-761.

Fornari, F.A., Randolph, J.K., Yalowich, J.C., Ritke, M.K. and Gewirtz, D.A. (1994) Interference by doxorubicin with DNA unwinding in MCF-7 breast tumor cells. Mol Pharmacol 45, 649-656.

Forth, W., Henschler, D. and Rummel, W. (2004). Allgemeine und spezielle Pharmakologie und Toxikologie. Urban & Fischer Verlag, München/ Jena, 9th Edition

Francescato, H.D., Costa, R.S., da Silva, C.G. and Coimbra, T.M. (2009) Treatment with a p38 MAPK inhibitor attenuates cisplatin nephrotoxicity starting after the beginning of renal damage. Life Sci 84, 590-597.

Frasconi, M., Chichiarelli, S., Gaucci, E., Mazzei, F., Grillo, C., Chinazzi, A. and Altieri, F. Interaction of ERp57 with calreticulin: Analysis of complex formation and effects of vancomycin. Biophys Chem 160, 46-53.

Frederick, C.A., Williams, L.D., Ughetto, G., van der Marel, G.A., van Boom, J.H., Rich, A. and Wang, A.H. (1990) Structural comparison of anticancer drug-DNA complexes: adriamycin and daunomycin. Biochemistry 29, 2538-2549.

French, L.E., Chonn, A., Ducrest, D., Baumann, B., Belin, D., Wohlwend, A., Kiss, J.Z., Sappino, A.P., Tschopp, J. and Schifferli, J.A. (1993) Murine clusterin: molecular cloning and mRNA localization of a gene associated with epithelial differentiation processes during embryogenesis. J Cell Biol 122, 1119-1130.

French, L.E., Wohlwend, A., Sappino, A.P., Tschopp, J. and Schifferli, J.A. (1994) Human clusterin gene expression is confined to surviving cells during in vitro programmed cell death. J Clin Invest 93, 877-884.

Fuchs, T.C., Frick, K., Emde, B., Czasch, S., von Landenberg, F. and Hewitt, P. (2012) Evaluation of Novel Acute Urinary Rat Kidney Toxicity Biomarker for Subacute Toxicity Studies in Preclinical Trials. Toxicol Pathol.

Fuchs, T.C. and Hewitt, P. (2011a) Preclinical perspective of urinary biomarkers for the detection of nephrotoxicity: what we know and what we need to know. Biomark Med 5, 763-79.

Fuchs, T.C. and Hewitt, P. (2011b) Biomarkers for Drug-Induced Renal Damage and Nephrotoxicity—An Overview for Applied Toxicology. AAPSJ 14, 615-631

Fuchs, T.C., Truisi, G. and Hewitt P. (planned for publication in 2013*) Chapter 35 "Toxicogenomics in Drug Development" in "A Comprehensive Guide to Toxicology in Preclinical Drug Development"* 1st Edition

Fukagawa, M., Noda, M., Shimizu, T. and Kurokawa, K. (1999) Chronic progressive interstitial fibrosis in renal disease--are there novel pharmacological approaches? Nephrol Dial Transplant 14, 2793-2795.

Furlanello, C., Serafini, M., Merler, S. and Jurman, G. (2003) Entropy-based gene ranking without selection bias for the predictive classification of microarray data. BMC Bioinformatics 4, 54.

Gasiewicz, T.A., Singh, K.P. and Casado, F.L. The aryl hydrocarbon receptor has an important role in the regulation of hematopoiesis: implications for benzene-induced hematopoietic toxicity. Chem Biol Interact 184, 246-251.

Gatanaga, H., Tachikawa, N., Kikuchi, Y., Teruya, K., Genka, I., Honda, M., Tanuma, J., Yazaki, H., Ueda, A., Kimura, S. and Oka, S. (2006) Urinary beta2-microglobulin as a possible sensitive marker for renal injury caused by tenofovir disoproxil fumarate. AIDS Res Hum Retroviruses 22, 744-748.

Geleilete, T.J., Melo, G.C., Costa, R.S., Volpini, R.A., Soares, T.J. and Coimbra, T.M. (2002) Role of myofibroblasts, macrophages, transforming growth factor-beta endothelin, angiotensin-II, and fibronectin in the progression of tubulointerstitial nephritis induced by gentamicin. J Nephrol 15, 633-642.

Gewurz, B.E., Towfic, F., Mar, J.C., Shinners, N.P., Takasaki, K., Zhao, B., Cahir-McFarland, E.D., Quackenbush, J., Xavier, R.J. and Kieff, E. Genome-wide siRNA screen for mediators of NF-kappaB activation. Proc Natl Acad Sci U S A 109, 2467-2472.

Gines, A., Escorsell, A., Gines, P., Salo, J., Jimenez, W., Inglada, L., Navasa, M., Claria, J., Rimola, A., Arroyo, V. and et al. (1993) Incidence, predictive factors, and prognosis of the hepatorenal syndrome in cirrhosis with ascites. Gastroenterology 105, 229-236.

Girton, R.A., Sundin, D.P. and Rosenberg, M.E. (2002) Clusterin protects renal tubular epithelial cells from gentamicin-mediated cytotoxicity. Am J Physiol Renal Physiol 282, F703-709.

Goetz, D.H., Holmes, M.A., Borregaard, N., Bluhm, M.E., Raymond, K.N. and Strong, R.K. (2002) The neutrophil lipocalin NGAL is a bacteriostatic agent that interferes with siderophore-mediated iron acquisition. Mol Cell 10, 1033-1043.

Goodison S, Urquidi V, Tarin D. (1999) CD44 cell adhesion molecules. Mol Pathol. 52(4), 189-196.

Goormaghtigh, E., Huart, P., Praet, M., Brasseur, R. and Ruysschaert, J.M. (1990) Structure of the adriamycin-cardiolipin complex. Role in mitochondrial toxicity. Biophys Chem 35, 247-257.

Gorbacheva, V.Y., Lindner, D., Sen, G.C. and Vestal, D.J. (2002) The interferon (IFN)-induced GTPase, mGBP-2. Role in IFN-gamma-induced murine fibroblast proliferation. J Biol Chem 277, 6080-6087.

Gottlieb, L.D. (2003) Plant polyploidy: gene expression and genetic redundancy. Heredity (Edinb) 91, 91-92.

Graham, G.G. and Scott, K.F. (2005) Mechanism of action of paracetamol. Am J Ther 12, 46-55.

Greaves, P. (2011) "Histopathology of Preclinical Toxicity Studies: Interpretation and Relevance in Drug Safety Evaluation", 4rd edition Elsevier Science

Greco, D.S., Turnwald, G.H., Adams, R., Gossett, K.A., Kearney, M. and Casey, H. (1985) Urinary gamma-glutamyl transpeptidase activity in dogs with gentamicin-induced nephrotoxicity. Am J Vet Res 46, 2332-2335.

Grollman, A.P., Shibutani, S., Moriya, M., Miller, F., Wu, L., Moll, U., Suzuki, N., Fernandes, A., Rosenquist, T., Medverec, Z., Jakovina, K., Brdar, B., Slade, N., Turesky, R.J., Goodenough, A.K., Rieger, R., Vukelic, M. and Jelakovic, B. (2007) Aristolochic acid and the etiology of endemic (Balkan) nephropathy. Proc Natl Acad Sci U S A 104, 12129-12134.

Grossman, I. (2009) ADME pharmacogenetics: current practices and future outlook. Expert Opin Drug Metab Toxicol 5, 449-462.

Gunderson, K.L., Kruglyak, S., Graige, M.S., Garcia, F., Kermani, B.G., Zhao, C., Che, D., Dickinson, T., Wickham, E., Bierle, J., Doucet, D., Milewski, M., Yang, R., Siegmund, C., Haas, J., Zhou, L., Oliphant, A., Fan, J.B., Barnard, S. and Chee, M.S. (2004) Decoding randomly ordered DNA arrays. Genome Res 14, 870-877.

Haan, C., Kreis, S., Margue, C. and Behrmann, I. (2006) Jaks and cytokine receptors--an intimate relationship. Biochem Pharmacol 72, 1538-1546.

Hagiwara, M., Yamagata, K., Capaldi, R.A. and Koyama, A. (2006) Mitochondrial dysfunction in focal segmental glomerulosclerosis of puromycin aminonucleoside nephrosis. Kidney Int 69, 1146-1152.

Hall, A. (1998) Rho GTPases and the actin cytoskeleton. Science 279, 509-514.

Han, S.W. and Roman, J. (2006) Fibronectin induces cell proliferation and inhibits apoptosis in human bronchial epithelial cells: pro-oncogenic effects mediated by PI3-kinase and NF-kappa B. Oncogene 25, 4341-4349.

Hara, I., Miyake, H., Gleave, M.E. and Kamidono, S. (2001) Introduction of clusterin gene into human renal cell carcinoma cells enhances their resistance to cytotoxic chemotherapy through inhibition of apoptosis both in vitro and in vivo. Jpn J Cancer Res 92, 1220-1224.

Harrigan, J.A., Vezina, C.M., McGarrigle, B.P., Ersing, N., Box, H.C., Maccubbin, A.E. and Olson, J.R. (2004) DNA adduct formation in precision-cut rat liver and lung slices exposed to benzo[a]pyrene. Toxicol Sci 77, 307-314.

Hasegawa, S., Kato, K., Takashi, M., Zhu, Y., Obata, K., Kinukawa, T. and Miyake, K. (1993) Increased levels of calbindin-D in serum and urine from patients treated by extracorporeal shock wave lithotripsy. J Urol 149, 1414-1418.

Haussecker, D., (2012), The RNAi Therapeutics Blog: http://1.bp.blogspot.com/-Hzgw0587ZSM/T0ZQqZ8rV0I/AAAAAAAABKA/ji01Qp1MgfQ/s400/glomerulus.jpg, Accessed 08.12.2012

Hayes, W.A. (2007) Principles and Methods of Toxicology, Informa Healthcare; 5th Edition

He, C., Imai, M., Song, H., Quigg, R.J. and Tomlinson, S. (2005) Complement inhibitors targeted to the proximal tubule prevent injury in experimental nephrotic syndrome and demonstrate a key role for C5b-9. J Immunol 174, 5750-5757.

Herget-Rosenthal, S., Bokenkamp, A., Hofmann, W., (2007) How to estimate GFR-serum creatinine, serum cystatinC or equations? Clin Biochem 40, 153–161

Hellman, N.E., Spector, J., Robinson, J., Zuo, X., Saunier, S., Antignac, C., Tobias, J.W. and Lipschutz, J.H. (2008) Matrix metalloproteinase 13 (MMP13) and tissue inhibitor of matrix metalloproteinase 1 (TIMP1), regulated by the MAPK pathway, are both necessary for Madin-Darby canine kidney tubulogenesis. J Biol Chem 283, 4272-4282.

Hemmingsen, C., Staun, M. (2009) Effect of parathyroid hormone on renal calbindin-D28k. 11(8), 1086-1093

Hewitt, S.M., Dear, J. and Star, R.A. (2004) Discovery of protein biomarkers for renal diseases. J Am Soc Nephrol 15, 1677-1689.

Hidaka, S., Kranzlin, B., Gretz, N. and Witzgall, R. (2002) Urinary clusterin levels in the rat correlate with the severity of tubular damage and may help to differentiate between glomerular and tubular injuries. Cell Tissue Res 310, 289-296.

Hidaka, S., Kranzlin, B., Gretz, N. and Witzgall, R. (2002) Urinary clusterin levels in the rat correlate with the severity of tubular damage and may help to differentiate between glomerular and tubular injuries. Cell Tissue Res 310, 289-296.

Hobson, S.J. (1997) Paracetamol in suicide and non-accidental overdose--are restrictions justified? J Epidemiol Community Health 51, 731-732.

Hodgson, E. (2010). "A Textbook of Modern Toxicology". John Wiley and Sons. 4th Edition

Hodgson, D.R., Whittaker, R.D., Herath, A., Amakye, D. and Clack, G. (2009) Biomarkers in oncology drug development. Mol Oncol 3, 24-32.

Hoffman, B., Amanullah, A., Shafarenko, M. and Liebermann, D.A. (2002) The proto-oncogene c-myc in hematopoietic development and leukemogenesis. Oncogene 21, 3414-3421.

Hoffmann, D., Fuchs, T.C., Henzler, T., Matheis, K.A., Herget, T., Dekant, W., Hewitt, P. and Mally, A. Evaluation of a urinary kidney biomarker panel in rat models of acute and subchronic nephrotoxicity. Toxicology 277, 49-58.

Hofstra, J.M., Deegens, J.K., Willems, H.L. and Wetzels, J.F. (2008) Beta-2-microglobulin is superior to N-acetyl-beta-glucosaminidase in predicting prognosis in idiopathic membranous nephropathy. Nephrol Dial Transplant 23, 2546-2551.

Honkanen, E.O., Teppo, A.M., Gronhagen-Riska, C. (2000) Decreased urinary excretion of vascular endothelial growth factor in idiopathic membranous glomerulonephritis. Kidney Int. 57(6), 2343-2349.

Horstrup, J.H., Gehrmann, M., Schneider, B., Ploger, A., Froese, P., Schirop, T., Kampf, D., Frei, U., Neumann, R. and Eckardt, K.U. (2002) Elevation of serum and urine levels of TIMP-1 and tenascin in patients with renal disease. Nephrol Dial Transplant 17, 1005-1013.

Hou, S.H., Bushinsky, D.A., Wish, J.B., Cohen, J.J. and Harrington, J.T. (1983) Hospital-acquired renal insufficiency: a prospective study. Am J Med 74, 243-248.

Hu, W.Y., Fukuda, N., Satoh, C., Jian, T., Kubo, A., Nakayama, M., Kishioka, H. and Kanmatsuse, K. (2000) Phenotypic modulation by fibronectin enhances the angiotensin II-generating system in cultured vascular smooth muscle cells. Arterioscler Thromb Vasc Biol 20, 1500-1505.

Huang, H., Woo, J., Alley, S.C. and Hopkins, P.B. (1995) DNA-DNA interstrand cross-linking by cis-diamminedichloroplatinum(II): N7(dG)-to-N7(dG) cross-linking at 5'-d(GC) in synthetic oligonucleotides. Bioorg Med Chem 3, 659-669.

Huang, Q., Dunn, R.T., 2nd, Jayadev, S., DiSorbo, O., Pack, F.D., Farr, S.B., Stoll, R.E. and Blanchard, K.T. (2001) Assessment of cisplatin-induced nephrotoxicity by microarray technology. Toxicol Sci 63, 196-207.

Huo, W., Zhang, K., Nie, Z., Li, Q. and Jin, F. Kidney injury molecule-1 (KIM-1): a novel kidney-specific injury molecule playing potential double-edged functions in kidney injury. Transplant Rev (Orlando) 24, 143-146.

Huzarewich, R.L., Siemens, C.G. and Booth, S.A. (2010) Application of "omics" to prion biomarker discovery. J Biomed Biotechnol, 613504.

Hynes, R.O. (1992) Integrins: versatility, modulation, and signaling in cell adhesion. Cell 69, 11-25.

Ichimura, T., Asseldonk, E.J., Humphreys, B.D., Gunaratnam, L., Duffield, J.S. and Bonventre, J.V. (2008) Kidney injury molecule-1 is a phosphatidylserine receptor that confers a phagocytic phenotype on epithelial cells. J Clin Invest 118, 1657-1668.

Ichimura, T., Bonventre, J.V., Bailly, V., Wei, H., Hession, C.A., Cate, R.L. and Sanicola, M. (1998) Kidney injury molecule-1 (KIM-1), a putative epithelial cell adhesion molecule containing a novel immunoglobulin domain, is up-regulated in renal cells after injury. J Biol Chem 273, 4135-4142.

Iguchi, S., Nishi, S., Ikegame, M., Hoshi, K., Yoshizawa, T., Kawashima, H., Arakawa, M., Ozawa, H. and Gejyo, F. (2004) Expression of osteopontin in cisplatin-induced tubular injury. Nephron Exp Nephrol 97, e96-105.

Ihle, J.N. (2001) The Stat family in cytokine signaling. Curr Opin Cell Biol 13, 211-217.

Ikeda, M., Bhattacharjee, A.K., Kondoh, T., Nagashima, T. and Tamaki, N. (2002) Synergistic effect of cold mannitol and Na(+)/Ca(2+) exchange blocker on blood-brain barrier opening. Biochem Biophys Res Commun 291, 669-674.

Ilangumaran, S., Briol, A. and Hoessli, D.C. (1998) CD44 selectively associates with active Src family protein tyrosine kinases Lck and Fyn in glycosphingolipid-rich plasma membrane domains of human peripheral blood lymphocytes. Blood 91, 3901-3908.

Illumina (2004). BeadStation 500X Gene Expression System Manual. http://www.rockefeller.edu/genomics/pdf/IlluminaGeneExpressionManual.pdf. Accessed: 29.05.2012

Illumina, Inc. (2006). RatRef-12 Expression BeadChip. http://www.switchtoi.com/pdf/GXRatRef-12DataSheet.pdf. Accessed: 29.05.2012

Illumina, Inc. (2010). Homepage Illumina. http://www.Illumina.com. Accessed: 29.05.2012

Imaizumi, T., Mechti, N., Matsumiya, T., Sakaki, H., Kubota, K., Yoshida, H., Kimura, H. and Satoh, K. (2008) Expression of interferon-stimulated gene 20 in vascular endothelial cells. Microbiol Immunol 52, 30-35.

Imamdi, R., de Graauw, M. and van de Water, B. (2004) Protein kinase C mediates cisplatin-induced loss of adherens junctions followed by apoptosis of renal proximal tubular epithelial cells. J Pharmacol Exp Ther 311, 892-903.

IMB Microarray Facility (2010) The University of Queensland. RNA Quality Information. http://microarray.imb.uq.edu.au/rna-qualityinformation. Accessed: 25.06.2010.

Inada, H., Togashi, H., Nakamura, Y., Kaibuchi, K., Nagata, K., Inagaki, M. (1999) Balance between activities of Rho kinase and type 1 protein phosphatase modulates turnover of phosphorylation and dynamics of desmin/vimentin filaments. J Biol Chem. 274(49), 34932-24939.

Inazaki, K., Kanamaru, Y., Kojima, Y., Sueyoshi, N., Okumura, K., Kaneko, K., Yamashiro, Y., Ogawa, H. and Nakao, A. (2004) Smad3 deficiency attenuates renal fibrosis, inflammation,and apoptosis after unilateral ureteral obstruction. Kidney Int 66, 597-604.

Innomed-PredTox Project (2005-2009). http://cordis.europa.eu/search/index.cfm?fuseaction=proj.document&CFID=23287&PJ_RCN=8330448&CFTOKEN=10725414. Accessed: 04.05.2011.

IPA White Paper (2011) Ingeuity Transcription Factor Analysis in IPA https://ingenuity.my.salesforce.com/articles/feature_description/Transcription-Factor Accessed: 15.06.2012

Ishigami, A., Fujita, T., Handa, S., Shirasawa, T., Koseki, H., Kitamura, T., Enomoto, N., Sato, N., Shimosawa, T. and Maruyama, N. (2002) Senescence marker protein-30 knockout mouse liver is highly susceptible to tumor necrosis factor-alpha- and Fas-mediated apoptosis. Am J Pathol 161, 1273-1281.

Ishii, A., Sakai, Y. and Nakamura, A. (2007) Molecular pathological evaluation of clusterin in a rat model of unilateral ureteral obstruction as a possible biomarker of nephrotoxicity. Toxicol Pathol 35, 376-382.

Islam, M., Burke, J.F., Jr., McGowan, T.A., Zhu, Y., Dunn, S.R., McCue, P., Kanalas, J. and Sharma, K. (2001) Effect of anti-transforming growth factor-beta antibodies in cyclosporine-induced renal dysfunction. Kidney Int 59, 498-506.

Jalkanen, S. and Jalkanen, M. (1992) Lymphocyte CD44 binds the COOH-terminal heparin-binding domain of fibronectin. J Cell Biol 116, 817-825.

Janeway, C.A., Travers, P., Walport, M., Shlomick, M.J. (2005). Immunobiology: The immune system in health and disease, New York: Garland Science Publishing. 6th Edition

Janicke, R.U., Lee, F.H. and Porter, A.G. (1994) Nuclear c-Myc plays an important role in the cytotoxicity of tumor necrosis factor alpha in tumor cells. Mol Cell Biol 14, 5661-5670.

Jaques, A., Daviskas, E., Turton, J.A., McKay, K., Cooper, P., Stirling, R.G., Robertson, C.F., Bye, P.T., Lesouef, P.N., Shadbolt, B., Anderson, S.D. and Charlton, B. (2008) Inhaled mannitol improves lung function in cystic fibrosis. Chest 133, 1388-1396.

Jeay, S., Sonenshein, G.E., Kelly, P.A., Postel-Vinay, M.C. and Baixeras, E. (2001) Growth hormone exerts antiapoptotic and proliferative effects through two different pathways involving nuclear factor-kappaB and phosphatidylinositol 3-kinase. Endocrinology 142, 147-156.

Jennings, P., Aydin, S., Bennett, J., McBride, R., Weiland, C., Tuite, N., Gruber, L.N., Perco, P., Gaora, P.O., Ellinger-Ziegelbauer, H., Ahr, H.J., Kooten, C.V., Daha, M.R., Prieto, P., Ryan, M.P., Pfaller, W. and McMorrow, T. (2009) Inter-laboratory comparison of human renal proximal tubule (HK-2) transcriptome alterations due to Cyclosporine A exposure and medium exhaustion. Toxicol In Vitro 23, 486-499.

Jones, S.E. and Jomary, C. (2002) Clusterin. Int J Biochem Cell Biol 34, 427-431.

Juliano, R.L. (1994) Integrin signals and tumor growth control. Princess Takamatsu Symp 24, 118-124.

Kanazawa, S., Soucek, L., Evan, G., Okamoto, T. and Peterlin, B.M. (2003) c-Myc recruits P-TEFb for transcription, cellular proliferation and apoptosis. Oncogene 22, 5707-5711.

Kang, D.H., Hughes, J., Mazzali, M., Schreiner, G.F. and Johnson, R.J. (2001) Impaired angiogenesis in the remnant kidney model: II. Vascular endothelial growth factor administration reduces renal fibrosis and stabilizes renal function. J Am Soc Nephrol 12, 1448-1457.

Kaplan, G., Totsuka, A., Thompson, P., Akatsuka, T., Moritsugu, Y. and Feinstone, S.M. (1996) Identification of a surface glycoprotein on African green monkey kidney cells as a receptor for hepatitis A virus. EMBO J 15, 4282-4296.

Kelland, L. (2007) The resurgence of platinum-based cancer chemotherapy. Nat Rev Cancer 7, 573-584.

Ken Pitts Science Page (2011): http://kenpitts.net/bio/human_anat/kidney_nephron.gif, Accessed 08.12.2012

Khan, S.R., Johnson, J.M., Peck, A.B., Cornelius, J.G. and Glenton, P.A. (2002) Expression of osteopontin in rat kidneys: induction during ethylene glycol induced calcium oxalate nephrolithiasis. J Urol 168, 1173-1181.

Kharasch, E.D., Schroeder, J.L., Bammler, T., Beyer, R. and Srinouanprachanh, S. (2006) Gene expression profiling of nephrotoxicity from the sevoflurane degradation product fluoromethyl-2,2-difluoro-1-(trifluoromethyl)vinyl ether ("compound A") in rats. Toxicol Sci 90, 419-431.

Khynriam, D. and Prasad, S.B. (2001) Hematotoxicity and blood glutathione levels after cisplatin treatment of tumor-bearing mice. Cell Biol Toxicol 17, 357-370.

Kihara, I., Yatoita, E., Kawasaki, K. and Yamamoto, T. (1995) Limitations of podocyte adaptation for glomerular injury in puromycin aminonucleoside nephrosis. Pathol Int 45, 625-634.

Kilty, C., Doyle, S., Hassett, B. and Manning, F. (1998) Glutathione S-transferases as biomarkers of organ damage: applications of rodent and canine GST enzyme immunoassays. Chem Biol Interact 111-112, 123-135.

Kim, N.H., Oh, J.H., Seo, J.A., Lee, K.W., Kim, S.G., Choi, K.M., Baik, S.H., Choi, D.S., Kang, Y.S., Han, S.Y., Han, K.H., Ji, Y.H. and Cha, D.R. (2005) Vascular endothelial growth factor (VEGF) and soluble VEGF receptor FLT-1 in diabetic nephropathy. Kidney Int 67, 167-177.

Kim, Y.O., Lim, S.W., Li, C., Kang, H.J., Ahn, K.O., Yang, H.J., Ghee, J.Y., Kim, S.H., Kim, J.Y., Choi, B.S., Kim, J. and Yang, C.W. (2007) Activation of intrarenal complement system in mouse model for chronic cyclosporine nephrotoxicity. Yonsei Med J 48, 517-525.

King, D.W. and Smith, M.A. (2004) Proliferative responses observed following vancomycin treatment in renal proximal tubule epithelial cells. Toxicol In Vitro 18, 797-803.

Kiss-Toth, E. and Roszer, T. (2008) PPARgamma in Kidney Physiology and Pathophysiology. PPAR Res 2008, 183108.

Kjeldsen, L., Johnsen, A.H., Sengelov, H. and Borregaard, N. (1993) Isolation and primary structure of NGAL, a novel protein associated with human neutrophil gelatinase. J Biol Chem 268, 10425-10432.

Kleinknecht D (1995) Interstitial nephritis, the nephrotic syndrome, and chronic renal failure secondary to nonsteroidal anti-inflammatory drugs. Semin Nephrol 15, 228–235

Klinke, R., Silbernagel, S. (2004) „Lehrbuch der Physiologie“, 4th Edition Georg Thieme Verlag

Knudsen S., (2004). Guide to Analysis of DNA Microarray Data. Wiley-VCH Verlag GmbH & Co. KGaA, Weinheim.

Koch Nogueira, P.C., Hadj-Aissa, A., Schell, M., Dubourg, L., Brunat-Mentigny, M. and Cochat, P. (1998) Long-term nephrotoxicity of cisplatin, ifosfamide, and methotrexate in osteosarcoma. Pediatr Nephrol 12, 572-575.

Koch, H.B., Zhang, R., Verdoodt, B., Bailey, A., Zhang, C.D., Yates, J.R., 3rd, Menssen, A. and Hermeking, H. (2007) Large-scale identification of c-MYC-associated proteins using a combined TAP/MudPIT approach. Cell Cycle 6, 205-217.

Kojetin, D.J., Venters, R.A., Kordys, D.R., Thompson, R.J., Kumar, R. and Cavanagh, J. (2006) Structure, binding interface and hydrophobic transitions of Ca2+-loaded calbindin-D(28K). Nat Struct Mol Biol 13, 641-647.

Kondo, C., Minowa, Y., Uehara, T., Okuno, Y., Nakatsu, N., Ono, A., Maruyama, T., Kato, I., Yamate, J., Yamada, H., Ohno, Y. and Urushidani, T. (2009) Identification of genomic biomarkers for concurrent diagnosis of drug-induced renal tubular injury using a large-scale toxicogenomics database. Toxicology 265, 15-26.

Koscianska, E., Baev, V., Skreka, K., Oikonomaki, K., Rusinov, V., Tabler, M. and Kalantidis, K. (2007) Prediction and preliminary validation of oncogene regulation by miRNAs. BMC Mol Biol 8, 79.

Kramer, J.A., Pettit, S.D., Amin, R.P., Bertram, T.A., Car, B., Cunningham, M., Curtiss, S.W., Davis, J.W., Kind, C., Lawton, M., Naciff, J.M., Oreffo, V., Roman, R.J., Sistare, F.D., Stevens, J., Thompson, K., Vickers, A.E., Wild, S. and Afshari, C.A. (2004) Overview on the application of transcription profiling using selected nephrotoxicants for toxicology assessment. Environ Health Perspect 112, 460-464.

Kroning, R., Lichtenstein, A.K. and Nagami, G.T. (2000) Sulfur-containing amino acids decrease cisplatin cytotoxicity and uptake in renal tubule epithelial cell lines. Cancer Chemother Pharmacol 45, 43-49.

Kuhn, K., Baker, S.C., Chudin, E., Lieu, M.H., Oeser, S., Bennett, H., Rigault, P., Barker, D., McDaniel, T.K. and Chee, M.S. (2004) A novel, high-performance random array platform for quantitative gene expression profiling. Genome Res 14, 2347-2356.

Kumarapeli, A.R., Su, H., Huang, W., Tang, M., Zheng, H., Horak, K.M., Li, M. and Wang, X. (2008) Alpha B-crystallin suppresses pressure overload cardiac hypertrophy. Circ Res 103, 1473-1482.

Lai, P., Yip, N.C. and Michelangeli, F. Regucalcin (RGN/SMP30) alters agonist- and thapsigargin-induced cytosolic [Ca2+] transients in cells by increasing SERCA Ca(2+)ATPase levels. FEBS Lett 585, 2291-2294.

Lambert, E., Dasse, E., Haye, B. and Petitfrere, E. (2004) TIMPs as multifacial proteins. Crit Rev Oncol Hematol 49, 187-198.

Lau, L.F. CCN1/CYR61: the very model of a modern matricellular protein. Cell Mol Life Sci 68, 3149-3163.

Le, Q.T., Sutphin, P.D., Raychaudhuri, S., Yu, S.C., Terris, D.J., Lin, H.S., Lum, B., Pinto, H.A., Koong, A.C. and Giaccia, A.J. (2003) Identification of osteopontin as a prognostic plasma marker for head and neck squamous cell carcinomas. Clin Cancer Res 9, 59-67.

Lebeau, C., Debelle, F.D., Arlt, V.M., Pozdzik, A., De Prez, E.G., Phillips, D.H., Deschodt-Lanckman, M.M., Vanherweghem, J.L. and Nortier, J.L. (2005) Early proximal tubule injury in experimental aristolochic acid nephropathy: functional and histological studies. Nephrol Dial Transplant 20, 2321-2332.

Lee, H.Y., Chung, J.W., Youn, S.W., Kim, J.Y., Park, K.W., Koo, B.K., Oh, B.H., Park, Y.B., Chaqour, B., Walsh, K. and Kim, H.S. (2007) Forkhead transcription factor FOXO3a is a negative regulator of angiogenic immediate early gene CYR61, leading to inhibition of vascular smooth muscle cell proliferation and neointimal hyperplasia. Circ Res 100, 372-380.

Lee, S.S., Buters, J.T., Pineau, T., Fernandez-Salguero, P. and Gonzalez, F.J. (1996) Role of CYP2E1 in the hepatotoxicity of acetaminophen. J Biol Chem 271, 12063-12067.

Lenderink, A.M., Liegel, K., Ljubanovic, D., Coleman, K.E., Gilkeson, G.S., Holers, V.M. and Thurman, J.M. (2007) The alternative pathway of complement is activated in the glomeruli and tubulointerstitium of mice with adriamycin nephropathy. Am J Physiol Renal Physiol 293, F555-564.

Leonard, E.C., Friedrich, J.L. and Basile, D.P. (2008) VEGF-121 preserves renal microvessel structure and ameliorates secondary renal disease following acute kidney injury. Am J Physiol Renal Physiol 295, F1648-1657.

Lesley, J., Hyman, R. and Kincade, P.W. (1993) CD44 and its interaction with extracellular matrix. Adv Immunol 54, 271-335.

Letavernier, E., Perez, J., Joye, E., Bellocq, A., Fouqueray, B., Haymann, J.P., Heudes, D., Wahli, W., Desvergne, B. and Baud, L. (2005) Peroxisome proliferator-activated receptor beta/delta exerts a strong protection from ischemic acute renal failure. J Am Soc Nephrol 16, 2395-2402.

Leussink, B.T., Baelde, H.J., Broekhuizen-van den Berg, T.M., de Heer, E., van der Voet, G.B., Slikkerveer, A., Bruijn, J.A. and de Wolff, F.A. (2003) Renal epithelial gene expression profile and bismuth-induced resistance against cisplatin nephrotoxicity. Hum Exp Toxicol 22, 535-540.

Li, S., Wu, P., Yarlagadda, P., Vadjunec, N.M., Proia, A.D., Harris, R.A. and Portilla, D. (2004) PPAR alpha ligand protects during cisplatin-induced acute renal failure by preventing inhibition of renal FAO and PDC activity. Am J Physiol Renal Physiol 286, F572-580.

Li, W. and Lee, M.K. (2005) Antiapoptotic property of human alpha-synuclein in neuronal cell lines is associated with the inhibition of caspase-3 but not caspase-9 activity. J Neurochem 93, 1542-1550.

Li, Y., Innocentin, S., Withers, D.R., Roberts, N.A., Gallagher, A.R., Grigorieva, E.F., Wilhelm, C. and Veldhoen, M. Exogenous stimuli maintain intraepithelial lymphocytes via aryl hydrocarbon receptor activation. Cell 147, 629-640.

Liangos, O., Perianayagam, M.C., Vaidya, V.S., Han, W.K., Wald, R., Tighiouart, H., MacKinnon, R.W., Li, L., Balakrishnan, V.S., Pereira, B.J., Bonventre, J.V. and Jaber, B.L. (2007) Urinary N-acetyl-beta-(D)-glucosaminidase activity and kidney injury molecule-1 level are associated with adverse outcomes in acute renal failure. J Am Soc Nephrol 18, 904-912.

Liangos, O., Perianayagam, M.C., Vaidya, V.S., Han, W.K., Wald, R., Tighiouart, H., MacKinnon, R.W., Li, L., Balakrishnan, V.S., Pereira, B.J., Bonventre, J.V. and Jaber, B.L. (2007) Urinary N-acetyl-beta-(D)-glucosaminidase activity and kidney injury molecule-1 level are associated with adverse outcomes in acute renal failure. J Am Soc Nephrol 18, 904-912.

Liangos, O., Wald, R., O'Bell, J.W., Price, L., Pereira, B.J. and Jaber, B.L. (2006) Epidemiology and outcomes of acute renal failure in hospitalized patients: a national survey. Clin J Am Soc Nephrol 1, 43-51.

Lim, B.J., Kim, P.K., Hong, S.W. and Jeong, H.J. (2004) Osteopontin expression and microvascular injury in cyclosporine nephrotoxicity. Pediatr Nephrol 19, 288-294.

Lin, Y.H. and Yang-Yen, H.F. (2001) The osteopontin-CD44 survival signal involves activation of the phosphatidylinositol 3-kinase/Akt signaling pathway. J Biol Chem 276, 46024-46030.

Liu, B.C., Zhang, L., Lv, L.L., Wang, Y.L., Liu, D.G. and Zhang, X.L. (2006) Application of antibody array technology in the analysis of urinary cytokine profiles in patients with chronic kidney disease. Am J Nephrol 26, 483-490.

Liu, L.L., Li, Q.X., Xia, L., Li, J. and Shao, L. (2007) Differential effects of dihydropyridine calcium antagonists on doxorubicin-induced nephrotoxicity in rats. Toxicology 231, 81-90.

Lofgren, S., Fernando, M.R., Xing, K.Y., Wang, Y., Kuszynski, C.A., Ho, Y.S. and Lou, M.F. (2008) Effect of thioltransferase (glutaredoxin) deletion on cellular sensitivity to oxidative stress and cell proliferation in lens epithelial cells of thioltransferase knockout mouse. Invest Ophthalmol Vis Sci 49, 4497-4505.

Loh, A.H. and Cohen, A.H. (2009) Drug-induced kidney disease--pathology and current concepts. Ann Acad Med Singapore 38, 240-250.

Lohr, J.W., Willsky, G.R. and Acara, M.A. (1998) Renal drug metabolism. Pharmacol Rev 50, 107-141.

Lu, C.Y., Winterberg, P.D., Chen, J. and Hartono, J.R. Acute kidney injury: a conspiracy of toll-like receptor 4 on endothelia, leukocytes, and tubules. Pediatr Nephrol.

Lu, L.H., Oh, D.J., Dursun, B., He, Z., Hoke, T.S., Faubel, S. and Edelstein, C.L. (2008) Increased macrophage infiltration and fractalkine expression in cisplatin-induced acute renal failure in mice. J Pharmacol Exp Ther 324, 111-117.

Luo, G., Ducy, P., McKee, M.D., Pinero, G.J., Loyer, E., Behringer, R.R. and Karsenty, G. (1997) Spontaneous calcification of arteries and cartilage in mice lacking matrix GLA protein. Nature 386, 78-81.

Lytle, C., Xu, J.C., Biemesderfer, D. and Forbush, B., 3rd. (1995) Distribution and diversity of Na-K-Cl cotransport proteins: a study with monoclonal antibodies. Am J Physiol 269, C1496-1505.

Malinin, N.L., Boldin, M.P., Kovalenko, A.V. and Wallach, D. (1997) MAP3K-related kinase involved in NF-kappaB induction by TNF, CD95 and IL-1. Nature 385, 540-544.
Manyike, P.T., Kharasch, E.D., Kalhorn, T.F. and Slattery, J.T. (2000) Contribution of CYP2E1 and CYP3A to acetaminophen reactive metabolite formation. Clin Pharmacol Ther 67, 275-282.

Manabe, K.E. (2011) Urinary L-FABP level as a predictive biomarker of contrast-induced acute kidney injury. Eur. J. Clin. Invest. 42 (5), 557-563

Mariat, C., Sanchez-Fueyo, A., Alexopoulos, S.P., Kenny, J., Strom, T.B. and Zheng, X.X. (2005) Regulation of T cell dependent immune responses by TIM family members. Philos Trans R Soc Lond B Biol Sci 360, 1681-1685.

Marquardt, H., S. Schaefer (2004) "Lehrbuch der Toxikologie" 2nd Edition Spektrum Akademischer Verlag

Marrer, E. and Dieterle, F. (2009) Impact of biomarker development on drug safety assessment. Toxicol Appl Pharmacol 243, 167-179.

Matheis, K.A., Com, E., Gautier, J.C., Guerreiro, N., Brandenburg, A., Gmuender, H., Sposny, A., Hewitt, P., Amberg, A., Boernsen, O., Riefke, B., Hoffmann, D., Mally, A., Kalkuhl, A., Suter, L., Dieterle, F. and Staedtler, F. (2011) Cross-study and cross-omics comparisons of three nephrotoxic compounds reveal mechanistic insights and new candidate biomarkers. Toxicol Appl Pharmacol 252, 112-122.

Matsumoto, H., Suzuki, K., Tsuyuguchi, K., Tanaka, E., Amitani, R., Maeda, A., Yamamoto, K., Sasada, M. and Kuze, F. (1997a) Interleukin-12 gene expression in human monocyte-derived macrophages stimulated with Mycobacterium bovis BCG: cytokine regulation and effect of NK cells. Infect Immun 65, 4405-4410.

Matsumoto, K. (1997b) Interleukin 10 inhibits vascular permeability factor release by peripheral blood mononuclear cells in patients with lipoid nephrosis. Nephron 75, 154-159.

Matsumoto, K. and Kanmatsuse, K. (2001) Transforming growth factor-beta1 inhibits vascular permeability factor release by T cells in normal subjects and in patients with minimal-change nephrotic syndrome. Nephron 87, 111-117.

Matsumoto, K., Ohi, H. and Kanmatsuse, K. (1997c) Interleukin 10 and interleukin 13 synergize to inhibit vascular permeability factor release by peripheral blood mononuclear cells from patients with lipoid nephrosis. Nephron 77, 212-218.

Matsumoto, K., Ohi, H. and Kanmatsuse, K. (1999) Effects of interleukin-15 on vascular permeability factor release by peripheral blood mononuclear cells in normal subjects and in patients with minimal-change nephrotic syndrome. Nephron 82, 32-38.

Matsumoto, M., Makino, Y., Tanaka, T., Tanaka, H., Ishizaka, N., Noiri, E., Fujita, T. and Nangaku, M. (2003) Induction of renoprotective gene expression by cobalt ameliorates ischemic injury of the kidney in rats. J Am Soc Nephrol 14, 1825-1832.

Mattson, M.P. and Chan, S.L. (2003) Calcium orchestrates apoptosis. Nat Cell Biol 5, 1041-1043.

Mazumder ' Indra, D., Mitra, S., Singh, R.K., Dutta, S., Roy, A., Mondal, R.K., Basu, P.S., Roychoudhury, S. and Panda, C.K. Inactivation of CHEK1 and EI24 are associated with the development of invasive cervical carcinoma: Clinical and prognostic implications. Int J Cancer.

Mazzali, M., Kipari, T., Ophascharoensuk, V., Wesson, J.A., Johnson, R. and Hughes, J. (2002) Osteopontin--a molecule for all seasons. QJM 95, 3-13.

McIntire, J.J., Umetsu, S.E., Macaubas, C., Hoyte, E.G., Cinnioglu, C., Cavalli-Sforza, L.L., Barsh, G.S., Hallmayer, J.F., Underhill, P.A., Risch, N.J., Freeman, G.J., DeKruyff, R.H. and Umetsu, D.T. (2003) Immunology: hepatitis A virus link to atopic disease. Nature 425, 576.

Mei, N., Guo, L., Zhang, L., Shi, L., Sun, Y.A., Fung, C., Moland, C.L., Dial, S.L., Fuscoe, J.C. and Chen, T. (2006) Analysis of gene expression changes in relation to toxicity and tumorigenesis in the livers of Big Blue transgenic rats fed comfrey (Symphytum officinale). BMC Bioinformatics 7 Suppl 2, S16.

Meighan-Mantha, R.L., Hsu, D.K., Guo, Y., Brown, S.A., Feng, S.L., Peifley, K.A., Alberts, G.F., Copeland, N.G., Gilbert, D.J., Jenkins, N.A., Richards, C.M. and Winkles, J.A. (1999) The mitogen-inducible Fn14 gene encodes a type I transmembrane protein that modulates fibroblast adhesion and migration. J Biol Chem 274, 33166-33176.

Mengs U, Lang W, Poch J-A. (1982) The carcinogenic action of aristolochic acid in rats. Arch Toxicol; 51, 107-119

Mengs, U. and Stotzem, C.D. (1993) Renal toxicity of aristolochic acid in rats as an example of nephrotoxicity testing in routine toxicology. Arch Toxicol 67, 307-311.

Merck Manuals Home Health Handbook (2007), New Jersey; Merck and Co., Inc.; http://www.merckmanuals.com/home/index.html. Accessed: 04.06.2012.

Minejima, E., Choi, J., Beringer, P., Lou, M., Tse, E. and Wong-Beringer, A. Applying new diagnostic criteria for acute kidney injury to facilitate early identification of nephrotoxicity in vancomycin-treated patients. Antimicrob Agents Chemother 55, 3278-3283.

Miner, J.H. (1999) Renal basement membrane components. Kidney Int 56, 2016-2024.
Minowa, Y., Kondo, C., Uehara, T., Morikawa, Y., Okuno, Y., Nakatsu, N., Ono, A., Maruyama, T., Kato, I., Yamate, J., Yamada, H., Ohno, Y. and Urushidani, T. Toxicogenomic multigene biomarker for predicting the future onset of proximal tubular injury in rats. Toxicology 297, 47-56.

Mishra, J., Ma, Q., Prada, A., Mitsnefes, M., Zahedi, K., Yang, J., Barasch, J. and Devarajan, P. (2003) Identification of neutrophil gelatinase-associated lipocalin as a novel early urinary biomarker for ischemic renal injury. J Am Soc Nephrol 14, 2534-2543.

Mishra, J., Mori, K., Ma, Q., Kelly, C., Barasch, J. and Devarajan, P. (2004) Neutrophil gelatinase-associated lipocalin: a novel early urinary biomarker for cisplatin nephrotoxicity. Am J Nephrol 24, 307-315.

Miyata, T., Jadoul, M., Kurokawa, K. and Van Ypersele de Strihou, C. (1998) Beta-2 microglobulin in renal disease. J Am Soc Nephrol 9, 1723-1735.

Miyamoto, Y., Koh, Y.H., Park, Y.S., Fujiwara, N., Sakiyama, H., Misonou, Y., Ookawara, T., Suzuki, K., Honke, K., Taniguchi, N. (2003) Oxidative stress caused by inactivation of glutathione peroxidase and adaptive responses. Biol Chem. 384(4), 567-574.

Mizushima, H., Koshikawa, N., Moriyama, K., Takamura, H., Nagashima, Y., Hirahara, F. and Miyazaki, K. (1998) Wide distribution of laminin-5 gamma 2 chain in basement membranes of various human tissues. Horm Res 50 Suppl 2, 7-14.

Moennikes, O., Loeppen, S., Buchmann, A., Andersson, P., Ittrich, C., Poellinger, L. and Schwarz, M. (2004) A constitutively active dioxin/aryl hydrocarbon receptor promotes hepatocarcinogenesis in mice. Cancer Res 64, 4707-4710.

Morel, G., Ban, M., Bonnet, P., Zissu, D. and Brondeau, M.T. (2005) Effect of beta-naphthoflavone and phenobarbital on the nephrotoxicity of chlorotrifluoroethylene and 1,1-dichloro-2,2-difluoroethylene in the rat. J Appl Toxicol 25, 153-165.

Mori, K., Lee, H.T., Rapoport, D., Drexler, I.R., Foster, K., Yang, J., Schmidt-Ott, K.M., Chen, X., Li, J.Y., Weiss, S., Mishra, J., Cheema, F.H., Markowitz, G., Suganami, T., Sawai, K., Mukoyama, M., Kunis, C., D'Agati, V., Devarajan, P. and Barasch, J. (2005) Endocytic delivery of lipocalin-siderophore-iron complex rescues the kidney from ischemia-reperfusion injury. J Clin Invest 115, 610-621.

Mork, C.N., Faller, D.V. and Spanjaard, R.A. (2007) Loss of putative tumor suppressor EI24/PIG8 confers resistance to etoposide. FEBS Lett 581, 5440-5444.

Mueller, O., Lightfoot, S., and Schroeder, A., (2010). Agilent Technologies booklet: "RNA Integrity Number (RIN) – Standardization of RNA Quality Control". http://gene-quantification.net/RIN.pdf. Accessed: 12.06.2012

Mundra, P., Rajapakse, J., Chetty, M., Ngom, A. & Ahmad, S. (2008). Support Vector Based T-Score for Gene Ranking Pattern Recognition in Bioinformatics, Vol. 5265, pp. 144-153. Springer Berlin / Heidelberg

Mundra, P., Rajapakse, J., Chetty, M., Ngom, A. & Ahmad, S. (2008). Support Vector Based T-Score for Gene Ranking Pattern Recognition in Bioinformatics, Springer Berlin / Heidelberg, Vol. 5265.

Murchison, D. and Griffith, W.H. (2000) Mitochondria buffer non-toxic calcium loads and release calcium through the mitochondrial permeability transition pore and sodium/calcium exchanger in rat basal forebrain neurons. Brain Res 854, 139-151.
Murray, P.J. (2007) The JAK-STAT signaling pathway: input and output integration. J Immunol 178, 2623-2629.

Mutschler, E., Geisslinger, G., Kroemer, H. K., Ruth, P. und Schafer-Korting, M. (2008). „Azneimittelwirkungen – Lehrbuch der Pharmakologie und Toxikologie". 9th Edition Wissenschaftliche Verlagsgesellschaft mbH, Stuttgart.

Naghibi, B., Ghafghazi, T., Hajhashemi, V., Talebi, A. and Taheri, D. (2007) The effect of 2,3-dihydroxybenzoic acid and tempol in prevention of vancomycin-induced nephrotoxicity in rats. Toxicology 232, 192-199.

Nakajima, K., Umino, K., Azuma, Y., Kosaka, S., Takano, K., Obara, T., Sato, K. (2009) Stimulating parathyroid cell proliferation and PTH release with phosphate in organ cultures obtained from patients with primary and secondary hyperparathyroidism for a prolonged period. J Bone Miner Metab. 27(2), 224-233

Nash, K., Hafeez, A. and Hou, S. (2002) Hospital-acquired renal insufficiency. Am J Kidney Dis 39, 930-936.

Nemes, Z., Dietz, R., Luth, J.B., Gomba, S., Hackenthal, E. and Gross, F. (1979) The pharmacological relevance of vital staining with neutral red. Experientia 35, 1475-1476.

Rached, E.K., (2009) Neue Ansätze zur Entwicklung von Alternativmethoden zur Prüfung auf chronische Nierentoxizität Dissertation University Wuerzburg.

Neufeld, G., Cohen, T., Gengrinovitch, S. and Poltorak, Z. (1999) Vascular endothelial growth factor (VEGF) and its receptors. FASEB J 13, 9-22.

Ng, C.F., Schafer, F.Q., Buettner, G.R. and Rodgers, V.G. (2007) The rate of cellular hydrogen peroxide removal shows dependency on GSH: mathematical insight into in vivo H2O2 and GPx concentrations. Free Radic Res 41, 1201-1211.

Nguyen, D.V. and Rocke, D.M. (2002) Tumor classification by partial least squares using microarray gene expression data. Bioinformatics 18, 39-50.

Nishikawa, K., Andres, G., Bhan, A.K., McCluskey, R.T., Collins, A.B., Stow, J.L. and Stamenkovic, I. (1993) Hyaluronate is a component of crescents in rat autoimmune glomerulonephritis. Lab Invest 68, 146-153.

Nishino, Y., Takemura, S., Minamiyama, Y., Hirohashi, K., Ogino, T., Inoue, M., Okada, S. and Kinoshita, H. (2003) Targeting superoxide dismutase to renal proximal tubule cells attenuates vancomycin-induced nephrotoxicity in rats. Free Radic Res 37, 373-379.

Nishino, Y., Takemura, S., Minamiyama, Y., Hirohashi, K., Tanaka, H., Inoue, M., Okada, S. and Kinoshita, H. (2002) Inhibition of vancomycin-induced nephrotoxicity by targeting superoxide dismutase to renal proximal tubule cells in the rat. Redox Rep 7, 317-319.

Nony, P.A. and Schnellmann, R.G. (2003) Mechanisms of renal cell repair and regeneration after acute renal failure. J Pharmacol Exp Ther 304, 905-912.

Nosaka, K., Takahashi, T., Nishi, T., Imaki, H., Suzuki, T., Suzuki, K., Kurokawa, K. and Endou, H. (1997) An adenosine deaminase inhibitor prevents puromycin aminonucleoside nephrotoxicity. Free Radic Biol Med 22, 597-605.

Nozaki, Y., Nikolic-Paterson, D.J., Yagita, H., Akiba, H., Holdsworth, S.R., Kitching, A.R. (2011) Tim-1 promotes cisplatin nephrotoxicity. Am J Physiol Renal Physiol. 301, F1098-104

Oberemm, A., Onyon, L. and Gundert-Remy, U. (2005). How can toxicogenomics inform risk assessment? Toxicol Appl Pharmacol 207, 592-598.

Ogutmen, B., Tuglular, S., Cakalagaoglu, F., Ozener, C. and Akoglu, E. (2006) Transforming growth factor-beta1, vascular endothelial growth factor, and bone morphogenic protein-7 expression in tacrolimus-induced nephrotoxicity in rats. Transplant Proc 38, 487-489.

Okamoto, K., Kamibayashi, C., Serrano, M., Prives, C., Mumby, M.C. and Beach, D. (1996) p53-dependent association between cyclin G and the B' subunit of protein phosphatase 2A. Mol Cell Biol 16, 6593-6602.

Okey, A.B. (2007) An aryl hydrocarbon receptor odyssey to the shores of toxicology: the Deichmann Lecture, International Congress of Toxicology-XI. Toxicol Sci 98, 5-38.

Oldberg, A., Franzen, A. and Heinegard, D. (1986) Cloning and sequence analysis of rat bone sialoprotein (osteopontin) cDNA reveals an Arg-Gly-Asp cell-binding sequence. Proc Natl Acad Sci U S A 83, 8819-8823.

Oleggini, R., Musante, L., Menoni, S., Botti, G., Duca, M.D., Prudenziati, M., Carrea, A., Ravazzolo, R. and Ghiggeri, G.M. (2000) Characterization of a DNA binding site that mediates the stimulatory effect of cyclosporin-A on type III collagen expression in renal cells. Nephrol Dial Transplant 15, 778-785.

Orr, M.S. and Scherf, U. (2002) Large-scale gene expression analysis in molecular target discovery. Leukemia 16, 473-477.

Ostendorf, T., Kunter, U., Eitner, F., Loos, A., Regele, H., Kerjaschki, D., Henninger, D.D., Janjic, N. and Floege, J. (1999) VEGF(165) mediates glomerular endothelial repair. J Clin Invest 104, 913-923.

Ozaki, N., Matheis, K.A., Gamber, M., Feidl, T., Nolte, T., Kalkuhl, A. and Deschl, U. Identification of genes involved in gentamicin-induced nephrotoxicity in rats--a toxicogenomic investigation. Exp Toxicol Pathol 62, 555-566.

Ozbek, E., Cekmen, M., Ilbey, Y.O., Simsek, A., Polat, E.C. and Somay, A. (2009) Atorvastatin prevents gentamicin-induced renal damage in rats through the inhibition of p38-MAPK and NF-kappaB pathways. Ren Fail 31, 382-392.

Pabla, N. and Dong, Z. (2008) Cisplatin nephrotoxicity: mechanisms and renoprotective strategies. Kidney Int 73, 994-1007.

Pabla, N., Dong, G., Jiang, M., Huang, S., Kumar, M.V., Messing, R.O. and Dong, Z. Inhibition of PKCdelta reduces cisplatin-induced nephrotoxicity without blocking chemotherapeutic efficacy in mouse models of cancer. J Clin Invest 121, 2709-2722.

Packham, G. and Cleveland, J.L. (1994) Ornithine decarboxylase is a mediator of c-Myc-induced apoptosis. Mol Cell Biol 14, 5741-5747.

Pan, H., Shen, Z., Mukhopadhyay, P., Wang, H., Pacher, P., Qin, X., Gao, B. (2009) Anaphylatoxin C5a contributes to the pathogenesis of cisplatin-induced nephrotoxicity. Am J Physiol Renal Physiol. 296(3), F496-504.

Panaretakis, T., Joza, N., Modjtahedi, N., Tesniere, A., Vitale, I., Durchschlag, M., Fimia, G.M., Kepp, O., Piacentini, M., Froehlich, K.U., van Endert, P., Zitvogel, L., Madeo, F. and Kroemer, G. (2008) The co-translocation of ERp57 and calreticulin determines the immunogenicity of cell death. Cell Death Differ 15, 1499-1509.

Pankov, R. and Yamada, K.M. (2002) Fibronectin at a glance. J Cell Sci 115, 3861-3863.

Paragas, N., Qiu, A., Zhang, Q., Samstein, B., Deng, S.X., Schmidt-Ott, K.M., Viltard, M., Yu, W., Forster, C.S., Gong, G., Liu, Y., Kulkarni, R., Mori, K., Kalandadze, A., Ratner, A.J., Devarajan, P., Landry, D.W., D'Agati, V., Lin, C.S. and Barasch, J. The Ngal reporter mouse detects the response of the kidney to injury in real time. Nat Med 17, 216-222.

Paragas, N., Qiu, A., Zhang, Q., Samstein, B., Deng, S.X., Schmidt-Ott, K.M., Viltard, M., Yu, W., Forster, C.S., Gong, G., Liu, Y., Kulkarni, R., Mori, K., Kalandadze, A., Ratner, A.J., Devarajan, P., Landry, D.W., D'Agati, V., Lin, C.S. and Barasch, J. The Ngal reporter mouse detects the response of the kidney to injury in real time. Nat Med 17, 216-222.

Park, J.K., Chung, Y.M., Kang, S., Kim, J.U., Kim, Y.T., Kim, H.J., Kim, Y.H., Kim, J.S. and Yoo, Y.D. (2002) c-Myc exerts a protective function through ornithine decarboxylase against cellular insults. Mol Pharmacol 62, 1400-1408.

Peng, W., Chen, J., Jiang, Y., Shou, Z., Chen, Y. and Wang, H. (2007) Non-invasive detection of acute renal allograft rejection by measurement of vascular endothelial growth factor in urine. J Int Med Res 35, 442-449.

Persy, V.P., Verstrepen, W.A., Ysebaert, D.K., De Greef, K.E. and De Broe, M.E. (1999) Differences in osteopontin up-regulation between proximal and distal tubules after renal ischemia/reperfusion. Kidney Int 56, 601-611.

Pfaller, W. and Gstraunthaler, G. (1998) Nephrotoxicity testing in vitro--what we know and what we need to know. Environ Health Perspect 106 Suppl 2, 559-569.

Picken, M.M. Amyloidosis-where are we now and where are we heading? Arch Pathol Lab Med 134, 545-551.

Poklar, N., Pilch, D.S., Lippard, S.J., Redding, E.A., Dunham, S.U. and Breslauer, K.J. (1996) Influence of cisplatin intrastrand crosslinking on the conformation, thermal stability, and energetics of a 20-mer DNA duplex. Proc Natl Acad Sci U S A 93, 7606-7611.

Prabhakar, R., Vreven, T., Morokuma, K. and Musaev, D.G. (2005) Elucidation of the mechanism of selenoprotein glutathione peroxidase (GPx)-catalyzed hydrogen peroxide reduction by two glutathione molecules: a density functional study. Biochemistry 44, 11864-11871.

Prescott, L.F. (2000) Paracetamol: past, present, and future. Am J Ther 7, 143-147.
Prozialeck, W.C., Edwards, J.R., Vaidya, V.S. and Bonventre, J.V. (2009) Preclinical evaluation of novel urinary biomarkers of cadmium nephrotoxicity. Toxicol Appl Pharmacol 238, 301-305.

PredictIV-webpage: www.predict-iv.toxi.uni-wuerzburg.de. Accessed: 04.02.2011

Prozialeck, W.C., Vaidya, V.S., Liu, J., Waalkes, M.P., Edwards, J.R., Lamar, P.C., Bernard, A.M., Dumont, X. and Bonventre, J.V. (2007) Kidney injury molecule-1 is an early biomarker of cadmium nephrotoxicity. Kidney Int 72, 985-993.

PSTC webpage, Predictive Safety Testing Cosortium of the Critical Path Institute. www.c-path.org/pstc.cfm. Accessed: 16.05.2010

Pujol, A., Mosca, R., Farres, J. and Aloy, P. (2010) Unveiling the role of network and systems biology in drug discovery. Trends Pharmacol Sci 31, 115-123.

Pulai, J.I., Chen, H., Im, H.J., Kumar, S., Hanning, C., Hegde, P.S. and Loeser, R.F. (2005) NF-kappa B mediates the stimulation of cytokine and chemokine expression by human articular chondrocytes in response to fibronectin fragments. J Immunol 174, 5781-5788.

Quigg, R.J. (2003) Complement and the kidney. J Immunol 171, 3319-3324.

Rached, E., Hoffmann, D., Blumbach, K., Weber, K., Dekant, W. and Mally, A. (2008) Evaluation of putative biomarkers of nephrotoxicity after exposure to ochratoxin a in vivo and in vitro. Toxicol Sci 103, 371-381.

Radi, R., Beckman, J.S., Bush, K.M. and Freeman, B.A. (1991) Peroxynitrite oxidation of sulfhydryls. The cytotoxic potential of superoxide and nitric oxide. J Biol Chem 266, 4244-4250.

Ramaswamy, S., Tamayo, P., Rifkin, R., Mukherjee, S., Yeang, C.H., Angelo, M., Ladd, C., Reich, M., Latulippe, E., Mesirov, J.P., Poggio, T., Gerald, W., Loda, M., Lander, E.S. and Golub, T.R. (2001) Multiclass cancer diagnosis using tumor gene expression signatures. Proc Natl Acad Sci U S A 98, 15149-15154.

Ramaswamy, S., Tamayo, P., Rifkin, R., Mukherjee, S., Yeang, C.H., Angelo, M., Ladd, C., Reich, M., Latulippe, E., Mesirov, J.P., Poggio, T., Gerald, W., Loda, M., Lander, E.S. and Golub, T.R. (2001) Multiclass cancer diagnosis using tumor gene expression signatures. Proc Natl Acad Sci U S A 98, 15149-15154.

Redl, H., Schlag, G., Paul, E. and Davies, J. (1995) Plasma glutathione S-transferase as an early marker of posttraumatic hepatic injury in non-human primates. Shock 3, 395-397.

Rennke, H.G., Denker, B.M. (2009). “Renal pathophysiology: The Essentials”. 3rd Edition, Lippincott Williams & Wilkins

Reynolds, P.E. (1989) Structure, biochemistry and mechanism of action of glycopeptide antibiotics. Eur J Clin Microbiol Infect Dis 8, 943-950.

Ridley, A.J. (2006) Rho GTPases and actin dynamics in membrane protrusions and vesicle trafficking. Trends Cell Biol 16, 522-529.

RNeasy Plus Mini User Manual, (2010)
http://www.qiagen.com/products/rnastabilizationpurification/rneasysystem/rneasyplusminikit.aspx#Tabs=t2. Accessed: 10.06.2012

Robinson, S., Pool, R. and Griffin, R. (2008) Emerging Safety Science: Workshop Summary Forum on Drug Discovery, Development, and Translation, Institute of Medicine, Chapter 7: Quaifying Biomarkers.

Roempp, H., Falbe, J., Regitz, M., (1992) „Römpp Lexikon Chemie“ 9th Edition Georg Thieme Verlag, Stuttgart

Rosenberg, M.E. and Silkensen, J. (1995) Clusterin: physiologic and pathophysiologic considerations. Int J Biochem Cell Biol 27, 633-645.

Rouse, R.L., Zhang, J., Stewart, S.R., Rosenzweig, B.A., Espandiari, P. and Sadrieh, N.K. Comparative profile of commercially available urinary biomarkers in preclinical drug-induced kidney injury and recovery in rats. Kidney Int 79, 1186-1197.

Rudd, G.N., Hartley, J.A. and Souhami, R.L. (1995) Persistence of cisplatin-induced DNA interstrand crosslinking in peripheral blood mononuclear cells from elderly and young individuals. Cancer Chemother Pharmacol 35, 323-326.

Rudolf, M. and Kuhlisch, W., (2008). Biostatistik- Eine Einführung für Biowissenschaftler, 1st Edition, Pearson Study, Munich.

Ruester, C., Wolf, G. (2006) Renin-angiotensin-aldosterone system and progression of renal disease. J Am Soc Nephrol 17(11), 2985-91.

Russell, W.M.S. and Burch, R.L. (1959). "The Principles of Humane Experimental Technique." Methuen, London, 1959

Ruster, C. and Wolf, G. (2006) Renin-angiotensin-aldosterone system and progression of renal disease. J Am Soc Nephrol 17, 2985-2991.

Rybak, M., Lomaestro, B., Rotschafer, J.C., Moellering, R., Jr., Craig, W., Billeter, M., Dalovisio, J.R. and Levine, D.P. (2009) Therapeutic monitoring of vancomycin in adult patients: a consensus review of the American Society of Health-System Pharmacists, the Infectious Diseases Society of America, and the Society of Infectious Diseases Pharmacists. Am J Health Syst Pharm 66, 82-98.

Draghici, S. (2003). Data Analysis Tools for DNA Microarrays Chapman and Hall/CRC Boca Raton.

Sakurai, H., Suzuki, S., Kawasaki, N., Nakano, H., Okazaki, T., Chino, A., Doi, T. and Saiki, I. (2003) Tumor necrosis factor-alpha-induced IKK phosphorylation of NF-kappaB p65 on serine 536 is mediated through the TRAF2, TRAF5, and TAK1 signaling pathway. J Biol Chem 278, 36916-36923.

Salahudeen, A.K., Haider, N., Jenkins, J., Joshi, M., Patel, H., Huang, H., Yang, M. and Zhe, H. (2008) Antiapoptotic properties of erythropoiesis-stimulating proteins in models of cisplatin-induced acute kidney injury. Am J Physiol Renal Physiol 294, F1354-1365.

Sands, J. M. und Verlander, J. W. (2005). Anatomy and physiology of the kidneys. In Toxicology of the kidney, 3rd Edition, CRC Press, Boca Raton.

Sanz, A.B., Sanchez-Nino, M.D. and Ortiz, A. TWEAK, a multifunctional cytokine in kidney injury. Kidney Int 80, 708-718.

Sanz, A.B., Sanchez-Nino, M.D., Ramos, A.M., Moreno, J.A., Santamaria, B., Ruiz-Ortega, M., Egido, J. and Ortiz, A. NF-kappaB in renal inflammation. J Am Soc Nephrol 21, 1254-1262.

Sastry, S.K. and Horwitz, A.F. (1993) Integrin cytoplasmic domains: mediators of cytoskeletal linkages and extra- and intracellular initiated transmembrane signaling. Curr Opin Cell Biol 5, 819-831.

Sauzeau, V., Carvajal-Gonzalez, J.M., Riolobos, A.S., Sevilla, M.A., Menacho-Marquez, M., Roman, A.C., Abad, A., Montero, M.J., Fernandez-Salguero, P. and Bustelo, X.R. Transcriptional factor aryl hydrocarbon receptor (Ahr) controls cardiovascular and respiratory functions by regulating the expression of the Vav3 proto-oncogene. J Biol Chem 286, 2896-2909.

Sawaya, B.P., Briggs, J.P. and Schnermann, J. (1995) Amphotericin B nephrotoxicity: the adverse consequences of altered membrane properties. J Am Soc Nephrol 6, 154-164.

Schaefer, L., Gilge, U., Heidland, A. and Schaefer, R.M. (1994) Urinary excretion of cathepsin B and cystatins as parameters of tubular damage. Kidney Int Suppl 47, S64-67.

Schaub, S., Wilkins, J.A., Antonovici, M., Krokhin, O., Weiler, T., Rush, D. and Nickerson, P. (2005) Proteomic-based identification of cleaved urinary beta2-microglobulin as a potential marker for acute tubular injury in renal allografts. Am J Transplant 5, 729-738.

Schmidt, R., F. Lang, et al. (2004) "Physiologie des Menschen". 29th Edition, Springer-Verlag GmbH

Schnaper, H.W., (1995) Balance between matrix synthesis and degradation: a determinant of glomerulosclerosis. Pediatr. Nephrol. 9(1), 104–111

Schrier, R.W. (2008) Blood urea nitrogen and serum creatinine: not married in heart failure. Circ Heart Fail 1, 2-5.

Schrijvers, B.F., Flyvbjerg, A. and De Vriese, A.S. (2004) The role of vascular endothelial growth factor (VEGF) in renal pathophysiology. Kidney Int 65, 2003-2017.

Schroeder, A., Mueller, O., Stocker, S., Salowsky, R., Leiber, M., Gassmann, M., Lightfoot, S., Menzel, W., Granzow, M. and Ragg, T. (2006) The RIN: an RNA integrity number for assigning integrity values to RNA measurements. BMC Mol Biol 7, 3.

Schurgers, L.J., Cranenburg, E.C. and Vermeer, C. (2008) Matrix Gla-protein: the calcification inhibitor in need of vitamin K. Thromb Haemost 100, 593-603.

Servais, H., Ortiz, A., Devuyst, O., Denamur, S., Tulkens, P.M. and Mingeot-Leclercq, M.P. (2008) Renal cell apoptosis induced by nephrotoxic drugs: cellular and molecular mechanisms and potential approaches to modulation. Apoptosis 13, 11-32.

Shannan, B., Seifert, M., Leskov, K., Willis, J., Boothman, D., Tilgen, W. and Reichrath, J. (2006) Challenge and promise: roles for clusterin in pathogenesis, progression and therapy of cancer. Cell Death Differ 13, 12-19.

Shen, Y., Yang, T., Wang, J., Xu, Q., Li, R., Pan, W., Li, G., Wang, Z., Tan, J., Wu, J., Wu, F., Wang, L. and Liu, Y. (2007) Indomethacin enhances the cytotoxicity of recombinant human lymphotoxin alpha on tumor cells by suppressing NFkappaB signaling. Cancer Biol Ther 6, 1428-1433.

Shi, L., Jones, W.D., Jensen, R.V., Harris, S.C., Perkins, R.G., Goodsaid, F.M., Guo, L., Croner, L.J., Boysen, C., Fang, H., Qian, F., Amur, S., Bao, W., Barbacioru, C.C., Bertholet, V., Cao, X.M., Chu, T.M., Collins, P.J., Fan, X.H., Frueh, F.W., Fuscoe, J.C., Guo, X., Han, J., Herman, D., Hong, H., Kawasaki, E.S., Li, Q.Z., Luo, Y., Ma, Y., Mei, N., Peterson, R.L., Puri, R.K., Shippy, R., Su, Z., Sun, Y.A., Sun, H., Thorn, B., Turpaz, Y., Wang, C., Wang, S.J., Warrington, J.A., Willey, J.C., Wu, J., Xie, Q., Zhang, L., Zhong, S., Wolfinger, R.D. and Tong, W. (2008) The balance of reproducibility, sensitivity, and specificity of lists of differentially expressed genes in microarray studies. BMC Bioinformatics 9 Suppl 9, S10.

Shihab, F.S., Andoh, T.F., Tanner, A.M. and Bennett, W.M. (1997) Sodium depletion enhances fibrosis and the expression of TGF-beta1 and matrix proteins in experimental chronic cyclosporine nephropathy. Am J Kidney Dis 30, 71-81.

Shihab, F.S., Bennett, W.M., Yi, H. and Andoh, T.F. (2001) Expression of vascular endothelial growth factor and its receptors Flt-1 and KDR/Flk-1 in chronic cyclosporine nephrotoxicity. Transplantation 72, 164-168.

Shui, H.A., Ka, S.M., Yang, S.M., Lin, Y.F., Lo, Y.F. and Chen, A. (2007) Osteopontin as an injury marker expressing in epithelial hyperplasia lesions helpful in prognosis of focal segmental glomerulosclerosis. Transl Res 150, 216-222.

Si, W., Kang, Q., Luu, H.H., Park, J.K., Luo, Q., Song, W.X., Jiang, W., Luo, X., Li, X., Yin, H., Montag, A.G., Haydon, R.C. and He, T.C. (2006) CCN1/Cyr61 is regulated by the canonical Wnt signal and plays an important role in Wnt3A-induced osteoblast differentiation of mesenchymal stem cells. Mol Cell Biol 26, 2955-2964.

Sibalic, V., Fan, X., Loffing, J. and Wuthrich, R.P. (1997) Upregulated renal tubular CD44, hyaluronan, and osteopontin in kdkd mice with interstitial nephritis. Nephrol Dial Transplant 12, 1344-1353.

Sieber, M., Hoffmann, D., Adler, M., Vaidya, V.S., Clement, M., Bonventre, J.V., Zidek, N., Rached, E., Amberg, A., Callanan, J.J., Dekant, W. and Mally, A. (2009) Comparative analysis of novel noninvasive renal biomarkers and metabonomic changes in a rat model of gentamicin nephrotoxicity. Toxicol Sci 109, 336-349.

Simerville, J.A., Maxted, W.C. and Pahira, J.J. (2005) Urinalysis: a comprehensive review. Am Fam Physician 71, 1153-1162.

Sin, W., Chen, X., Leung, T., Lim, L. (1998) RhoA-Binding Kinase α Translocation Is Facilitated by the Collapse of the Vimentin Intermediate Filament Network Mol. Cell. Biol. 18, 11

Singal, P.K., Deally, C.M. and Weinberg, L.E. (1987) Subcellular effects of adriamycin in the heart: a concise review. J Mol Cell Cardiol 19, 817-828.

Singh, A., Jayaraman, A. and Hahn, J. (2006) Modeling regulatory mechanisms in IL-6 signal transduction in hepatocytes. Biotechnol Bioeng 95, 850-862.

Solichova, P., Karpisek, M., Ochmanova, R., Hanulova, Z., Humenanska, V., Stejskal, D. and Bartek, J. (2007) Urinary clusterin concentrations--a possible marker of nephropathy? Pilot study. Biomed Pap Med Fac Univ Palacky Olomouc Czech Repub 151, 233-236.

Standford School of Medicine Homepage (2012), Nephrology in the Department of Medicine: http://med.stanford.edu/nephrology/images/Kidney05-custom.jpg; Accessed 08.12.2012

Steemers, F.J. and Gunderson, K.L. (2005) Illumina, Inc. Pharmacogenomics 6, 777-782.

Steitz, S.A., Speer, M.Y., Curinga, G., Yang, H.Y., Haynes, P., Aebersold, R., Schinke, T., Karsenty, G. and Giachelli, C.M. (2001) Smooth muscle cell phenotypic transition associated with calcification: upregulation of Cbfa1 and downregulation of smooth muscle lineage markers. Circ Res 89, 1147-1154.

Stemmer, K., Ellinger-Ziegelbauer, H., Ahr, H.J. and Dietrich, D.R. (2007) Carcinogen-specific gene expression profiles in short-term treated Eker and wild-type rats indicative of pathways involved in renal tumorigenesis. Cancer Res 67, 4052-4068.

Stevens, L.A., Coresh, J., Greene, T. and Levey, A.S. (2006) Assessing kidney function--measured and estimated glomerular filtration rate. N Engl J Med 354, 2473-2483.

Stiborova, M., Frei, E., Arlt, V.M. and Schmeiser, H.H. (2009) The role of biotransformation enzymes in the development of renal injury and urothelial cancer caused by aristolochic acid: urgent questions and difficult answers. Biomed Pap Med Fac Univ Palacky Olomouc Czech Repub 153, 5-11.

Sugimoto, H., Hamano, Y., Charytan, D., Cosgrove, D., Kieran, M., Sudhakar, A. and Kalluri, R. (2003) Neutralization of circulating vascular endothelial growth factor (VEGF) by anti-VEGF antibodies and soluble VEGF receptor 1 (sFlt-1) induces proteinuria. J Biol Chem 278, 12605-12608.

Sumanasekera, W.K., Tien, E.S., Turpey, R., Vanden Heuvel, J.P. and Perdew, G.H. (2003) Evidence that peroxisome proliferator-activated receptor alpha is complexed with the 90-kDa heat shock protein and the hepatitis virus B X-associated protein 2. J Biol Chem 278, 4467-4473.

Suter, L., Schroeder, S., Meyer, K., Gautier, J.C., Amberg, A., Wendt, M., Gmuender, H., Mally, A., Boitier, E., Ellinger-Ziegelbauer, H., Matheis, K. and Pfannkuch, F. EU framework 6 project: predictive toxicology (PredTox)--overview and outcome. Toxicol Appl Pharmacol 252, 73-84.

Tacchini, L., De Ponti, C., Matteucci, E., Follis, R. and Desiderio, M.A. (2004) Hepatocyte growth factor-activated NF-kappaB regulates HIF-1 activity and ODC expression, implicated in survival, differently in different carcinoma cell lines. Carcinogenesis 25, 2089-2100.

Tadagavadi, R.K. and Reeves, W.B. (2010) Endogenous IL-10 attenuates cisplatin nephrotoxicity: role of dendritic cells. J Immunol 185, 4904-4911.

Taher, T.E., Smit, L., Griffioen, A.W., Schilder-Tol, E.J., Borst, J. and Pals, S.T. (1996) Signaling through CD44 is mediated by tyrosine kinases. Association with p56lck in T lymphocytes. J Biol Chem 271, 2863-2867.

Takahara, P.M., Rosenzweig, A.C., Frederick, C.A. and Lippard, S.J. (1995) Crystal structure of double-stranded DNA containing the major adduct of the anticancer drug cisplatin. Nature 377, 649-652.

Takahashi, Y., Li, L., Kamiryo, M., Asteriou, T., Moustakas, A., Yamashita, H. and Heldin, P. (2005) Hyaluronan fragments induce endothelial cell differentiation in a CD44- and CXCL1/GRO1-dependent manner. J Biol Chem 280, 24195-24204.

Takashi, M., Hasegawa, S., Ohmuta, M., Ohshima, S. and Kato, K. (1998) Significant elevation of urinary 28-kD calbindin-D and N-acetyl-beta-D-glucosaminidase levels in patients undergoing extracorporeal shock wave lithotripsy. Int Urol Nephrol 30, 407-415.

Takeda, K., Kaisho, T., Yoshida, N., Takeda, J., Kishimoto, T. and Akira, S. (1998) Stat3 activation is responsible for IL-6-dependent T cell proliferation through preventing apoptosis: generation and characterization of T cell-specific Stat3-deficient mice. J Immunol 161, 4652-4660.

Tanaka, Y., Engelender, S., Igarashi, S., Rao, R.K., Wanner, T., Tanzi, R.E., Sawa, A., V, L.D., Dawson, T.M. and Ross, C.A. (2001) Inducible expression of mutant alpha-synuclein decreases proteasome activity and increases sensitivity to mitochondria-dependent apoptosis. Hum Mol Genet 10, 919-926.

Tao, Y., Hu, L., Li, S., Liu, Q., Wu, X., Li, D., Fu, P., Wei, D. and Luo, Z. Tranilast prevents the progression of chronic cyclosporine nephrotoxicity through regulation of transforming growth factor beta/Smad pathways. Transplant Proc 43, 1985-1988.

Tarloff, J.B., Khairallah, E.A., Cohen, S.D. and Goldstein, R.S. (1996) Sex- and age-dependent acetaminophen hepato- and nephrotoxicity in Sprague-Dawley rats: role of tissue accumulation, nonprotein sulfhydryl depletion, and covalent binding. Fundam Appl Toxicol 30, 13-22.

Teomed Homepage (2012), http://www.teomed.ch/de/labor/luminex-technologie, Accessed 08.12.2012

Theilhaber, J., Connolly, T., Roman-Roman, S., Bushnell, S., Jackson, A., Call, K., Garcia, T. and Baron, R. (2002) Finding genes in the C2C12 osteogenic pathway by k-nearest-neighbor classification of expression data. Genome Res 12, 165-176.

Thermo Scientific (2008). NanoDrop 1000 Spectrophotometer V3.7 User's Manual. Stand: Juli 2008. http://www.nanodrop.com/Library/nd-1000-v3.7-users-manual-8.5x11.pdf. Accessed: 25.06.2010.

Thompson, K.L., Afshari, C.A., Amin, R.P., Bertram, T.A., Car, B., Cunningham, M., Kind, C., Kramer, J.A., Lawton, M., Mirsky, M., Naciff, J.M., Oreffo, V., Pine, P.S. and Sistare, F.D. (2004) Identification of platform-independent gene expression markers of cisplatin nephrotoxicity. Environ Health Perspect 112, 488-494.

Thukral, S.K., Nordone, P.J., Hu, R., Sullivan, L., Galambos, E., Fitzpatrick, V.D., Healy, L., Bass, M.B., Cosenza, M.E. and Afshari, C.A. (2005) Prediction of nephrotoxicant action and identification of candidate toxicity-related biomarkers. Toxicol Pathol 33, 343-355.

Todorovic, V., Chen, C.C., Hay, N. and Lau, L.F. (2005) The matrix protein CCN1 (CYR61) induces apoptosis in fibroblasts. J Cell Biol 171, 559-568.

Togashi, Y., Sakaguchi, Y., Miyamoto, M. and Miyamoto, Y. Urinary cystatin C as a biomarker for acute kidney injury and its immunohistochemical localization in kidney in the CDDP-treated rats. Exp Toxicol Pathol.

Tong, X., Xie, D., O'Kelly, J., Miller, C.W., Muller-Tidow, C. and Koeffler, H.P. (2001) Cyr61, a member of CCN family, is a tumor suppressor in non-small cell lung cancer. J Biol Chem 276, 47709-47714.

Toxicogenomics Project in Japan (2002-2007) http://wwwtgp.nibio.go.jp/index-e.html. Accessed: 22.08.2011

Toyoguchi, T., Takahashi, S., Hosoya, J., Nakagawa, Y. and Watanabe, H. (1997) Nephrotoxicity of vancomycin and drug interaction study with cilastatin in rabbits. Antimicrob Agents Chemother 41, 1985-1990.

Tran, N.L., McDonough, W.S., Savitch, B.A., Sawyer, T.F., Winkles, J.A. and Berens, M.E. (2005) The tumor necrosis factor-like weak inducer of apoptosis (TWEAK)-fibroblast growth factor-inducible 14 (Fn14) signaling system regulates glioma cell survival via NFkappaB pathway activation and BCL-XL/BCL-W expression. J Biol Chem 280, 3483-3492.

Trougakos, I.P., Lourda, M., Agiostratidou, G., Kletsas, D. and Gonos, E.S. (2005) Differential effects of clusterin/apolipoprotein J on cellular growth and survival. Free Radic Biol Med 38, 436-449.

Tuschl, G., Lauer, B., Mueller, S.O. (2008) Primary hepatocytes as a model to analyze species-specific toxicity and drug metabolism Expert Opin Drug Metab Toxicol 4 (7), 855-870

Tyagi, S., Gupta, P., Saini, A.S., Kaushal, C., Sharma, S. (2011). The peroxisome proliferator-activated receptor: A family of nuclear receptors role in various diseases. J Adv Pharm Technol Res 2 (4), 236–40.

Uchida, K. and Gotoh, A. (2002) Measurement of cystatin-C and creatinine in urine. Clin Chim Acta 323, 121-128.

Uchino, S., Kellum, J.A., Bellomo, R., Doig, G.S., Morimatsu, H., Morgera, S., Schetz, M., Tan, I., Bouman, C., Macedo, E., Gibney, N., Tolwani, A. and Ronco, C. (2005) Acute renal failure in critically ill patients: a multinational, multicenter study. JAMA 294, 813-818.

Usuda, K., Kono, K., Dote, T., Nishiura, K., Miyata, K., Nishiura, H., Shimahara, M. and Sugimoto, K. (1998) Urinary biomarkers monitoring for experimental fluoride nephrotoxicity. Arch Toxicol 72, 104-109.

Usuda, K., Kono, K., Dote, T., Nishiura, K., Miyata, K., Nishiura, H., Shimahara, M. and Sugimoto, K. (1998) Urinary biomarkers monitoring for experimental fluoride nephrotoxicity. Arch Toxicol 72, 104-109.

Vaidya, V.S., Waikar, S.S., Ferguson, M.A., Collings, F.B., Sunderland, K., Gioules, C., Bradwin, G., Matsouaka, R., Betensky, R.A., Curhan, G.C. and Bonventre, J.V. (2008) Urinary biomarkers for sensitive and specific detection of acute kidney injury in humans. Clin Transl Sci 1, 200-208.

van Timmeren, M.M., Vaidya, V.S., van Ree, R.M., Oterdoom, L.H., de Vries, A.P., Gans, R.O., van Goor, H., Stegeman, C.A., Bonventre, J.V. and Bakker, S.J. (2007) High urinary excretion of kidney injury molecule-1 is an independent predictor of graft loss in renal transplant recipients. Transplantation 84, 1625-1630.

Vanherweghem, J.L., Depierreux, M., Tielemans, C., Abramowicz, D., Dratwa, M., Jadoul, M., Richard, C., Vandervelde, D., Verbeelen, D., Vanhaelen-Fastre, R. and et al. (1993) Rapidly progressive interstitial renal fibrosis in young women: association with slimming regimen including Chinese herbs. Lancet 341, 387-391.

Varlam, D.E., Siddiq, M.M., Parton, L.A. and Russmann, H. (2001) Apoptosis contributes to amphotericin B-induced nephrotoxicity. Antimicrob Agents Chemother 45, 679-685.

Vayssiere, B., Zalcman, G., Mahe, Y., Mirey, G., Ligensa, T., Weidner, K.M., Chardin, P. and Camonis, J. (2000) Interaction of the Grb7 adapter protein with Rnd1, a new member of the Rho family. FEBS Lett 467, 91-96.

Viracore Homepage (2012), http://www.viracor.com/Learning-Lab/Luminex, Accessed 08.12.2012

Wagener, G., Gubitosa, G., Wang, S., Borregaard, N., Kim, M. and Lee, H.T. (2008) Urinary neutrophil gelatinase-associated lipocalin and acute kidney injury after cardiac surgery. Am J Kidney Dis 52, 425-433.

Wakelin, S.J., Marson, L., Howie, S.E., Garden, J., Lamb, J.R. and Forsythe, J.L. (2004) The role of vascular endothelial growth factor in the kidney in health and disease. Nephron Physiol 98, p73-79.

Walev, I. and Bhakdi, S. (1996) Possible reason for preferential damage to renal tubular epithelial cells evoked by amphotericin B. Antimicrob Agents Chemother 40, 1116-1120.

Walisser, J.A., Glover, E., Pande, K., Liss, A.L. and Bradfield, C.A. (2005) Aryl hydrocarbon receptor-dependent liver development and hepatotoxicity are mediated by different cell types. Proc Natl Acad Sci U S A 102, 17858-17863.

Walker, P.D., Barri, Y. and Shah, S.V. (1999) Oxidant mechanisms in gentamicin nephrotoxicity. Ren Fail 21, 433-442.

Wang, E.J., Snyder, R.D., Fielden, M.R., Smith, R.J. and Gu, Y.Z. (2008) Validation of putative genomic biomarkers of nephrotoxicity in rats. Toxicology 246, 91-100.

Wang, J., Huo, K., Ma, L., Tang, L., Li, D., Huang, X., Yuan, Y., Li, C., Wang, W., Guan, W., Chen, H., Jin, C., Wei, J., Zhang, W., Yang, Y., Liu, Q., Zhou, Y., Zhang, C., Wu, Z., Xu, W., Zhang, Y., Liu, T., Yu, D., Chen, L., Zhu, D., Zhong, X., Kang, L., Gan, X., Yu, X., Ma, Q., Yan, J., Zhou, L., Liu, Z., Zhu, Y., Zhou, T., He, F. and Yang, X. (2011) Toward an understanding of the protein interaction network of the human liver. Mol Syst Biol 7, 536.

Wang, S., Zhan, M., Yin, J., Abraham, J.M., Mori, Y., Sato, F., Xu, Y., Olaru, A., Berki, A.T., Li, H., Schulmann, K., Kan, T., Hamilton, J.P., Paun, B., Yu, M.M., Jin, Z., Cheng, Y., Ito, T., Mantzur, C., Greenwald, B.D. and Meltzer, S.J. (2006) Transcriptional profiling suggests that Barrett's metaplasia is an early intermediate stage in esophageal adenocarcinogenesis. Oncogene 25, 3346-3356.

Wang, T. (2006) Flow-activated transport events along the nephron. Curr Opin Nephrol Hypertens 15, 530-536.

Wapstra, F.H., van Goor, H., de Jong, P.E., Navis, G. and de Zeeuw, D. (1999) Dose of doxorubicin determines severity of renal damage and responsiveness to ACE-inhibition in experimental nephrosis. J Pharmacol Toxicol Methods 41, 69-73.

Wasilewska, A.M. and Zoch-Zwierz, W.M. (2008) Urinary levels of matrix metalloproteinases and their tissue inhibitors in nephrotic children. Pediatr Nephrol 23, 1795-1802.

Waters, M.D. and Fostel, J.M. (2004) Toxicogenomics and systems toxicology: aims and prospects. Nat Rev Genet 5, 936-948.

Weber, G.F., Ashkar, S., Glimcher, M.J. and Cantor, H. (1996) Receptor-ligand interaction between CD44 and osteopontin (Eta-1). Science 271, 509-512.

Webster, N.L. and Crowe, S.M. (2006) Matrix metalloproteinases, their production by monocytes and macrophages and their potential role in HIV-related diseases. J Leukoc Biol 80, 1052-1066.

Wesson, J.A., Johnson, R.J., Mazzali, M., Beshensky, A.M., Stietz, S., Giachelli, C., Liaw, L., Alpers, C.E., Couser, W.G., Kleinman, J.G. and Hughes, J. (2003) Osteopontin is a critical inhibitor of calcium oxalate crystal formation and retention in renal tubules. J Am Soc Nephrol 14, 139-147.

Wheeler, D.S., Devarajan, P., Ma, Q., Harmon, K., Monaco, M., Cvijanovich, N. and Wong, H.R. (2008) Serum neutrophil gelatinase-associated lipocalin (NGAL) as a marker of acute kidney injury in critically ill children with septic shock. Crit Care Med 36, 1297-1303.

White, L.E. and Hassoun, H.T. Inflammatory Mechanisms of Organ Crosstalk during Ischemic Acute Kidney Injury. Int J Nephrol 2012, 505197.

Wieser, M., Stadler, G., Jennings, P., Streubel, B., Pfaller, W., Ambros, P., Riedl, C., Katinger, H., Grillari, J. and Grillari-Voglauer, R. (2008) hTERT alone immortalizes epithelial cells of renal proximal tubules without changing their functional characteristics. Am J Physiol Renal Physiol 295, F1365-1375.

Wiesinger, M., Mayer, B., Jennings, P. and Lukas, A. Comparative analysis of perturbed molecular pathways identified in in vitro and in vivo toxicology studies. Toxicol In Vitro.

Wilcox, C.S, (1999) Metabolic and adverse effects of diuretics. Semin Nephrol 19, 557–568

Wiley, S.R., Cassiano, L., Lofton, T., Davis-Smith, T., Winkles, J.A., Lindner, V., Liu, H., Daniel, T.O., Smith, C.A. and Fanslow, W.C. (2001) A novel TNF receptor family member binds TWEAK and is implicated in angiogenesis. Immunity 15, 837-846.

Willson, R.A. (2002) Nephrotoxicity of interferon alfa-ribavirin therapy for chronic hepatitis C. J Clin Gastroenterol 35, 89-92.

Winckler, J. (1974) [Vital staining of lysosomes and other cell organelles of the rat with neutral red (author's transl)]. Prog Histochem Cytochem 6, 1-91.

Witzgall, R., Brown, D., Schwarz, C. and Bonventre, J.V. (1994) Localization of proliferating cell nuclear antigen, vimentin, c-Fos, and clusterin in the postischemic kidney. Evidence for a heterogenous genetic response among nephron segments, and a large pool of mitotically active and dedifferentiated cells. J Clin Invest 93, 2175-2188.

Woodrum, D.T., Ford, J.W., Ailawadi, G., Pearce, C.G., Sinha, I., Eagleton, M.J., Henke, P.K., Stanley, J.C., Upchurch, G.R. Jr. (2005) Gender differences in rat aortic smooth muscle cell matrix metalloproteinase-9. J Am Coll Surg 201, 398-404

Wu, H., Ma, J., Wang, P., Corpuz, T.M., Panchapakesan, U., Wyburn, K.R. Chadban, S.J., (2010) HMGB1 Contributes to Kidney Ischemia Reperfusion Injury J Am Soc Nephrol. 21(11), 1878–1890.

Xie, J. and Shaikh, Z.A. (2006) Cadmium-induced apoptosis in rat kidney epithelial cells involves decrease in nuclear factor-kappa B activity. Toxicol Sci 91, 299-308.

Xie, Y., Nishi, S., Iguchi, S., Imai, N., Sakatsume, M., Saito, A., Ikegame, M., Iino, N., Shimada, H., Ueno, M., Kawashima, H., Arakawa, M. and Gejyo, F. (2001) Expression of osteopontin in gentamicin-induced acute tubular necrosis and its recovery process. Kidney Int 59, 959-974.

Xiong, X.L., Jia, R.H., Yang, D.P. and Ding, G.H. (2006) Irbesartan attenuates contrast media-induced NRK-52E cells apoptosis. Pharmacol Res 54, 253-260.

Wright, E.M., Hirayama, B.A., Loo, D.F. (2007) Active sugar transport in health and disease. J. Intern. Med. 261, 32–43.

Yang, A., Trajkovic, D., Illanes, O. and Ramiro-Ibanez, F. (2007) Clinicopathological and tissue indicators of para-aminophenol nephrotoxicity in sprague-dawley rats. Toxicol Pathol 35, 521-532.

Yang, L., Li, X. and Wang, H. (2007) Possible mechanisms explaining the tendency towards interstitial fibrosis in aristolochic acid-induced acute tubular necrosis. Nephrol Dial Transplant 22, 445-456.

Yang, Y., Ji, S., Wang, C. and Hou, Y. (2001) Apoptosis of renal tubular cells in congenital hydronephrosis. Chin Med J (Engl) 114, 502-505.

Yao, X., Panichpisal, K., Kurtzman, N. and Nugent, K. (2007) Cisplatin nephrotoxicity: a review. Am J Med Sci 334, 115-124.

Yoneda, T., Imaizumi, K., Oono, K., Yui, D., Gomi, F., Katayama, T. and Tohyama, M. (2001) Activation of caspase-12, an endoplastic reticulum (ER) resident caspase, through tumor necrosis factor receptor-associated factor 2-dependent mechanism in response to the ER stress. J Biol Chem 276, 13935-13940.

Yuen, P.S., Jo, S.K., Holly, M.K., Hu, X. and Star, R.A. (2006) Ischemic and nephrotoxic acute renal failure are distinguished by their broad transcriptomic responses. Physiol Genomics 25, 375-386.

Zhan, Y., Cleveland, J.L. and Stevens, J.L. (1997) A role for c-myc in chemically induced renal-cell death. Mol Cell Biol 17, 6755-6764.

Zhang, D., Ai, D., Tanaka, H., Hammock, B.D. and Zhu, Y. DNA methylation of the promoter of soluble epoxide hydrolase silences its expression by an SP-1-dependent mechanism. Biochim Biophys Acta 1799, 659-667.

Zhang, J., Goering, P.L., Espandiari, P., Shaw, M., Bonventre, J. V., Vaidya, V. S., Brown, R. P., Keenan, J., Kilty, C. G., Sadrieh, N., and Hanig, J. P. (2009). Differences in immunolocalization of Kim-1, RPA-1, and RPA-2 in kidneys of gentamicin-, cisplatin-, and valproic acid-treated rats: potential role of iNOS and nitrotyrosine. Toxicol Pathol 37, 629–43.

Zhou, Y., Vaidya, V.S., Brown, R.P., Zhang, J., Rosenzweig, B.A., Thompson, K.L., Miller, T.J., Bonventre, J.V. and Goering, P.L. (2008) Comparison of kidney injury molecule-1 and other nephrotoxicity biomarkers in urine and kidney following acute exposure to gentamicin, mercury, and chromium. Toxicol Sci 101, 159-170.

Zhu, B., Suzuki, K., Goldberg, H.A., Rittling, S.R., Denhardt, D.T., McCulloch, C.A. and Sodek, J. (2004) Osteopontin modulates CD44-dependent chemotaxis of peritoneal macrophages through G-protein-coupled receptors: evidence of a role for an intracellular form of osteopontin. J Cell Physiol 198, 155-167.

Zhu, G., Xiang, X., Chen, X., Wang, L., Hu, H. and Weng, S. (2009) Renal dysfunction induced by long-term exposure to depleted uranium in rats. Arch Toxicol 83, 37-46.

5 Annexes

5.1 Annex 1 Immunohistochemical observations of control animals

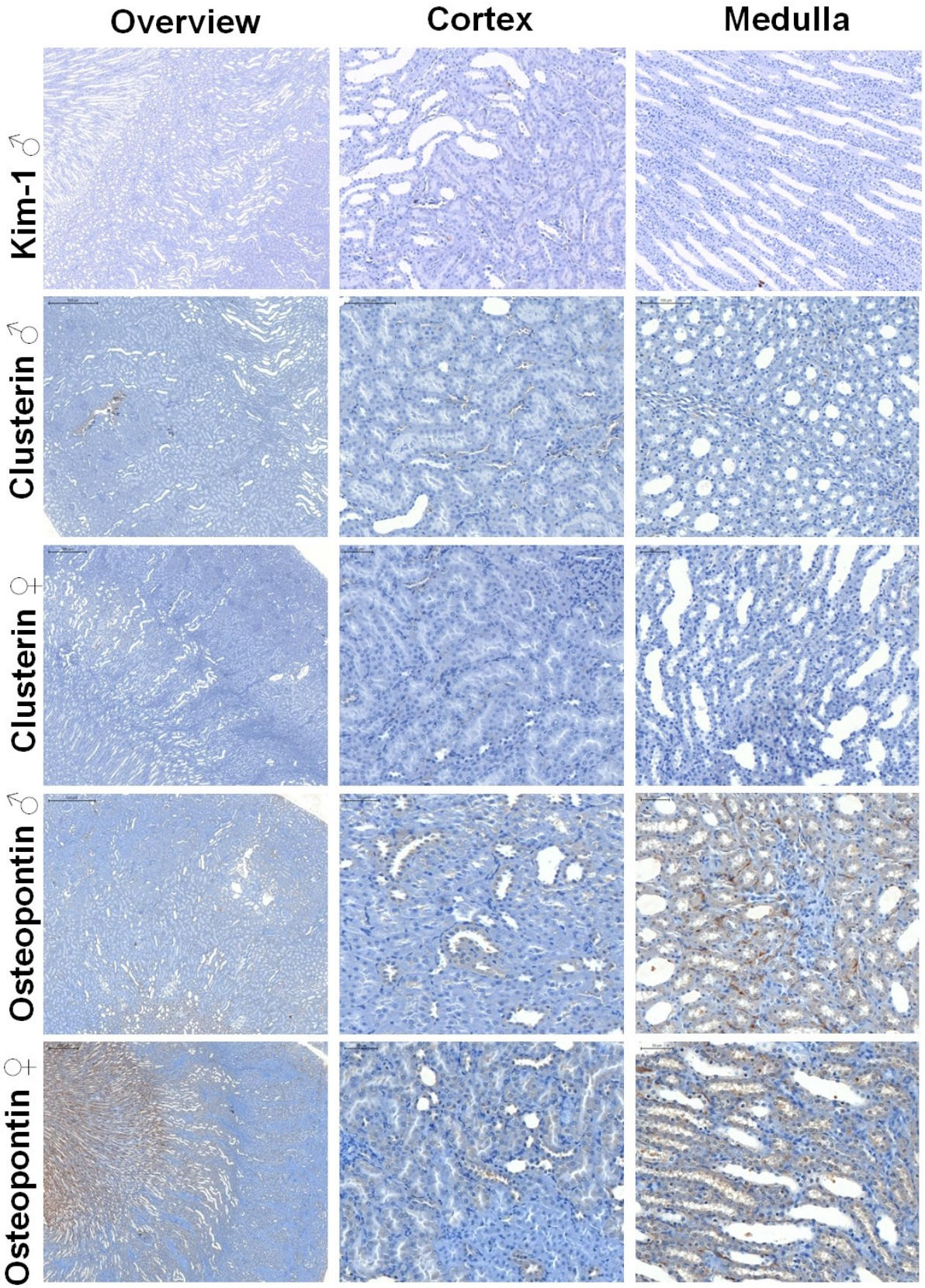

Figure 5-1 Displayed are the immunhistochemical staining of renal Kim-1, Clusterin and Osteopotin protein in representativ male and female control rats. No to minimal protein staining could be observed for Kim-1 and Clusterin, while Osteopontin showed some background staining formally in the medullary region.

A

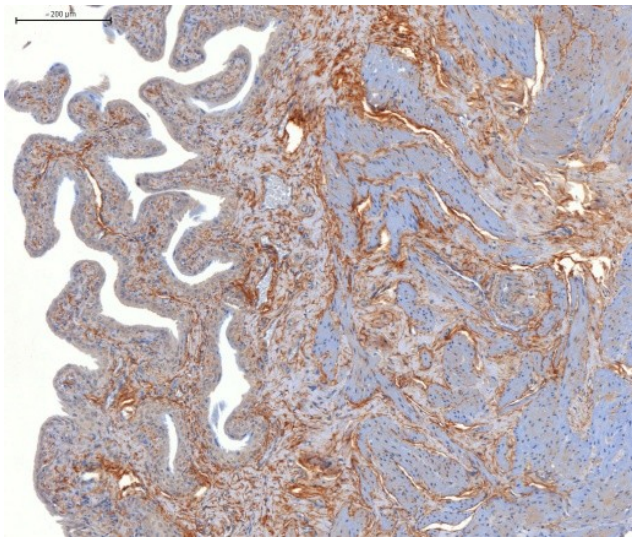

B

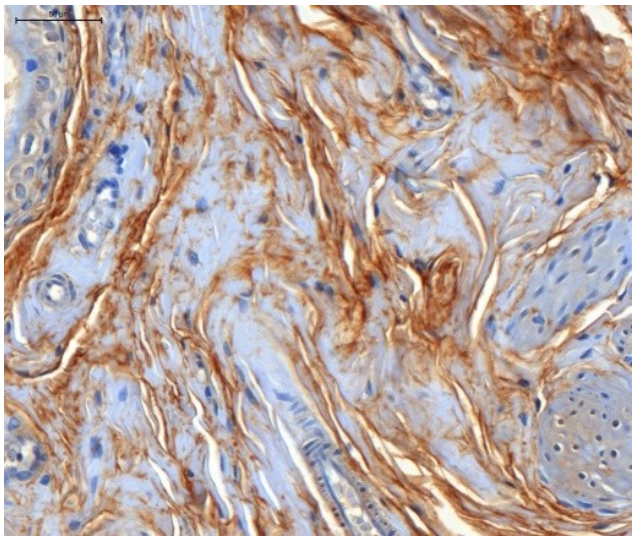

C

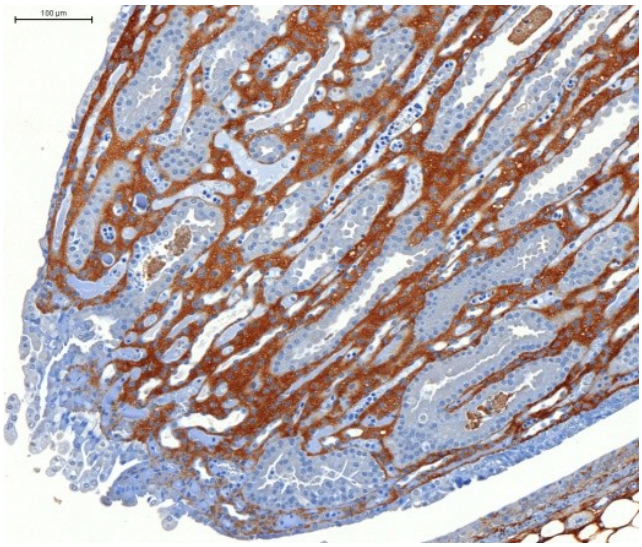

Figure 5-2 Shown is the expression/ accumulation of Osteopontin protein in the (A+B) bladder and (C) renal papilla of untreated rats.

5.2 Annex 2 Signaling pathway related fold-change values of Vancomycin treated rats

Table 5-1 Given are the fold-changes (average of treated rats against average of corresponding control rats) of components of the complement system of male rats treated with either 50 mg/kg (LD) or 300 mg/kg (HD) Vancomycin for up to 28 days. Genes were selected by t-test of HD treated rats ($p \leq 0.01$, $q \leq 0.01$, fold-change $\geq 1.5 / \leq -1.5$).

Symbol	Entrez Gene Name	Gene Entrez	Day 4		Day 8		Day 15		Day 29	
			LD	HD	LD	HD	LD	HD	LD	HD
C2	complement component 2	24231	-1,15	5,92	1,25	7,97	-1,19	13,58	-1,03	4,42
C3	complement component 3	24232	1,17	11,78	1,29	8,35	-1,48	6,16	-1,01	3,15
C6	complement component 6	24237	1,22	1,90	1,11	1,95	-1,05	2,11	1,11	1,60
C7	complement component 7	117517	1,50	5,48	1,23	5,66	-1,28	8,41	1,10	4,73
C1QA	complement component 1, q subcomponent, A chain	298566	-1,37	2,88	1,25	4,49	-1,37	6,75	-1,16	2,45
C1QB	complement component 1, q subcomponent, B chain	29687	-1,05	5,72	1,15	7,09	-1,40	12,11	-1,15	4,25
C1QC	complement component 1, q subcomponent, C chain	362634	-1,20	4,33	1,09	4,98	-1,47	9,12	-1,11	3,47
C1R	complement component 1, r subcomponent	312705	-1,39	1,99	1,41	3,39	-1,44	3,26	-1,30	1,58
C1S	complement component 1, s subcomponent	192262	-1,20	1,71	1,60	4,28	-1,31	3,49	-1,02	1,54
C4B	complement component 4B (Chido blood group)	24233|406161	1,67	9,07	-1,19	9,35	-1,40	10,46	-1,30	8,01
C4BPA	complement component 4 binding protein, alpha	24235	1,30	7,08	-1,08	2,10	-1,08	2,36	-1,02	1,95
C8G	complement component 8, gamma polypeptide	296545	-1,59	-2,02	/	/	-1,21	-1,70	/	/
CFI	complement factor I	79126	2,05	5,92	1,06	5,96	-1,27	10,42	-1,21	7,31
SERPING1	serpin peptidase inhibitor, clade G, member 1	295703	-1,47	1,82	-1,31	2,90	-1,06	2,47	-1,55	1,78

Table 5-2 Given are the fold-changes (average of treated rats against average of corresponding control rats) of components of the complement system of female rats treated with either 50 mg/kg (LD) or 300 mg/kg (HD) Vancomycin for up to 28 days. Genes were selected by t-test of HD treated rats ($p \leq 0.01$, $q \leq 0.01$, fold-change $\geq 1.5 / \leq -1.5$).

Symbol	Entrez Gene Name	Gene Entrez	Day 4		Day 8		Day 15		Day 29	
			LD	HD	LD	HD	LD	HD	LD	HD
C2	complement component 2	24231	-1.15	3.64	1.52	15.50	1.16	2.49	1.45	4.48
C3	complement component 3	24232	-1.06	2.77	1.05	5.48	-1.02	1.77	1.04	3.50
C7	complement component 7	117517	1.39	7.87	-1.06	8.47	-1.00	2.44	1.97	3.91
C1QA	complement component 1, q subcomponent, A chain	298566	1.23	3.25	1.34	7.74	1.20	2.23	1.73	4.20
C1QB	complement component 1, q subcomponent, B chain	29687	1.05	4.95	1.06	12.69	1.19	3.05	1.93	8.29
C1QC	complement component 1, q subcomponent, C chain	362634	1.36	4.85	1.17	10.38	1.17	2.87	1.77	6.45
C1R	complement component 1, r subcomponent	312705	1.38	3.05	1.32	5.17	1.16	1.91	2.08	3.47
C1S	complement component 1, s subcomponent	192262	1.66	2.79	1.83	4.67	1.24	1.66	2.71	3.32
C4B	complement component 4B (Chido blood group)	24233|406161	-1.05	6.33	1.23	12.25	-1.03	2.13	1.39	6.53

Symbol	Entrez Gene Name	Gene Entrez	Day 4		Day 8		Day 15		Day 29	
CFI	complement factor I	79126	-1.17	8.59	1.07	11.06	1.01	2.44	2.11	7.19
SERPING1	serpin peptidase inhibitor, clade G, member 1	295703	1.21	3.59	1.45	5.67	1.04	1.61	1.37	2.41

Table 5-3 Given are the fold-changes (average of treated rats against average of corresponding control rats) of leukocyte extravasations of male rats treated with either 50 mg/kg (LD) or 300 mg/kg (HD) Vancomycin for up to 28 days. Genes were selected by t-test of HD treated rats ($p \leq 0.01$, $q \leq 0.01$, fold-change $\geq 1.5 / \leq -1.5$).

Symbol	Entrez Gene Name	Entrez Gene ID	Day 4		Day 8		Day 15		Day 29	
			LD	HD	LD	HD	LD	HD	LD	HD
ABL1	c-abl oncogene 1, non-receptor tyrosine kinase	311860	/	/	-1.30	1.99	1.36	2.58	/	/
ACTB	actin, beta	81822	/	/	-1.38	2.05	-1.09	2.25	-1.35	1.94
ACTN1	actinin, alpha 1	81634	1.24	2.69	1.02	3.60	-1.02	1.95	1.17	4.82
ACTN4	actinin, alpha 4	63836	-1.53	-1.15	/	/	1.10	1.62	/	/
ARHGAP1	Rho GTPase activating protein 1	311193	/	/	-1.22	1.71	1.02	1.91	/	/
ARHGAP8	Rho GTPase activating protein 8	300115	/	/	-1.23	1.73	1.14	2.39	/	/
ARHGAP9	Rho GTPase activating protein 9	362893	-1.20	1.58	-1.10	2.60	1.17	2.48	1.04	1.77
BTK	Bruton agammaglobulinemia tyrosine kinase	367901	1.22	1.55	-1.02	1.87	1.07	1.67	/	/
CD44	CD44 molecule (Indian blood group)	25406	1.08	4.19	-1.02	8.18	1.07	4.72	1.15	5.22
CLDN1	claudin 1	65129	/	/	-1.11	2.63	1.13	2.05	1.12	2.49
CLDN2	claudin 2	300920	-1.84	1.05	/	/	-1.36	1.82	-1.51	1.52
CLDN3	claudin 3	65130	-1.70	1.55	-1.24	2.64	-1.01	3.52	-1.45	1.76
CLDN4	claudin 4	304407	-1.12	3.32	-1.17	6.22	1.09	3.95	-1.12	3.21
CLDN9	claudin 9	287099	-1.31	1.55	-1.07	3.52	1.17	2.24	-1.10	1.83
CLDN19	claudin 19	298487	/	/	-1.13	2.37	1.15	1.77	-1.30	1.90
CTNNB1	catenin, beta 1, 88kDa	84353	/	/	-1.24	1.86	1.09	2.25	-1.21	1.63
CTTN	cortactin	60465	/	/	-1.19	1.77	-1.03	1.56	-1.21	1.51
CXCR4	chemokine (C-X-C motif) receptor 4	60628	/	/	-1.00	2.31	1.04	2.03	-1.07	1.73
CYBB	cytochrome b-245, beta polypeptide	66021	1.12	2.53	1.03	3.90	1.25	3.16	1.12	2.28
GNAI2	guanine nucleotide binding protein, alpha inhibiting activity polypeptide 2	81664	/	/	-1.32	2.19	1.12	2.29	-1.31	1.52
ICAM1	intercellular adhesion molecule 1	25464	-1.08	2.53	-1.31	4.43	1.19	3.88	1.10	3.40
ITGA4	integrin, alpha 4	311144	1.11	1.66	-1.10	3.29	1.14	3.10	-1.02	2.14
ITGB1	integrin, beta 1	24511	-1.23	1.71	-1.28	2.96	1.16	3.36	-1.20	2.42
JAM3	junctional adhesion molecule 3	315509	/	/	-1.10	1.74	1.21	2.05	/	/
MAPK1	mitogen-activated protein kinase 1	116590	/	/	/	/	1.08	2.00	/	/

Symbol	Entrez Gene Name	Entrez Gene ID	Day 4		Day 8		Day 15		Day 29	
			LD	HD	LD	HD	LD	HD	LD	HD
MLLT4	myeloid/lymphoid or mixed-lineage leukemia; translocated to, 4	26955	/	/	/	/	1.03	1.58	/	/
MMP7	matrix metallopeptidase 7	25335	1.13	1.67	1.10	13.45	1.09	5.54	1.20	2.81
MMP11	matrix metallopeptidase 11	25481	/	/	-1.09	2.52	-1.02	1.65	/	/
MMP12	matrix metallopeptidase 12	117033	1.13	2.13	1.11	13.72	1.03	8.57	1.39	6.90
MMP14	matrix metallopeptidase 14	81707	-1.29	1.67	-1.27	4.20	1.34	4.33	-1.11	2.03
MSN	moesin	81521	/	/	-1.16	2.03	1.02	2.51	-1.17	2.36
PIK3R1	phosphoinositide-3-kinase, regulatory subunit 1 (alpha)	25513	1.16	1.59	-1.16	2.97	1.24	2.35	-1.20	2.98
PLCG1	phospholipase C, gamma 1	25738	/	/	-1.23	1.70	1.35	2.54	/	/
PRKCB	protein kinase C, beta	25023	1.12	1.93	-1.32	3.14	1.09	2.90	1.13	1.89
PRKCD	protein kinase C, delta	170538	/	/	/	/	1.25	2.25	/	/
PRKCH	protein kinase C, eta	81749	/	/	-1.23	2.03	1.20	2.72	/	/
PRKCI	protein kinase C, iota	84006	/	/	-1.08	1.51	-1.04	1.64	-1.00	1.78
PRKD3	protein kinase D3	313834	/	/	-1.10	1.72	1.08	1.74	/	/
RAC1	ras-related C3 botulinum toxin substrate 1	363875	/	/	-1.24	2.04	1.08	2.16	-1.23	1.58
RAC2	ras-related C3 botulinum toxin substrate 2	366957	-1.99	-1.10	-1.17	2.63	1.07	2.42	-1.20	1.52
RHOA	ras homolog family member A	117273	1.23	2.02	1.61	3.68	2.22	3.98	1.56	1.77
RHOH	ras homolog family member H	305341	/	/	-1.15	2.12	1.02	2.39	/	/
ROCK2	Rho-associated, coiled-coil containing protein kinase 2	25537	/	/	-1.16	1.59	1.02	1.64	/	/
SIPA1	signal-induced proliferation-associated 1	361710	/	/	1.00	1.88	1.01	1.64	/	/
TEC	tec protein tyrosine kinase	84492	/	/	/	/	1.18	2.17	/	/
TIMP1	TIMP metallopeptidase inhibitor 1	116510	1.32	15.30	-1.03	33.24	1.57	12.73	2.53	26.73
TIMP2	TIMP metallopeptidase inhibitor 2	29543	/	/	-1.17	1.81	1.02	1.59	/	/
VASP	vasodilator-stimulated phosphoprotein	361517	/	/	-1.03	1.89	1.16	1.69	/	/
VCAM1	vascular cell adhesion molecule 1	25361	/	/	-1.32	3.34	1.16	2.72	-1.18	1.51
WAS	Wiskott-Aldrich syndrome (eczema-thrombocytopenia)	317371	1.18	2.21	-1.03	2.43	1.09	2.02	1.09	2.00
WIPF1	WAS/WASL interacting protein family, member 1	117538	/	/	-1.37	2.65	1.40	3.25	-1.22	1.58

Table 5-4 Given are the fold-changes (average of treated rats against average of corresponding control rats) of leukocyte extravasations of female rats treated with either 50 mg/kg (LD) or 300 mg/kg (HD) Vancomycin for up to 28 days. Genes were selected by t-test of HD treated rats ($p \leq 0.01$, $q \leq 0.01$, fold-change $\geq 1.5 / \leq -1.5$).

Symbol	Entrez Gene Name	Entrez Gene ID	Day 4		Day 8		Day 15		Day 29	
			LD	HD	LD	HD	LD	HD	LD	HD
ABL1	c-abl oncogene 1, non-receptor tyrosine kinase	311860	1.05	2.22	1.69	3.45	1.16	1.78	1.52	2.83
ACTB	actin, beta	81822	-1.11	2.84	1.19	3.47	-1.02	2.04	1.50	3.82
ACTN1	actinin, alpha 1	81634	-1.06	2.52	-1.10	1.98	1.08	1.65	1.11	4.90
ACTN4	actinin, alpha 4	63836	-1.12	1.75	1.44	2.28	1.06	1.58	1.26	2.32
ARHGAP8	Rho GTPase activating protein 8	300115	1.02	1.85	1.94	3.06	1.09	1.71	1.63	2.82
CD44	CD44 molecule (Indian blood group)	25406	-1.11	4.31	1.17	5.28	1.02	1.82	1.40	5.14
CLDN2	claudin 2	300920	-1.05	2.74	1.11	3.41	1.16	1.76	1.27	3.52
CLDN3	claudin 3	65130	-1.08	3.01	1.60	4.11	1.19	2.04	1.79	4.30
CLDN4	claudin 4	304407	1.07	5.95	1.31	5.29	1.07	2.82	1.74	6.50
CLDN9	claudin 9	287099	-1.03	2.28	1.35	2.59	-1.02	1.66	1.05	2.47
CTNNB1	catenin, beta 1, 88kDa	84353	1.05	2.38	1.29	3.04	1.00	1.61	1.28	2.72
CTTN	cortactin	60465	1.01	2.24	1.22	1.96	1.04	1.54	1.16	2.34
CYBB	cytochrome b-245, beta polypeptide	66021	1.02	2.61	-1.09	3.68	-1.00	1.67	1.11	1.81
GNAI2	guanine nucleotide binding protein, alpha inhibiting activity polypeptide 2	81664	1.14	1.99	1.52	3.05	1.18	1.64	1.74	3.06
ICAM1	intercellular adhesion molecule 1	25464	1.11	3.80	1.67	5.67	1.18	2.57	1.68	5.87
ITGA4	integrin, alpha 4	311144	1.16	2.38	1.24	4.06	1.12	1.73	1.53	2.44
ITGB1	integrin, beta 1	24511	1.06	2.88	1.34	3.50	1.01	1.89	1.50	3.86
MAPK1	mitogen-activated protein kinase 1	116590	1.14	1.91	1.47	2.28	1.16	1.52	1.38	2.15
MMP11	matrix metallopeptidase 11	25481	-1.09	2.19	1.17	3.08	1.07	1.60	1.15	2.02
MMP12	matrix metallopeptidase 12	117033	-1.10	2.08	-1.10	8.50	-1.10	2.07	1.22	4.42
MMP14	matrix metallopeptidase 14	81707	1.08	3.31	1.87	5.51	1.14	2.13	2.02	4.09
MSN	moesin	81521	1.06	2.58	1.31	2.86	1.13	1.63	1.61	3.87
PLCG1	phospholipase C, gamma 1	25738	1.02	1.87	1.80	3.10	1.11	1.76	1.72	2.59
PRKCB	protein kinase C, beta	25023	1.15	2.25	1.23	4.71	-1.00	1.94	1.33	2.41
PRKCH	protein kinase C, eta	81749	1.21	1.57	1.52	2.48	1.26	1.51	1.64	2.49
PRKD3	protein kinase D3	313834	1.14	2.18	1.28	2.36	1.06	1.52	1.40	2.00
RAC1	ras-related C3 botulinum toxin substrate 1	363875	1.03	2.34	1.41	2.82	1.12	1.79	1.74	3.36
RAC2	ras-related C3 botulinum toxin substrate 2	366957	-1.07	2.14	1.53	4.96	1.10	1.57	1.67	2.69
RHOA	ras homolog family member A	117273	2.39	3.64	2.23	2.02	1.66	1.50	2.49	2.57
RHOH	ras homolog family member H	305341	-1.01	1.53	1.22	3.09	1.02	1.51	1.26	1.71
TIMP1	TIMP metallopeptidase inhibitor 1	116510	1.32	21.76	1.26	24.56	1.19	5.32	4.72	64.51
VCAM1	vascular cell adhesion molecule 1	25361	1.21	2.88	1.11	3.44	1.15	1.91	1.76	3.28

Symbol	Entrez Gene Name	Entrez Gene ID	Day 4		Day 8		Day 15		Day 29	
			LD	HD	LD	HD	LD	HD	LD	HD
WIPF1	WAS/WASL interacting protein family, member 1	117538	1.03	2.39	1.71	4.39	1.15	1.92	1.61	3.58

Table 5-5 Given are the fold-changes (average of treated rats against average of corresponding control rats) of IL-6 Signaling of male rats treated with either 50 mg/kg (LD) or 300 mg/kg (HD) Vancomycin for up to 28 days. Genes were selected by t-test of HD treated rats ($p \leq 0.01$, $q \leq 0.01$, fold-change $\geq 1.5 / \leq -1.5$).

Symbol	Entrez Gene Name	Entrez Gene ID	Day 4		Day 8		Day 15		Day 29	
			LD	HD	LD	HD	LD	HD	LD	HD
A2M	alpha-2-macroglobulin	24153	-1.04	5.31	1.03	15.68	-1.01	5.32	1.27	9.20
CD14	CD14 molecule	60350	-1.04	2.53	-1.21	5.72	1.20	4.73	1.14	4.45
COL1A1	collagen, type I, alpha 1	29393	1.65	2.25	-1.18	7.16	1.21	3.31	1.24	4.10
FOS	FBJ murine osteosarcoma viral oncogene homolog	314322	1.62	3.50	1.04	4.33	1.05	2.48	1.24	3.18
HSPB1	heat shock 27kDa protein 1	24471	1.24	1.66	-1.21	3.40	1.15	2.49	-1.17	2.07
IL1R2	interleukin 1 receptor, type II	117022	1.17	1.54	1.09	3.78	1.05	1.66	1.23	1.76
IL1RN	interleukin 1 receptor antagonist	60582	1.13	2.00	-1.01	3.30	1.08	1.96	1.09	1.89
JUN	jun proto-oncogene	24516	1.03	2.20	-1.09	2.96	1.22	3.37	-1.15	2.08
KRAS	v-Ki-ras2 Kirsten rat sarcoma viral oncogene homolog	24525	-1.21	-1.89	/	/	/	/	-1.37	-2.04
LBP	lipopolysaccharide binding protein	29469	1.24	3.69	-1.21	2.62	1.34	5.19	1.10	6.36
NFKB1	nuclear factor of kappa light polypeptide gene enhancer in B-cells 1	81736	1.22	1.62	1.07	1.57	/	/	1.18	1.73
NFKB2	nuclear factor of kappa light polypeptide gene enhancer in B-cells 2	309452	-1.21	1.88	-1.18	2.45	1.00	2.19	-1.09	1.97
NRAS	neuroblastoma RAS viral (v-ras) oncogene homolog	24605	-1.16	1.70	-1.18	2.95	1.16	2.71	-1.10	2.37
RRAS	related RAS viral (r-ras) oncogene homolog	361568	-1.38	1.78	-1.42	2.36	-1.07	2.31	-1.27	1.91
TNFRSF11B	tumor necrosis factor receptor superfamily, member 11b	25341	-1.57	-8.49	-1.32	-5.09	/	/	-3.19	-10.08
TNFRSF1A	tumor necrosis factor receptor superfamily, member 1A	25625	-1.20	2.24	-1.19	4.09	-1.02	3.03	1.06	3.29

Table 5-6 Given are the fold-changes (average of treated rats against average of corresponding control rats) of IL-6 Signaling of female rats treated with either 50 mg/kg (LD) or 300 mg/kg (HD) Vancomycin for up to 28 days. Genes were selected by t-test of HD treated rats ($p \leq 0.01$, $q \leq 0.01$, fold-change $\geq 1.5 / \leq -1.5$).

Symbol	Entrez Gene Name	Entrez Gene ID	Day/4		Day/8		Day/15		Day/29	
			LD	HD	LD	HD	LD	HD	LD	HD
A2M	alpha-2-macroglobulin	24153	-1.07	7.03	1.03	13.68	1.00	1.79	1.12	9.23
CD14	CD14 molecule	60350	-1.10	2.16	1.49	4.25	-1.02	1.94	1.36	4.66
CEBPB	CCAAT/enhancer binding protein (C/EBP), beta	24253	1.08	2.24	1.21	2.98	1.07	1.78	2.16	5.29

Symbol	Entrez Gene Name	Entrez Gene ID	Day/4		Day/8		Day/15		Day/29	
			LD	HD	LD	HD	LD	HD	LD	HD
COL1A1	collagen, type I, alpha 1	29393	1.16	3.28	1.05	4.69	1.04	1.73	1.20	4.72
CSNK2A1	casein kinase 2, alpha 1 polypeptide	116549	/	/	1.18	1.67	/	/	1.17	1.52
CSNK2A2	casein kinase 2, alpha prime polypeptide	307641	1.07	1.92	1.13	1.94	/	/	1.18	1.97
FOS	FBJ murine osteosarcoma viral oncogene homolog	314322	1.05	2.52	1.05	2.71	/	/	1.20	4.33
HSPB1	heat shock 27kDa protein 1	24471	1.21	2.91	1.67	2.77	1.01	1.95	1.34	4.02
IKBKB	inhibitor of kappa light polypeptide gene enhancer in B-cells, kinase beta	84351	1.03	2.10	1.18	2.03	1.01	1.77	1.34	2.50
IKBKE	inhibitor of kappa light polypeptide gene enhancer in B-cells, kinase epsilon	363984	1.06	1.50	1.25	1.83	/	/	/	/
IL18	interleukin 18	29197	-1.06	1.60	1.26	2.39	/	/	1.40	2.15
IL1B	interleukin 1, beta	24494	1.22	2.05	1.27	3.76	/	/	1.19	1.78
IL1R2	interleukin 1 receptor, type II	117022	/	/	-1.05	1.87	/	/	/	/
IL1RN	interleukin 1 receptor antagonist	60582	-1.03	1.84	-1.09	2.54	/	/	-1.04	2.08
IL6R	interleukin 6 receptor	24499	/	/	-1.00	1.58	/	/	/	/
JUN	jun proto-oncogene	24516	1.11	2.61	1.45	3.10	-1.01	1.62	1.45	3.38
LBP	lipopolysaccharide binding protein	29469	1.17	2.41	1.06	4.10	1.08	1.67	1.31	4.97
MAP2K1	mitogen-activated protein kinase kinase 1	170851	1.06	1.74	1.82	2.73	1.21	1.55	1.60	3.00
MAP4K4	mitogen-activated protein kinase kinase kinase kinase 4	301363	-1.07	1.91	-1.03	2.29	-1.08	1.51	-1.18	1.98
MAPK1	mitogen-activated protein kinase 1	116590	1.14	1.91	1.47	2.28	1.16	1.52	1.38	2.15
MAPK12	mitogen-activated protein kinase 12	60352	/	/	1.24	1.53	/	/	1.12	1.52
NFKB2	nuclear factor of kappa light polypeptide gene enhancer in B-cells 2	309452	-1.14	2.39	1.21	2.94	1.05	2.01	1.30	3.78
NGFR	nerve growth factor receptor	24596	/	/	1.00	1.71	/	/	/	/
NRAS	neuroblastoma RAS viral (v-ras) oncogene homolog	24605	-1.07	2.44	1.25	2.94	1.08	1.75	1.30	3.38
RELA	v-rel reticuloendotheliosis viral oncogene homolog A	309165	-1.01	1.67	1.28	1.97	1.10	1.54	1.30	2.06
RRAS	related RAS viral (r-ras) oncogene homolog	361568	-1.15	2.24	1.30	2.80	1.02	1.79	1.36	3.66
SRF	serum response factor	501099	1.01	1.69	1.59	2.43	/	/	1.44	2.68
STAT3	signal transducer and activator of transcription 3	25125	-1.04	2.10	1.46	3.12	1.18	1.75	1.79	3.55
TNFRSF11B	tumor necrosis factor receptor superfamily, member 11b	25341	-1.14	-2.81	2.22	-2.53	1.10	-1.57	-1.14	-5.45
TNFRSF1A	tumor necrosis factor receptor superfamily, member 1A	25625	1.12	2.96	1.23	3.92	1.09	2.16	1.73	5.68
TRAF2	TNF receptor-associated factor 2	311786	1.07	1.53	1.08	1.71	/	/	1.23	1.82

Table 5-7 Given are the fold-changes (average of treated rats against average of corresponding control rats) of Apoptosis Signaling of male rats treated with either 50 mg/kg (LD) or 300 mg/kg (HD) Vancomycin for up to 28 days. Genes were selected by t-test of HD treated rats ($p \leq 0.01$, $q \leq 0.01$, fold-change ≥ 1.5/ ≤ -1.5).

Symbol	Entrez Gene Name	Entrez Gene ID	Day 4		Day 8		Day 15		Day 29	
			LD	HD	LD	HD	LD	HD	LD	HD
BAK1	BCL2-antagonist/killer 1	116502	-1.19	1.75	-1.27	3.50	1.32	3.69	-1.12	2.27
BCL2A1	BCL2-related protein A1	170929	-1.01	2.34	-1.12	6.35	1.09	4.32	1.01	3.29
BID	BH3 interacting domain death agonist	64625	/	/	-1.19	1.73	-1.07	1.79	-1.12	1.65
BIRC2	baculoviral IAP repeat containing 2	60371	/	/	-1.12	1.54	1.25	2.04	/	/
BIRC3	baculoviral IAP repeat containing 3	78971	1.05	3.74	-1.06	7.09	-1.01	4.33	1.36	3.99
CAPN2	calpain 2, (m/II) large subunit	29154	/	/	-1.29	2.24	1.22	2.70	-1.46	1.56
CAPNS1	calpain, small subunit 1	29156	/	/	-1.42	1.69	-1.05	2.21	-1.44	1.54
CASP2	caspase 2, apoptosis-related cysteine peptidase	64314	/	/	-1.29	2.03	1.31	2.69	/	/
CASP3	caspase 3, apoptosis-related cysteine peptidase	25402	1.08	1.71	-1.32	2.84	1.08	2.93	-1.05	2.26
CASP6	caspase 6, apoptosis-related cysteine peptidase	83584	/	/	-1.10	1.62	1.08	1.73	/	/
CASP8	caspase 8, apoptosis-related cysteine peptidase	64044	/	/	-1.13	1.60	1.07	1.61	1.01	1.52
CASP12	caspase 12 (gene/pseudogene)	156117	1.23	4.14	-1.08	8.45	1.11	5.05	1.18	5.01
CASP9	caspase 9, apoptosis-related cysteine peptidase	58918	/	/	/	/	1.11	1.69	/	/
CDK1	cyclin-dependent kinase 1	54237	-1.54	6.01	-1.26	11.09	1.18	4.53	1.98	5.76
IKBKB	inhibitor of kappa light polypeptide gene enhancer in B-cells, kinase beta	84351	/	/	-1.24	1.75	-1.02	1.92	/	/
IKBKE	inhibitor of kappa light polypeptide gene enhancer in B-cells, kinase epsilon	363984	/	/	/	/	1.14	1.51	/	/
MAP2K1	mitogen-activated protein kinase kinase 1	170851	/	/	-1.32	1.66	1.32	2.35	/	/
MAP4K4	mitogen-activated protein kinase kinase kinase kinase 4	301363	/	/	-1.18	2.30	-1.04	1.82	-1.12	1.82
MAPK1	mitogen-activated protein kinase 1	116590	/	/	/	/	1.08	2.00	/	/
MCL1	myeloid cell leukemia sequence 1 (BCL2-related)	60430	/	/	-1.48	1.76	-1.01	1.90	/	/
NFKB2	nuclear factor of kappa light polypeptide gene enhancer in B-cells 2	309452	-1.21	1.88	-1.18	2.45	1.00	2.19	-1.09	1.97
NRAS	neuroblastoma RAS viral (v-ras) oncogene homolog	24605	-1.16	1.70	-1.18	2.95	1.16	2.71	-1.10	2.37
PARP1	poly (ADP-ribose) polymerase 1	25591	/	/	-1.43	1.92	1.28	2.43	/	/
PLCG1	phospholipase C, gamma 1	25738	/	/	-1.23	1.70	1.35	2.54	/	/
RELA	v-rel reticuloendotheliosis viral oncogene homolog A	309165	/	/	-1.27	1.61	-1.01	1.67	/	/
RRAS	related RAS viral (r-ras) oncogene homolog	361568	-1.38	1.78	-1.42	2.36	-1.07	2.31	-1.27	1.91
TNFRSF1A	tumor necrosis factor receptor superfamily, member 1A	25625	-1.20	2.24	-1.19	4.09	-1.02	3.03	1.06	3.29

Table 5-8 Given are the fold-changes (average of treated rats against average of corresponding control rats) of Apoptosis Signaling of female rats treated with either 50 mg/kg (LD) or 300 mg/kg (HD) Vancomycin for up to 28 days. Genes were selected by t-test of HD treated rats ($p \leq 0.01$, $q \leq 0.01$, fold-change ≥ 1.5/ ≤ -1.5).

Symbol	Entrez Gene Name	Entrez Gene ID	Day/4		Day/8		Day/15		Day/29	
			LD	HD	LD	HD	LD	HD	LD	HD
ACIN1	apoptotic chromatin condensation inducer 1	305884	1.07	1.60	1.27	1.95	1.02	1.59	1.22	1.94
BAK1	BCL2-antagonist/killer 1	116502	1.17	2.90	1.79	4.77	1.19	1.93	2.14	5.23
BCL2A1	BCL2-related protein A1	170929	-1.00	3.12	1.19	6.61	1.08	2.07	1.24	3.28
BID	BH3 interacting domain death agonist	64625	1.05	1.97	1.11	1.92	-1.08	1.61	1.07	2.08
BIRC2	baculoviral IAP repeat containing 2	60371	1.12	1.54	1.56	1.88	/	/	1.30	1.68
BIRC3	baculoviral IAP repeat containing 3	78971	-1.03	4.70	1.08	5.97	1.02	2.04	1.25	4.34
CAPN2	calpain 2, (m/II) large subunit	29154	-1.05	2.05	1.51	2.84	1.14	1.79	1.52	2.82
CAPNS1	calpain, small subunit 1	29156	-1.12	2.55	1.11	2.97	1.01	1.88	1.30	3.71
CASP2	caspase 2, apoptosis-related cysteine peptidase	64314	-1.00	1.92	1.84	2.91	1.08	1.58	1.50	2.86
CASP3	caspase 3, apoptosis-related cysteine peptidase	25402	1.05	2.29	1.42	3.26	1.03	1.83	1.41	3.35
CASP6	caspase 6, apoptosis-related cysteine peptidase	83584	1.01	1.66	1.46	2.11	1.18	1.73	1.28	1.93
CASP8	caspase 8, apoptosis-related cysteine peptidase	64044	/	/	1.01	1.58	/	/	1.10	1.81
CASP12	caspase 12 (gene/pseudogene)	156117	1.19	5.32	1.02	5.72	1.03	2.11	1.32	5.66
CASP9	caspase 9, apoptosis-related cysteine peptidase	58918	/	/	1.38	1.76	/	/	1.30	2.03
CDK1	cyclin-dependent kinase 1	54237	-1.09	6.63	1.01	9.85	1.12	2.72	1.39	6.55
IKBKB	inhibitor of kappa light polypeptide gene enhancer in B-cells, kinase beta	84351	1.03	2.10	1.18	2.03	1.01	1.77	1.34	2.50
IKBKE	inhibitor of kappa light polypeptide gene enhancer in B-cells, kinase epsilon	363984	1.06	1.50	1.25	1.83	/	/	/	/
MAP2K1	mitogen-activated protein kinase kinase 1	170851	1.06	1.74	1.82	2.73	1.21	1.55	1.60	3.00
MAP4K4	mitogen-activated protein kinase kinase kinase kinase 4	301363	-1.07	1.91	-1.03	2.29	-1.08	1.51	-1.18	1.98
MAPK1	mitogen-activated protein kinase 1	116590	1.14	1.91	1.47	2.28	1.16	1.52	1.38	2.15
MCL1	myeloid cell leukemia sequence 1	60430	-1.19	1.79	1.13	1.86	/	/	1.44	2.71
NFKB2	nuclear factor of kappa light polypeptide gene enhancer in B-cells 2	309452	-1.14	2.39	1.21	2.94	1.05	2.01	1.30	3.78
NRAS	neuroblastoma RAS viral (v-ras) oncogene homolog	24605	-1.07	2.44	1.25	2.94	1.08	1.75	1.30	3.38
PARP1	poly (ADP-ribose) polymerase 1	25591	-1.06	2.15	1.72	3.24	1.06	1.72	1.57	3.70
PLCG1	phospholipase C, gamma 1	25738	1.02	1.87	1.80	3.10	1.11	1.76	1.72	2.59
RELA	v-rel reticuloendotheliosis viral oncogene homolog A	309165	-1.01	1.67	1.28	1.97	1.10	1.54	1.30	2.06
RPS6KA1	ribosomal protein S6 kinase, 90kDa, polypeptide 1	81771	/	/	1.05	1.96	/	/	1.12	1.88
RRAS	related RAS viral (r-ras) oncogene homolog	361568	-1.15	2.24	1.30	2.80	1.02	1.79	1.36	3.66

Symbol	Entrez Gene Name	Entrez Gene ID	Day/4		Day/8		Day/15		Day/29	
			LD	HD	LD	HD	LD	HD	LD	HD
TNFRSF1A	tumor necrosis factor receptor superfamily, member 1A	25625	1.12	2.96	1.23	3.92	1.09	2.16	1.73	5.68
TP53	tumor protein p53	24842	1.11	1.57	1.32	1.69	/	/	1.23	1.88

Table 5-9 Given are the fold-changes (average of treated rats against average of corresponding control rats) of Death-receptor Signaling of male rats treated with either 50 mg/kg (LD) or 300 mg/kg (HD) Vancomycin for up to 28 days. Genes were selected by t-test of HD treated rats ($p \leq 0.01$, $q \leq 0.01$, fold-change $\geq 1.5/ \leq -1.5$).

Symbol	Entrez Gene Name	Entrez Gene ID	Day/4		Day/8		Day/15		Day/29	
			LD	HD	LD	HD	LD	HD	LD	HD
BID	BH3 interacting domain death agonist	64625	/	/	-1.19	1.73	-1.07	1.79	-1.12	1.65
BIRC2	baculoviral IAP repeat containing 2	60371	/	/	-1.12	1.54	1.25	2.04	/	/
BIRC3	baculoviral IAP repeat containing 3	78971	1.05	3.74	-1.06	7.09	-1.01	4.33	1.36	3.99
CASP2	caspase 2, apoptosis-related cysteine peptidase	64314	/	/	-1.29	2.03	1.31	2.69	/	/
CASP3	caspase 3, apoptosis-related cysteine peptidase	25402	1.08	1.71	-1.32	2.84	1.08	2.93	-1.05	2.26
CASP6	caspase 6, apoptosis-related cysteine peptidase	83584	/	/	-1.10	1.62	1.08	1.73	/	/
CASP8	caspase 8, apoptosis-related cysteine peptidase	64044	/	/	-1.13	1.60	1.07	1.61	1.01	1.52
CASP9	caspase 9, apoptosis-related cysteine peptidase	58918	/	/	/	/	1.11	1.69	/	/
FADD	Fas (TNFRSF6)-associated via death domain	266610	-1.51	1.11	/	/	1.09	2.53	/	/
HSPB1	heat shock 27kDa protein 1	24471	1.24	1.66	-1.21	3.40	1.15	2.49	-1.17	2.07
IKBKB	inhibitor of kappa light polypeptide gene enhancer in B-cells, kinase beta	84351	/	/	-1.24	1.75	-1.02	1.92	/	/
IKBKE	inhibitor of kappa light polypeptide gene enhancer in B-cells, kinase epsilon	363984	/	/	/	/	1.14	1.51	/	/
MAP4K4	mitogen-activated protein kinase kinase kinase kinase 4	301363	/	/	-1.18	2.30	-1.04	1.82	-1.12	1.82
NFKB2	nuclear factor of kappa light polypeptide gene enhancer in B-cells 2	309452	-1.21	1.88	-1.18	2.45	1.00	2.19	-1.09	1.97
RELA	v-rel reticuloendotheliosis viral oncogene homolog A	309165	/	/	-1.27	1.61	-1.01	1.67	/	/
TBK1	TANK-binding kinase 1	299827	/	/	/	/	1.12	1.56	/	/
TNFRSF1A	tumor necrosis factor receptor superfamily, member 1A	25625	-1.20	2.24	-1.19	4.09	-1.02	3.03	1.06	3.29
TNFSF10	tumor necrosis factor (ligand) superfamily, member 10	246775	-1.07	1.70	-1.22	2.80	1.01	2.71	1.06	1.68

Table 5-10 Given are the fold-changes (average of treated rats against average of corresponding control rats) of Death-receptor Signaling of female rats treated with either 50 mg/kg (LD) or 300 mg/kg (HD) Vancomycin for up to 28 days. Genes were selected by t-test of HD treated rats ($p \leq 0.01$, $q \leq 0.01$, fold-change $\geq 1.5/\leq -1.5$).

Symbol	Entrez Gene Name	Entrez Gene ID	Day/4		Day/8		Day/15		Day/29	
			LD	HD	LD	HD	LD	HD	LD	HD
BID	BH3 interacting domain death agonist	64625	1.05	1.97	1.11	1.92	-1.08	1.61	1.07	2.08
BIRC2	baculoviral IAP repeat containing 2	60371	1.12	1.54	1.56	1.88	/	/	1.30	1.68
BIRC3	baculoviral IAP repeat containing 3	78971	-1.03	4.70	1.08	5.97	1.02	2.04	1.25	4.34
CASP2	caspase 2, apoptosis-related cysteine peptidase	64314	-1.00	1.92	1.84	2.91	1.08	1.58	1.50	2.86
CASP3	caspase 3, apoptosis-related cysteine peptidase	25402	1.05	2.29	1.42	3.26	1.03	1.83	1.41	3.35
CASP6	caspase 6, apoptosis-related cysteine peptidase	83584	1.01	1.66	1.46	2.11	1.18	1.73	1.28	1.93
CASP8	caspase 8, apoptosis-related cysteine peptidase	64044	/	/	1.01	1.58	/	/	1.10	1.81
CASP9	caspase 9, apoptosis-related cysteine peptidase	58918	/	/	1.38	1.76	/	/	1.30	2.03
FADD	Fas (TNFRSF6)-associated via death domain	266610	-1.04	1.51	1.54	3.12	1.05	1.56	1.32	2.45
HSPB1	heat shock 27kDa protein 1	24471	1.21	2.91	1.67	2.77	1.01	1.95	1.34	4.02
IKBKB	inhibitor of kappa light polypeptide gene enhancer in B-cells, kinase beta	84351	1.03	2.10	1.18	2.03	1.01	1.77	1.34	2.50
IKBKE	inhibitor of kappa light polypeptide gene enhancer in B-cells, kinase epsilon	363984	1.06	1.50	1.25	1.83	/	/	/	/
MAP4K4	mitogen-activated protein kinase kinase kinase kinase 4	301363	-1.07	1.91	-1.03	2.29	-1.08	1.51	-1.18	1.98
NFKB2	nuclear factor of kappa light polypeptide gene enhancer in B-cells 2	309452	-1.14	2.39	1.21	2.94	1.05	2.01	1.30	3.78
RELA	v-rel reticuloendotheliosis viral oncogene homolog A	309165	-1.01	1.67	1.28	1.97	1.10	1.54	1.30	2.06
TBK1	TANK-binding kinase 1	299827	1.07	1.62	1.42	1.81	/	/	1.30	1.94
TNFRSF1A	tumor necrosis factor receptor superfamily, member 1A	25625	1.12	2.96	1.23	3.92	1.09	2.16	1.73	5.68
TNFSF10	tumor necrosis factor (ligand) superfamily, member 10	246775	-1.03	2.43	1.25	3.43	-1.01	1.83	1.49	2.22
TRAF2	TNF receptor-associated factor 2	311786	1.07	1.53	1.08	1.71	/	/	1.23	1.82

Table 5-11 Given are the fold-changes (average of treated rats against average of corresponding control rats) of Cell Cycle Control Signaling of male rats treated with either 50 mg/kg (LD) or 300 mg/kg (HD) Vancomycin for up to 28 days. Genes were selected by t-test of HD treated rats ($p \leq 0.01$, $q \leq 0.01$, fold-change $\geq 1.5/\leq -1.5$).

Symbol	Entrez Gene Name	Entrez Gene ID	Day/4		Day/8		Day/15		Day/29	
			LD	HD	LD	HD	LD	HD	LD	HD
CDC6	cell division cycle 6 homolog (S. cerevisiae)	360621	1.01	1.61	-1.04	1.98	1.02	1.59	1.16	2.41
CDK4	cyclin-dependent kinase 4	94201	-1.46	1.72	-1.32	2.74	1.02	2.45	-1.27	2.09
CDK6	cyclin-dependent kinase 6	114483	/	/	-1.11	1.55	/	/	-1.09	1.53

Symbol	Entrez Gene Name	Entrez Gene ID	Day/4		Day/8		Day/15		Day/29	
			LD	HD	LD	HD	LD	HD	LD	HD
CHEK2	checkpoint kinase 2	114212	-1.02	1.56	-1.14	1.90	1.07	1.66	-1.01	1.53
DBF4	DBF4 homolog (S. cerevisiae)	312046	-1.06	1.79	-1.06	2.61	-1.07	1.69	1.03	1.72
MCM2	minichromosome maintenance complex component 2	312538	-1.20	2.53	-1.17	4.06	1.12	3.34	1.40	4.64
MCM3	minichromosome maintenance complex component 3	316273	1.13	2.48	1.14	3.07	-1.02	1.91	1.46	4.33
MCM4	minichromosome maintenance complex component 4	29728	1.07	2.09	1.09	2.75	1.03	2.04	1.46	3.55
MCM5	minichromosome maintenance complex component 5	291885	1.30	1.97	1.15	1.93	1.02	1.59	1.41	2.73
MCM6	minichromosome maintenance complex component 6	29685	-1.13	4.21	-1.22	6.64	1.09	4.78	1.93	9.03
MCM7	minichromosome maintenance complex component 7	288532	-1.20	1.77	-1.24	2.62	-1.07	2.45	1.04	2.90
ORC1	origin recognition complex, subunit 1	313479	1.17	1.65	1.01	1.70	/	/	1.28	2.43
ORC6	origin recognition complex, subunit 6	291927	/	/	-1.13	2.21	1.11	2.14	1.05	2.03
RPA2	replication protein A2, 32kDa	59102	/	/	-1.24	2.31	-1.08	2.30	-1.08	2.29

Table 5-12 Given are the fold-changes (average of treated rats against average of corresponding control rats) of Cell Cycle Control Signaling of female rats treated with either 50 mg/kg (LD) or 300 mg/kg (HD) Vancomycin for up to 28 days. Genes were selected by t-test of HD treated rats ($p \leq 0.01$, $q \leq 0.01$, fold-change $\geq 1.5/ \leq -1.5$).

Symbol	Entrez Gene Name	Entrez Gene ID	Day 4		Day 8		Day 15		Day 29	
			LD	HD	LD	HD	LD	HD	LD	HD
CDC6	cell division cycle 6 homolog (S. cerevisiae)	360621	-1.02	1.63	-1.03	1.59	/	/	1.04	2.71
CDK4	cyclin-dependent kinase 4	94201	1.00	2.57	1.49	3.87	1.07	1.95	1.43	4.12
CDK5	cyclin-dependent kinase 5	140908	1.01	1.65	1.27	2.00	/	/	1.21	1.98
CHEK2	checkpoint kinase 2	114212	1.03	1.86	1.02	2.25	/	/	1.11	1.86
DBF4	DBF4 homolog (S. cerevisiae)	312046	1.02	1.91	1.02	2.07	/	/	1.12	2.20
MCM2	minichromosome maintenance complex component 2	312538	-1.10	3.19	1.17	4.15	1.07	2.29	1.56	6.51
MCM3	minichromosome maintenance complex component 3	316273	-1.03	2.19	-1.08	2.34	-1.03	1.54	-1.07	4.02
MCM4	minichromosome maintenance complex component 4	29728	-1.01	1.90	-1.06	2.12	/	/	1.11	2.94
MCM5	minichromosome maintenance complex component 5	291885	-1.02	1.63	-1.06	1.65	/	/	-1.16	2.52
MCM6	minichromosome maintenance complex component 6	29685	-1.06	4.69	1.18	6.45	1.10	3.07	1.87	13.58
MCM7	minichromosome maintenance complex component 7	288532	-1.08	2.31	1.23	3.10	1.22	1.90	1.56	4.82
ORC2	origin recognition complex, subunit 2	301430	1.05	1.61	1.25	1.93	1.03	1.50	1.32	2.49
ORC6	origin recognition complex, subunit 6	291927	1.09	1.91	1.32	2.54	1.11	1.71	1.35	3.42
RPA2	replication protein A2, 32kDa	59102	1.07	2.00	1.41	2.93	1.05	2.06	1.52	4.50

Table 5-13 Given are the fold-changes (average of treated rats against average of corresponding control rats) of Integrin Signaling of male rats treated with either 50 mg/kg (LD) or 300 mg/kg (HD) Vancomycin for up to 28 days. Genes were selected by t-test of HD treated rats ($p \leq 0.01$, $q \leq 0.01$, fold-change ≥ 1.5/ ≤ -1.5).

Symbol	Entrez Gene Name	Entrez Gene ID	Day 4		Day 8		Day 15		Day 29	
			LD	HD	LD	HD	LD	HD	LD	HD
ABL1	c-abl oncogene 1, non-receptor tyrosine kinase	311860	/	/	-1.30	1.99	1.36	2.58	/	/
ACTB	actin, beta	81822	/	/	-1.38	2.05	-1.09	2.25	-1.35	1.94
ACTN1	actinin, alpha 1	81634	1.24	2.69	1.02	3.60	-1.02	1.95	1.17	4.82
AKT1	v-akt murine thymoma viral oncogene homolog 1	24185	/	/	-1.18	2.03	-1.05	1.85	-1.19	1.67
Arf2	ADP-ribosylation factor 2	79119	/	/	-1.25	1.64	1.27	2.25	/	/
ARPC3	actin related protein 2/3 complex, subunit 3, 21kDa	288669	/	/	-1.43	2.02	1.06	2.17	/	/
ARPC4	actin related protein 2/3 complex, subunit 4, 20kDa	297518	/	/	-1.39	1.66	1.17	2.06	/	/
ARPC5	actin related protein 2/3 complex, subunit 5, 16kDa	360854	/	/	-1.23	1.75	1.14	2.26	/	/
ARPC1B	actin related protein 2/3 complex, subunit 1B, 41kDa	54227	-1.05	2.09	-1.28	2.96	1.24	2.95	1.15	3.07
ASAP1	ArfGAP with SH3 domain, ankyrin repeat and PH domain 1	314961	/	/	-1.11	2.01	1.06	1.70	/	/
CAPN2	calpain 2, (m/II) large subunit	29154	/	/	-1.29	2.24	1.22	2.70	-1.46	1.56
CAPNS1	calpain, small subunit 1	29156	/	/	-1.42	1.69	-1.05	2.21	-1.44	1.54
CAV1	caveolin 1, caveolae protein, 22kDa	25404	/	/	1.12	1.59	/	/	/	/
CTTN	cortactin	60465	/	/	-1.19	1.77	-1.03	1.56	-1.21	1.51
ILK	integrin-linked kinase	170922	/	/	-1.21	1.61	1.05	1.75	/	/
ITGA1	integrin, alpha 1	25118	-1.33	1.56	-1.25	2.26	1.39	2.84	/	/
ITGA4	integrin, alpha 4	311144	1.11	1.66	-1.10	3.29	1.14	3.10	-1.02	2.14
ITGA5	integrin, alpha 5	315346	/	/	-1.08	2.34	-1.01	1.68	-1.07	1.73
ITGAM	integrin, alpha M	25021	/	/	1.09	1.71	/	/	/	/
ITGAX	integrin, alpha X	499271	/	/	1.02	1.66	/	/	/	/
ITGB1	integrin, beta 1	24511	-1.23	1.71	-1.28	2.96	1.16	3.36	-1.20	2.42
ITGB4	integrin, beta 4	25724	1.16	1.67	-1.03	3.44	1.08	3.46	-1.01	3.28
ITGB6	integrin, beta 6	311061	/	/	-1.43	2.37	1.33	2.85	1.07	2.23
ITGB7	integrin, beta 7	25713	/	/	1.07	1.60	1.07	1.53	/	/
MAP2K1	mitogen-activated protein kinase kinase 1	170851	/	/	-1.32	1.66	1.32	2.35	/	/
MPRIP	myosin phosphatase Rho interacting protein	116504	/	/	-1.33	1.87	1.23	1.97	/	/
MYL9	myosin, light chain 9, regulatory	296313	1.36	1.66	1.00	2.94	1.21	1.58	1.01	1.82
NCK2	NCK adaptor protein 2	316369	/	/	-1.34	1.73	1.19	2.07	/	/
NRAS	neuroblastoma RAS viral (v-ras) oncogene homolog	24605	-1.16	1.70	-1.18	2.95	1.16	2.71	-1.10	2.37
PIK3R1	phosphoinositide-3-kinase, regulatory subunit 1 (alpha)	25513	1.16	1.59	-1.16	2.97	1.24	2.35	-1.20	2.98
PIK3R6	phosphoinositide-3-kinase, regulatory subunit 6	497932	/	/	1.17	1.53	/	/	/	/
PLCG1	phospholipase C, gamma 1	25738	/	/	-1.23	1.70	1.35	2.54	/	/

Symbol	Entrez Gene Name	Entrez Gene ID	Day 4		Day 8		Day 15		Day 29	
			LD	HD	LD	HD	LD	HD	LD	HD
RAC1	ras-related C3 botulinum toxin substrate 1	363875	/	/	-1.24	2.04	1.08	2.16	-1.23	1.58
RAC2	ras-related C3 botulinum toxin substrate 2	366957	-1.99	-1.10	-1.17	2.63	1.07	2.42	-1.20	1.52
RALB	v-ral simian leukemia viral oncogene homolog B	116546	/	/	-1.40	1.51	1.31	2.07	/	/
RGD1309537	similar to Myosin regulatory light chain 2-A, smooth muscle isoform	501203	-1.31	1.59	-1.32	2.83	1.19	2.98	-1.15	2.28
RHOA	ras homolog family member A	117273	1.23	2.02	1.61	3.68	2.22	3.98	1.56	1.77
RHOB	ras homolog family member B	64373	-1.27	2.53	-1.51	4.07	1.27	3.39	-1.13	2.30
RHOC	ras homolog family member C	295342	/	/	1.01	1.79	1.72	2.92	-1.54	1.31
RHOG	ras homolog family member G	308875	/	/	-1.22	2.05	1.10	2.32	-1.23	1.58
RHOH	ras homolog family member H	305341	/	/	-1.15	2.12	1.02	2.39	/	/
RHOJ	ras homolog family member J	299145	/	/	-1.31	3.33	1.40	2.87	-1.27	1.66
RHOQ	ras homolog family member Q	85428	/	/	-1.22	2.12	1.43	2.33	/	/
RND3	Rho family GTPase 3	295588	/	/	-1.24	2.15	1.10	1.96	-1.10	1.82
RRAS	related RAS viral (r-ras) oncogene homolog	361568	-1.38	1.78	-1.42	2.36	-1.07	2.31	-1.27	1.91
TLN1	talin 1	313494	/	/	-1.23	1.85	1.23	2.25	-1.31	1.51
TSPAN4	tetraspanin 4	293627	/	/	-1.06	1.63	1.08	2.02	1.07	1.70
VASP	vasodilator-stimulated phosphoprotein	361517	/	/	-1.03	1.89	1.16	1.69	/	/
WAS	Wiskott-Aldrich syndrome	317371	1.18	2.21	-1.03	2.43	1.09	2.02	1.09	2.00
WIPF1	WAS/WASL interacting protein family, member 1	117538	/	/	-1.37	2.65	1.40	3.25	-1.22	1.58

Table 5-14 Given are the fold-changes (average of treated rats against average of corresponding control rats) of Integrin Signaling of female rats treated with either 50 mg/kg (LD) or 300 mg/kg (HD) Vancomycin for up to 28 days. Genes were selected by t-test of HD treated rats ($p \leq 0.01$, $q \leq 0.01$, fold-change ≥ 1.5/ ≤ -1.5).

Symbol	Entrez Gene Name	Entrez Gene ID	Day 4		Day 8		Day 15		Day 29	
			LD	HD	LD	HD	LD	HD	LD	HD
ABL1	c-abl oncogene 1, non-receptor tyrosine kinase	311860	1.05	2.22	1.69	3.45	1.16	1.78	1.52	2.83
ACTB	actin, beta	81822	-1.11	2.84	1.19	3.47	-1.02	2.04	1.50	3.82
ACTN1	actinin, alpha 1	81634	-1.06	2.52	-1.10	1.98	1.08	1.65	1.11	4.90
ACTN4	actinin, alpha 4	63836	-1.12	1.75	1.44	2.28	1.06	1.58	1.26	2.32
ACTR3	ARP3 actin-related protein 3 homolog	81732	-1.10	1.98	1.31	2.56	1.06	1.65	1.19	2.30
AKT1	v-akt murine thymoma viral oncogene homolog 1	24185	-1.09	2.19	1.04	2.17	-1.04	1.68	1.05	2.73
Arf2	ADP-ribosylation factor 2	79119	-1.10	1.69	1.13	2.53	1.15	1.60	1.31	2.44
ARPC3	actin related protein 2/3 complex, subunit 3, 21kDa	288669	-1.15	1.94	1.50	3.03	1.17	1.72	1.53	4.01
ARPC4	actin related protein 2/3 complex, subunit 4, 20kDa	297518	-1.08	2.03	1.39	2.99	1.11	1.67	1.39	2.95

Symbol	Entrez Gene Name	Entrez Gene ID	Day 4		Day 8		Day 15		Day 29	
			LD	HD	LD	HD	LD	HD	LD	HD
ARPC5	actin related protein 2/3 complex, subunit 5, 16kDa	360854	-1.09	1.92	1.53	2.47	1.07	1.54	1.39	2.86
ARPC1B	actin related protein 2/3 complex, subunit 1B, 41kDa	54227	1.03	2.68	1.38	3.89	1.04	1.97	1.56	5.20
CAPN2	calpain 2, (m/II) large subunit	29154	-1.05	2.05	1.51	2.84	1.14	1.79	1.52	2.82
CAPNS1	calpain, small subunit 1	29156	-1.12	2.55	1.11	2.97	1.01	1.88	1.30	3.71
CTTN	cortactin	60465	1.01	2.24	1.22	1.96	1.04	1.54	1.16	2.34
ILK	integrin-linked kinase	170922	-1.10	1.95	1.11	2.02	-1.04	1.58	1.20	2.11
ITGA1	integrin, alpha 1	25118	-1.04	2.10	1.52	3.13	1.02	1.59	1.51	1.79
ITGA4	integrin, alpha 4	311144	1.16	2.38	1.24	4.06	1.12	1.73	1.53	2.44
ITGB1	integrin, beta 1	24511	1.06	2.88	1.34	3.50	1.01	1.89	1.50	3.86
MAP2K1	mitogen-activated protein kinase kinase 1	170851	1.06	1.74	1.82	2.73	1.21	1.55	1.60	3.00
MAPK1	mitogen-activated protein kinase 1	116590	1.14	1.91	1.47	2.28	1.16	1.52	1.38	2.15
MPRIP	myosin phosphatase Rho interacting protein	116504	1.14	2.30	1.52	2.95	1.11	1.55	1.36	2.42
NRAS	neuroblastoma RAS viral (v-ras) oncogene homolog	24605	-1.07	2.44	1.25	2.94	1.08	1.75	1.30	3.38
PAK1	p21 protein (Cdc42/Rac)-activated kinase 1	29431	1.01	2.15	1.32	2.81	1.05	1.56	1.32	3.29
PLCG1	phospholipase C, gamma 1	25738	1.02	1.87	1.80	3.10	1.11	1.76	1.72	2.59
RAC1	ras-related C3 botulinum toxin substrate 1	363875	1.03	2.34	1.41	2.82	1.12	1.79	1.74	3.36
RAC2	ras-related C3 botulinum toxin substrate 2	366957	-1.07	2.14	1.53	4.96	1.10	1.57	1.67	2.69
RALB	v-ral simian leukemia viral oncogene homolog B	116546	1.03	1.93	1.63	2.70	1.12	1.66	1.31	2.64
RGD1309537	similar to Myosin regulatory light chain 2-A, smooth muscle isoform	501203	-1.03	2.35	1.64	3.01	1.04	1.63	1.60	4.30
RHOA	ras homolog family member A	117273	2.39	3.64	2.23	2.02	1.66	1.50	2.49	2.57
RHOB	ras homolog family member B	64373	1.02	4.49	1.26	4.50	1.14	2.39	1.90	5.26
RHOC	ras homolog family member C	295342	-1.07	1.93	2.07	4.69	1.23	1.83	1.81	3.89
RHOG	ras homolog family member G	308875	1.24	2.23	1.43	3.30	1.21	1.76	1.46	2.56
RHOH	ras homolog family member H	305341	-1.01	1.53	1.22	3.09	1.02	1.51	1.26	1.71
RHOJ	ras homolog family member J	299145	1.24	1.97	1.64	3.02	1.15	1.56	1.71	2.88
RHOQ	ras homolog family member Q	85428	1.00	1.88	1.77	2.98	1.16	1.57	1.68	2.94
RND3	Rho family GTPase 3	295588	1.09	1.90	1.25	2.13	1.08	1.61	1.33	2.80
RRAS	related RAS viral (r-ras) oncogene homolog	361568	-1.15	2.24	1.30	2.80	1.02	1.79	1.36	3.66
TLN1	talin 1	313494	1.11	1.99	1.70	2.93	1.19	1.62	1.62	2.53
WIPF1	WAS/WASL interacting protein family, member 1	117538	1.03	2.39	1.71	4.39	1.15	1.92	1.61	3.58

Table 5-15 Given are the fold-changes (average of treated rats against average of corresponding control rats) of Signaling by Rho Family GTPases of male rats treated with either 50 mg/kg (LD) or 300 mg/kg (HD) Vancomycin for up to 28 days. Genes were selected by t-test of HD treated rats ($p \leq 0.01$, $q \leq 0.01$, fold-change ≥ 1.5/ ≤ -1.5).

Symbol	Entrez Gene Name	Entrez Gene ID	Day 4		Day 8		Day 15		Day 29	
			LD	HD	LD	HD	LD	HD	LD	HD
ACTB	actin, beta	81822	/	/	-1.38	2.05	-1.09	2.25	-1.35	1.94
ACTR3	ARP3 actin-related protein 3 homolog	81732	/	/	/	/	1.13	1.97	/	/
ARHGEF2	Rho/Rac guanine nucleotide exchange factor (GEF) 2	310635	/	/	-1.26	2.49	1.41	3.18	/	/
ARPC3	actin related protein 2/3 complex, subunit 3, 21kDa	288669	/	/	-1.43	2.02	1.06	2.17	/	/
ARPC4	actin related protein 2/3 complex, subunit 4, 20kDa	297518	/	/	-1.39	1.66	1.17	2.06	/	/
ARPC5	actin related protein 2/3 complex, subunit 5, 16kDa	360854	/	/	-1.23	1.75	1.14	2.26	/	/
ARPC1B	actin related protein 2/3 complex, subunit 1B, 41kDa	54227	-1.05	2.09	-1.28	2.96	1.24	2.95	1.15	3.07
CDC42EP2	CDC42 effector protein (Rho GTPase binding) 2	309175	-1.08	1.82	-1.20	2.79	1.05	2.63	-1.53	1.52
CDC42EP5	CDC42 effector protein (Rho GTPase binding) 5	361505	/	/	-1.10	1.92	-1.02	1.82	-1.18	1.58
CDH17	cadherin 17, LI cadherin (liver-intestine)	117048	/	/	1.09	1.66	-1.00	1.52	1.20	1.76
CFL2	cofilin 2 (muscle)	366624	/	/	-1.20	1.73	1.24	2.24	/	/
CYBB	cytochrome b-245, beta polypeptide	66021	1.12	2.53	1.03	3.90	1.25	3.16	1.12	2.28
CYFIP1	cytoplasmic FMR1 interacting protein 1	308666	/	/	-1.35	1.61	1.09	2.12	/	/
DES	desmin	64362	/	/	-1.14	2.48	1.06	2.36	-1.11	1.98
FOS	FBJ murine osteosarcoma viral oncogene homolog	314322	1.62	3.50	1.04	4.33	1.05	2.48	1.24	3.18
GNA15	guanine nucleotide binding protein , alpha 15	89788	/	/	1.12	2.14	1.04	1.56	1.14	1.82
GNAI2	guanine nucleotide binding protein , alpha inhibiting activity polypeptide 2	81664	/	/	-1.32	2.19	1.12	2.29	-1.31	1.52
GNB2L1	guanine nucleotide binding protein , beta polypeptide 2-like 1	83427	-1.52	1.14	-1.26	2.22	1.15	2.39	/	/
GNG10	guanine nucleotide binding protein, gamma 10	114119	-1.18	1.64	-1.30	2.62	1.11	2.50	-1.24	1.96
GNG13	guanine nucleotide binding protein, gamma 13	685451	1.06	2.01	-1.05	2.28	-1.05	1.58	1.26	2.19
ITGA4	integrin, alpha 4	311144	1.11	1.66	-1.10	3.29	1.14	3.10	-1.02	2.14
ITGA5	integrin, alpha 5	315346	/	/	-1.08	2.34	-1.01	1.68	-1.07	1.73
ITGB1	integrin, beta 1	24511	-1.23	1.71	-1.28	2.96	1.16	3.36	-1.20	2.42
JUN	jun proto-oncogene	24516	1.03	2.20	-1.09	2.96	1.22	3.37	-1.15	2.08
LIMK1	LIM domain kinase 1	65172	/	/	-1.12	1.95	1.12	1.90	-1.02	1.71
MAP2K1	mitogen-activated protein kinase kinase 1	170851	/	/	-1.32	1.66	1.32	2.35	/	/
MAPK1	mitogen-activated protein kinase 1	116590	/	/	/	/	1.08	2.00	/	/
MSN	moesin	81521	/	/	-1.16	2.03	1.02	2.51	-1.17	2.36
MYL9	myosin, light chain 9, regulatory	296313	1.36	1.66	1.00	2.94	1.21	1.58	1.01	1.82
NFKB2	nuclear factor of kappa light polypeptide gene enhancer in B-cells 2	309452	-1.21	1.88	-1.18	2.45	1.00	2.19	-1.09	1.97

Symbol	Entrez Gene Name	Entrez Gene ID	Day 4		Day 8		Day 15		Day 29	
			LD	HD	LD	HD	LD	HD	LD	HD
NOX4	NADPH oxidase 4	85431	-1.63	-2.98	-1.37	-3.26	1.08	-1.52	-1.19	-3.05
PAK1	p21 protein (Cdc42/Rac)-activated kinase 1	29431	/	/	/	/	1.04	1.77	/	/
PAK2	p21 protein (Cdc42/Rac)-activated kinase 2	29432	/	/	/	/	1.04	1.58	/	/
PARD3	par-3 partitioning defective 3 homolog (C. elegans)	81918	/	/	-1.28	1.59	1.02	1.84	/	/
PIK3R1	phosphoinositide-3-kinase, regulatory subunit 1 (alpha)	25513	1.16	1.59	-1.16	2.97	1.24	2.35	-1.20	2.98
PRKCI	protein kinase C, iota	84006	/	/	-1.08	1.51	-1.04	1.64	-1.00	1.78
RAC1	ras-related C3 botulinum toxin substrate 1	363875	/	/	-1.24	2.04	1.08	2.16	-1.23	1.58
RELA	v-rel reticuloendotheliosis viral oncogene homolog A	309165	/	/	-1.27	1.61	-1.01	1.67	/	/
RHOA	ras homolog family member A	117273	1.23	2.02	1.61	3.68	2.22	3.98	1.56	1.77
RHOB	ras homolog family member B	64373	-1.27	2.53	-1.51	4.07	1.27	3.39	-1.13	2.30
RHOC	ras homolog family member C	295342	/	/	1.01	1.79	1.72	2.92	-1.54	1.31
RHOG	ras homolog family member G	308875	/	/	-1.22	2.05	1.10	2.32	-1.23	1.58
RHOH	ras homolog family member H	305341	/	/	-1.15	2.12	1.02	2.39	/	/
RHOJ	ras homolog family member J	299145	/	/	-1.31	3.33	1.40	2.87	-1.27	1.66
RHOQ	ras homolog family member Q	85428	/	/	-1.22	2.12	1.43	2.33	/	/
RND3	Rho family GTPase 3	295588	/	/	-1.24	2.15	1.10	1.96	-1.10	1.82
ROCK2	Rho-associated, coiled-coil containing protein kinase 2	25537	/	/	-1.16	1.59	1.02	1.64	/	/
SEPT9	septin 9	83788	/	/	-1.31	1.77	1.07	1.72	/	/
STMN1	stathmin 1	29332	-1.55	1.31	-1.40	1.94	1.03	1.94	/	/
VIM	vimentin	81818	/	/	-1.25	3.54	1.28	2.62	-1.08	1.75
WAS	Wiskott-Aldrich syndrome	317371	1.18	2.21	-1.03	2.43	1.09	2.02	1.09	2.00
WIPF1	WAS/WASL interacting protein family, member 1	117538	/	/	-1.37	2.65	1.40	3.25	-1.22	1.58

Table 5-16 Given are the fold-changes (average of treated rats against average of corresponding control rats) of Signaling by Rho Family GTPases of female rats treated with either 50 mg/kg (LD) or 300 mg/kg (HD) Vancomycin for up to 28 days. Genes were selected by t-test of HD treated rats ($p \leq 0.01$, $q \leq 0.01$, fold-change ≥ 1.5/ ≤ -1.5).

Symbol	Entrez Gene Name	Entrez Gene ID	Day 4		Day 8		Day 15		Day 29	
			LD	HD	LD	HD	LD	HD	LD	HD
ACTB	actin, beta	81822	-1.11	2.84	1.19	3.47	-1.02	2.04	1.50	3.82
ACTR3	ARP3 actin-related protein 3 homolog	81732	-1.10	1.98	1.31	2.56	1.06	1.65	1.19	2.30
ARHGEF2	Rho/Rac guanine nucleotide exchange factor (GEF) 2	310635	-1.11	2.10	1.70	3.74	1.15	1.74	1.73	3.14
ARPC3	actin related protein 2/3 complex, subunit 3, 21kDa	288669	-1.15	1.94	1.50	3.03	1.17	1.72	1.53	4.01
ARPC4	actin related protein 2/3 complex, subunit 4, 20kDa	297518	-1.08	2.03	1.39	2.99	1.11	1.67	1.39	2.95
ARPC5	actin related protein 2/3 complex, subunit 5, 16kDa	360854	-1.09	1.92	1.53	2.47	1.07	1.54	1.39	2.86

Symbol	Entrez Gene Name	Entrez Gene ID	Day 4		Day 8		Day 15		Day 29	
			LD	HD	LD	HD	LD	HD	LD	HD
ARPC1B	actin related protein 2/3 complex, subunit 1B, 41kDa	54227	1.03	2.68	1.38	3.89	1.04	1.97	1.56	5.20
CDC42EP1	CDC42 effector protein (Rho GTPase binding) 1	315121	1.04	1.59	-1.01	1.55	/	/	1.09	1.83
CDC42EP2	CDC42 effector protein (Rho GTPase binding) 2	309175	1.01	2.70	1.23	3.52	1.00	1.56	1.38	3.19
CDC42EP5	CDC42 effector protein (Rho GTPase binding) 5	361505	1.04	1.52	1.43	2.15	/	/	1.29	2.31
CDH11	cadherin 11, type 2, OB-cadherin (osteoblast)	84407	1.18	1.60	1.06	1.83	/	/	1.16	1.51
CFL2	cofilin 2 (muscle)	366624	-1.02	1.67	1.56	2.02	/	/	1.45	2.79
CYBB	cytochrome b-245, beta polypeptide	66021	1.02	2.61	-1.09	3.68	-1.00	1.67	1.11	1.81
CYFIP1	cytoplasmic FMR1 interacting protein 1	308666	1.05	1.78	1.51	2.56	/	/	1.33	2.38
DES	desmin	64362	-1.05	2.14	1.41	2.14	1.06	1.66	1.40	3.85
DIAPH3	diaphanous homolog 3 (Drosophila)	290396	-1.00	1.66	-1.13	1.65	/	/	-1.09	1.56
FOS	FBJ murine osteosarcoma viral oncogene homolog	314322	1.05	2.52	1.05	2.71	/	/	1.20	4.33
GNA15	guanine nucleotide binding protein, alpha 15	89788	/	/	-1.11	1.72	/	/	-1.03	1.56
GNAI2	guanine nucleotide binding protein, alpha inhibiting activity polypeptide 2	81664	1.14	1.99	1.52	3.05	1.18	1.64	1.74	3.06
GNB2L1	guanine nucleotide binding protein, beta polypeptide 2-like 1	83427	-1.06	2.10	1.29	3.11	1.14	1.69	1.59	3.31
GNG10	guanine nucleotide binding protein, gamma 10	114119	1.00	2.46	1.50	3.72	1.07	1.84	1.27	3.34
GNG13	guanine nucleotide binding protein, gamma 13	685451	-1.04	1.71	-1.05	1.86	/	/	1.11	2.44
ITGA4	integrin, alpha 4	311144	1.16	2.38	1.24	4.06	1.12	1.73	1.53	2.44
ITGA5	integrin, alpha 5	315346	-1.00	1.86	-1.04	1.85	/	/	1.14	2.11
ITGB1	integrin, beta 1	24511	1.06	2.88	1.34	3.50	1.01	1.89	1.50	3.86
JUN	jun proto-oncogene	24516	1.11	2.61	1.45	3.10	-1.01	1.62	1.45	3.38
LIMK1	LIM domain kinase 1	65172	1.08	1.75	1.07	1.73	/	/	1.13	3.02
MAP2K1	mitogen-activated protein kinase kinase 1	170851	1.06	1.74	1.82	2.73	1.21	1.55	1.60	3.00
MAPK1	mitogen-activated protein kinase 1	116590	1.14	1.91	1.47	2.28	1.16	1.52	1.38	2.15
MAPK12	mitogen-activated protein kinase 12	60352	/	/	1.24	1.53	/	/	1.12	1.52
MSN	moesin	81521	1.06	2.58	1.31	2.86	1.13	1.63	1.61	3.87
MYL9	myosin, light chain 9, regulatory	296313	1.14	1.97	1.12	1.79	/	/	1.16	2.40
NFKB2	nuclear factor of kappa light polypeptide gene enhancer in B-cells 2	309452	-1.14	2.39	1.21	2.94	1.05	2.01	1.30	3.78
PAK1	p21 protein (Cdc42/Rac)-activated kinase 1	29431	1.01	2.15	1.32	2.81	1.05	1.56	1.32	3.29
PAK2	p21 protein (Cdc42/Rac)-activated kinase 2	29432	/	/	1.25	1.59	/	/	1.29	1.61
PARD3	par-3 partitioning defective 3 homolog (C. elegans)	81918	1.10	1.70	1.28	1.86	/	/	1.38	2.44
PIK3R1	phosphoinositide-3-kinase, regulatory subunit 1 (alpha)	25513	-1.11	1.97	1.25	2.15	/	/	1.03	2.99
RAC1	ras-related C3 botulinum toxin substrate 1	363875	1.03	2.34	1.41	2.82	1.12	1.79	1.74	3.36

Symbol	Entrez Gene Name	Entrez Gene ID	Day 4		Day 8		Day 15		Day 29	
			LD	HD	LD	HD	LD	HD	LD	HD
RELA	v-rel reticuloendotheliosis viral oncogene homolog A	309165	-1.01	1.67	1.28	1.97	1.10	1.54	1.30	2.06
RHOA	ras homolog family member A	117273	2.39	3.64	2.23	2.02	1.66	1.50	2.49	2.57
RHOB	ras homolog family member B	64373	1.02	4.49	1.26	4.50	1.14	2.39	1.90	5.26
RHOC	ras homolog family member C	295342	-1.07	1.93	2.07	4.69	1.23	1.83	1.81	3.89
RHOG	ras homolog family member G	308875	1.24	2.23	1.43	3.30	1.21	1.76	1.46	2.56
RHOH	ras homolog family member H	305341	-1.01	1.53	1.22	3.09	1.02	1.51	1.26	1.71
RHOJ	ras homolog family member J	299145	1.24	1.97	1.64	3.02	1.15	1.56	1.71	2.88
RHOQ	ras homolog family member Q	85428	1.00	1.88	1.77	2.98	1.16	1.57	1.68	2.94
RND3	Rho family GTPase 3	295588	1.09	1.90	1.25	2.13	1.08	1.61	1.33	2.80
ROCK2	Rho-associated, coiled-coil containing protein kinase 2	25537	-1.17	1.56	1.50	1.93	/	/	1.20	1.74
SEPT9	septin 9	83788	1.04	1.87	1.38	2.40	/	/	1.56	2.46
STMN1	stathmin 1	29332	1.19	2.93	1.70	4.41	1.25	1.86	1.75	3.48
VIM	vimentin	81818	-1.01	1.82	1.77	2.99	/	/	1.77	3.42
WAS	Wiskott-Aldrich syndrome	317371	-1.09	2.11	-1.05	2.54	/	/	1.04	1.68
WASF1	WAS protein family, member 1	294568	-1.02	1.51	1.20	1.79	/	/	1.12	1.74
WIPF1	WAS/WASL interacting protein family, member 1	117538	1.03	2.39	1.71	4.39	1.15	1.92	1.61	3.58

Table 5-17 Given are the fold-changes (average of treated rats against average of corresponding control rats) of Signaling by HMGB1 Signaling of male rats treated with either 50 mg/kg (LD) or 300 mg/kg (HD) Vancomycin for up to 28 days. Genes were selected by t-test of HD treated rats ($p \leq 0.01$, $q \leq 0.01$, fold-change $\geq 1.5 / \leq -1.5$).

Symbol	Entrez Gene Name	Entrez Gene ID	Day 4		Day 8		Day 15		Day 29	
			LD	HD	LD	HD	LD	HD	LD	HD
AKT1	v-akt murine thymoma viral oncogene homolog 1	24185	/	/	-1.18	2.03	-1.05	1.85	-1.19	1.67
CCL2	chemokine (C-C motif) ligand 2	287562	/	/	1.06	2.26	/	/	1.11	1.84
FOS	FBJ murine osteosarcoma viral oncogene homolog	314322	1.62	3.50	1.04	4.33	1.05	2.48	1.24	3.18
HAT1	histone acetyltransferase 1	296501	/	/	-1.25	1.67	1.02	2.16	/	/
ICAM1	intercellular adhesion molecule 1	25464	-1.08	2.53	-1.31	4.43	1.19	3.88	1.10	3.40
IFNGR1	interferon gamma receptor 1	116465	-1.29	1.65	-1.42	2.43	1.07	2.77	-1.17	1.76
IFNGR2	interferon gamma receptor 2	360697	-1.26	1.58	-1.31	2.64	1.15	2.80	-1.23	1.64
JUN	jun proto-oncogene	24516	1.03	2.20	-1.09	2.96	1.22	3.37	-1.15	2.08
KAT2A	K(lysine) acetyltransferase 2A	303539	/	/	-1.20	1.63	1.02	1.67	/	/
MAP2K1	mitogen-activated protein kinase kinase 1	170851	/	/	-1.32	1.66	1.32	2.35	/	/
NFKB1	nuclear factor of kappa light polypeptide gene enhancer in B-cells 1	81736	1.22	1.62	1.07	1.57	/	/	1.18	1.73

Symbol	Entrez Gene Name	Entrez Gene ID	Day 4		Day 8		Day 15		Day 29	
			LD	HD	LD	HD	LD	HD	LD	HD
NFKB2	nuclear factor of kappa light polypeptide gene enhancer in B-cells 2	309452	-1.21	1.88	-1.18	2.45	1.00	2.19	-1.09	1.97
NRAS	neuroblastoma RAS viral (v-ras) oncogene homolog	24605	-1.16	1.70	-1.18	2.95	1.16	2.71	-1.10	2.37
PIK3R1	phosphoinositide-3-kinase, regulatory subunit 1 (alpha)	25513	1.16	1.59	-1.16	2.97	1.24	2.35	-1.20	2.98
PIK3R6	phosphoinositide-3-kinase, regulatory subunit 6	497932	/	/	1.17	1.53	/	/	/	/
PLAT	plasminogen activator, tissue	25692	/	/	-1.21	2.44	1.39	3.06	-1.05	1.70
RAC1	ras-related C3 botulinum toxin substrate 1	363875	/	/	-1.24	2.04	1.08	2.16	-1.23	1.58
RBBP7	retinoblastoma binding protein 7	83712	-1.14	-2.55	-1.07	-1.59	1.05	-1.69	-1.07	-1.87
RELA	v-rel reticuloendotheliosis viral oncogene homolog A	309165	/	/	-1.27	1.61	-1.01	1.67	/	/
RHOA	ras homolog family member A	117273	1.23	2.02	1.61	3.68	2.22	3.98	1.56	1.77
RHOB	ras homolog family member B	64373	-1.27	2.53	-1.51	4.07	1.27	3.39	-1.13	2.30
RHOC	ras homolog family member C	295342	/	/	1.01	1.79	1.72	2.92	-1.54	1.31
RHOG	ras homolog family member G	308875	/	/	-1.22	2.05	1.10	2.32	-1.23	1.58
RHOH	ras homolog family member H	305341	/	/	-1.15	2.12	1.02	2.39	/	/
RHOJ	ras homolog family member J	299145	/	/	-1.31	3.33	1.40	2.87	-1.27	1.66
RHOQ	ras homolog family member Q	85428	/	/	-1.22	2.12	1.43	2.33	/	/
RND3	Rho family GTPase 3	295588	/	/	-1.24	2.15	1.10	1.96	-1.10	1.82
RRAS	related RAS viral (r-ras) oncogene homolog	361568	-1.38	1.78	-1.42	2.36	-1.07	2.31	-1.27	1.91
SERPINE1	serpin peptidase inhibitor, clade E, member 1	24617	1.09	1.93	1.13	4.84	1.14	2.15	1.24	6.63
TLR4	toll-like receptor 4	29260	/	/	1.10	1.56	/	/	/	/
TNFRSF11B	tumor necrosis factor receptor superfamily, member 11b	25341	-1.57	-8.49	-1.32	-5.09	/	/	-3.19	-10.08
TNFRSF1A	tumor necrosis factor receptor superfamily, member 1A	25625	-1.20	2.24	-1.19	4.09	-1.02	3.03	1.06	3.29
VCAM1	vascular cell adhesion molecule 1	25361	/	/	-1.32	3.34	1.16	2.72	-1.18	1.51

Table 5-18 Given are the fold-changes (average of treated rats against average of corresponding control rats) of Signaling by HMGB1 Signaling of female rats treated with either 50 mg/kg (LD) or 300 mg/kg (HD) Vancomycin for up to 28 days. Genes were selected by t-test of HD treated rats ($p \leq 0.01$, $q \leq 0.01$, fold-change ≥ 1.5/ ≤ -1.5).

Symbol	Entrez Gene Name	Entrez Gene ID	Day 4		Day 8		Day 15		Day 29	
			LD	HD	LD	HD	LD	HD	LD	HD
AKT1	v-akt murine thymoma viral oncogene homolog 1	24185	-1.09	2.19	1.04	2.17	-1.04	1.68	1.05	2.73
HAT1	histone acetyltransferase 1	296501	-1.28	1.62	1.31	2.19	-1.08	1.59	1.32	3.39
ICAM1	intercellular adhesion molecule 1	25464	1.11	3.80	1.67	5.67	1.18	2.57	1.68	5.87
IFNGR1	interferon gamma receptor 1	116465	-1.03	2.56	-1.08	3.02	1.09	1.67	1.30	2.96

Symbol	Entrez Gene Name	Entrez Gene ID	Day 4		Day 8		Day 15		Day 29	
			LD	HD	LD	HD	LD	HD	LD	HD
IFNGR2	interferon gamma receptor 2	360697	1.15	2.53	1.47	3.97	1.01	1.66	1.34	3.04
JUN	jun proto-oncogene	24516	1.11	2.61	1.45	3.10	-1.01	1.62	1.45	3.38
KAT2A	K(lysine) acetyltransferase 2A	303539	1.02	1.71	1.24	1.98	1.10	1.53	1.16	2.43
MAP2K1	mitogen-activated protein kinase kinase 1	170851	1.06	1.74	1.82	2.73	1.21	1.55	1.60	3.00
MAPK1	mitogen-activated protein kinase 1	116590	1.14	1.91	1.47	2.28	1.16	1.52	1.38	2.15
NFKB2	nuclear factor of kappa light polypeptide gene enhancer in B-cells 2	309452	-1.14	2.39	1.21	2.94	1.05	2.01	1.30	3.78
NRAS	neuroblastoma RAS viral (v-ras) oncogene homolog	24605	-1.07	2.44	1.25	2.94	1.08	1.75	1.30	3.38
RAC1	ras-related C3 botulinum toxin substrate 1	363875	1.03	2.34	1.41	2.82	1.12	1.79	1.74	3.36
RELA	v-rel reticuloendotheliosis viral oncogene homolog A	309165	-1.01	1.67	1.28	1.97	1.10	1.54	1.30	2.06
RHOA	ras homolog family member A	117273	2.39	3.64	2.23	2.02	1.66	1.50	2.49	2.57
RHOB	ras homolog family member B	64373	1.02	4.49	1.26	4.50	1.14	2.39	1.90	5.26
RHOC	ras homolog family member C	295342	-1.07	1.93	2.07	4.69	1.23	1.83	1.81	3.89
RHOG	ras homolog family member G	308875	1.24	2.23	1.43	3.30	1.21	1.76	1.46	2.56
RHOH	ras homolog family member H	305341	-1.01	1.53	1.22	3.09	1.02	1.51	1.26	1.71
RHOJ	ras homolog family member J	299145	1.24	1.97	1.64	3.02	1.15	1.56	1.71	2.88
RHOQ	ras homolog family member Q	85428	1.00	1.88	1.77	2.98	1.16	1.57	1.68	2.94
RND3	Rho family GTPase 3	295588	1.09	1.90	1.25	2.13	1.08	1.61	1.33	2.80
RRAS	related RAS viral (r-ras) oncogene homolog	361568	-1.15	2.24	1.30	2.80	1.02	1.79	1.36	3.66
TNFRSF11B	tumor necrosis factor receptor superfamily, member 11b	25341	-1.14	-2.81	2.22	-2.53	1.10	-1.57	-1.14	-5.45
TNFRSF1A	tumor necrosis factor receptor superfamily, member 1A	25625	1.12	2.96	1.23	3.92	1.09	2.16	1.73	5.68
VCAM1	vascular cell adhesion molecule 1	25361	1.21	2.88	1.11	3.44	1.15	1.91	1.76	3.28

5.3 Annex 3 Overview of viability values of NRK-52E cells

Table 5-19 Given are the viability ± Standarddeviation (SD) values in percentage of vehicle control of NRK-52E cells treated with one of five concentrations of either Puromycin Paracetamol, Doxorubicin, AphotericinB, Metformin, d-Mannitol for 72h. Values are presented for ATP-depletion as well as neutral red uptake assay over five concentration [µM].

		conc. [µM]				
Puromycin		**0,025**	**0,25**	**2,5**	**25**	**250**
ATP	mean (viability)	99%	68%	0%	2%	3%
	SD (viability)	2%	2%	0%	0%	0%
NRU	mean (viability)	104%	90%	0%	0%	0%
	SD (viability)	8%	7%	0%	0%	0%

		conc. [µM]				
Paracetamol		**50**	**250**	**500**	**1000**	**2000**
ATP	mean (viability)	114%	100%	113%	103%	83%
	SD viability	6%	13%	7%	8%	10%
NRU	mean (viability)	109%	111%	119%	96%	73%
	SD (viability)	30%	22%	19%	16%	14%

		conc. [µM]				
Doxorubicin		**0,0005**	**0,005**	**0,05**	**0,5**	**5**
ATP	mean (viability)	97%	91%	64%	21%	6%
	SD (viability)	2%	2%	2%	11%	1%
NRU	mean (viability)	116%	123%	68%	10%	0%
	SD (viability)	34%	37%	26%	3%	2%

		conc. [µM]				
Amphotericin B		**0,05**	**0,5**	**5**	**50**	**125**
ATP	mean (viability)	105%	115%	84%	0%	3%
	SD (viability)	3%	7%	9%	0%	0%
NRU	mean (viability)	130%	112%	110%	118%	9%
	SD (viability)	41%	18%	30%	51%	4%

		conc. [µM]				
Metforimin		**50**	**100**	**250**	**500**	**1000**
ATP	mean (viability)	102%	103%	104%	96%	84%
	SD (viability)	5%	3%	2%	10%	11%
NRU	mean (viability)	125%	127%	134%	133%	131%
	SD (viability)	25%	68%	58%	63%	37%

d-Mannitol		conc. [µM] 0,5	5	50	500	5000
ATP	mean (viability)	104%	104%	106%	107%	107%
	SD viability	1%	8%	3%	1%	6%
NRU	mean (viability)	132%	141%	131%	132%	141%
	SD viability	58%	64%	54%	48%	51%

5.4 Annex 4 Transcriptional FC values of NRK-52E cells after treatment with (non-)nephrotoxic compounds

Table 5-20 Given are the fold-changes (FC; average of treatment against average of corresponding vehicle control) of significant altered transcripts (t-test $p \leq 0.01$, fold-change $\geq 1.5 / \leq -1.5$) in NRK-52E cells after treatment with either the TC_{20} or the NOAEC of Puromycin, Paracetamol, Doxorubicin, or AmphotericinB. In addition the transcriptional alterations of the identified transcripts after treatment with two negative compounds, Metformin and d-Mannitol are displayed.

Gene symbol	Accession No.	AmphotericinB		Doxorubicin		Puromycin		Paracetamol		Metformin		d-Mannitol	
		LD	HD	LD	HD	LD	HD	LD	HD	LD	HD	LD	HD
Aars	XM_001077503.1	1,45	1,93	1,12	1,64	1,00	1,72	1,29	1,69	-1,10	1,05	-1,05	-1,04
Abcc3	NM_080581.1	-1,18	-1,68	-1,12	-1,41	-1,10	-1,58	-1,29	-1,83	-1,00	1,02	-1,04	-1,16
Abtb1	NM_001005902.1	-1,36	-1,81	-1,12	-1,13	-1,13	-1,58	-1,33	-1,60	-1,10	-1,12	-1,14	-1,07
Adhfe1	NM_001025423.1	-1,54	-2,37	-1,46	-1,67	-1,07	-1,94	-1,64	-2,27	1,16	1,04	-1,10	-1,07
Aldoc	NM_012497.1	-1,69	-2,56	-1,22	-2,00	-1,05	-2,34	-2,06	-2,99	-1,09	-1,09	-1,06	-1,04
Ampd3	NM_031544.1	-1,06	-2,01	-1,30	-1,55	-1,15	-2,09	-1,44	-3,31	-1,05	-1,13	-1,06	-1,08
Ankrd1	NM_013220.1	1,10	6,99	1,24	9,03	-1,02	2,65	1,56	18,18	-1,19	-1,22	-1,08	-1,07
Arhgef19_predicted	XM_342965.3	-1,35	-2,57	-1,21	-1,68	1,03	-1,76	-1,37	-2,38	1,00	-1,02	-1,08	-1,08
Armcx1	NM_001024367.1	-1,27	-2,07	-1,22	-2,24	-1,04	-1,89	-1,43	-3,83	1,01	-1,10	1,02	1,07
Asns	NM_013079.1	1,57	2,48	1,25	1,82	1,12	2,04	1,64	2,75	1,08	1,18	1,22	1,19
Atf4	NM_024403.1	1,36	1,85	1,16	1,59	-1,01	1,70	1,19	1,87	1,05	1,00	-1,01	1,02
Atp8b3_predicted	XM_001076355.1	-1,41	-2,25	-1,30	-1,55	-1,12	-1,79	-1,37	-2,54	-1,19	-1,09	-1,33	-1,24
B4galt4	NM_001012018.1	-1,32	-2,24	-1,10	-2,05	-1,05	-1,62	-1,30	-2,93	-1,07	-1,09	-1,11	-1,03
Baz1a_predicted	XM_001079067.1	1,32	1,90	1,25	1,42	1,05	1,71	1,44	1,91	1,09	1,15	1,10	1,04
Bhmt	NM_030850.1	-1,29	-1,67	-1,16	-1,28	-1,05	-1,72	-1,34	-1,86	-1,03	-1,11	-1,01	1,01
Boc_predicted	XM_001060215.1	-1,51	-3,25	-1,35	-2,13	-1,03	-1,80	-1,57	-3,67	-1,03	-1,03	-1,16	-1,17
C1qtnf1	NM_001007675.1	-1,66	-3,93	-1,30	-2,00	-1,03	-2,36	-1,55	-3,23	1,04	1,04	-1,02	-1,06
Calcoco1	NM_139190.1	-1,42	-2,88	-1,33	-1,20	-1,06	-1,74	-1,38	-1,84	-1,02	-1,12	-1,16	-1,30
Cars_predicted	XM_001065753.1	1,46	1,59	1,07	1,50	1,04	1,53	1,30	1,70	-1,02	1,02	1,03	1,03
Ccne2_predicted	XM_001064132.1	1,55	2,00	1,24	-1,11	1,08	1,96	2,27	2,68	1,11	1,16	1,17	1,06
Ccng1	NM_012923.1	1,16	2,20	1,60	2,51	1,16	1,71	1,74	2,73	1,07	1,07	1,06	-1,00
Cd44	NM_012924.2	1,35	2,15	1,18	2,17	-1,00	1,79	1,36	3,43	-1,02	-1,08	-1,05	-1,02
Cdc6_predicted	XM_340896.3	1,30	2,22	1,14	-1,26	1,04	1,71	1,79	2,25	-1,15	-1,02	1,07	1,08
Cdkn1a	NM_080782.3	1,18	2,65	2,17	4,04	1,10	2,11	2,02	5,40	1,15	1,24	1,16	-1,02
Cep70	NM_001017470.1	-1,30	-1,80	-1,21	-1,76	-1,11	-1,66	-1,49	-2,33	1,01	-1,04	-1,02	-1,04
Cfd	XM_001077068.1	-1,64	-1,93	-1,48	-1,57	-1,10	-2,19	-1,85	-2,12	-1,07	-1,13	-1,04	1,02
Cln6_predicted	XM_236325.3	-1,49	-3,57	-1,32	-2,91	-1,10	-2,38	-1,70	-5,10	-1,08	-1,14	-1,18	-1,11
Cnksr3	NM_001012061.1	1,21	1,95	1,34	2,09	1,12	1,93	1,50	2,58	1,06	1,10	1,10	1,17

Gene symbol	Accession No.	AmphotericinB		Doxorubicin		Puromycin		Paracetamol		Metformin		d-Mannitol	
		LD	HD	LD	HD	LD	HD	LD	HD	LD	HD	LD	HD
Col16a1	XM_345584.3	-1,35	-1,95	1,00	-1,51	1,03	-1,54	-1,15	-2,11	1,06	1,01	-1,06	1,05
Col3a1	NM_032085.1	-2,56	-5,97	-1,35	-3,05	-1,09	-4,60	-1,83	-6,29	1,09	1,02	-1,12	-1,04
Coro2a_predicted	XM_575819.1	-1,25	-1,74	-1,19	-1,28	-1,06	-1,56	-1,27	-1,78	1,04	-1,02	1,10	1,01
Cryab	NM_012935.2	1,13	2,28	1,19	3,80	1,07	1,75	1,16	4,61	-1,04	1,00	1,01	-1,04
Csad	NM_021750.1	-1,34	-2,86	-1,19	-1,98	-1,05	-1,94	-1,47	-2,65	1,04	1,05	1,03	-1,01
Csdc2	XM_001077363.1	-1,31	-1,98	-1,16	-1,39	-1,05	-1,75	-1,30	-1,96	-1,02	1,00	-1,07	-1,17
Cxcl1	NM_030845.1	1,34	11,43	1,61	1,67	-1,02	1,03	1,35	2,99	1,08	1,06	1,21	1,28
Cxcl13	NM_001017496.1	-1,91	-3,25	-1,25	-1,88	-1,02	-2,71	-1,96	-3,28	1,06	-1,12	-1,03	1,05
Cycs	NM_012839.2	1,35	2,24	1,19	1,74	1,04	1,53	1,34	2,20	1,04	1,08	1,13	1,12
Cyr61	NM_031327.2	1,03	3,16	1,67	2,61	1,02	1,61	1,56	3,39	1,01	1,03	1,02	1,14
Dci	NM_017306.3	-1,33	-2,11	-1,22	-2,99	-1,02	-1,89	-1,57	-2,49	1,03	-1,08	-1,00	1,08
Ddah1	NM_022297.2	1,26	3,33	1,28	2,39	1,13	1,79	1,39	3,16	-1,11	1,02	1,00	-1,02
Donson	NM_001008287.1	1,25	1,64	1,17	-1,14	1,08	1,56	1,70	2,17	1,05	1,06	1,18	1,00
Ech1	NM_022594.1	-1,49	-3,00	-1,23	-1,48	-1,06	-1,85	-1,58	-2,10	1,00	-1,00	-1,06	-1,12
Edn1	NM_012548.1	-1,06	4,22	1,74	4,18	-1,00	1,70	1,72	6,37	1,09	1,07	1,04	1,06
Elmo3	NM_001030028.1	-1,17	-2,09	1,01	-1,40	-1,08	-1,61	-1,09	-1,48	1,00	-1,02	-1,03	-1,12
Enc1	NM_001003401.1	1,19	1,68	1,32	1,41	1,13	1,66	1,44	2,38	1,06	1,07	1,10	1,08
Enpp3	NM_019370.1	-1,21	-2,24	-1,34	-2,09	-1,19	-2,57	-1,28	-2,82	-1,09	-1,09	-1,24	-1,31
Ephx2	NM_022936.1	-1,22	-1,88	-1,07	-1,81	1,12	-1,59	-1,13	-1,88	1,17	1,07	1,08	1,09
Ergic3_predicted	XM_001066442.1	-1,71	-1,96	-1,31	-1,28	-1,24	-1,72	-1,70	-2,02	-1,09	-1,15	-1,22	-1,35
Eva_predicted	XM_236197.3	-1,21	-1,79	1,03	-1,70	-1,07	-1,72	-1,12	-2,22	-1,07	-1,10	-1,00	1,00
Fah	NM_017181.2	-1,56	-1,98	-1,33	-1,83	-1,07	-1,59	-1,70	-2,92	-1,04	-1,07	-1,18	-1,03
Fbxo2	NM_053511.1	-1,36	-1,70	-1,24	-1,77	-1,15	-1,54	-1,36	-1,74	-1,21	-1,26	-1,16	-1,19
Fbxo6b	NM_138917.2	-1,39	-1,90	-1,23	-1,14	-1,10	-1,71	-1,60	-2,12	-1,09	-1,10	-1,28	-1,15
Fcgrt	NM_033351.1	-1,63	-2,67	-1,19	-1,28	-1,11	-1,79	-1,40	-1,89	1,02	1,02	-1,07	-1,10
Fhl1	NM_145669.2	1,48	3,64	1,27	2,49	1,13	2,46	1,96	5,23	1,09	1,05	1,05	1,02
Flot1	NM_022701.1	-1,33	-2,23	-1,32	-1,67	-1,02	-1,30	-1,51	-2,00	1,00	-1,01	-1,10	-1,14
Flrt3_predicted	XM_001080226.1	1,30	2,65	1,20	2,03	1,04	2,24	1,65	3,71	-1,03	1,07	1,01	-1,03
Fmo4	NM_144562.1	-1,07	-1,63	-1,17	-1,23	-1,05	-1,51	-1,21	-1,62	-1,05	-1,11	-1,20	1,00
Fn1	NM_019143.1	1,21	2,55	1,34	2,88	1,08	1,55	1,68	3,49	1,06	-1,01	1,14	1,28
Fst	NM_012561.1	1,20	2,29	1,72	3,72	1,07	2,04	1,93	4,57	-1,07	1,16	1,11	1,10
Gamt	NM_012793.1	-1,44	-1,74	-1,25	-1,55	-1,04	-1,78	-1,46	-1,70	-1,01	-1,05	-1,10	1,00
Gars	XM_216152.4	1,40	1,42	1,10	1,51	-1,01	1,58	1,47	1,69	-1,05	-1,04	-1,11	-1,15
Gja12_predicted	XM_573100.2	-1,64	-1,99	-1,08	-1,48	-1,21	-1,64	-1,56	-1,65	-1,17	-1,14	-1,15	-1,17
Gpc3	NM_012774.1	-1,05	-1,90	1,04	-7,31	1,01	-1,99	-1,19	-10,15	-1,01	-1,05	1,07	1,11

Gene symbol	Accession No.	AmphotericinB		Doxorubicin		Puromycin		Paracetamol		Metformin		d-Mannitol	
		LD	HD	LD	HD	LD	HD	LD	HD	LD	HD	LD	HD
Gpr126_predicted	XM_001071417.1	1,26	2,42	1,24	2,74	1,09	1,87	1,19	3,60	1,04	1,05	-1,02	1,01
Gsta4	XM_001059683.1	-1,28	-2,19	-1,01	-1,54	-1,15	-1,95	-1,37	-2,09	1,08	-1,06	1,06	1,07
Gstm1	NM_017014.1	-1,82	-2,31	-1,20	-1,56	-1,13	-2,40	-1,81	-2,10	-1,09	-1,11	-1,15	-1,09
Hist1h2ao_predicted	XM_344599.2	1,19	1,96	1,30	2,11	1,10	2,52	1,41	5,45	1,03	1,04	1,03	1,03
Htra1	NM_031721.1	1,06	2,71	1,49	3,80	1,05	1,51	1,32	4,60	-1,08	-1,11	1,01	1,08
Idh1	NM_031510.1	-1,17	-2,05	-1,22	-1,90	1,02	-1,68	-1,33	-2,25	-1,03	-1,04	1,01	-1,10
Ifi35	NM_001009625.1	-1,39	-1,57	-1,13	-1,54	1,05	-1,71	-1,30	-1,36	-1,05	-1,10	-1,07	-1,00
Igfbp6	NM_013104.2	-1,75	-6,64	-1,36	-4,08	-1,08	-3,25	-1,98	-6,79	1,13	1,11	1,12	1,01
Isg20l1_predicted	XM_341874.3	1,13	3,34	1,89	2,78	1,17	1,71	1,59	3,81	1,02	-1,05	1,07	1,21
Itga3_predicted	XM_340884.2	1,23	1,18	-1,05	1,87	1,05	1,95	1,29	1,96	1,07	1,31	-1,07	-1,14
Ivns1abp_predicted	XM_213898.4	1,30	1,72	1,13	1,21	1,02	1,54	1,63	1,59	-1,00	1,01	1,07	1,05
Kazald1	NM_001033064.1	-1,73	-3,52	-1,36	-2,47	-1,07	-2,84	-1,91	-4,00	-1,03	-1,02	-1,12	-1,03
Kcnmb4	NM_023960.2	-1,28	-2,07	-1,21	-1,11	-1,10	-1,71	-1,22	-1,58	-1,03	-1,07	-1,14	-1,13
KIFC2	NM_198752.1	-1,54	-2,11	-1,22	-1,71	-1,14	-2,11	-1,45	-2,56	-1,08	-1,19	-1,16	-1,11
Klc4	NM_001009601.1	-1,43	-1,89	-1,06	-1,32	-1,06	-1,68	-1,34	-1,95	-1,15	-1,16	-1,12	-1,03
Krt15	NM_001004022.2	-1,37	-2,19	-1,04	-1,43	-1,05	-1,83	-1,04	-2,65	-1,07	-1,09	1,07	1,03
Krt19	NM_199498.1	-1,73	-6,54	-1,46	-3,61	-1,13	-4,60	-1,40	-9,09	-1,07	-1,25	-1,05	-1,08
LOC304500	XM_222190.3	-1,29	-1,68	-1,16	-1,37	1,02	-1,59	-1,25	-1,64	-1,05	-1,07	-1,16	-1,04
LOC360228	NM_001003706.1	-1,75	-2,01	-1,05	-1,41	1,03	-1,71	-1,54	-1,78	-1,04	-1,23	-1,04	1,03
LOC497685	XM_579547.1	-1,31	-2,30	-1,28	-1,27	-1,11	-1,75	-1,53	-1,91	-1,04	-1,11	-1,18	-1,19
LOC497723	XM_579534.1	1,40	1,41	1,41	1,59	1,15	1,62	1,57	1,72	1,36	1,24	1,27	1,24
LOC497767	XM_579388.1	-1,54	-3,16	-1,14	-1,62	-1,04	-2,07	-1,51	-2,69	1,00	-1,12	-1,05	-1,04
LOC499120	XM_001078762.1	-1,26	-1,69	-1,31	-1,67	-1,03	-1,54	-1,31	-2,23	-1,05	-1,09	-1,04	-1,06
LOC499201	XM_579934.1	1,54	1,85	1,30	1,53	1,15	1,15	1,29	3,13	1,18	1,06	1,11	1,08
LOC679409	XM_001054960.1	-1,06	-1,79	-1,21	-1,86	-1,08	-1,61	-1,51	-3,01	-1,04	-1,09	-1,10	-1,13
LOC684490	XM_001067912.1	1,58	3,70	1,36	1,69	1,07	2,03	1,87	3,40	-1,07	1,04	1,10	1,13
LOC687840	XM_001080312.1	-1,36	-2,33	-1,02	-1,75	-1,09	-2,35	-1,41	-2,11	1,00	-1,04	1,02	1,01
Loxl3_predicted	XM_232107.4	-1,36	-1,64	-1,18	-1,37	-1,18	-1,65	-1,31	-1,69	-1,12	-1,05	-1,29	-1,25
Lrp8_predicted	XM_342877.2	1,31	1,61	1,18	1,32	1,11	1,69	1,44	2,04	1,06	1,11	1,08	1,06
Lrrc56	NM_001024902.1	-1,58	-2,19	-1,15	-1,83	-1,10	-2,07	-1,50	-2,63	-1,13	-1,25	-1,04	-1,03
Lztfl1	NM_001024266.1	-1,41	-1,95	-1,22	-1,45	-1,05	-1,61	-1,54	-2,08	-1,04	-1,06	-1,05	-1,01
Maged2	NM_080479.2	-1,28	-1,74	-1,13	-1,37	-1,02	-1,72	-1,35	-2,19	-1,05	-1,11	-1,18	-1,18
Map2k6	NM_053703.2	-1,04	-1,66	-1,30	-1,65	-1,06	-2,17	-1,25	-2,20	1,02	1,03	-1,04	1,01
Mcm10_predicted	XM_001071383.1	1,44	1,69	1,03	-1,51	1,09	1,53	1,75	1,35	-1,02	1,06	1,03	-1,06
Mettl7a	NM_001037355.1	-1,52	-2,67	-1,55	-1,74	-1,19	-2,22	-1,98	-2,58	-1,10	-1,04	-1,28	-1,27

Gene symbol	Accession No.	AmphotericinB		Doxorubicin		Puromycin		Paracetamol		Metformin		d-Mannitol	
		LD	HD	LD	HD	LD	HD	LD	HD	LD	HD	LD	HD
Mettl7a	NM_001037355.1	-1,44	-1,85	-1,27	-1,55	-1,17	-1,81	-1,64	-2,13	-1,20	-1,20	-1,11	-1,15
MGC94199	NM_001007746.1	-1,28	-1,96	-1,21	-2,06	1,04	-1,55	-1,44	-2,74	-1,02	-1,10	-1,07	-1,00
Mgp	NM_012862.1	-2,17	-3,45	-1,84	-2,31	-1,17	-3,66	-2,56	-3,74	1,11	1,01	-1,01	1,23
Mgst1	NM_134349.2	-1,22	-2,19	-1,11	-1,81	-1,02	-1,77	-1,30	-1,70	1,05	1,04	1,03	-1,01
Mmp11	NM_012980.1	-1,39	-2,27	-1,23	-1,85	1,01	-1,58	-1,47	-2,50	1,17	1,10	-1,06	-1,07
Mpst	NM_138843.1	-1,42	-1,97	-1,21	-1,70	-1,04	-1,73	-1,45	-1,72	-1,06	1,01	-1,07	-1,13
Ms4a11_predicted	XM_001075502.1	-1,18	-1,52	1,09	1,02	-1,05	-1,56	1,09	1,55	1,03	-1,02	1,06	1,02
Mthfd1	NM_022508.1	1,21	1,79	1,24	1,62	1,04	1,72	1,50	2,24	-1,02	1,01	1,06	1,04
Mybl1_predicted	XM_232620.3	1,15	1,78	1,28	1,16	1,04	1,75	1,75	2,90	1,08	1,09	1,03	1,05
Myc	NM_012603.2	1,30	2,64	1,20	2,03	-1,01	2,12	1,50	2,62	-1,02	-1,06	1,08	1,02
Myh14	XM_001080622.1	-1,58	-2,68	-1,24	-1,84	-1,07	-1,90	-1,57	-2,68	1,01	-1,16	-1,17	-1,08
Myh6	NM_017239.1	-1,71	-2,65	1,05	-1,61	-1,05	-1,63	1,04	-2,01	-1,03	-1,06	1,08	1,16
Ndrg2	NM_133583.1	-1,55	-2,30	-1,11	-1,41	-1,09	-1,94	-1,64	-2,70	-1,15	-1,14	-1,08	1,04
Nme3	NM_053507.1	-1,45	-1,55	-1,15	-2,27	-1,10	-1,84	-1,41	-1,68	-1,07	-1,10	-1,13	-1,02
Nme7	NM_138532.1	-1,30	-2,07	-1,29	-1,59	1,00	-1,51	-1,47	-2,23	1,00	-1,05	1,01	-1,06
Nol5a	NM_001025732.1	1,25	2,47	1,20	1,42	-1,00	1,71	1,51	1,88	-1,14	-1,04	1,08	1,01
Nppb	NM_031545.1	1,17	5,60	1,48	12,85	-1,05	2,19	1,55	23,09	-1,07	-1,08	1,10	1,10
Nrep	NM_178096.2	-1,45	-1,74	-1,21	-2,09	-1,07	-1,69	-1,31	-2,53	-1,14	-1,07	-1,02	1,05
Odc1	NM_012615.1	1,38	1,77	1,02	1,50	1,01	1,93	1,58	2,68	1,01	1,04	-1,03	-1,08
Oplah	NM_053904.1	-1,16	-1,76	1,07	-1,51	1,04	-2,28	-1,28	-2,16	-1,02	-1,06	1,09	1,24
Pcolce	NM_019237.1	-1,35	-1,63	-1,15	-1,06	-1,10	-1,57	-1,33	-1,61	-1,07	-1,07	-1,16	-1,14
Pdk2	NM_030872.1	-1,50	-2,45	-1,04	-1,30	-1,01	-1,85	-1,41	-1,82	-1,00	-1,08	-1,03	1,05
Phyh	NM_053674.1	-1,31	-2,24	-1,08	-2,24	1,06	-1,90	-1,68	-3,52	-1,00	1,14	1,13	1,09
Phyhd1	NM_001013081.1	-1,91	-4,55	-1,24	-1,60	-1,16	-3,46	-1,80	-2,95	-1,09	-1,12	-1,12	-1,09
Pik3ip1	NM_001017453.1	-1,20	-2,90	-1,33	-2,96	-1,06	-2,25	-1,73	-5,48	1,03	1,13	-1,15	-1,09
Pink1_predicted	XM_216565.4	-1,21	-1,92	-1,12	-1,24	-1,02	-1,58	-1,36	-1,79	1,04	-1,06	-1,09	-1,12
Pomgnt1	NM_001007747.1	1,23	1,96	1,28	2,77	1,07	1,78	1,30	2,76	1,04	1,06	1,10	1,22
Ptpru	XM_342930.2	-1,55	-2,14	-1,06	-1,43	-1,02	-1,60	-1,21	-2,38	-1,03	-1,07	-1,02	-1,02
Pus7_predicted	XM_001061692.1	1,33	1,75	1,18	1,06	1,08	1,73	1,51	1,67	-1,03	1,12	1,13	1,10
Rbp1	NM_012733.4	-2,06	-6,27	-1,31	-4,91	-1,06	-1,90	-1,28	-4,58	1,02	1,01	-1,05	-1,04
Rcbtb2	NM_199084.1	-1,18	-2,10	-1,26	-2,28	-1,06	-1,66	-1,26	-2,90	1,01	1,04	-1,04	-1,10
Rcn3_predicted	NM_001008694.1	-1,50	-1,92	1,11	-1,84	1,05	-2,21	-1,14	-2,28	1,10	1,05	1,12	1,16
RGD1304580	NM_001009283.1	-1,50	-2,19	-1,22	-1,49	-1,09	-2,25	-1,34	-2,12	-1,05	-1,05	-1,10	1,07
RGD1306063_predicted	XM_214137.3	-1,32	-1,60	-1,24	-1,43	-1,12	-1,54	-1,59	-1,79	-1,07	-1,13	-1,09	-1,07
RGD1306107_predicted	XM_227412.4	-1,18	-1,96	-1,17	-1,50	-1,08	-1,64	-1,25	-2,25	-1,06	-1,12	-1,02	-1,10

Gene symbol	Accession No.	AmphotericinB		Doxorubicin		Puromycin		Paracetamol		Metformin		d-Mannitol	
		LD	HD	LD	HD	LD	HD	LD	HD	LD	HD	LD	HD
RGD1307392_predicted	XM_001060869.1	-1,45	-1,65	-1,26	-1,70	-1,16	-1,50	-1,43	-1,87	-1,06	-1,14	-1,14	-1,11
RGD1307396_predicted	XM_341029.3	-1,30	-2,34	-1,13	-1,97	1,01	-1,79	-1,21	-3,05	1,00	-1,07	1,09	-1,04
RGD1307493_predicted	XM_001080742.1	1,27	2,08	1,24	1,21	-1,02	1,71	1,47	1,91	-1,08	1,06	1,07	1,08
RGD1307524_predicted	XM_219909.4	-1,64	-2,52	-1,37	-1,69	1,02	-1,66	-1,46	-1,90	1,02	-1,08	-1,20	-1,19
RGD1307682	NM_001024760.1	-1,43	-1,92	-1,19	-1,48	-1,08	-1,76	-1,33	-1,59	-1,15	-1,11	-1,16	-1,15
RGD1308013_predicted	XM_001068272.1	-1,33	-4,02	-1,20	-3,14	-1,06	-2,79	-2,28	-8,64	1,06	1,09	1,04	-1,02
RGD1309263_predicted	XM_214574.4	-1,17	-1,27	-1,02	-1,53	1,00	-1,53	-1,25	-1,54	-1,10	-1,08	-1,06	-1,08
RGD1311307	NM_001025719.1	1,02	2,04	1,27	3,21	1,09	1,88	1,24	3,68	-1,02	-1,04	-1,01	1,09
RGD1560177_predicted	XM_001057282.1	1,04	2,06	1,16	2,03	-1,03	1,55	1,18	2,81	-1,11	-1,06	-1,12	-1,06
RGD1560453_predicted	XM_574890.2	-1,17	-1,61	-1,22	-1,65	-1,07	-1,60	-1,27	-2,00	-1,14	-1,04	1,01	-1,01
RGD1560673_predicted	XM_001078819.1	-1,23	-1,52	-1,12	-1,43	-1,07	-1,69	-1,53	-1,94	-1,06	-1,10	-1,07	-1,03
RGD1560911_predicted	XM_001062704.1	-1,46	-1,75	-1,05	-1,33	-1,04	-2,06	-1,43	-1,48	1,06	-1,10	1,10	1,16
RGD1561254_predicted	XM_001065019.1	1,18	1,75	1,28	1,71	1,05	1,51	1,39	2,16	1,01	1,05	1,14	1,07
RGD1562852_predicted	XM_001067836.1	-1,33	-1,86	-1,21	-1,55	-1,08	-1,86	-1,60	-2,05	-1,08	-1,17	-1,02	-1,02
RGD1563521_predicted	XR_007378.1	1,23	2,27	1,11	1,28	-1,04	1,81	1,37	2,02	-1,05	-1,06	1,00	1,01
RGD1564040_predicted	XM_001062502.1	1,48	3,12	1,17	1,54	1,01	1,99	1,69	2,81	-1,02	-1,03	-1,04	1,01
RGD1565950_predicted	XM_001071965.1	-1,47	-1,84	-1,04	-1,34	1,10	-1,75	-1,58	-2,42	1,08	-1,00	1,10	1,23
Rgs2	NM_053453.1	1,33	2,53	1,71	2,03	1,16	2,69	2,36	2,84	1,14	1,16	1,37	1,29
Rilpl2	NM_001004205.1	-1,28	-1,79	-1,35	-1,67	-1,04	-1,72	-1,53	-2,16	-1,01	-1,05	-1,16	-1,00
Rnd1	NM_001013222.1	1,03	2,28	1,32	5,10	-1,08	1,87	1,45	7,57	-1,04	-1,08	-1,04	-1,04
Rnu3ip2_predicted	XM_343469.3	1,04	1,98	1,05	1,44	-1,08	1,51	1,20	1,69	-1,06	-1,03	-1,11	-1,08
Rragd_predicted	XM_001063809.1	1,07	-1,91	-1,23	-1,57	-1,02	-2,05	-1,68	-2,59	-1,01	1,05	-1,02	-1,14
Rrm2	NM_001025740.1	1,72	2,49	1,40	-1,88	1,11	1,92	2,21	2,77	1,06	1,20	1,23	1,13
RT1-S3	XM_001072449.1	-1,34	-2,34	-1,23	-1,49	-1,07	-1,89	-1,43	-2,03	1,01	-1,02	1,02	1,01
Rtn1	NM_053865.1	-1,33	-1,61	-1,25	-1,54	1,00	-1,51	-1,01	-1,19	-1,02	-1,08	-1,18	-1,21
S100a1	NM_001007636.1	-1,95	-3,88	-1,37	-2,16	-1,17	-2,24	-1,87	-2,05	1,01	-1,03	1,02	1,01
S100a13_predicted	XM_215607.3	-1,85	-3,20	-1,41	-2,53	-1,07	-2,09	-1,88	-2,71	-1,07	-1,13	-1,14	-1,06
S100a16_predicted	XM_342291.3	-1,29	-2,17	-1,19	-1,34	-1,08	-1,74	-1,91	-2,26	1,01	-1,06	-1,08	-1,06
Sec11c	NM_153628.1	1,39	1,65	1,33	2,45	1,10	1,54	1,59	2,53	1,14	1,09	1,20	1,08
Selenbp1	NM_080892.1	-1,57	-3,16	-1,53	-2,88	-1,10	-3,15	-1,58	-3,88	-1,00	-1,12	-1,03	-1,03
Serpinf1	NM_177927.2	-1,52	-1,67	-1,02	-1,38	-1,04	-1,57	-1,25	-1,55	-1,03	-1,06	1,02	1,05
Serping1	NM_199093.1	-2,24	-4,44	-1,17	-1,95	-1,05	-3,52	-1,66	-3,62	1,04	-1,02	-1,05	1,02
Sfxn1	NM_001012213.1	1,29	1,56	1,13	1,27	1,19	1,77	1,52	1,82	1,14	1,24	1,20	1,10
Skap2	NM_130413.1	-1,18	-1,70	-1,14	-1,36	-1,05	-1,62	-1,30	-1,55	-1,09	-1,06	-1,11	-1,08
Slc12a5	NM_134363.1	-1,19	-1,88	-1,37	-1,39	-1,21	-1,55	-1,47	-1,86	-1,00	-1,02	-1,17	-1,11

Gene symbol	Accession No.	AmphotericinB		Doxorubicin		Puromycin		Paracetamol		Metformin		d-Mannitol	
		LD	HD	LD	HD	LD	HD	LD	HD	LD	HD	LD	HD
Slc17a6	NM_053427.1	1,46	2,24	1,50	2,45	1,06	1,62	1,66	1,34	1,04	-1,17	1,20	1,10
Slc20a1	NM_031148.1	1,29	2,04	1,17	2,10	-1,05	1,61	1,56	2,20	-1,15	-1,12	-1,12	-1,10
Slc27a1	NM_053580.2	-1,37	-1,97	-1,35	-1,24	-1,12	-1,74	-1,49	-1,99	-1,15	-1,12	-1,16	-1,13
Slc7a5	NM_017353.1	1,66	2,75	1,11	1,13	-1,01	2,36	1,55	1,88	1,01	1,14	1,05	1,12
Slc7a7	NM_031341.1	-1,17	-1,60	1,03	-1,20	-1,01	-1,58	-1,27	-1,53	1,07	1,01	1,10	1,07
Sox11	NM_053349.1	1,25	2,33	1,04	1,05	1,03	1,62	1,26	1,96	1,04	1,08	1,10	1,05
Tagln	NM_031549.1	-1,01	5,50	1,32	3,60	1,02	2,51	1,34	7,15	-1,15	-1,12	1,03	1,15
Tcea3	NM_001015008.1	-1,63	-1,91	-1,03	-1,55	1,02	-2,11	-1,58	-1,91	1,06	-1,02	1,09	1,22
Tekt1	NM_053508.2	-1,61	-1,92	-1,31	-1,51	-1,21	-1,76	-1,43	-1,80	-1,17	-1,16	-1,17	-1,26
Tf	NM_001013110.1	-1,68	-2,46	-1,18	-1,90	1,01	-2,40	-1,71	-3,08	1,09	-1,06	-1,00	1,12
Thra	NM_031134.2	-1,19	-2,47	-1,19	-2,82	-1,05	-1,61	-1,44	-4,01	1,10	-1,02	1,03	-1,03
Tle2	NM_001039013.1	-1,13	-1,61	-1,10	-1,30	-1,07	-1,56	-1,30	-2,10	-1,01	-1,11	-1,04	1,03
Tm7sf2	NM_001013071.1	-1,40	-1,89	-1,04	-1,61	-1,05	-1,73	-1,15	-1,67	-1,04	1,07	1,08	1,00
Tm7sf2	NM_001013071.1	-1,31	-2,20	-1,10	-1,69	-1,03	-1,67	-1,16	-1,86	-1,10	1,04	-1,01	-1,05
Tmem176b	NM_134390.2	-1,97	-3,78	-1,25	-2,07	1,00	-5,41	-1,62	-2,18	1,06	-1,07	-1,03	1,08
Tnfrsf12a	NM_181086.2	1,09	1,55	1,27	2,42	1,09	1,62	1,28	2,74	1,04	1,10	1,09	-1,03
Tnfsf12	NM_001001513.2	-1,50	-2,02	-1,54	-1,54	-1,20	-1,66	-1,42	-1,91	-1,12	-1,02	-1,22	-1,22
Tnfsf13	NM_001009623.1	-1,52	-2,58	-1,29	-2,10	-1,06	-2,65	-1,41	-2,64	1,03	-1,14	-1,01	1,03
Tnfsf18_predicted	XM_344166.3	1,37	3,99	1,17	2,03	1,11	1,94	1,76	7,30	1,03	1,10	1,12	1,01
Tst	NM_012808.1	-1,58	-1,98	-1,27	-1,48	-1,09	-1,80	-1,50	-2,15	-1,12	-1,22	-1,14	-1,10
Vkorc1	NM_203335.2	-1,37	-1,81	-1,11	-1,66	-1,03	-1,54	-1,29	-1,53	1,13	1,08	1,09	1,09
Vwf	XM_001066203.1	-1,13	-1,70	-1,09	-1,57	1,05	-1,17	-1,18	-2,15	1,01	-1,02	1,03	1,09
Xpa_predicted	XM_001071899.1	-1,18	-1,59	-1,07	-1,41	1,00	-1,56	-1,46	-1,91	1,13	1,11	1,07	1,07
Yars	NM_001025696.1	1,29	2,33	1,13	1,35	1,05	1,58	1,33	1,94	-1,04	-1,03	1,04	1,08

CURRICULUM VITAE

Personal information

Name: Tobias Christian Fuchs

Date of birth: April 23rd 1983
Birthplace: Darmstadt
Marital status: Married
Nationality: German

Since July 2012 Regulatory Affairs Manager

BASF SE, Performance Products, Performance Chemicals

Position: Regulatory Affairs Manager.

Task: Coordination of projects related to European chemical legislation (REACH)

2009 to 2012 PhD student

TU Darmstadt/ Merck Serono, Toxicology

Topic: Nephrotoxicity biomarkers in vivo and in vitro: Identification and validation of biomarkers for the detection of substance-induced acute and sub-acute renal damage.

Main area: Toxicology

2003 to 2008 Study of biology

TU Darmstadt

Diploma thesis: Establishment of an in vitro system for the detection of nephrotoxicity.

Main area: Biochemistry, Cell- and Developmental Biology, Ecology.
Grade: Passed with distinction

1999 to 2003 Education and social services

July 2003 - Sept. 2003 Voluntary activities in the childcare service in Eberstadt
Aug. 2002 - May 2003 Alternative national service at the sheltered workshop, Darmstadt

Aug. 1999 - June 2002 Bertolt-Brecht-School, high school diploma (grade 1.8)
Aug. 1993 - June 1999 Bernhard-Adelung-school, school-leaving certificate (grade 1.3)

Awards

Awards: “Toxicologic and Exploratory Pathology Specialty Section Charles Capen Award” of the “International Academy of Toxicologic Pathology” (IATP) (2011)

Member of the Student Excellence Program (STEP) of the Merck KGaA (2008-2012)

LIST OF PUBLICATIONS

Peer-Review Articles/Reviews:

- Analysis of transcriptional and urinary kidney biomarker for the early prediction of aristolochic acid induced nephrotoxicity.
  Accepted for publication in Veterinary Pathology, December 9th 2012
  Tobias Christian Fuchs, Assaf Wool, Angela Mally, Merav Beiman, and Philip Hewitt

- Evaluation of acute urinary rat kidney toxicity biomarker for sub-acute toxicity studies in pre-clinical trails
  Toxicologic Pathology, May 13th 2012
  Tobias Christian Fuchs, Katharina Frick, Stephanie Czasch, Barbara Emde, Friedrich von Landenberg, Philip Hewitt

- Preclinical perspective of urinary biomarkers for the detection of nephrotoxicity: what we know and what we need to know.
  Biomarker in Medicine. November 25th 2011
  Tobias Christian Fuchs, Philip Hewitt

- Biomarkers for Drug-Induced Renal Damage and Nephrotoxicity—An Overview for Applied Toxicology
  AAPS J Oktober 4th 2011
  Tobias Christian Fuchs, Philip Hewitt

- Evaluation of a urinary kidney biomarker panel in rat models of acute and subchronic nephrotoxicity
  Toxicology, September 9th 2010
  Dana Hoffmann, Tobias Christian Fuchs, Tanja Henzler, Katja Matheis, Thomas Herget, Wolgang Dekant, Philip Hewitt, Angela Mally

Book Chapter:

- Toxicogenomics in Pre-clinical safety assessment (Buchkapitel)
  A Comprehensive Guide to Toxicology in Preclinical Drug Development (Buchtitel)
  Elseviert, Published December 2012
  Tobias Christian Fuchs, Germaine Truisi, Philip Hewitt

Study Report:

- MSC2362412A (AFC-5261) – single dose oral toxicity study in rats
  Study Report T16207, Merck Serono, Toxicology April 2011 (confidential)
  Barbara Emde, Philip Hewitt, Tobias Christian Fuchs

- Cisplatin, Vancomycin and Puromycin – 28 days intraperitoneal injection pilot toxicity study in rats
  Study Report T16188, Merck Serono, Toxicology, 2011 (confidential)
  Barbara Emde, Stephanie Czasch, Tobias Christian Fuchs

- Vancomycin – 28 days intraperitoneal injection repeated dose toxicity study in rats
  Study Report T16206, Merck Serono, Toxicology 2012 (confidential)
  Barbara Emde, Stephanie Czasch, Tobias Christian Fuchs

- Cisplatin – 28 days intraperitoneal injection repeated dose toxicity study in rats
  Study Report T16215, Merck Serono, Toxicology 2013, (confidential)
  Barbara Emde, Stephanie Czasch, Tobias Christian Fuchs, Stefan Weigt

- Puromycin – 28 days intraperitoneal injection repeated dose toxicity study in rats
  Study Report T16222, Merck Serono, Toxicology 2013 (confidential)
  Barbara Emde, Stephanie Czasch, Tobias Christian Fuchs

Posters:

- Analysis of Urinary Proteins, miRNA, and Transcriptional Biomarkers for the Detection of Vancomycin-Induced Nephrotoxicity
  Toxicologist 126 (Suppl 2): 260, March 11th 2012 (SOT Annual Meeting 2012, San Francisco)
  Tobias Christian Fuchs, Barbara Emde, Esther Johann, Stefan Mueller, Philip Hewitt

- Identifying Biomarkers of Kidney and Liver Toxicity by Integrating Toxicogenomics Dataset
  Toxicologist 126, (Suppl 2): 260, März 15th 2012 (SOT Annual Meeting 2012, San Francisco)
  Philip Hewitt, Tobias Christian Fuchs, Rob Russell, Dragana Mitic Potkrajac, Gordana Apic

- Establishment of an in vitro screening system for the early detection of nephrotoxicity.
  Toxicology Letter 205, (Suppl), S159, August 28th 2011 (EuroTox Annual Meeting 2011, Paris)
  Tobias Christian Fuchs, Birthe Lauer, Philip Hewitt

- Detection of Vancomycin Induced Nephrotoxicity in Rat by Urinary Protein Biomarkers
  NDT Plus 4 (Suppl 2) s2.46; June 23rd 2011 (ERA-EDTA Annual Meeting 2011, Prague)
  Tobias Christian Fuchs, Barbara Emde, Stephanie Czasch, Friedrich von Landenberg, Philip Hewitt

- A Toxicogenomics approach for the establishment of an in vitro nephrotoxicity screening system.
  Naunyn-Schmiedeberg´s Arch Pharmacol. 383 (Suppl 1), 88; March 30th 2011 (DGPT Annual Meeting 2011, Frankfurt a. M.)
  Tobias Christian Fuchs, Philip Hewitt

- State-of-the-art Detection of Nephrotoxicity by Urinary Protein Biomarkers.
  Toxicologist 120 (Suppl 2):160, March 6th 2011 (SOT Annual Meeting 2011, Washington D.C.)
  Barbara Emde, Philip Hewitt, Stephanie Czasch, Friedrich von Landberg, Tobias Christian Fuchs

- Detection of Aristolochic acid induced renal damage by new urinary and transcriptional biomarkers.
  Toxicology Letter 196, (Suppl), S244-S245, July 19th 2010 (IUTox Meeting 2010, Barcelona)
  Tobias Christian Fuchs, Angela Mally, Merav Beiman, Assaf Wool, Philip Hewitt

- Nephrotoxicity biomarkers: An inter-platform comparison for the detection of renal damage
  Naunyn-Schmiedeberg´s Arch Pharmacol. 381 (Suppl 1), 64; March 23rd 2010 (DGPT Annual Meeting 2010, Mainz)
  Tobias Christian Fuchs, Merav Beiman, Assaf Wool, Tanja Henzler, Katja Matheis, Angela Mally, Philip Hewitt

Projects:

- Robert Russel, Gordana Apic, Philip Hewitt, Tobias Christian Fuchs,. August 2009 – June 2012; ”Development and industrial validation of new identification systems for biomarkers predicting hepato- and nephrotoxicity”; BMBF funded BioRN Project of the Biomarker Center (BMC-08).

- Assaf Wool, Merav Beiman, Philip Hewitt, Tobias Christian Fuchs, January 2009 – April 2010; “Evaluation of transcriptional biomarkers in pre-clinical safety assessment”; Cooperation project of Compugen Ltd. and Merck Serono.

EHRENWÖRTLICHE ERKLÄRUNG

Ich erkläre hiermit ehrenwörtlich, dass ich die vorliegende Arbeit entsprechend den Regeln guter wissenschaftlicher Praxis selbstständig und ohne unzulässige Hilfe Dritter angefertigt habe.

Sämtliche aus fremden Quellen direkt oder indirekt übernommenen Gedanken sowie sämtliche von Anderen direkt oder indirekt übernommenen Daten, Techniken und Materialien sind als solche kenntlich gemacht. Die Arbeit wurde bisher bei keiner anderen Hochschule zu Prüfungszwecken eingereicht.

_____ _____

Ort, Datum Unterschrift